LEABHARLANN CHOLÁISTE NA TRÍONÓIDE, BAILE ÁTHA CLIATH | TRINITY COLLEGE LIBRARY DUBLIN
Ollscoil Átha Cliath | The University of Dublin

Terms and Conditions of Use of Digitised Theses from Trinity College Library Dublin

Copyright statement

All material supplied by Trinity College Library is protected by copyright (under the Copyright and Related Rights Act, 2000 as amended) and other relevant Intellectual Property Rights. By accessing and using a Digitised Thesis from Trinity College Library you acknowledge that all Intellectual Property Rights in any Works supplied are the sole and exclusive property of the copyright and/or other IPR holder. Specific copyright holders may not be explicitly identified. Use of materials from other sources within a thesis should not be construed as a claim over them.

A non-exclusive, non-transferable licence is hereby granted to those using or reproducing, in whole or in part, the material for valid purposes, providing the copyright owners are acknowledged using the normal conventions. Where specific permission to use material is required, this is identified and such permission must be sought from the copyright holder or agency cited.

Liability statement

By using a Digitised Thesis, I accept that Trinity College Dublin bears no legal responsibility for the accuracy, legality or comprehensiveness of materials contained within the thesis, and that Trinity College Dublin accepts no liability for indirect, consequential, or incidental, damages or losses arising from use of the thesis for whatever reason. Information located in a thesis may be subject to specific use constraints, details of which may not be explicitly described. It is the responsibility of potential and actual users to be aware of such constraints and to abide by them. By making use of material from a digitised thesis, you accept these copyright and disclaimer provisions. Where it is brought to the attention of Trinity College Library that there may be a breach of copyright or other restraint, it is the policy to withdraw or take down access to a thesis while the issue is being resolved.

Access Agreement

By using a Digitised Thesis from Trinity College Library you are bound by the following Terms & Conditions. Please read them carefully.

I have read and I understand the following statement: All material supplied via a Digitised Thesis from Trinity College Library is protected by copyright and other intellectual property rights, and duplication or sale of all or part of any of a thesis is not permitted, except that material may be duplicated by you for your research use or for educational purposes in electronic or print form providing the copyright owners are acknowledged using the normal conventions. You must obtain permission for any other use. Electronic or print copies may not be offered, whether for sale or otherwise to anyone. This copy has been supplied on the understanding that it is copyright material and that no quotation from the thesis may be published without proper acknowledgement.

Dual acting nuclear receptor targeting conjugates:

Design, synthesis and

biochemical evaluation

A thesis submitted to the University of Dublin for the degree of doctor of philosophy

By

Patrick M. Kelly

Under the supervision of Prof. Mary J. Meegan, B. Sc., PhD (N.U.I.), M.R.S.C., C. Chem.

School of Pharmacy and Pharmaceutical Sciences

Trinity College Dublin

2013

TRINITY COLLEGE
- 4 MAR 2014
LIBRARY DUBLIN

Thesis 10231

DECLARATION

I declare that this thesis has not been submitted as an exercise for a degree at this or any other university and it is entirely my own work.

I agree to deposit this thesis in the University's open access institutional repository or allow the library to do so on my behalf, subject to Irish Copyright legislation and Trinity College Library conditions of use and acknowledgement.

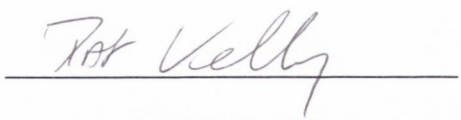

Patrick M. Kelly

Abstract

Breast cancer has become the second most common cancer worldwide after lung cancer, the fifth most common cause of cancer death, and the foremost cause of cancer death in women. Worldwide, breast cancer exceeds all other cancers and the incidence rates of breast cancer are increasing steadily. The vast majority of early stage breast cancers, in both pre- and postmenopausal women, are hormone-dependent. The human hormone estradiol (E2) plays an important role in the progression and development of the tumour. One of the major therapeutic advances in clinical treatment of breast cancer has been the introduction of selective estrogen receptor modulators (SERMs). The key feature of the SERMs, which are chemically diverse compounds, is that they contain a tertiary structure that enables them to bind to the estrogen receptor. Another important chemotherapy class are vascular targeting agents such as antimitotic drugs which target the microtubules and their dynamics. They interact with various tubulin binding sites and disrupt the role that microtubules play in the tumour cell cycle. Microtubules play a major part in mitosis and cell division, and for this reason they are an important target for anticancer drugs.

This thesis describes the design and synthesis of novel conjugates that contain both SERM type ligands and a 'warhead' cytotoxic agent. The SERM pharmacophore will selectively target the estrogen receptor in hormone dependent breast cancers. The cytotoxic agent will be selectively delivered to the site of the tumour and should reduce indiscriminate damage to perishable tissue. In chapter 1, a comprehensive overview of cancer is presented and the chemotherapy agents used to fight the disease with particular interest to breast cancer and breast cancer therapies are discussed. Chapter 2 describes the synthesis of SERM type ligands that would be incorporated into the conjugate scaffolds required. The cytotoxic agents which are based on combretastatin A4 (CA4) are synthesised in chapter 3. A novel approach for the synthesis of the cytotoxic agents which utilized microwave assisted organic synthesis (MAOS), and a series of piperazine derivatives of the CA4 are also discussed in this chapter. Chapter 4 describes a series of routes for the synthesis of two aromatase inhibitor type ligands that would be incorporated into the conjugate scaffold. The chemistry of the aromatase inhibitor type ligands led to the synthesis of a novel hybrid molecule based on CA4 and the aromatase inhibitor letrozole. The synthesis of the SERM type conjugates with cytotoxic agents is described in chapter 5, and the incorporation of aromatase inhibitors type ligands as part of the conjugate scaffold is also presented. The conjugate compounds synthesised within this project were evaluated for antiproliferative activity in MCF-7 (ER overexpressing breast cancer cell line) and for ER binding activity and the results are discussed in chapter 6 with the observations from the biochemical analysis rationalized using molecular modelling studies.

Acknowledgements

Foremost, I would like to express my sincere gratitude to my advisor Prof. Mary J. Meegan for the continuous support of my PhD study and research, for her patience, motivation, enthusiasm, and immense knowledge. Her guidance helped me in all the time of research and writing of this thesis. I could not have imagined having a better advisor and mentor for my PhD study.

Dr. John O'Brien of the NMR unit at Trinity College has been a major contributor to this work, as a cursory examination of the spectra included will confirm, and has my eternal gratitude for all his kind help and enthusiasm. Also a special thanks to Dr. Manuel Ruether who may not always get the credit he deserves.

The biochemistry evaluation was carried out in the laboratory of Dr. Daniela Zisterer in the School of Biochemistry, Trinity College, and I wish to thank Dr. Daniela Zisterer and all her group for their help. Most especially, thanks are due to Dr. Sandra Bright, Jade Pollock, Dr. Seema Nathwani and Dr. Lisa Greene. It was any interesting experience! Thanks to the staff of School, especially Ray, Rhona, Brian, Irene and Joe for technical support.

I am truly indebted and thankful to my fellow postgraduates and post-doctoral researchers who have borne with me in the laboratories, and thought the school, over the years. Niall, Yvonne, Niamh, Billy, Shu, Tadhg, Siddig, Andy, Conor, Feri, Jason, Gary, Adrain, Brian, Claire, Keith, Susan, Stephany, Vilmar, Shane, Juan and Jun in particular have provided welcome doses of sanity and friendship at bleak moments, which can hardly be repaid, and also to Mike and Gabor for the knowledge and guidance that I received from you both, I will never forget it. It has to be said we had an interesting ride through my time, from 'USB keys' to 'POF' it was thoroughly enjoyable. The friendships I have gained here I will be cherished forever.

Finally, I wish to thank the most loving, understanding patient family in the world. My parents, Stephen and Mary who supported me through my endeavours and kept patients when I when it looked like I was never going to leave. I would also like to thank my uncle Paddy and his wife Geraldine for the endless support and assistance that I received from them; I am eternally grateful and showed me the true meaning of family. And last but not least Lynn what can I say.... you showed the patience of a saint (most of the time) and keeping me sane for the most part, thank you.

The PhD. journey has been full of emotion with ups and downs from columns to reactions mixtures but one thing I have discovered which is very applicable to a medicinal chemistry PhD. and is best phrased by Albert Einstein-

'Insanity is doing the same thing over and over again and expecting different results'

Abbreviation

^{13}C-NMR	Carbon-^{13} NMR
^{1}H-NMR	Proton NMR
4-OHT	4-Hydroxytamoxifen
ADCs	Antibody-drug conjugates
AEBS	Antiestrogen binding site
AF1	Activation Function 1
AF2	Activation Function 2
AI	Aromatase inhibitor
AML	Acute myeloid leukaemia
AR	Androgen receptor
B:	Base
CA4	Combretastatin A-4
CML	Chronic myelogenous leukaemia
CoA	Co-activator
CoR	Co-repressor
COX	Cyclooxygenase
CYP	Cytochrome P450 enzyme
DASIs	Dual aromatase-sulfatase inhibitors
DBD	DNA-binding domain
DCC	*N,N'*-Dicyclohexylcarbodiimide
DCM	Dichloromethane
DHA	Docosahexaenoic acid
DHU	Dicyclohexylurea
DMAP	Dimethylaminepyridine
DMEM	Dulbecco's modified eagles medium
DMF	Dimethylformamide
DMSO	Dimethylsulfoxide
DNA	Deoxyribonucleic acid
DOX	Doxorubicin
E_1	Estrone
E_2	Estradiol
E_3	Estriol
EDC	1-Ethyl-3-(3-dimethylaminopropyl) carbodiimide hydrochloride
EPR	Enhanced permeability and retention
ER	Estrogen receptor
ERE	Estrogen receptor element
IR	Infrared
LBD	Ligand binding domain
LDH	Lactate dehydrogenase
Lit.	Literature
M.O.E.	Molecular Operating Environment
m.p.	Melting point
MAPs	Microtubule associated proteins
MCF-7	ER-positive human breast cancer cell line
MDA	ER-negative human breast cancer cell line
MeOH	Methanol
MMPs	Matrix metalloproteinases
MTT	3-(4,5-Dimethylthiazol-2-yl)-2,5-diphenyltetrazoliumbromide
NBS	*N*-bromo succinimide
*n*BuLi	*n*-Butyllithium
NF-κB	Nuclear factor kappa-light-chain-enhancer of activated B cells
NMR	Nuclear magnetic resonance
NOE	Nuclear Overhauser Effect
PBD	Pyrrolobenzodiazepine
Pd/C	Palladium on carbon
pdb	Protein databank file
ppm	Part per million
PUFAs	Polyunsaturated fatty acids
RBA	Relative binding affinity
Rf	Retention Factor
SAR	Structure–activity relationship
S.E.M.	Standard error of the mean
SERD	Selective estrogen receptor down-regulator
SERM	Selective estrogen receptor modulator
SERSM	Selective estrogen receptor subtype modulator
SI	Sulfatase inhibitor
SSRI	Serotonin-specific reuptake inhibitor
STS	Steroid sulfatase
TAM	Tamoxifen
TBAF	Tetrabutylammonium fluoride
TBDMS	*tert*-Butyldimethylsilyl
TBDPS	*t*-butyldiphenylsilyl
T-DM1	TrastuzumabDM1

ERR	Estrogen receptor-related
EtOAc	Ethyl acetate
EtOH	Ethanol
GISTs	Gastrointestinal stromal tumours
HER2	Human Epidermal Growth Factor Receptor 2
HOBt	Hydroxbenzotriazole
HRMS	High resolution mass spectrometry
IC_{50}	Maximal concentration of drug to cause 50% inhibition
GI_{50}	Concentration of drug to cause 50% reduction in proliferation
THF	Tetrahydrofuran
TIPS	Triisopropyl silane
TLC	Thin layer chromatography
TPS	Triphenylsilyl
TTP	Time to progression
UV	Ultra-violet
VDAs	Vascular disrupting agents

Table of contents

1	Chapter 1	1
1.1	Cancer	2
1.2	Chemotherapy	4
1.3	Breast Cancer	14
1.4	Estrogens	16
1.5	Selective Estrogen Receptors Modulators (SERMs)	26
1.6	Tamoxifen Metabolism	41
1.7	Aromatase Inhibitors	43
1.8	Sulfatase Inhibitors	49
1.9	Antimitotic agents	53
1.10	Combretastatins	54
1.11	Tumour-Targeting conjugates of cytotoxic agents	58
1.12	ER-targeting conjugates	65
1.13	Project Objectives	76
2	Chapter 2	77
2.1	Overview	78
2.2	Synthesis of cyclofenil-based analogues	94
2.3	Synthesis of 2-phenylindole-based analogues	98
3	Chapter 3	130
3.1	Introduction	131
3.2	Synthesis plan	131
3.3	Combretastatin analogues	132
4	Chapter 4	161
4.1	Overview	162
4.2	Synthesis of the anastrozole pharmacophore	162
4.3	Letrozole derivative as a conjugate ligand.	169
4.4	Aromatase Inhibitor – Combretastatin CA4 hybrid compounds	182
5	Chapter 5	186
5.1	Overview	187
5.2	Conjugate Strategy	187
5.3	Direct amide conjugates	189
5.4	Conjugate synthesis with cinnamic and 3-phenylpropanoic acids	196
5.5	Cyclofenil-based conjugates	200

5.6 2-Phenylindole conjugates 204
5.7 Synthesis of aromatase inhibitor containing conjugate prototype 211
6 Chapter 6 218
6.1 Biochemical evaluation 219
6.2 Molecular modelling studies 252
7 Chapter 7 272
7.1 Summary and Conclusion 273
8 Chapter 8 278
8.1 General experimental details 279
8.2 Synthesis of protected endoxifen 280
8.3 Synthesis of cyclofenil derivatives 282
8.4 Synthesis of 2-phenylindole derivatives 289
8.5 Synthesis of the acrylic acid analogues 312
8.6 Synthesis of the anastrozole derivative 331
8.7 Synthesis of endoxifen-acrylic acid conjugates 341
8.8 Synthesis of endoxifen-cinnamic acid/-3-phenylpropanoic acid conjugates 352
8.9 Synthesis of Cyclofenil-acrylic acid conjugates 356
8.10 Synthesis of Indole-acrylic acid conjugates 361
8.11 Synthesis of Endoxifen-anastrozole conjugate 367
8.12 Synthesis of letrozole-cytotoxic agent conjugate 368
9 Bibliography 369

Table of Figures

Figure 1-1 Fludarabine [1], Methotrexate [2], 5-Fluorouracil [3], ... 7
Figure 1-2. Dacarbazine [4], Procarbazine [5], Temozolomide [6] 8
Figure 1-3. Chlorambucil [7]), Mitomycin C [8], Cisplatin [9], Psoralens [10] 8
Figure 1-4 Anthramycin [11] 8
Figure 1-5 DSB-120 [12] and Bizelesin [13] 9
Figure 1-6 Doxorubicin[14] and Mitoxantrone[15] 10
Figure 1-7 Topotecan [16], Etoposide [17]) and ICRF 193 [18] 10
Figure 1-8 Bleomycin A_2 [19] 11
Figure 1-9 Paclitaxel [20], Vinblastine [21] and Combretastatin A-4 [22] 12
Figure 1-10 ZD6126 [23], CA4P [24], NPI-2358 [25] and Vadimezan [26] 12
Figure 1-11 Imatinib [27] 13
Figure 1-12. Summary of main enzymatic pathways for biosynthesis of estradiol 15
Figure 1-13. Evolutive transformation of the breast cell from normal to carcinogen[56] 16
Figure 1-14. Ovarian Synthesis, Transport, and Metabolism of Estrogens.[65] 17
Figure 1-15. Tamoxifen (R_1 = CH_3= R_3 = CH_3, R_2 = H) [34]; 4-Hydroxytamoxifen (R_1 = R_3 =, CH_3, R_2 = OH) [35]; 18
Figure 1-16. Classic Pathway of Estrogen Signal Transduction[65] 19
Figure 1-17. Sequence organization of the two isoforms, ERα and ERβ[95] 21
Figure 1-18 (A) Empty LBD of the ERα and (B) with E2 docked into the empty ligand binding cavity of ERα[96] 21
Figure 1-19. Schematic of observed ER LDB conformational states and activation role[99] 22
Figure 1-20. Structural basis of estrogen receptor (ER) activation: major conformations induced by ER agonists[97] 23
Figure 1-21 Orientation of estradiol [28] in the ligand binding pocket of the estrogen receptor ligand binding domain[100] 25
Figure 1-22. Selection of Triphenylethylenes [34], [37]-[40] 28
Figure 1-23. Cyclofenil [41], GW5638 [42] and GW7604 [43] 29
Figure 1-24. Raloxifene [45] and Arzoxifene [46] 30
Figure 1-25. Lasofoxifene [47], Nafoxidine [48] and Trioxifene [49] 30
Figure 1-26. Bazedoxifene [50] and Pipendoxifene [51] 31
Figure 1-27. Manipulation of the indole to increase selectivity and RBA, [52] and [53] 31
Figure 1-28 X-ray crystal structure interation A) 2QTU.pdb and B) 2POG.pdb 32
Figure 1-29. Ormeloxifene [54], levormeloxifene [55], SP500263 [56], EM-800 [57] & EM-652 [58] 33
Figure 1-30. Compound [59] 33
Figure 1-31. Novel chromane analogues, [60]-[63] 34
Figure 1-32. 2-Phenylquinoline derivative [64] and 6*H*-chromeno[4,3-*b*]quinoline derivatives [65],[66] 35
Figure 1-33. Dihydrobenzoxathiins [67] / Dihydrobenzodithiins [68] 35
Figure 1-34. Tetrahydrofluorenone derivatives [69]-[72] 37
Figure 1-35. Tetrahydrobenzo[*a*]fluorenes and Hexahydrochrysenes analogues 37
Figure 1-36. Pyrazoles, Indazoles and Furans derivatives [75]-[78] 38
Figure 1-37. Phenyl-2*H*-indazole analogues [79] and [80], and benzimidazole derivative [81] 38
Figure 1-38.ERB-041 [82] and C-3 monophenolic variation [83] 39

Figure 1-39. Novel Flexible Ligands, [84] and [85] 40
Figure 1-40. Fulvestrant [86] 41
Figure 1-41. Tamoxifen metabolites and relevant CYP genes 42
Figure 1-42 First- and Second- generation of Aromatase Inhibitors [90]-[94] 44
Figure 1-43 Third generation Aromatase Inhibitors [96]-[98] 45
Figure 1-44 Xanthone derivative [99] and chromone analogue [100] 47
Figure 1-45 COX-2 inhibitors derivatives as Aromatase Inhibitors, Nimesulide and [101]-[103] 48
Figure 1-46 Tamoxifen metabolite - norendoxifen 48
Figure 1-47 STS Steroid inhibitors [104]-[106] 50
Figure 1-48 Steroid sulfamate based inhibitors of STS [107]-[111] 50
Figure 1-49 Steroid sulfamate based inhibitors of STS [112]-[113] 50
Figure 1-50 Non steroid sulfamate based inhibitors of STS [114]-[117] 51
Figure 1-51 Steroid non sulfamate based inhibitors of STS [118]-[119] 51
Figure 1-52 Non steroid non sulfamate based inhibitors of STS [120]-[122] 51
Figure 1-53 Biphenyl derivatives [123]-[125] 52
Figure 1-54 Isolated natural products with anticancer properties [22], [126]-[131] 55
Figure 1-55 Function modification of the Combretastatin structure [133]-[139] 56
Figure 1-56 Combretastatin with significant structural variation [140]-[150] 56
Figure 1-57 Novel compounds based on the combretastatin structure [152]-[160] 57
Figure 1-58 Increased solubility Combretastatin [161] & VTA in clinical trials [24] and [163] 58
Figure 1-59 BR96-DOX [164] 60
Figure 1-60 Gemtuzumab Ozogamicin (Mylotarg®) [165] 61
Figure 1-61 Trastuzumab DM1 (T-DM1) 62
Figure 1-62 DHA–paclitaxel (Taxoprexin®) [166] 62
Figure 1-63 Folic acid [167] & hyaluronic acid monomer unit [168] 63
Figure 1-64 Targets of chemotherapeutic agents[394] 66
Figure 1-65 Estradiol-Ellipticine Conjugate [169] & CNU-estradiol conjugates [170] 67
Figure 1-66 Geldanamycin conjugate [171], Chlorambucil conjugate [172] & ICI 164,384 [173] 68
Figure 1-67 Examples of Estradiol–Anthracycline conjugate [174], Estradiol–Paclitaxel conjugates [175] and Estradiol–cisplatin conjugate [176] 69
Figure 1-68 Antiestrogen-Mitomycin conjugate [177] and AE-Dox conjugate [178] 70
Figure 1-69 Novel ER targeting conjugates [180]-[184] 73
Figure 1-70 Potent conjugate containing an dihydroxyendoxifen coupled to CA4 [185] 74
Figure 1-71 Conjugates of radioligands, [186]-[188] 74
Figure 1-72 Conjugates with improved pharmaceutical properties, [186]-[188] 75
Figure 2-1 Tamoxifen [34] and metabolites: 4-hydroxytamoxifen [35], endoxifen [36] and norendoxifen [36a] 78
Figure 2-2 ^{1}H-NMR spectrum for [193] 87
Figure 2-3 ^{1}H-NMR spectrum of [196] 90
Figure 2-4 Bromoethyl CH_2 signals for ^{1}H-NMR spectrum of [196] 91
Figure 2-5 ^{1}H-NMR spectrum of [197] 92
Figure 2-6 ^{13}C, DEPT 135 and DEPT 90 NMR spectrums of [197] 93
Figure 2-7 *E*-and *Z*- isomers of [197] 94
Figure 2-8 ^{1}H-NMR spectrum of [222] 97
Figure 2-9 ^{13}C and DEPT135 NMR spectras of [222] 97

Figure 2-10 2-Phenylindoles with biological activity 98
Figure 2-11 Flexible alignment of 2-(4-hydroxyphenyl)-3-methyl-1H-indol-5-ol [228] (green) and estradiol [28] (yellow) 99
Figure 2-12 ^{1}H NMR spectrum of [231] 102
Figure 2-13 ^{13}C NMR spectrum of [231] 102
Figure 2-14 ^{1}H NMR spectrum of [235] 104
Figure 2-15 ^{13}C NMR spectrum of [235] 104
Figure 2-16 ^{1}H NMR spectrum of [238] 106
Figure 2-17 ^{13}C NMR spectrum of [238] 107
Figure 2-18 ^{1}H NMR spectrum of [241] (MeOD-d_4) 111
Figure 2-19 ^{13}C NMR and DEPT-135 spectras of [241] (MeOD-d_4) 112
Figure 2-20 ^{1}H NMR spectrum of [263] 113
Figure 2-21 ^{13}C NMR and DEPT-135 spectras of [263] 114
Figure 2-22 ^{1}H NMR spectrum of [269] 116
Figure 2-23 ^{13}C NMR spectrum of [269] 116
Figure 2-24 ^{1}H NMR spectrum comparison (above, rearranged product S2 [273], below [251]) 117
Figure 2-25 ^{13}C NMR spectrum comparison (above rearranged product S2 [273], below [251]) 118
Figure 2-26 ^{1}H NMR spectrum of [285] 125
Figure 2-27 ^{13}C NMR and DEPT-135 spectras of [285] 126
Figure 2-28 ^{1}H NMR spectrum of [299] 127
Figure 2-29 ^{13}C NMR and DEPT 135 spectras of [299] 128
Figure 3-1 Combretastatin A4 [22] and Combretastatin A4 acrylic acid [150] 132
Figure 3-2 Yield comparisons of Microwave and Reflux methods for the acrylic acids synthesised 142
Figure 3-3 ^{1}H-NMR spectrum of [310] 142
Figure 3-4 ^{13}C-NMR spectrum of [310] 143
Figure 3-5 Combretastatin A-4 and [150] 144
Figure 3-6 ^{1}H-NMR spectrum of [342] 150
Figure 3-7 ^{13}C-NMR spectrum of [342] 150
Figure 3-8 ^{1}H-NMR spectrum of [343] 151
Figure 3-9 ^{13}C-NMR and DEPT-135 spectrums of [343] 152
Figure 3-10 ^{1}H-NMR spectrum of [349] 159
Figure 3-11 ^{13}C-NMR and DEPT-135 spectras of [349] 159
Figure 4-1 ^{1}H NMR spectrum of [373] 166
Figure 4-2 ^{13}C NMR and DEPT-135 spectrums of [373] 166
Figure 4-3 ^{1}H NMR spectrum of [375] 168
Figure 4-4 ^{13}C NMR and DEPT-135 spectrum of [375] 168
Figure 4-5 Open vessel microwave chamber - Dean-Stark[543] 177
Figure 4-6 ^{1}H NMR spectrum of [384] 178
Figure 4-7 ^{13}C NMR and DEPT-135 spectrums of [384] 178
Figure 4-8 ^{1}H NMR spectrum of [387] 181
Figure 4-9 ^{13}C NMR and DEPT-135 spectrum of [387] 181
Figure 4-10 ^{1}H-^{13}C COSY experiment of compound [387] 182
Figure 4-11 ^{1}H NMR spectrum of [413] 185
Figure 4-12 ^{13}C NMR spectrum of [413] 185

Figure 5-1 General prototype structure and example of CA type cytotoxic agent [150] and ER-ligand endoxifen [36] 188
Figure 5-2 ^{1}H-NMR spectrum for [418] 194
Figure 5-3 ^{13}C-NMR spectrum for [418] 194
Figure 5-4 ^{1}H NMR spectrum for [418], A - DCC method, B - EDC method 195
Figure 5-5 Enlarged ^{1}H NMR spectrum between 1-2 ppm for [418], A - DCC method 196
Figure 5-6 ^{1}H-NMR spectrum of [436] 199
Figure 5-7 ^{13}C-NMR and DEPT-135 spectrums of [436] 200
Figure 5-8 ^{1}H-NMR spectrum of [443] 202
Figure 5-9 ^{1}H-NMR spectrum for [448] 203
Figure 5-10 ^{13}C-NMR spectrum for [448] 204
Figure 5-11 ^{1}H-NMR spectrum of [454] - (CD_3OD) 207
Figure 5-12 ^{13}C-NMR and DEPT-135 spectrums of [454] (CD_3OD) 208
Figure 5-13 Compound [458] 208
Figure 5-14 ^{1}H-NMR spectrum of [458] as part of VT NMR experiment (DMSO-d_6) 209
Figure 5-15 Expanded regions of the ^{1}H-NMR spectra of [458], above and the ^{1}H-NMR spectra of [458] processed *via* Gaussian multiplication 210
Figure 5-16 Synthesis of the methoxy-2-phenylindole conjugates 210
Figure 5-17 ^{1}H-NMR spectrum of [463] ($CDCl_3$) 213
Figure 5-18 ^{13}C-NMR and DEPT-135 spectrums for [463] 214
Figure 5-19 ^{1}H-NMR spectrum of [464] ($CDCl_3$) 215
Figure 5-20 ^{13}C-NMR and DEPT-135 spectrums of [464] ($CDCl_3$) 216
Figure 6-1 Antiproliferative effects of tamoxifen and combretastatin A4 in the MCF-7 human breast cancer cell line. 225
Figure 6-2 The antiproliferative effects of an endoxifen-combretastatin conjugate in the MCF-7 human breast cancer cell line (compound [427]). 228
Figure 6-3 Antiproliferative effects of endoxifen-modified combretastatin conjugates [435] and [436] in the MCF-7 human breast cancer cell line (compounds [435] and [436]) 230
Figure 6-4 A representative graph of the antiproliferative effects of a cyclofenil-based analogue in the MCF-7 human breast cancer cell line (compound [223]). 231
Figure 6-5 A representative graph of the antiproliferative effects of cyclofenil-combretastatin conjugates in the MCF-7 human breast cancer cell line (compounds [447] and [448]). 233
Figure 6-6 The antiproliferative effects of a 2-phenylindole analogue in the MCF-7 human breast cancer cell line (compound [243]) 234
Figure 6-7 A representative graph of the antiproliferative effects of a 2-phenylindole-combretastatin conjugate in the MCF-7 human breast cancer cell line (compound [458]) 236
Figure 6-8 A representative graph of the antiproliferative effects of a bis-2-phenylindole analogue in the MCF-7 human breast cancer cell line (compound [268]). 237
Figure 6-9 Antiproliferative effects of the aromatase inhibitor containing conjugates ([464] & [463]) in the MCF-7 human breast cancer cell line 239
Figure 6-10 Antiproliferative effects of the letrozole derivative [413] in the MCF-7 human breast cancer cell line. 241
Figure 6-11 Tubulin polymerization assay for compound [413] (10 μM) with EtOH 242
Figure 6-12 Tubulin polymerization assay for CA4 (10 μM) with EtOH 242

Figure 6-13 Antiproliferative effects of the selected piperazine acrylic acid derivative [349] in the MCF-7 human breast cancer cell line. 243
Figure 6-14 Selected cohort of the most active compounds from each set of synthesised compounds, Conjugate (Red), ER type ligands (orange) and VTA/ letrozole-CA4 (blue) 246
Figure 6-15 Flow cytometry to determine the percentage of (A.) apoptosis, as assessed by quantification of the pre-G1 peak and (B.) G2/M-arrested cells. Values represent the mean ± S.E.M. of three independent experiments. 247
Figure 6-16 Flow cytometry to determine the percentage of (A.) apoptosis, as assessed by quantification of the pre-G1 peak and (B.) G2/M-arrested cells. 247
Figure 6-17 Inhibition of NF-κB activity after treatment with novel ER ligand [297]. 251
Figure 6-18 WAY-169916 [465] 252
Figure 6-19 Estradiol agonist in the human ERα ligand binding domain, 1ERE.pdb 255
Figure 6-20 4-Hydroxytamoxifen antagonist in the human ERα ligand binding domain, 3ERT.pdb. 255
Figure 6-21 Antagonistic side chain interaction of raloxifene in rERβ (1QKN.pdb) 256
Figure 6-22 Antagonistic side chain interaction of ICI 164,384 (B) within the rERβ LBD (1HJ1.pdb)..257
Figure 6-23 Top-ranking docked conformation of [414] in ERα, 3ERT.pdb. 259
Figure 6-24 Superposition of 4-OHT (pink) and [414] (grey) docked conformations in ERα (3ERT.pdb) 259
Figure 6-25 Top-ranking docked conformation of [435] in the LBD of ERα, 3ERT.pdb. 260
Figure 6-26 Superimposition of 4-OHT (pink) and [436] (grey) docked conformations in ERα, 3ERT.pdb 261
Figure 6-27 Top-ranking docked conformation of [448] in 3ERT (ERα). 262
Figure 6-28 Orientation of [448] cyclofenil ligand fragment docked within the ERα 262
Figure 6-29 Top-ranking docked conformation of [243] in 1ERR, (ERα). 263
Figure 6-30 Superposition of ICI 164,384 (pink) and [243] (grey) docked conformations in ERβ 1HJ1.pdb 264
Figure 6-31 Top-ranking docked conformation of [458] in ERα, 1ERR.pdb. 265
Figure 6-32 Top-ranking docked conformation of [458] in 1QKN (rERβ). 265
Figure 6-33 Top-ranking docked conformation of [268] in ERα, 1ERR.pdb. 266
Figure 6-34 Top-ranking docked conformation of [463] in ERα, 3ERT.pdb. 267
Figure 6-35 Top-ranking docked conformation of [349] in colchicine binding site of tubulin (1SA0.pdb). 268
Figure 6-36 Superposition of DAMA Colchicine (green) and [349] (grey) docked conformations in tubulin (1SA0) 269
Figure 6-37 Top-ranking docked conformation of [413] in colchicine binding site of tubulin (1SA0,pdb). 269
Figure 6-38 Superposition of DAMA Colchicine (green) and [413] (grey) docked conformations in 1SA0 270
Figure 6-39 Top-ranking [413] docked conformation in 3EQM with androstenedione (ligand). 271
Figure 6-40 Androstenedione [466] 271
Figure 7-1 Example of synthesised compounds which would be ideal candidates for further anti-cancer studies 277

Table of Schemes

Scheme 1-1 Outline of the synthesis of steps to obtain [179] (i) DIPEA, THF sealed tube, 60 °C; hydrazine, EtOH, 60 °C; (iii) TFA, EtOH, water. 72
Scheme 2-1 4-Hydroxytamoxifen synthesis route by McCague *et al*[434] 79
Scheme 2-2 Tamoxifen synthesis route by Miller[435] 79
Scheme 2-3 Tamoxifen synthesis route by Shimizu[438] 80
Scheme 2-4 Tamoxifen synthesis route by Studemann[439] 80
Scheme 2-5 Tamoxifen synthesis by Zhou[440] 80
Scheme 2-6 Tamoxifen synthesis by Itami[442] 80
Scheme 2-7 Tamoxifen synthesis route by McKinley and O'Shea[432] 81
Scheme 2-8 Mechanism of the McMurry reaction for the formation of the triarylethylene 83
Scheme 2-9 Synthetic strategy of endoxifen analogue 84
Scheme 2-10 TBAF deprotection step 86
Scheme 2-11 Formation of [193] *via* the McMurry reaction. (ii) $TiCl_4$, Zn, THF, 4 h reflux 86
Scheme 2-12 Synthesis of the bromoethyl triarylethylene product [196] 88
Scheme 2-13 Phase-transfer catalysed ethylbromination reaction mechanism 89
Scheme 2-14 Amination reaction to afford [197] 92
Scheme 2-15 Synthesis of cyclofenil-endoxifen analogues [216] - [225] 95
Scheme 2-16 Synthesis of 2-phenylindole analogues [229] - [243] 100
Scheme 2-17 Mechanism for Fischer indole synthesis of [231] 101
Scheme 2-18 Bromination of [231] 103
Scheme 2-19 Mechanism for bromination of [231] 103
Scheme 2-20 Amination reaction to afford products [238]-[240] 105
Scheme 2-21 Proposed mechanism of demethylation 107
Scheme 2-22 Synthesis of 2-phenylindole analogues [241]-[243] and [261]-[262] 108
Scheme 2-23 Synthesis of 4-Benzoxyphenylhydrazine 109
Scheme 2-24 Synthesis of by-products S1 [263]-[267] 112
Scheme 2-25 Synthesis of [268]-[272] 114
Scheme 2-26 2-Phenyl-3*H*-indole analogue synthesis 115
Scheme 2-27 Proposed reaction mechanism for the formation of the 2-phenyl-3*H*-indole [273] 119
Scheme 2-28 Synthesis of [279] and [282] 121
Scheme 2-29 Synthesis of [281] 121
Scheme 2-30 Bromination of [281] 122
Scheme 2-31 Synthetic route for the potential selective inhibitors of NF-κB [292]-[297] and S2 product [298],[299],[301], [302], RBr = [278]-[283] 123
Scheme 2-32 Attempted debenzylation of [299] 128
Scheme 3-1 Synthesis combretastatin A4 [22] 132
Scheme 3-2 Perkin reaction mechanism (formation of [310]) 133
Scheme 3-3 Synthesis of the acrylic acid combretastatin analogue [310] 134
Scheme 3-4 Formation of the acetate ester [323]. 137
Scheme 3-5 Cleavage of the acetate ester [318] 138
Scheme 3-6 Synthetic route for the preparation of phenylacetic acid [328] and [329] 144
Scheme 3-7 Synthesis of benzylic nitrile [339] 146

Scheme 3-8 Synthesis of cinnamic acids and 3-phenylpropanoic acids....147
Scheme 3-9 Mechanism for the formation of cinnamic acids [342] and [344] *via* the Doebner modification of the Knoevenagel condensation....149
Scheme 3-10 Reduction of the cinnamic acids....151
Scheme 3-11 Attempted synthesis of the hydroxamic acid [362] *via* the methyl ester....153
Scheme 3-12 Synthesis of the piperazine derivatives [347]-[360]....154
Scheme 3-13 DCC coupling reaction mechanism for amide synthesis....155
Scheme 4-1 Aromatase inhibitors [96]-[97] and target conjugates [463]-[464]....163
Scheme 4-2 Route to the anastrozole derivative [376]....163
Scheme 4-3 Mechanism for the 1,2,4-triazole substitution....167
Scheme 4-4 Attempted synthesis of [378]....169
Scheme 4-5 Synthesis of letrozole [97]....170
Scheme 4-6 Proposed synthesis of the letrozole derivative [387]....171
Scheme 4-7 Synthesis of [382]....171
Scheme 4-8 Proposed synthesis of the letrozole derivative [385]....172
Scheme 4-9 General mechanism of formation of the aryl zinc bromide....173
Scheme 4-10 General mechanism of transition metal-catalysed crosscoupling reaction....174
Scheme 4-11 Mechanism for the formation of [384]....175
Scheme 4-12 Alternative synthesis route for [396]....176
Scheme 4-13 General mechanism for preparation of [396]....176
Scheme 4-14 Altered route for the synthesis of [386]....179
Scheme 4-15 Synthesis of the letrozole derivative [387]....180
Scheme 4-16 Synthetic route for the AI-CA4-hybrid compounds....183
Scheme 5-1 General mechanism for amide synthesis with EDC....190
Scheme 5-2 Endoxifen direct-amide conjugates....191
Scheme 5-3 Amide resonance: partial double bond character....195
Scheme 5-4 Synthesis of endoxifen conjugates [435]-[438]....198
Scheme 5-5 Cyclofenil-based conjugates....201
Scheme 5-6 2-Phenylindole based direct-amide conjugates....205
Scheme 5-7 Endoxifen-anastrozole conjugate [463]....212
Scheme 5-8 Synthesis of letrozole conjugate [464]....215

Table of Tables

Table 1 Cyclofenil analogues[469] 94
Table 2 Endoxifen-cyclofenil analogue reaction yeilds (*=novel compound) 96
Table 3 2-Phenylindole analogue reaction yields (*=novel compound) 110
Table 4 Bis-2-phenylindole analogue reaction yields 115
Table 5 2-Phenyl-3*H*-indole analogues 118
Table 6 Various chains utilized for the synthesis of potential selective inhibitors of NF-κB 123
Table 7 Potential selective inhibitors of NF-κB [292]-[297] 125
Table 8 Effect of reaction time on the isolated yields of compound [310] 135
Table 9 Effect of reaction temperature on the isolated yields of [310] in microwave reaction synthesis 136
Table 10 Structure and yields of acrylic acids synthesised (* novel compounds) 141
Table 11 Synthesis of the phenylacetic acids [328] and [329] 146
Table 12 Synthesised cinnamic acids [342] and [344], and 3-phenylpropanoic acids [343] and [345] 148
Table 13 Piperazine derivatives [347] - [360] (*novel compounds) 158
Table 14 Aromatase inhibitor – combretastatin CA4 hybrid [394], [411]-[413] and [402] 184
Table 15 Yields for amide conjugate reaction (DCC and EDC as coupling agent) 193
Table 16 Direct amide conjugate reaction yields (DCC and EDC as coupling agent) 199
Table 17 Direct amide conjugate reaction yields and deprotection yields 202
Table 18 Direct amide conjugate reaction yields and deprotection yields 206
Table 19 Volume of reagents required per well for the NF-κB study 223
Table 20 Antiproliferative data for reference compounds [22], [34] and [36] 225
Table 21 Antiproliferative data for novel endoxifen-combretastatin conjugates 228
Table 22 Antiproliferative data for the structurally modified combretastatin-endoxifen conjugates 229
Table 23 Antiproliferative data for cyclofenil-based analogues as potential ER-ligand 231
Table 24 Antiproliferative data of combretastatin-cyclofenil based conjugates 232
Table 25 Antiproliferative data for 2-phenylindole-based analogues as potential ER-ligands 234
Table 26 Antiproliferative data of combretastatin-2-phenylindole-based conjugates 235
Table 27 Antiproliferative data of for bis-2-phenylindole-based analogues as potential ER-ligand ..237
Table 28 Antiproliferative data of for the Aromatase inhibitor containing conjugates 239
Table 29 Antiproliferative data for the letrozole derivatives 240
Table 30 Antiproliferative data for selected piperazine acrylic acid derivative 243
Table 31 ERα and ERβ binding data for the most active novel compounds 244
Table 32 Antiproliferative data for the selected compounds synthesised for the NF-κB study 249
Table 33 ERα and ERβ binding data for the novel compounds selected for the NF-κB study 250
Table 34 Crystal structure codes with corresponding ligand and protein 253
Table 35 Correlation of key binding residues in human and rat ERβ isoforms 257

Chapter 1
Introduction

1.1 Cancer

1.1.1 Cancer Statistics

The objective of this project is to investigate, synthesize and evaluate new chemotherapeutic agents which are specifically designed to target breast cancer cells.

Over the three year (2007-2009) period in Ireland, an average of 29,745 cancer cases was diagnosed annually.[1] Over this three year period, a 12% average increase in the incidence of cancer cases was shown when compared to that of the years 2004-2006. Furthermore, this statistic shows a 50% increase when compared to the annual average in the mid 1990s. The incidence of cancer was higher in men than in women: cumulative lifetime risk for invasive cancer (excluding Non-Melanoma Skin Cancer NMSC) was approximately 1 in 3 for men and 1 in 4 for women.

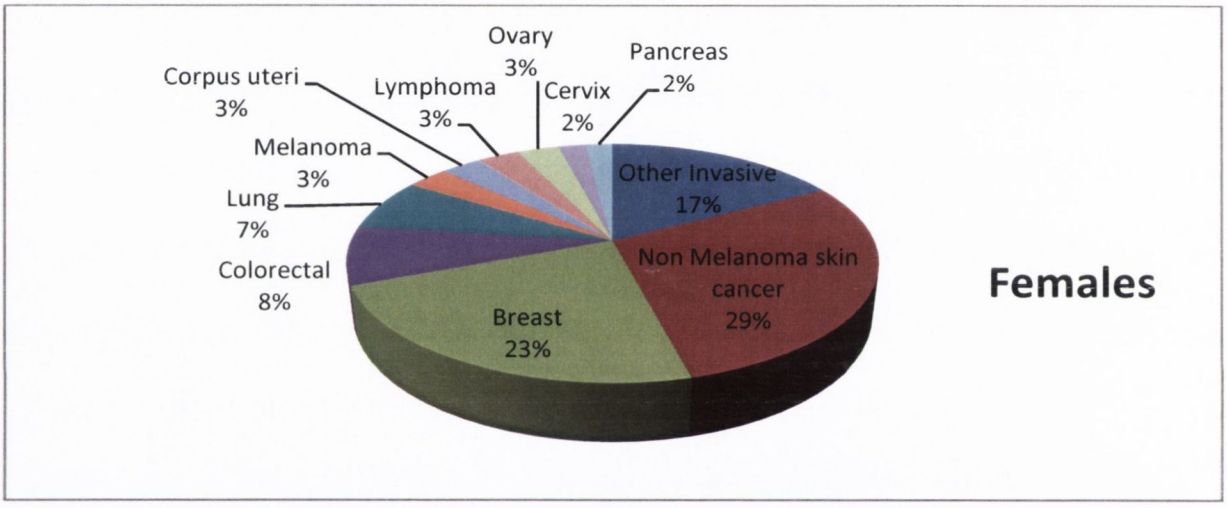

Chart 1-1 Relative frequency of the main invasive cancers diagnosed in females (2007-2009)

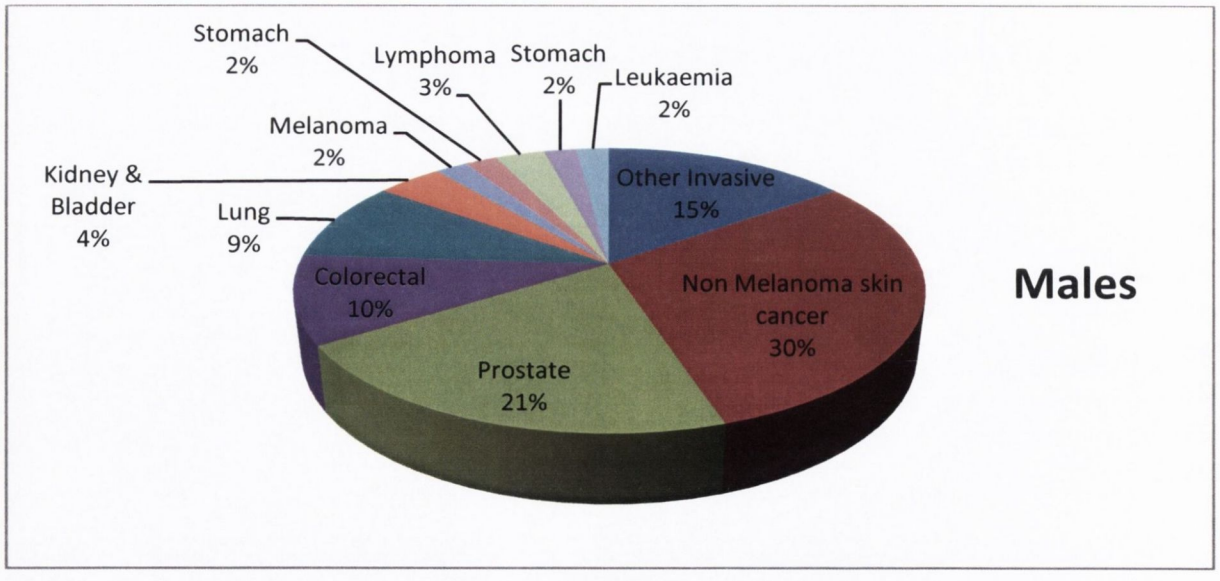

Chart 1-2 Relative frequency of the main invasive cancers diagnosed in females (2007-2009)

Incidents of cancer in a population are usually categorized firstly by gender; male and female. Excluding NMSC, the female breast cancer and prostate cancers in males account for nearly a third of the all cancers diagnosed (see Chart 1-1 and Chart 1-2).

Three factors are believed to contribute to the increase in cancer incidence[2]:

- Demographic factor

Ageing Population – with the advances in medicine and treatments, there is an increasing number of the population now living beyond their 65th birthday.

- Independent of demographic factor

Increase in underlying cancer rates – breast and gynaecological cancers have seen a significant increase in women and prostate cancer has also seen a significant increase in males.

- Improvements in screening techniques and cancer awareness

1.1.2 Cancer overview

Cancer is a disease in which abnormal cells divide without control and are able to invade other tissues, which can lead to a solid mass of cells known as a tumour.[3] Cancer is not just one disease but many diseases, characterised by similar uncontrolled cell growth. There are more than 100 different types of cancer and the majority are named according to the organ or type of cell in which they originate, i.e. breast cancer. A tumour (or neoplasm) is an abnormal tissue mass which results from neoplasia, a state in which the control mechanism governing cell growth becomes damaged, leading to cell proliferation. The cells can experience an abnormal growth pattern prior to neoplasia, such as metaplasia or dysplasia.[4] Cells which undergo metaplasia or dysplasia do not always result in neoplasia. The tumour (or neoplasm) may be benign, pre-malignant (carcinoma in situ) or malignant (cancer).

The cancer generally originates in a single cell in a tissue, which is genetically damaged to produce a cancer stem cell containing a malignant phenotype. This cell then undergoes abnormal mitosis which is uncontrolled, eventually leading to the formation of a neoplasm at that location; this is known as the primary tumour. Metastasis enables the tumour to spread to new sites within that tissue or other sites around the body. Some tumour cells can easily penetrate to the circulatory system which allows access to distant sites in the body. The metastatic spread of cancer cells in the blood or lymph vessels will often form secondary tumour in organs which have a large blood supply. Cancers can often result in death, as the tumour growth in an organ can inhibit the natural function of this organ.

Dynamic changes in the genome caused by possible internal and external factors are often associated with the initiation of cancer. Internal factors include mutations in DNA sequences, addition or loss of genetic material and uncontrolled gene expression or amplification. External factors include bacterial infections, viruses, carcinogenic chemicals, exposure to radiation (UV light, gamma rays, X-rays, radioactive particles) and hereditary factors (inherited genes can predispose individuals to develop certain forms of cancer).

As cancer is not just one disease but many diseases that have similar uncontrolled cell growth, so too are there many treatments. The treatment often depends on the type of cancer and the degree of tumour progression. Often a patient may receive more than one course of treatment such as a combination of the following: surgery, radiotherapy, chemotherapy. More recent advances in the treatment such as cancer genomics, gene therapy, immunotherapy and photodynamic therapies are becoming more widely used in the clinical environment. Surgery can often be the only treatment a patient may require. The surgery can remove the tumour completely and the cancer is contained in one area and has not spread to the surrounding tissue or organs. Non-localised cancer requires treatments such as chemotherapy, biological or hormone therapy.

Radiotherapy is a treatment used for the treatment of localised cancer. Like surgery it is often used in conjunction with other treatments. A patient may be prescribed radiotherapy pre/post surgery to decrease the size of the tumour. Some radiotherapy utilize X-rays or radiopharmaceuticals (radionuclides) which emit γ-rays. As the radiation can kill healthy cell along with cancer cells, the radiotherapy can be given locally to limit damage to healthy tissue.

Chemotherapy is the use of cytotoxic anti-neoplastic drugs to selectively target the cancer cells or limit growth. The use of non-toxic light-sensitive drugs that when exposed selectivity to light can become toxic to selectively target the malignant cells is known as photodynamic therapy.[5] Immuno- and gene therapy are called biological therapies. It has been found that a number of neoplasms produce specific antigens and has led to the development of monoclonal antibodies specific to those tumours. There are two types of monoclonal antibodies are used in cancer treatments "Naked mAbs" which are antibodies are effective (no drug or radioactive material attached) and "Conjugated mAbs" which contain either a chemotherapy drug, radioactive particle, or a toxin as conjugate. These act as homing devices which can selectively deliver the substances directly to the cancer cells.[6]

1.2 Chemotherapy

The available anticancer drugs have distinct mechanisms of action which can vary the effect they have on different types of normal and cancer cells. A single "cure" for cancer has proved elusive

since there is not a single type of cancer but as many as 100 different types of cancer. In addition, there are very few demonstrable biochemical differences between cancerous cells and normal cells.[7] A final problem is that cancerous cells which are initially suppressed by a specific drug may develop a resistance to that drug. For this reason cancer chemotherapy may consist of using several drugs in combination for varying lengths of time.

Small tumours which are relatively well supplied by the circulatory system are more susceptible to drug treatment when compared with larger tumours which can be hypoxic and necrotic which can make the cancers much more difficult to treat as they can be less responsive to the available cancer drugs.[8] Hence the importance of early detection of tumours when they are smaller and the chemotherapeutic agents are much more effective.

As with treatments of other diseases, drug resistance in cancer chemotherapy is becoming more and more of a problem. The resistance of anticancer drugs in the treatment of cancer tumours may be caused by a variety of factors including individual variations in patients and somatic cell genetic differences in tumours, even those from the same tissue of origin.[9] In recent years, the treatments of cancers has become more aimed towards molecular targets of the oncogenes and tumour suppressors as compared to that of the general cytotoxic agents, such as nitrogen mustard (1940's) to *Vinca* alkaloids (1970's) and anthracyclines (1960's) used in the early days of cancer treatments.[10, 11] The early treatments work by being more cytotoxic to cancer cells than healthy cells but cause many side effects. In recent times treatments have tended in the direction of specific monoclonal antibodies[11] and immunotoxins[12] targeted to cell surface receptors and specific agents that inactivate specific enzyme such as kinases in growth promoting pathways [13]. This move to more modern treatments has seen the improved response rate of the active drug and a decrease in side effects but yet has yielded no cure for the majority of patients. As these more modern treatments fail, research has been following the mechanism by which the cancers elude treatments and this has given a wealth of knowledge – investigation and research into why treatments fail and how to tackle the drug resistance issue aids in the design of new anti-cancer agent which do not become inhibited by traditional resistance mechanism.[9]

1.2.1 Mechanism of action of chemotherapeutic agents

Chemotherapy drugs can be divided into several groups based on factors such as how they work, their chemical structure, and their relationship to another drug. Some chemotherapy drugs are grouped together because they were derived from the same plants. Some drugs act by modulating more than one biochemical pathway and they may belong to more than one category.[14]

The cancer chemotherapy agents generally act by disrupting the cancer cell cycle. Disrupting this cell cycle can be done in many ways such as targeting one or more of a different series of molecular and biochemical signalling pathways. Chart 1-3 shows the four main phases in a cancer cell life-cycle and illustrate where pharmaceutically produced inhibitors target the different phases to stop the reproduction in the cell.

The first phase in the cycle is known as the G1 phase or gap and here the cell grows and prepares to synthesize DNA. This is followed by the S phase or synthesis; this is where the cell synthesises DNA. The G2 phase or second gap is where the cell prepares to divide. Then finally the M phase or mitosis, this is responsible for cell division. The cell cycle involves a complex series of molecular and biochemical signalling pathways which are controlled by a variety of enzymes and receptors.

Different chemotherapeutic agents have various targets in the body and therefore exert their different effects by utilising different mechanistic pathways (see Chart 1-3). [3, 15, 16]

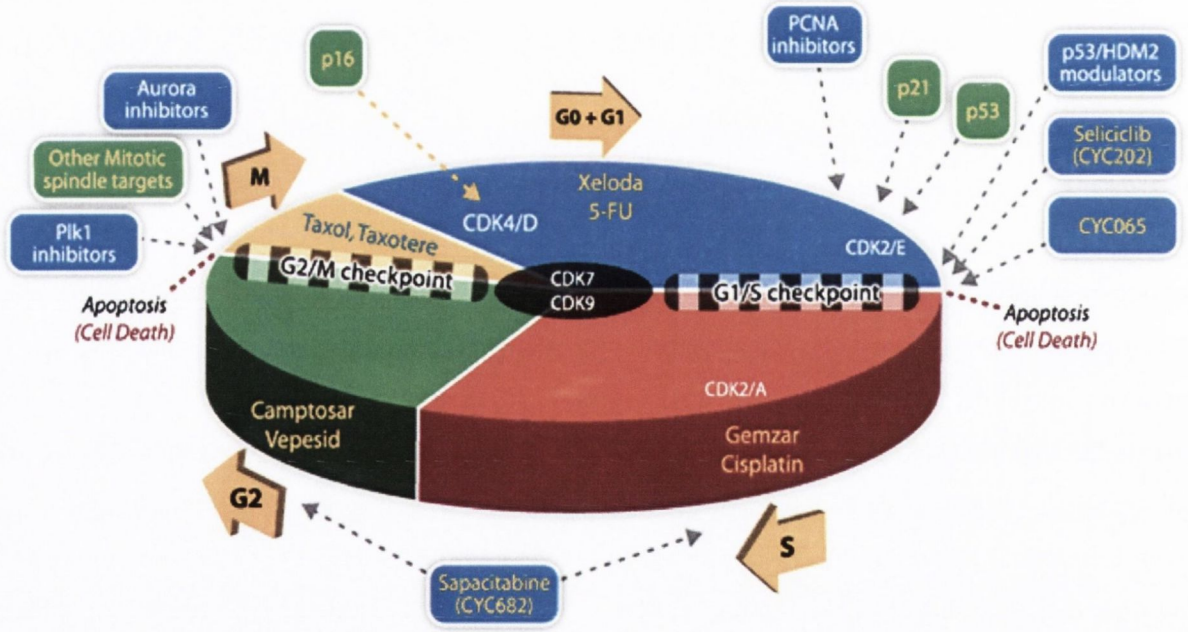

Chart 1-3 Molecular and biochemical signalling pathways which can be targeted by cancer chemotherapeutic drugs[17]

1.2.1.1 Antimetabolites[18]

Antimetabolites were among the first effective chemotherapy agents discovered. This type of chemotherapy agent works by inhibiting the use of metabolites[19] by mimicking naturally occurring molecules required in nucleic acid (DNA and RNA) synthesis such as folic acid, pyrimidine or purine analogues. These antimetabolities slightly differ from the natural nucleic acids and their

components, so that they can obstruct the normal cell function. Generally, antimetabolites induce cell death during the S phase of cell growth when incorporated into RNA and DNA or they inhibit enzymes needed for nucleic acid production.[20] Selectivity is obtained due to the fact that cancer cells often grow more rapidly than the surrounding healthy cells. Antimetabolite drugs include purine analogues (Fludarabine) [1], dihydrofolate reductase inhibitors (Methotrexate) [2], pyrimidine analogues (5-Fluorouracil) [3], thymidylate synthesis inhibitors and adenosine deaminase inhibitors (see Figure 1-1).

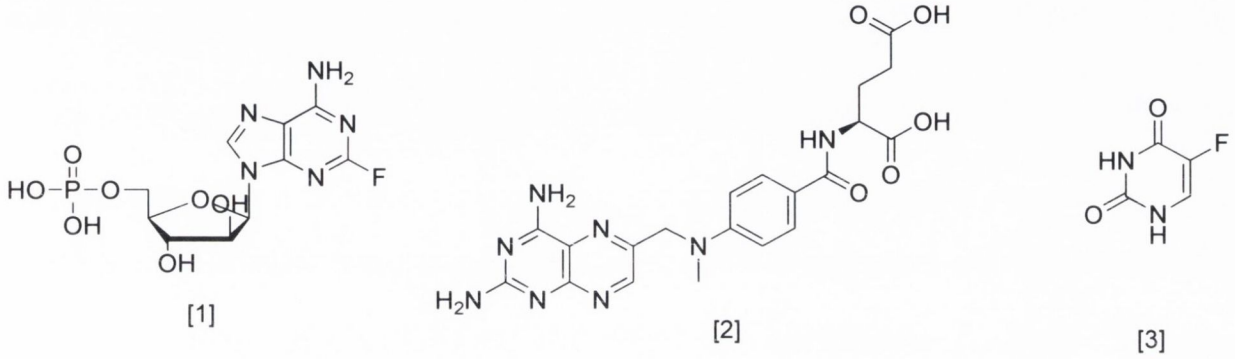

Figure 1-1 Fludarabine [1], Methotrexate [2], 5-Fluorouracil [3],

1.2.1.2 Drugs which interact with DNA

DNA binding compounds have become very useful for the visualization of DNA both *in vitro* and inside the cell. Not only are DNA binding drugs used as a visualization tool but have served as a very important classification of anticancer agents which binds and/or modify DNA.[21] Drug–DNA interactions can be classified into two major categories: intercalation and groove binding. Intercalation involves the insertion of a planar molecule between DNA base pairs, which results in a decrease in the DNA helical twist and lengthening of the DNA.[22] Groove binding agents will not bring about large conformational changes in DNA and may be considered similar to macromolecular binding.[23] Chemotherapy agents which involve DNA alkylating pathways include nitrogen mustards (aziridines)[24-26], alkylsulfonate esters[27], nitroureas[28], carbinolamines[29] and mitomycin C[30].

Methylating agents (dacarbazine [4], procarbazine [5], temozolomide [6], etc.) shown in Figure 1-2, work by methylating guanine bases within the major and (less predominantly) minor, grooves of DNA. Many of these types of drugs produce a transient methyldiazonium ion which is a DNA-methylating species.

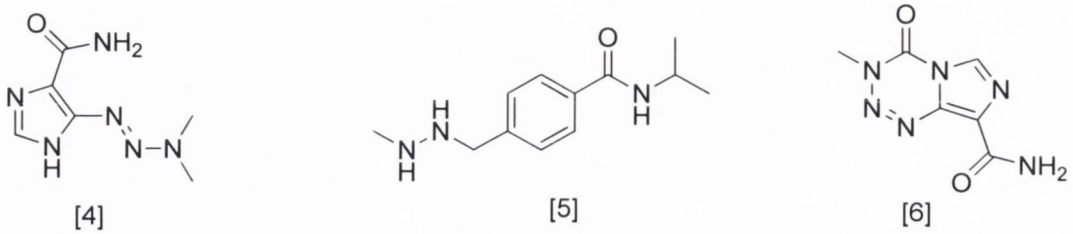

Figure 1-2. Dacarbazine [4], Procarbazine [5], Temozolomide [6]

Crosslinking agents (nitrogen mustard (Chlorambucil [7]), mitomycin C [8], cisplatin [9], psoralens [10], etc.) work as antitumor drugs that react with DNA by inducing DNA inter- and intra-strand cross-links, which can block DNA transcription and replication, Figure 1-3.

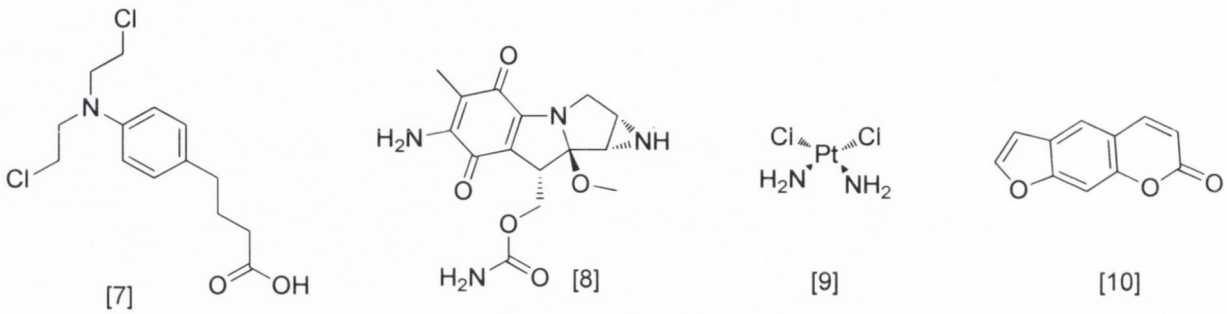

Figure 1-3. Chlorambucil [7]), Mitomycin C [8], Cisplatin [9], Psoralens [10]

The pyrrolobenzodiazepine (PBD) family of antitumour agents are based on anthramycin [11] (natural product). They exert their antitumour activity by covalently binding to DNA in the minor grooves where they covalently attach to the guanine base, and due to their shape, cause minimal disruption to the DNA helix, Figure 1-4.

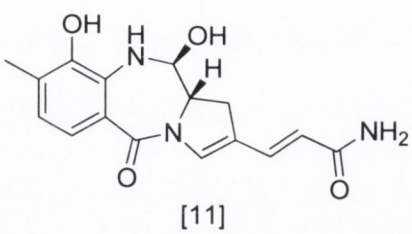

Figure 1-4 Anthramycin [11]

It is believed that the formation of the DNA-PBD adduct inhibits nucleic acid synthesis and causes excision-dependent single and double stranded breaks in the DNA helix.[31] While many alkylating compounds are relatively small in size, larger sequence-selective alkylating agents have been reported.[32] The PBD dimer enables the molecule to retain its natural properties but due to its greater length improves the sequence selectivity (compound [12]). Two covalent adducts to guanine

bases can be formed thus increasing the ability for crosslinking the DNA. An example of a PBD dimer has been reported that incorporated two DC-81 monomers (DSB-120 [12]) through their aromatic A-ring phenol C8-positions *via* a flexible propyldioxy linker and was found to be highly cytotoxic *in vitro* and to produce DNA interstrand crosslinks with high efficiency.[33, 34] Bizelesin [13] is a bifunctional cyclopropylpyrroloindole containing two reactive chloromethyl moieties that can be converted to cyclopropyl alkylating species, allowing for noncovalent and covalent (alkylated) bonds in the minor grooves with adenines on opposite DNA strands. Bizelesin inhibits both cellular and viral (SV40) DNA replication in whole cells and has exhibited activity against colorectal cancer, Figure 1-5.[35]

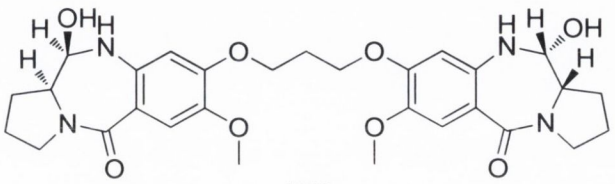

[12]

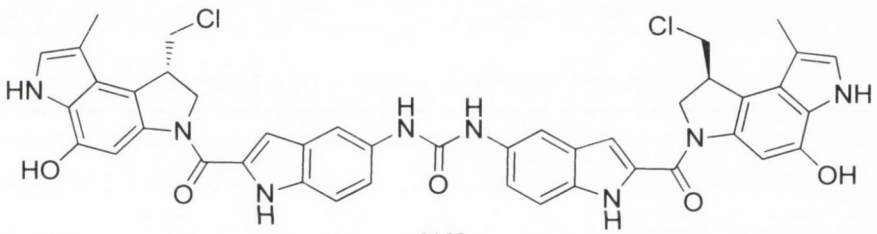

[13]

Figure 1-5 DSB-120 [12] and Bizelesin [13]

Intercalating drugs are widely used as antitumour agents (anthracycline, anthracenes and phenoxazines). Their scaffold generally consists of three or four fused aromatic rings and are planar in shape. Their mechanism of action requires the intercalating agent to be inserted between base pairs of the DNA perpendicular to the axis of the helix. Hydrogen bonding and Van der Waals forces keep the intercalating agent in place, which then affects the structure of the DNA, preventing polymerase and other DNA binding proteins from functioning correctly. The result is inhibition of DNA synthesis, prevention of transcription and facilitating the generation of mutations.[7] Doxorubicin [14] (anthracycline-based anticancer drug) is used to treat a wide variety of solid tumours including carcinoma of the breast, lung, thyroid and ovary as well as soft tissue carcinomas. Mitoxantrone [15] (anthracene based anticancer drug) has been used in the treatment of metastatic breast cancers, acute myeloid leukaemia and non-Hodgkin's lymphoma, Figure 1-6.[36]

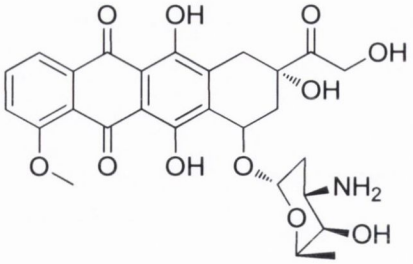

[14]

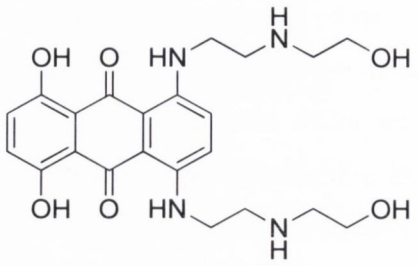

[15]

Figure 1-6 Doxorubicin[14] and Mitoxantrone[15]

Topoisomerases in recent times have become popular targets for cancer chemotherapy treatments. It is believed that topoisomerase inhibitors have the ability to kill all cells undergoing DNA replication, reading of the DNA for protein production or experiencing repair of DNA damage by generating single and double stranded breaks that harm the integrity of the genome. Introduction of these breaks consequently lead to apoptosis and cell death. Topoisomerase inhibitors are classified according to which type of enzyme is inhibited, known as I and II. Topotecan [16] is a topo I inhibitor which is a water-soluble derivative of camptothecin. It is used as the hydrochloride (hycamtin) to treat ovarian cancer and lung cancer, as well as other types of cancers. Topotecan intercalates between DNA bases. This intercalation disrupts the DNA duplication mechanism when it reaches a site where topotecan is intercalated. The type II topoisomerase inhibitors are furthermore broken into two sub categories - topoisomerase poisons (Etoposide [17])[37], which target the topoisomerase-DNA complex, and topoisomerase inhibitors (ICRF 193[18])[38], which disrupts catalytic turnover, Figure 1-7.

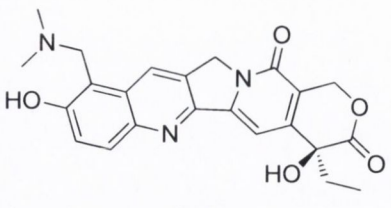

[16]

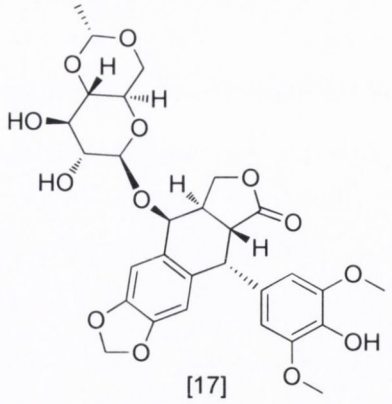

[17]

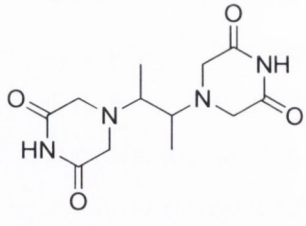

[18]

Figure 1-7 Topotecan [16], Etoposide [17]) and ICRF 193 [18]

DNA-cleaving anti-cancer agents act by binding tightly to guanine bases in DNA, predominantly in G-T and G-C-rich sequences. When the ternary complex of Fe(II), DNA-cleaving anti-cancer agent and oxygen attacks DNA, it removes hydrogen atoms. The resultant radicals react

with oxygen to form peroxy-species which then undergo degradation, resulting in chain cleavage.[39] Bleomycin is a glycopeptide antibiotic isolated from the bacterium *Streptomyces verticillus* and is a classical example of DNA-cleaving anti-cancer agent which is used for the treatment of Hodgkin's lymphoma, squamous cell carcinomas, and testicular cancer.[40] Bleomycin is isolated as a mixture of related antibiotics but the major component of which is Bleomycin A_2 [19], Figure 1-8.

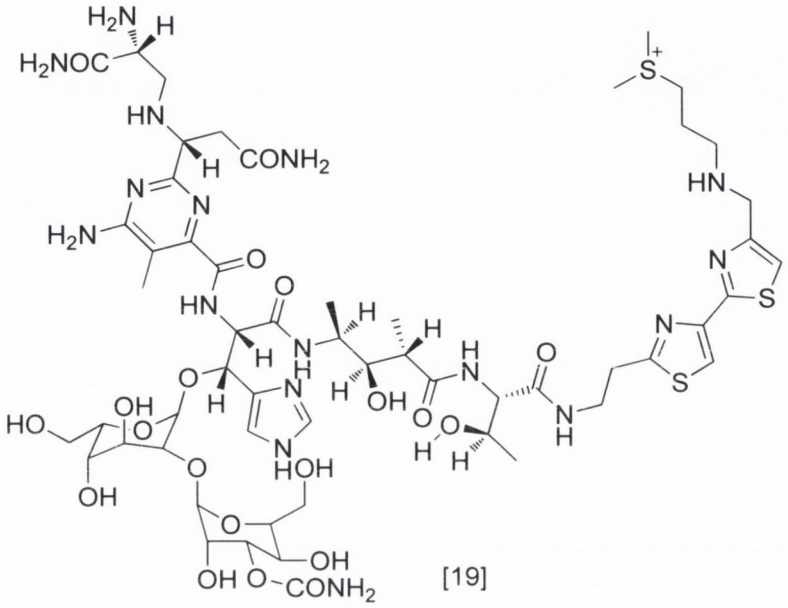

Figure 1-8 Bleomycin A_2 [19]

1.2.1.3 Antitubulin agents

Anticancer agents that exert their activity by interfering with microtubulin function are in common use in the treatment of cancer.[41] These antitubulin agents have shown a broad spectrum of activity against both hematological malignancies and solid tumours.[42, 43] The tubulin dimers and microtubule-associated proteins comprise the main backbone of microtubules.[44] The cell division and cell function of eukaryotic cells requires the microtubule system which is a highly dynamic structure and plays an essential role.[45, 46] Thus tubulin is an attractive target for the development of new compounds that impede cell function. Tubulin-binding agents constitute a large family of natural occurring and semi-synthetic agents that inhibit cell division through their inhibition of microtubule dynamics. In general the tubulin-binding agents can be classified by the mechanism of tubulin interaction. The agents are classified into one of three groups although exceptions do exist, microtubule stabilizing compounds (paclitaxel [20] and docetaxel), vinca alkaloid site interacting agents (vincristine, vinblastine[21], and vinorelbine) and colchicine site binders (Combretastatin A-4[22], ZD6126), Figure 1-9.[47]

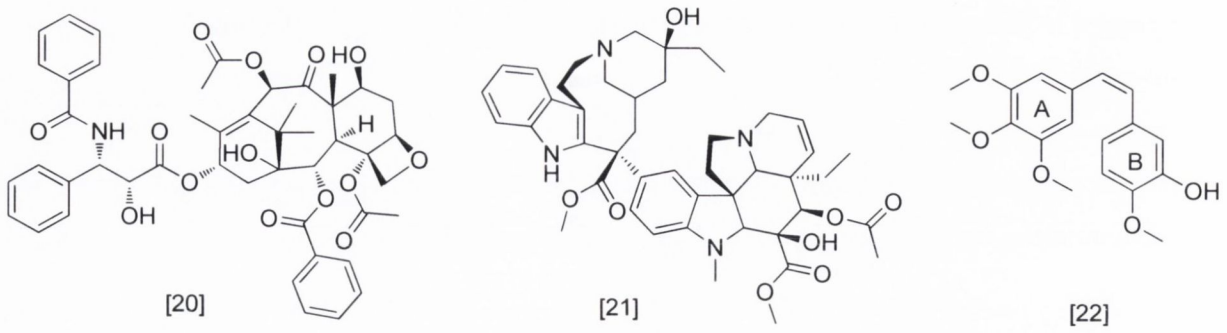

Figure 1-9 Paclitaxel [20], Vinblastine [21] and Combretastatin A-4 [22]

1.2.1.4 Vascular disrupting agents

Vascular disrupting agents (VDAs) are a relatively new class of anticancer drugs that show encouraging results in treating an array of solid tumours.[48] VDAs can selectively target the existing tumour vasculature which differs from antiangiogenic therapies which hinder the outgrowth of new blood vessels. There are a few small VDAs that are currently in clinical trials or undergoing preclinical testing which have achieved promising results (ZD6126 [23], CA4P [24], NPI-2358 [25] and vadimezan [26]), Figure 1-10.[49]

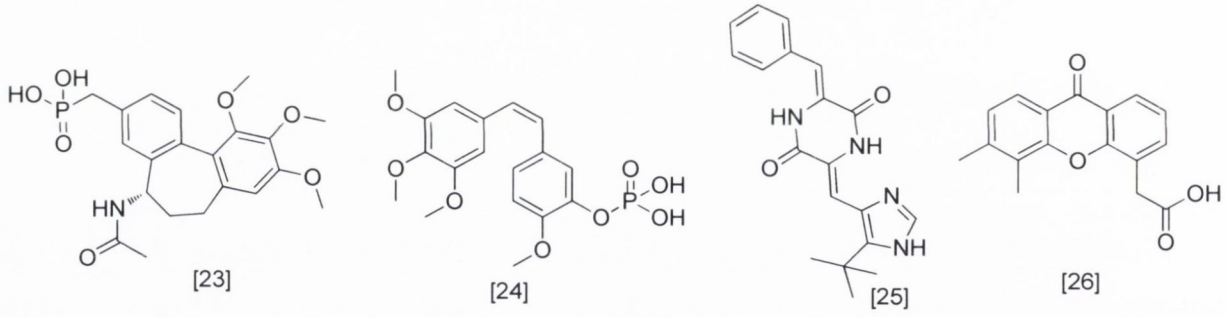

Figure 1-10 ZD6126 [23], CA4P [24], NPI-2358 [25] and Vadimezan [26]

1.2.1.5 Signal transduction inhibitors

In recent years, the knowledge of growth factor signalling pathways and the study of how these pathways are often altered in human cancers have led to the development of highly specific inhibitors for these pathways.[50] Due to the up-regulation of certain cellular pathways in cancer cells, inhibition can lead to an anticancer effect. It was discovered that a viral oncogene was also a mutated receptor tyrosine kinase in human cancer and this has implicated receptor tyrosine kinase in cancer pathogenesis.[50] A number of inhibitors of receptor tyrosine kinase signalling pathways have been discovered. Receptor tyrosine kinases have been blocked *via* different mechanisms *in vitro* such as blocking ligand binding, inhibiting receptor tyrosine kinase expression and inhibiting receptor tyrosine kinase activity. Imatinib [27] is an example of signal inhibition drug (tyrosine kinase

inhibitor) used to treat ten different cancers including chronic myelogenous leukaemia (CML) and gastrointestinal stromal tumours (GISTs), Figure 1-11.

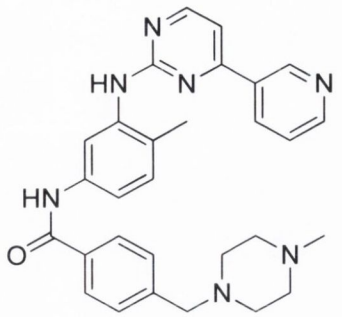

Figure 1-11 Imatinib [27]

1.2.1.6 Hormonal therapies

Hormonal therapy involves the manipulation of the endocrine system through exogenous administration of specific hormones, predominantly steroid hormones, or drugs which inhibit the manufacture or action of such hormones (hormone antagonists). In hormone-dependent tissue such as the breast, endometrium and testes, tumours can arise which are themselves dependent on the same hormone. Depriving hormone-dependent tumours of hormone stimulation can cause tumour regression. Prostate cancer is usually androgen-dependent and can be treated with estrogens and/or antiandrogens (i.e. cyproterone acetate). Anitestrogens (i.e. Raloxifene and Tamoxifen) can also reduce cell growth in breast cancer. Aromatase inhibitors (i.e. anastrozole and letrozole) can be used to treat advanced post-menopausal breast cancer.

1.2.1.7 Biologicals

Tumour-targeting therapy that involves use of monoclonal antibodies which can attach to the cancer cell. In doing so they can expose the cancer cell to be more visible to the immune system, block growth signals, stop formation of new blood vessels and/or deliver a radiation (Ibritumomab)/cytotoxic drug to cancer cells.[51] The use of antibodies to deliver cytotoxic drugs will be disused in more detail in Section 1.11.1.1. In principle the antibody should selectively deliver the drug to the tumour cells. Examples of tumour-target approaches are antibody-directed enzyme prodrug therapy (ADEPT) and gene-directed enzyme prodrug therapy (GDEPT). Trastuzumab is a humanized monoclonal antibody that interferes with the HER2/neu (erbB2) receptor.[52] The cell proliferation is stimulated by the HER proteins. In some cancers, notably certain types of breast cancer, HER2 is over-expressed, and causes cancer cells to reproduce uncontrollably.[53] Amplification of the HER2/neu (erbB2) occurs in 20-30% of early-stage breast cancer. Trastuzumab induces HER2 receptor downmodulation and, as a result, inhibits critical signalling pathways and blocks cell progression. It also inhibits angiogenesis and induces antibody-dependent cellular cytotoxicity.[54]

1.3 Breast Cancer

1.3.1 Overview

Breast cancer has become the second most common cancer worldwide after lung cancer, the fifth most common cause of cancer death, and the foremost cause of cancer death in women. Worldwide, breast cancer exceeds all other cancers and the incidence rates of breast cancer are increasing steadily.[55] The vast majority (95%) of breast cancer in early stage, in both pre- and postmenopausal women, are hormone-dependent. The remaining 5% of breast cancer, denoted BRCA-1 and BRCA-2, are considered hereditary.[56] The human hormone estradiol (E2)[28] plays an important role in the progression and development of the tumour. The hormone and estrogen receptor complex can control activation of proto-oncogenes, oncogenes, nuclear proteins, as well as other target genes. In contrast to the hormone-dependent tumours, triple-negative breast cancers (in which this tumour subgroup lacks expression of HER2), the estrogen receptor and progesterone receptor do not respond to hormonal therapies or HER2-targeted therapies and these tumours are associated with a poor prognosis.[57]

During the postmenopausal period when the ovaries have ceased to function, the majority of breast cancers occur. Despite resulting low levels of circulating estrogens, the concentration of estrone (E1) [29], estradiol (E2) [28] and their sulfates (E1S [30], E2S [31]) in the breast cancer tissue are several times higher than those found in the plasma or in the area of the breast considered as normal tissue, suggesting specific tumoral biosynthesis and accumulation of these hormones.[58, 59]

Human breast cancer tissue contains enzymes involved in the last steps of E2 biosynthesis: estrone sulfatase, 17β-hydroxysteroid dehydrogenase and aromatase (Figure 1-12).[56] The tumours can be affected by the binding of different ER-ligands (e.g. antiestrogens) which mimic the role of estradiol at the estrogen receptor (ER) or by gaining control over intracellular concentrations of estradiol. The estrogens, which are converted by sulfotransferases to the biologically inactive estrogen sulfate, are present in this tissue. To target the enzymatic pathways in the biosynthesis of estradiol could lead to successful therapy. Quantitative determinations have shown that the sulfatase pathway , which converts the estrogens sulfates to the unconjugated bioactive derivate E2 [28], has shown an increase to between 40–500 times higher than that of aromatase pathway.[56] Antiestrogens (i.e. Tamoxifen), progestins, tibolone and its metabolites, as well as other steroids (i.e. sulfamates) and non-steroidal compounds have being investigated as possible inhibitors for the sulfatase enzyme and this has lead to the identification of more potent, selective, metabolically stable and less estrogenic agents.[56] Quantitative data show that the sulfatase pathway, which

transforms estrogen sulfates into the bioactive unconjugated E2, is 100–500 times more effective than the aromatase pathway.

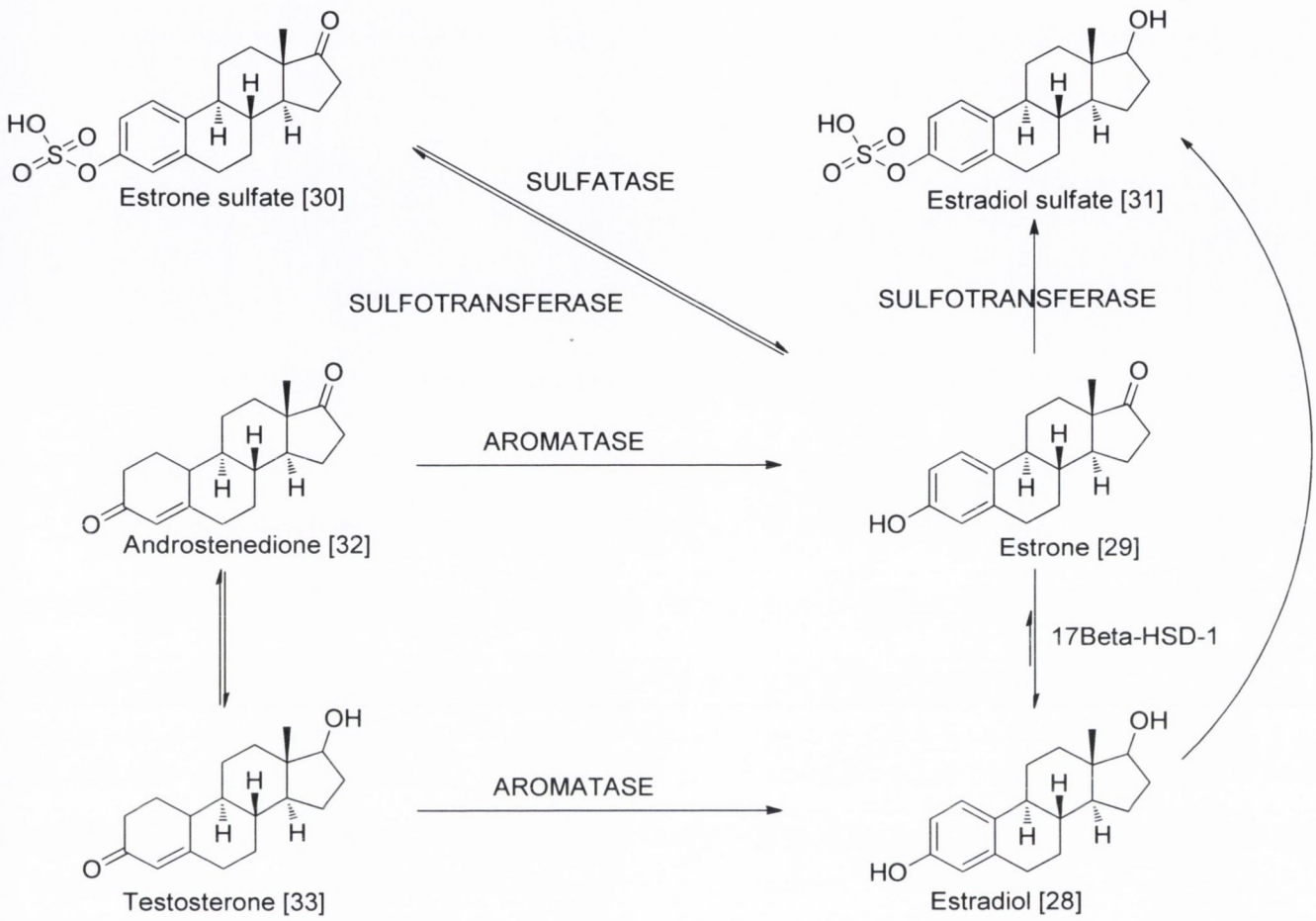

Figure 1-12. Summary of main enzymatic pathways for biosynthesis of estradiol

The ER receptor gene is prone to truncations, mutations and deletions as the cancer cell evolves.[60-62] Therefore the ER becomes 'non-functional', and the hormone fails to stimulate the cells despite binding in the ER pocket. This 'non-functional' ER possibly explains why a relativity high number of patients with ER positive tumours do not respond to antiestrogen therapy.[63, 64] Shown in Figure 1-13 is the transition to the hormone-independent carcinoma as a direct mutation from the hormone-dependent carcinoma that itself is a mutation of the normal mammary tissue.

Prognosis of the disease evolution is at two stages; when the breast cancer is hormone-dependent (I) period when prognosis is very good, but when the breast cancer is hormone-independent (II) phase then it becomes very poor. ER+ refer to estrogen receptor positive (detectable and functional); ER mutants refers to estrogen receptor detectable but non-functional; ER– refers to estrogen receptor negative (not detectable).[56]

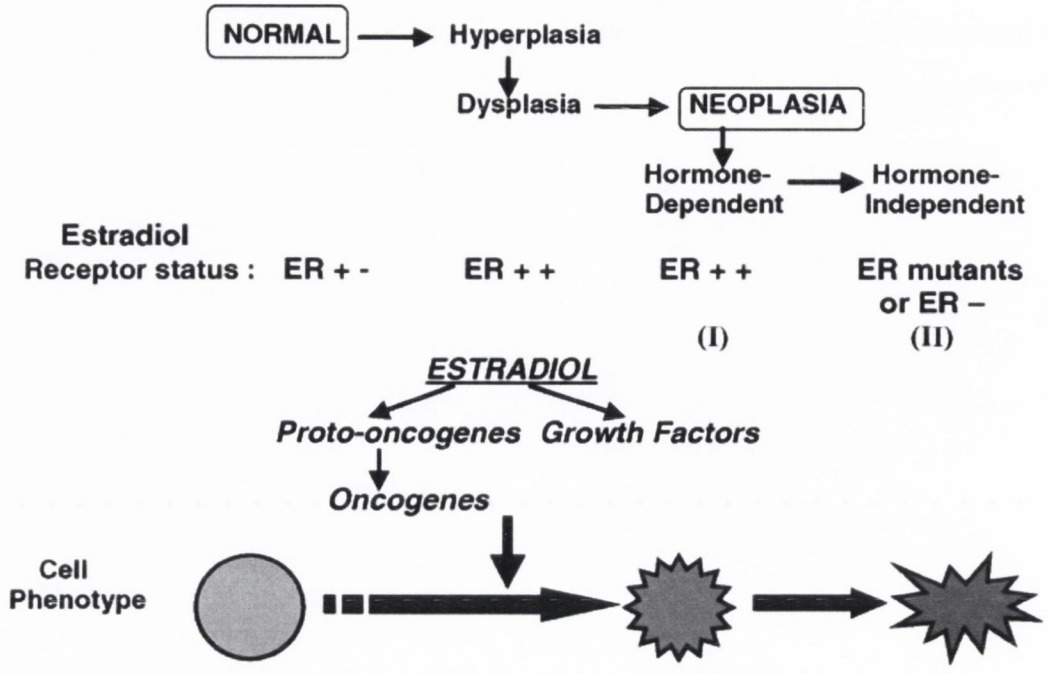

Figure 1-13. Evolutive transformation of the breast cell from normal to carcinogen[56]

1.4 Estrogens

Estrogens (oestrogen) are a group of compounds named for their importance in the estrous cycle of humans. Estrogens have extensive biologic actions, and there are naturally occurring phytoestrogens that mimic some of the actions of endogenously produced estrogens.[65] They are the primary female sex hormones. The naturally occurring estrogens 17β-estradiol (E2) [28], estrone (E1) [29], and estriol (E3) are C_{18} steroids derived from cholesterol (Figure 1-14). After cholesterol is bound to the lipoprotein receptor it taken up by the steroidogenic cells, stored and moved to the sites of steroid synthesis. The cytoskeleton and the intracellular carrier proteins such as the sterol carrier protein-2 can facilitate the intercellular movement.[66] Different steroids are formed by reducing the number of carbons atoms from 27 to 18. Cholesterol is transferred from the cytosol to the inner membrane of the mitochondrion, where the cytochrome P450 enzymes that catalyze the cleavage of the side chain of cholesterol are identified as the rate limiting step in the steroid production.[67] The last step in the estrogen formation is aromatization. This reaction is catalyzed by the P450 aromatase monooxygenase enzyme complex. In three consecutive hydroxylating reactions, estrone and estradiol are produced from their obligatory precursor's androstenedione and testosterone, respectively. The final hydroxylating step in aromatization does not require enzymatic action.[65]

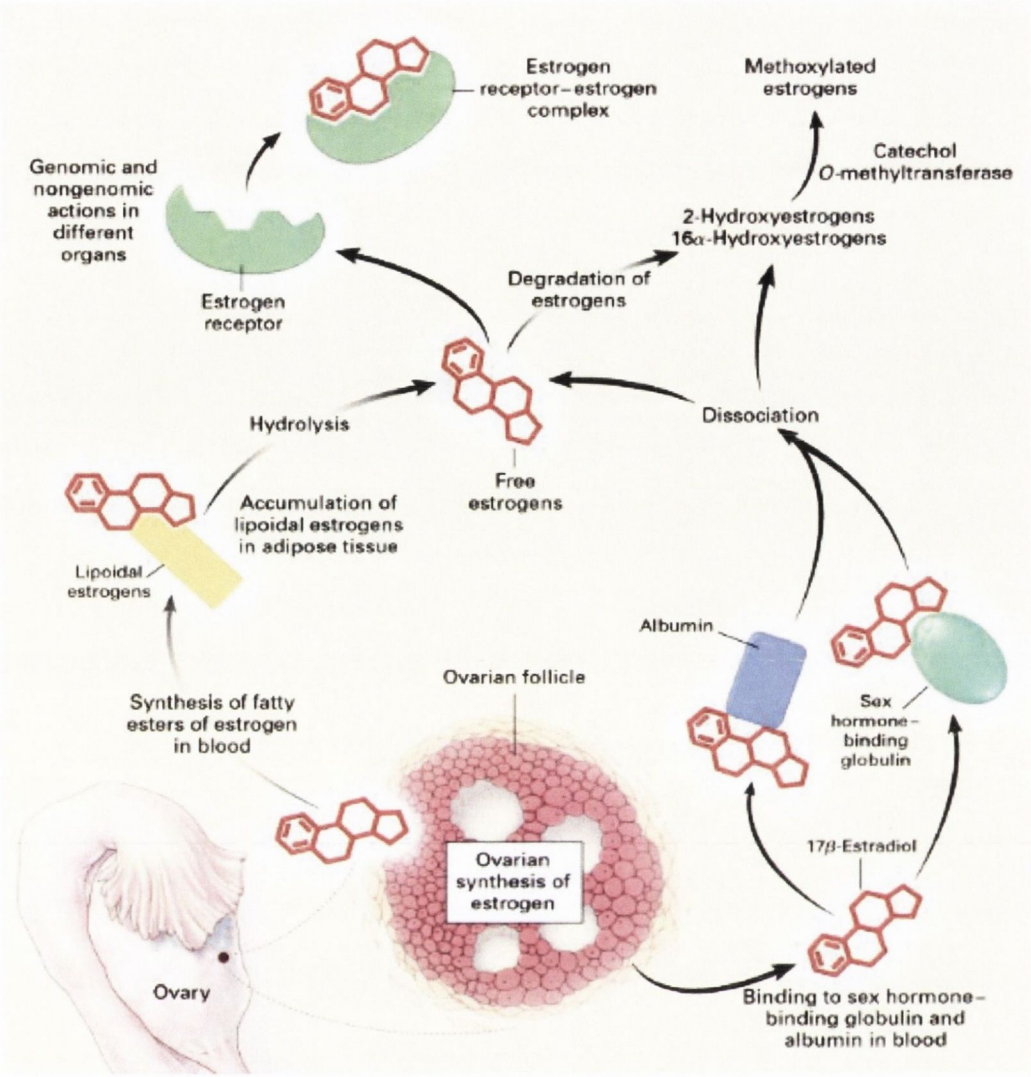

Figure 1-14. Ovarian Synthesis, Transport, and Metabolism of Estrogens.[65]

Normally in women, the rate of estradiol production varies during the menstrual cycle with plasma levels varying from 50 – 850 pg/mL.[15, 16] Estrogens exert their effects by entering target cells and binding to specific cytoplasmic proteins known as estrogen receptors (ERs). McGuire *et al.* showed that the ERs were present in breast cancer tumours.[60] This provided rationale for the development of antiestrogens for the treatment of breast cancer.

In premenopausal non pregnant women the ovaries are the principal source of systemic estrogen. The synthesis, transport and metabolism of estrogen is quite complex and is demonstrated in Figure 1-14. Other sites of estrogen biosynthesis are present throughout the body and these become main sources of estrogen after menopause. These sites include the mesenchymal cells of the adipose tissue and skin[68], osteoblasts[69] and possibly chondrocytes in bone, vascular endothelial[70] and aortic smooth muscle cells[71] as well as various sites in the brain[72]. These extragonadal sites of estrogen biosynthesis have a number of fundamental characteristics that differ from those of the

ovaries. The estrogen synthesised within these localised site is almost certainly biologically active only at local tissue level.[73] The total amount of estrogen produced by these extragonadal sites may be miniscule, but the local tissue concentrations achieved are probably quite high and exert significant biological influence within that site. Thus, these sources of oestrogen play an important physiological and pathophysiological role after menopause and adipose tissue becomes the main source of estrogen.[68, 74]

1.4.1 Antiestrogens

This is a class of substance that blocks the production or utilization of estrogens or inhibits their effects. In the late 1950s tamoxifen [34] emerged from research aimed at developing an antiestrogen oral contraceptive. The finding that a metabolite of tamoxifen, 4-hydroxytamoxifen (4-OHT) [35], was a potent antiestrogen with the binding affinity for the ER equivalent to that of estradiol stimulated research for novel anticancer agents with high binding affinity for the ER that would act as potential antagonists of the ER. The metabolites of tamoxifen acts as antiestrogens which can promote an invasive phenotype in ER+ breast cancer cells with deficient intercellular adhesion.[75]

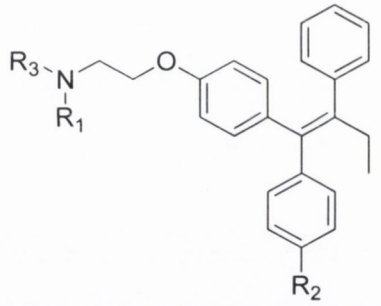

Figure 1-15. Tamoxifen (R_1 = CH_3= R_3 = CH_3, R_2 = H) [34]; 4-Hydroxytamoxifen (R_1 = R_3 =, CH_3, ,R_2 = OH) [35]; Endoxifen (R_1 = CH_3, R_2 = OH, R_3 = H) [36]; Norendoxifen (R_1/R_3 = H, R_2 = OH) [36a]

The active metabolites, 4-OHT [35], endoxifen [36] and norendoxifen [36a] (Figure 1-15), all boast a much greater binding affinity for the ER than that of the parent drug tamoxifen, and because of this fact tamoxifen can be classified as an antiestrogen prodrug.[76] The identification of selective estrogen receptor modulators and the opportunity of developing multifunctional medicines have resulted in the successful development of selective estrogen receptor modulators (SERMs) to treat and prevent ER-related diseases.[76, 77] Although aromatase inhibitors could be considered antiestrogens, they are often considered to be a distinct class. Aromatase inhibitors reduce the 'production' of estrogen, while the term "antiestrogen" is typically retained for agents that reduce the 'response' to estrogen.

1.4.2 Mode of estrogenic action

In recent years, new information regarding the ER structures, intra- and intermolecular interactions, post translational modifications, and several other factors pertaining to the ER actions has emerged.[78-80]. In Figure 1-16, shows the proposed mechanisms of ER stimulation (stabilization of the preinitiation complex), chromatin remodelling, and interaction with other transcription factors.[65]

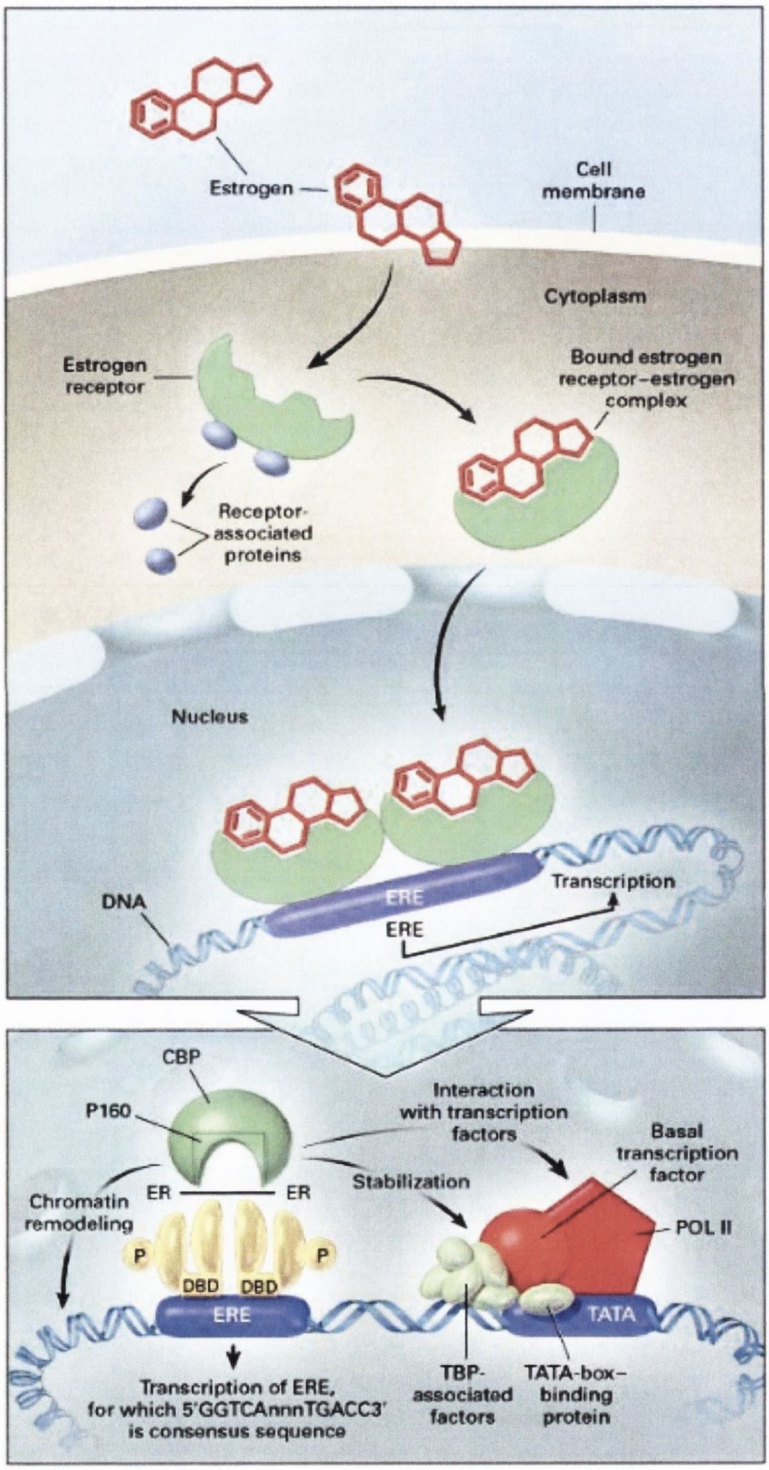

Figure 1-16. Classic Pathway of Estrogen Signal Transduction[65]

When an estrogen molecule binds to an estrogen receptor (ER), the receptor can then breaks from its cytoplasmic chaperones (receptor-associated proteins). The hormone–receptor complex then moves to the nucleus, where it binds to DNA and initiates transcription. Transcription is catalyzed by RNA polymerase II (POL II) and requires the assembly of various proteins and other transcription factors join thereafter, completing the preinitiation complex. Activated, phosphorylated (P) estrogen receptors interact with several proteins. This complex binds to the estrogen-response element (ERE) through the DNA-binding domain (DBD) of the receptor and stimulates transcription.[65] A transcription species is produced by interaction with co-activator (CoA) peptide to initiate RNA synthesis and ultimately, the estrogen-specific cellular response. Co-repressor (CoR) peptides are believed to prevent transcription by interacting with antiestrogen ER complex. There is increasing evidence to suggest that the recruitment of the cofactor (CoA and CoR) entities have a key role in defining the action of SERMs.[81]

1.4.3 Structural biology of estrogen receptors

There are two subtypes of estrogen receptor each with several isoforms and splice variants of each subtype. The first subtype, the classic estrogen receptor α (ERα)[82] and the second subtype, estrogen receptor β (ERβ)[83]. The structure of the α and β subtypes differs and their encoding genes are on different chromosomes. Although the α and β estrogen receptor have very similar DNA binding domains, the overall degree of homology of the receptors is low. This is particularly true for the ligand-binding domain, of which, only 55 percent of the amino acid sequence is shared.[84] The distributions of ERα and ERβ differ depending on tissue type, but some overlap does occur. ERα is mostly present in the endometrium, breast-cancer cells, and ovarian stroma. In contrast, ERβ is mainly found in several non-classic target tissues (kidney, intestinal mucosa, lung parenchyma, bone marrow, bone, brain, endothelial cells, and prostate gland).[85]

Figure 1-17 illustrates the sequence organization of both isoforms of the estrogen receptor. The amino acid sequence is given for the different domains. NTD (amino terminal domain) which is involved in transactivation (A/B) and is highlighted in red; DBD (DNA binding domain), (C) are highlighted in green; hinge region involved in dimerisation and Hsp90 binding (D) are highlighted in blue, LBD (ligand binding domain) which synergises with transactivation function in the NTD region are highlighted in yellow and the F region located towards the C-terminal end is highlighted in grey.

The ER isoforms contain two regions called activation functions (AFs) domains, AF1 and AF2 which are located within NTD and LBD, and are responsible for regulating transcriptional activity.[86] AF1 is known to function independent of estrogen whereas AF2 requires the presence of estrogen.[86, 87] It is believed that the two AFs act in synergy to achieve transcription activity. Their activity is also believed to be promoter and cell specific.[88] The DBD in both ERα and ERβ, show more than 95 %

sequence homology.[83] The response element (associated with the DNA-binding domain) can either reside proximally to the promoter or enhancer regions which are located distant from the transcription site.[89] The DBD of both ERα and ERβ isoforms shares the identical DNA response elements. The ERE sequence plays an important regulatory role as it dictates the binding affinity of the ER and also modulate the recruitment of coactivators.[90, 91] ERE transcriptional regulation can be controlled *via* two separate mechanisms of ER action. Ligand bound ER can directly associate with specific response element sequences or the ER may contribute in a multiprotein, pre-initiation complex and regulate gene transcription without direct interaction with any DNA sequence.[92-94] Collectively, these mechanisms highlight the complex role of coactivators and response elements in eliciting specificity in transcriptional output.[95]

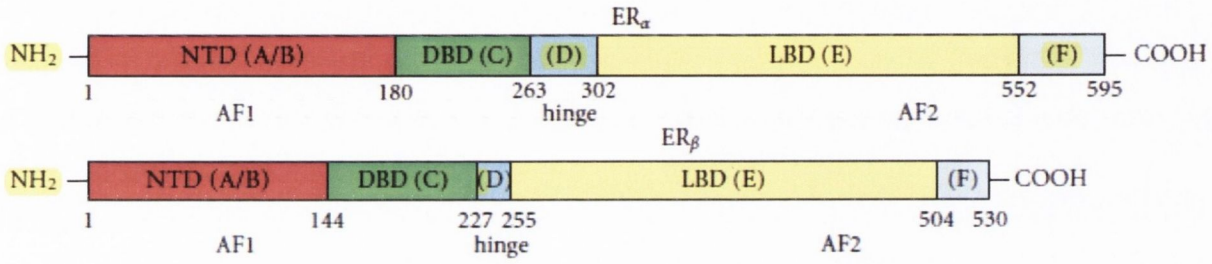

Figure 1-17. Sequence organization of the two isoforms, ERα and ERβ[95]

1.4.4 Overall structure of the ER

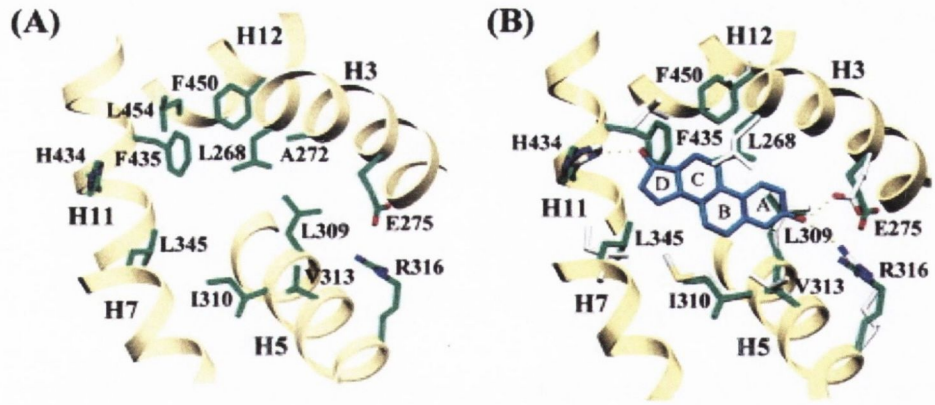

Figure 1-18 (A) Empty LBD of the ERα and (B) with E2 docked into the empty ligand binding cavity of ERα[96]

X-ray crystallography of ligand bound ER has shown that the ER LBD adopts a classical helical sandwich fold, common to all nuclear receptors LDBs.[97] The three dimensional structure of isolated LDBs and DBDs are known.[98] The molecular scaffold has a 'wedge-shape' with a considerable ligand-binding cavity at the narrower end of the domain. The molecular scaffold comprises of three α-helices (H5-6, H9, and H10) as a central core layer sandwiched between two further α-helices layers (H1-4, H7, H8, and H11).[98] The cavity is completely buried within the core of the LDB and flanked by a small β-hairpin (S1 and S2) and the C-terminal helix (H12).[98] The H8/H11 layer of the LBD fold

creates head-to-head dimers forming an interface with the ER monomers. LBD dimerisation is identical for both ER subtypes and independent of the nature of the bound ligand (i.e. agonist/antagonist-dimers are similar). The ERβ quaternary structure appears to be slightly more flexible.[98] The ability of a SERM to regulate expression is influenced by the relative expression of CoA and CoR with a cell.

1.4.5 Molecular mechanism

The complexity of the mechanism of action of estrogen and antiestrogens is due to the presence of two ERs (ERα and ERβ). The belief is that the ER LBD is capable of existing in multiple response states depending on the nature of the bound-ligand.[97, 98] The shape of the ligands that bind to both ERα and ERβ, programmes the complex to produce estrogenic or anti-estrogenic signals. The context of the ER complex influences expression of the response through the numbers of co-repressors (CoR) or coactivators (CoA). Binding of receptor agonists favours CoA recruitment, whereas binding of antagonists - both full (i.e. AF1/AF2) and AF2 - favours CoR interaction.[97] The relative expression of CoA and CoR within a cell influences the ability of a SERM to regulate gene expression. While ERs bind a variety of ligands with similar affinity and interact with the same ERE, their transcription activity is different.[98] The expression of estrogenic action is not simply the binding of the receptor complex to the promoter of the estrogen-responsive gene, but a dynamic process of CoA complex assembly and destruction, Figure 1-19.

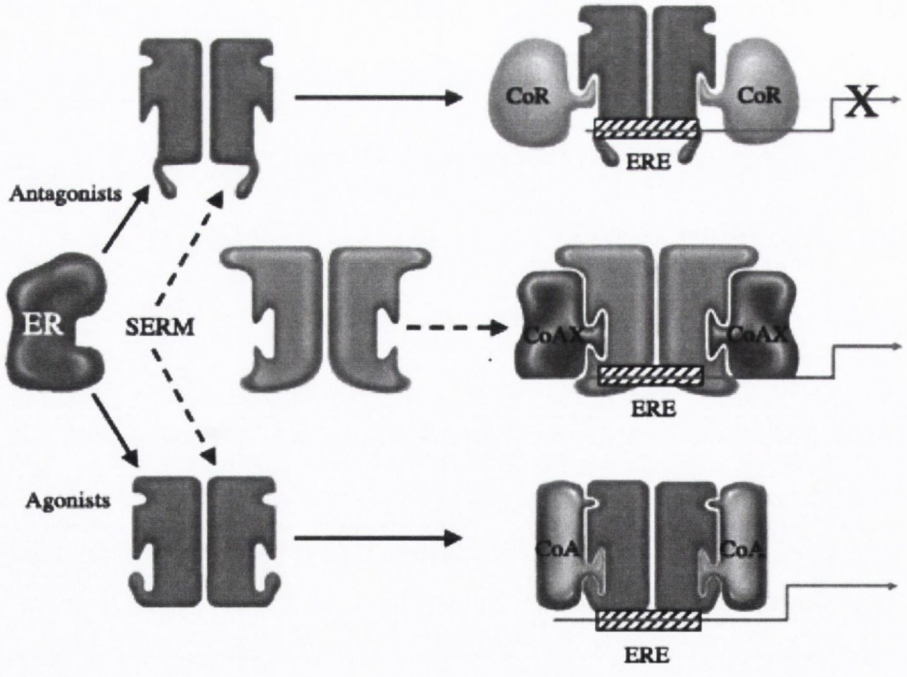

Figure 1-19. Schematic of observed ER LDB conformational states and activation role[99]

Upon binding an agonist or an antagonist, the ER undergoes a conformational change that permits its spontaneous dimerization and facilitates the subsequent interaction of the dimer with ERE located within target genes. The functional consequences of different ligand-induced conformational changes were revealed with the discovery of receptor (CoA) and (CoR). Coactivators (CoAX = coactivator "X") interact with agonist-activated ER and facilitate transcriptional activation, whereas corepressors interact with the antagonist-activated receptor and help to maintain it in a quiescent state. SERMs permit the receptor to adopt a structure that is intermediate between that observed following the binding of agonists or antagonists.[99] The target tissue is programmed to express a spectrum of responses between full oestrogen action and anti-oestrogen action on the basis of the shape of the ligand and the complexity of the tissue-modulating network such as NFκB, nuclear factor κB.

1.4.6 Receptor agonism

ER's ligand-dependent transactivation function (AF2) is formed by helices H3, H4, H5 and H12. Shallow hydrophobic grooves are formed by the residues that serve as the docking site of the co-regulators. The agonist, when binding, stabilises a receptor conformation in which H12 is aligned across the LBD fold and seals the ligand within the buried cavity (Figure 1-20A). In this arrangement, H12 completes the AF2 region and represents the most favourable geometry for co-activator recruitment.[100]

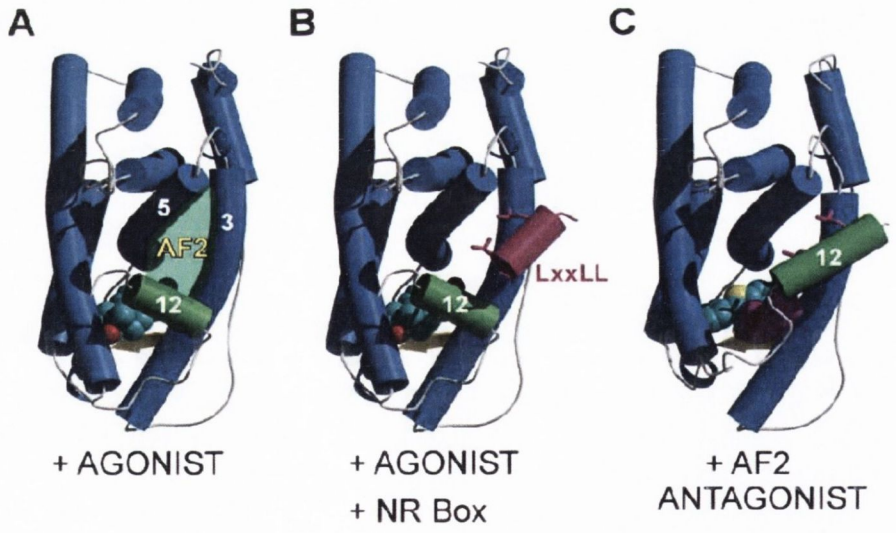

Figure 1-20. Structural basis of estrogen receptor (ER) activation: major conformations induced by ER agonists[97]

Helix-12 stabilization in this agonist bound orientation does not rely on direct contacts between the ligand and Helix-12 but is dependent on the interactions made by the ligand within the cavity. Co-activators bind to ERβ in a manner similar to that described for the ERα LDB.[97, 98] The structural basis of coactivator recruitment has been exposed by cocrystallisation of ER with short peptides. These Leu-Xxx-Xxx-Leu-Leu, Leu-Xxx-Xxx-Met-Leu and Leu-Xxx-Xxx-Try-Leu peptide motifs

(Xxx= any amino acid) adopt a helical conformation and bind along the hydrophobic AF2 coactivator groove.[101] The helical nature of the LxxLL motif presents the first and third leucine residues on the same face so that they can bind in shallow depressions in the AF2 groove (Figure 1-20B). The key event in the creation of the AF2 interaction site and subsequent stabilization of LxxLL binding is the correct positioning of Helix-12, as it bears the conserved glutamate residue of the 'charge clamp' that interacts with the N-terminal end of the short LxxLL helical motif. Therefore, Helix-12 is often referred to as the 'molecular switch', as its orientation with respect to the rest of the LBD determines whether ER is 'on' or 'off'.

1.4.7 Receptor Antagonism

The molecular basis of antagonist effects is not well understood. It is believed to derive from a total blockage of the AF2 activity together with tissue specific activation mediated by other regions of ER, including AF1. ER antagonists are characterised by a hydrophobic core that mimics the steroid nucleus of E2 with an extended moiety of varying length that is oriented approximately perpendicular to the core. The ER LBD allows the phenolic core to bind in a similar manner in the cavity, due to shared characteristics mimicked between that of the antagonist ligands and that of natural hormones. As a direct result of the mimicked binding, the basic side-chain moiety is too large to be contained within the cavity and protrudes between H3 and H11. This then inhibits H12 to bind across the LBD in the agonist orientation and alternatively binds along the hydrophobic grove between H3 and H5.[100, 102] AF2 is incorrectly formed thus preventing co-activation recruitment (Figure 1-20C). Antagonist basic moieties can strongly interact with the Asp351 carboxylate group within the LBD cavity, anchoring the ligand in the LBD and precisely redirecting the H12 into the AF2 groove.[100] In ERβ particularly, passive antagonism can occur without the need for the bulky substituent.[103] In this case, the ligand fails to make appropriate contact with the binding cavity so the antagonist rather than the agonist orientation of H12 is preferred. Full antagonist ligands, such as ICI 182,780 and ICI 164,384, are able to inactivate AF1 and AF2. H12 is prevented from either lying over the LBD or occluding the Leu motif binding groove.[104] Full antagonists appear to induce a distinct conformation of the receptor in which H12 is not stably associated with the LBD. As such, in fully antagonised state, AF2 is highly accessible and may favour efficient co-repressor recruitment.

Similar to the Co-activator (CoA) in the case of agonists, the AF2 grooves serves as a docking site for co-repressors (CoR). The CoR-bound ER LBD remains the most structurally ill-defined of all the conformation states outlined above. Accessibility of H3 and H5 grooves appears to be a requirement for CoR docking, while the elimination of H12 favours co-repressor binding. There is increased evidence that the occlusion of AF2 groove may contribute to the tissue selective action of SERMs.[97, 100]

1.4.8 Key aspects of an ER pharmacophore and its steroid ligands

A more detailed discussion of ligand molecular binding is discussed in Chapter 6. A synopsis of the key structural aspects of the ER pharmacophore is presented here. The characteristics for the ER binding site E2, are based on the collection of relative binding affinity (RBA) values, data from affinity-labelling and site directed mutagenesis studies. These data establish the binding site as hydrophobic, apart from at the termini, and practically envelops the native ligand. The specific sites do show some flexibility, although these receptor regions do not act independently.[105]

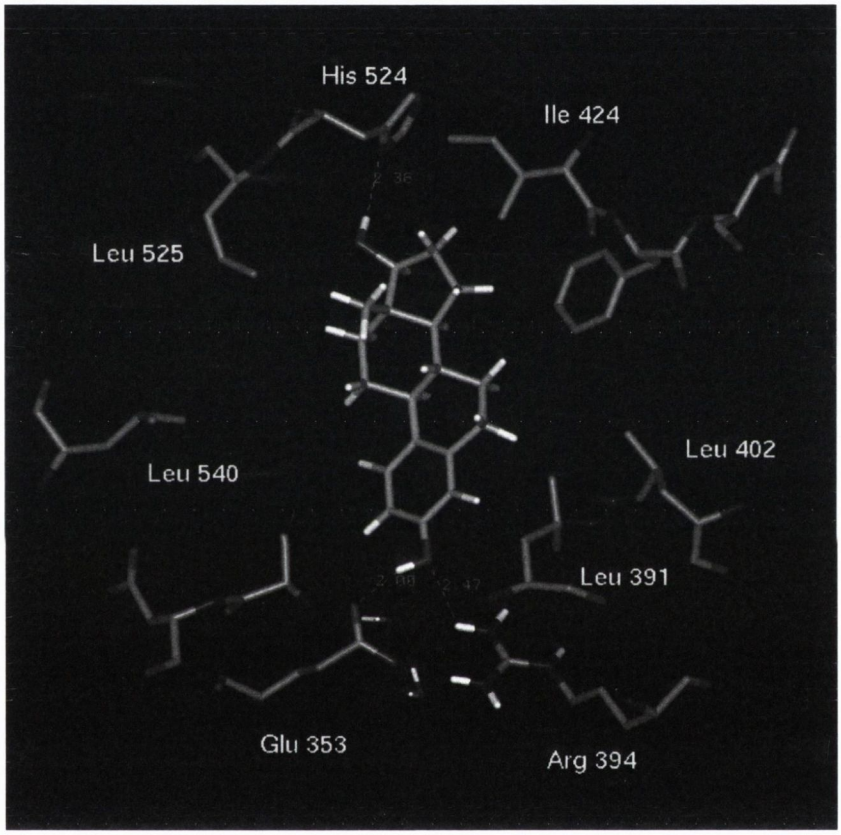

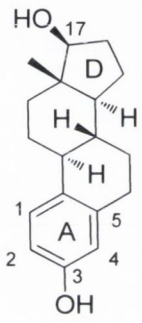

[28]

Figure 1-21 Orientation of estradiol [28] in the ligand binding pocket of the estrogen receptor ligand binding domain[100]

The ER binding site can be divided into 4 ring regions based on estradiol [28], A, B, C and D – rings (Figure 1-21). The A-ring (position 1) is believed to be in close contact with the receptor as estradiol is intolerant of both hydrophobic and polar substituents. The hydroxyl group of position-3 donates a hydrogen bond to a weakly charged receptor residue, and this bond is donated *syn* to the C2-C3 bond. Position 4 may be in close proximity to a cysteine residue, based on the inactivation of the receptor by 4-mercuri-E2[106]. The A-ring electron cloud may be engaged in a weak polar interaction with a slightly positively charged receptor residue, situated on the 13-face of the steroid.[105] The B-ring at position 6 again suggests close approximation of this area to the receptor essential volume as it seems to be intolerant of both polar and nonpolar substituents, however the α-substituents at position-7 are well tolerated and a hydrophobic pocket at the 7α-position with

minimum volume of 17 $Å^3$ is suggested. It has being shown that a pentenyl group, with a volume of 85 $Å^3$, can be accommodated at 7α-position with high RBA. The 9α-position has low steric tolerance, indicating close approach to the receptor essential volume. The 7β and 8α-positions are unexplored.[105] Finally, the C- and D-rings require a hydrophobic pocket (45 $Å^3$) at the 11β-site. This pocket has shown a high steric tolerance that could accommodate aromatic substituents but at the same time retain good RBA, it is however, intolerant of polar groups. The 12β-site can accommodate small nonpolar groups (e.g. methyl). The 14α/β-position can accept small, nonpolar groups without noticeable loss of RBA. The 15-position is intolerant of small hydrophobic substituents such as methyl or replacement with oxygen. The 16α-position accommodates large nonpolar groups such as iodine but the β-position is sterically less accommodating. The receptor accepts only small nonpolar groups in the 17α- location such as ethynyl or groups with chains directed in an endo-manner.[107] The 17β-hydroxyl group probably acts as a H-bond acceptor from the receptor residue either directly or *via* a water molecule.[105]

1.5 Selective Estrogen Receptors Modulators (SERMs)

One of the major therapeutic advances in clinical treatment of breast cancer has been the introduction of selective estrogen receptor modulators (SERMs). Contrasting these with estrogens, which are uniformly agonists, and antiestrogens, which are uniformly antagonists, the SERMs exert selective agonist or antagonist effects on various estrogen target tissues. The key feature of the SERMs which are chemically diverse compounds is that they contain a tertiary structure that enables them to bind to the estrogen receptor. It is also worth noticing that SERMs do not have the same steroid structure found in estrogens.

1.5.1 The evolution of SERMs

Since the first clinical use of tamoxifen (as it was known, ICI-46474) as a SERM in 1971 there has been substantial interest in this area. There are now multiple 'generations' of SERMs developed. Tamoxifen belongs to the first-generation of SERMs. It has been shown to maintain bone mineral density in postmenopausal women, decrease low-density lipoprotein cholesterol levels (LDL) and antagonise estradiol-stimulated tumour growth in the breast. It is an endocrine therapy standard for ER-positive breast cancers in both the neoadjuvant and postoperative adjuvant settings and a first-line therapy for the treatment of pre/postmenopausal women with estrogen-responsive advanced (stage IV) breast cancer. Tamoxifen has been a prototype for other SERMs with improved therapeutic profiles.[108, 109]

Second-generation SERMs were developed with the intention of obtaining ER targeted pharmaceuticals that do not have the uterotrophic effects of tamoxifen. The best known second-

generation SERM is raloxifene [45]. This compound functions as an agonist in bone and the cardiovascular system but acts as a pure antagonist in the breast and uterine tissue. Raloxifene has higher efficacy in maintaining bone mineral density compared with first generation SERMs, which is likely due to the unique manner in which it alters the ER structure. Raloxifene was found to decrease the risk of all ER positive breast cancers by 90% and invasive breast cancers by 72%.[110] The generally positive effects of raloxifene in the uterus are likely to make it the agent of choice for use as a chemo-preventative in postmenopausal women at high risk of breast cancer.

Third-generation SERMs should retain the favourable qualities of raloxifene including the superior enhancement of bone mineral density while decreasing the serum low-density lipoprotein cholesterol levels but, with a reduced tendency to induce hot flushes. Two of the most advanced third-generation SERMs are bazedoxifene and lasofoxifene. Both of these drugs have improved pharmaceutical properties. Their mechanisms of action differ slightly from each other and to that of existing SERMs. Bazedoxifene exhibited an improved vasomotor profile in phase III clinical trials compared with tamoxifen or raloxifene.[111, 112]

Future development of fourth-generation SERMs are focussed on primarily the following desired characteristics: 1) Estrogen antagonist action in the breast, 2) No uterotrophic activity, 3) Protection of bone to the full extent of estrogen, 4) Better cardiovascular and central nervous system side effect profiles than current SERMs, 5) Possession of superior bioavailability than current SERMs, 6) Potential benefits for men in protection against age-related bone loss and 7) increase in cholesterol levels, without displaying estrogenic proliferative effects in the prostate.[113]

1.5.2 SERMs chemical groups

To date, a large number of steroidal and non-steroidal molecules are known which exhibit SERM activity and in some cases selective estrogen receptor subtype modulation (SERSM) activity, and which display selectivity towards either ERα or ERβ.[114] These compounds can be subdivided in to a number of distinct chemical groups.[77, 114, 115]

1.5.2.1 Triarylethylenes

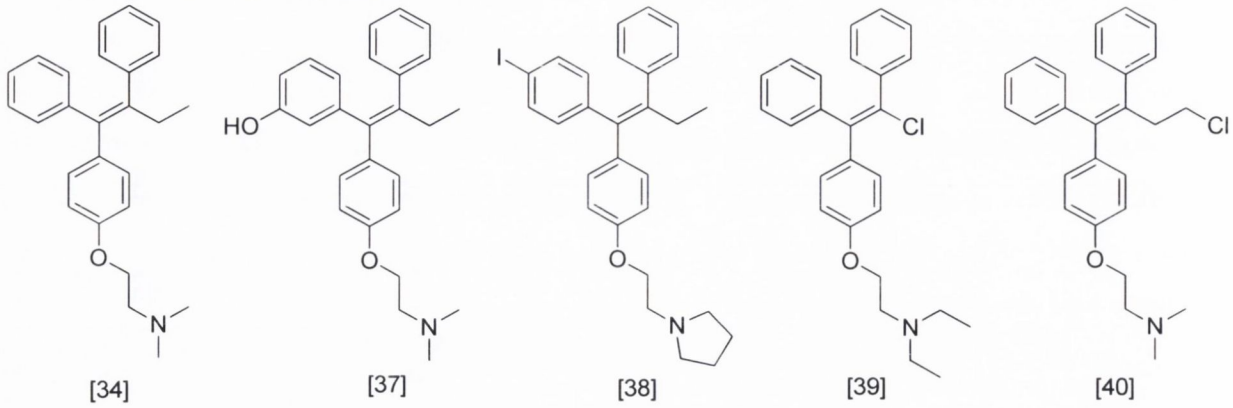

[34] [37] [38] [39] [40]

Figure 1-22. Selection of Triphenylethylenes [34], [37]-[40]

The triarylethylene group all contain a central ethylene double bond linked to three aryl rings and an ethyl group (i.e. tamoxifen [34]). A basic tertiary nitrogen moiety is also a common motif amongst this SERM subgroup. Members of this set of compounds have antagonistic activity. While tamoxifen displays antagonistic activity in breast tissue it can induce positive effects on bone density whereas toremifene [40] use is accompanied by slight reductions in bone density[116]. Both toremifene and tamoxifen have an estrogen-agonistic effect on the endometrium[117, 118]. Other compounds of the group of the triphenylethylenes also induce uterine stimulation and, for this reason, their development has been limited and their use restricted to cases of advanced breast cancer. Others are still in the early phases of development ([49]-[52]).[119] Also shown on Figure 1-22 are Droloxifene [37], Idoxifene [38] and Clomiphene [39] as further examples of compounds in this class.

Among the structural class of triarylethylene ligands there are many examples of ligands in which rigidity and in some cases bulk has been introduced by inclusion of an additional ring structure. This ring, however, has always linked carbon atoms of the ethyl group back to the *proximal* phenyl ring, which in tamoxifen would prevent *cis–trans* isomerism, a process that affects the antagonist character of this antiestrogen.[120] Cyclofenil [41] and its derivatives are non steroidal biphenol variants of the triarylethylene structure with high affinity for ER and partial antagonist activity.[121] The structure of the molecules retains the ethylene double bond and also a cyclohexylidine ring making the compound symmetrical and thus preventing *cis-trans* isomerism.

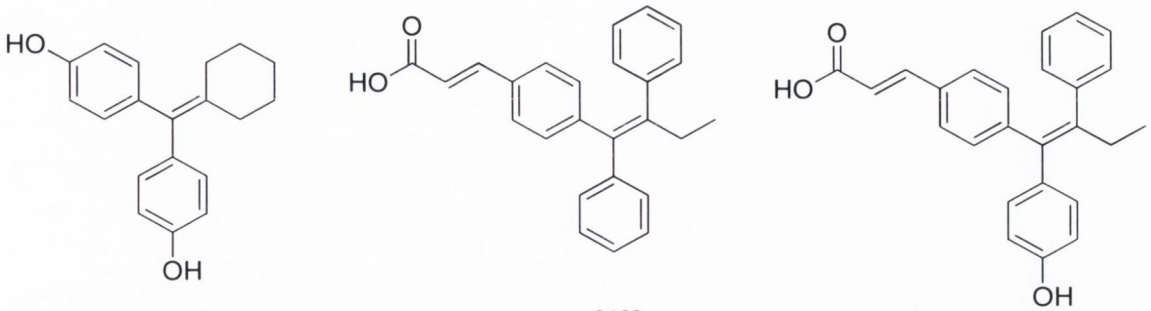

[41] [42] [43]

Figure 1-23. Cyclofenil [41], GW5638 [42] and GW7604 [43]

Triarylethylene carboxylic acids have also been reported as a new class of SERMs. Willson *et al.*[122] reported GW5638 [42] as an estrogen agonist containing an acrylic acid moiety with selectivity in bone over unterine tissue in rats. Both GW5638 [42] and GW7604 [43] were patented for possible use in tamoxifen resistant cancers. It is proposed that the carboxylic acid group could alter the environment associated with the Asp351 residue in the ER thus reducing estrogenic activity when compared with 4-OHT [35] (Figure 1-23).

1.5.2.2 Benzothiophenes

Benzothiophenes constitute an important chemical class in the treatment of ER dependent breast cancer (Figure 1-24). Conformationally restricted analogues of tamoxifen were investigated as potential antiestrogens because of problems associated with the isomerisation of the triarylethylene double bond. Raloxifene [45] is the main example of the restricted structure-type, benzothiophene class and is currently the most widely used drug for osteoporosis treatment and as a preventative agent. Raloxifene therapy has been associated with improvement in the levels of serum lipoprotein cholesterol, fibrinogen and homocysteine. This class of SERMS is antiresorptive on bone. It has shown no stimulatory effect on the endometrium[123] and an estrogen-like effect on lipids[123, 124]. It has also shown an inhibitory effect on ER(+) breast cancer cells[125]. Since the discovery of raloxifene, many structural modifications have been examined leading to a comprehensive SAR of this group. Arzoxifene [46] is another SERM of this group. In breast cancer cells lines, arzoxifene has a more potent effect than raloxifene but is similar or more potent in the skeletal system. However arzoxifene failed to meet secondary endpoints of reduction in non-vertebral fractures and cardiovascular events and improvements in cognitive function. Based on these results, further development of the drug has been discontinued and regulatory approval was not sought.[126]

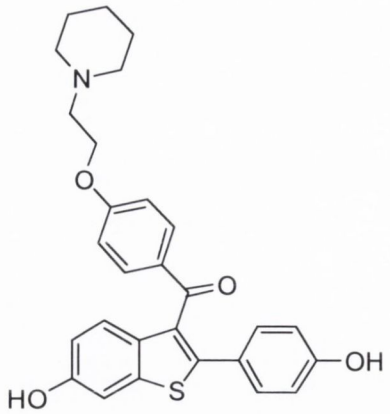

[45]

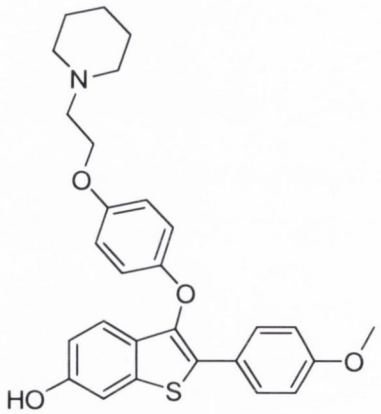

[46]

Figure 1-24. Raloxifene [45] and Arzoxifene [46]

1.5.2.3 Tetrahydronaphthalenes

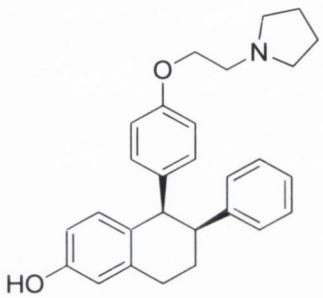

[47]

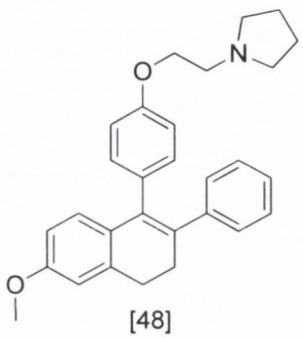

[48]

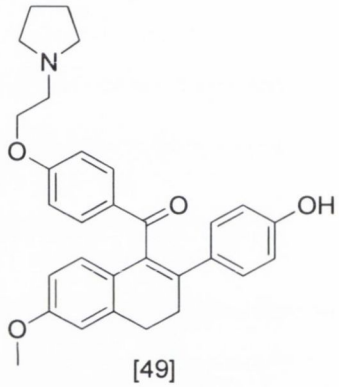

[49]

Figure 1-25. Lasofoxifene [47], Nafoxidine [48] and Trioxifene [49]

Lasofoxifene [47] is the main representative of the tetrahydronaphthalenes SERM group. Lasofoxifene is a desmethyl dihydro analogue of nafoxidine [48]. It was shown to have a high affinity towards ERα, *in vivo* animal experiments.[127] Lasofoxifene is approved as a SERM for the prevention of osteoporosis. Trioxifene [49], another member of the tetrahydronaphthalenes SERM group, was abandoned due to adverse side effects (Figure 1-25).[128]

1.5.2.4 Indoles

Both bazedoxifene [50] and pipendoxifene [51] were developed by Wyeth and are the two main examples of the indole group of SERMs. Bazedoxifene demonstrated bone protective and cholesterol lowering effects with no adverse uterine effects in OVX and intact rat models. This class of SERMS antagonizes the C3 gene and counteracts naloxone-induced vasomotor responses in rats. In addition, mechanical strength of bone is improved in treated animals, Figure 1-26.[76, 77, 114]

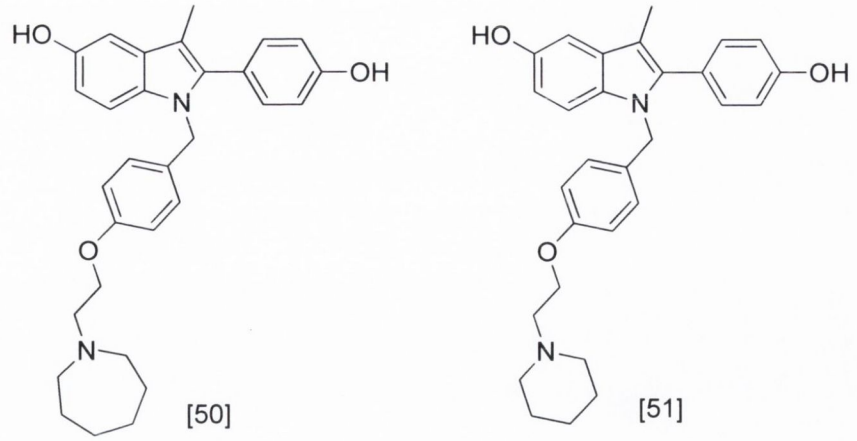

Figure 1-26. Bazedoxifene [50] and Pipendoxifene [51]

Ji *et al.* modified the benzothiophene scaffold and synthesised a series of benzothieno[3,2-*b*]indole ER ligands.[129] By altering the benzothiophene core to a tetracycle core-motif, rotation of the two phenolic groups is simultaneously restricted, so that the core is more coplanar and perhaps better mimics the endogenous steroidal ligand. While these novel ligands did not display improved binding affinities compared to raloxifene (ERα IC_{50} value = 0.9 nM; ERβ IC_{50} value = 11.6 nM) however, they did demonstrate good binding values (ERα IC_{50} value = 3-60 nM; ERβ IC_{50} value = 11-54 nM) and some derivatives showed stimulation of bone density.

A series of 2-arylindene-1-ones based on genistein, an ER agonist, were also synthesised which displayed good binding affinities (ERα IC_{50} value = 1-9 nM; ERβ IC_{50} value = 2-12 nM) which are comparable to estradiol and had nearly a 4-fold selectivity towards ERα.[130] In an attempt to design ERβ selective ligands, the team developed a series of 2-phenylisoindole-1,3-diones. Molecular modelling was used extensively to predict the optimisation point on the scaffold. The C-7-position of the indole six-membered ring appeared as a viable optimisation target. In doing so, it was hoped to improve binding affinity by producing favourable interaction with the discriminating residue Ile373. A bromo substituent was introduced to the indole core at 7-position and resulted in improved ERβ binding two-fold with compound [52] displaying a 45-fold selectivity towards ERβ (IC_{50}=36 nM).[131]

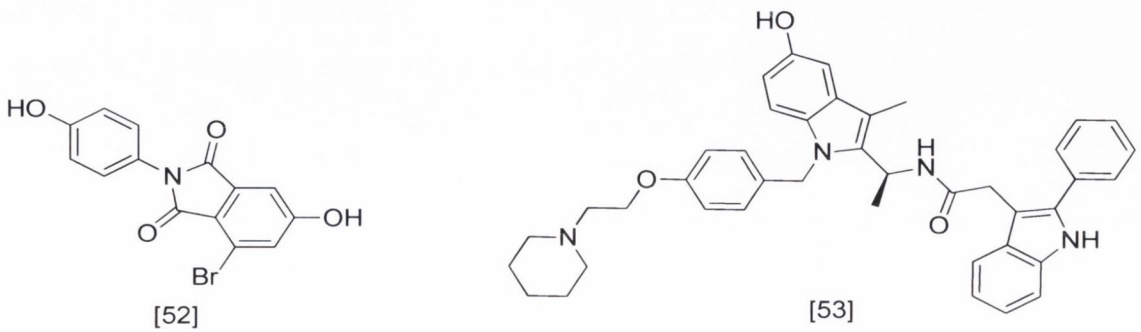

Figure 1-27. Manipulation of the indole to increase selectivity and RBA, [52] and [53]

Merck successfully modified the bazedoxifene scaffold to produce a novel ligand [53] with high binding affinity and selectivity towards ERα (ERα binding IC_{50} value = 2 nM (130-fold selectivity)). This compound [53] displayed 76 % antagonism in a uterine weight assay and good antiproliferative results in MCF-7 (IC_{50} value = 30 nM), Figure 1-27.[132]

1.5.2.5 Benzopyrans

A number of benzopyran containing SERMs have been reported. Ormeloxifene [54] is used as a contraceptive (Figure 1-29). The development of levormeloxifene [55] was stopped because of uterine safety issues.[133] Other molecules in active development include are SP500263 [56][134], EM-800 [57] and EM-652 [58][135, 136]. Benzopyrans can bind to both ERα and ERβ with the D-ring phenol interacting with hydrogen bond network (Glu353-Arg394-H_2O triad). This can be seen with the X-ray crystal structures, (2QTU.pdb, ER-benzopyran ligand)[137] and (2POG.pdb, benzopyran SAR studies)[138] (Figure 1-28).

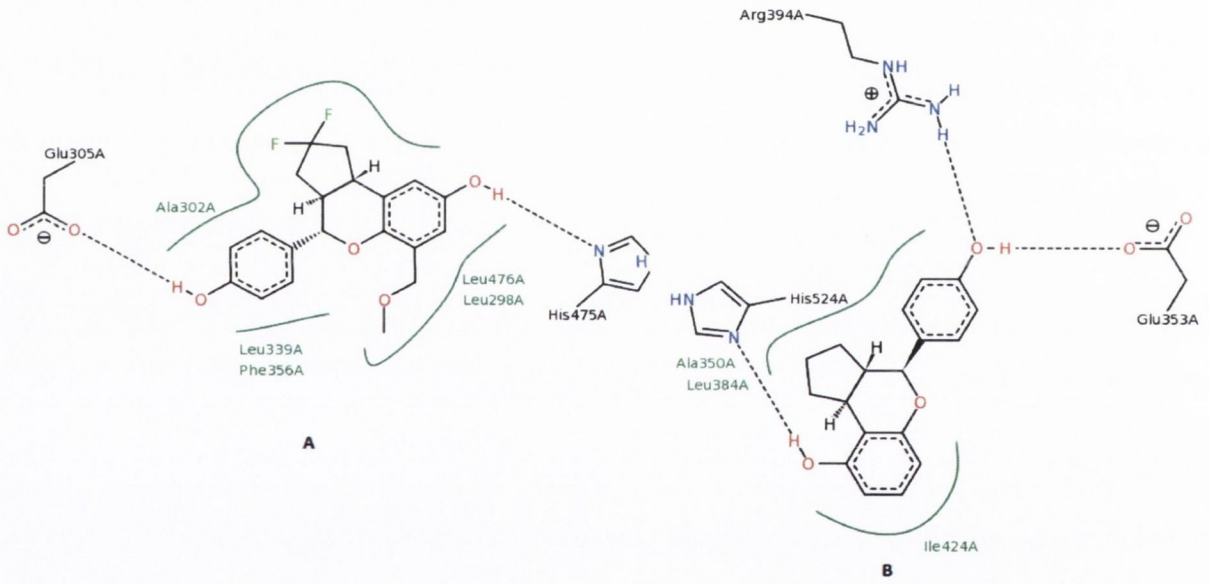

Figure 1-28 X-ray crystal structure interation A) 2QTU.pdb and B) 2POG.pdb

The A-ring phenol on the benzopyran core [54] interacts with His524/ His475 in ERα/ERβ respectively. The two rings (A and D) both bind in the same place in the LBD. The benzopyran scaffold is orientated 180 ° to the bisphenol axis with the A-ring phenol to the left of the residue (His524) in ERα or shifted to the right in ERβ. It was also seen that the C-ring in ERα pointed at Leu384 but pointed at Ile373 in ERβ. As expected any A-ring modification will place functional groups in the vicinity of Met421 and Met336 in ERα and ERβ respectively, Figure 1-29.[138, 139]

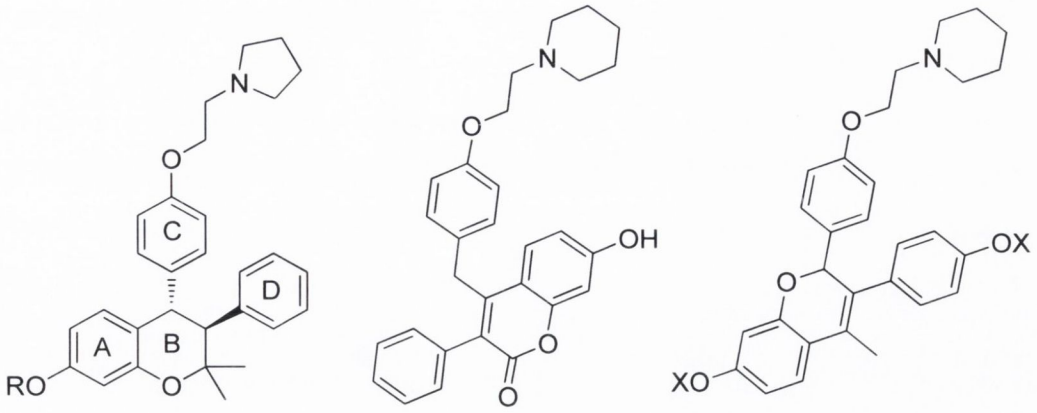

Figure 1-29. Ormeloxifene [54], levormeloxifene [55], SP500263 [56], EM-800 [57] and EM-652 [58]

The researchers at Lilly were able make a combination of modifications to the C and A rings to increase the ER selectivity of the benzopyran scaffold. Fluorination of the C-ring could increase the selectivity of the compound. Methoxymethyl group addition to the A-ring in combination with fluorination on the C-ring [55] gave an 83-fold increase in selectivity for ERβ [59][139]. The analysis of crystal structure (2QTU.pdb) showed that the C-ring addition (difluoromethylene group) was orientated towards the residue Ile373 and the A-ring addition (methoxy group) was orientated towards the residue Met336, to explain ER selectivity observed, Figure 1-30.[138, 139]

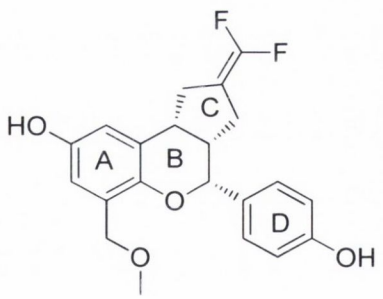

Figure 1-30. Compound [59]

1.5.2.6 Chromans/isochromans/Chromaquinolines

Phenylbenzopyran ER ligands can be separated into 4 distinct classes based on the position of the aromatic B-ring on the benzopyran or chromene moiety; 2-phenylbenzopyrans (flavonoids), 3-phenylbenzopyrans (isoflavonoids), 4-phenylbenzopyrans (neoflavonoids) and miscellaneous flavonoids generally without the pyran C-ring (chalcones and phenyl benzofurans).[140] The discovery that 8-prenylation of naringenin led to one of the most potent phytoestrogens with preferential binding to the ERα, suggested that prenylation of flavonoids might increase their estrogenic activity.[141]

Several studies with nonprenylated and various prenylated genistein and daidzein derivatives reported for both isoflavones a major decrease in agonistic activity, or a decrease in binding affinity, towards both ERα and ERβ upon prenylation.[142-146] The non-prenylated glycinol (pterocarpan) is a very potent agonist, whereas the pyran ring-substituted analogue of glycinol, glyceollin I, appeared to be a potent ERα antagonist. The use of molecular modelling, showed that glyceollin I docks in the ERα cavity occupying the same position as the side chain of ERα antagonists such as 4-OHT.[140] The investigation into isoflavonoids is still relatively new and no SERM based isoflavonoid is known. The ability of some prenylated isoflavonoids to act both as agonists and antagonists, strongly suggests that they might be classified as phytoSERMs.[140]

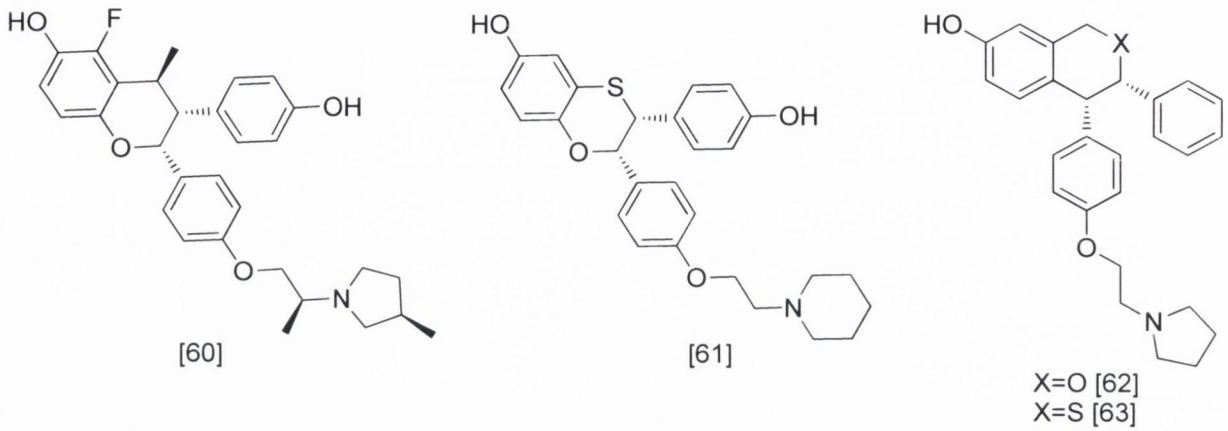

Figure 1-31. Novel chromane analogues, [60]-[63]

Tan *et al.* synthesised a series of novel chromane analogues with variations of the antagonist side chain with one of the derivatives [60] displaying potent inhibition in the MCF-7 cell line (IC_{50}= 70 pM) and with high binding affinity in ERα (IC_{50}= 0.7 nM) and ERβ (IC_{50}= 4.1 nM), Figure 1-31. This compound also exhibited impressive antagonistic properties in uterine weight assay of 124 % antagonism and -13 % agonism.[147] Novel "chromane" type analogues were also synthesised by this group with the carbon para to the oxygen in the ring exchanged with the larger sulphur atom. They believed that an interaction between the sulphur atom and the discriminating residues in the binding pocket of both ER isoforms (Leu384 for ERα, Met354 for ERβ) was responsible for the increase in selectivity. The sulphur containing compound [61] also showed increased selectivity which supported the hypothesis, i.e. replacement of the sulphur atom by the smaller carbon atom resulted in a complete loss of α-selectivity. Based on SARs, it was hoped that either oxygen or sulphur substitution in the ring might offer the same discrimination between the ERα and ERβ as is seen in [61]. Isochroman and isothiochroman scaffold derivatives were synthesised by modifying the lasofoxifene core using oxygen [62] and sulphur [63] respectively. These analogues showed similar

inhibition IC_{50} values in MCF-7 cell line (0.15-0.25 nM), but exhibited higher agonism when compared with lasofoxifene.[148]

A series of 6-phenylnaphthalenes were developed as a simplified structure which could mimic genistein framework. Docking studies suggested that the 6-phenylnaphthalene scaffold could exploit several binding orientations to achieve selectivity. The appropriate substituents placed at various positions were shown to be essential to gain ERβ selectivity by interacting favourably with ERβ Ile373 and/or repulsively with ERα Met421 using two different binding orientations.[149] Investigation into the 2-phenylquinoline scaffold which had a similar motif to 6-phenylnaphthalenes resulted in the synthesis of a series of 2-phenylquinoline derivatives with the best analogue [64] exhibiting ERβ binding (IC_{50}= 3.4 nM) and selectivity for ERβ (83-fold).[149] Docking studies of the ERβ LBD placed the bromine in close proximity to the ERβ Ile373 (ERα Met421) residue. Locking the dihedral angle seen in docking studies, by introducing a ring system, would generate a more rigid quinoline framework to mimic the docking of the lead compound. This inclusion led to the synthesis of 6*H*-chromeno[4,3-*b*]quinoline derivatives. The C7- chloro [65] and bromo [66] derivatives displayed good ERβ binding affinities (IC_{50}= 4.3-4.6 nM), with ERβ 46 to 50 fold selectivity, Figure 1-32.[150]

Figure 1-32. 2-Phenylquinoline derivative [64] and 6*H*-chromeno[4,3-*b*]quinoline derivatives [65],[66]

1.5.2.7 Dihydrobenzoxathiins / Dihydrobenzodithiins

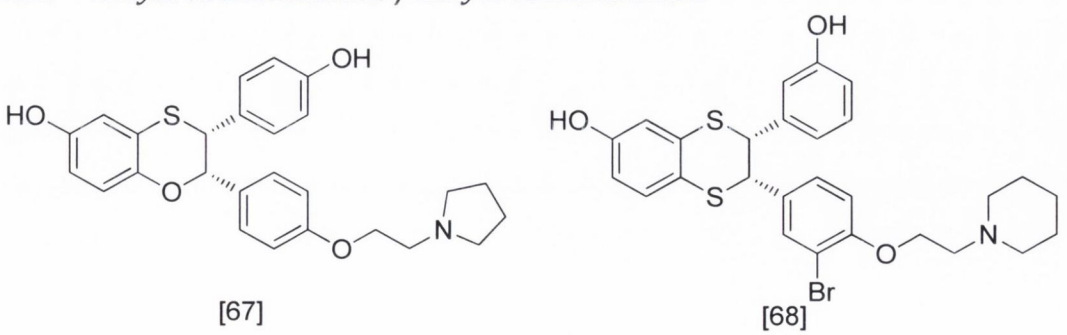

Figure 1-33. Dihydrobenzoxathiins [67] / Dihydrobenzodithiins [68]

A group of novel dihydrobenzoxathiins[151] and dihydrobenzodithiins[152] ring isoteres of the flavanone scaffold was developed through SAR studies based on the flavanone scaffold which

demonstrated selectivity towards ERα. The *cis*-[2*S*,3*R*] enantiomer [67] was found to have 50-fold selectivity towards ERα, exhibiting ERα binding (IC_{50}= 0.8 nM). The racemic mixture of the corresponding ligand displayed an IC_{50} at ERα of 3 nM and 143 nM at ERβ, Figure 1-33. It has been shown that dihydrobenzoxathiin, with different alkyl substitutions at the pyrrolidine ring or at the side chain resulted in diastereomeric mixtures.[151, 153] These diastereomers showed different effects in their agonist or antagonist activities in uterine tissues, resulting in full antagonism and mixed-functional agonism/antagonism.[151, 153] The crystal structure of ERα in complex with four dihydrobenzoxathiin derivatives is reported, in human ERα. It was found that the uterine antagonism/ agonism profile of the dihydrobenzoxathiin SERMs is highly dependent on the size and location of side chain substituents.[153] The dihydrobenzodithiin compounds displayed 16- to 40- fold ERα selectivity with a binding affinity between 4-20 nM (ERα) and are less active compared with the dihydrobenzoxathiin group.[152]

1.5.2.8 Tetrahydrofluorenone, Hexahydrochrysene and Tetrahydrobenzofluorene

The tetrahydrofluorenone derivatives were identified in a high throughput screen as ERβ selective ligands. Compound [69] was identified as an ERβ selective ligand, Figure 1-34. The ERβ binding of [69] gave an IC_{50} of 218 nM with 12 fold selectivity towards ERβ.[154] A number of related derivatives with selectivity towards ERβ and binding affinity in the low nanomolar region were developed. Further investigation into the structure of the tetrahydrofluorenone was carried out and it was then postulated that if a constrained ring system could be included it would conformationally restrict this key binding element thus increasing the selectivity. This led to the discovery of [70] which had ERβ binding of IC_{50} of 1 nM with 97-fold selectivity.[155] A series of fused pyrazole-tetrahydrofluorenone analogs which are potent, ERβ selective ligands, some with picomolar ERβ binding with >100-fold selectivity have been reported. Compound [71] demonstrated binding affinity in ERβ (IC_{50} = 5 nM) with a 400-fold selectivity.[156] Tetrahydrofluorenone derivatives perform well *in vitro* in ER binding and cell based tranactivation assays but display poor pharmacokinetic properties, (rapid clearance and low oral bioavailability). One approach to counteract this was to add 7-hydroxy functionality to heterocycles which act as phenol bioisosteres. The triazole tetrahydrofluorenone analogs displayed improved oral bioavailability with excellent and selective ERβ affinity, while retaining full ERβ agonism. The lead compound [72] combined potent affinity for ERβ (IC_{50} = 5.7 nM) and excellent selectivity versus ERα (333-fold) with a substantially improved pharmacokinetic profile.[157]

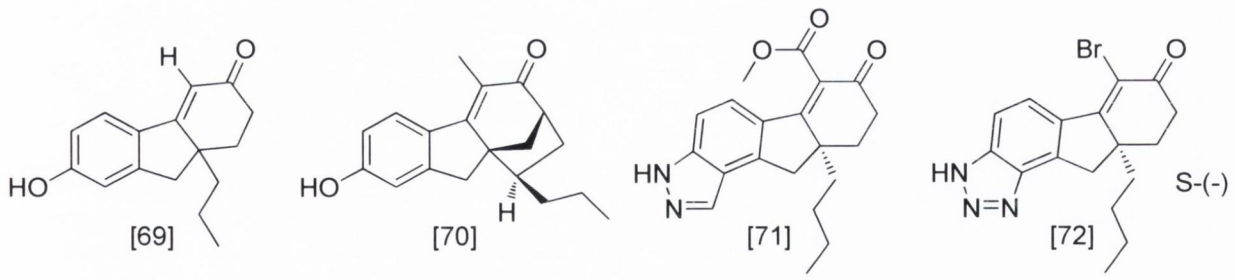

Figure 1-34. Tetrahydrofluorenone derivatives [69]-[72]

Tetrahydrochrysenes (THCs) were first developed as fluorescent ER ligands[158] but the *cis*-isomers display remarkable ER subtype selectivity with agonist activity on ERα and antagonist activity on ERβ.[159] Tedesco *et al.* reported the synthesis of hexahydrochrysenes which are saturated analogues of the THCs and tetrahydrobenzo[*a*]fluorenes which are saturated analogues of the related benzo[*a*]fluorene core but these analogues proved to be unstable.[160] The lead compound in both series contained the tetrahydrobenzo[*a*]fluorene or hexahydrochrysene core, with a piperidinyl-ethoxyphenyl substituent attached, [73] and [74] respectively, Figure 1-35. The lead compounds from each group were quite similar but had considerably different 3D conformation/shape (confirmed by X-ray crystallography) resulting in a different topological display of substituents around the rigid ligand core. Compounds [73] and [74] behaved as antagonists on both ERα and ERβ, but [74] displayed a more complete antagonism and higher potency. This was rationalised using molecular modelling which demonstrated that changes in this orientation could preclude the basic side chain of [73] interacting with the Asp354 residue.

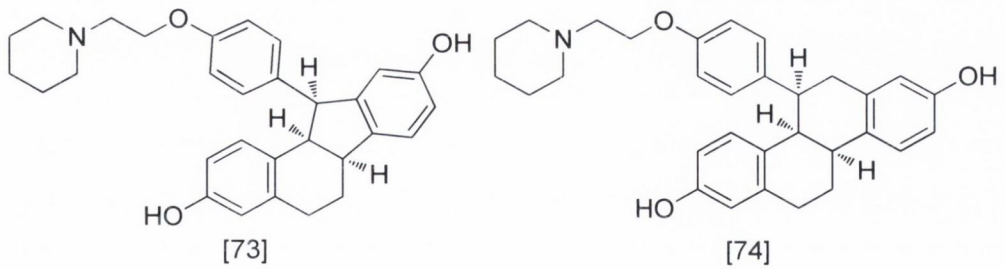

Figure 1-35. Tetrahydrobenzo[*a*]fluorenes and Hexahydrochrysenes analogues, [73] and [74] respectively

1.5.2.9 Pyrazoles, Indazoles and Furans

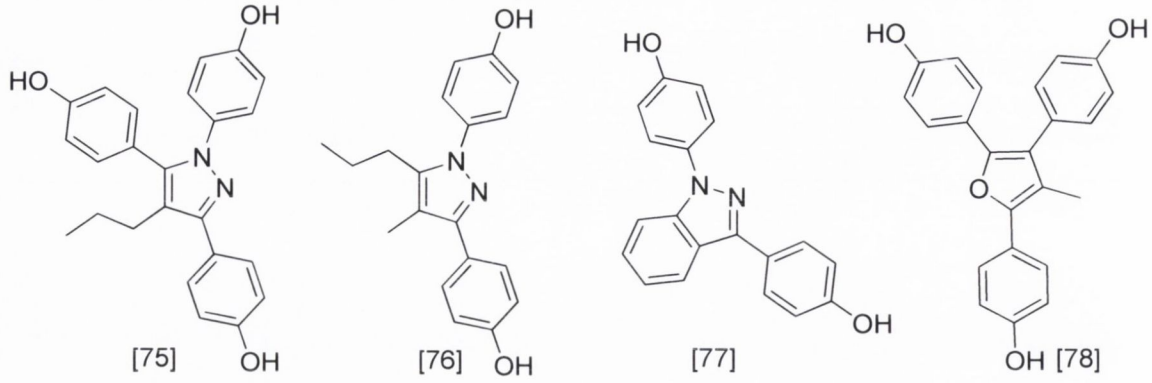

Figure 1-36. Pyrazoles, Indazoles and Furans derivatives [75]-[78]

It has been reported that ER binding selectivity and transcription-regulating potency can be changed by substitution on the phenolic pyrazoles. 1,3,5-Triphenolic-4-propyl pyrazole [75] acts as selective ERβ agonist, while the 1,3-diphenolic-4-methyl pyrazole [76] with a extended moiety at C5 (MPP), behaves as a selective ERα antagonist, Figure 1-36.[161, 162] Other pyrazole derivatives have been shown to be full ERα/ERβ agonist/antagonists, Compound [77] is a full ERα agonist and ERβ antagonist. Molecular modelling studies have shown that two different binding orientations, providing for ligand interactions with Met421 in ERα and Thr299 in ERβ, could explain this ERα agonism and ERβ antagonism respectively.[163] Tetrasubstituted furans proved to be potent SERMs with binding selectivity ERα /ERβ of 50-70 % with one analogue [78] displaying selective ER agonist activity with no agonist or antagonist activity on ERβ.[114] The phenyl-2*H*-indazole core structure was investigated as this heterocyclic system would allow the introduction of different steric and polar groups at an internal position of the heterocyclic system. This led to two lead compounds [79] and [80] with RBA for ERα between 18 and 32% and affinity selectivity over 100-fold and were found to be agonists, Figure 1-37.[164] Researchers at Pfizer synthesised and evaluated a series of benzimidazole derivatives, the lead compound [81] in the series exhibited 105-fold selectivity for ERβ and also acts as a functional agonist in whole cells.

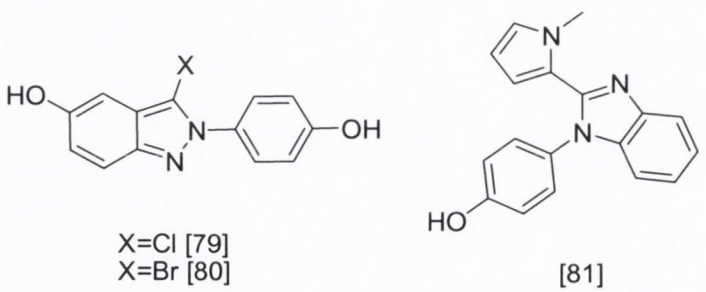

Figure 1-37. Phenyl-2*H*-indazole analogues [79] and [80], and benzimidazole derivative [81]

1.5.2.10 Benzisoxazole and Benzoxazole

Novel diphenolic benzisoxazoles and benzoxazoles with good potency and selectivity towards ERβ were reported with the most potent and selective analogues of this series have binding affinities of 1-5 nM at ERβ and selectivities relative to ERα of greater than 100-fold. The use of X-ray cocrystal structures (in ERα) along with docking calculations made it possible to obtain a single conservative residue substitution in the LBD, Met421 and Ile373, in ERα and ERβ respectively. Benzoxazole with a variation at the 7-position was the most selective of the azole series, with its lead compound ERB-041 [82] being 920-fold more selective for ERβ (human full length ERβ), Figure 1-38.[165]

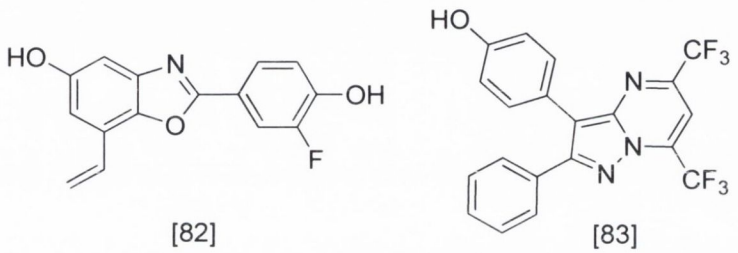

[82] [83]

Figure 1-38.ERB-041 [82] and C-3 monophenolic variation [83]

1.5.2.11 Pyrimidines

The synthesis of pyrazolo[1,5-*a*]pyrimidine core analogues have been shown to have unique profiles when binding to the ER.[166] These analogues showed relatively low binding affinities but selectivity for ERβ. The analogues were seen to act as passive antagonists on both ERα and ERβ, with some obvious selective antagonism on ERβ. These were the first series of compounds found to act as passive antagonists on ERα. The modelling studies provide no definitive answer to the mechanism of antagonism, but it is believed that the antagonistic character is due to the analogues presenting themselves differently in ERα and ERβ. The lead compound in the series was the C-3 monophenolic variation [83] with 36-fold selectivity for ERβ, and it was effective as an ERβ antagonist while showing no considerable agonism on ERα or ERβ.[166]

1.5.2.12 Novel Flexible Ligands

Reports have suggested that incorporating flexibility into the rigid backbone of antiestrogens could enhance the desired effects of that ligand at the estrogen receptor. The tolerance of estrogen receptors to triarylethylene structures with added flexibility was investigated by previous research within the Meegan research group.[167, 168] The compounds synthesised were related structurally to tamoxifen but incorporated a spacing methylene group between the aryl and vinylic systems into the traditional triarylethylene structure, which gave novel flexibility to this rigid class of antagonist. The spacing methylene group was moved around the vinylic system to generate a series of novel flexible ligands. These compounds have demonstrated high antiestrogenic potency, low cytotoxicity profiles

and high ER binding affinity (ERα binding affinity in the range of 157-508 nM), with the most potent compound [84] in the series having an IC_{50} value of 3.57 μM in MCF-7 cell line.[114, 169] Further optimization of [84] was also performed to investigate the effect of substituent addition to the now flexible benzylic substituent. One of the compounds [85] with a *p*-methoxy substituent on the aryl ring demonstrated 17-fold ERα selectivity with a high ERα binding affinity IC_{50} value of 72 nM, Figure 1-39.[168]

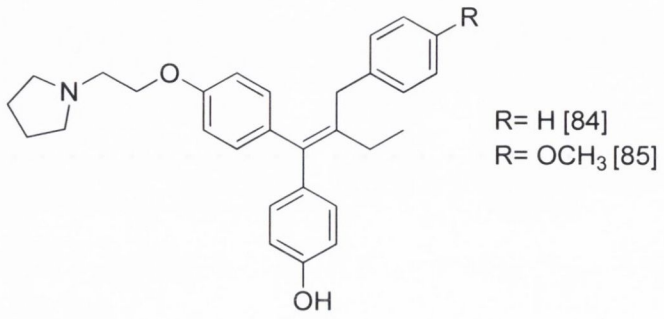

Figure 1-39. Novel Flexible Ligands, [84] and [85]

1.5.2.13 Steroidal Ligands

A number of estradiol-based compounds were studied as possible 'pure' antiestrogens (possessing only estrogen antagonistic activity). While the compounds in this class demonstrated effective antiproliferative character, they did not protect against bone density loss or promote lipid reduction commonly associated with SERMs. Research into steroidal ligands found that the attachment of a motif at the C-7 atom of estradiol, provided the optimum site on the steroid nucleus for substituents to retain a high affinity for ER.[170] The synthesis of 7 alpha-alkylamide analogues of estradiol (ICI-182,780, fulvestrant) [86] led to the discovery of a pure novel antiestrogen that competitively binds to ER and blocks receptor dimerisation, Figure 1-40.[171] Fulvestrant competitively binds to the ER but with a much greater affinity than tamoxifen, approximately 89% that of estradiol, compared with 2.5% for tamoxifen.[172] Fulvestrant forms an unstable complex with the ER which then undergoes accelerated degradation, resulting in downregulation of the ER with subsequent inhibition of ER-DNA binding and abrogation of the expression of genes associated with tumour progression, metastasis, and angiogenesis [173, 174] It has also been shown to reduce dose dependence at the cellular level of ERs and progesterone receptors, resulting in more profound effects in tumours that express both hormonal receptors.[175, 176] An additional benefit of fulvestrant is that it has a distinct mechanism of action allowing it to bypass tumour resistance found with other hormonal agents. There is also no known estrogen agonist effects associated with its use. Fulvestrant is classified as SERM but it is more correctly classified as a Selective Estrogen Receptor Downregulater (SERD).

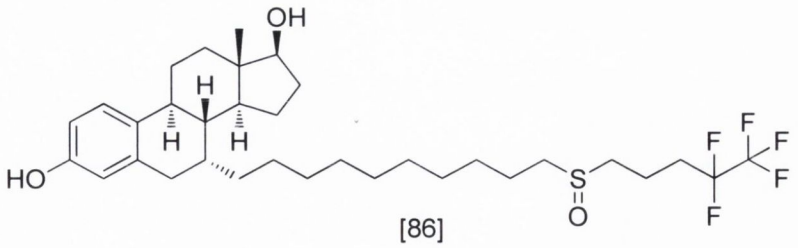

[86]

Figure 1-40. Fulvestrant [86]

1.6 Tamoxifen Metabolism

The metabolism and elimination may determine the safety and efficacy for a particular drug. The metabolism of a drug may be performed by one or more enzymes, and its activity could therefore be influenced by genetic variants and drug interactions which could lead to an enzyme with reduced or no activity.

Tamoxifen [34] itself has a relatively poor affinity to the ER and simultaneously is metabolized to several compounds; some exhibit estrogen-like activity whereas others are strong antiestrogens with high ER affinity. The metabolism of tamoxifen is complex involving *N*-demethylation, aromatic α-hydroxylation, side chain hydroxylation and *N*-oxidation, Figure 1-41.[177] *N*-Demethylation is predominantly performed by cytochrome (CYP) P450 isoenzymes CYP3A4 and CYP3A5. *N*-Desmethyltamoxifen [87] is less effective in its ability to bind to the ER when compared to 4-OH-tamoxifen [35] and endoxifen [36] (highly potent metabolite), and to subsequently suppress the estrogen-dependent cell growth and gene expression[178]. *N*-Desmethyltamoxifen may be transformed to endoxifen *via* 4 hydroxylation which is nearly exclusively accomplished *via* CYP2D6.[179]. The formation of 4-OHT represents a minor route of the metabolism to endoxifen and is achieved by various CYP450 enzymes.[179] The most prevalent route for metabolizing tamoxifen to endoxifen is mostly dependent on the function of one enzyme, CYP2D6.

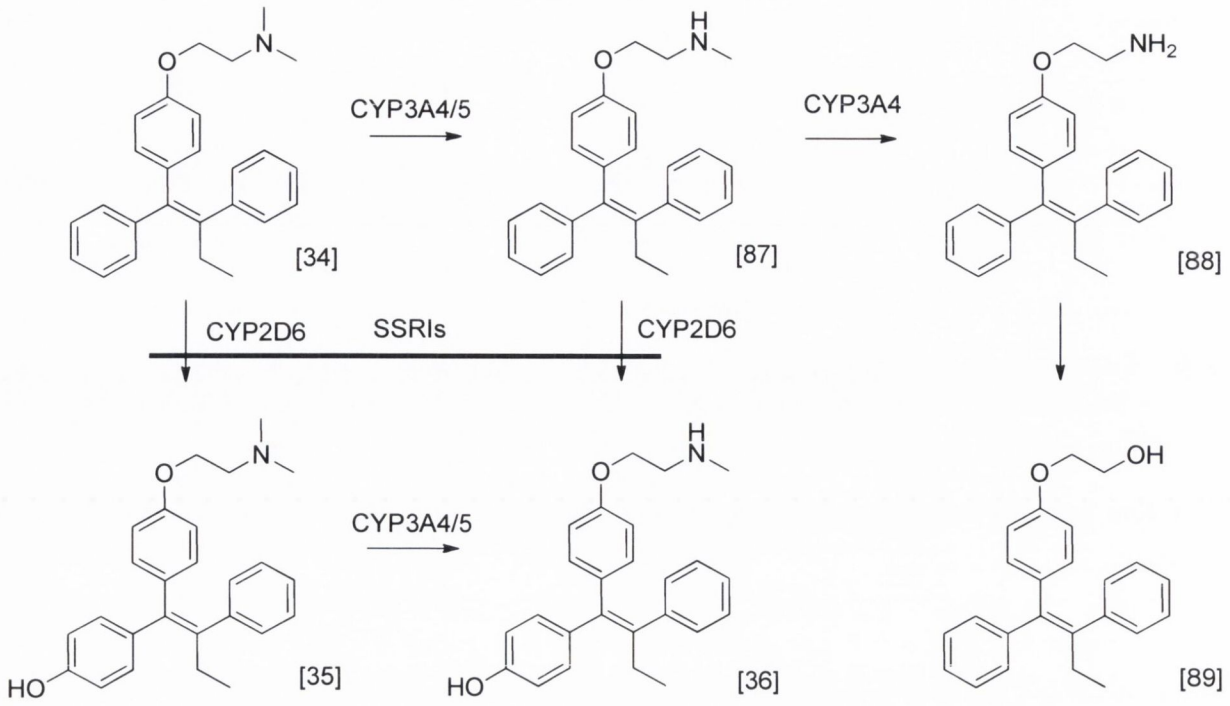

Figure 1-41. Tamoxifen metabolites and relevant CYP genes

Although CYP2D6 represents less than 2% of the total CYP450, it is believed to account for 25% of the metabolism of commonly used drugs.[180] 4-OHT and endoxifen are thought to exist as an equilibrium of *cis* and *trans* isomers, which are known to differ in their ability to operate either as an agonist or an antagonist towards the ER. The final steps in the metabolism of tamoxifen are sulphate conjugation and glucuronidation, resulting in an increase in solubility in order to facilitate the excretion of the drug. N-Desmethyltamoxifen is further demethylated to N-desdimethyltamoxifen [88] and then deaminated to metabolite Y [89], a glycol derivative. Levels of endoxifen are twice those seen for 4-hydroxytamoxifen, which in turn are about 5% of those observed for tamoxifen.[181] 4-OHT and endoxifen have increased affinity for the ER and both metabolites have been shown to be equipotent with respect to ER binding and inhibition of 17β-estradiol induced cell proliferation of T47D and BT474 human breast tumour cell lines. Both metabolites are significantly superior *in vitro* to the pro-drug tamoxifen.

Enzyme variants of CYP2D6 do not promote the metabolism of tamoxifen to endoxifen and this means that a significant number of women might not receive optimal benefit from tamoxifen treatment. Specific selective serotonin reuptake inhibitors (SSRIs) have been reported to bind to CYP2D6 and prevent the hydroxylation of tamoxifen and N-desmethyltamoxifen. This prevents the metabolic activation of tamoxifen. It was found that some of the prescribed SSRIs (fluoxetine and paroxetine) are potent inhibitors of the CYP2D6. Ongoing studies show that potent inhibitors of

CYP2D6 in the SSRI family significantly decrease levels of the tamoxifen metabolite endoxifen.[181] Another SSRI, Venlafaxine, has a low affinity for the CYP2D6 enzyme and is therefore recommended as an alternative to ameliorate menopausal symptoms during endocrine therapy.[100]

1.7 Aromatase Inhibitors

1.7.1 Role of Aromatase

Aromatase is an enzyme required for the biosynthesis of estradiol. In women, the incidence of the precursor C19 steroids for aromatisation to estrogen in extragonadal sites is more prevalent than in the male.[182] The primary source of C19 steroids production is the adrenal cortex through androstenedione, dehydroepiandrosterone (DHEA) and DHEA sulphate (DHEAS) but the secretion of these steroids and their plasma concentrations reduces significantly with age.[183] Preceding aromatisation, DHEA must first be converted to androstenedione. Another important step is the reduction of the 17-keto group to 17-hydroxyl, catalysed by 17-hydroxysteroid dehydrogenase type I, which is essential for formation of the active estrogen, estradiol. This enzyme is known to be distributed in a number of extragonadal sites of aromatisation around the body, although it is expressed in tumourous breast epithelium[184] and in bone[71].

1.7.2 Aromatase in breast cancer tissue

The mechanism of aromatisation which gives rise to amplified local concentration of estrogen in breast cancer *via* aromatase overexpression within the tumour tissue has been well reported.[185-187] Alarming findings from these studies showed noticeably increased local levels of estrone, estrone sulfate, and estradiol in breast tumour tissue compared with circulating estrogen levels.[185-187] *In-vivo* studies on mice where MCF7 breast cancer cells (stably transfected to express a mouse mammary tumour virus promoter-driven human aromatase cDNA and inoculated into oophorectomized nude mice) remained dependent on circulating androstenedione for their rapid growth.[188]

1.7.3 Aromatase Inhibitors

Aromatase inhibitors (AIs) can be classified by their mechanism of action: Type I inhibitors which are steroidal compounds that may be purely competitive inhibitors, or more commonly in the case of those compounds that are used clinically, irreversible 'suicide substrates'[189] Type II inhibitors are nonsteroidal compounds and bind to the haem group of the aromatase enzyme by co-ordination through a basic nitrogen atom[189]. They are also often classified into first-, second-, third- and fourth-generation subgroups in chronological order to their clinical development.[3, 15, 190] AIs have a different toxicity profile to other endocrine therapies, although some that mimic menopausal symptoms due to depletion of estrogen are the same, such as hot flushes and sweating.

Although type I and type II AIs interfere with the final step in estrogens biosynthesis, they do so by different mechanisms.

Type I inhibitors have an androgen structure and compete with the natural aromatase substrate androstenedione. At the catalytic site of aromatase, the Type I inhibitors bind covalently to the enzyme inducing aromatase inactivation, and more aromatase enzyme must be produced before estrogen biosynthesis can resume, hence the term suicide inhibitors. Exemestane [90] is one such example of a Type I inhibitor; exemestane and its 17-hydroexemestane metabolite have the potential for androgenic effects. The binding of exemestane to the androgen receptor (AR) is about 0.2% of that of dihydrotestosterone[191], but when exemestane becomes metabolised to 17-hydroexemestane, the affinity for the AR becomes enhanced by about 100-fold that of pre-metabolised parent compound[192].

Type II inhibitors lack a steroidal core (nonsteroidal), and interact with the CYP450 moiety of the enzyme, by binding through the basic nitrogen atom to the iron atom of the haem group of the enzyme[193]. Estrogen biosynthesis is prevented but activity is dependent on the continued presence of the nonsteroidal agent.[194]

1.7.4 Early Aromatase Inhibitors

The first generation aromatase inhibitor, aminoglutethimide [91], has been available for therapeutic use for breast cancer for over four decades. In clinical studies, aminoglutethimide was as effective as tamoxifen in advanced disease, as its mechanism of action inhibited several CYP450 enzymes involved in adrenal steroidogenesis. However the toxicity, lack of selectivity and inconvenient dosing regimen posed serious problems for its use, Figure 1-42.[195, 196]

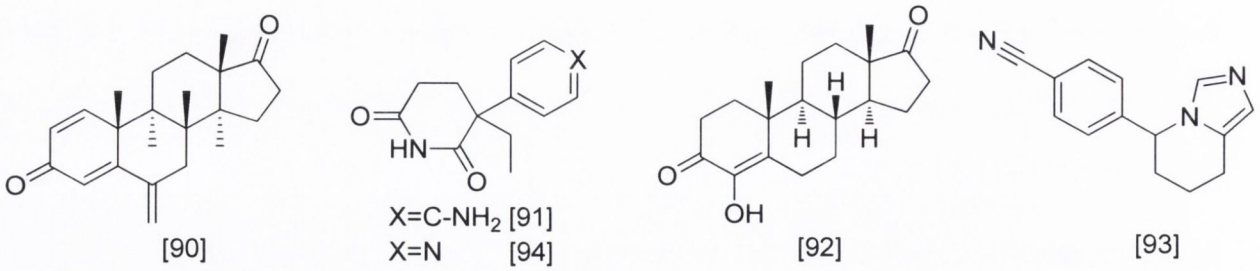

Figure 1-42 First- and Second- generation of Aromatase Inhibitors [90]-[94]

Second-generation aromatase inhibitors include formestane/4-hydroxyandrostenedione (4-OHA) [92][197] (a type I inhibitor), fadrozole [93][198] and rogletimide [94], both type II inhibitors. 4-OHA binds irreversibly to the enzyme active site and acts as a suicide inhibitor with prolonged action on the enzyme. While fadrozole is a CYP19 inhibitor, effectively inhibiting brain aromatase activity,

estradiol biosynthesis and vitellogenin production.[199] Similar to the first generation AI's they were not without their disadvantages. 4-OHA required intramuscular injection, and fadrozole causes aldosterone suppression which limited the quantity of the doses which only produced about 90% inhibition.[200] Other second-generation aromatase inhibitors have been investigated clinically but have never been approved for clinical use. Research on novel A,D ring modified steroid analogues of formestane and testolactone was relatively unsuccessful as the new analogues were less active than the parent compound. This research discovered that the binding pocket of the active site of aromatase required planarity in the region of the steroid A,B-rings and the D-ring structure was critical for binding.[201]

1.7.5 Third generation Aromatase Inhibitors

A number of non-steroidal aromatase inhibitors were developed based on the structure of antifungal agents that inhibit the CYP450 enzyme. This development led to a third generation of inhibitors comprising of mostly imidazole and triazole derivatives. Third-generation AIs are highly selective for enzyme aromatase and are fairly well tolerated. Three third generation AIs are approved for clinical use, one type I (Exemestane [90]); and two type II (anastrozole [96] and letrozole [97]). Both of the type II AIs contain the triazole motif. Another AI in this class was vorozole [98] contains a triazole and benzotriazole rings but was withdrawn from testing when no difference was detected in the duration of median survival as compared to the progestational agent megestrol acetate, Figure 1-43.[202] It has been shown that all three AIs reduce systemic estrogen levels by as much as 98%.

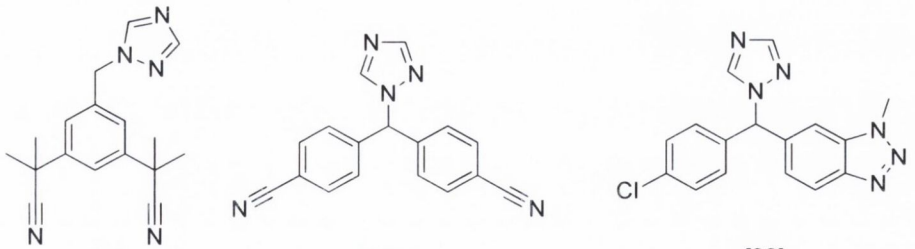

[96] [97] [98]

Figure 1-43 Third generation Aromatase Inhibitors [96]-[98]

Prior to the development of the third generation compounds, trials showed tamoxifen was better than first and second generation aromatase inhibitors. The development of third generation drugs, letrozole and anastrozole have been demonstrated in trials to be superior to tamoxifen as first line treatment for advanced breast cancer.[203, 204]

The use of experimental and molecular modelling data has given a footprint which the ligands should contain for the selective inhibition of aromatase enzyme. The structure should

incorporate a moiety that is able to interact strongly with the iron atom of the heme group (imidazole/triazole ring, etc)[205], a hydrophobic spacer group between heme coordinating groups and hydrogen bond acceptor moiety[206], and a ligand that is able to accept a H-bond from S478 present in active site (CN group)[207].

1.7.5.1 Anastrozole

Anastrozole [96] is a potent, orally active, selective, non-steroidal AI that markedly reduces the levels of circulating oestrogens in postmenopausal women with breast cancer.[208, 209] It has been used for adjuvant therapy in postmenopausal women with advanced breast cancer, and has exhibited significant benefits over tamoxifen with respect to time to progression (TTP)[210, 211] when given as first line treatment of postmenopausal women with hormone dependent breast cancer. Anastrozole is highly effective in reducing tumour volume in the neoadjuvant therapy of breast cancer in postmenopausal women.[212] Bone weakness has been associated with anastrozole. Women who switched to anastrozole after two years on tamoxifen reported twice as many fractures as those who continued to take tamoxifen.[213]

1.7.5.2 Letrozole

Letrozole [97] is a highly potent and selective AI that inhibits the enzyme activity of intracellular aromatase at the major sites where it is found, resulting in almost complete suppression of whole body aromatization.[214] Letrozole is highly selective for aromatase and unlike previous generation AIs and does not drastically affect cortisol, aldosterone, or thyroxine.[215] Studies have shown that it is over three orders of magnitude more selective than aminoglutethimide in its effects on progesterone and corticosterone production, and greater than 300-fold more selective against aldosterone than fadrozole.[216, 217] Letrozole has been shown *in vivo* to inhibit the growth or induces the regression of hormone-responsive breast tumours. Letrozole was evaluated using *in vitro* and *in vivo* models and was shown to be the most potent of the third-generation AIs. The superiority of letrozole over tamoxifen has been consistently demonstrated in advanced and early breast cancer.[218, 219]

1.7.5.3 Fourth generation Aromatase Inhibitors

Although third generation aromatase inhibitors are viable substitute for tamoxifen, but there is scope for enhancement. The fourth generation of AIs will require more specific inhibition and lower toxicity profiles especially for addressing musculoskeletal disorders. The development of the new generation of AIs will lead to multipotent compounds that can deal with complexity and multiplicity of factors involved in the development of hormone-dependent breast cancer.[220-222]

Recanatini *et al.* have reported the use of different oxygenated heterocycles such as flavone, chromone, and xanthone as aromatase inhibitors.[223] This group synthesised a library of compounds with several concerted structural modifications on these scaffolds which were shown to be very potent and selective for CYP enzymes, mainly 17R-hydroxylase/17,20-lyase (CYP17), a cytochrome P450 enzyme[223]. The early appropriately substituted xanthones synthesised showed that the heterocyles were essential for inhibitory effects previously observed[205]. Further development on the xanthone core showed that substitution of the oxygen by a sulphur atom always enhanced the potency (increase in lipophilicity) and that the presence of either a ketone or nitro group was essential for H-bond interaction, with compound [99] exhibiting a slight increase in potency (CYP19 IC_{50} 3.98 nM), Figure 1-44.

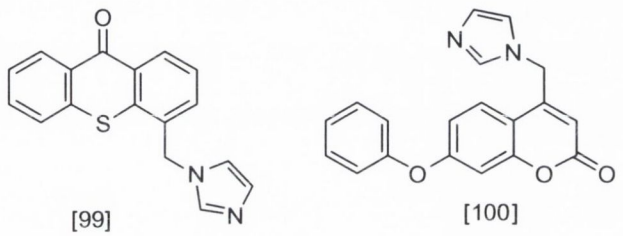

Figure 1-44 Xanthone derivative [99] and chromone analogue [100]

The use of 3D-QSAR studies has been applied to the discovery of novel potent and selective AIs.[224] A series of compounds were synthesised by covalently linking a hetrocycle ring to a flourene, indenodiazine or coumarin scaffold. Overall the coumarin based analogues displayed the highest potency and CYP17/CYP19 selectivity as was seen in compound [100], Figure 1-44.

Nonsteroidal anti-inflammatory drugs (NSAIDs) have been shown to have beneficial effects in breast cancer treatment.[225] It was reported that in rats the use of the COX-2 inhibitor nimesulide could suppress the development of 2-amino-1-methyl-6-phenylimidazo [4,5-*b*] pyridine (PhIP)-induced mammary gland carcinogenesis.[226] Further studies has shown that nimesulide could reduce the aromatase activity and expression in several breast cancer cell lines[227]. Several new nimesulide analogues showed selectivity to inhibit cell proliferation in Her2 overexpressing breast cancer[228] and these compounds could induce long term estrogen deprived (LTEDaro) cell apoptosis[229]. These characteristics suggests that nimeslide analogues may potentially overcome AI resistant breast cancer cell growth and overcome AI resistance for hormone-dependent breast cancer respectively.[228, 229] Nimesulide derivatives which do not have COX-2 inhibitory activity were more active than nimesulide to target aromatase.[229, 230]

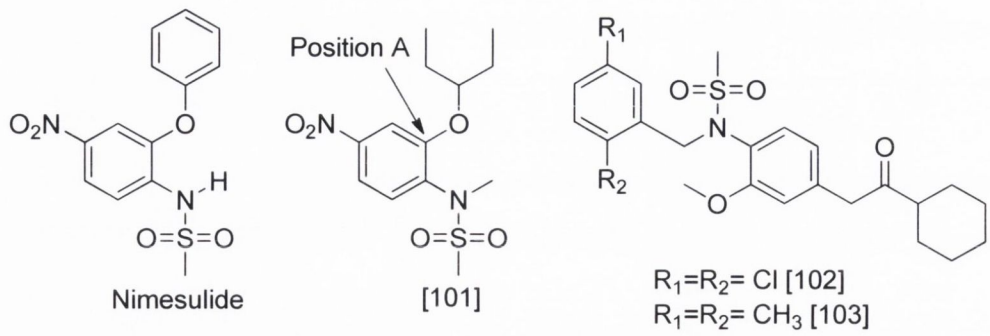

Figure 1-45 COX-2 inhibitors derivatives as Aromatase Inhibitors, Nimesulide and [101]-[103]

Su *et al.* evaluated a series of sulfonanilide analogues of nimesulide for their effects on aromatase activity and COX-2 inhibition as aromatase levels in breast cancer are enhanced by prostaglandins and reduced by COX inhibitors[230]. One compound [101] from the sulfonanilide series showed the most suppression of aromatase activity in SK-BR-3 cells with an IC_{50} of 230 nM, Figure 1-45. The SAR study found no link between aromatase and COX-2 inhibition in SK-BR-3 breast cancer cells but did show that the decrease in aromatase gene expression was independent to COX-2 inhibition. Further work performed by Su *et al.* optimized the nimesulide structure and developed several more potent analogues; the lead compound [102] inhibited LTEDaro cell growth with IC50 of 1 μM.[231] The SAR study suggests that position A needs 2,5-dimethyl [103] or dichloro [102] benzyl subsistent to increase the biological activity.[231 232]

1.7.6 Tamoxifen metabolites and Aromatase Inhibition

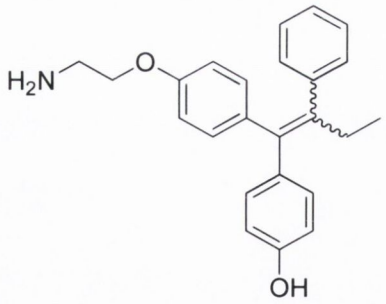

[36a]

Figure 1-46 Tamoxifen metabolite - norendoxifen

Two tamoxifen metabolites have been recently documented as AIs, norendoxifen and 4,4-dihydroxy-tamoxifen.[233] Norendoxifen (the demethylated metabolite) is potent and selective inhibitor of human aromatase, more so than 4,4'-dihydroxy-tamoxifen. Norendoxifen was shown to inhibit recombinant aromatase *via* a competitive mechanism with a Ki of 35 nM. Norendoxifen inhibited placental aromatase with an IC_{50} of 90 nM, while it inhibited human liver CYP2C9 and CYP3A with IC_{50} values of 990 and 908 nM, respectively. Inhibition of human liver CYP2C19 by

norendoxifen appeared even weaker. The tamoxifen metabolite (norendoxifen) exists at notably lower concentrations than the parent drug or its major metabolites, endoxifen and *N*-desmethyltamoxifen, but it is a more potent inhibitor of aromatase than the major metabolites.[234, 235, 236] Norendoxifen merits further investigation as a clinical aromatase inhibitor and may be able to serve as a lead compound for the rational design of novel AIs.

1.8 Sulfatase Inhibitors

1.8.1 Estrogen sulfate and estrone sulfatase

Studies have shown that the main source of estrogen in breast tumours cells is through the conversion of estrone sulfate to estrone which is catalyzed by a specific sulfohydrolase (estrone sulfatase) or, in general, sterylsulfatase [STS]). Estrone sulfate, the main substrate for estrone sulfatase is the most abundant circulating estrogen in the plasma of postmenopausal women.[237]

The significance of estrone sulfate in breast carcinomas was investigated using a tumour model. The chosen tumour model was nitrosomethylurea induced mammary tumours in rats which contain estrone sulfatase activity. It was seen that the estrone sulfate could stimulate tumour cell growth and not only this, but the estrone sulfate could also be converted to estrone and estradiol.[237] This indicated the significance of estrone sulfate as a probable source of estrogen to support the growth of estrogen-dependent breast cancer.[238] Inhibitors of estrone sulfatase may be potential agents for breast cancer treatment.

1.8.2 Sulfatase Inhibitors

These inhibitors are divided into four categories: those which are sulfamoylated or not or those having a steroid nucleus or not. STS inhibition has been reported since the 1970's but the development of STS inhibitors started much more recently in the early 1990's.[239-241] This research into early STS inhibitors demonstrated that a modified version of the natural substrate E1S generated estrone-O-sulfamate (EMATE) [104], a potent STS inhibitor, Figure 1-47.[242] It was discovered that if the OH of the sulfate group was replaced with NH_2, generating a steroidal- or non-steroidal aryl sulfamate group (OSO_2NH_2), these products could efficiently inactivate the enzyme.[243]

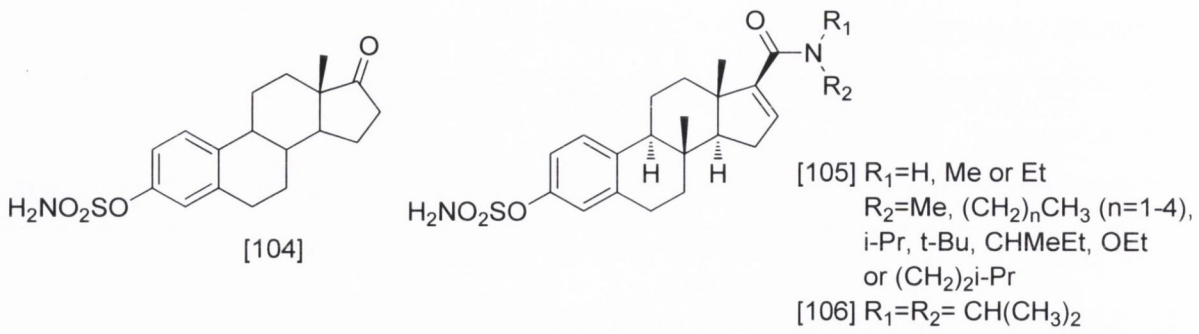

Figure 1-47 STS Steroid inhibitors [104]-[106]

Modifications to the steroid core have been reported as steroid sulfamate based inhibitors and representative of this class are shown in Figure 1-47, Figure 1-48 and Figure 1-49.[244-251] This group exhibited good potency with [112] and [113] displaying sub nanomolar activity.[252-255]

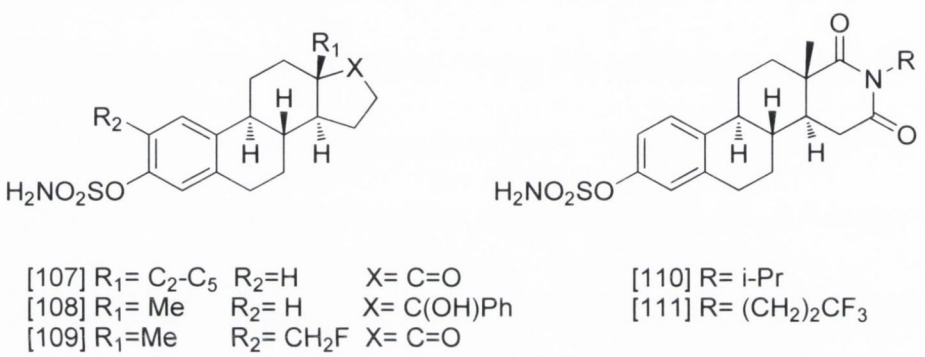

Figure 1-48 Steroid sulfamate based inhibitors of STS [107]-[111]

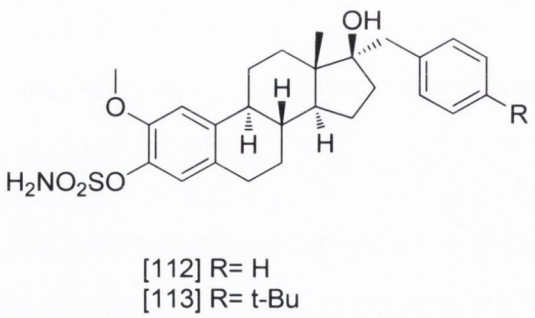

Figure 1-49 Steroid sulfamate based inhibitors of STS [112]-[113]

Another class of STS inhibitors reported in the literature are non-steroid sulfamate based inhibitors. This group differ from the previous STS inhibitors mentioned previously as they do not contain a steroidal core. In Figure 1-50, shows representatives of the non-steroid sulfamate based inhibitors reported.[256-265]

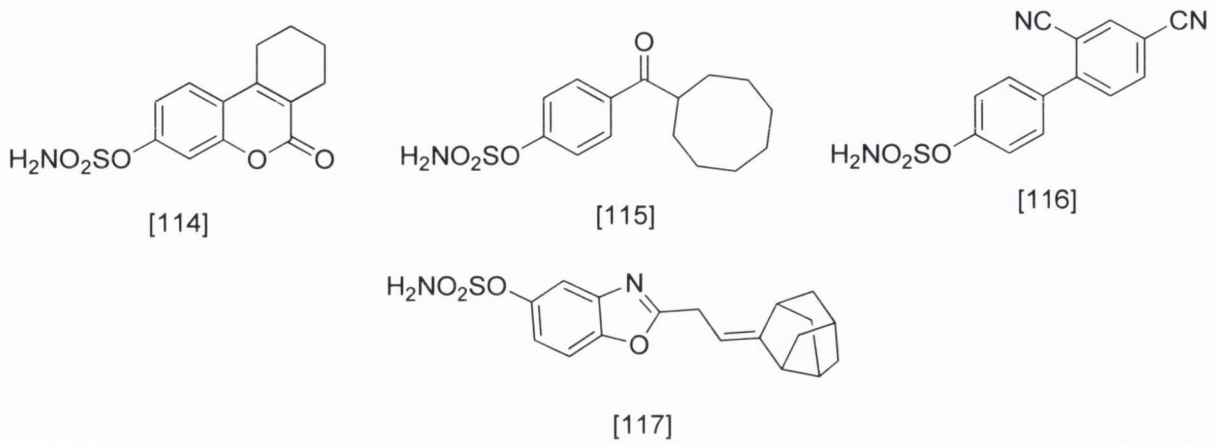

Figure 1-50 Non steroid sulfamate based inhibitors of STS [114]-[117]

The previous two types of steroid and non steroid inhibitors of STS were based upon sulfamate, while the next type STS inhibitor contains a steroid core however are not based on sulfamate. SAR examination on 17α-subsistuted estradiol derivatives as possible STS inhibitors led to the synthesis of compounds containing either linear or ramified alkyl moieties. Of these compounds evaluated as STS inhibitors, it was clear that the addition of a hydrophobic substituent on the estradiol scaffold brings about a reversible potent inhibition.[266] A number of this type of STS inhibitors have been reported and representatives of this class are shown in Figure 1-51.[267] [268] Similar to two types of steroid and non steroid type inhibitors of STS based upon sulfamate, a further type of inhibitor not based on sulfamate and not containing the steroidal core have been reported and representative of this class is shown in Figure 1-52.[269] [270]

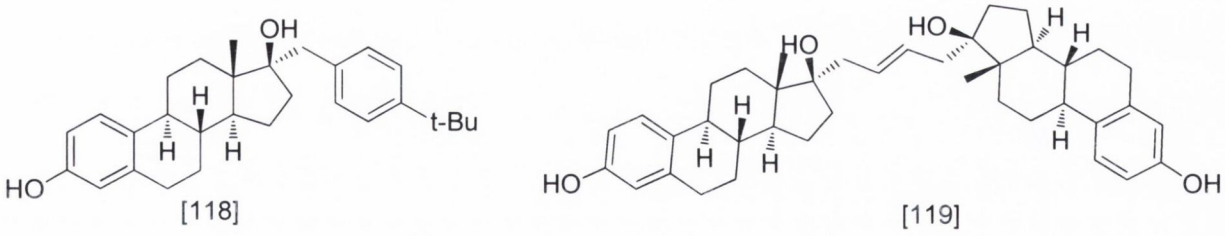

Figure 1-51 Steroid non sulfamate based inhibitors of STS [118]-[119]

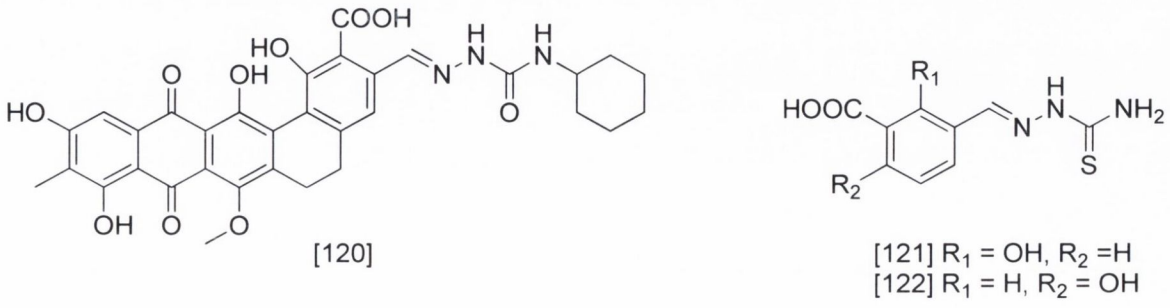

Figure 1-52 Non steroid non sulfamate based inhibitors of STS [120]-[122]

1.8.3 Dual aromatase-sulfatase inhibitors (DASIs)

Designing hybrid molecules that target multiple biological targets is an emerging and attractive strategy in drug design and discovery. The combined therapeutic potential of sulfatase(STS) inhibitors and aromatase inhibitors (AIs) could lead to a more comprehensive estrogen deprivation to target hormone dependent breast cancer.

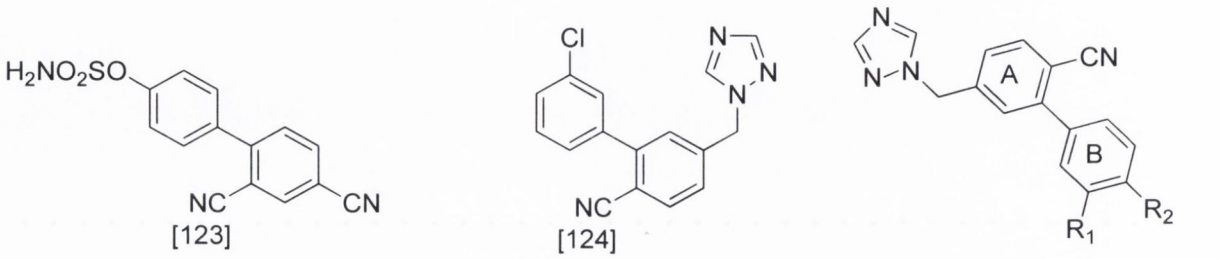

Figure 1-53 Biphenyl derivatives [123]-[125]

A common approach has been used in the design of DASIs. The STS inhibitory pharmacophore could be incorporated into an established or experimental AI with minimal structural change incurred to the original scaffold in order to retain and maximize aromatase inhibition. More recently, the opposite approach has been examined, one which introduces an aromatase inhibitory pharmacophore into a template that has been designed primarily for STS inhibition. Okada *et al.* reported a series of biphenyl STS inhibitors which incorporated the aromatase inhibitory pharmacophore.[271] The lead compound [123] was shown to be a highly potent STS inhibitor. Another similar approach used the biphenyl motif to successfully design a new class of nonsteroidal aromatase inhibitor. The most potent compound [124] was shown to have an IC_{50} of 0.22 nM against aromatase in JEG-3 cells and was shown to be a highly potent STS inhibitor, Figure 1-53.[272]

In designing new DASIs, Woo *et al.* developed a modified derivative of [123] which potentially could introduce the aromatase inhibitory pharmacophore to the series.[273] A large library of biphenyl compounds was designed with different substitution patterns on the A and B rings. The use of SAR studies identified that the most potent compounds would require a specific substitution pattern on the A ring (CN group at 2-position and triazol-1-ylmethyl at 5-position) and B ring contain a chlorine atom in the meta position [124]. Compound [124] was evaluated and exhibited very promising aromatase inhibition results IC_{50} = 2.0 nM and STS inhibition IC_{50} = 35 nM. The addition of a chlorine at the 3-position on the B-ring lead to the most potent compound [125] of this series with aromatase inhibition IC_{50} = 0.5 nM and STS inhibition IC_{50} = 5.5 nM. Both compounds were shown *in*

vivo to inhibit aromatase strongly 3 h after dosing, rendering a reduction in estradiol plasma levels by 63% and 60%.

1.9 Antimitotic agents

1.9.1 Tubulin and microtubules

During mitosis, the final stage of the cell cycle, chromosomes segregate and cell replication occurs. The involvement of a dynamic pipe-like protein fibre, known as microtubule, is essential in this process. The microtubules are built from a basic α/β-tubulin building block, yet subpopulations of microtubules can be differentially marked by a number of post-translational modifications.[274] These modifications are believed to act individually or in combination to control specific microtubule-based functions such as cell signalling, division, migration, cellular transport, signal transduction and mitosis. The α-tubulin and β-tubulin heterodimers are found in virtually all nucleated cells and posses a high degree of homology (40-50 %) to each other. The functional diversity of microtubules is achieved in several ways: through the binding of various regulatory proteins, including microtubule associated proteins (MAPs), to soluble tubulin and to the microtubule surfaces and ends; by expression of different tubulin isotypes, which have different functions; and through several post-translational modifications of tubulin.[275] Upon binding to GTP, an energy rich guanosine triphosphate, and through a succession of events that are still not fully understood, tubulin polymerises into microtubules. Any discrepancy in the pace of polymerisation can greatly influence cellular replication. Affected cells become locked in mitosis phase and subsequently enter apoptosis. There are a variety of MAPs involved, including the dynein and kinesin motor proteins, as well microtubule-regulatory proteins, such as survivin, stathmin, TOG, MCAK, MAP4, EB1, dynactin 1, RAC1 and FHIT.[275]

Microtubules play a major part of mitosis and cell division, and for this reason they are an important target for anticancer drugs. The ligands that target the microtubules and their dynamics are known as antimitotic drugs which interact with various tubulin binding sites. Three distinct small molecule binding sites are known and characterised for these ligands: the colchicine site, vinca alkaloid domain and the taxoid domain.[275] The colchicine site and vinca alkaloid domains are located on monomeric unpolymerised α/β-tubulin and the taxoid domain is located on polymerised microtubules. Ligands which bind at the vinca domain (i.e. vinblastine, vincristine) or colchicine binding site (i.e. colchicine, combretastatin A-4) disrupt the polymerisation of tubulin into microtubule while ligands which bind at the taxoid domain (i.e. paclitaxel, epothilone) stabilise microtubule. These ligands affect the dynamic instability of microtubules system and lead to cellular division arrest.[275]

1.10 Combretastatins

1.10.1 Discovery and initial work

The *Combretaceae* family of shrubs and trees are well exploited in tradition medical practices in India and Africa. The plants are used in the treatment of a variety of illness such as respiratory infection, hepatitis, malaria, uterine cancer, anthelminic treatment, leprosy, dysentery and vermifuge. From the examination of primitive medical treatments of cancer in Africa and Asia, eight species have been identified for their anticancer properties.[276] In 1979, a thorough study of the constituents of the South African willow tree for anticancer properties was reported by Pettit *et al.*[277]. This lead to the discovery of several natural products with extraordinary activity as inhibitors of tubulin polymerization (phenanthrenes, dihydrophenanthrene, stilbenes, and bibenzyls), exhibiting potent *in vitro* inhibition against human cancer cell lines, and *in vivo* efficacy as vascular targeting agents (VTAs) and antiangiogensis agents. The combretastatins showed extreme promise due to the remarkably simple structures and their robust activity in biological systems. The bibenzyl combretastatin [126] was isolated, the crystal structure was determined and it was screened as a possible anticancer agent in the National Cancer Institute (NCI).[278] Continuation of this work lead to further combretastatins being discovered and structurally determined (A-1 [127], A-2 [128], A-3 [129], B-1 [130], and B-2 [131]), Figure 1-54.[277, 279] In 1989, Pettit *et al.* successfully isolated and structurally determined the structure of combretastatin A-4 (CA4) [22].[280] When the combretastatins A-1 & A-4 were evaluated, they were both shown to be extremely prolific inhibitors of tubulin polymerisation with strong binding affinity to the colchicine binding site.[280] Structure activity relationship analysis showed that the *cis*-configuration of the stilbene moiety was a very important factor for inhibition of cancer cell growth.[281] The E-stilbenes show a considerable decrease in their biological activity compared to the Z-stilbenes. Combretastatins, in particular CA4, have become lead compounds for drug design and development studies of tubulin targeting agents.[282, 283]

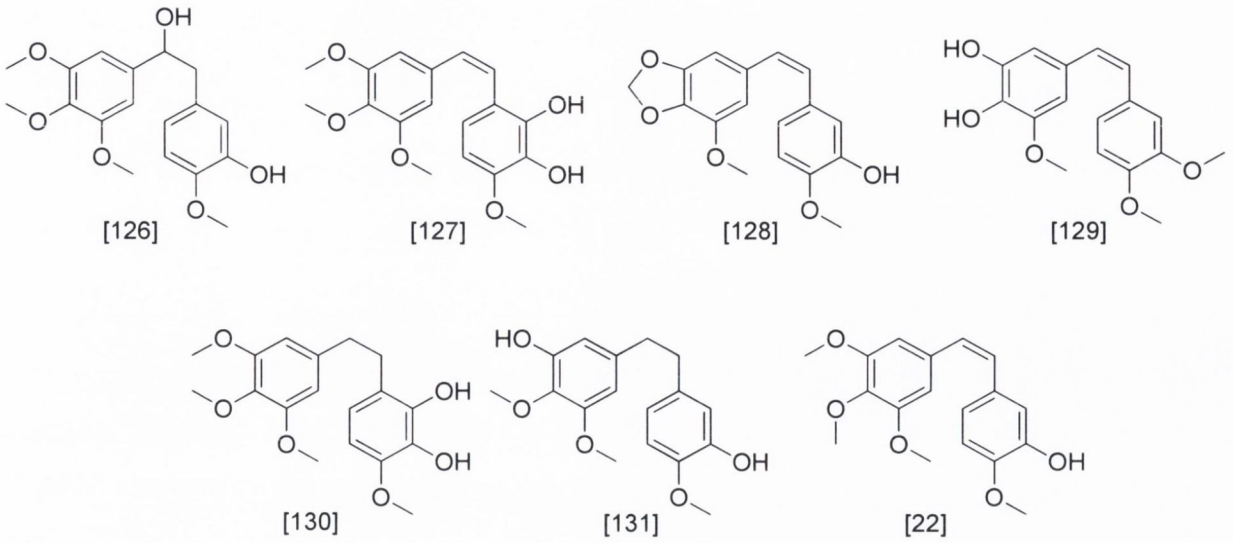

Figure 1-54 Isolated natural products with anticancer properties [22], [126]-[131]

1.10.2 Combretastatins mode of action

CA4 is believed to induce apoptosis in cancer cells but the *in vitro* studies have not yet explained the mechanism[284], which suggests that it may activate at least one specific intracellular signalling pathway. *In vivo* studies support the suggestion that CA4 induces a rapid vascular collapse by increasing tumour-vessel permeability.[285] The antimetastatic potential of CA4 has also been examined with evidence of significant shrinkage (up to 30%) of the metastatic mass in mice with vascularised liver metastases.[286] Other studies have shown that tumour vessels are more susceptible to the disruptive effects of CA4 than normal vasculature and it is relatively inactive in normal tissues. CA4 is said to be tumour specific but studies have shown it can cause side effects in cancer treatment.[287]

1.10.3 Modifications of combretastatin ring substituent's

Since the discovery of its anticancer properties, the combretastatin motif has become the focus of considerable research in order to increase its biological activity. A wide variety of combretastatin analogues with varying substitutions pattern on the A and B ring, while retaining the ethylene linker, have been reported e.g. 3-nitro [133][288, 289], 3-amino [134][288, 289], 3-amino acid salts [135][289, 290], 2-nitrogen substituted derivatives[291], 3-azido [136][288], 3,4-methylenedioxy-3-amino derivatives [137][292], 3-fluoro [138][293], 4-methyl [139][294] and 3,4,5-trimethyl[295] combretastatin analogues, Figure 1-55.

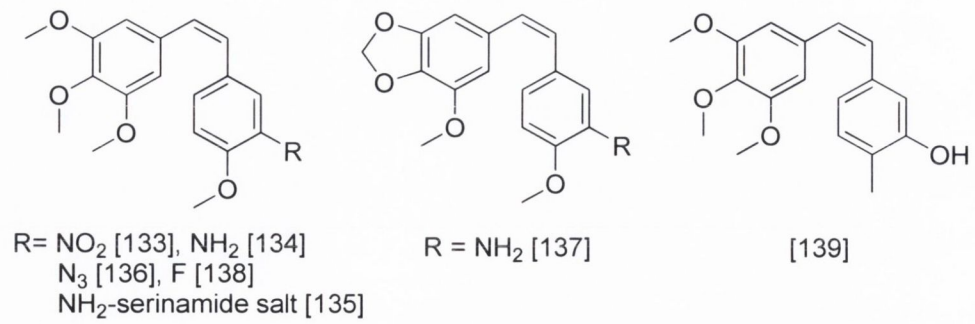

Figure 1-55 Function modification of the Combretastatin structure [133]-[139]

In addition to the functional modification, combretastatins with significant structural variation from the basic stilbenoid motif have also been reported, e.g. phenstatin [140][296], hydrophenstatin [141][297], hetercombretastatins [142][298], combretatropones [143][299], aza-combretastatin [144][300], bridge-modified vicinal diols [145][301], combretadioxolane analogues [146][302], chalcone derivatives [147][303], disubstituted imidazole analogues [148][304], pyridone analogues [149][305], acrylic acid analogues [150][306] and sulfonamide analogues [151][307], Figure 1-56.

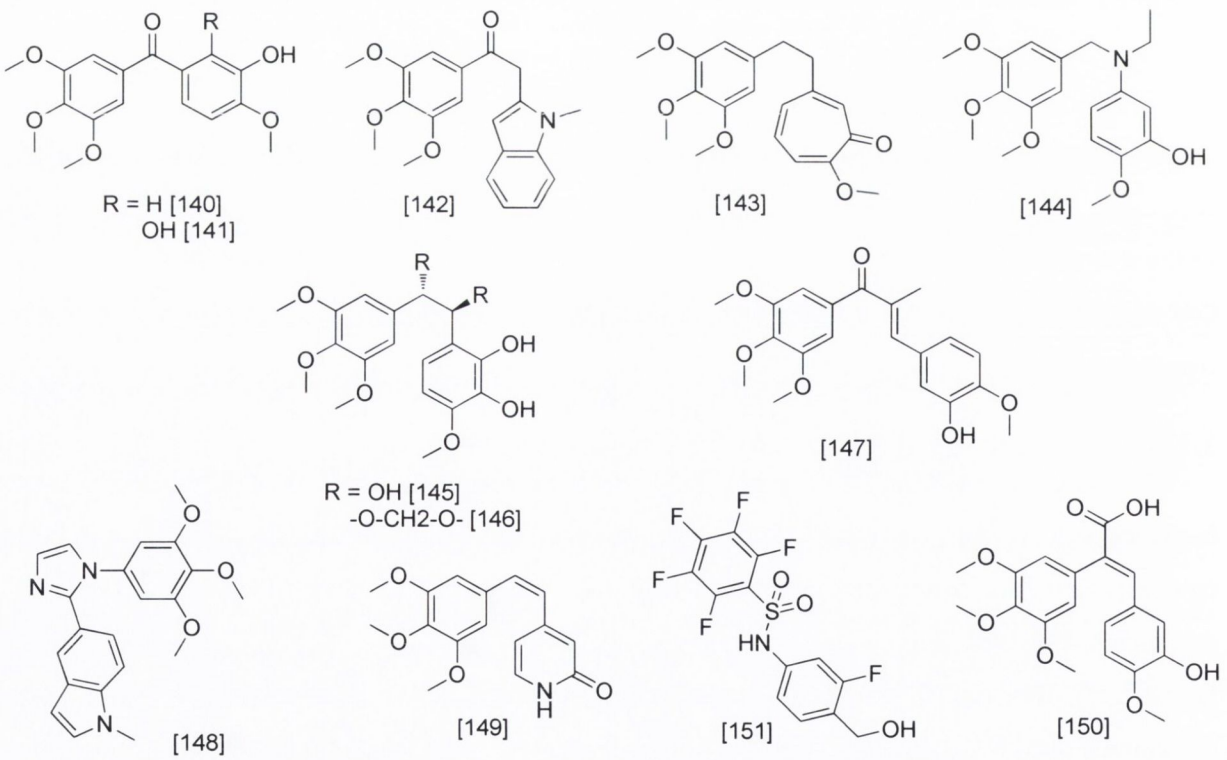

Figure 1-56 Combretastatin with significant structural variation [140]-[150]

Many novel compounds based on the combretastatin structure incorporating the substitution pattern of the A and/or B ring on the new scaffold core structures have been reported e.g. 3-aroyl-2-arylindoles [152][308], 2,3-diaryl indoles [153][308], 3-formyl indoles [154][309],

benzo[b]thiophene [155][310], benzofuran analogues [156][308], dihydronaphthalenes [157][311], dihydroindolo[2,1-α]isoquinolines [158][312], indolyoxazoline analogues [159][313] and β-Lactam analogues [160][314], Figure 1-57.

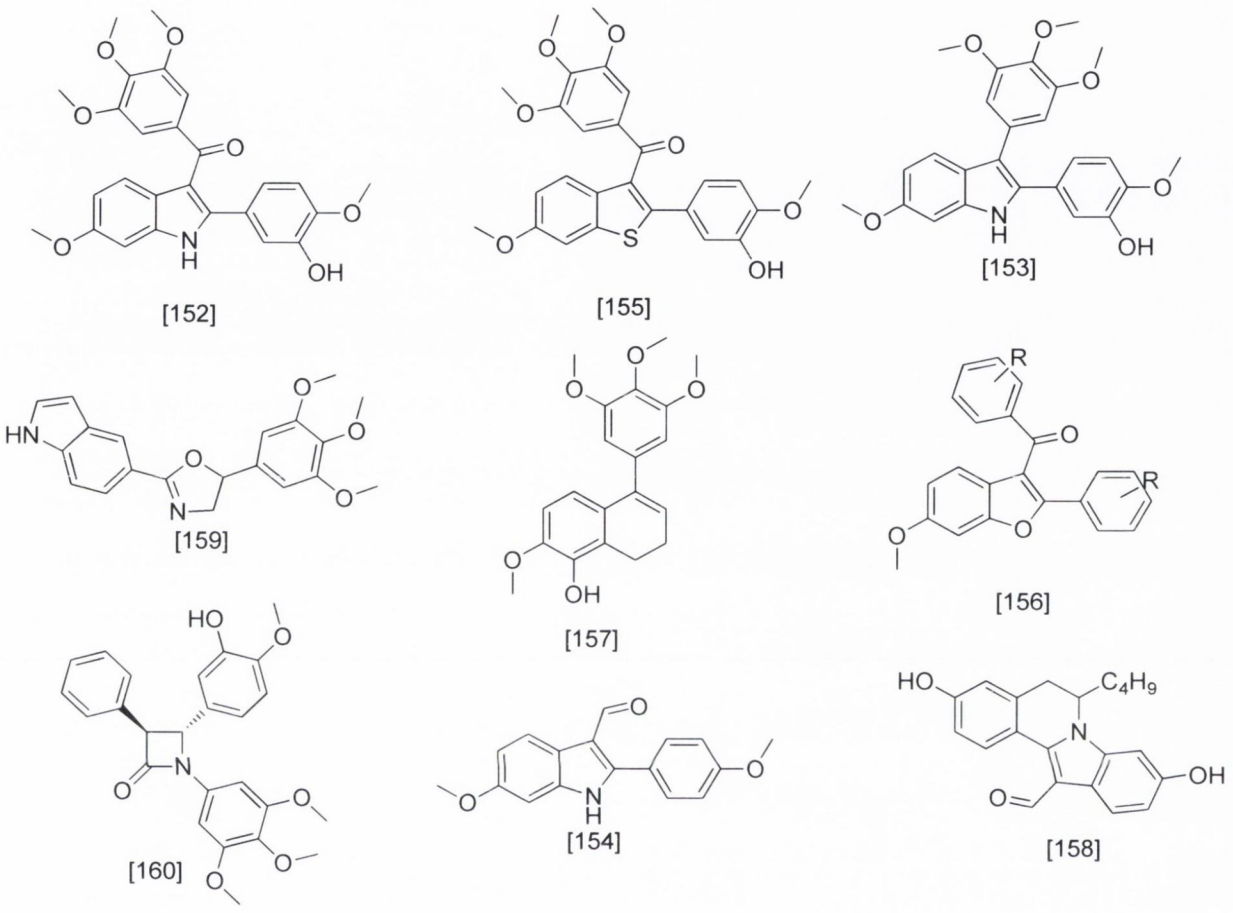

Figure 1-57 Novel compounds based on the combretastatin structure [152]-[160]

1.10.4 Prodrug combretastatin derivatives

The CA4 stilbene compound initially showed great promise as an antitumour agent but due to its lack of solubility in pharmaceutical accepted solvents, it was prevented from entering phase I clinical trials.[315] Pre-clinical development was performed to increase the water-solubility; salts of the 3'-phenol of CA4 were synthesised for evaluation as possible water-soluble derivatives.[316] The synthesis yielded three derivatives, ammonium, potassium and sodium phosphate salts which exhibited the best enhanced solubility. The sodium salt was selected for drug formulation and further pre-clinical development. Other attempts to increase the solubility have been reported; Brown *et al.* reported the synthesis of water-soluble glycosides of CA4, two of which displayed potent cytotoxic properties[317]; Ohsumi *et al.* reported the synthesis of a series of CA4 analogues containing an amino group in order to increase solubility[318], with the lead compound [161] showing potent antitumour activity against Colon 38 and 3LL murine tumour models in mice. It also displayed

antitumour activity against HCT-15 human xenographs in nude mice, was superior to cisplatin in Colon 38, 3LL and HCT-15 tumour models, and displayed improved solubility, Figure 1-58.

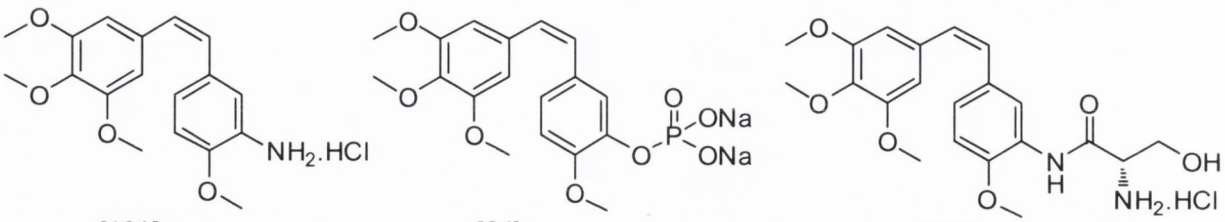

Figure 1-58 Increased solubility Combretastatin [161] & VTA in clinical trials [24] and [163]

Currently there are two small VTA compounds in human clinical development which function through a biological mechanism ultimately targeting tubulin. These drugs include CA4P [162] which has shown to stop rapid and selective blood flow within the tissue (synthesised by Pettit *et al.*)[319] and AVE8062 [163][320, 321] which is a more soluble and active analogue of combretastatin A-4 (discovered by Ajinomoto). Another VTA drug, ZD-6126 [23], which is based on the natural compound colchicine, was in trials but these were stopped as it became apparent that ZD6126 was too cardiotoxic at the required doses.[322]

1.11 Tumour-Targeting conjugates of cytotoxic agents

1.11.1 Overview

To circumvent the problems associated with non specific cytotoxic agents, many delivery protocols and systems designed to selectivity target the tumour tissue have been reported. Examples include utilising tumour overexpressed enzymes, tumour overexpressed receptors, ADEPT, photo-responsive prodrugs, conjugates with docohexaenoic acid and polymer conjugates (*via* hyaluronic acid, poly(ethylene glycol), carboxymethylcyclodextran, poly(*L*-glutamic acid), *N*-(2-hydroxypropyl)methacrylamide), protein conjugates and dendrimers).[323-326] Enhancing the time for which tumour is exposed to therapeutic agent by increasing the amount of drug at the tumour site and/or local delivery, could improve treatment either by increasing efficacy or reducing side effects. It is foreseen that new conjugate delivery systems that can target the tumour tissue could allow the use of anticancer agents which would otherwise not be useable for cancer therapy due toxicity or side effects. The pharmacological properties of the conjugate compounds can differ drastically to that of the low weight cytotoxic drugs whose actions are governed by the physicochemical properties, physiology and anatomy of the body at both tissue and cellular level. These different properties can bring about drug delivery barriers which must be overcome or exploited to enhance specificity.[327]

The morphological and physiological differences between malignant and normal tissues play an essential role in development of effective tumour-specific drug delivery. In some cases, tumour cells overexpress many receptors and biomarkers, which can be used to deliver cytotoxic agents selectively to the site of the tumours. The rapid cell proliferation of cancer cells necessitates rapid creation of new blood vessels and the tumour vasculature has numerous deficiencies allowing large molecules and lipids to penetrate the extravascular space in tumours. In contrast, the lymphatic system is underdeveloped in tumours, preventing large molecules and lipid being released from the tumour thus leading to an accumulation of macromolecules. This phenomenon is termed 'enhanced permeability and retention' (EPR) effects.[327-329] The cancer cells can induce hypoxicity due to their enhanced metabolic rate, instigating anaerobic metabolism that generates lactate and consequently lowering the intracellular pH.[327] Therefore, many tumour targeting conjugates contain a motif that upon acidification, the cytotoxic agent becomes released into the tumour site.

In general, drug delivery systems for tumour-targeting consist of a tumour recognition moiety and a cytotoxic 'warhead' connected directly or through an appropriate linker to form a conjugate. The conjugate, which can be regarded as 'prodrug', should be systemically non-toxic. This means that the linker must be stable in circulation. Upon internalization into the cancer cell the conjugate should be readily cleaved to rejuvenate the active cytotoxic agent. Tumour-targeting conjugates bearing cytotoxic agents can be classified into several groups based on the type of cancer recognition moieties.[327]

The use of conjugate drugs as tumour-targeting delivery systems can offer many advantages over delivery of physical mixture of multiple drugs; prolonged drug circulation half-life mediated by the carrier, reduced nonspecific uptake, increased accumulation at the tumour site through passive EPR effect and/or active targeting by incorporation of targeting ligands[330], predominantly endocytotic uptake with the potential to bypass mechanisms of multidrug resistance, and ratiometric dosing, i.e. ability to tailor the relative ratios of each agent based on its pharmacological disposition.[331]

1.11.1.1 Monoclonal antibody-based tumour targeting

Unique or overexpressed tumour-specific antigens can found in a wide range of human tumour cells.[332] Antibody-drug conjugates (ADCs) have become very promising candidates for tumour-targeting delivery systems. This approach incorporates a cytotoxic drug linked to monoclonal antibodies (mAbs), which have high binding specificity for tumour-specific antigens, hence mAbs can be used as vehicles to target cytotoxic agents to tumour cells. Several mAbs have the ability to distinguish and specifically bind to these tumour-associated antigens. The use of mAbs

as single agents for the treatment of cancer have been reported, through specific binding to the cancer-cell antigen can stimulate the immunological response against the target cancer cell.[333] The insufficient efficiency of most mAbs in cancer therapy has been circumvented by conjugating the immunoglobulin with radioactive isotopes[334] or cytotoxic drugs[335-337], yielding highly specific ADCs.[338]

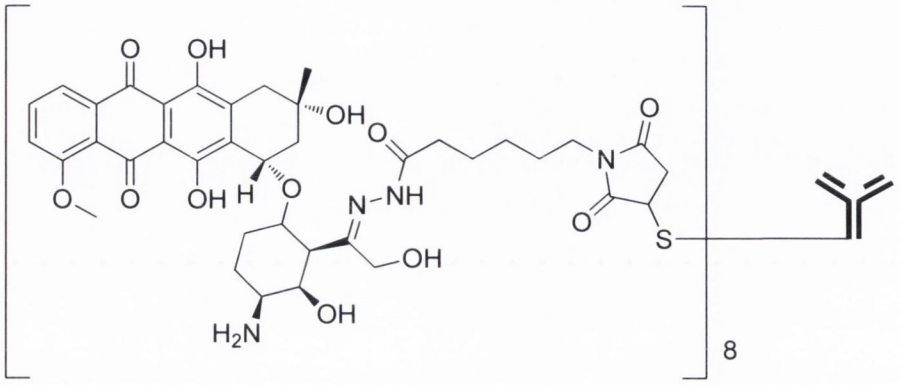

Figure 1-59 BR96-DOX [164]

Doxorubicin (DOX), an intercalating agent that blocks DNA replication, was covalently linked *via* (6-maleimidocaproyl)hydrazone linker to cysteine residues to humanized mAb BR96.[339] The pre-clinical data for BR96-DOX [164] (Figure 1-59) was remarkable, but despite the use of eight DOX per mAb molecule, the dose required *in vivo* was high presumably due to the relatively low potency of doxorubicin (IC50 = 0.1-0.2 μM)[340]. Another problem was that the half-life of the drug in the blood was approximately 43 h, which was considerably shorter than that of naked BR96 mAb, which has the half-life of several days to weeks in humans. The compound later failed to show sufficient clinical efficacy.[338]

The first mAb linked to a cytotoxic agent that received regulatory approval was gemtuzumab ozogamicin (Mylotarg®) [165] (Figure 1-60)[341-343] for the treatment of relapsed acute myelocytic leukaemia (AML). Gemtuzumab ozogamicin consists of N-acetyl-γ-calicheamicin (an enediyne antibiotic that binds to the minor groove of DNA and causes double-strand breaks leading to apoptosis) covalently attached to humanized anti-CD33 IgG4 κ antibody (hP67.6) *via* a bifunctional linker. The 4-(4-acetylphenoxy)butanoic acid moiety allows for attachment to surface-exposed lysines of the antibody over an amide bond and forms an acyl hydrazone linkage with N-acetyl-γ-calicheamicin dimethyl hydrazide. Upon internalization of the ADC, the calicheamicin prodrug is released by hydrolysis of the hydrazone in lysosomes of the CD33-positive target cells. The enediyne drug is then activated by reductive cleavage of the disulfide bond. This disulfide linkage has been stabilized by two methyl groups to prevent premature release of calicheamicin by circulating reduced thiols, such as glutathione.

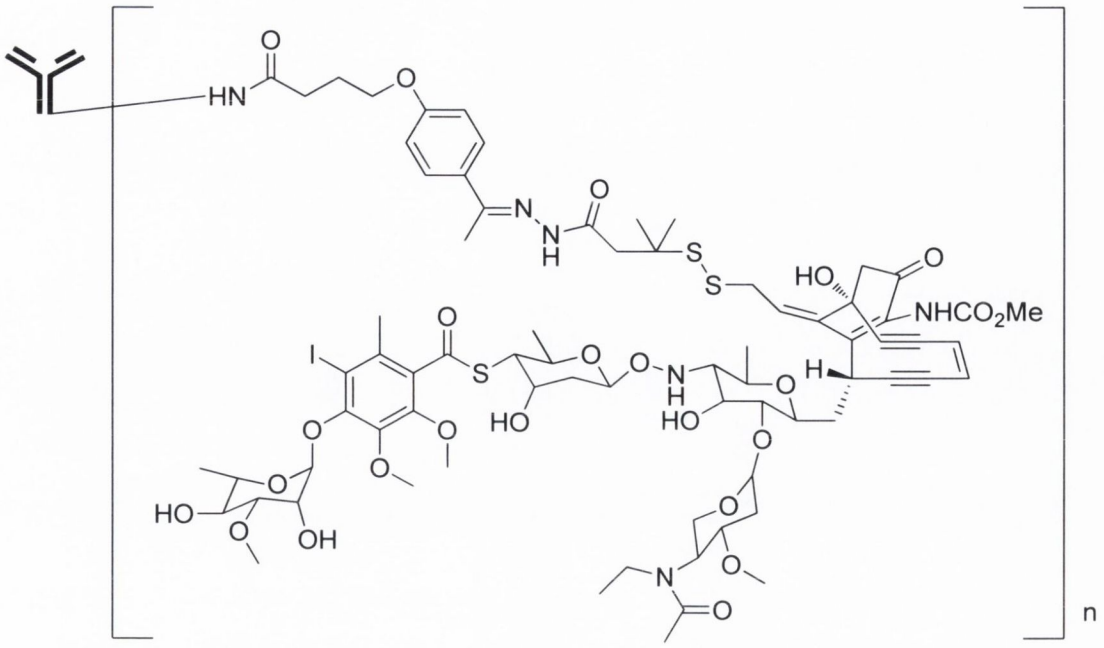

Figure 1-60 Gemtuzumab Ozogamicin (Mylotarg®) [165]

In February 2013, the immuno-conjugate TrastuzumabDM1 (T-DM1) (Figure 1-61) which was designed to combine the biological activity of trastuzumab (Herceptin) with the targeted delivery of a highly potent antimicrotubule agent, DM1, a maytansine derivative, to HER2-expressing breast cancer cells was approved for the treatment of advanced HER2-expressing breast cancer. Trastuzumab is a monoclonal antibody that specifically targets the HER2 tyrosine kinase receptor quite successfully. However, the majority of patients with metastatic HER2 overexpressing breast cancer who initially respond to trastuzumab develop resistance within one year of initiation of treatment, and in the adjuvant setting, progress despite trastuzumab-based therapy. The antimitotic drug, maytansine was chosen for use in the conjugate as exhibited high potency *in vitro*, binds to tubulin competitively with vinca alkaloids and is approximately 100 times more potent than vincristine.[344-348] To link maytansinoids to antibodies through disulfide bonds, a thiol containing maytansinoid, DM1 (*N*-methyl-*N*-[3-mercapto-1-oxopropyl]-*L*-alanine ester of maytansinol), an analogue of the clinically-studied drug maytansine) was used.[349] The immuno-conjugate T-DM1 has displayed significant *in vitro* and *in vivo* potency.[349] Each antibody contains an average of 3.5 drugs, however the product contains a distribution from 0 to 8 drugs per antibody.[350] The T-DM1 was found to effectively target HER2 overexpressing breast cancer, even after trastuzumab was ineffective due to resistance.

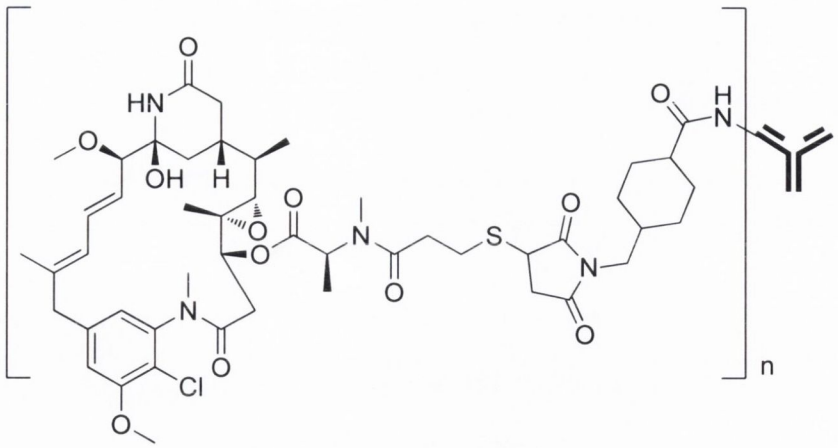

Figure 1-61 Trastuzumab DM1 (T-DM1)

1.11.1.2 Tumour-targeting with polyunsaturated fatty acids (PUFAs)

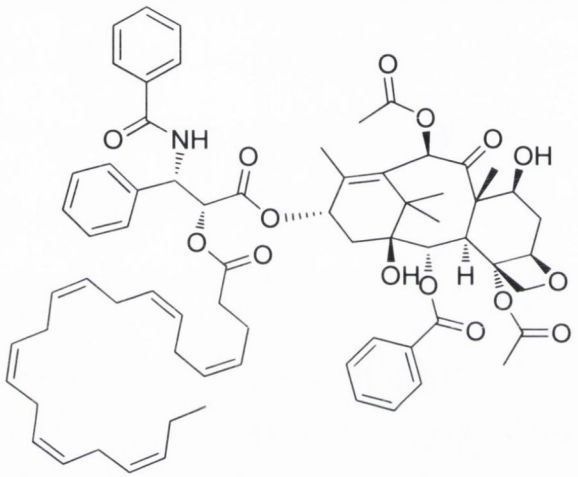

Figure 1-62 DHA–paclitaxel (Taxoprexin®) [166]

Many of the polyunsaturated fatty acids (PUFAs) can be found in vegetable oils, coldwater fish, and meat. The use of the PUFAs and their metabolites are considered to be safe to humans.[351, 352] It has been shown that PUFAs are extensively metabolised by tumour cells, incorporating into the lipid bilayer of cells, disrupting membrane structure and fluidity and possibly influencing the chemosensitivity of tumour cells.[327] Bradley *et al.* synthesised a DHA–paclitaxel (Taxoprexin®) [166] (Figure 1-62) linking docosahexaenoic acid (DHA) to the C-2' position of paclitaxel.[353] This DHA–paclitaxel conjugate was shown to be much more stable in plasma that paclitaxel on its own and could slowly release paclitaxel. The DHA–paclitaxel achieved complete tumour regression in mice when paclitaxel caused neither complete nor partial regression. Although DHA–paclitaxel exhibits an impressive antitumor activity against drug sensitive tumours, this conjugate would not be effective against multidrug-resistant (MDR) tumours. DHA-paclitaxel was found to be a weak substrate of P-glycoprotein (Pgp) as compared to paclitaxel. Paclitaxel molecules released slowly were still caught

by the Pgp efflux pump and eliminated from the cancer cell.[354] The DHA-paclitaxel conjugate in currently undergoing clinical trials.[353]

1.11.1.3 Tumour-targeting with folic acid

Folate receptors (FR-α & FR-β) are highly expressed in a range of solid tumours, particularly in ovarian and endometrial cancer.[355] The reported frequency of folate receptor overexpression in these forms of cancer compared to other cancer cells is 40-80%. Both isoforms bind folic acid [167] with high affinity (KD < 1 nM), Figure 1-63.[356] The expression of FR in normal tissues is low and restricted to various epithelial cells,[357, 358] while they are overexpressed in many epithelial cancer cells.[358] Tumour-selective targeting has been achieved by an FR-targeted PEG-gemcitabine prodrug[359], an FR-conjugated multiarm-block copolymer-doxorubicin[360], FR-conjugated liposomes encapsulating an antineoplastic drug[361] or antisense oligonucleotides[362], an FR-conjugated protein toxin[363], and FR-derivatized antibodies or their Fab/scFv fragments binding to the T-cell receptor[364]. Hong *et al.* reported dendrimer-methotrexate conjugates that exhibited significantly lower toxicity and a 10 fold enhancement in efficacy compared to free methotrexate.[365]

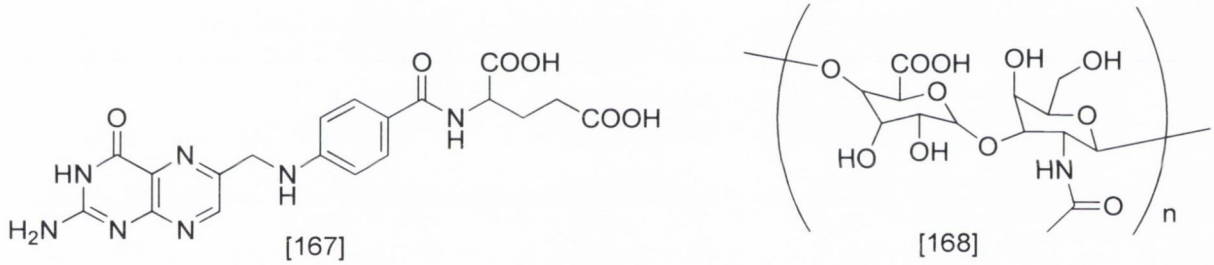

Figure 1-63 Folic acid [167] & hyaluronic acid monomer unit [168]

1.11.1.4 Tumour-targeting with hyaluronic acid

Hyaluronic acid (HA) [168] has a function in cell growth, differentiation, and migration within the cellular matrix, Figure 1-63. HA is also closely associated with angiogenesis in many types of tumours, in which HA receptors (CD44 & RHAMM) are overexpressed on the surface. [366] Thus, malignant cells with high metastatic activities often exhibit enhanced binding and uptake of HA.[367] Lee *et al.* reported the synthesis and evaluation of HA-paclitaxel conjugates which in an aqueous solution would form nanosized spherical micelles.[368] HA-paclitaxel conjugate micelles exhibited greater cytotoxicity to HA recognizable CD44 overexpressing cells than the conventional paclitaxel formulation, suggesting that they could be efficiently delivered to cancer cells that overexpress HA receptors.

1.11.1.5 Tumour-targeting with peptides

Angiogenesis plays an essential role in tumour growth because it enriches the tumour with nutrients and oxygen, and removes waste products. Matrix metalloproteinases (MMPs) are secreted

in excess from cancer cells during tumour angiogenesis. The MMPs degrade the extracellular matrix (ECM) which consists of primarily collagen which aids in tumour progression, invasion and metastasis.[369, 370] Two MMPs (MMP-2 and MMP-9) have been reported to play important roles in this process[371], as they are observed in several different types of solid tumours, such as stomach, colorectal, breast, prostate, lung, and ovarian cancers.[372] The use of MMP-2 or MMP-9 as targets for cancer diagnosis and therapy has also been reported recently. MMP-2 peptides have been used for an MMP-2-sensitive tumour imaging probe[373]; albumin-binding doxorubicin (specificity for MMP-2 and MMP-9)[374] and an MMP-2 cleavable melittin/avidin conjugate[375] have been found useful. A peptide–doxorubicin conjugate, Gly-Pro-Leu-Gly-Val (GPLGV)-DOX were found to be cleaved by MMPs secreted by cancer cells and was shown to have significantly lower cytotoxicity compared with doxorubicin. In an *in vivo* study, GPLGV– DOX was found to suppress tumour growth as much as doxorubicin and showed reduced toxicity.[376] Burkhart *et al.* reported the use of cyclic-(N-Me-VRGDf) (Cilengitide), an αvβ3 targeting peptide conjugate linked to 5"-formyldoxsaliform tethered through a hydroxylamine ether.[377] This was found to have low nM activity in MDA-MB-435 cell lines and it was shown that while the prodrug was unable to penetrate through the plasma membrane, the active metabolite can however be released from the targeting group, with reduced toxicity.

1.11.1.6 Tumour-targeting with polymers

The use of biodegradable polymeric nanoparticles has been extensively employed as an effective drug delivery system to enhance the efficacy and safety of encapsulated drugs. Nanoparticle carriers provide a better accumulation in tumour tissues through an EPR effect[378], ability to overcome multidrug resistance[379], and better pharmacokinetics of drug *in vivo*[380]. Nanoparticles composed of poly(ε-caprolactone) (PCL) and poly(ethylene glycol) (PEG) have been shown as suitable carriers for the delivery of anti-cancer agents. It has been reported that amphiphilic triblock copolymers consisting of PEG as hydrophilic segment, and PCL as hydrophobic block, have been used as drug delivery systems, e.g. for 4′-demethyl-epipodophyllotoxin[381], honokiol[382], folic acid[383], nimodipine[384] and doxorubicin[385, 386].

1.11.1.7 Tumour-targeting with receptor ligands

The use of receptor ligands as a delivery device for anticancer agents has been investigated in the past few decades. Targeting ligand receptors overexpressed in tumours can lead to selective conjugates with enhanced biological activity. The target receptor should have a high density on the surface of the target cells, e.g. a receptor density of 10^5 ERBB2 receptors per cell was required for an improved therapeutic effect of anti-ERBB2-targeted liposomal doxorubicin over non-targeted liposomal doxorubicin in a metastatic breast cancer model.[387] A review of the many estrogen-receptor tumour-targeting conjugates which been investigated are presented in the next section.

1.12 ER-targeting conjugates

The ER is a suitable target for selective treatment of ER-positive breast cancer tumours as there are 10^5 ERBB2 ER molecules per cell.[388] The ER targeting ligands should retain high affinity for ER, with a relative binding affinity (RBA) ≥ 10% compared to that of estradiol. The conjugate should be capable of achieving an intracellular concentration, either by active uptake or passive diffusion, sufficient to promote the anticancer effect. The conjugate should provide a mechanism by which the therapeutic component is effectively available to its site of action (Figure 1-64). That effect should occur at levels below those at which toxicity is generated in normal cells, or non ER selective cells.[76, 389, 390] Katzenellenbogen *et al.* described the characteristics that novel ER-targeting conjugates should demonstrate, such as effectiveness as a ligand with high binding affinity for ER, potent efficacy in an appropriate assay and selective activity in ER-dependent but not ER-negative breast cancer cells that is reversible by exposure to estradiol.[391]

1.12.1 Conjugates of cytotoxic agents

1.12.1.1 Steroid conjugates

Delbarre *et al.* synthesised estradiol-ellipticine conjugates.[392] Ellipticine is a DNA intercalating agent that has been evaluated as a breast cancer chemotherapeutic agent but it has shown lack of selectivity and severe side effects which negated its clinical utility. The conjugates comprised of a 17α-substituted estradiol linked through a moiety to the ellipicine drug. The first conjugate contained a propionic acid residue to conjugate ellipticine as its quaternary salt. Conjugation of the estradiol and ellipticine exhibited no enhancement of cytotoxicity in the MCF-7 breast cancer cell line when compared to untargeted ellipticine. This lack of significant effect was explained by the low binding affinity of the conjugate to the ER receptors. It can be seen from the crystal structure of 17α substituted estradiol-ER-LBD complexes that the binding pocket was unable to accommodate the large bulky group hence reducing the binding affinity. The interactions of the conjugate with DNA demonstrated that the steroidal group did not significantly interfere with DNA intercalation.[392] The estradiol-ellipticine conjugate was shown to exert both cytostatic and cytotoxic effects, which was primarily due to the pyridocarbazole moiety. The use of SAR of the estrogen indicated that the most crucial units required for binding were the free 3-OH and 17β-OH groups. Devraj *et al.* synthesized a series of E2–ellipticine conjugates with longer linkers and neutral ellipticine derivatives (linked at various positions), Figure 1-65.[393] The longer linker was used so that the position of the ellipticine nucleus was further from the 17β-hydroxyl group of estradiol. The evaluation of the conjugates showed that the longer chain lengths had the greatest effect and the highest RBA. It was also seen that attaching estradiol to the 2-position of ellipticine promoted the enhancement of potency and DNA binding affinity when compared to the 6- and the 9- [169]

positional derivatives of the ellipticine. However, the E2–2-ellipticine conjugate displayed no selectivity toward the ER+ breast cancer cells, suggesting that conjugation did not impart significant ER recognition properties.

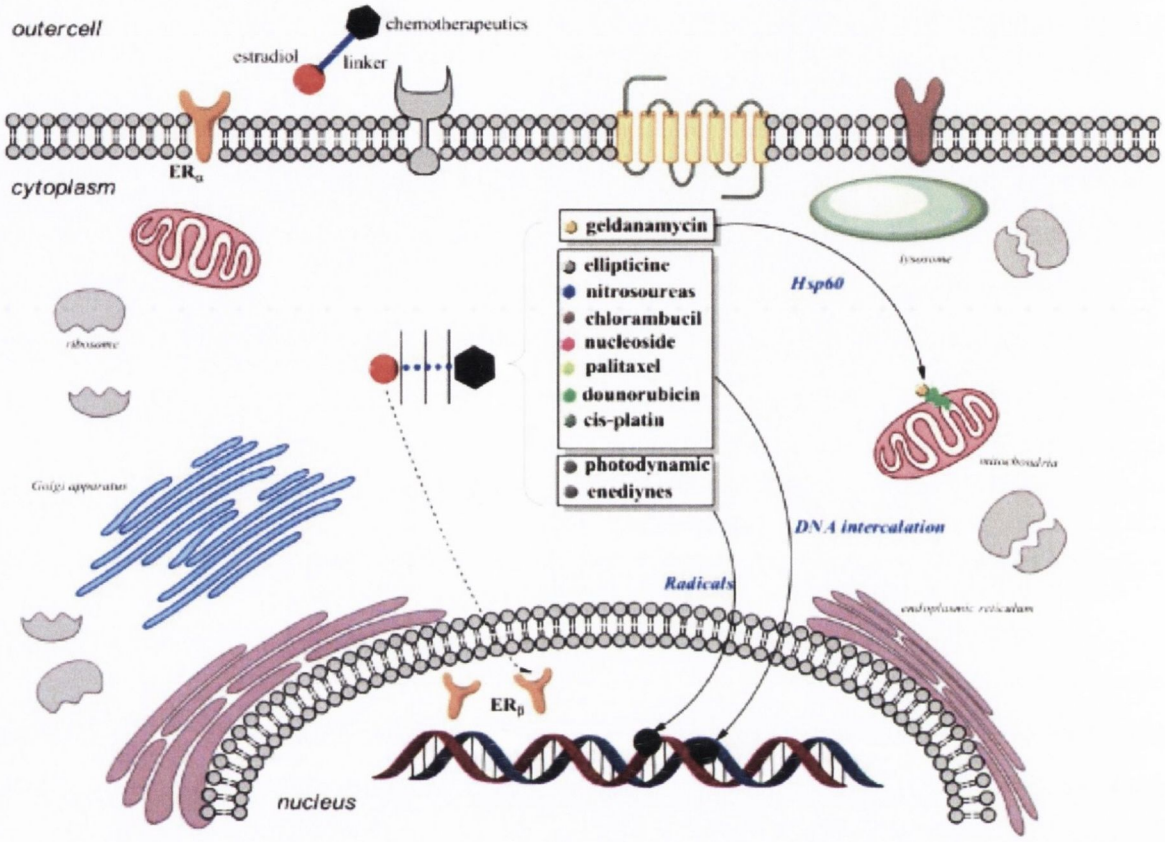

Figure 1-64 Targets of chemotherapeutic agents[394]

The 2-chloroethylnitrosourea (CNU) is highly reactive component found in many antineoplastic chemotherapeutic agents.[395] The clinical use of CNU is limited by the nonselective mechanism of cytotoxicity. Eisenbrand *et al.* prepared a series of 2-chloroethylnitrosourea-alanyl (CNU-ala)-estradiol conjugates [170], which is linked through a 3/17-O ether linkage, or at 6α-position.[396] When the conjugates were evaluated they showed a 3-fold longer terminal plasma half-life when compared to CNU-Ala and E2-CNU conjugates possibly due to their higher lipophilicity. The E2-CNU–17-ester conjugate exhibited enhanced cytotoxicity and antineoplastic potency. The experimental evidence suggested the CNU-estradiol conjugates may have played a role in its anticancer activity in hormone-dependent tumours but possibly not through the ER as the RBA values were relatively low for all CNU-E2 conjugates (0.05 - 4.7 %).

Geldanamycin (GDA) is an ansamycin benzoquinone antibiotic that is well known for its cancer chemotherapy properties, including breast cancer.[397] Geldanamycin exerts its antineoplastic

effect by binding to chaperone-heat shock proteins (HSPs) of cancer cells, leading to degradation of the Hsp90 complex. Its uses are limited as it shows poor selectivity and systemic toxicity.[398] Kuduk *et al.* prepared a series of 7-*N*-geldanamycin conjugates linked through the 16α position of estradiol.[399] The linkers were alkyl groups that varied in length, some of which contained an embedded alkene group. The lead compound 2-butynyl-linked estradiol-geldanamycin conjugate [171] displayed the highest RBA but it was very low when compared to estradiol, Figure 1-66. The evaluation of the conjugate with the butanyl linkage showed significant inhibition in ER+ cancer cells. The estradiol-GDA conjugate showed no effect on IGF1R and reduced activity against Raf-1, signifying some degree of selectivity for ER vs non ER responses. The cytotoxic activity of the estradiol-GDA conjugate was less than that of GDA alone, and the biological effects were not blocked by coadministration of estradiol.

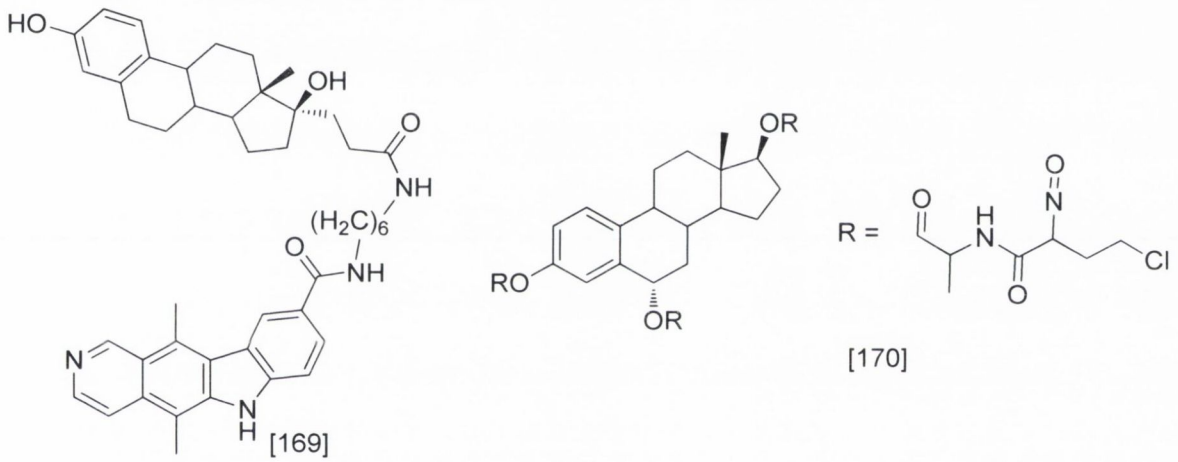

Figure 1-65 Estradiol-Ellipticine Conjugate [169] & CNU-estradiol conjugates [170]

Chlorambucil is a member of the nitrogen mustard family and is used for the treatment of chronic lymphocytic leukaemia. Its mechanism of reaction involves cross-linking DNA, leading ultimately to cell death. Chlorambucil has been shown to be effective against certain cancers but the nonselectivity of its mechanism of action renders it useless against breast cancer.[400] Sharma *et al.* synthesised a series of chlorambucil analogues attached to estradiol at the 7α-position *via* a series of linkers.[401] The biological evaluation of the series indicated that the carbamate group [172] and amino conjugate [172a] retained the highest ER affinity, RBA = 46% and 40%, respectively. The high ER affinity was credited to the conjugate which could adopt a binding mode similar to that observed for ICI 164,384 [173], Figure 1-66.[402] This conformation would allow the terminal chlorambucil group to be available for reaction with the DNA. It was shown that the lead conjugate interacted with DNA initially and recruitment of ER was happening later. The result was that the treated cells were less

likely to repair the defects caused by alkylation with the chlorambucil moiety in the presence of ER, leading to enhanced cell death.[401]

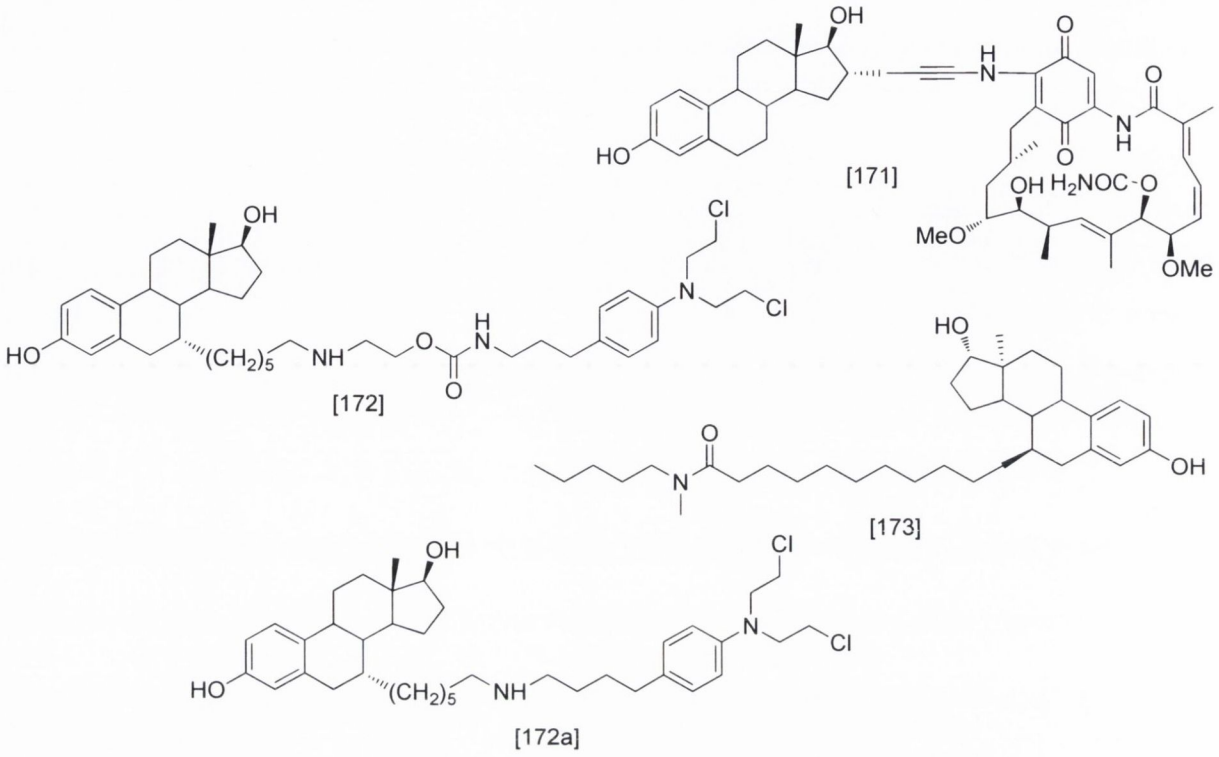

Figure 1-66 Geldanamycin conjugate [171], Chlorambucil conjugate [172] & ICI 164,384 [173]

Daunorubicin is a member of the anthracycline antibiotics family and is often used for the treatment of advanced breast cancer.[403] Daunorubicin is known to cause cardiotoxicity at high doses, but it is still preferred due to is beneficial effects in metastatic breast cancer.[404] Hartman *et al.* reported the synthesis of an estradiol–anthracycline conjugate which was linked *via* a 17-oxime moiety but this compound displayed negligible ER binding affinity and no ER-responsive cancer selectivity.[405] In another approach, Kasiotis *et al.* synthesised estradiol which was conjugated through an 17α-aminopropynyl group [174] to the sugar moiety of the anthracycline.[406] The conjugate had an RBA value of <1% that of E2 and was significantly less active than daunorubicin in both ER+ and ER– breast cancer cell lines, Figure 1-67.

Paclitaxel (Taxol) is a potent antimitotic cancer drug, and because the mechanism of action is different from that of other chemical agents, it has become a valuable component in combination therapy. In particular, it has established a major role in the treatment of recurrent, metastatic breast cancer.[407] Paclitaxel has poor solubility characteristics and its inherent toxicity reduces its clinical application in the treatment of cancer patients. Liu *et al.*[408] reported a series of estradiol–paclitaxel conjugates which were linked *via* a moiety at position 11β or 16α of the estradiol and at the 2', 7', or

10-hydroxyls of paclitaxel.[16] The use of the 2'-hemisuccinate or 7-hemisuccinate ester group was intended to improve the conjugate solubility but when they were evaluated with the moiety at position 11β or 16α of the estradiol they were less active than Taxol and established no significant selectivity for ER+ MCF-7 cells when compared to the ER- MDA-MB-231 cells. All conjugates had low ER binding affinity and were less active *in vitro* than paclitaxel, (16α-estradiol ether linkage at 7'-O-Taxol [175]), Figure 1-67.

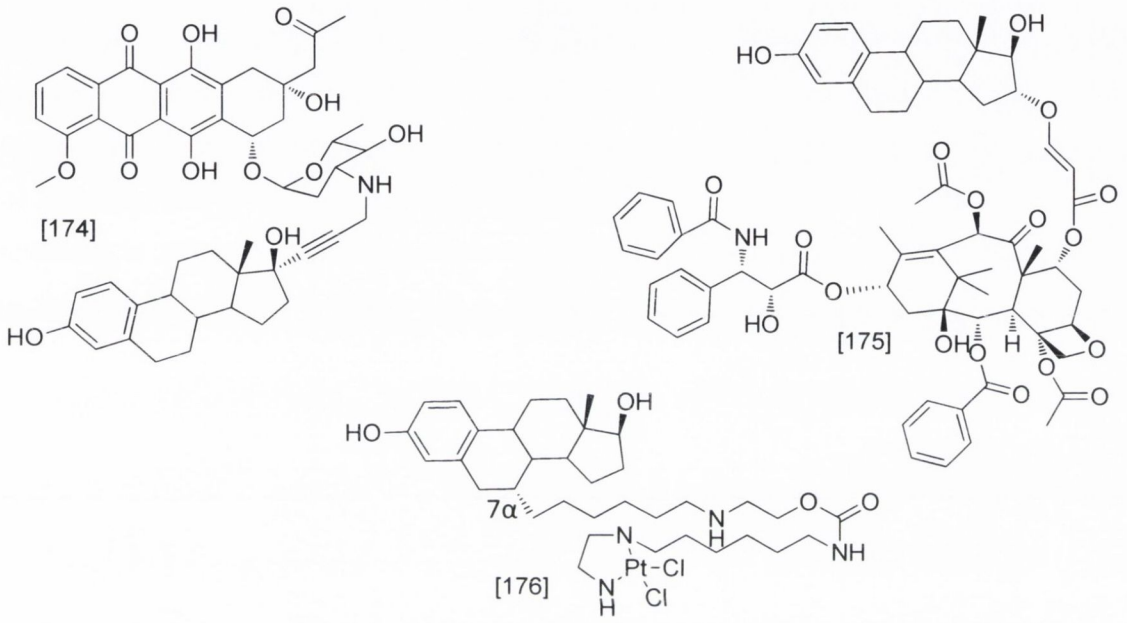

Figure 1-67 Examples of Estradiol–Anthracycline conjugate [174], Estradiol–Paclitaxel conjugates [175] and Estradiol–cisplatin conjugate [176]

Cisplatin and its derivatives comprise a major component in the treatment regimens for many forms of cancer, including breast cancer. Cisplatin's usefulness is limited, as with many anticancer drugs, by its lack of tissue selectivity and systemic toxicity. With estradiol-cisplatin conjugates, it would be desired that cisplatin would retain its anticancer activity and at the same time display the ER-selectivity of estradiol. A substantial number of estradiol-cisplatin conjugates have been reported and evaluated as potential therapeutic agents. As with the previous example of conjugates where the substituent was ligated at the 3- or 17β-position, the estradiol-cisplatin conjugates exhibited low ER-binding activity but significant cytotoxic activity was retained. Barnes *et al.* reported novel Pt(IV) complex but was unable to acquire significant ER+ selectivity.[409] Kim *et al.* synthesised a series of (Est-en)$PtCl_2$, a bifunctional cisplatin conjugate consisting of ethylendiamine dichloridoplatinum (II) tethered to the 7α-position of estradiol [176], Figure 1-67.[410] This estradiol–platin conjugate reserved significant ER-binding affinity and demonstrated enhanced cytotoxicity in ER+ breast cancer cell lines as compared to cisplatin alone. However the conjugate efficacy in ER- breast cancer cells was not reported so the cell selectivity was indeterminate.

Mitomycin C belongs to the class of compounds that require metabolic activation, i.e., quinone reduction, prior to alkylation of the DNA[411], and it also displays a degree of sequence selectivity based upon its molecular structure[412]. Dao *et al.* reported the synthesis of an antiestrogen-mitomycin conjugate [177] that incorporated structural features in an attempt to improve selectivity and cytotoxicity, the antiestrogenic 11β-(4-alkoxyaryl) estradiol for ER binding, the alkylamino mitomycin C for DNA binding, and the hydrophilic, biologically compatible tri(ethylene glycol) linker to the two functional groups, Figure 1-68.[394, 413] The conjugate competitively displaced estradiol from ERα-LBD with RBA value of 7 %. The conjugate did not stimulate the production of alkaline phosphatase, an efficacy assay, at any dose level but the compound potently inhibited the stimulation caused by 1 nM estradiol. It was also shown on ER+ MCF-7 and ER- MDA-231 breast cancer cell lines that the cytotoxicity activity was comparable to that of mytomicin C alone. The conjugate showed that it retained the high ER affinity of estradiol and antiestrogen efficacy, but it was unable to improve the cytotoxicity effect and demonstrate selectivity for ER-expressing cells.

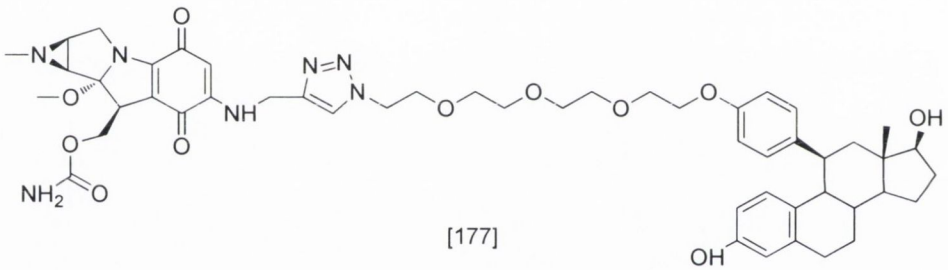

[177]

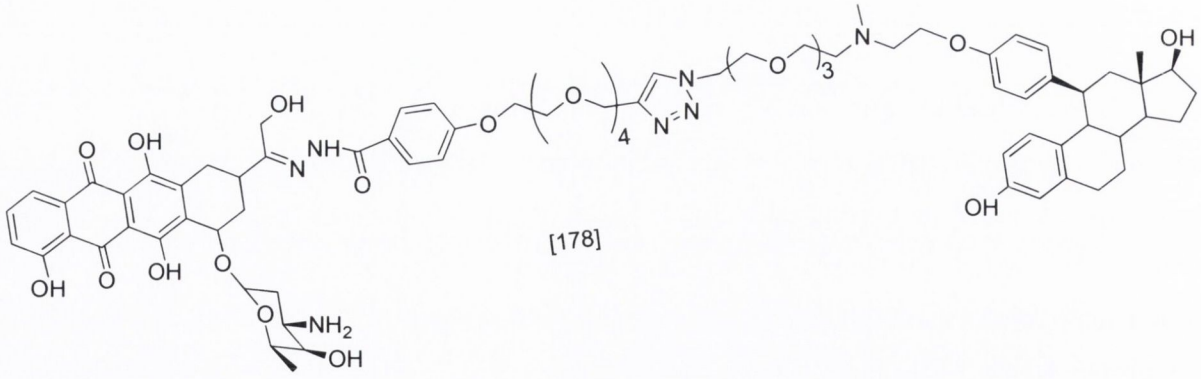

[178]

Figure 1-68 Antiestrogen-Mitomycin conjugate [177] and AE-Dox conjugate [178]

Doxorubicin is widely used for treatment of advanced breast cancer and is a favourite scaffold in conjugation studies. Dao *et al.* designed the antiestrogen (AE)-doxorubicin (Dox) conjugate [178] connected through a pH-sensitive hydrazone moiety, Figure 1-68.[394] The antiestrogen was a steroidal antagonist RU39411 as the ER targeting component. The AE-Dox conjugate showed a significant improvement of cytotoxicity (approximately 70-fold, IC_{50} = 11 nM) in

ER+ MCF-7 cells compared to doxorubicin (IC_{50} = 0.602 μM) alone or the doxorubicin–hydrazone (IC_{50} = 0.597 μM). Studies showed the participation of ER-mediated events in the cytotoxicity process in the ER+ cell line. When the AE-Dox cytotoxicity was evaluated in ER- MDA-MB-231 cell lines, it exhibited no differences among the three doxorubicin formulations. It was also demonstrated that the AE-Dox cytotoxicity in this cell line was an ER-independent process.

1.12.1.2 Non-Steroid conjugates

Krohn *et al.* synthesised a number of ER targeting conjugates based on diethylstilbestrol (DES) and hexestrol (HEX) analogues with a C4 side chain at the double bond attached to a number of functional and/or potential alkylating groups such as carboxylic acids, hydroxyl groups, esters, nitrogen mustards and varied haloalkyl groups.[414, 415] The group concluded that the coupling of the cytotoxic agents tended to have a detrimental effect of their bioactivity.

The use of tamoxifen and its metabolites in conjugate development has been reported. It is envisioned that the known ER binding ligand will increase the conjugate's selectivity to the tumour tissue and reduce indiscriminate tissue damage and this has been well documented.[416] Both doxorubicin and daunorubicin were reported to be activated through the catalytic production of formaldehyde and for this reason analogues of doxorubicin and daunorubicin containing a masked formaldehyde moiety, termed Doxoform and Daunoform, were synthesised.[416] The induction of oxidative stress culminating in the production of formaldehyde gives rise to many drug side effects, the most serious of which is chronic cardiotoxicity. While both novel analogues were hydrolytically unstable, they both demonstrated improved cytotoxicity against the MCF-7 cancer cell line and a resistant strain, MCF-7/ADR cells. Doxoform was 150-fold more cytotoxic to MCF-7 cancer cells and 1000-fold more cytotoxic to MCF-7/ADR. Burke *et al.* reported the synthesis of a third generation of doxorubicin-formaldehyde conjugate that bears the doxsaliform moiety tethered to 4-hydroxytamoxifen as a targeting group in an attempt to circumvent the resistance mechanisms (Scheme 1-1).[416, 417] The use of the non-steroidal ligand was preferred to a growth-stimulation hormone ligand (estradiol) as it would target the tissue where the ER is overexpressed but without the growth-stimulation. The masked formaldehyde was integrated in the form of an *N*-Mannich base between the amide function of the salicylamide moiety and the amine of doxorubicin. The salicylamide triggering molecule, previously developed to release the doxorubicin-formaldehyde metabolite, is tethered *via* derivatised ethylene glycols for enhanced solubility to an equimolar mixture of *E*- and *Z*- 4-hydroxytamoxifen.

The antiestrogen binding site (AEBS) is a known secondary binding site where non competitive binding of triarylethylene antiestrogens has been demonstrated.[418] Antiestrogen binding

sites are cytosolic, membrane-bound protein complexes that tightly bind tamoxifen and 4-OHT but exhibit virtually no affinity for estradiol but in contrast 4-OHT shows a much tighter affinity in the ER. The cellular distribution of AEBS is quite uncertain. However, there is evidence for the presence of AEBS in MCF-7 and MDA-MB-231 cell lines where the expression levels have been reported as 140000 sites/cell and 82000 sites/cell for ER+ MCF-7 and ER- MDA-MB-231, respectively.[418]

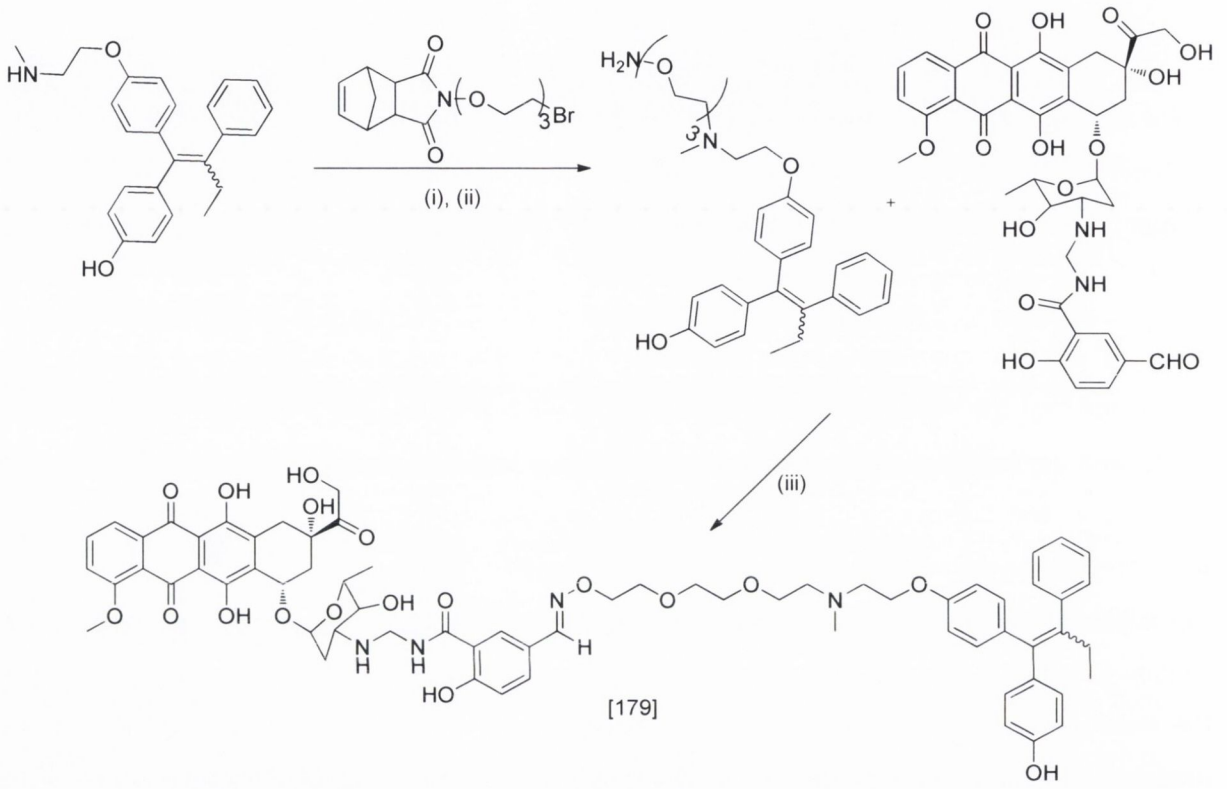

[179]

Scheme 1-1 Outline of the synthesis of steps to obtain [179] (i) DIPEA, THF sealed tube, 60 °C; hydrazine, EtOH, 60 °C; (iii) TFA, EtOH, water.

In Burke's study, the target doxorubicin-formaldehyde conjugates estrogen receptor binding and *in vitro* growth inhibition was evaluated as a function of tether length. The lead compound, DOX-TEG-TAM [179] (doxsaliform moiety tethered to 4-hydroxytamoxifen bearing a triethlene glycol (TEG) tether), was synthesised as shown in Scheme 1-1. It binds the ER (IC_{50} = 200 nM) with a binding affinity of 2.5 % relative to 4-OHT and inhibits the growth of four breast cancer cell lines with 4-fold up to 140-fold enhanced activity relative to doxorubicin, Scheme 1-1. The hydrolysis and stability studies of [179] displayed half-lives of 76 min (pH 7.4), 68 min (pH 7.6) at 37 °C and 180 h (pH 7.4), 119 h (pH 7.6) at 4 °C. The group concluded that the longer the tether the better the binding affinities. As the conjugate [179] exhibited activity in both ER+ and ER- cell line, further investigation was undertaken on the AEBS affinity. It was demonstrated that the conjugate targeting ability was

mediated through the AEBS as well as the ER, with [179] demonstrating approximately 60% of the AEBS binding affinity relative to 4-OHT.[419]

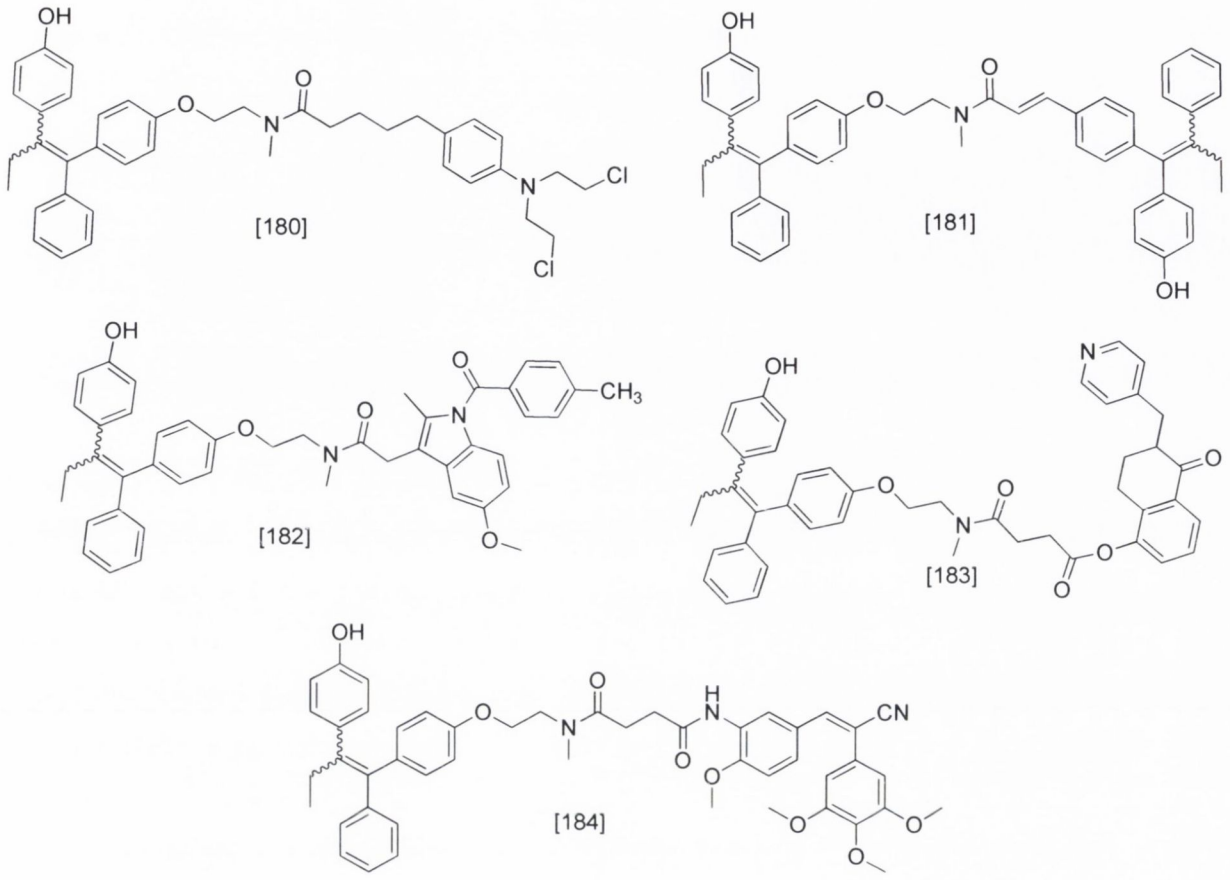

Figure 1-69 Novel ER targeting conjugates [180]-[184]

The development of novel ER targeting conjugates was performed within the Meegan research group in TCD. Keely *et al.* reported the design, synthesis and evaluation of a series of dual acting estrogen receptor binding conjugates.[420] The conjugates contained the ER-ligand endoxifen, a tamoxifen metabolite, tethered through an amide bond to components with known anticancer activity; chlorambucil [180], indomethacin [182], GW7604 [182], tetralone AI [183] and a CA4 analogue [184]. The conjugates showed promising antiproliferative activity in MCF-7 cell line and good ER binding activity with the one compound [181] exhibiting IC_{50} values of 35.6 nM (ERα), 19.5 nM (ERβ) and RBA values of 16 (ERα) and 29 (ERβ). In further research performed by Keely[421], a series of conjugates containing the ER-ligands endoxifen and dihydroxyendoxifen covalently bonded to a low weight VTA based on the combretastatin A-4 were synthesised. The lead compound [185] exhibited potent ER binding affinity [(IC_{50} values of 0.9 nM (ERα), 4.7 nM (ERβ)] and exhibited very potent antiproliferative activity of IC_{50} = 5.1 nM in MCF-7 cell line. The conjugate was shown to be stable at physiological conditions, therefore is believed not to act as a prodrug. The use of SAR and

molecular modelling studies showed that the cytotoxic drug was effective as an extension of the endoxifen moiety and was able to inhibit the action of Helix-12 in the LBD of the ER.

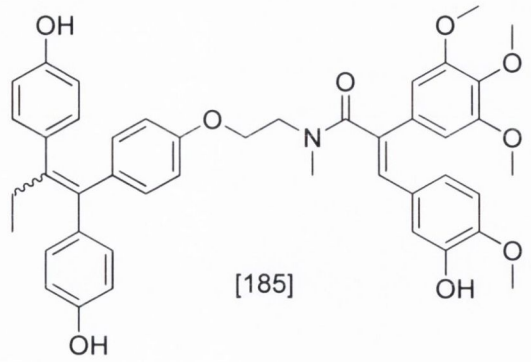

[185]

Figure 1-70 Potent conjugate containing an dihydroxyendoxifen coupled to CA4 [185]

1.12.1.3 Conjugates of radioligands

The use of selective radioligands could help in distinguishing between ER positive or ER negative breast cancer tumours and could aid in the selection of appropriate therapy. Top *et al.* reported a rhenium-based estradiol conjugate [186] with a RBA of 172 %.[422] The high RBA affinity was attributed to the presence of a chloromethyl substituent located on the 11β-position of the estradiol. The use of SAR rationalized that the chloromethyl substituent could interact with Cys381 and Cys530 residues in the LBD. Another ER-targeting radioligand conjugate [187] reported incorporated a ^{177}Lutetium, using a bifunctional chelating agent to sequester the radioisotope.[423] The ^{177}Lu conjugate was successfully taken up by MCF-7 cells. The breast cancer imaging agent [188] was synthesised by coupling an amino derivative of tamoxifen to an N_2S_2 bifunctional chelator for both rhenium and technetium-99m.[424] However, [188] showed very poor ER binding affinities *in vivo* and *in vitro* with RBA value of 0.009 %, Figure 1-71.

1.12.1.4 Conjugates with improved pharmaceutical properties

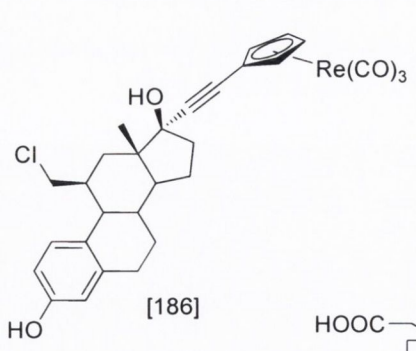

[186]

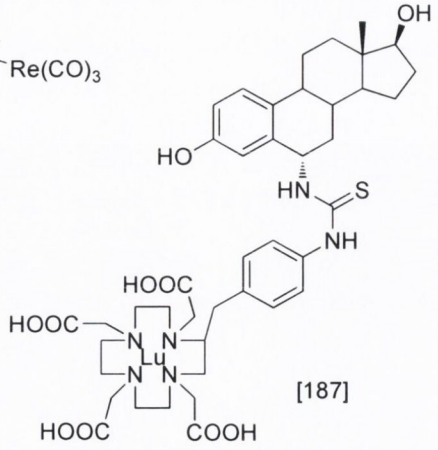

[187]

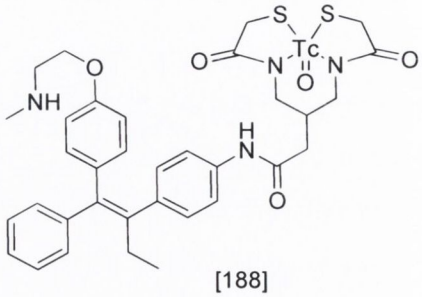

[188]

Figure 1-71 Conjugates of radioligands, [186]-[188]

Fulvestrant (ICI 182,780) [86], is a 7α substituted estradiol derivative and pure antagonist of the ER. It is an effective treatment for advanced postmenopausal ER positive breast cancer, however, its low oral bioavailability and the requirement of intramuscular administration has led to various attempts to increase the water solubility and bioavailability. One such approach is the synthesis of sugar conjugates *via* glycosylation reactions at the phenolic 3-and hindered 17-positions of the steroid structure, e.g. [189][425], Figure 1-72.

A polymer-estradiol conjugate was reported that could act as a hydro-soluble estradiol prodrug which could be further investigated as means of drug delivery.[426] Using a carbamate linkage estradiol-3-benzoate [190] was covalently bonded to the polymer PAHA (poly(α,β-(*N*-2-hydroxyethyll-*DL*-aspartamide))-poly(α,β-(*N*-2-aminoethyl-*DL*-aspartamide)) copolymer. It was noted that attachment of estrogen derivatives to the polymer will reduce the cellular uptake to the endocytic route.

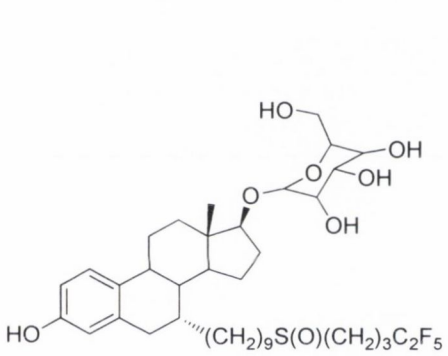

[189]

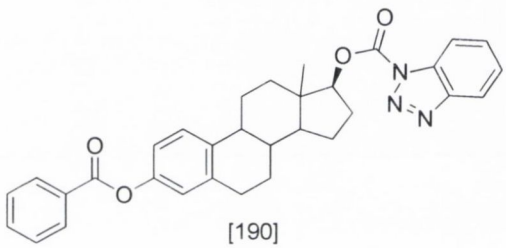

[190]

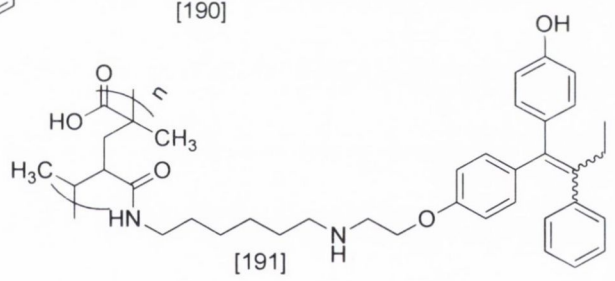

[191]

Figure 1-72 Conjugates with improved pharmaceutical properties, [186]-[188]

An endoxifen-macromolecular conjugate [191] was synthesised which displayed good binding affinity for both the ERα and ERβ. The antagonistic properties of this conjugate were shown to be similar to that of endoxifen.[427] The endoxifen analogue was conjugated to a diaminoalkyl linker and then conjugated to activated esters of a poly(methacrylic acid) polymer by atom transfer radical polymerization. The evaluation of the conjugate in an estradiol competition assay showed IC_{50} values were 11 ± 9 nM of ERα and 33 ± 10 nM of ERβ, while the endoxifen exhibited IC_{50} values were 15 ± 5 nM of ERα and 9 ± 5 nM of ERβ.[427]

1.13 Project Objectives

The ER is an attractive target for the design of drugs to treat hormonal-dependent diseases. Currently, there is an unmet need for good ER-ligands for many therapeutic applications. The main overall objectives are to design, synthesise and evaluate novel ER-targeting compounds and investigate their possible application as useful therapies. The specific objectives of the thesis are:-

- To utilise molecular modelling techniques in order to aid the design of novel estrogen receptor (ER) ligands and associated conjugates.
- To synthesise a library of suitable ER ligands and conjugates, based on endoxifen [36], cyclofenil [198] and bazedoxifene [50] which will exert a selective antagonistic effect in breast cancer cells while demonstrating good ER-binding affinity.
- To biochemically evaluate a number of compounds synthesised for anti-proliferative activity and cytotoxicity in MCF-7 and MDA human breast cancer cell line
- To assess both ERα and ERβ binding affinity properties of a selection of the compounds synthesised in order to determine ligand ER-subtype selectivity.
- To select suitable candidate compounds for further evaluation and development as potential anticancer drugs.

Chapter 2
Estrogen receptor ligands

2.1 Overview

Many studies have been reported which demonstrate that 4-hydroxytamoxifen, endoxifen and norendoxifen (the major metabolites of tamoxifen), also possess potent antiestrogen activity (Figure 2-1).[428] The endoxifen molecule will provide the conjugates to be synthesised with the selectivity to target the estrogen receptor expressed in ER positive breast cancer cells, such as MCF-7 cells. Endoxifen is an ER antagonist and binds at the estrogen receptor with the IC_{50} value of 29.0 nM in ERα. The use of the endoxifen scaffold in the novel conjugate design should allow the selectivity to deliver a cytotoxic agent directly to the tumour site. Previous studies by Burke[429] and Keely[421] have demonstrated the use of the antiestrogen endoxifen for the delivery of cytotoxic drugs such as doxorubicin. Estradiol has also been used as the ER targeting ligand in related studies.[430]

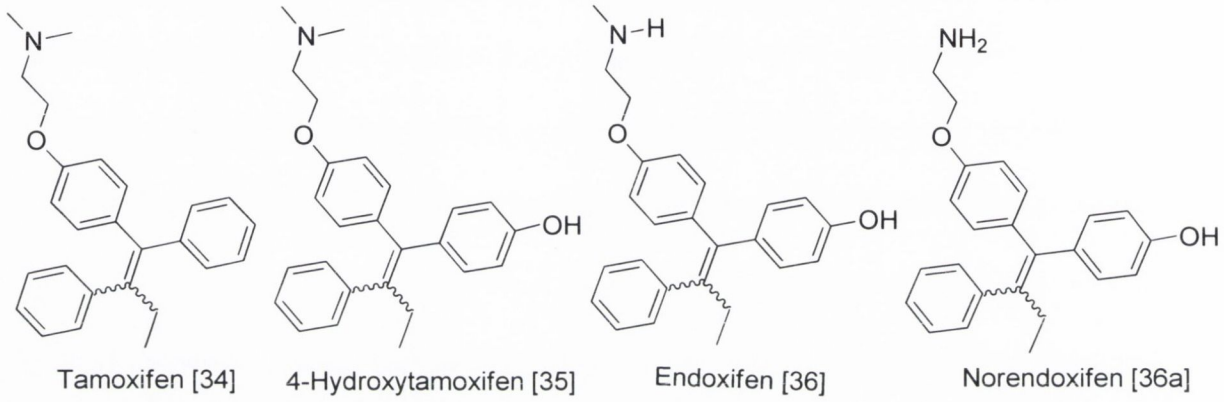

Figure 2-1 Tamoxifen [34] and metabolites: 4-hydroxytamoxifen [35], endoxifen [36] and norendoxifen [36a]

2.1.1 Synthesis of triarylethylene analogues

Stereochemistry is a key factor when synthesising tamoxifen analogues, and a reaction that produces predominantly the Z-isomer is desirable. Studies performed by Robertson et al.[431] found that the two isomers exerted different effects on the same tissue. Using rat uterus, *Z*-tamoxifen (*cis*-isomer), was shown to express an antagonist effect while the *E*-tamoxifen (*trans*-isomer), exhibited an agonistic effect in the same tissue.[431] The study also demonstrated that for tamoxifen and related metabolites, the relative binding affinity (RBA) was significantly higher for the *Z*-isomer in rat uterine ER. Where the RBA of estradiol is taken to be as 100, *Z*-4-hydroxytamoxifen had a RBA of 285, while the *E*-isomer had a value of 5.

A large number of synthetic routes utilising either carbometalation reactions or palladium-mediated cross coupling reactions, or a combination of the both, were reported to construct the tetrasubstituted olefin backbone of tamoxifen and related triarylethylene analogues.[432]

Tamoxifen and its derivatives were initially synthesised by reaction of aryl Grignard reagents with 1,2-diarylbutanone. Potter[433] and McCague[434], later reported the synthesis of an equal ratio mixture of isomeric triarylethylene phenols. The synthesis involved the use of a ketone compound, which was reacted with 4-(tetrahydropyranloxy)phenyl-lithium followed by an acid treatment, (Scheme 2-1).

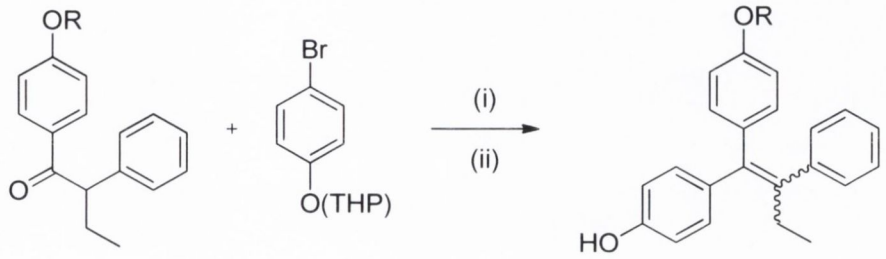

(i) *n*BuLi, THF (ii) HCl, EtOH

Scheme 2-1 4-Hydroxytamoxifen synthesis route by McCague *et al*[434]

Miller's group[435] exploited a carbometalation of phenyl(trimethylsilyl)acetylene with diethylaluminum chloride/titanocene dichloride to yield an organometallic intermediate, which was reacted with *N*-bromosuccinimide (NBS) and is subsequently reacted to generate diphenylbut-1-enyltrimethylsilane. This was subsequently converted in two steps to analogues of tamoxifen [34], Scheme 2-2.

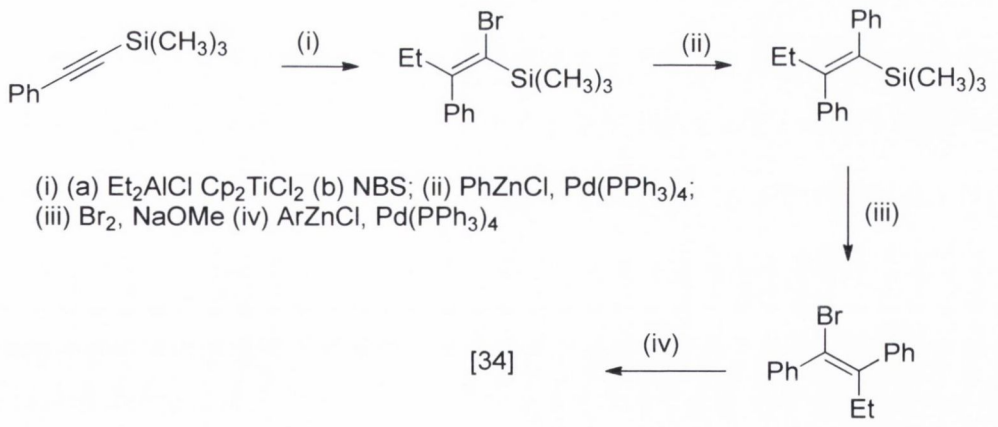

Scheme 2-2 Tamoxifen synthesis route by Miller[435]

Minato et al.[436] and Liron et al.[437] investigated the palladium-catalysed stereoselective synthesis of arylated olefins. Both groups were able to utilise arylstannane derivatives to sequentially arylate 1,1-dihaloalkenes that gave rise to a number of coupled products, including tamoxifen derivatives in good yields.

Shimizu et al.[438] exploited a geminal diborylation of 2,2-dibromo-1-ethylvinylbenzene with *bis*-(pinacolato)diboron (Bpin-Bpin) generating the 1,1-diboryl-1-alkene, which underwent successive cross couplings with two different aryl iodidies to afford tamoxifen (Scheme 2-3).

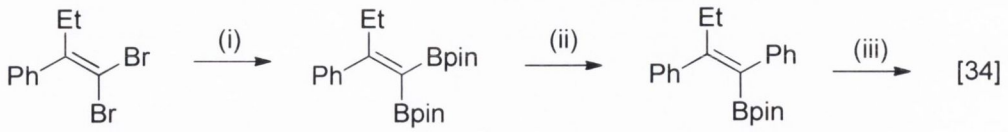

(i) (a) *n*BuLi (b) Bpin-Bpin; (ii) PhI, Pd_2dba_2, P(*t*-Bu)$_3$; (iii) Ar-I, Pd_2dba_2, P(*t*-Bu)$_3$

Scheme 2-3 Tamoxifen synthesis route by Shimizu[438]

Studemann et al.[439] used Ni-catalyzed carbozincation of 1-phenyl-1-butyne, followed by addition of iodine to generate the (*Z*)-iodoalkene, which could be converted to tamoxifen by Pd catalysed cross-coupling reaction with an arylzinc bromide (Scheme 2-4).

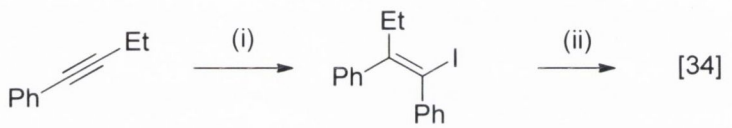

(i) (a) Ph_2Zn, $Ni(acac)_2$ (b) I_2; (ii) ArZnBr, $Pd(dba)_2$,PPh_3

Scheme 2-4 Tamoxifen synthesis route by Studemann[439]

Zhou et al.[440, 441] described the three-component coupling of 1-phenyl-1-butyne with iodobenzene and an arylboronic acid to provide a direct synthesis of tamoxifen (Scheme 2-5).

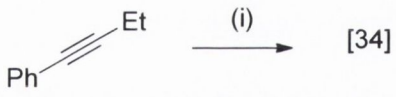

(i) PhI, $ArB(OH)_2$, $PdCl_2(PhCN)_2$

Scheme 2-5 Tamoxifen synthesis by Zhou[440]

Itami et al.[442] reported the utilisation of an alkynyl(2-pyridyl)silane (derived from but-1-ynyl-chlorodimethylsilane) to effect a regio- and stereo-selective carbomagnesation/cross-coupling sequence to generate the 1,2-diaryl-1-butenyl(2-pyridyl)silane. Subsequent conversion to an alkenylboronate ester and Suzuki-Miyaura coupling yielded tamoxifen (Scheme 2-6).

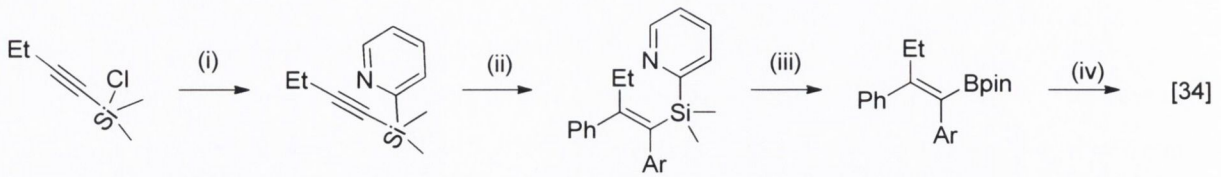

(i) *o*-C_5H_4NMgBr; (ii) (a) PhMgI, CuI (b) ArI, Pd[P(*t*-Bu)$_3$]$_2$; (iii) (a) BCl_3 (b) pinacol; (iv) PhI, Pd[P(*t*-Bu)$_3$]$_2$

Scheme 2-6 Tamoxifen synthesis by Itami[442]

Shiina et al.[443] developed a three component coupling reaction between aromatic aldehydes, cinnamyltrimethylsilane and anisole using a Lewis acids catalyst to afford tetra-substituted ethylenes. After migration of the double bond functionality using potassium *tert*-butoxide and the addition of a basic side chain, tamoxifen derivatives are afforded.

McKinley and O'Shea[432] reported a route to synthesis *Z*-tamoxifen through the carbolithation of diphenylacetylene generating (*E*)-1-lithio-1,2-diphenylalkyl-1-enes which can be reacted *in situ* with triisopropylborate to stereoselectively provide (*E*)-1,2-diphenyl-1alkylene boronic acids. The tetrasubstituted vinylboronic acids served as versatile intermediates for the generation of tetrasubstituted olefins while retaining the stereochemistry (Scheme 2-7).

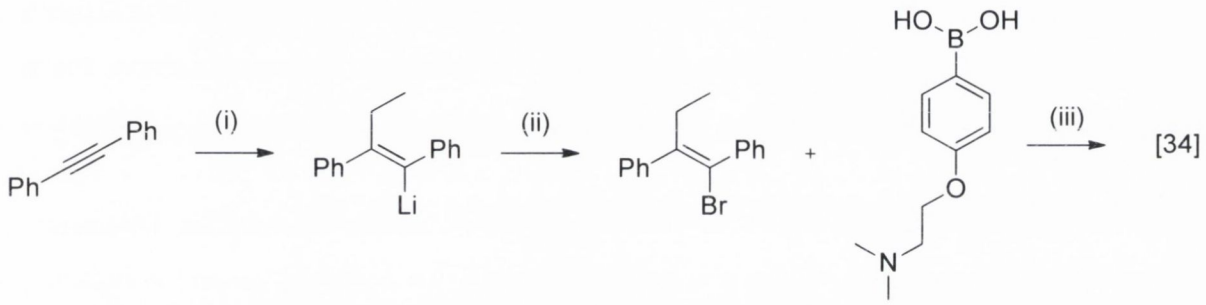

(i) EtLi; (ii) (a) $Br(CH_2)_2Br$ (b) HCl; (iii) $Pd(PPh_3)_4$ Na_2CO_3, DME, H_2O

Scheme 2-7 Tamoxifen synthesis route by McKinley and O'Shea[432]

Coe et al.[444] first reported the use of the McMurry reaction for the stereoselective synthesis of tamoxifen. The McMurry reaction is a low valent titanium mediated crossed coupling of substituted benzophenones. The route tended to favour the synthesis of the desired Z-isomer for a number of analogues. The reaction has become very popular because of the impressive stereoselectivity and relative ease of reaction, and has been utilised by many groups to propose different tamoxifen analogues as the desired isomer in high yields.[445, 446] Within the Meegan research group, the McMurry reaction has been the route of choice for the synthesis of the triarylethylene scaffold as it commonly leads to good E:Z isomer ratios and optimisation of the reaction has been investigated by previous researchers.[447-449]

2.1.2 McMurry Reaction

2.1.2.1 Background

In the 1970's, two research groups discovered that carbonyl compounds could be reductively coupled to produce alkenes upon treatment with low-valent titanium reagents.[450] Tyrlik and Wolochowicz described the coupling of aliphatic and aromatic aldehydes and ketones by means of the $TiCl_3$-Mg system[451], and suggested that tetraarylethylene was obtained *via* the carbene

species Me_2C. Mukaiyama *et al.*[452] used the $TiCl_4$-Zn combination in the reductive coupling of aromatic aldehydes and ketones. This combination showed that the benzaldehyde and acetophenone were selectively transformed into the corresponding pinacols and alkenes, respectively, when the reaction was performed in appropriate solvent at either low temperature or under reflux, and proposed the intermediary of a metallopinacolate species. The latter was envisaged as being formed either by dimerisation of ketyl radical resulting from one electron transfer from the low-valent metal species to the carbonyl and/or, in the case of the more easily reducible and reactive aromatic ketones, by nucleophilic attack of a ketone dianion on the C=O bond. McMurry and Fleming reported on the reductive coupling of carbonyls to form olefins using $TiCl_3$ and $LiAlH_4$ and came to a similar conclusion that the mechanism of the reaction went through the metallopinacol intermediates.[453] The reductive coupling of carbonyls to give pinacols and alkenes by means of low-valent titanium compounds was called the McMurry reaction. The very broad scope of the McMurry reaction allows a large array of ketones, aldehydes, acylsilanes, keto esters, and oxamides to be efficiently coupled, in a inter- and intramolecular fashion, to produce a variety of products, including strained or sterically hindered olefins, macrocycles, polymers and heterocycles.[454, 455] The application of the McMurry reaction has been well utilized in organic and organometallic chemistry, biochemistry and material science.

2.1.2.2 Mechanism of carbonyl coupling

The McMurry reaction is of particular importance as a synthetic method in this thesis as it permits the reductive coupling of ketones to yield alkenes by reaction with low-valent titanium as the reducing agent. The initial step of the coupling reaction is the binding of the carbonyl substrate to the titanium surface, and the transfer of an electron to the carbonyl group. The carbonyl group is reduced to a radical species, and the titanium is oxidized. Two such ketyl radicals can dimerize to form a pinacolate-like intermediate that is coordinated to titanium. Cleavage of the C-O bonds leads to formation of an alkene and a titanium oxide (Scheme 2-8). The low-valent titanium reagents used are not soluble under the reaction conditions, thus heterogenous reaction conditions apply. Low-valent titanium such as $TiCl_4$ is used as the reducing agent in the presence of Zinc. Depending on molar ratio and the reductive agent used, a reagent is obtained that contains titanium of different oxidation states; however Ti(0) appears to be the active species. The coupling of unsymmetrical ketones leads to formation of stereoisomeric alkenes; the ratio depending mainly on steric demand of substituents.[456]

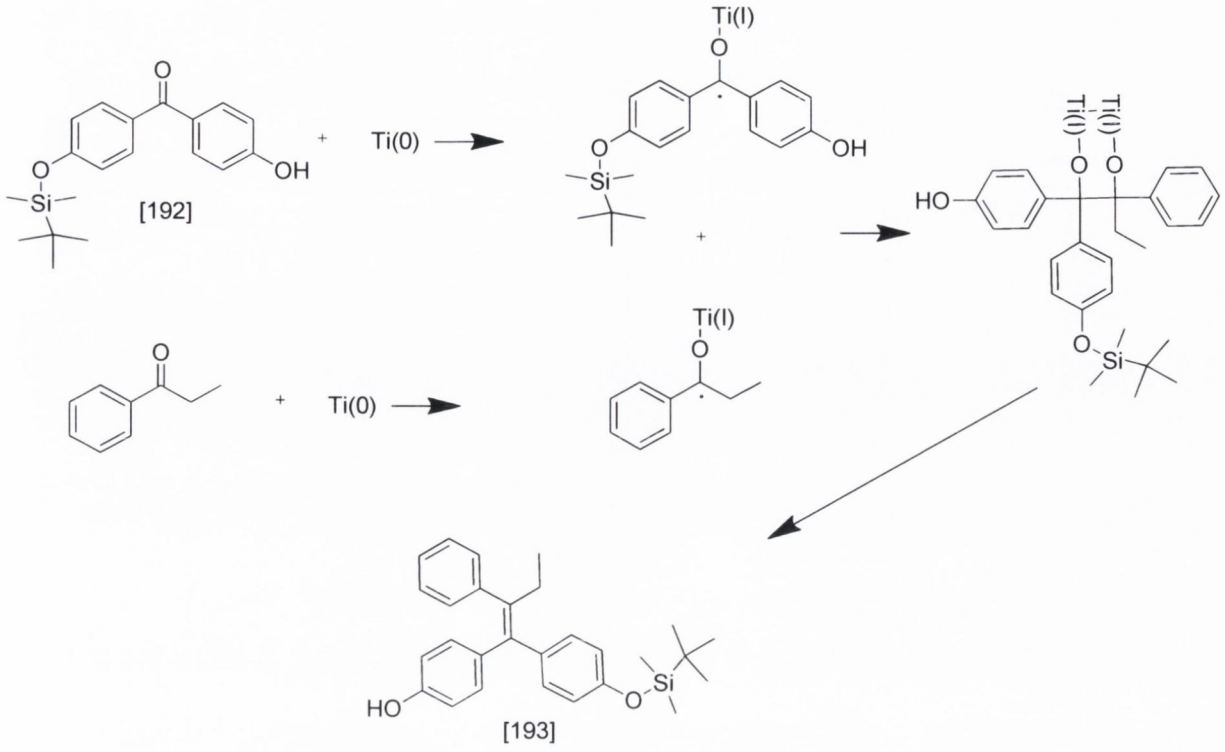

Scheme 2-8 Mechanism of the McMurry reaction for the formation of the triarylethylene

2.1.3 Synthesis of endoxifen analogues

2.1.3.1 General reaction scheme

Endoxifen was chosen as a suitable ER-ligand scaffold due to its high affinity ER-binding properties. Additionally, the secondary amine group present on the basic side chain can undergo acid coupling reactions to synthesise the prototype conjugated compounds. The general strategy for the synthesis of endoxifen is shown in Scheme 2-9

The main steps involve (including conditions):-

(i) The single protection of specific phenols groups present on the starting materials (*tert*-butyldimethylsilylchloride, imidazole, DMF)

(ii) The McMurry reaction, whereby two ketones are coupled to form a alkene bridge resulting in the desired triarylethylene backbone structure ($TiCl_4$, THF, Zn, reflux)

(iii) An alkylation reaction of the phenolic product *via* phase-transfer catalysis (1,2-dibromoethane, NaOH (aq.), $(n\text{Bu})_4\text{NHSO}_3$))

(iv) An amination reaction whereby the bromide product is reacted with different primary amines to form a set of analogues (R-NH_2, sealed tube at 60 °C)

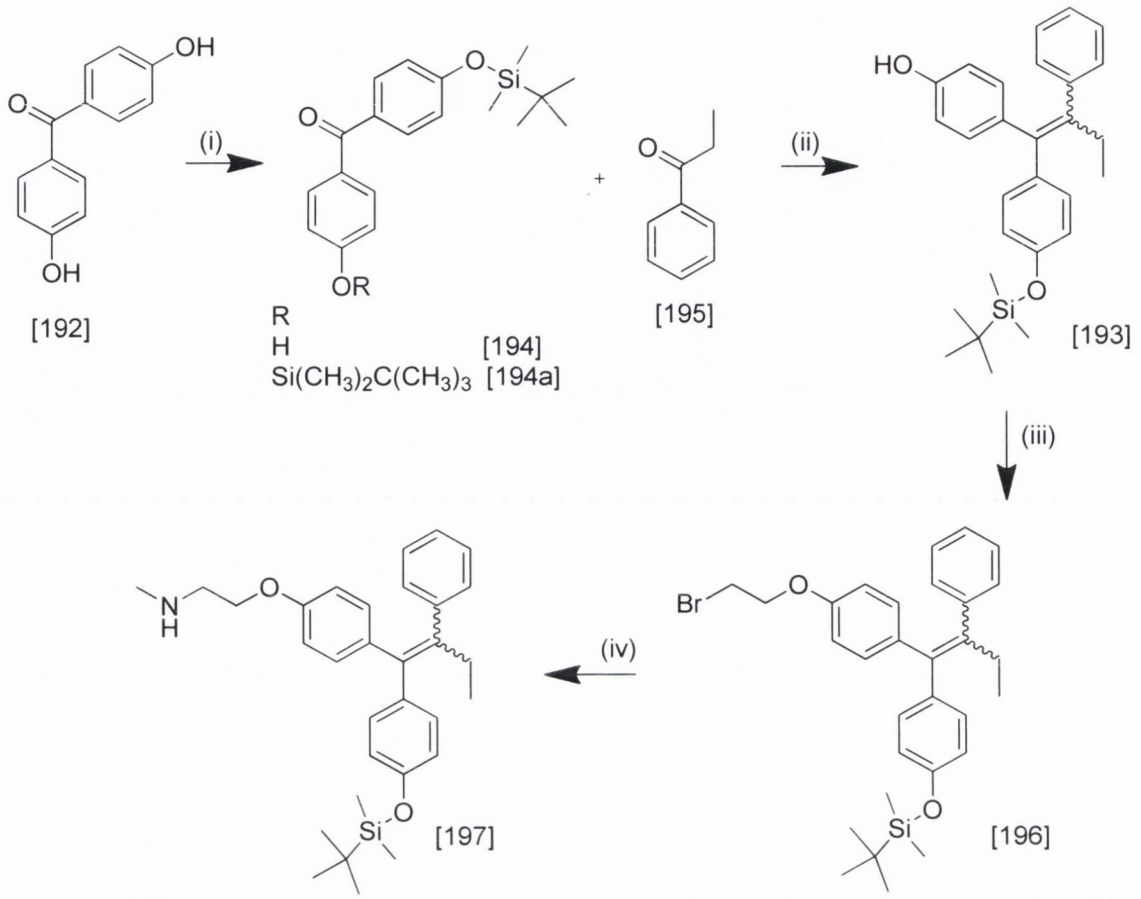

(i) TBDMSCl, imidazole, DMF; (ii) Zn, $TiCl_4$; (iii) $Br_2(CH_2)_2$, NaOH (aq.), $(n\text{Bu})_4NHSO_3$, DCM; (iv) $MeNH_2$, sealed tube, 60 °C

Scheme 2-9 Synthetic strategy of endoxifen analogue

2.1.4 Silyl-ether protection group reaction

The initial step in the synthetic route involved the mono protection of one the phenolic group present on the starting material, 4,4-dihydroxybenzophone [193]. Throughout the project, the protection of the hydroxyl functional group was essential and was achieved by formation of the *tert*-butyldimethysilyl (TBDMS) ether. The silyl ether was chosen as a suitable protecting group as it is tolerant to a wide array of reaction conditions. The reaction route chosen to synthesise the endoxifen analogue involved a number of harsh and basic reactions conditions in which the TBDMS ether is generally stable. TBDMS ether is more stable to hydrolysis than trimethylsilyl ether, but is still readily cleaved by a variety of selective conditions.

The silyl ether protection was performed by the addition of one equivalent of the hydroxylated benzophenone with one equivalent of the *tert*-butyldimethylsilyl chloride in the presence of 10 % equivalent excess of imidazole in DMF solvent. The imidazole acts as a base and promotes the formation of phenolic anions. This phenolic anion can react with the silyl chloride presumably *via* S_N2 type mechanism to form the silyl ether product. The excess imidazole helps

scavenge hydrochloric acid by-product as it is produced in the reaction while also recycling itself for further promotion of phenolic anion formation.

The sequence and rate of addition of the starting material was important for the dihydroxylated starting material. Firstly, a mixture of benzophenone [192] and excess imidazole are stirred for sufficient time to allow for the formation of phenolic anions. The addition of the silyl chloride is then carried out slowly to ensure that the concentration ratio of phenolic anions to chloride is large and that a greater proportion of mono-protected material [194] is generated in the early stages of the reaction. When the reaction had gone to completion (monitored *via* TLC), two new distinct products appeared on TLC; a mixture mono- ([194] 27 % yield) and di-protected ([194a] 34 % yield) products were afforded (Scheme 2-9).

The TBDMS protecting group has distinctive and characteristic signals observed in the ^{1}H-NMR spectrum. Both methyl groups present on the silicon atom are highly shielded, therefore are positioned upfield in the NMR spectrum. These methyl groups are chemically and magnetically equivalent. For compound [194], the protons and carbons of these methyl groups are observed at 0.27 ppm in the ^{1}H-NMR spectrum and at -4.78 ppm in the ^{13}C-NMR spectrum respectively. The *tert*-butyl moiety of the TBDMS group is also shielded due to the proximity to the silicon atom while the proton and carbon atoms of the methyl groups are also chemically and magnetically equivalent. Therefore, the protons of the methyl groups of the *tert*-butyl moiety are found as a singlet at 1.02 ppm in the ^{1}H-NMR spectrum while the carbons appear at 25.16 ppm in the ^{13}C-NMR spectrum. The quaternary carbon of the *tert*-butyl moiety is observed at 17.80 ppm in the ^{13}C-NMR spectrum.

The cleavage (deprotection) step of the silyl protecting group utilised throughout the project is discussed here. The cleavage of the TBDMS group is slow under hydrolytic conditions. When required, the silyl ether group was removed by treatment with *tetra-n*-butylammoniumfluoride (TBAF). Other reagents have been used for the cleavage of the silyl ether such as methanolic NH_4F, aqueous HF, BF_3, or SiF_4. Bulkier silyl group can be utilised where more stability of the protecting group is required. Triisopropyl (TIPS), triphenylsilyl (TPS) and *tert*-butyldiphenylsilyl (TBDPS) are example of other silyl ether protecting groups with increased steric bulk. All these groups are susceptible to TBAF cleavage, however, TPS and TBDPS groups are cleaved much more slowly. TBAF produces a source of fluoride ions that can react with the silicon to form a pentavalent intermediate which cleaves to free the hydroxyl group (Scheme 2-10). The reaction is high yielding and the by-products can be removed by an acidic aqueous wash, often affording a relatively clean, crude product. Direct column chromatography over silica gel could be achieved without the acidic workup to yield the pure product.

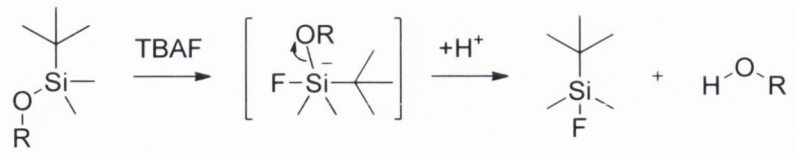

Scheme 2-10 TBAF deprotection step

2.1.5 McMurry reaction

The next step involved the formation of the triarylethylene backbone. The McMurry reaction was chosen as a suitable pathway to form the olefin [193] from the monosilyl protected benzophenone [194] and propiophenone [195] (Scheme 2-11).

The diversity in behaviour of different low-valent titanium reagent systems is likely due to variations in the particle size, surface area, physical nature of the surface and the solvent. The solvent is believed to stabilise the zero-valent particles during the initial formation of the reagent system. The presence of functional groups in the reaction mixture which are easily reducible is not compatible due to the strong reducing power of Ti(0). There has not been a full study of functional group compatibility reported to date, however, it appears that three categories exist: compatible (i.e. alcohol, amine, alkyl silane, ether), semicompatible (i.e. amides, ester, alkyne) and incompatible (i.e. nitro, allylic alcohol, oxime).[454] All functional groups in the incompatible category undergo rapid reduction upon treatment with low-valent titanium to such a degree that they cannot survive the carbonyl coupling. Optimization of reaction conditions with a variety of low valent titanium carbonyl coupling reagent systems has been performed. The main variables when optimising the reaction conditions include: the selection of reducing agent and solvent, the molar ratio of titanium to reducing agent and the molar ratio of titanium to ketone.[457]

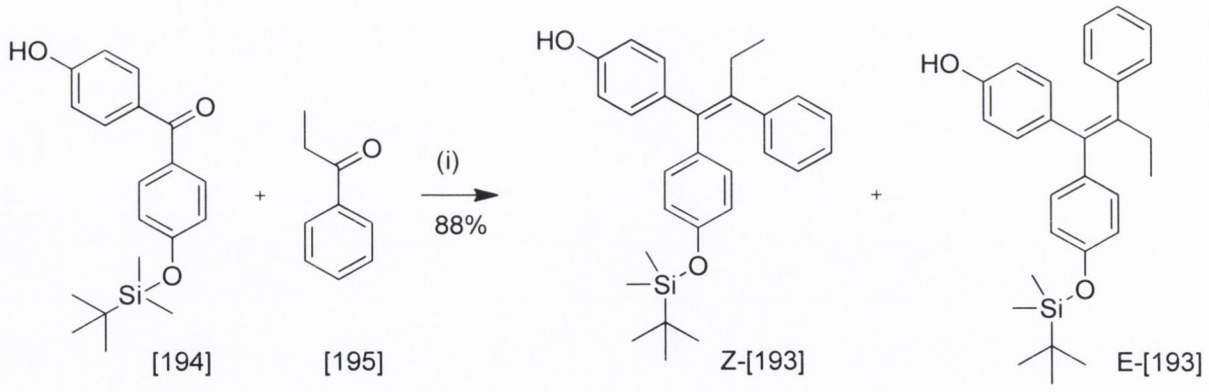

Scheme 2-11 Formation of [193] *via* the McMurry reaction. (ii) $TiCl_4$, Zn, THF, 4 h reflux

The McMurry reaction system employed in this project for the carbonyl-coupling reactions comprises of titanium (IV) tetrachloride and zinc in THF.[444] The optimal condition for this specific

McMurry reaction system was investigated by previous research at Trinity College Dublin.[421] Determined chemometrically through experimental design[458], the optimum conditions required titanium(IV) tetrachloride (4.5eq.) and zinc dust (9eq.) to be refluxed in the dark prior to the addition of the relevant benzophenone (1eq.) and propiophenone (1eq.) to allow for the formation of the reactive titanium species. The reaction mixture was further refluxed for 3 h under nitrogen and in complete darkness. Following work-up procedures, the material is purified *via* flash chromatography on silica gel to afford a *cis* (33 %) and *trans* (66 %) as a mixture of the required olefin [193] in a 88 % yield. The reaction sequence is illustrated in Scheme 2-11.

In the ^{1}H-NMR spectrum of [193] shown in Figure 2-2, the presence of both *E*- and *Z*- isomers can be observed by the overlap of the silyl protecting group signals resulting in a complex spectrum peaks. The signal for the methyl group on the ethyl side chain is overlapped with the signal peaks from *tert*-butyl moiety of the silyl protecting group also. Further signal overlapping occurred with the CH_2 group of both isomers overlapping and are observed as a quartet at 2.50 ppm with a coupling constant of 7.5 Hz. The aromatic region is complex due to the presence of both isomers and resulting in multiplet signals peaks between 6.49 - 7.19 ppm, Figure 2-2.

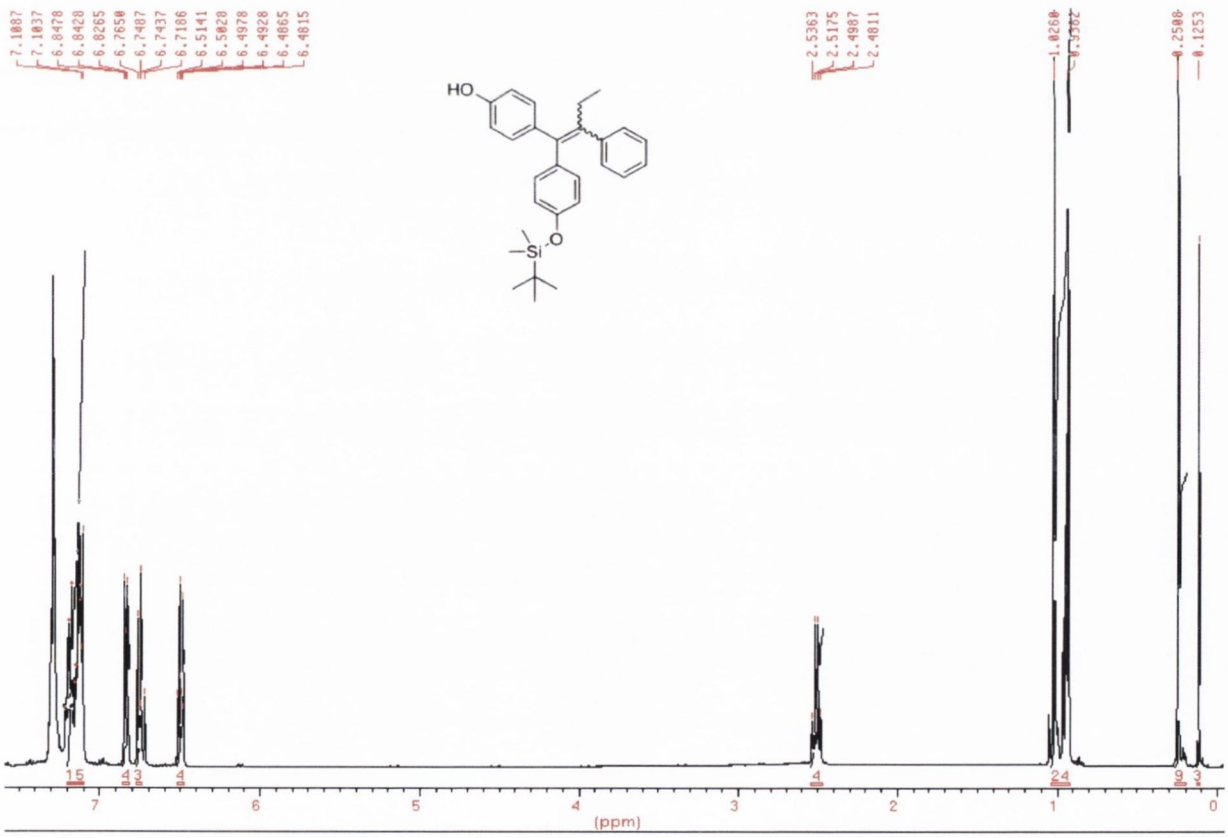

Figure 2-2 ^{1}H-NMR spectrum for [193]

It has been reported that phenolic benzophenone-derived ketones used in coupling reactions have been shown to favour the configuration of product which has a *trans* arrangement of the ethyl side chain relative to the original phenolic system across the double bond.[444, 445, 457] As it was not possible to separate the isomeric compounds using column chromatography, the use of ^{1}H-NMR was used to determine the ratio of E- to Z-isomers through the comparison of the peak integrals between the two CH_3 substituents on the silane atom, 1 to 1.2 respectively.

2.1.6 Phase transfer catalysis reaction

The synthesised olefin [193] contains the triarylethylene structure required for the endoxifen scaffold. The next step in the synthesis of endoxifen is the addition of a bromoethyl moiety. The free phenolic hydroxyl group on [193] undergoes an ethyl-bromination step *via* a phase-transfer catalysis method[417] to afford [196]. The phase transfer catalyst facilitates the migration of the reactants in a heterogeneous system from one phase into another phase where reaction can take place (Scheme 2-13). Ionic reactants are often soluble in an aqueous phase but insoluble in an organic phase unless the phase transfer catalyst is present.[459] The ionic substance (phase-transfer catalyst) contains hydrocarbon groups in the cation which are large enough to convey good solubility of salt in the organic solvent (highly lipophilic). The organic reactants are dissolved in the water-immiscible solvent in this case DCM. The salt containing the nucleophile is dissolved in the aqueous phase. The lipophilic cations are transferred to the non-polar phase and the anions are transferred from the water to the organic phase, which enhances the nucleophilicity (Scheme 2-13), allowing the substitution reaction to occur at mild conditions to afford product [196] (Scheme 2-12).

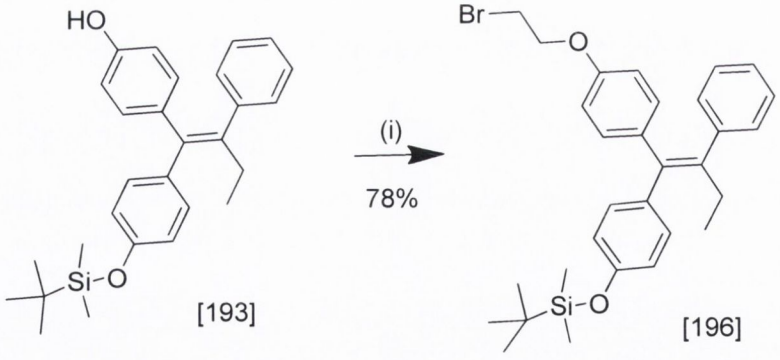

(i) tetra-*n*-butyl ammonium hydrogen sulfate, 1M NaOH, 1,2-dibromoethane, 16h RT

Scheme 2-12 Synthesis of the bromoethyl triarylethylene product [196]

In this project the organic phase consisted of excess of dibromoethane starting material and solvent wherein the triarylethylene and phase-transfer catalyst, tetra-*n*-butylammonium hydrogen sulfate reside and the aqueous phase, consisting of sodium hydroxide and acts as a reservoir of reacting base for generation of the triarylethylene anions. To ensure the maximum interaction is

achieved between the two phases the mixture is stirred vigorously for 16 h. Following work-up procedure and purification *via* flash chromatography over silica gel, the E/Z isomeric mixture of [196] was afforded in a 78 % yield.

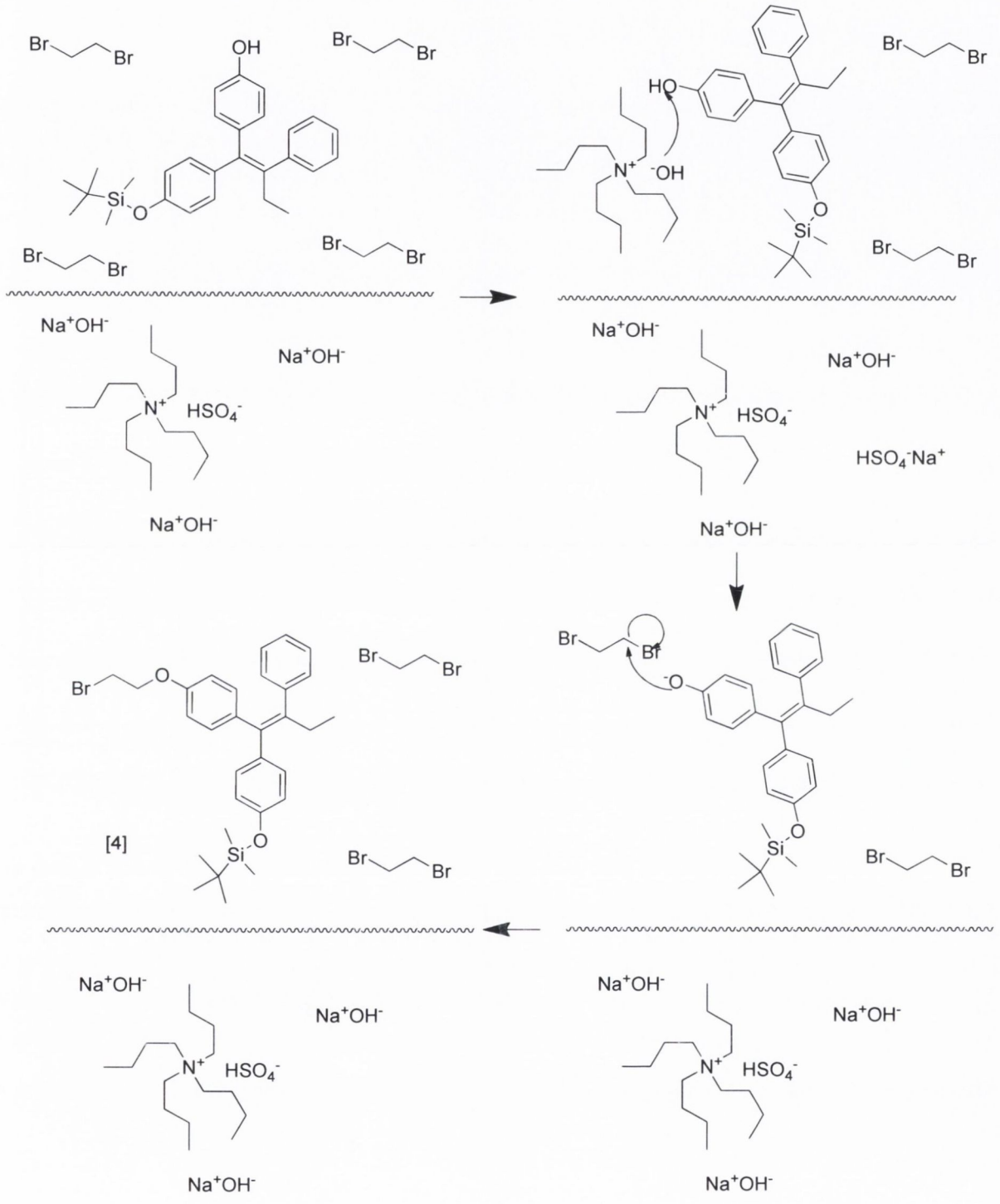

Scheme 2-13 Phase-transfer catalysed ethylbromination reaction mechanism

Bedford and Richardson determined that the Z-isomer basic side chain methylene proton signals of tamoxifen are shifted further downfield compared to that of the E-isomer.[460] With many

tamoxifen derivatives, spectral isomeric assignment interpretations can be made based on the relative positions of the aryl proton signal arising from the A_2B_2 para system of the 4-substituted phenyl ring and/or on the relative chemical shift observed for the OCH_2 signal arising from protons in the basic side chain.[169] Throughout this project, the calculation of the E/Z isomeric ratios were based on the intergration of the side chain OCH_2 and NCH_2 signals.

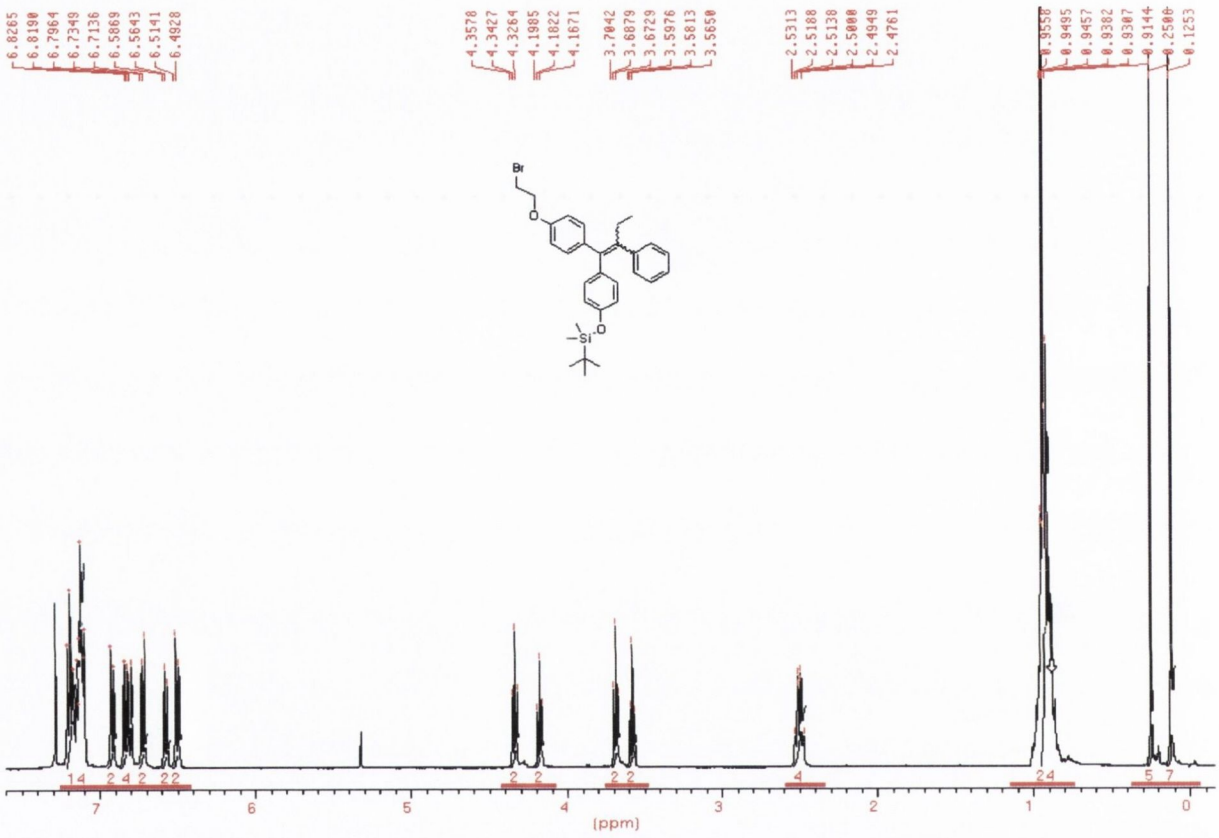

Figure 2-3 ^{1}H-NMR spectrum of [196]

In the ^{1}H-NMR spectrum of [196] as illustrated in Figure 2-3, the E-isomer CH_2N signals are observed as a triplet (J= 6.5 Hz) at 3.56 ppm while the *Z*-isomer CH_2N signals are observed as a triplet (J= 6.5 Hz) further downfield at 3.66ppm. The CH_2O signals are observed as a triplet (J= 6.5 Hz) at 4.18 ppm while the *Z*-isomer CH_2O signal are observed as a triplet (J= 6.5 Hz) further downfield at 4.34 ppm. The OCH_2 and the NCH_2 signals are more clearly defined than other signals in Figure 2-3, hence they are used to assign the *E:Z* ratio of the product. For compound [196], the *E:Z* isomeric ratio is calculated as 1:1.3 based on the integral of the signal peaks shown in Figure 2-4

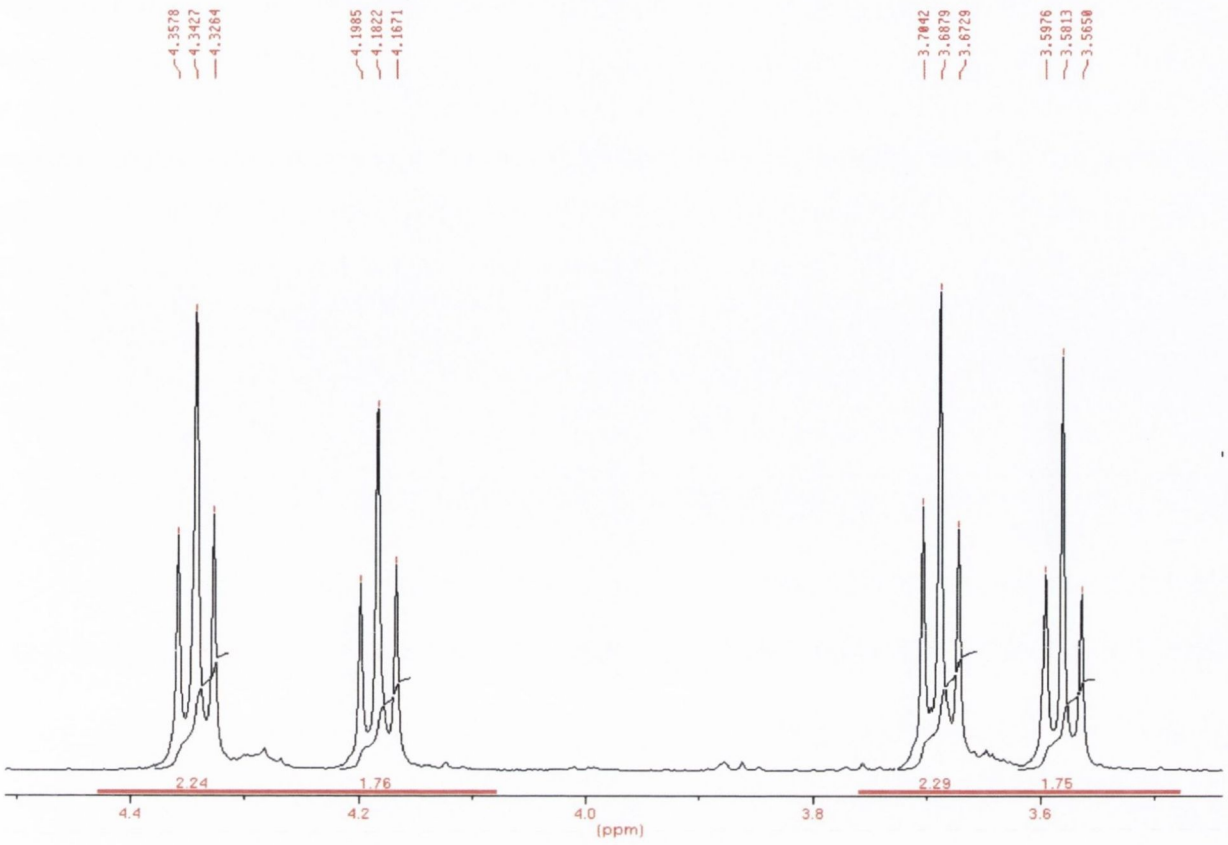

Figure 2-4 Bromoethyl CH_2 signals for ^{1}H-NMR spectrum of [196]

2.1.7 Amination reaction

The amination reaction is a key reaction in this study as it allows the synthesis of endoxifen analogue with the basic side chain on the triarylethylene core structure. The amine is required for effective binding of endoxifen to the estrogen receptor site. The basic side chain plays a key role in ensuring ER antagonist mechanism of action. The amine was introduced onto the bromide compound [196] through a high pressure amination reaction[417] to afford the silyl protected endoxifen analogue [197]. There is a solid and gaseous component on each side of the generalised balanced chemical equation for the amination reaction involved methylamine and [196] shown below (Scheme 2-14). When examining this reaction it is important to understand the principles that required the use of pressure for the formation the desired product.

$$\text{Bromide}_{(s)} + \text{MeNH}_{2\,(g)} \leftrightarrow \text{Amine}_{(s)} + \text{HBr}_{(g)}$$

Following Le Chatelier's principle which states that if a chemical system at equilibrium experiences a change in concentration, temperature, volume, or partial pressure, then the equilibrium shifts to counteract the imposed change and a new equilibrium is established.[461] This principle is relevant in the context of pressure. Methylamine is in excess and has a slightly higher molar volume compared with hydrobromic acid. If the reaction is carried out under increased

pressure it should drive the shift in equilibrium to form the lower volume gas in this case the hydrobromic acid, therefore leading to an equilibrium shift that will favour the formation of amine compound (silyl-protected endoxifen) [197]. For the amination reaction, excess methylamine is dissolved in THF together with the bromide [196] and sealed in a high pressure tube and the reaction mixture is heated with stirring for 24-48 h at 60 °C. The use of the pressure tube in this reaction was successful in producing the silyl-protected endoxifen [197] with a high yield (94%) of the E/Z isomeric mixture, 1 to 1.15 respectively.

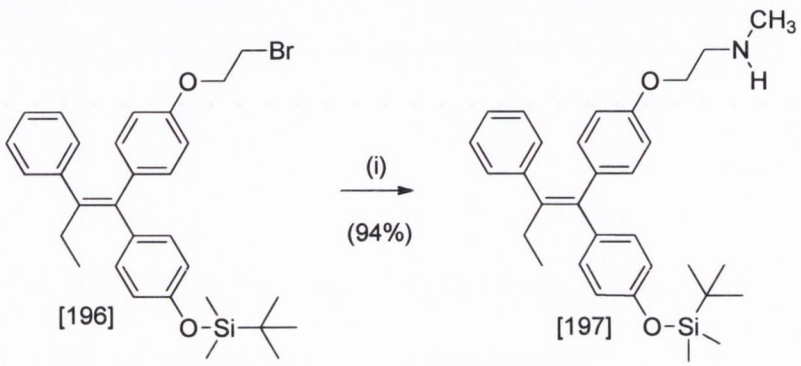

(i) NH_2Me, THF, 65 °C, 48 h

Scheme 2-14 Amination reaction to afford [197]

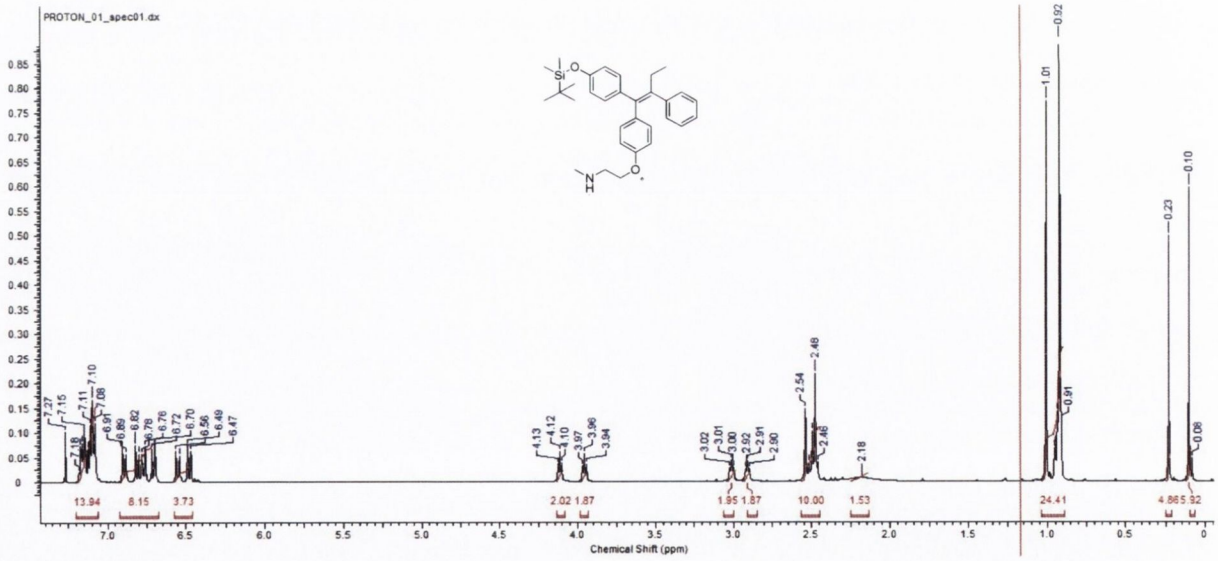

Figure 2-5 ^{1}H-NMR spectrum of [197]

The ^{1}H-NMR and ^{13}C-NMR spectra for the *E/Z* isomeric mixture of [197] are shown in Figure 2-5 and Figure 2-6. The CH_3 group protons of the ethyl side chain and the methyls of the *t*-butyl group located on the silyl moiety are observed between 0.92 - 1.01 ppm as a multiplet as the peaks overlap, while the CH_2 of the ethyl branch and the amine CH_3 protons signals overlap and are observed between 2.46 – 2.54 ppm. The basic side chain proton signals are observed at 2.90 - 3.02

ppm (CH_2N) and 3.94 - 4.13 ppm (CH_2O). The aromatic protons are observed between 6.47 – 7.18 ppm. In the ^{13}C-NMR spectrum the methyl carbon adjacent to the nitrogen are identified at 35.26 and 35.39 ppm.

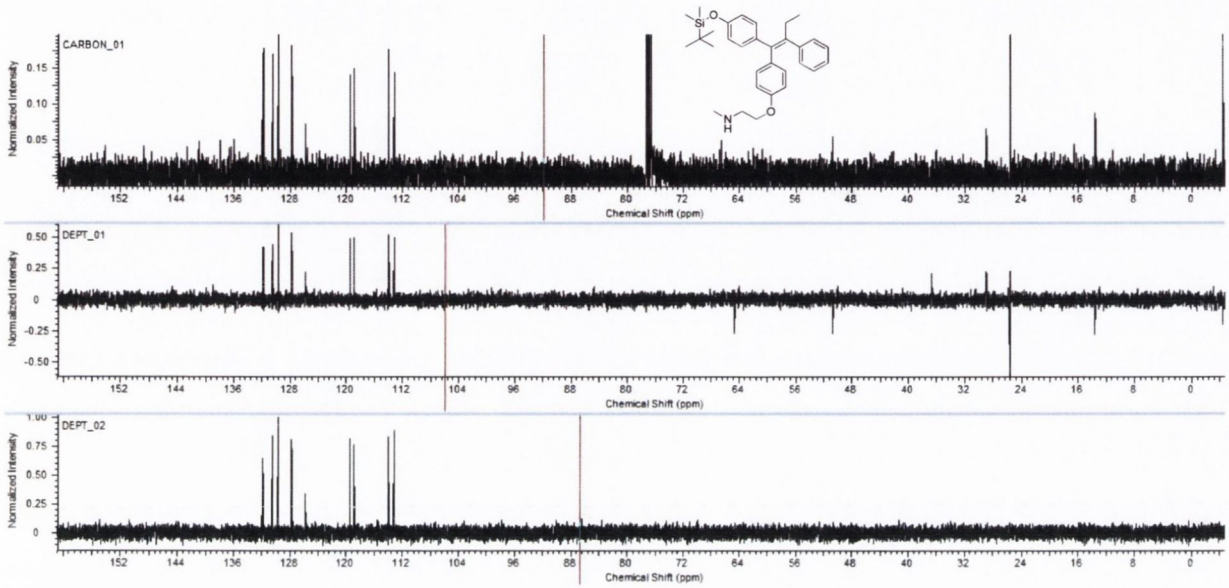

Figure 2-6 ^{13}C, DEPT 135 and DEPT 90 NMR spectrums of [197]

2.1.7.1 Isomeric mixture of the silyl-E/Z -protected endoxifen.

The formation of an isomeric mixture occurs as the carbonyl coupling step (ii) in the synthesis of endoxifen result in either *E* or *Z* configurations. This *E/Z* mixture was insepararable at all stages during the synthesis. The difficulty of purifying and separation of *E/Z* isomeric mixtures of tamoxifen derivatives and analogues into pure isomers have been well documented.[462]

The *Z* (*cis*)-isomer of 4-hydroxytamoxifen is well known to be a more potent anti-estrogen than the *E* (*trans*)-isomer[120, 463] Although *E*-isomer of 4-hydroxytamoxifen is known to be estrogenic[464] or weakly antiestrogenic[464, 465], there are several reports[120, 431, 463] that *E*-isomers could be converted readily to more potent anti-estrogenic *Z*-isomers in an *in vitro* cell system and *Z*-isomers are bound preferentially to the nuclear estrogen receptors, despite the possible conversion of *Z*- to *E*-isomer. This could explain why *E/Z*-4-hydroxytamoxifen has similar anti-estrogenic action to the pure *Z*-isomers analogues. For 4-hydroxytamoxifen, the *E/Z* isomers interconvert *in vivo,* and so can be progressed as an isomertic mixture without effect on the anti-estrogenic actions of compounds.[466] Therefore, the *E/Z* isomer mixture of [197] obtained in the present work will be used without further separation in the formation of the subsequent conjugates (Figure 2-7). Deprotection of [197] would afford the endoxifen compound [36]; however the subsequent coupling/ conjugation reactions required the TBDMS protecting group to be retained (see Chapter 5).

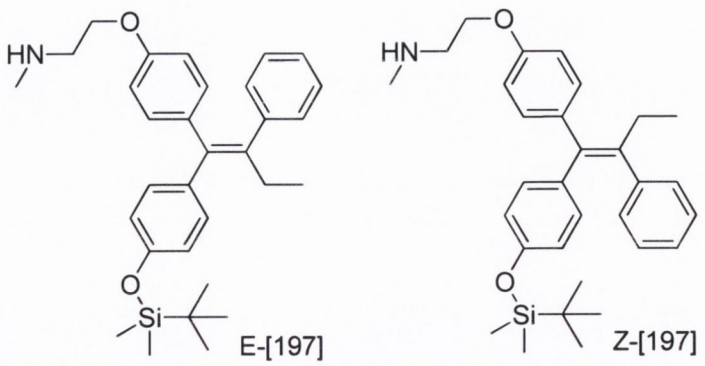

Figure 2-7 *E*-and *Z*- isomers of [197]

2.2 Synthesis of cyclofenil-based analogues

The anti-estrogen cyclofenil diphenol (F6060) is generally used as a stimulant of ovarian function. Cyclofenil and its derivatives have high binding affinity for ER, often comparable to/or greater than that of estradiol, and 4,4'-((4-methylcyclohexylidene)methylene)diphenol [200] showed the highest ERβ to ERα ratio.[467] Notably, it has mixed agonist-antagonist activity typical for a nonsteroidal selective ER modulator such as tamoxifen or raloxifene.[468, 469] F6060 and analogues have been shown to inhibit [35S]proteoglycan synthesis[470] and induce fragmentation of the Golgi apparatus into small vesicles[471] in cultures of Swarm chondrosarcoma chondrocutes. Tamoxifen is also a potent inhibitor of [35S]proteoglycan synthesis. Seo *et al.* reported good ER-subtype binding and selectivity in a number of cyclofenil analogues.[469] The best reported ER-binding results were for the three cyclofenil analogues [198], [199] and [200] shown in Table 1.

		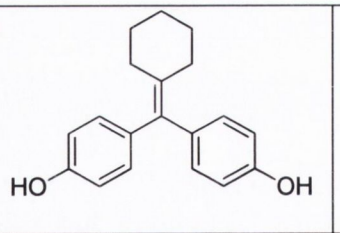	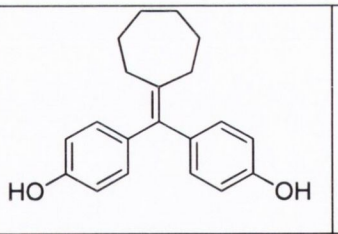	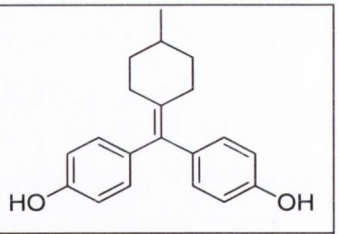
		[198]	[199]	[200]
RBA (E_2=100)	ERα	124	110	66.5
	ERβ	285	354	274
β/α		2.3	3.2	4.1

Table 1 Cyclofenil analogues[469]

In the present study, the cyclofenil analogues chosen for synthesis retain the cycloalkyl group of the cyclofenil parent structure, while in addition, include the basic side chain moiety of the endoxifen parent structure [36]. Unlike the previous synthesis of the triarylethylene scaffold for the endoxifen analogues, the use of closed ring systems eliminates any issue of *E*- and *Z*- isomers. It was envisioned that the elimination of the *E/Z* isomers could lead to a simpler purification step and

would result in a less complex NMR spectra. The synthetic route is similar to that employed for the synthesis of the endoxifen analogue [197] (see Scheme 2-15). The benzophenone [194] was reacted with the appropriate cyclic ketone (cyclopentanone [201], cyclohexanone [202], cycloheptanone [203], cyclooctanone [204] and 4-methylcyclohexanone [205]) in the McMurry reaction to give the compounds [206]-[210] respectively. Compounds [206]-[210] then undergo an ethylbromination reaction to give [211]-[215]. Following an amination reaction step, analogues [216]-[220] are afforded. Compounds [216]-[220] will be used in the formation of novel conjugates later in Chapter 5. Compounds [216]-[220] are also deprotected to afford the endoxifen-type cyclofenil analogues [221]-[225] (Table 2).

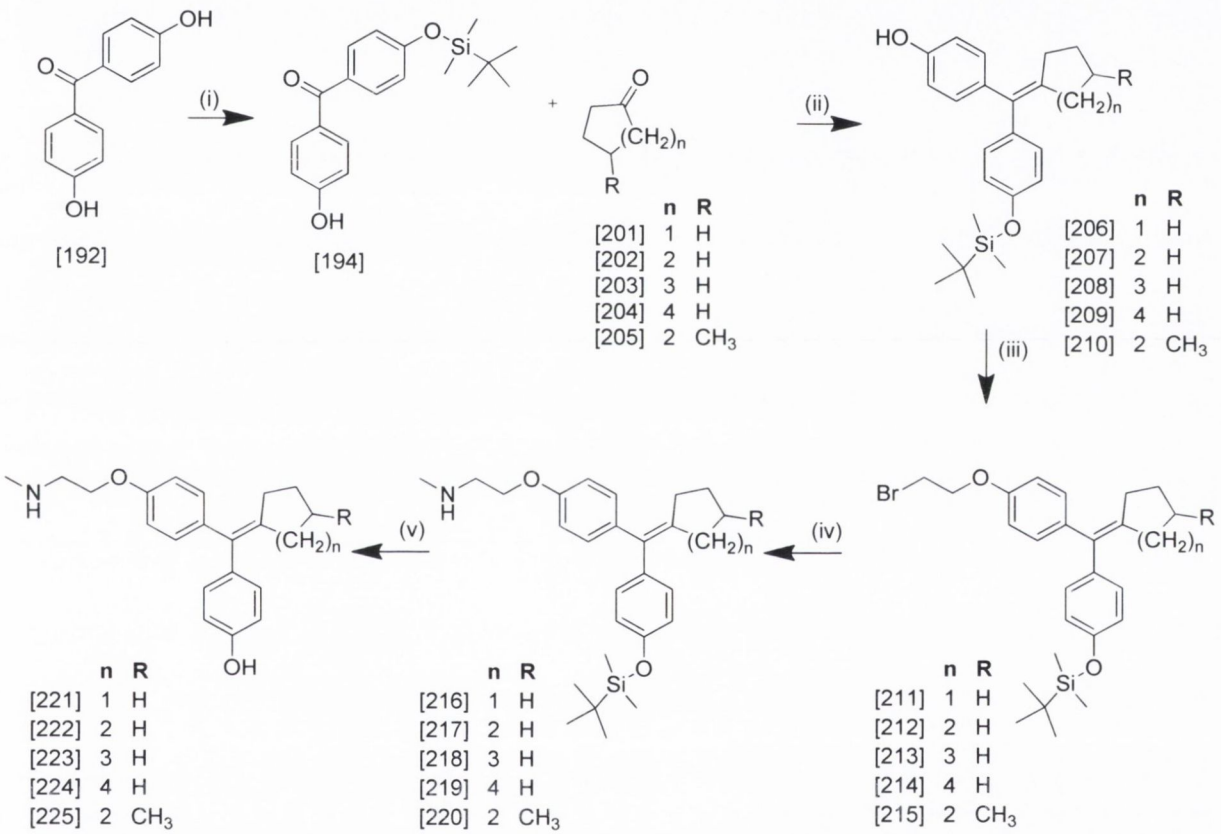

(i) TBDMSCl, imidazole, DMF; (ii) Zn, $TiCl_4$; (iii) $Br_2(CH_2)_2$, NaOH (aq.), $(nBu)_4NHSO_3$, DCM; (iv) $MeNH_2$, sealed tube, 60 °C; (v) TBAF, THF

Scheme 2-15 Synthesis of cyclofenil-endoxifen analogues [216] - [225]

In general, the reaction yields compared well to those yields obtained for the previous endoxifen analogues discussed in Section 2.1.3. The ^{1}H-NMR spectra for this series of intermediates and analogues [221]-[225] were more defined due to the absence of overlapping *E/Z* isomeric proton signals. In the ^{1}H-NMR spectrum of [222] (Figure 2-8), the CH_2 protons from the cycloalkane ring appears as two multiplets at 1.54 and 2.16 ppm which integrate for 6 and 4 hydrogens respectively. The CH_2 protons from the basic side chain appear as two triplets at 2.80 and 3.97 ppm

with *J*= 5.5 and 5.6 Hz respectively. The amine methyl protons appear as a multiplet which integrates for 3 hydrogens between 3.15-3.19 ppm. The aromatic protons appear between 6.66-6.83 ppm. The secondary amine proton is not visible in this spectrum.

Starting Material	Yields (%) + Compound ID			
	McMurry	Ethylbromination	Amination	Deprotection
Cyclopentanone [201]	97 % [206]*	93 % [211]*	82 % [216]*	73 % [221]*
Cyclohexanone [202]	87 % [207]*	91 % [212]*	86 % [217]*	78 % [222]*
Cycloheptanone [203]	84 % [208]*	94 % [213]*	90 % [218]*	81 % [223]*
Cyclooctanone [204]	89 % [209]*	94 % [214]*	84 % [219]*	78 % [224]*
Methylcyclohexanone [205]	86 % [210]*	90 % [215]*	80 % [220]*	82 % [225]*

Table 2 Endoxifen-cyclofenil analogue reaction yeilds (*=novel compound)

In the ^{13}C-NMR spectrum (Figure 2-9), the various CH_2 peaks of the cyclohexyl ring and the methyl carbon signal are observed between 23.5-36.6 ppm. The basic side chain carbons are identified at 50.8 (NCH_2) and 67.5 ppm (OCH_2). The aromatic carbons are observed between 114.3-137.0 ppm while the carbons adjacent to the oxygen are found at 157.0 and 157.3 ppm. In the IR spectrum, the hydroxyl group is observed as a broad band at 3438.2 cm^{-1}. The characterisation of [122] was confirmed through HRMS where a mass of 338.2104 $(M+H)^+$ was found for the required molecular ion $C_{22}H_{28}NO_2$.

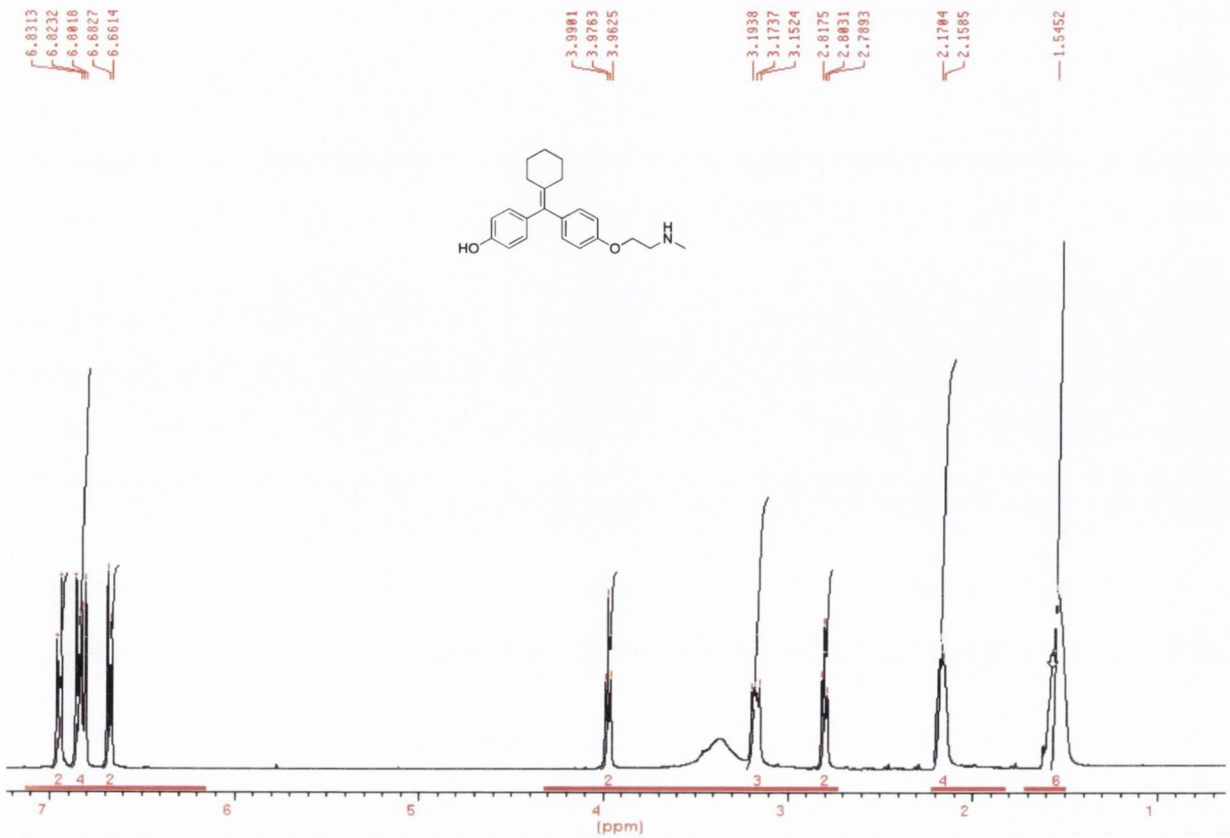

Figure 2-8 ^{1}H-NMR spectrum of [222]

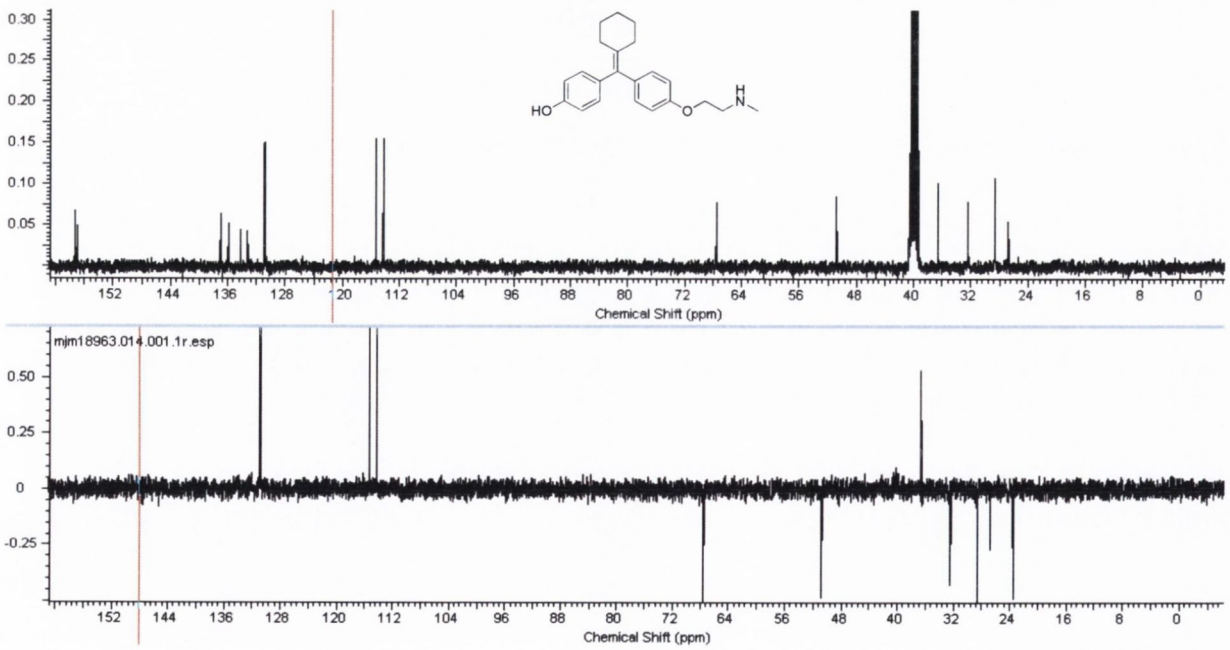

Figure 2-9 ^{13}C and DEPT135 NMR spectras of [222]

2.3 Synthesis of 2-phenylindole-based analogues

Another ER-ligand of interest within the scope of the project is conjugate formation with the 2-phenylindole based SERM bazedoxifene acetate [50] (WAY-140424, TSE-424).[472] This indole-based ER ligand has unique structural characteristics with respect to tamoxifen [34] and raloxifene [45], and was specifically selected to ensure an improved profile when compared to the older classes of SERMs.[111, 473, 474] Bazedoxifene exerts significant estrogenic and antiestrogenic activity, both *in vitro* and *in vivo*, targeting any tissues that possess ERs, such as bone, uterus, breast, blood vessels, and liver. This SERM binds to both ERα and ERβ, with a slight higher affinity for ERα.[472] The molecule was designed by using raloxifene as a template and substituting an indole ring for the benzothiophene core.[475] Many related 2-phenylindoles have shown pharmacological activity and the covalent attachment of various aminoalkyl substituents provided products with good ER binding. The 2-phenylindoles have been evaluated as inhibitors of mammary tumour growth. Selected 2-phenylindoles (see Figure 2-10) have been discovered to bind selectively to ERα over ERβ. Compound [226] for example has a relative binding affinity (RBA) of 2.17 in ERα and 0.24 in ERβ. Compound [227] has a RBA value of 0.314 in ERα and ERβ. RBA values are given with respect to estradiol which is given a RBA value of 100.

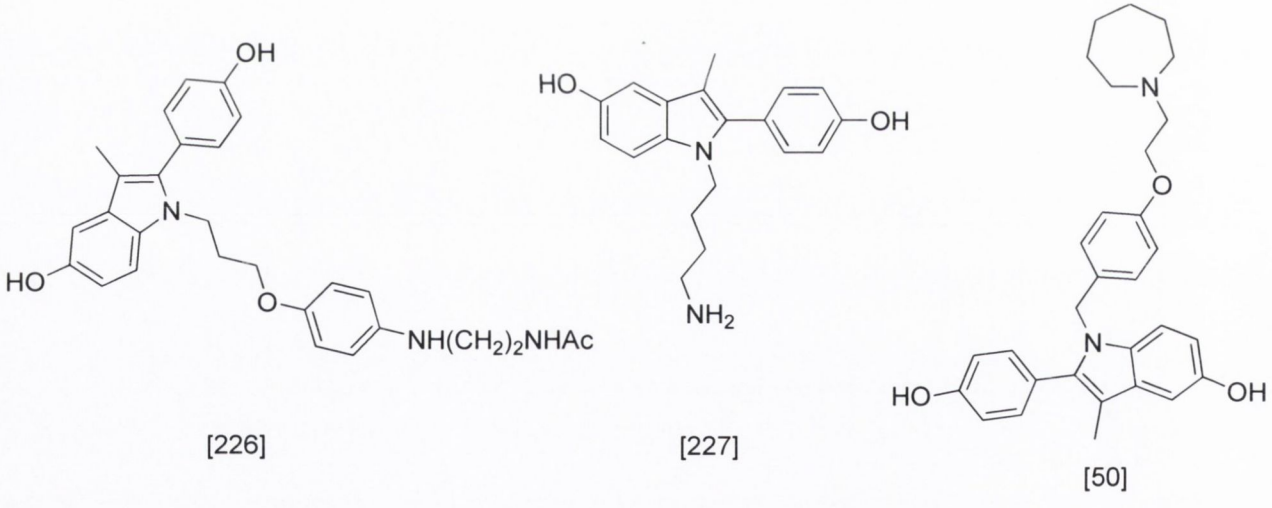

[226] [227] [50]

Figure 2-10 2-Phenylindoles with biological activity

It has been found that various 2-phenylindoles with an *n*- alkyl substituent show moderate to strong affinity for the ER.[476] It was also reported that a methyl or ethyl substituent at position 3 of the indole nucleus and an ethyl or propyl substituent on the indole nitrogen is the most favourable structure for estrogen binding. When the *n*-alkyl chain was increased to more than 3 carbons in length a decrease in affinity was observed. The phenylindoles also displayed estrogenic and antiestrogenic affects. These phenylindoles were found to be weak estrogen receptor agonists with

antagonistic activity due to prevention of endogenous estradiol binding to the receptor. Mammary tumour growth was also shown to be inhibited as shown by studies in rats.[476] The introduction of a terminal amino group was discovered to possess anti-estrogen activity. The introduction of an amino alkyl group also leads to increased binding affinity and loss of agonist activity in some cases.[477] The use of phenylindole conjugate to deliver the cytotoxic agents to breast cancer tumours was developed as far back as 1988 when Von Angerer et al developed phenylindole-platinum conjugates. They found binding affinity was only slightly decreased using a conjugate when compared to the phenyl-indole itself.[478] The position of hydroxyl groups is an important feature with respect to SAR of the 2-phenylindoles. These two phenolic groups are shown to overlap with the two phenols of estradiol when examined using flexible alignment (see Figure 2-11). Structure activity relationships for estradiol have been extensively studied. The aromatic A ring and C_3 hydroxy group are essential for estrogenic activity. The 17β-hydroxyl and the distance between the C_3 and C_{17} groups are also important for activity. Ideally the distance between the oxygen atoms of C_3 and C_{17} should be between 10.3 and 12.1 angstroms (Å).[479] The distance between the 2-phenylindole hydroxyl groups was shown to be 11.54 Å which is within the range of 10.3-12.1 Å required for estrogen receptor activity. The 2-phenylindole also possesses an aromatic A ring similar to that seen in estradiol. Therefore the 2-phenylindole combines all the key structural requirements for binding to the estrogen receptor.

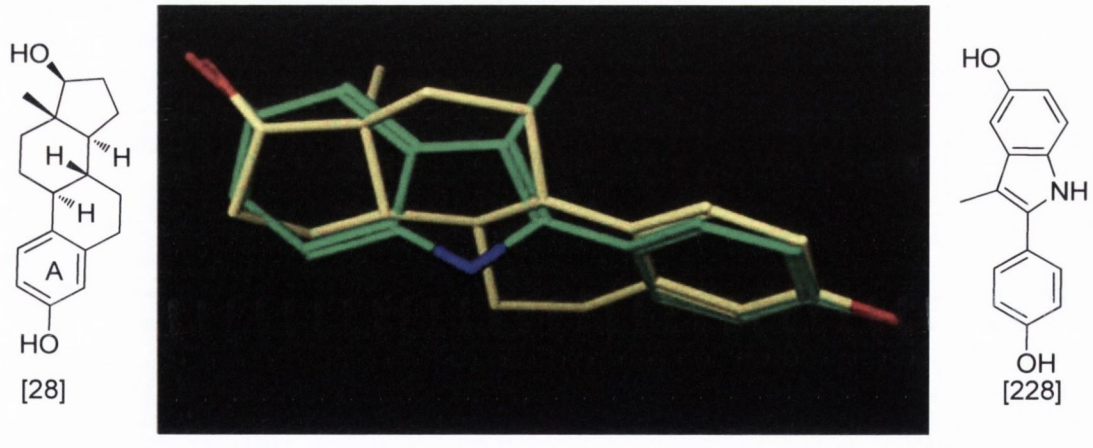

Figure 2-11 Flexible alignment of 2-(4-hydroxyphenyl)-3-methyl-1H-indol-5-ol [228] (green) and estradiol [28] (yellow)

In the present study, the corresponding 2-phenylindole analogues synthesised will contain the indole core from bazedoxifene but the basic side chain will be similar to that of tamoxifen. The 2-phenylindole analogues also contain the two phenols essential for binding to the ER but are initially protected as methoxy ethers which can be cleaved at a later stage to afford the free phenols. The synthetic route for the synthesis of the 2-phenylindoles analogue is shown in Scheme 2-16.

2.3.1 Synthesis of the indole core

The first step in the synthesis of the required 2-phenylindole analogues was the preparation of the indole scaffold *via* the Fischer indole synthesis using 4-methoxyphenylhydrazine hydrochloride [230] and 4-methoxypropiophenone [229] (Scheme 2-16). The Fischer indole synthesis is the most widely used route for the formation of indoles. The reaction involves the treatment of phenylhydrazine in acid with an aldehyde or ketone. The first step proposed in the mechanism is the formation of phenylhydrazone (an imine), when phenylhydrazine attacks a carbonyl group. The hydrazone then tautomerises to an enamine, which then undergoes a cyclic rearrangement with the formation of a C-C bond. Re-aromatization of the benzene ring creates an aromatic amine which immediately attacks the available imine. This gives an aminal, the nitrogen equivalent of a hemiacetal. Finally acid-catalysed elimination of ammonia gives the aromatic indole.[480, 481] The reaction mechanism is illustrated in Scheme 2-17. The 2-phenylindole synthesised was characterised using ^{1}H NMR, ^{13}C NMR, chromatography, IR spectroscopy and HRMS (75% yield).

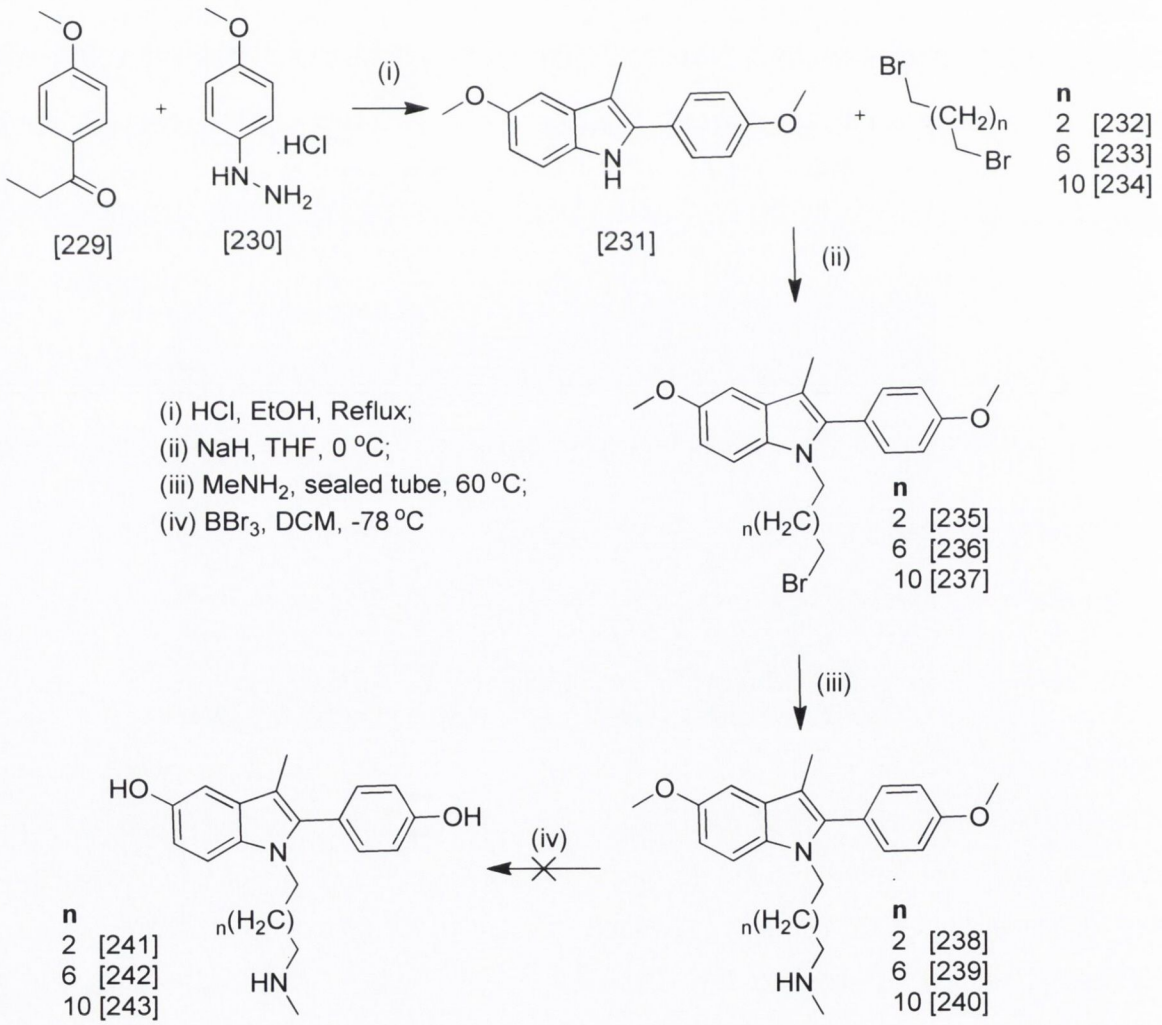

Scheme 2-16 Synthesis of 2-phenylindole analogues [229] - [243]

In the ^{1}H-NMR spectrum for [231] shown in Scheme 2-12, the large singlet at 2.44 ppm corresponds to the C-3 methyl group of the indole. The two singlet signals at 3.89 and 3.93 ppm relate to the two methoxy group protons. The signals in the aromatic region of the spectrum integrate for the 7 aromatic protons in the aromatic region. The signal furthest downfield at 7.88 ppm is assigned to the N-H proton in the indole ring. The ^{13}C NMR spectrum for [231] is shown in Figure 2-13. The first signal at 9.27ppm corresponds to the methyl group at C-3 of the indole. The two methoxy groups signals are observed at 54.92 and 55.54 ppm respectively. The signals in the region 100.28 - 134.55 ppm represent the aromatic carbons. The two signals furthest downfield at 153.63 and 158.48 ppm represent the carbons bearing the methoxy group.

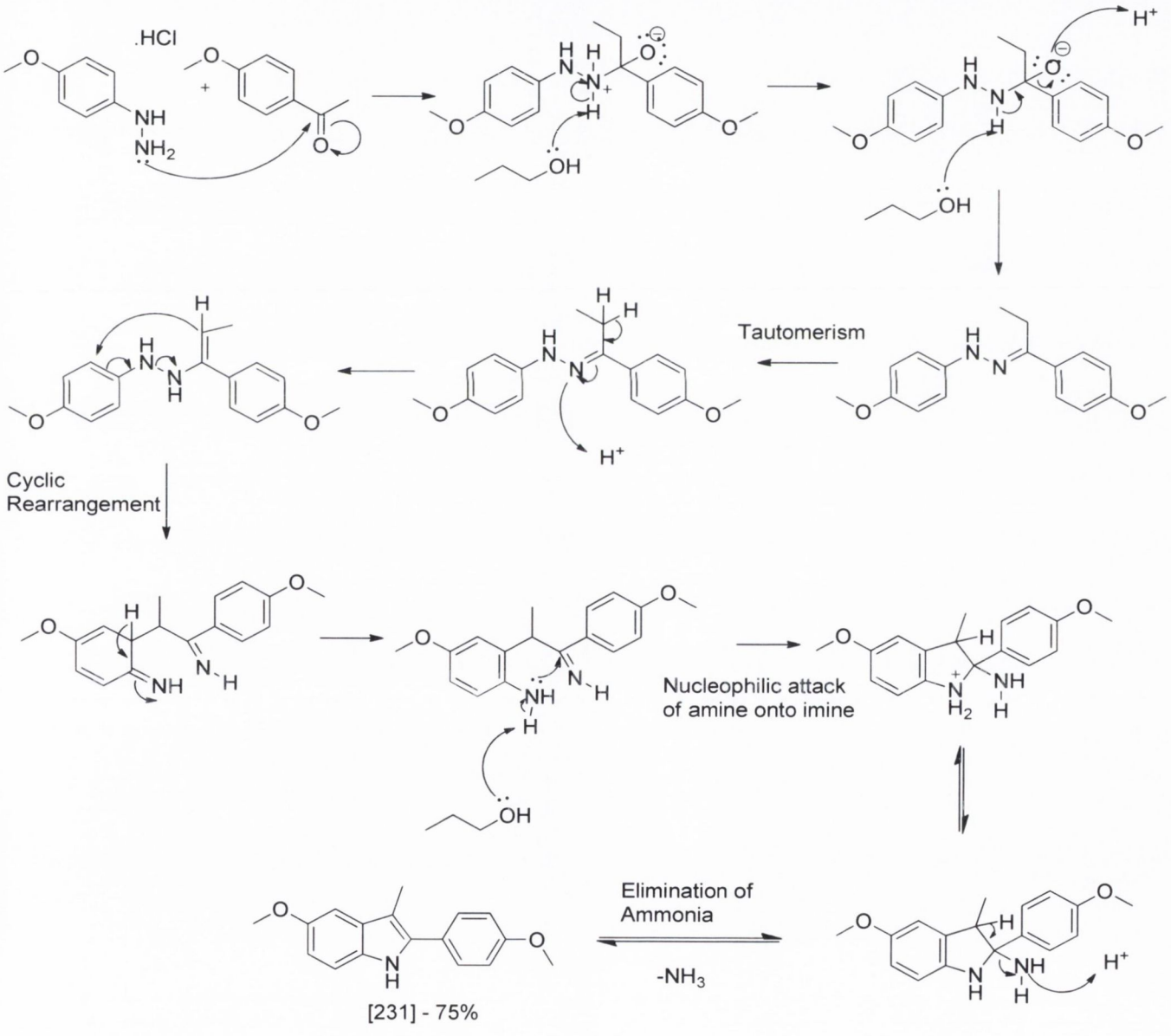

Scheme 2-17 Mechanism for Fischer indole synthesis of [231]

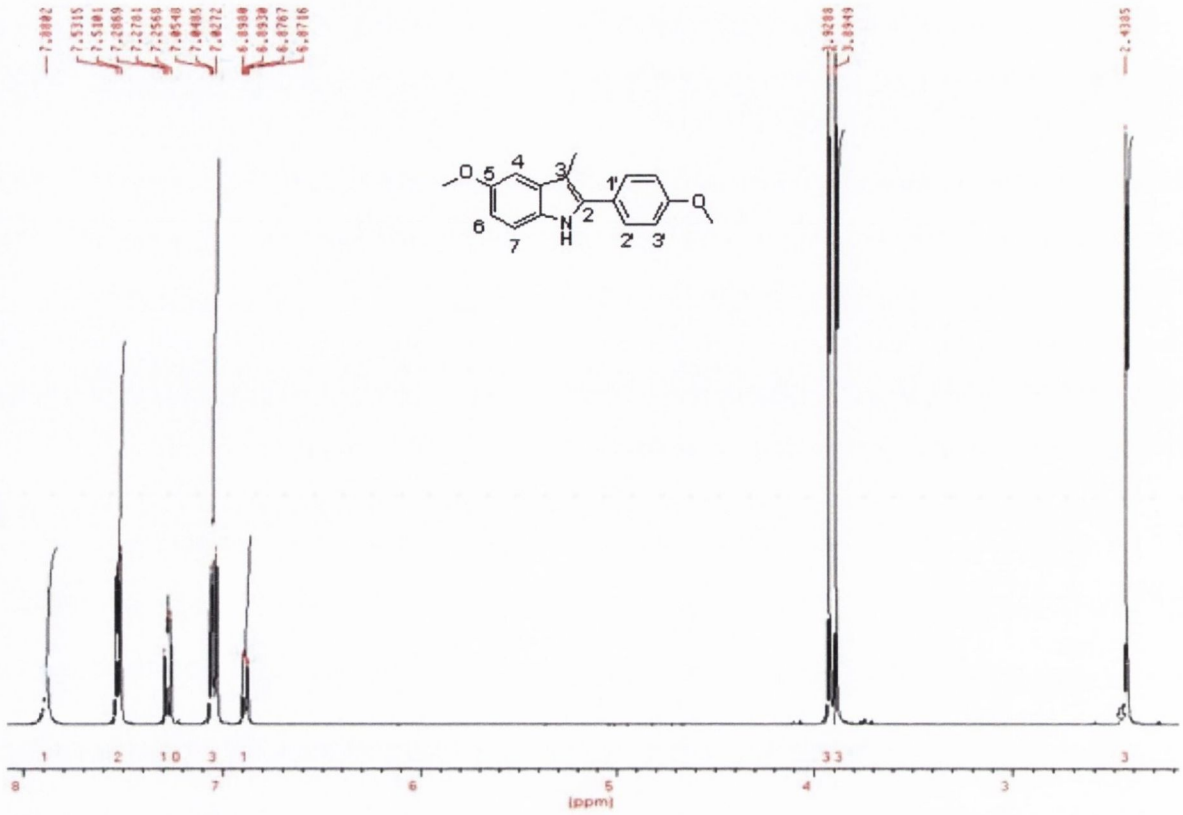

Figure 2-12 ^{1}H NMR spectrum of [231]

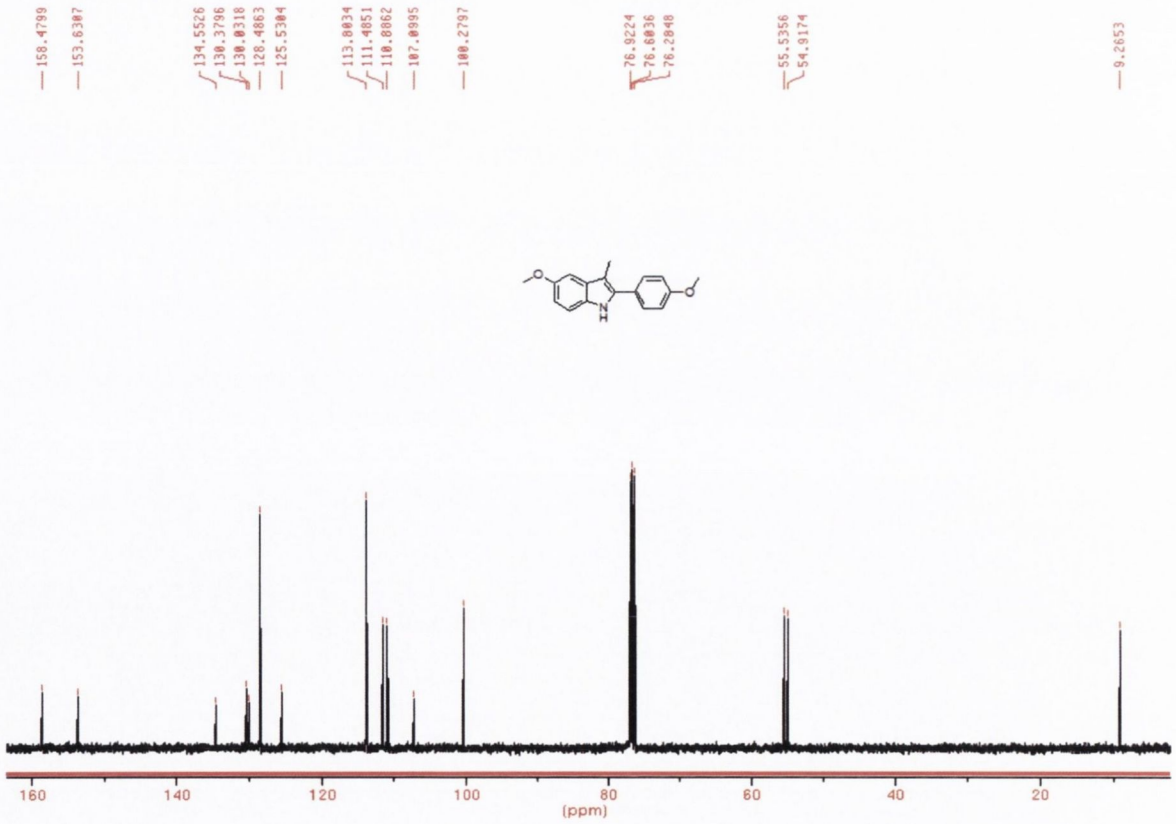

Figure 2-13 ^{13}C NMR spectrum of [231]

2.3.2 Bromoalkylation

The second step in the synthesis was the addition of a bromoalkyl chain to the indole nitrogen to afford the product [235]-[237] (see Scheme 2-18). This reaction requires the use of sodium hydride (60 % in mineral oil) in tetrahydrofuran (THF). Sodium hydride deprotonates the indole nitrogen. The anion attacks the positive dipole in the dibromoalkyl compound displacing bromine which acts as a good leaving group. The proposed mechanism for this reaction is illustrated in Scheme 2-19.

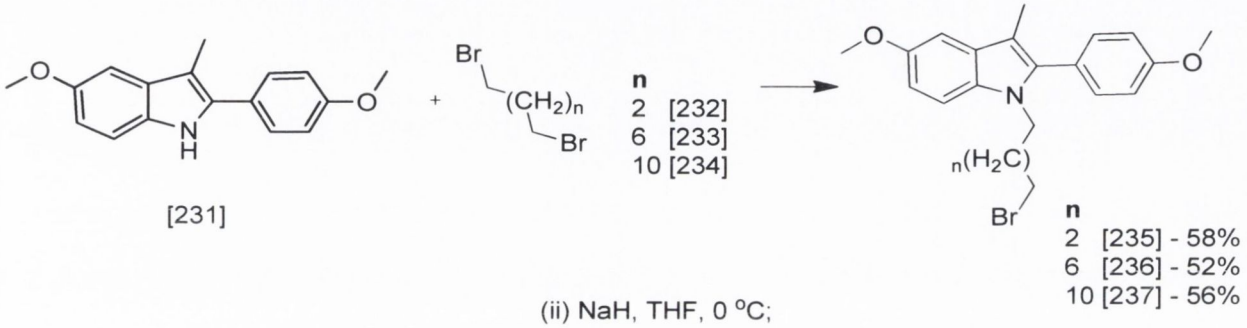

Scheme 2-18 Bromination of [231]

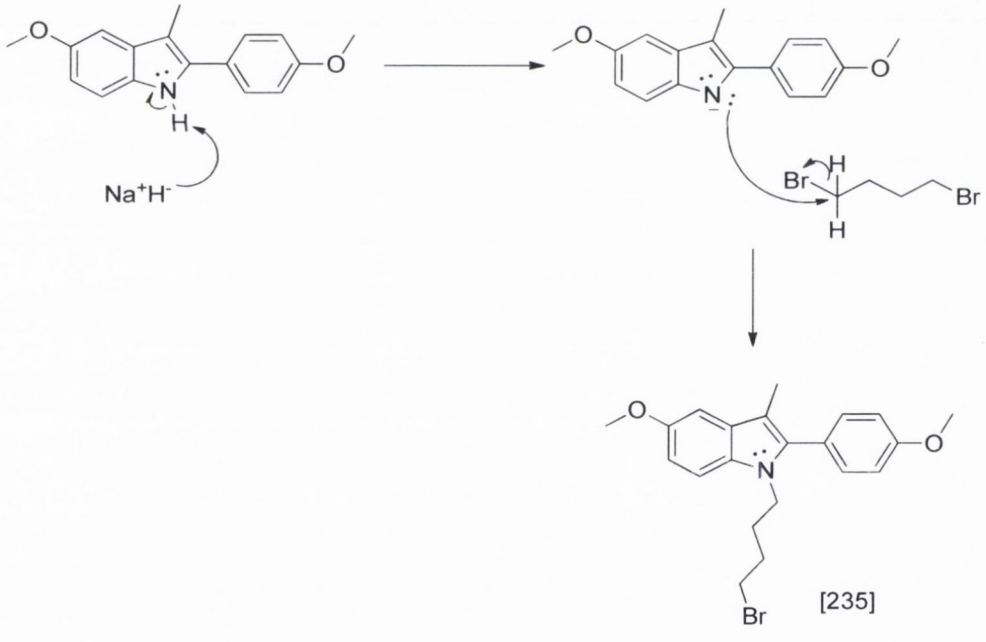

Scheme 2-19 Mechanism for bromination of [231]

The ^{1}H NMR spectrum of [235] is shown in Figure 2-14. The major difference in structure to [231] is the addition of the alkyl chain leading to 4 extra signals. The first two CH_2 signals appear as quintets at 1.63 and 1.76 ppm respectively. The CH_2 protons adjacent to the bromine are observed as a triplet at 3.20 ppm. The CH_2 adjacent to indole nitrogen is observed in this spectrum as a triplet at 4.02 ppm (J= 6.5 Hz). The ^{13}C NMR spectrum for compound [235] is shown in Figure 2-15. The

additional signals corresponding to the CH_2 of the alkyl chain are clearly seen in the DEPT 135 and appear at 28.09, 29.32, 32.61 and 42.42 ppm.

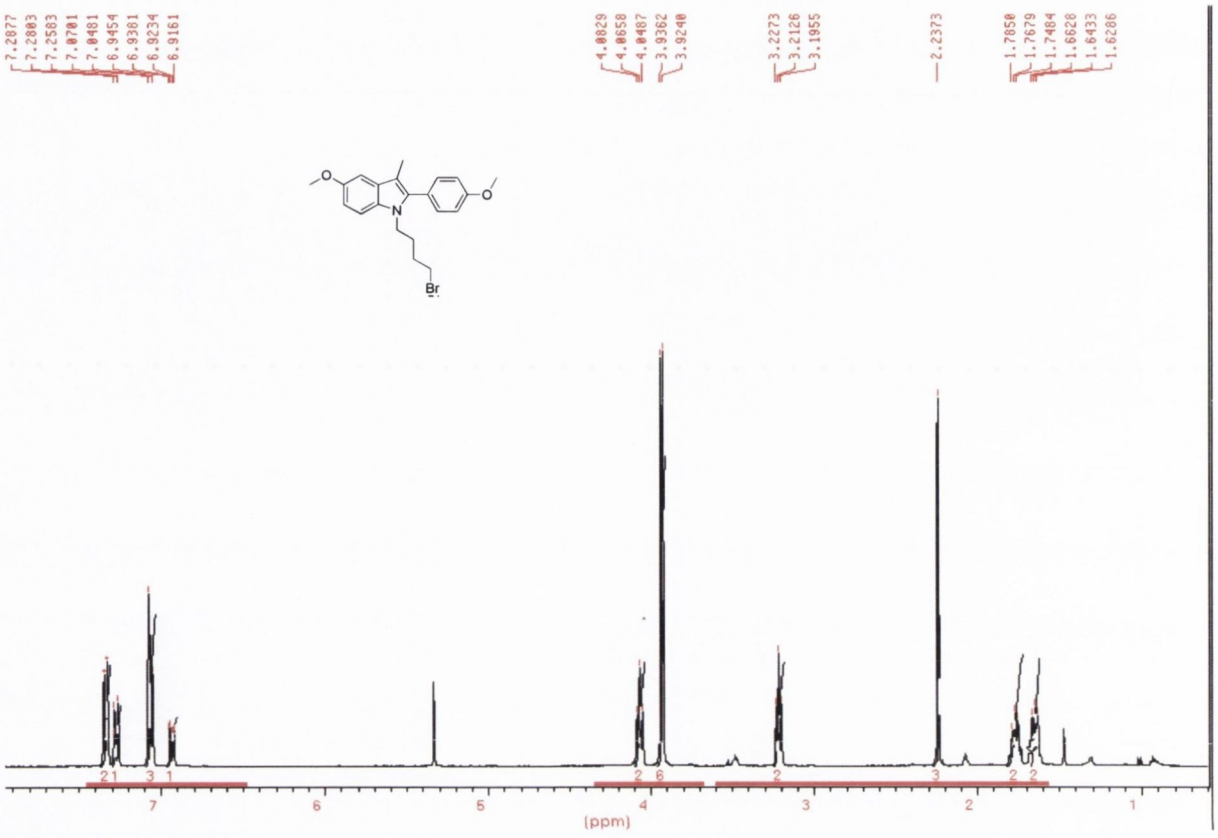

Figure 2-14 ^{1}H NMR spectrum of [235]

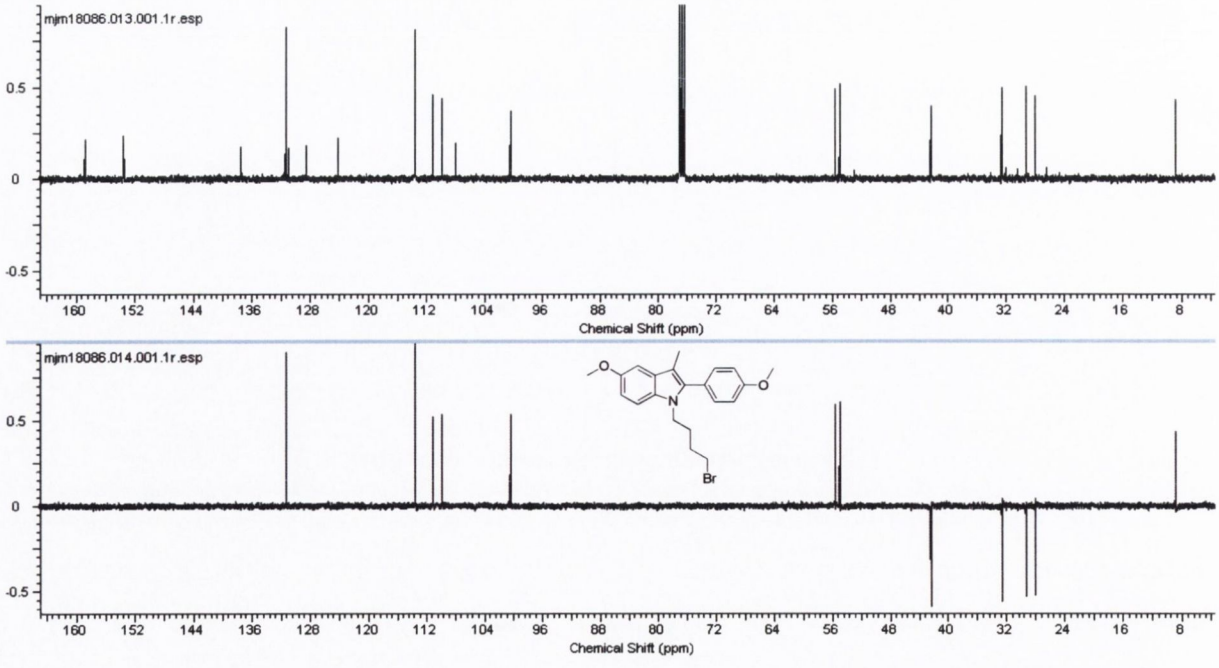

Figure 2-15 ^{13}C NMR spectrum of [235]

2.3.3 Amination reaction

The third step is the amination of the alkyl bromide using methylamine. This reaction is similar to the one employed for the synthesis of the endoxifen analogue [197]. This reaction is achieved by treatment of the bromides [235]-[237] with methylamine under pressure in a sealed tube to afford products [238]-[240] respectively in good yield (Scheme 2-20).

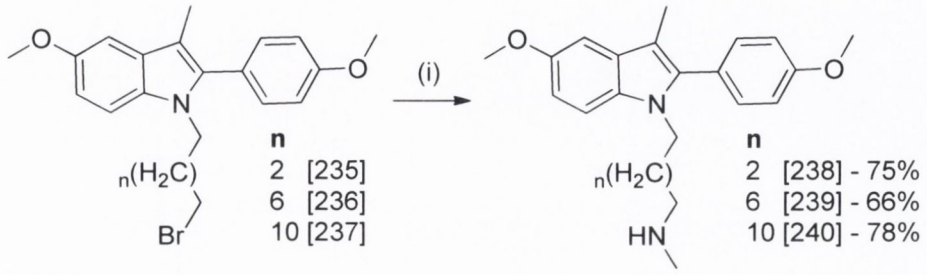

(i) NH_2Me, THF, 65 °C, 48 h

Scheme 2-20 Amination reaction to afford products [238]-[240]

The ^1H NMR spectrum for [238] is shown in Figure 2-16. The ^1H NMR spectrum of [238] is similar to it precursor (the brominated 2-phenylindole [235]) except the protons adjacent to the alkyl nitrogen, which were adjacent to the bromo group in [235] now has an upfield shift (2.42 ppm compared to 3.20 ppm). The methyl group adjacent to the secondary amine appears as a singlet at 2.35 ppm. In the ^1H NMR spectrum 7 aromatic protons are observed as before together with the singlet signals for the methoxy and methyl group protons. The ^{13}C NMR spectrum for compound [238] is shown in Figure 2-17. The ^{13}C NMR spectrum of [238] again is very similar to the spectrum for the brominated 2-phenylindole [235]. The only main difference is that the chemical shift for the methylene carbon next to the alkylated nitrogen is observed at 43.17 ppm compared to 32.61 ppm for the carbon next to bromine in [235]. There is also a signal at 35.68 ppm for the methyl group.

2.3.4 Demethylation

It is possible to cleave the methoxy ether of [238]-[240] to afford the phenols [241]-[243] using boron tribromide. Since compounds [238]-[240] contain two methoxy groups, one on each of the phenyl rings, it was desired to perform such a reaction on these compounds. This is because the free hydroxyl groups are essential for ER ligand binding. Boron tribromide acts as a Lewis acid which forms a complex with the methoxy group (Scheme 2-21). Hydrolysis is carried out using excess methanol to cleave the boron complex and quench any excess boron tribromide present in the reaction mixture.

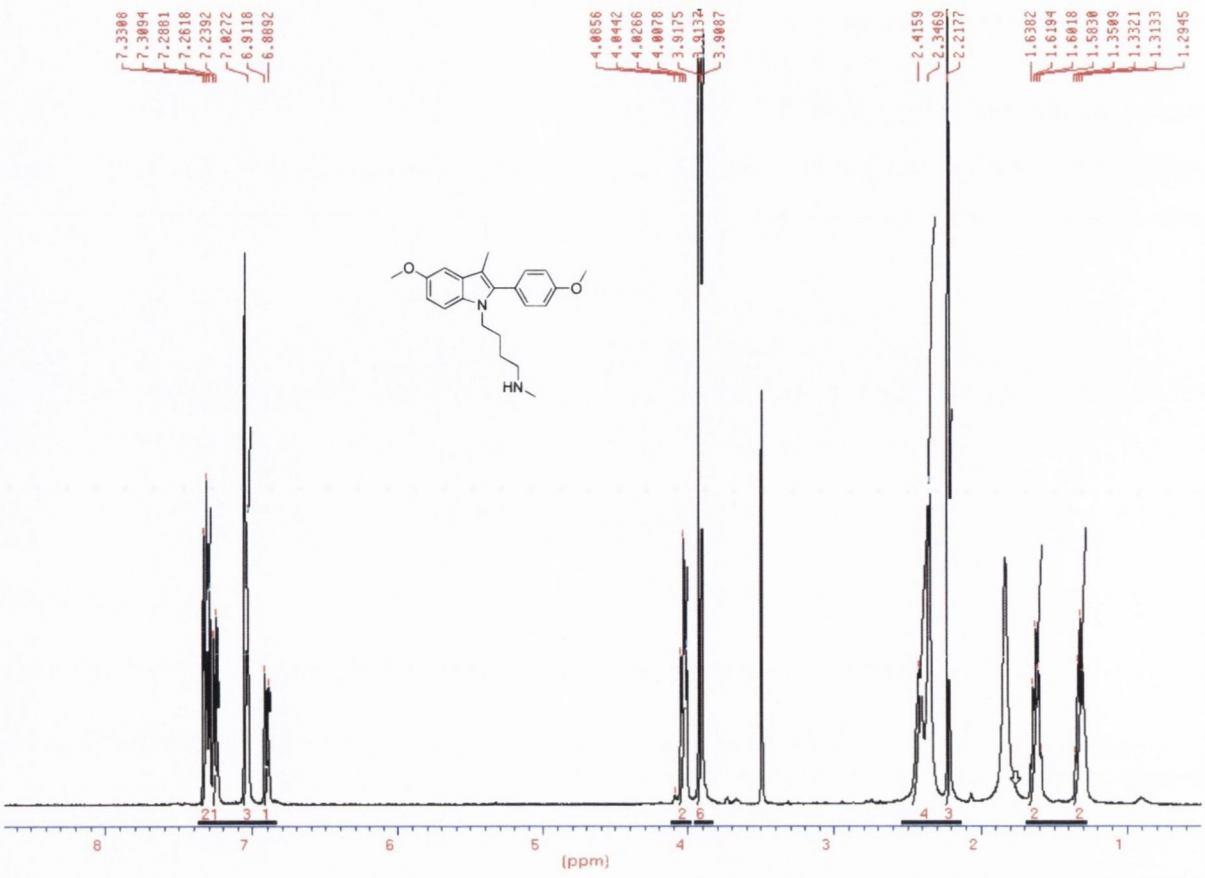

Figure 2-16 ^{1}H NMR spectrum of [238]

In the case of the methoxy ether containing compound, [238] the cleavage of the methoxy ether group was successful but only in trace amounts of the desired product [241]. When the reaction mixture was monitored *via* TLC and the starting material remained constant except for the formation of a faint product with a lower R.F. Following chromatography the isolated material was examined by mass spectrometry which confirmed the formation of the demethylated compound [241] (Found 325.1916 $(M+H)^+$, $C_{20}H_{25}N_2O_2$ requires 325.1911). This reaction was repeated for [239] and [240], similar results were observed. It was then decided to protect the hydroxyl group using benzyl protecting group as it could be removed with a hydrogenation to afford the free hydroxyl groups required for the binding to the ER. Miller *et al.*[482] reported the synthesis of bazedoxifene [50] had been achieved with the utilization of benzyl ether protection, for this reason it was decided that the new approach could incorporate the benzyl ethers required for novel indoles in the present work. The synthetic route is similar to that employed for the synthesis of the 2-phenylindole analogue [238]-[240] (see Scheme 2-22).

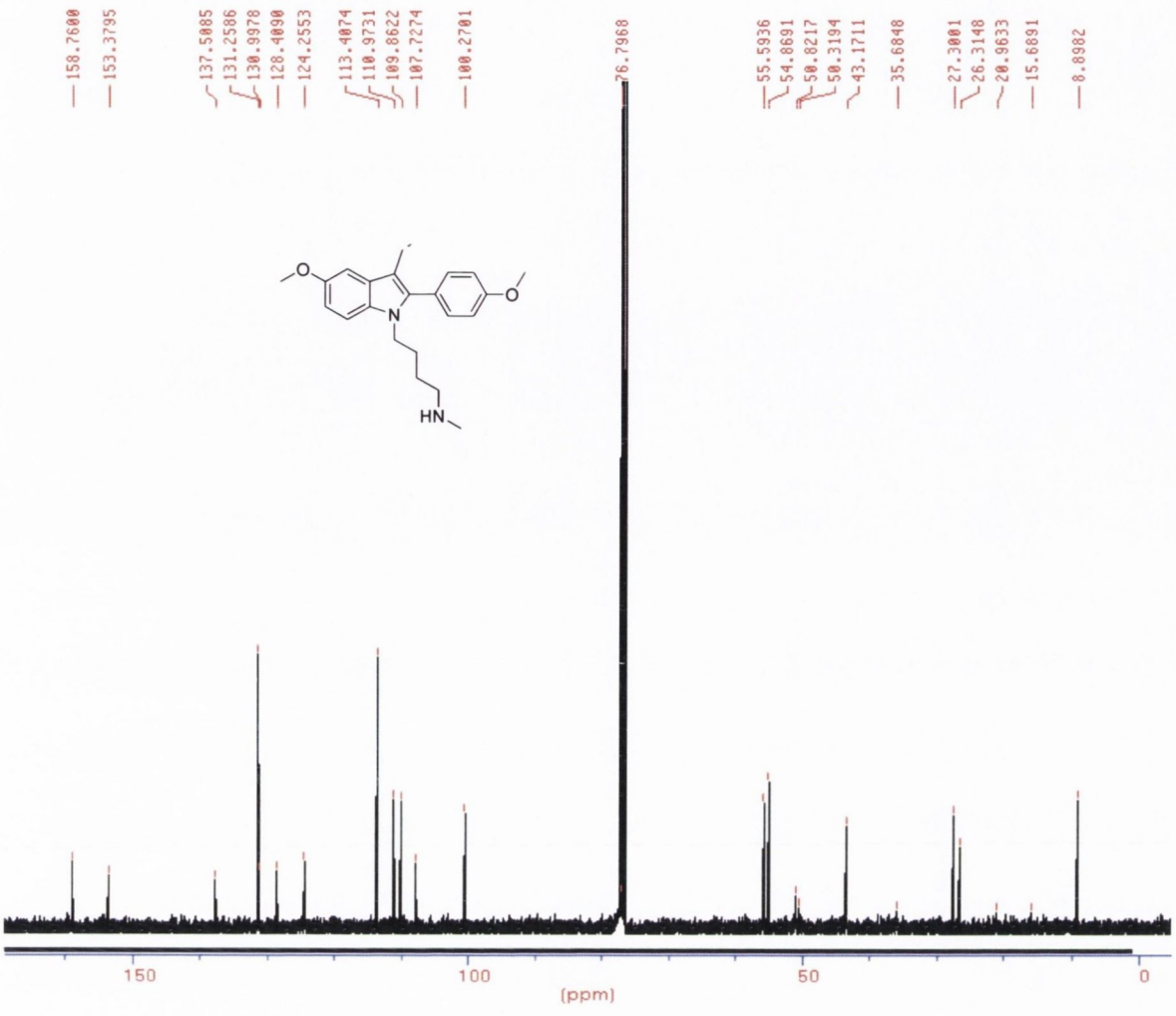

Figure 2-17 ^{13}C NMR spectrum of [238]

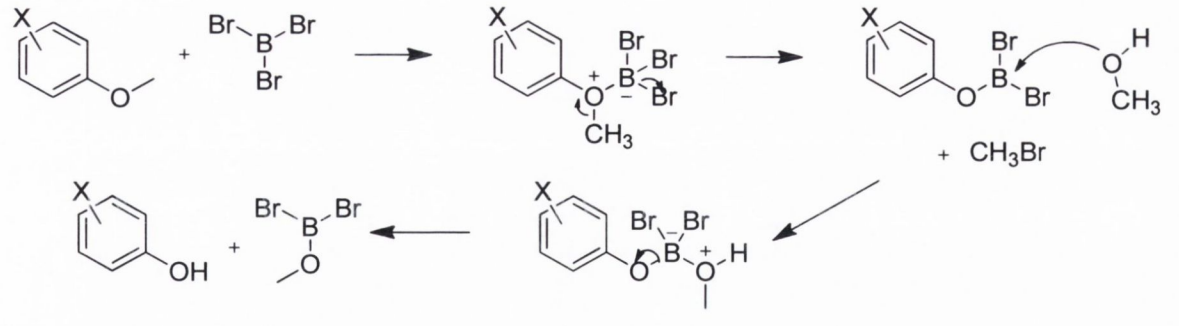

Scheme 2-21 Proposed mechanism of demethylation

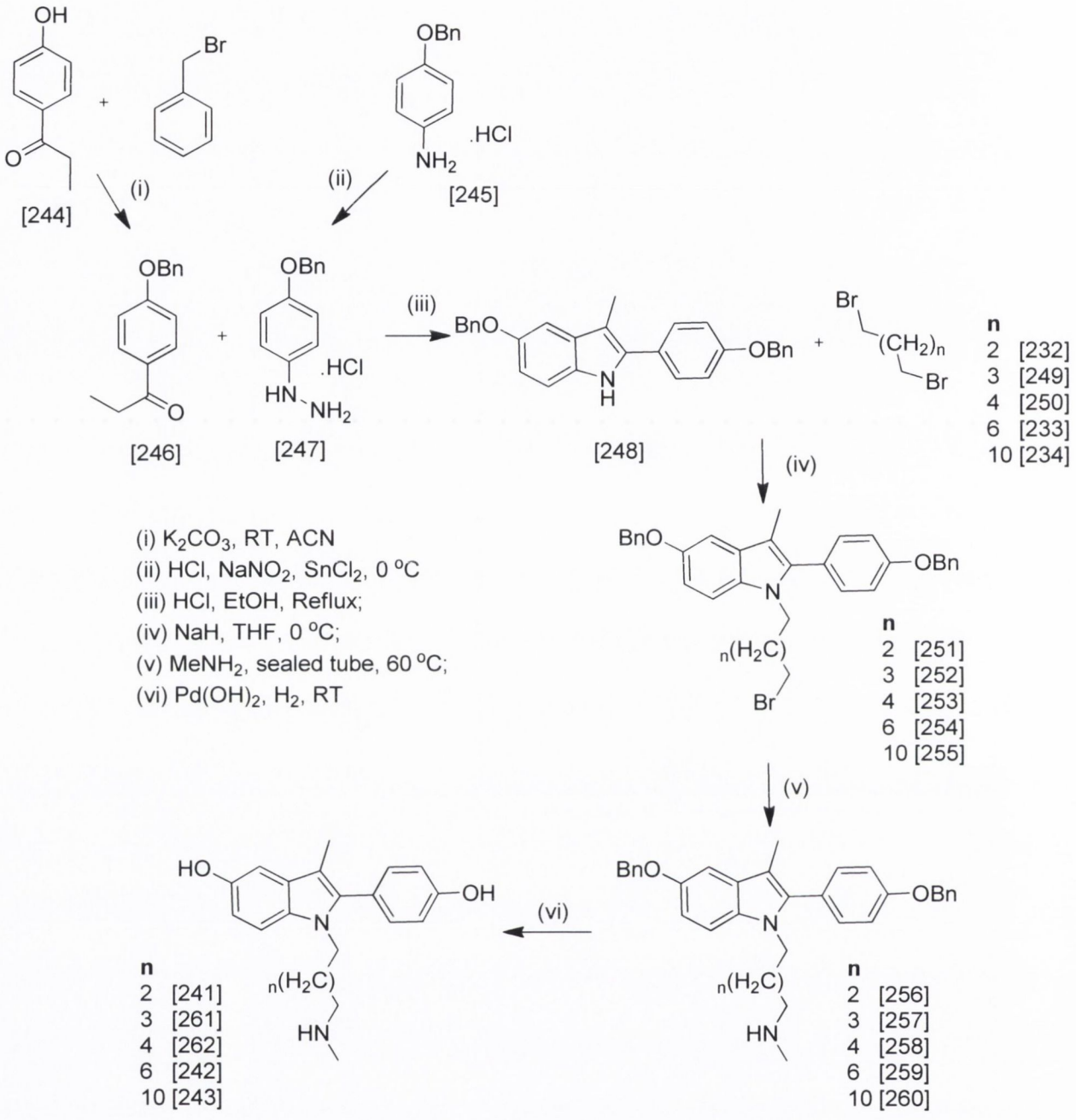

Scheme 2-22 Synthesis of 2-phenylindole analogues [241]-[243] and [261]-[262]

2.3.5 Benzylation of 4-Benzoxyprophenone [244]

The first step of the synthetic route involved is the benzylation of the 4-hydroxypropiophenone [244] to form the 4-benzyloxyprophenone [246]. In this Williamson ether synthesis, the phenoxide ion is generated first following deprotonation of the phenol using a base and subsequent reaction with benzyl bromide delivers the protected alcohol (Scheme 2-22).

2.3.6 Synthesis of 4-Benzoxyphenylhydrazine

The second step required the preparation of 4-benzyloxyphenylhydrazine [247] from 4-benzyloxyaniline hydrochloride [245]. The preparation of the [247] starts with a 4-benzyloxyaniline hydrochloride [245] which is converted into the corresponding phenylhydrazine by diazotization with $NaNO_2$ in concentrated HCl solution at low temperature and subsequently reduced with $SnCl_2$ (Scheme 2-23).

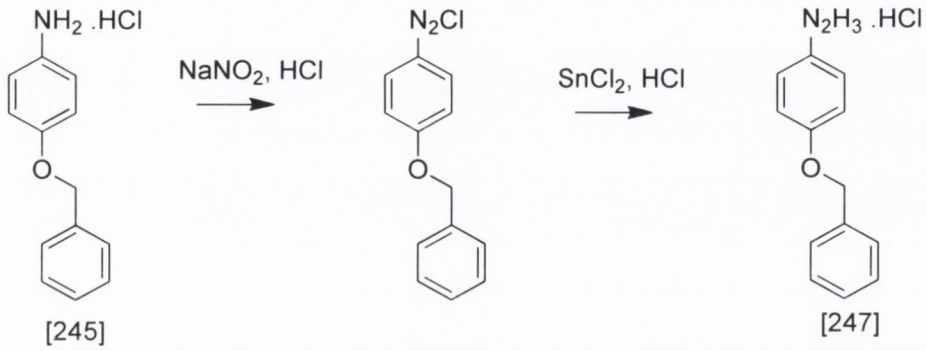

Scheme 2-23 Synthesis of 4-Benzoxyphenylhydrazine

2.3.7 2-Phenylindole derivatives with the benzyl ether protecting group

The 4-benzoxyprophenone [246] was reacted with the 4-benzyloxyphenylhydrazine [247] in a Fisher indole synthesis reaction to give the compound [248] with a yield of 84 % (Scheme 2-22). Compound [248] then undergoes the addition of the bromoalkyl reagent of varying chain length (1,4-dibromobutane [232], 1,5-dibromopentane [249], 1,6-dibromohexane [250], 1,8-dibromooctane [233] and 1,12-dibromododecane [234]) to give the products [251]-[255]. At this step two side products of interest were isolated and they will be discussed later in this chapter. Following the usual amination reaction step with methyl amine, analogues [256]-[260] are afforded. Compounds [256]-[260] will be used in the formation of novel conjugates later in Chapter 5.

2.3.8 Debenzylation of 2-phenylindoles

The synthesis required removal of the benzyl protecting groups from compounds [256]-[260] to afford ER targeting phenolic products. Compounds [256]-[260] will also be used in the formation of novel conjugates later in Chapter 5. Compounds [256]-[260] are deprotected to afford the 2-phenylindole analogues [261]-[265]. The most frequently used procedure for removal of the benzyl protecting group required a hydrogenation over Pd/C catalyst.[483] This reaction was attempted initially for 3 h and monitored *via* TLC. However after 3 h all starting material still remained. This reaction was subsequently repeated with the use of a higher surface area Pd/C catalyst (Palladium black) for the duration of a week constantly monitoring *via* TLC. The TLC showed that the majority of starting material remained. It was clear that this was not going to be a feasible deprotection method under these conditions. After a substantial review on the deprotection of benzyl group, it was

unclear why this reaction was not successful as this is the preferred route for the removal of the benzyl group. It was decided to try a pressurised hydrogenation (Parr reactor) over Pd/C.[483] The benzyl protected compound [256] was dissolved in the minimum quantity of ethyl acetate and to this solution palladium black (high surface area Pd/C, 40-60 m^2/g) was added. The reaction vessel was place under 3bar of hydrogen gas and was allowed to react for 24h. After the 24h the mixture was analysed *via* TLC, it showed the formation of a product identified as the deprotected compound [241] with a yield of 80%. Further investigation into the deprotection reaction lead to the use of another platinum based catalyst, 20 % palladium hydroxide (Pearlman's catalyst) also effective for hydrogenation and debenzylation.[484] The benzyl protected compounds [256]-[260] were dissolved in MeOH:EtOAc (1:4) (20 mL) and to this palladium hydroxide (20 %) was added. The mixture was placed under a hydrogen at 1 atmosphere and the reaction was monitored *via* TLC. After 30 min, reaction complete was achieved to afford the 2-phenylindole analogues [241]-[243] and [261]-[262] (Scheme 2-22, Table 3). In general, the reaction yields compared well to those yields obtained for the previous methoxy 2-phenylindoles analogues discussed in Section 2.3.2. The yields for the alkyl bromination step were lower and this was due to the formation of side products and this will be discussed later in this chapter.

Starting Material	Yields + Compound ID		
	Alkylbromination	Amination	Deprotection
1,4-dibromobutane [232]	63 % [251]	92 % [256]	80 % [241]
1,5-dibromopentane [249]*	65 % [252]	93 % [257]	71 % [261]
1,6-dibromohexane [250]	66 % [253]	95 % [258]	76 % [262]
1,8-dibromooctane [233]*	60 % [254]	91 % [259]	91 % [242]
1,12-dibromododecane [234]*	59 % [255]	87 % [260]	88 % [243]

Table 3 2-Phenylindole analogue reaction yields (*=novel compound)

In the ^{1}H-NMR spectrum for [241] is shown in Figure 2-18, the two CH_2 signals (2 and 3) from the alkyl chain appear as multiplets at 1.39-1.40 ppm and 1.54-1.65 ppm, the large singlet at 2.13 ppm corresponds to the methyl group at C-3 of the indole. The amine methyl protons appear as a singlet which integrates for 3 hydrogens at 2.54 ppm. The two triplet signals at 2.70 and 4.12 ppm relate to the CH_2 adjacent to the methylamine and the CH_2 adjacent to the indole nitrogen, respectively. The aromatic region of the spectrum contains signals which integrate for the 7 protons. The amine (NH) and the phenol (OH) signals were not observed in this spectrum. The ^{13}C NMR spectrum for [241] is shown in Figure 2-19. The signal at 7.6 ppm corresponds to the methyl

substituent in C-3 of the indole. The signals assigned to the CH_2 groups of the alkyl chain appear at 22.6, 26.0, 41.9 and 48.0 ppm, and these are observed as negative signal in the DEPT-135. The signal at 31.5 ppm relates to the amine methyl. The signals in the region 102.0 - 137.6 ppm represent the aromatic tertiary and quaternary carbons. The two signals furthest downfield at 149.7 and 156.7 ppm represent the chemical shift for the phenolic carbons C-5 and C-4'.

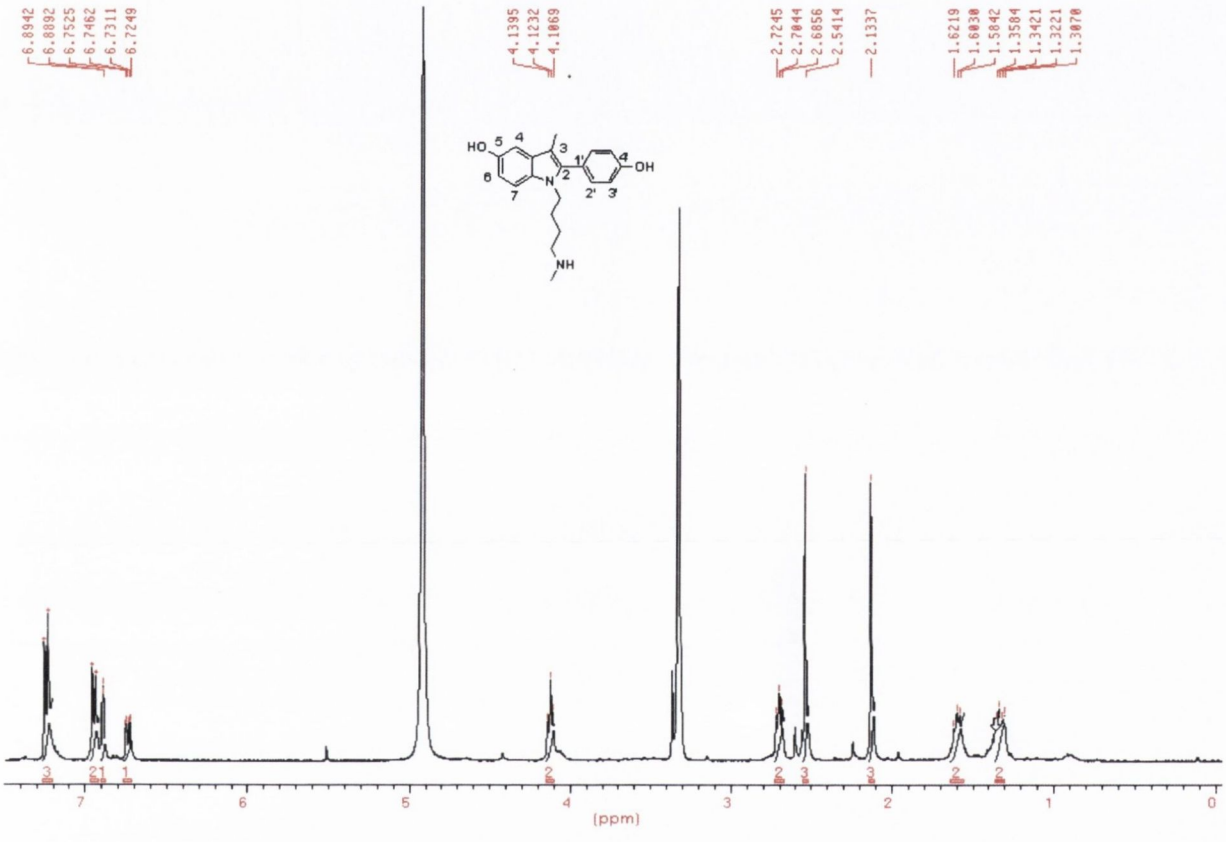

Figure 2-18 ^{1}H NMR spectrum of [241] (MeOD-d_4)

2.3.8.1 Further products isolated from the bromoalkylation reaction

When the crude product from each of the previous bromoalkylation reactions was isolated and purified using column chromatography over silica gel the alkyl bromine products [251]-[255] were afforded in yields ranging from 59-66 %. When the TLC plate were examined (*n*-Hexane:DCM, gradient 4:1 to 2:1) it showed that all of the starting material 2-phenylindole [248] had reacted and hence it would have been correct to assume that the yields would be higher (60%). Further development of the TLC on the crude mixtures using different mobile phases showed the presence of two additional products. One of the products (S1) with an Rf= 0.65 was present in moderate quantity and the second product (S2) which remained on the base line of the TLC until a strong polar mobile phase was used. Another notable characteristic of S2 was that it gave a bright blue florescence at 366 nm which was not attributed to the other indole products. In each case, isolation

and purification of S1 and S2 afforded two indole based compounds, a bis-indole S1 and a rearranged indole S2.

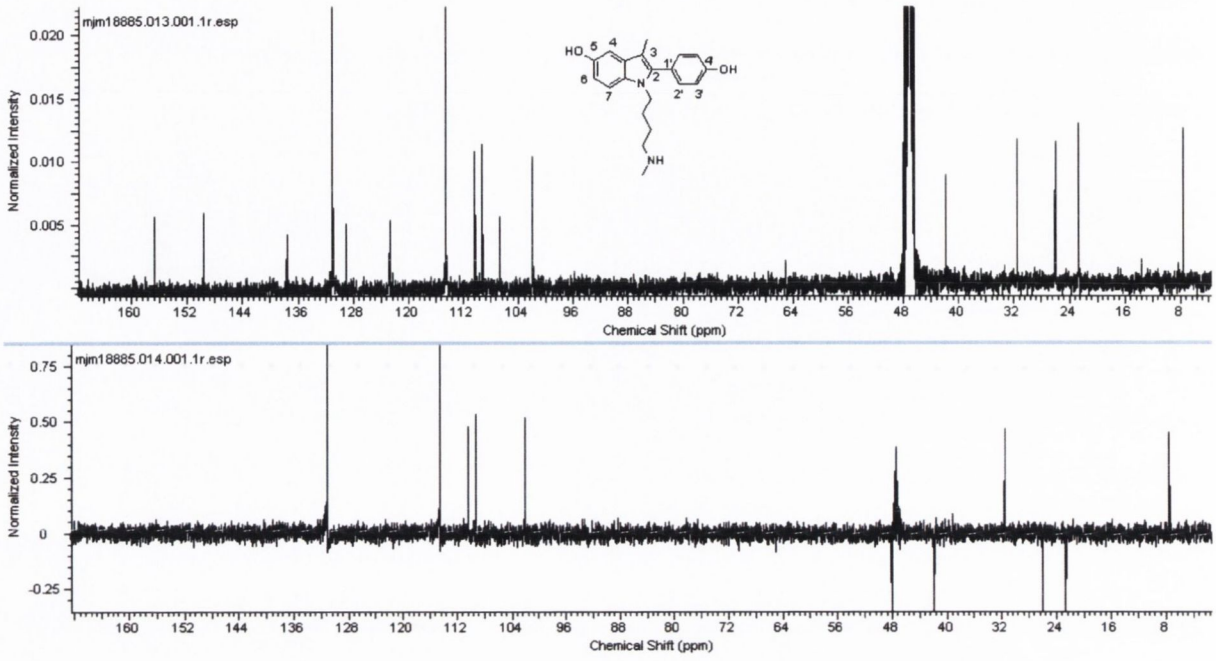

Figure 2-19 ^{13}C NMR and DEPT-135 spectras of [241] (MeOD-d_4)

The isolated by-products S1 was identified as the bis-2-phenylindole series [263]-[267]. These products are formed when further reaction of the initially formed bromo alkylated indole and a second 2-phenyindole molecule occurs in the reaction conditions to produce the bis-2-phenylindole. The identification of these compounds was performed by ^{1}H and ^{13}C NMR, and HRMS.

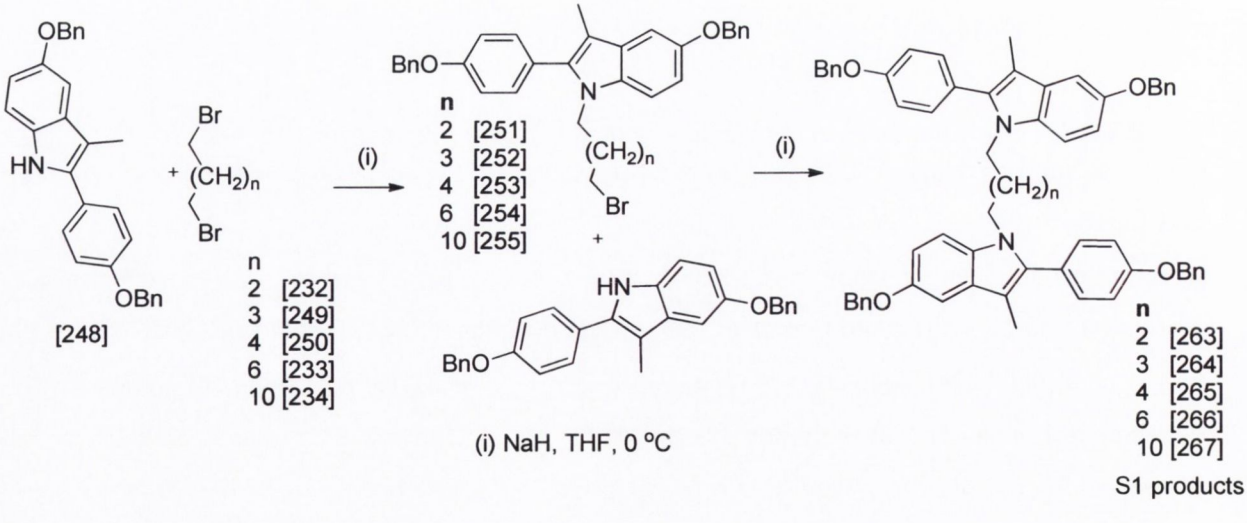

Scheme 2-24 Synthesis of by-products S1 [263]-[267]

The proton signals are easily defined in the ^{1}H-NMR spectrum of [263], shown in Figure 2-20. The signal at 1.24 - 1.37 ppm appears as a multiplet, corresponding to the two centre CH_2 groups in

the alkyl chain. The large singlet at 2.17 ppm corresponds to the methyl groups at C-3 of the indoles. The remaning two CH_2s from the alkyl chain appear as a multiplet at 3.70 - 3.86 ppm. The signals for the four CH_2s of the benzyl aryl ethers are found as two singlets at 5.13 and 5.16 ppm. The aromatic signals appear between 6.93 – 7.39 ppm. The ^{13}C NMR spectrum for [263] is shown in Figure 2-21, the signal at 8.9 ppm corresponds to the methyl group carbons at C-3 of the indoles. The signals correspond with the CH_2 of the alkyl chain appear at 26.5 and 42.6 ppm inverted in the DEPT 135 spectrum. The benzyl CH_2 groups give rise to the signals at 69.9 and 70.6 ppm. The signals in the range 101.9 - 137.4 ppm represent the aromatic tertiary carbons and quaternary carbons. The two signals furthest downfield at 152.6 and 157.9 ppm represent the chemical shift for the carbons attached to the benzyl ethers, C-5 and C-4' of the indole rings.

These *bis*-2-phenylindole compounds have an interesting structure as either of the 2-phenylindole termini could potentially bind in the estrogen receptor. The second 2-phenylindole could interact within the ER binding pocket and may exhibit enhanced ER binding activity. It has been reported that bis-indole type compounds have demonstrated cytotoxic activity in cultures of PC-3 (prostate), U251 (CNS), K562 (leukaemia), Hep-2 (Liver), HeLa (cervix), and HCT-15 (colon) cells.[485, 486] The isolated [263]-[267] compounds were deprotected, to remove the benzyl protecting ethers, and affording the free phenolics which are essential for ER binding.

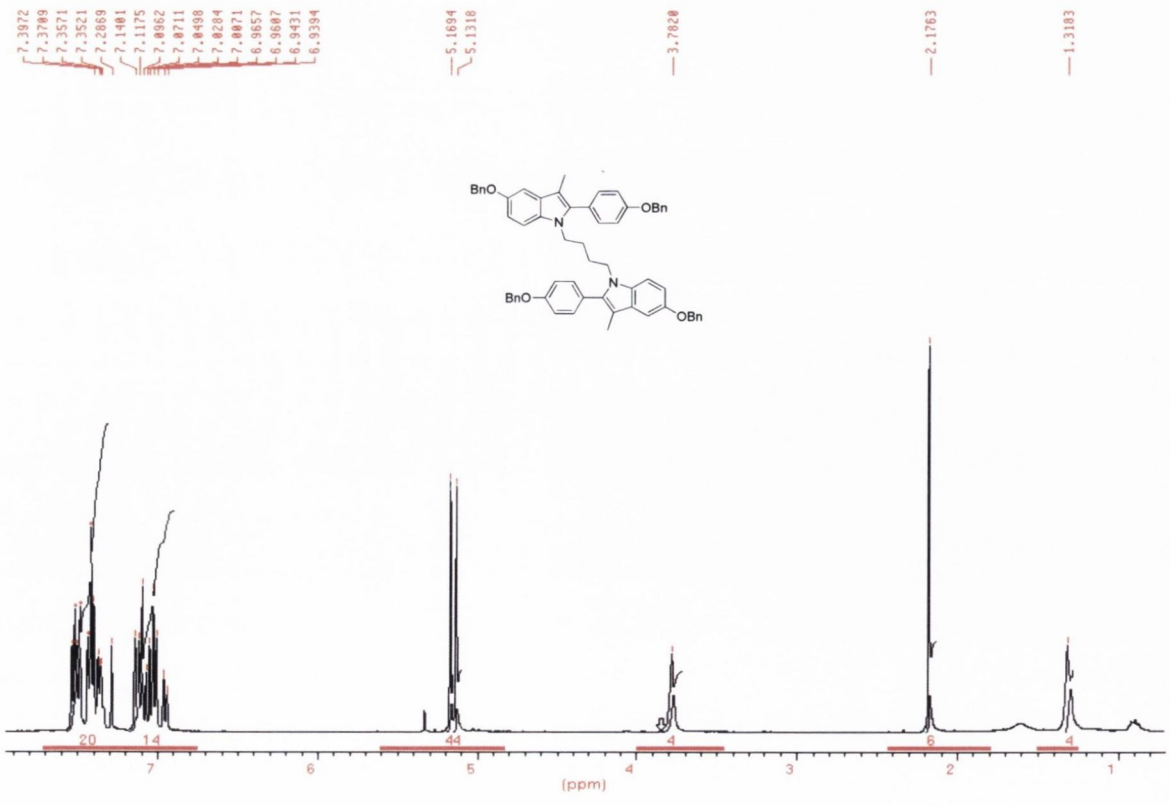

Figure 2-20 ^1H NMR spectrum of [263]

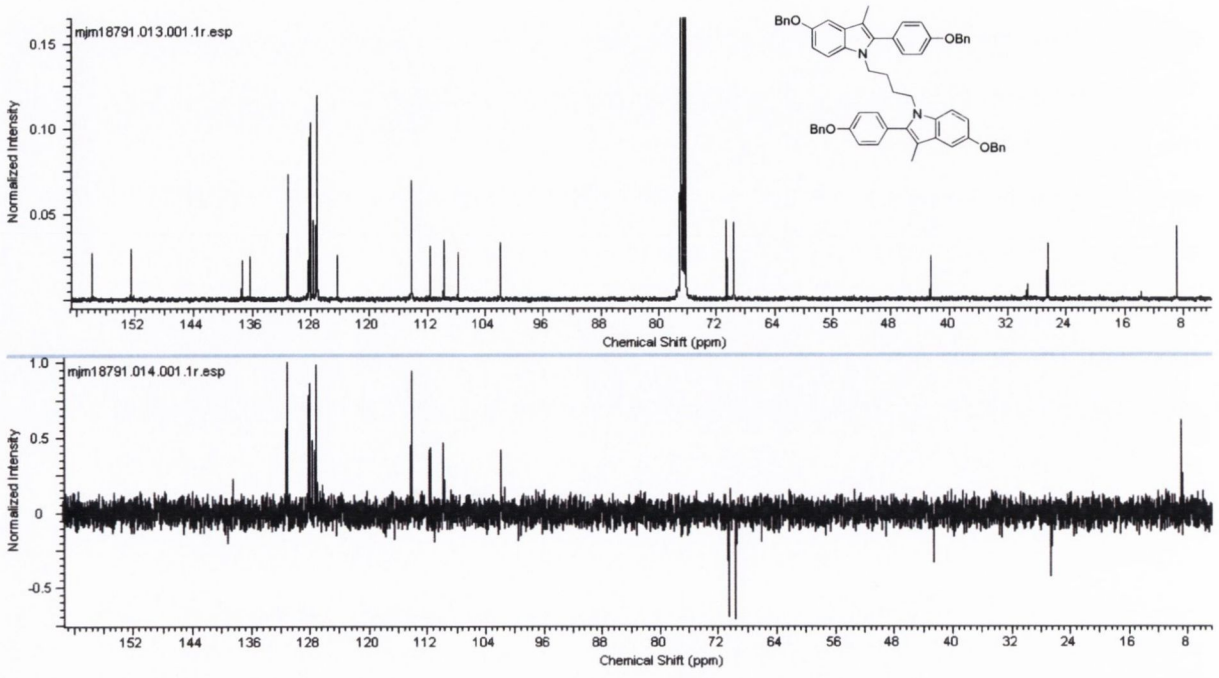

Figure 2-21 ^{13}C NMR and DEPT-135 spectras of [263]

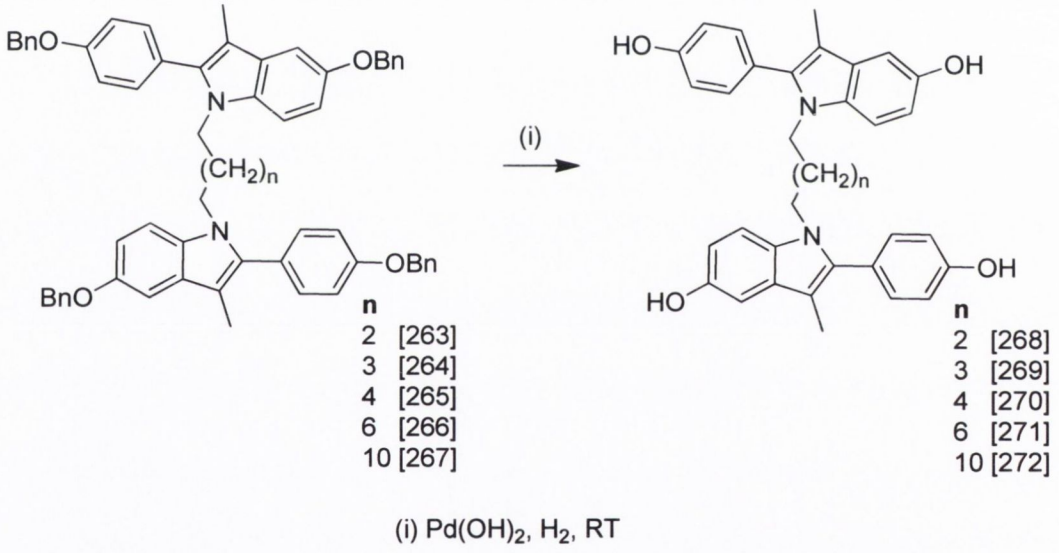

Scheme 2-25 Synthesis of [268]-[272]

Compounds [263]-[267] are deprotected, affording the bis-2-phenylindole analogues [267]-[271]. The benzyl protected compounds [263]-[267] were dissolved in MeOH:EtOAc (1:4) and to this palladium hydroxide (20 %) was added. The reaction vessel was place under a hydrogen atmosphere and the reaction monitored *via* TLC. After 30 min all traces of starting material had reacted. The use of palladium hydroxide as the hydrogenation catalyst afforded the bis-2-phenylindole analogues [268]-[272] in moderate yields (Table 4).

Linking alkyl chain	Compound ID & yield (%)	
	Side product isolated	Deprotection
$-(CH_2)_4-$	20 [263]	67 [268]
$-(CH_2)_5-$	22 [264]	53 [269]
$-(CH_2)_6-$	26 [265]	74 [270]
$-(CH_2)_8-$	22 [266]	61 [271]
$-(CH_2)_{12}-$	30 [267]	58 [272]

Table 4 Bis-2-phenylindole analogue reaction yields

The ^{1}H-NMR spectrum of [269] shown in Figure 2-22, is similar to that of the protected compound [263] as shown in Figure 2-20. The key differences are the presence of an additional CH_2 signal at 0.39 ppm due to the increase in chain length when compared to [263]. The two signals corresponding to the CH_2's of the benzyl ethers are no longer present and the integral for the aromatic region has been decreased to 14 hydrogens. Similarly, in the ^{13}C NMR spectrum of [269] shown in Figure 2-23, the additional CH_2 from the alkyl chain appears at 23.7 ppm, and the benzyl CH_2 signals appearing at 69.9 and 70.6 ppm are no longer present. The two signals furthest downfield at 151.3 and 158.2 ppm represent the chemical shift for the C-4' and C-5 carbons having the phenolic hydroxyl groups.

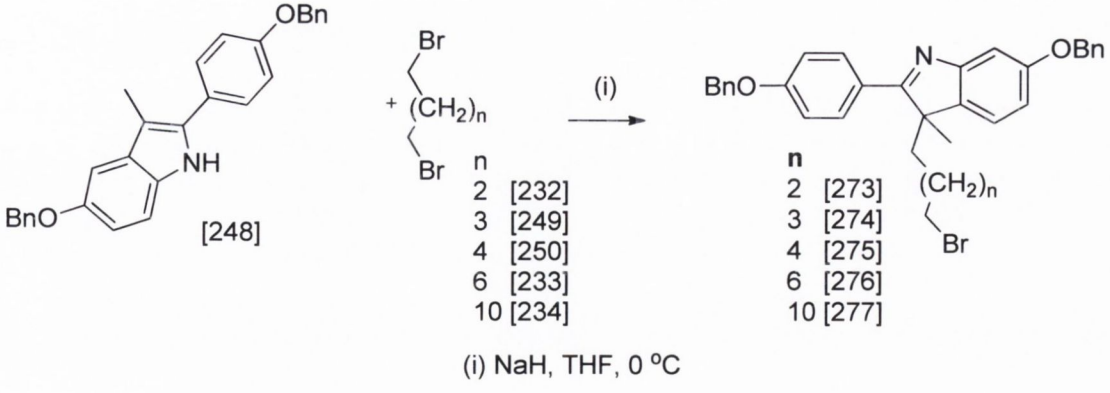

Scheme 2-26 2-Phenyl-3*H*-indole analogue synthesis

The isolation of a second byproduct in the bromoalkylation of indole [248] reaction S2 was identified as an unexpected product [273]. Determination of the structure was achieved using ^{1}H and ^{13}C NMR spectra, and it is possible to confirm that the bromo alkyl chain was present but not as

expected. The ^{1}H-NMR spectrum showed the required number of signals but the pattern of the signals appears different compared to the ^{1}H-NMR spectrum of the expected product [251] (see Figure 2-24).

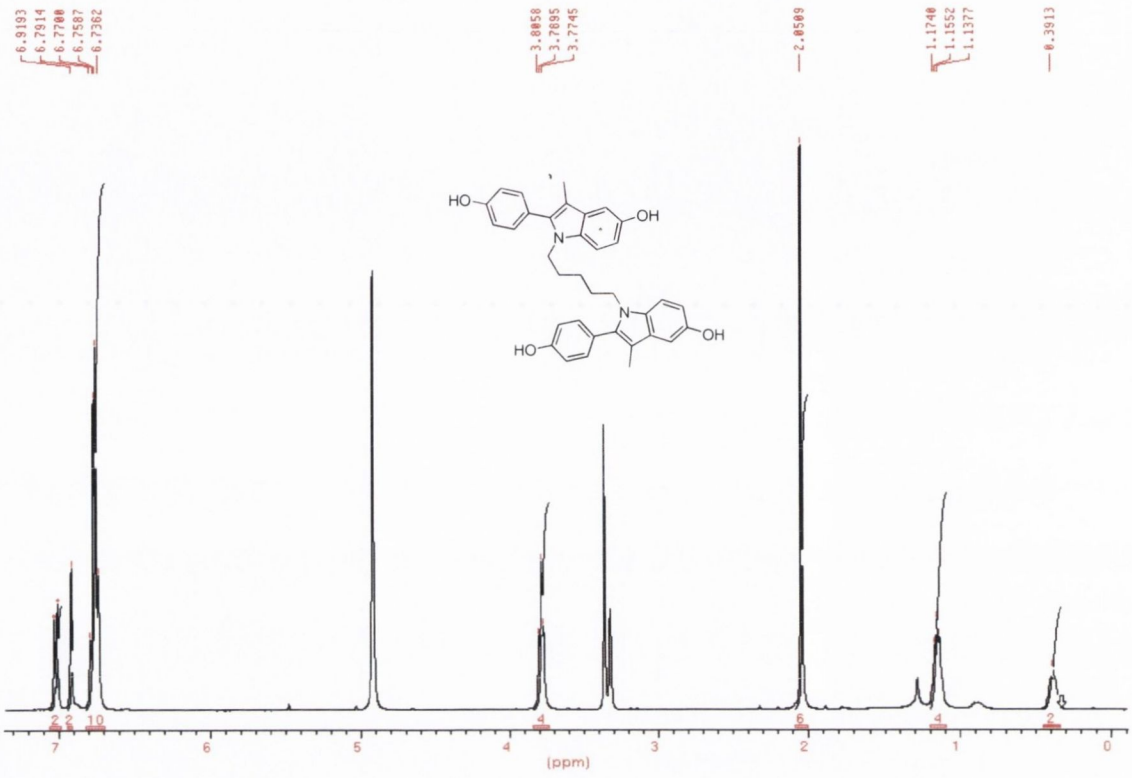

Figure 2-22 ^{1}H NMR spectrum of [269]

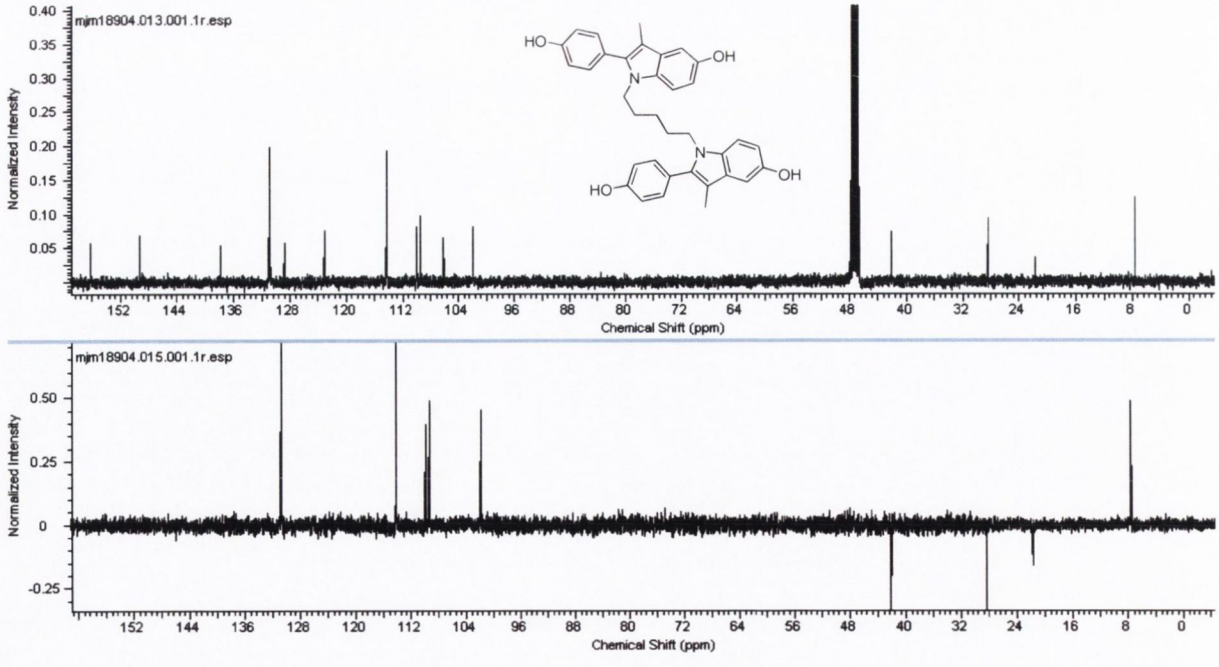

Figure 2-23 ^{13}C NMR spectrum of [269]

When the two spectra for [251] and [273] are examined it is possible to see that the molecules are significantly different (Figure 2-24). The signal attributed to the methyl group attached to the indole core has changed its chemical shift significantly from 2.24 to 1.58 ppm. In the rearranged product the methyl signal appear much more upfield at 1.58 ppm. The alkyl chain also displayed different signal pattern when compared to the ^{1}H-NMR spectrum of [251]. The ^{13}C NMR spectrum (Figure 2-25) also confirmed the presence of the alkyl chain. In the spectrum of the [273], two signals were difficult to characterise; the signal appearing further downfield at 179.3 ppm and the quaternary carbon at 57.5 ppm. This side product was also found to have the same HRMS molecular ion peak as compound [251] which was surprising. From the elemental analysis it was determined that the isolated product was a structural isomer of [251], with molecular formula $C_{33}H_{32}BrNO_2$.

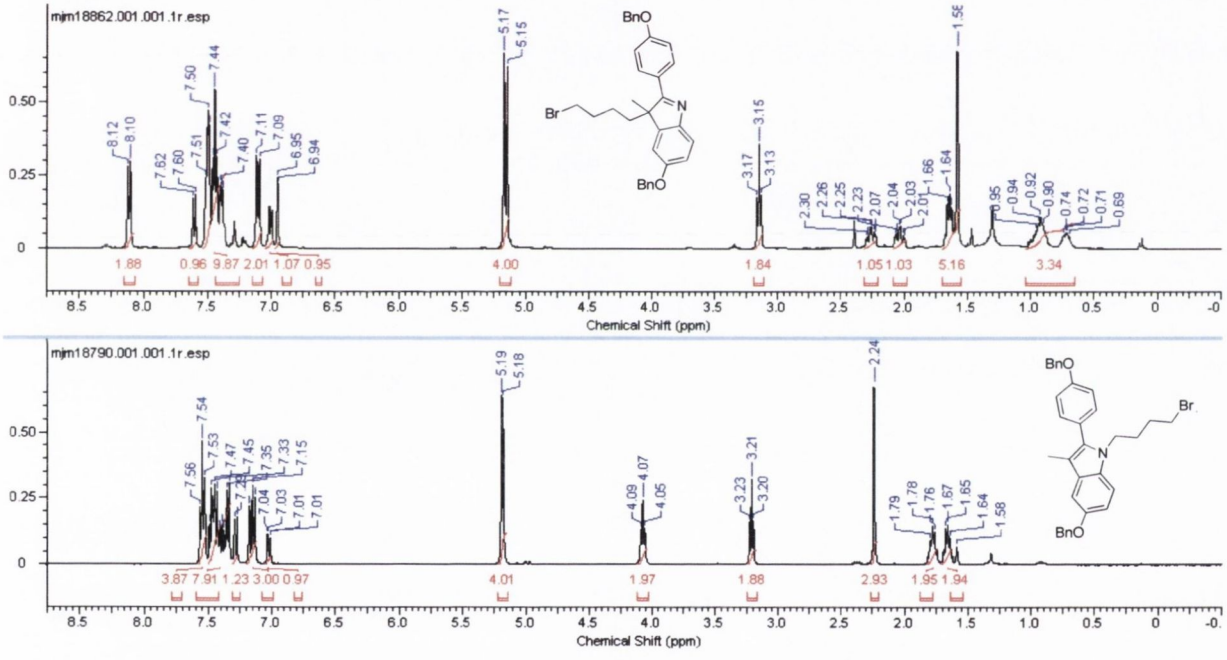

Figure 2-24 ^{1}H NMR spectrum comparison (above, rearranged product S2 [273], below [251])

In the ^{1}H NMR spectrum for [273] is shown in Figure 2-24, the methyl signal appears more upfield at 1.58 ppm when compare to the ^{1}H spectrum for [251]. The alkyl CH_2 signals appear very different to that of [251]. The CH_2 signals appear as a multiplet between 0.84-1.03 ppm, as a multiplet between 1.53-170 ppm and as 2 double triplets which correspond to one CH_2 at 2.03 and 2.26 ppm. The benzyl CH_2 signals appear in the same region as [252] at 5.15 and 5.17 ppm. The aromatic hydrogen adjacent to the imine carbon on the 3*H*-indole core appears more downfield and appears as a doublet at 8.11 ppm. Similarly in the ^{13}C NMR spectrum for [273] shown in Figure 2-25, the methyl group on the 3H-indole core has moved much more downfield to 24.6 ppm. The signal at 57.6 ppm is assigned to quaternary carbon C-3 on which the methyl and the alkyl chain are located.

The imine carbon on the 3*H*-indole core appears more upfield at 179.1 ppm. Similar products [273]-[277] were isolated on reaction of indole [248] with the dibromoalkenes [232]-[234]. See Scheme 2-26 and Table 5.

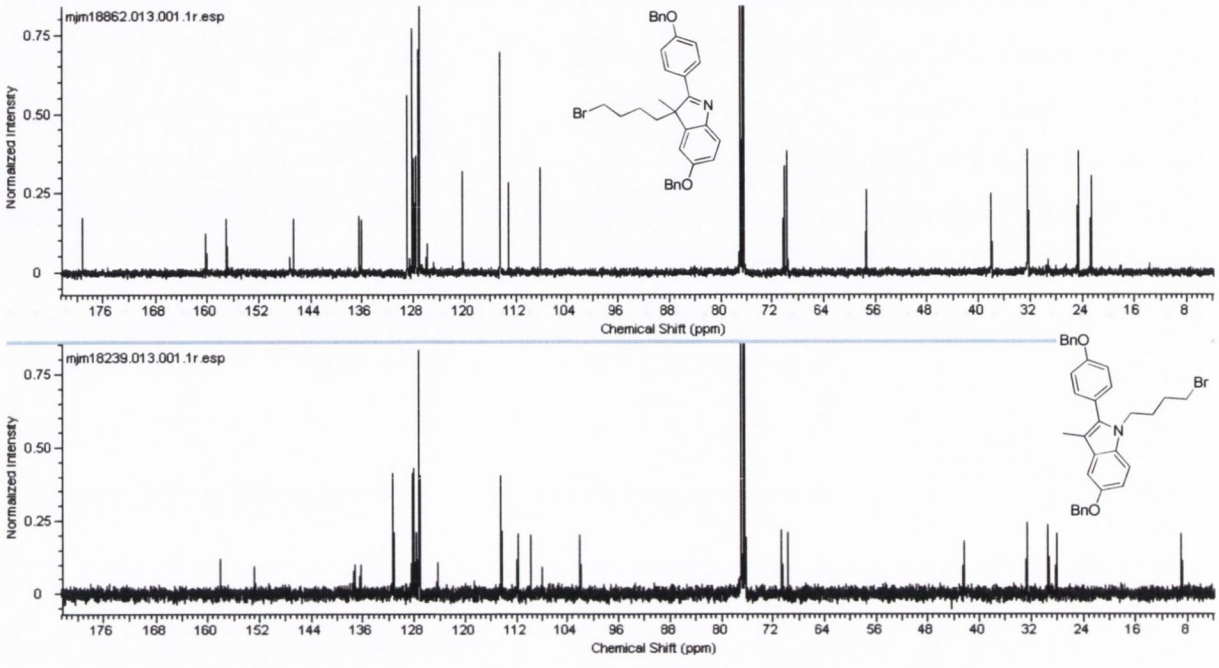

Figure 2-25 ^{13}C NMR spectrum comparison (above rearranged product S2 [273], below [251])

Linking alkyl chain	Compound ID & yield (%)
	Side product isolated, S2
$-(CH_2)_4-$	17 [273]
$-(CH_2)_5-$	9 [274]
$-(CH_2)_6-$	12 [275]
$-(CH_2)_8-$	13 [276]
$-(CH_2)_{12}-$	11 [277]

Table 5 2-Phenyl-3*H*-indole analogues

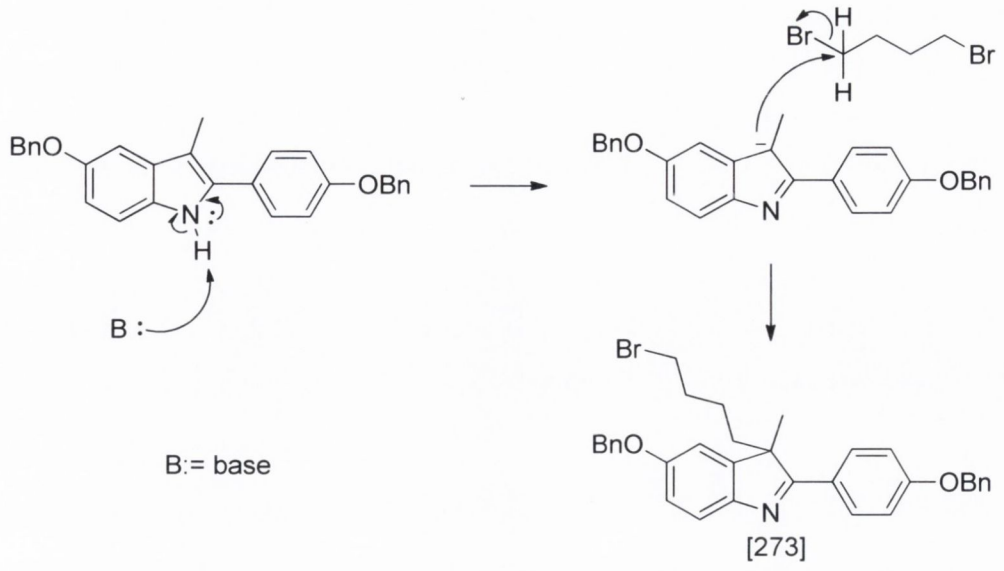

Scheme 2-27 Proposed reaction mechanism for the formation of the 2-phenyl-3*H*-indole [273]

A plausible mechanism for the dearomative alkylation reaction to form the 2-phenyl-3*H*-indole [273] is depicted in Scheme 2-27. The base deprotonates the indole nitrogen. Assisted by base, the indole acts as nucleophile through C-3 position to attack the dibromoalkyl compound displacing bromine. This proposed mechanism is similar to that documented by Ke-Jia *et al* for the palladium(0)-catalyzed dearomative arylation of indoles.[487]

2.3.9 Potential selective inhibitors of NF-κB

17β-Estradiol (E2) is known to have anti-inflammatory activity which is believed to be a result of interference with NF-κB activity.[488] Binding of estradiol to the estrogen receptor induces inhibition of NF-κB and previous studies have shown that NF-κB activation is only present in ER-negative cancers.[489] In ER-positive breast cancers, NF-κB activation is absent and this could be due to inhibitory crosstalk between NF-κB and ER signalling.[490] The mechanism for this interaction has not been fully elucidated but is believed to be through either direct protein-protein interactions, the inhibition of NF-κB binding to DNA, increased NF-κB expression or through a co-activator. The identification of pathway-selective estrogen receptor ligands that inhibit NF-κB transcriptional activity is likely to have potential application as potent anti-inflammatory agents that do not induce the classic effects of estradiol and estrogen ligands including ER-mediated gene expression and proliferation of uterine cells.

The aim of this section of the project was to elucidate if novel indole containing ER ligands acting as pathway-selective inhibitors of NF-κB can display anti-inflammatory effects. NF-κB can function as a tumour promoter in inflammation associated cancer and is therefore a potential target for cancer prevention in chronic inflammatory diseases. The inhibition of NF-κB transcriptional activity by estradiol (E2) bound to the estrogen receptor (ERα or ERβ) has been known for several

years and is well documented.[488] Some ER ligands have also shown effects on selective expression of NF-κB.[491, 492] As an additional aim of this project, a selected number of novel ER ligands with varying effects on the ER (both agonistic and antagonistic) have been synthesised and evaluated, some of which also were previously demonstrated to have potent anti-proliferative effects on the human breast carcinoma MCF-7 cell line. The identification of more selective ligands for the ER has been sought due to the associated risks of endometrial cancer and venous thrombosis with the use of estrogens. More selective ligands are those which would retain the beneficial outcomes of estrogen therapy, while eliminating the unwanted side effects.

The novel ER ligands selected for evaluation all contain the 2-phenylindole core that was synthesised previously (Section 2.3.7). For the synthesis of novel SERMs, this scaffold was required for successful binding of the molecule to the ER. Bazedoxifene [50] binds to both ER receptor α and β, and displays low binding IC_{50} values of 23 nM and 89 nM respectively, with a greater affinity for ERα. The addition of a basic side groups is then required to give the molecule potential anti-proliferative activity. It is also a potent inhibitor of cell proliferation, with an IC_{50} value of 3.7 nM in MCF-7 cells. This drug acts as an antagonist in mammary tissue and prevents the binding of estradiol.

2.3.9.1 Potential selective inhibitors of NF-κB

A series of indole compounds was prepared for evaluation as dual ER/NF-κB ligands. The synthetic route is outlined in Scheme 2-31. Compounds designed with a 2-phenylindole-3-methlyindole with a variety of alkyl and benzyl substituents located on the N-1 position. These compounds will be used as novel substrates for ER/NF-κB activity. The synthesis of 2-phenylindole [248] was discussed previously in (Section 2.3.7) from the appropriate 4-benzyloxyphenylhydrazine [247] and 4-benzyloxypropiophenone [246]. The variety of brominated precursors used for the synthesis of [284]-[289], where possible were obtained from commercial sources however, some of the proposed alkyl bromides were not available and required synthesis from the aldehyde or alcohol. This synthesis of these precursors is discussed in (Section 2.3.9.2). The alkyl bromides [232]-[234] and [249]-[250], and benzyl bromides [279]-[283] were reacted with the indole [248] to afford products [253]-[254] and [284]-[289]. The deprotection of the benzyl ethers was performed using $Pd(OH)_2$ under an hydrogen atmosphere affording the phenolic compounds [290]-[297], (see Scheme 2-31).

2.3.9.2 Synthesis of alkylbromide and benzylbromides.

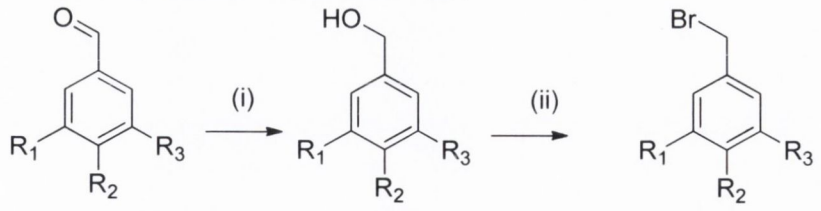

R_1	R_2	R_3		R_1	R_2	R_3		R_1	R_2	R_3	
H	OBn	H	[302]	H	OBn	H	[303] - 95%	H	OBn	H	[279] - 92%
OMe	OMe	OMe	[304]	OMe	OMe	OMe	[305] - 98%	OMe	OMe	OMe	[282] - 91%

(i) $NaBH_4$, MeOH, RT; (ii) PBr_3, DCM, 0 °C

Scheme 2-28 Synthesis of [279] and [282]

The preparation of 1-(benzyloxy)-4-(bromomethyl)benzene [297] and 5-(bromomethyl)-1,2,3-trimethoxybenzene [282] following the synthetic route shown in Scheme 2-28. 1-(benzyloxy)-4-(bromomethyl)benzene [279] was first prepared. The free *p*-phenol on the benzyl side chain was required for the preparation of the final compound [293]. To inhibit any side reaction that may occur during the synthesis, the phenol was protected as the benzyl ether. As this compound was not available from a commercial source it was synthesised from the appropriate 4-(benzyloxy)benzaldehyde [302] shown in Scheme 2-28, which was reduced using $NaBH_4$ to afford the benzyl alcohol [303] in good yield (95%). The second step required the bromination of the benzyl alcohol [303] using PBr_3 to afford the 1-((4-(bromomethyl)phenoxy)methyl)benzene [279].

The mechanism involves initial activation of the alcohol oxygen by the electrophilic phosphorus, followed by an S_N2 substitution at the benzylic carbon. The synthesis for the 5-(bromomethyl)-1,2,3-trimethoxybenzene [282] was carried out *via* the same procedure as for [279]. The 3,4,5-trimethoxybenzaldehyde was reduced with $NaBH_4$ followed by the bromination of the benzyl alcohol to afford [282].

Then the synthesis of 1-((2-bromoethoxy)methyl)benzene [281] was prepared from the bromination of the alcohol [306] was achieved using PPh_3 and NBS at -78 °C in the dark (Scheme 2-29). This reaction afforded the desired product [281] with a good yield (88%). Attempted bromination of [306] using PBr_3 in DCM was not successful.

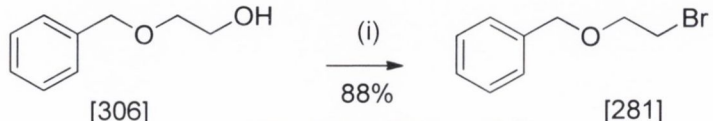

[306] [281]

(i) NBS, PPh_3, DCM, -78 °C

Scheme 2-29 Synthesis of [281]

The mechanism for this bromination reaction is shown in Scheme 2-30. Formation of the phosphonium salt is followed by deprotonation of the alcohol, to yield an alkoxide ion pair. Nucleophilic displacement of the bromide by the alkoxide yields an intermediate. The halide reacts in a S_N2 process forming the alkyl halide and triphenylphosphine oxide.

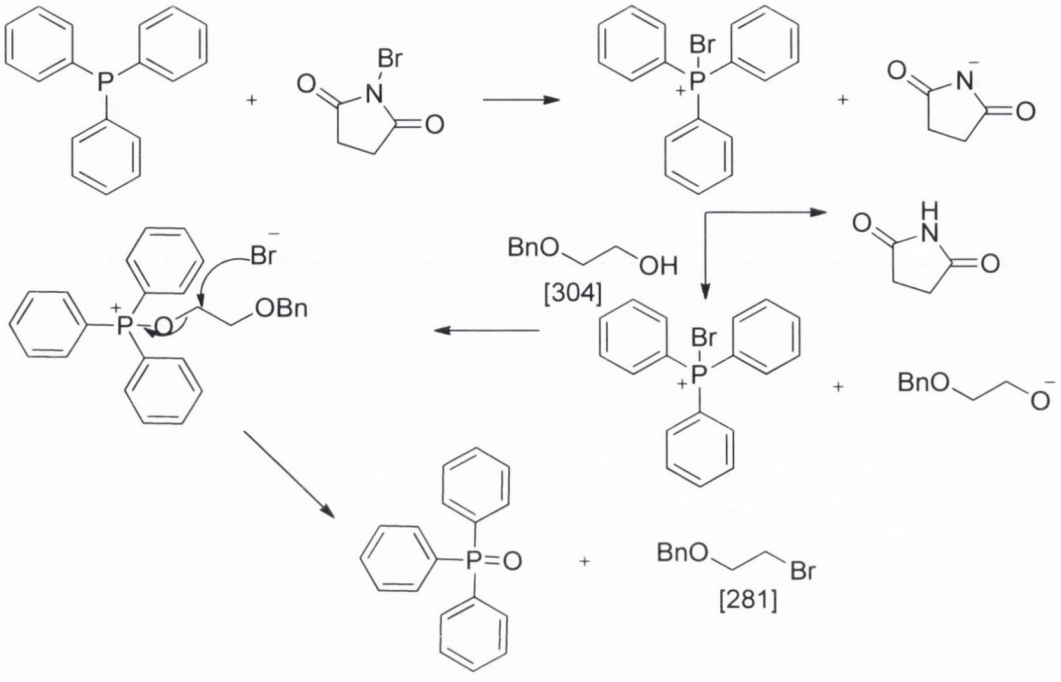

Scheme 2-30 Bromination of [281]

The substituents used in the formation of the dual ER/NF-κB ligands were selected due to the diversity of structural type. The proposed screen was to incorporate a wide range of side chains to investigate the differences in activity observed. This allowed for use of alkylbromide and benzylbromides and dibenzylbromides affording a diverse array of 2-phenylindole derivatives [282]-[297] to be evaluated for dual ER/NF-κB activity.

2.3.10 Synthesis of potential selective inhibitors of NF-κB

The potential selective inhibitors of NF-κB were synthesised *via* the route shown in Scheme 2-31. As seen with the alkyl bromination step in (Section 2.3.7), the addition reaction leads to the formation of S2 type 2-phenyl-3*H*-indole side products. The synthesis of [285], [286],[288] and [289] (Scheme 2-31) were also accompanied by the formation of the corresponding 2-phenyl-3H-indole side products, [298]-[299] and [300],[301], Table 7. The formation of the 2-phenyl-3H-indole side products was also observed with the benzylbromides used during the synthesis of the potential selective inhibitors of NF-κB and this suggests that this rearrangement reaction could be seen for any alkyation under these conditions.

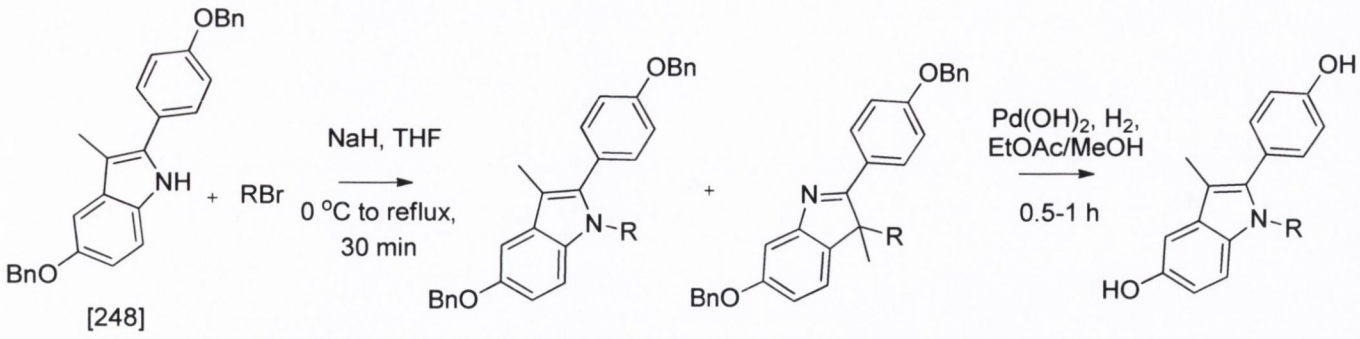

Scheme 2-31 Synthetic route for the potential selective inhibitors of NF-κB [292]-[297] and S2 product [298],[299],[301], [302], RBr = [278]-[283]

RBr	Alkyl bromide	Alkylation (i)	Deprotection (ii)
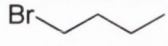	[278]	[284] – 50%	[292] – 70%
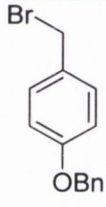	[279]	[285] – 68%	[293] – 82%
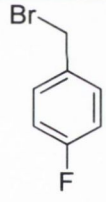	[280]	[286] – 68%	[294] – 78%
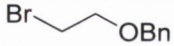	[281]	[287] – 43%	[295] – 71%
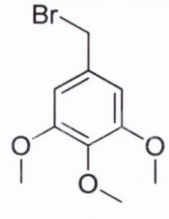	[282]	[288] – 51%	[296] – 88%
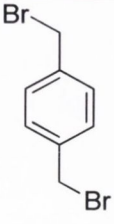	[283]	[289] – 63%	[297] – 71%

Table 6 Various chains utilized for the synthesis of potential selective inhibitors of NF-κB [292]-[297]

Starting material	Compound ID & yield (%)		
	Alkylation	Deprotection	Side product
[278]	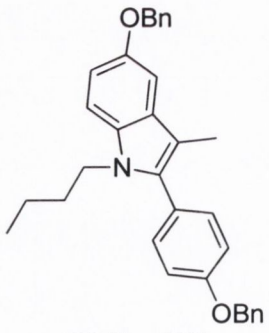 [284] – 43%	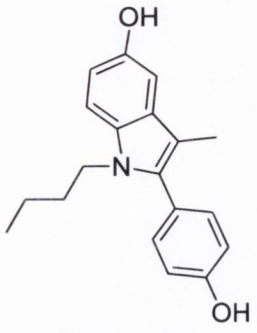 [292] - 71%	Side product not isolated
[279]	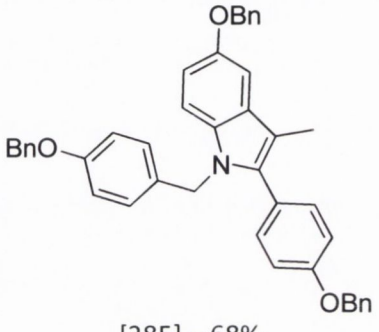 [285] – 68%	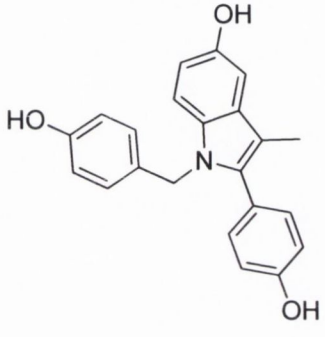 [293] – 82%	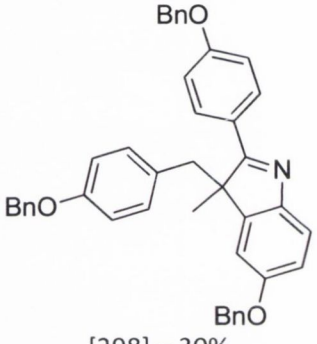 [298] – 30%
[280]	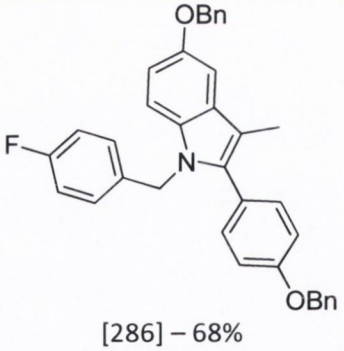 [286] – 68%	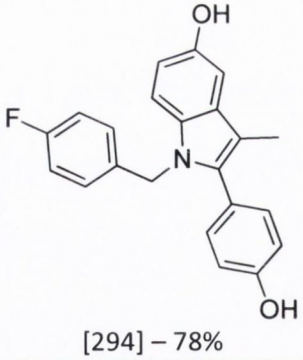 [294] – 78%	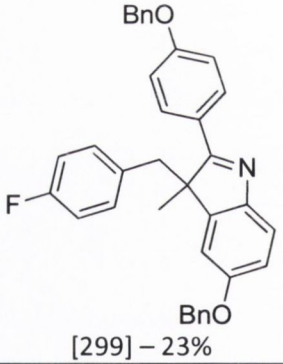 [299] – 23%
[281]	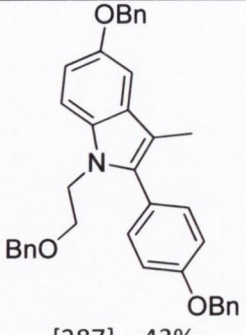 [287] – 43%	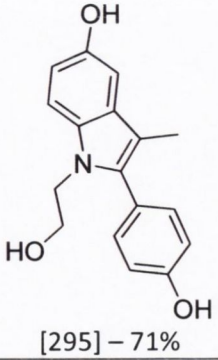 [295] – 71%	Side product not isolated

[282]	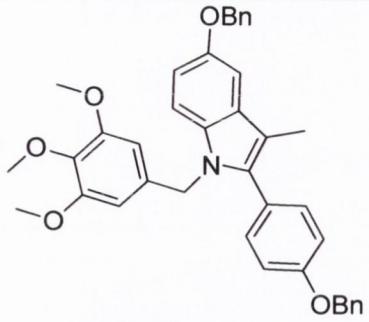 [288] – 51%	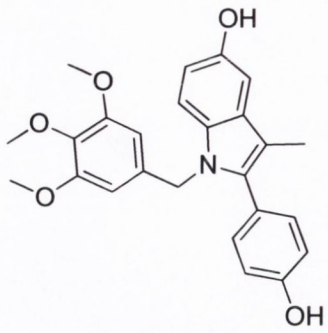 [296] – 88%	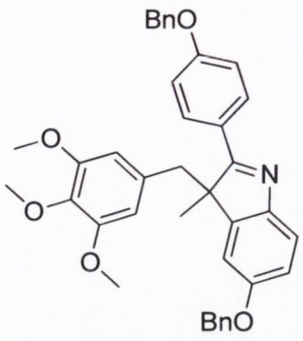 [300] – 17%
[283]	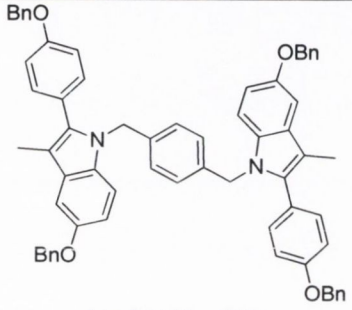 bis-[289] - 63%	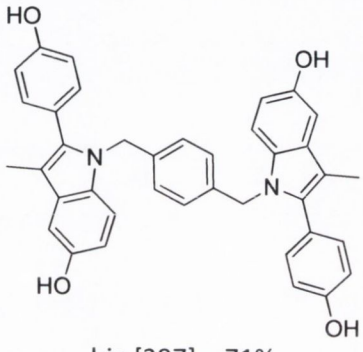 bis-[297] – 71%	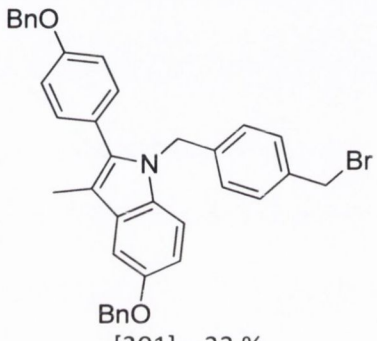 [301] – 22 %

Table 7 Potential selective inhibitors of NF-κB [292]-[297]

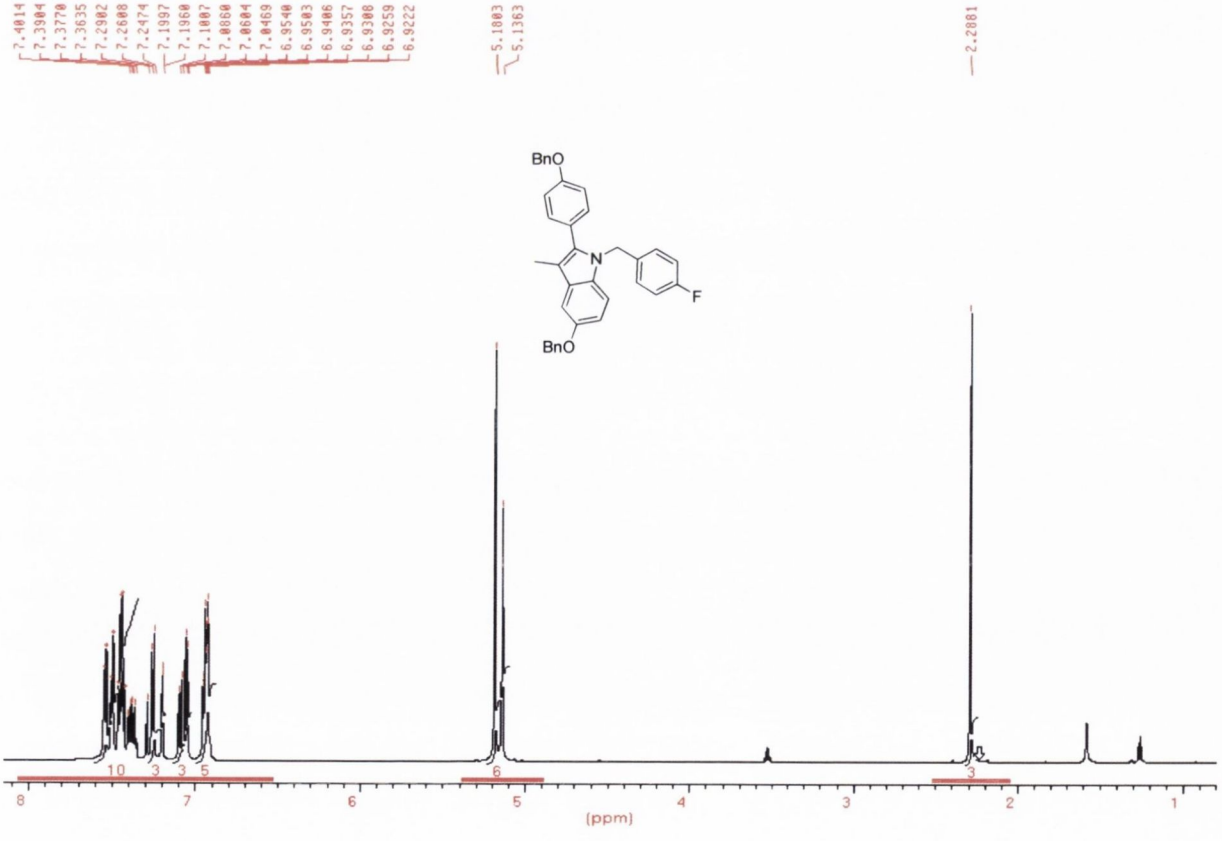

Figure 2-26 ^{1}H NMR spectrum of [285]

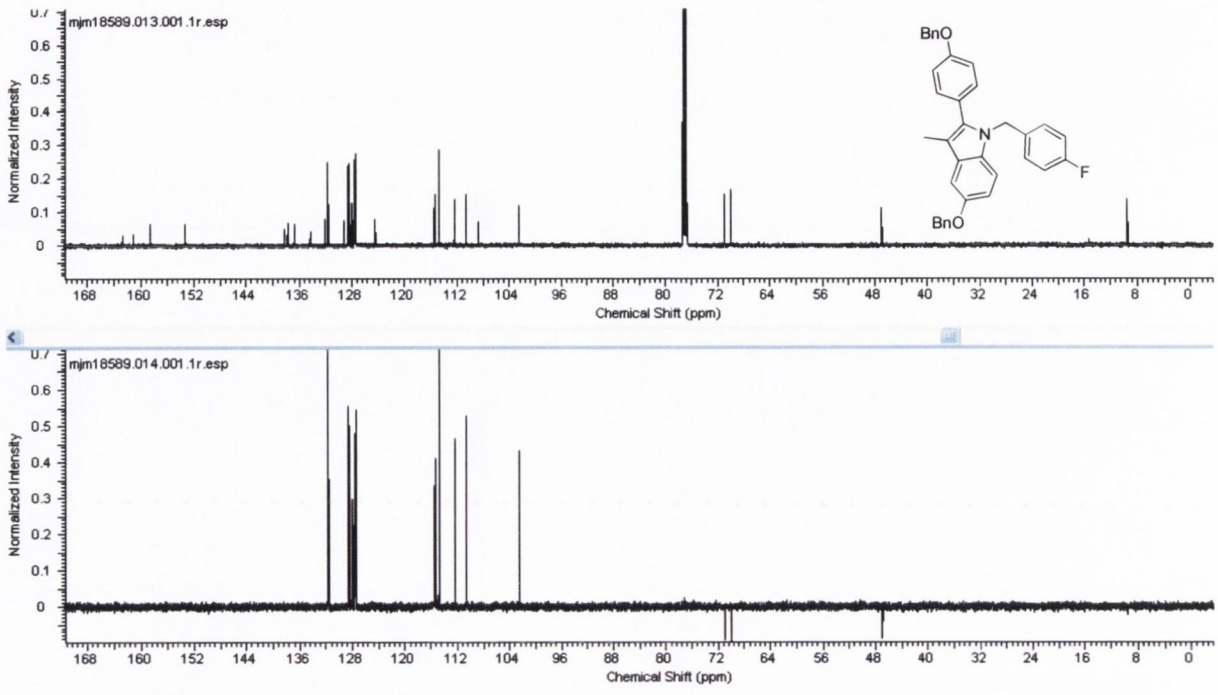

Figure 2-27 ^{13}C NMR and DEPT-135 spectras of [285]

The ^{1}H NMR spectra for [285] is shown in Figure 2-26, and is similar to that of the previous 2-phenylindole compounds examined. The signal appearing a singlet at 2.28 ppm corresponds to the methyl substituent on the C-3 of indole core. The benzyl CH_2 signals are seen at 5.13 and 5.18 ppm. The region between 6.92 and 7.40 ppm shows the aromatic protons signals which integrate for 21 hydrogens. The ^{13}C NMR and DEPT-135 spectra for [285] is shown in Figure 2-27. The C-3 methyl of the indole core appears at 9.5 ppm. The benzyl CH_2 signals are observed at 46.9, 70.0 and 71.0 ppm. The carbon (C-4') C-F can be seen at 162.6. The carbons aromatic C-O benzyl ether signals can be seen at 161.0 and 158.6 ppm. The remaining signals correspond to the aromatic tertiary carbons and quaternary carbons.

The isolation of the isomeric 2-phenyl-3*H*-indole side product was achieved in the majority of the alkylation and benzylation reactions investigated using NaH as a base. This side product reaction occur readily under these conditions but until now was unreported. The ^{1}H and ^{13}C NMR spectra of both the desired and side product differ significantly (as discussed later in this chapter) and can be seen from Figure 2-24 and Figure 2-25. The ^{1}H spectrum for [299] is shown in Figure 2-28, the C-3 methyl signal appears as a singlet more upfield when compared to the C-3 methyl signal in the ^{1}H-NMR spectrum for [280] (Figure 2-28). The benzyl CH_2 located on C-3 carbon appears as a multiplet as a double doublet at 3.26-3.40 ppm, this splitting is due to long range coupling of the methyl substituent located on the C-3 carbon. The benzyl ether signals appear as a multiplet between 5.03 - 5.26. The aromatic hydrogen adjacent to the imine carbon (C-7) on the 3*H*-indole

core appears downfield as a singlet at 8.15 ppm. In the ^{13}C NMR spectrum for [299] shown in Figure 2-29, the C-3 methyl group on the 3*H*-indole core is shifted downfield to 24.3 ppm compared with compound [285]. The signal at 57.8 ppm is assigned to the quaternary carbon (C-3) on which the methyl and the benzyl group are located. The imine carbon of (C-2) the 3*H*-indole core appears more upfield as a singlet at 178.6 ppm.

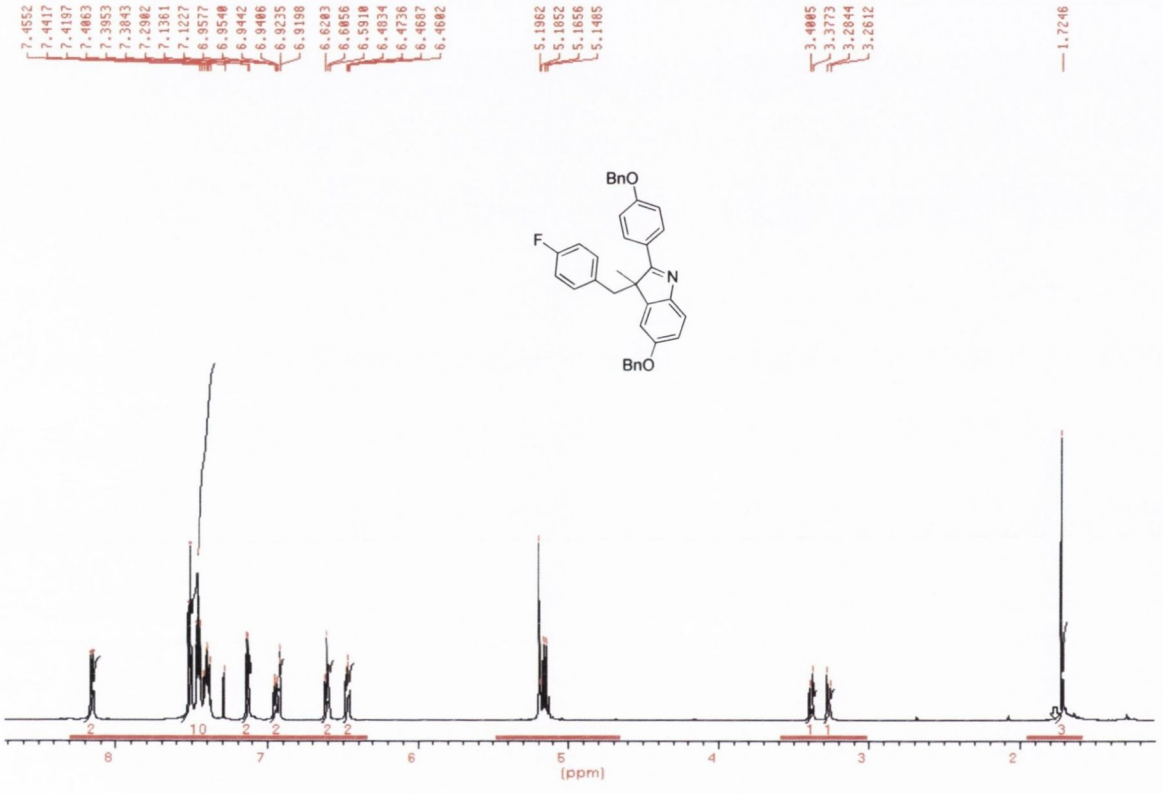

Figure 2-28 ^{1}H NMR spectrum of [299]

The 2-phenyl-3*H*-indole products [298], [299], [301] and [302] were identified. It was then proposed that these compounds could be evaluated as potential selective inhibitors of NF-κB however these compounds would require debenzylation. The debenzylation reaction was performed in a similar method as debenzylation of the 2-phenylindole discussed earlier in this chapter. This reaction was unsuccessful as the desired compound was not obtained but the deprotected 2-phenylindole [290] was obtained (Scheme 2-32), which was verified *via* mass spectrometry: found ion 240.0946 $[M+H]^+$, 240.0940 required for $C_{15}H_{14}NO_2$. The attempted debenzylation of [298], [299], [301] and [302] was discontinued. Under hydration conditions the p-flouro benzyl substituent [299] undergoes rearrangement to locate on the nitrogen and subsequently debenzylates to afford [228].

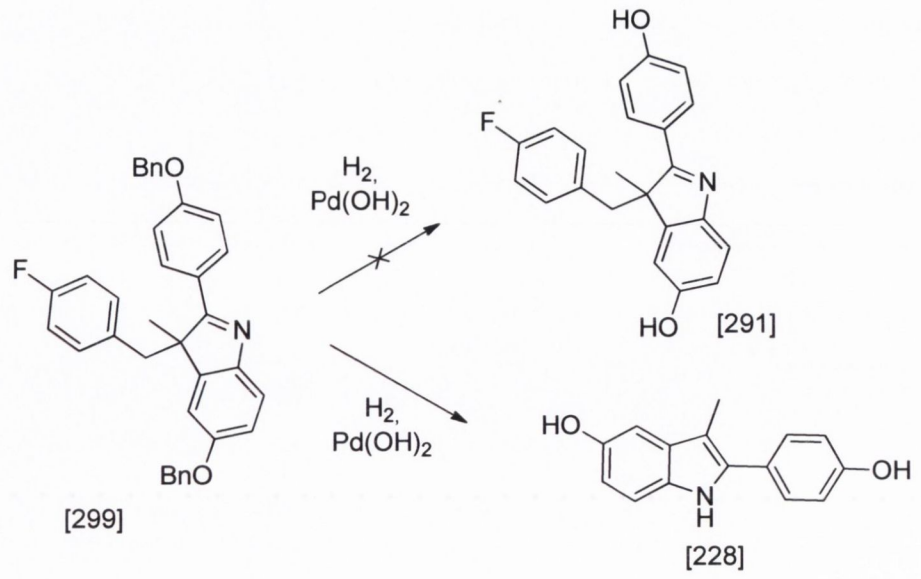

Scheme 2-32 Attempted debenzylation of [299]

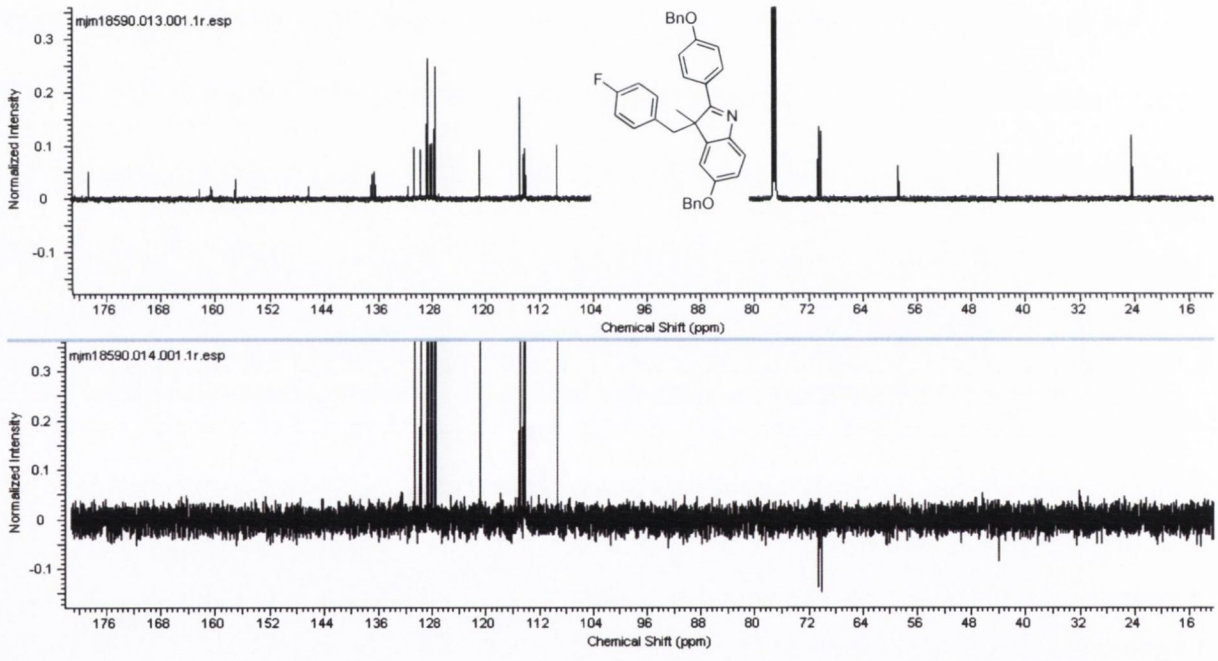

Figure 2-29 ^{13}C NMR and DEPT 135 spectras of [299]

The estrogen receptor ligands that were synthesised in this chapter were fundamental development for use in the conjugates scaffolds (Chapter 5). The ER ligands are required to give the novel conjugates the selectivity towards the ER overexpressing breast cancer cells. The vast array of ER binding type ligands that were synthesised contain structural similarities and are modelled on endoxifen, cyclofenil and bazedoxifene which are all known potent binding ligands in the ER. The bis-indoles will be evaluated for antiproliferative and ER binding activity. The novel bis-2-phenylindole [297] could potentially bind *via* one of the 2-phenylindole within the ER binding site and the other

unbound indole has the potential to interact with or interfere with the H-12 and potentially act as an ER antagonist. The isolation of the 2-phenyl-3*H*-indoles was unexpected and previously unreported using this method. Further optimisation could potentially allow for the novel and inexpensive method for the formation of various 2-phenyl-3*H*-indoles of interest.

3 Chapter 3
Combretastatin analogues

3.1 Introduction

Tubulin is composed of a heterodimer of two closely related 55 kDa proteins designated as α and β tubulin. Tubulin polymerises to form structures called microtubules. Microtubules consist of 13 protofilaments and are 25 nm in diameter, each μm of microtubule length is composed of 1650 heterodimers.[493] Microtubules are highly ordered fibres that have an intrinsic polarity. Tubulin can polymerise from both ends *in vitro*, however the rate of polymerisation is not equal. It has therefore become the convention to refer to the rapidly polymerising end, as the plus-end of a microtubule, and the slowly polymerizing end as the minus-end. *In vivo* the plus end of a microtubule is distal to the microtubule organizing centre. Microtubules are involved in several basic cellular processes such as segregation of genetic material, intracellular transport, maintenance of cell morphology, cell organelle localisation, extracellular transport by cilia, and movement of cells be means of flagella and cilia.[282] Microtubules are essential for the replication of cells. Hence, if formation of the microtubules in a tumour cell can be inhibited, the chromosomes cannot separate, the cell cannot divide and hence the tumour cannot grow.[494] Thus, agents who can interfere with the dynamics of tubulin may also act as inhibitors of cell division.

A number of active compounds known as combretastatin were isolated from the South African Willow, *Combretum Caffrum*.[495] These different combretastatin analogues, in particular combretastatin A-4 [22] is one of the simpler compounds to show antimitotic effects by interaction with the colchicine binding site of tubulin. Combretastatin A4 is one of the most potent inhibitors of colchicine binding presently known.[496] Combretastatin A-4 [22] exhibits an impressive spectrum of activity as it is also not recognized by the multidrug resistance (MDR) pump, a cellular pump which rapidly ejects foreign molecules, including many anticancer drugs from the cell. It has also been documented that combretastatin A-4 [22] can inhibit angiogenesis, a process essential for tumour growth.[497] Consequently, to date, a large number of combretastatin A-4 [22] analogues and other combretastatin analogues have been synthesised and analysed, resulting in detailed structure-activity relationship (SAR) information.[283]

3.2 Synthesis plan

Due to its high potency and effects on tumour vasculature, combretastatin CA4 [22] was chosen as a suitable cytotoxic agent for the synthesis of the novel ER-conjugates designed to target ER-positive breast tumours. The development of novel ER targeting conjugates had been reported by Keely who synthesised a series of ER-ligand conjugates consisting of endoxifen, a tamoxifen metabolite, tethered to CA4 *via* an ester linkage. Direct amide linkage *via* the acid functional group of the acrylic acid analogue of CA4 [150] was also achieved (Figure 3-1) and the direct amide conjugates resulted in interesting biological activity.[421] Therefore, in present work, the use of acrylic

acid analogue of combretastatin will be employed as the cytotoxic agent in the novel ER-conjugates designed to target ER-positive breast tumours.

3.3 Combretastatin analogues

The combretastatin acrylic acid analogues are to be included as structural components of the proposed endoxifen conjugates. It is proposed that the endoxifen will selectivity target the ER-positive cancer cells, while the combretastatin analogue acts as the cytotoxic agent in the conjugate and will cause vascular disruption in the tumour resulting in apoptosis. Synthesis of a group of structural analogues of combretastatin containing acrylic acid variation is now presented as this functional group is required for the construction of the designed conjugate structure.

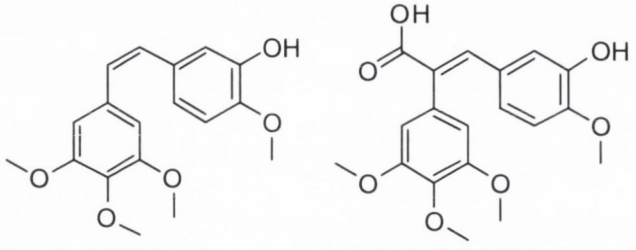

[22] [150]

Figure 3-1 Combretastatin A4 [22] and Combretastatin A4 acrylic acid [150]

3.3.1 Synthetic route for combretastatin analogues.

The synthesis of combretastatin type compounds has been widely reported in literature. Some of the routes of synthesis include use of Wittig reactions[498], Ramberg-Backlund reaction[499] Suzuki reactions[500], Lindlar's catalysts reduction of the corresponding alkyne[501], Sonogashira reaction and reduction with Ti(II)-complexes[502]. However many of these routes have associated complications, such as lack of stereoselectivity, and require difficult separation procedures.

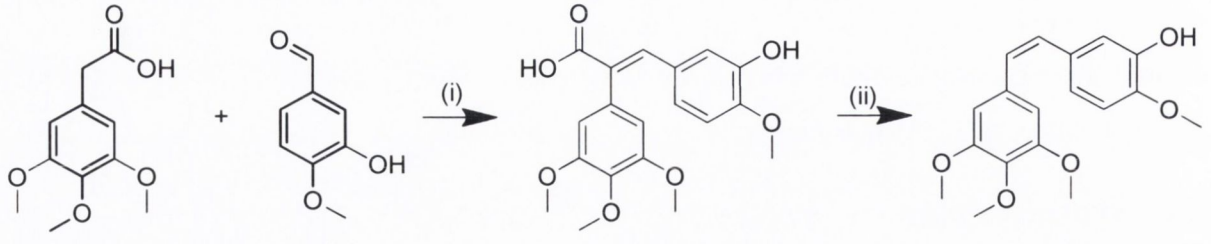

[307] [308] [150] [22]

(i) acetic anhydride, triethylamine, reflux (ii) copper powder, quinoline, 220 °C

Scheme 3-1 Synthesis combretastatin A4 [22]

Gaukroger *et al* reported a stereoselective route to CA4 [22] in high yields using the Perkin reaction followed by a decarboxylation at high temperature, as illustrated in Scheme 3-1.[281] The condensation of an aromatic aldehyde with an acid anhydride in the presence of the sodium or

potassium salt of the acid corresponding to the anhydride to yield an α,β-unsaturated acid is known as the Perkin reaction.[503] The mechanism involves a form of aldol condensation (Scheme 3-2).

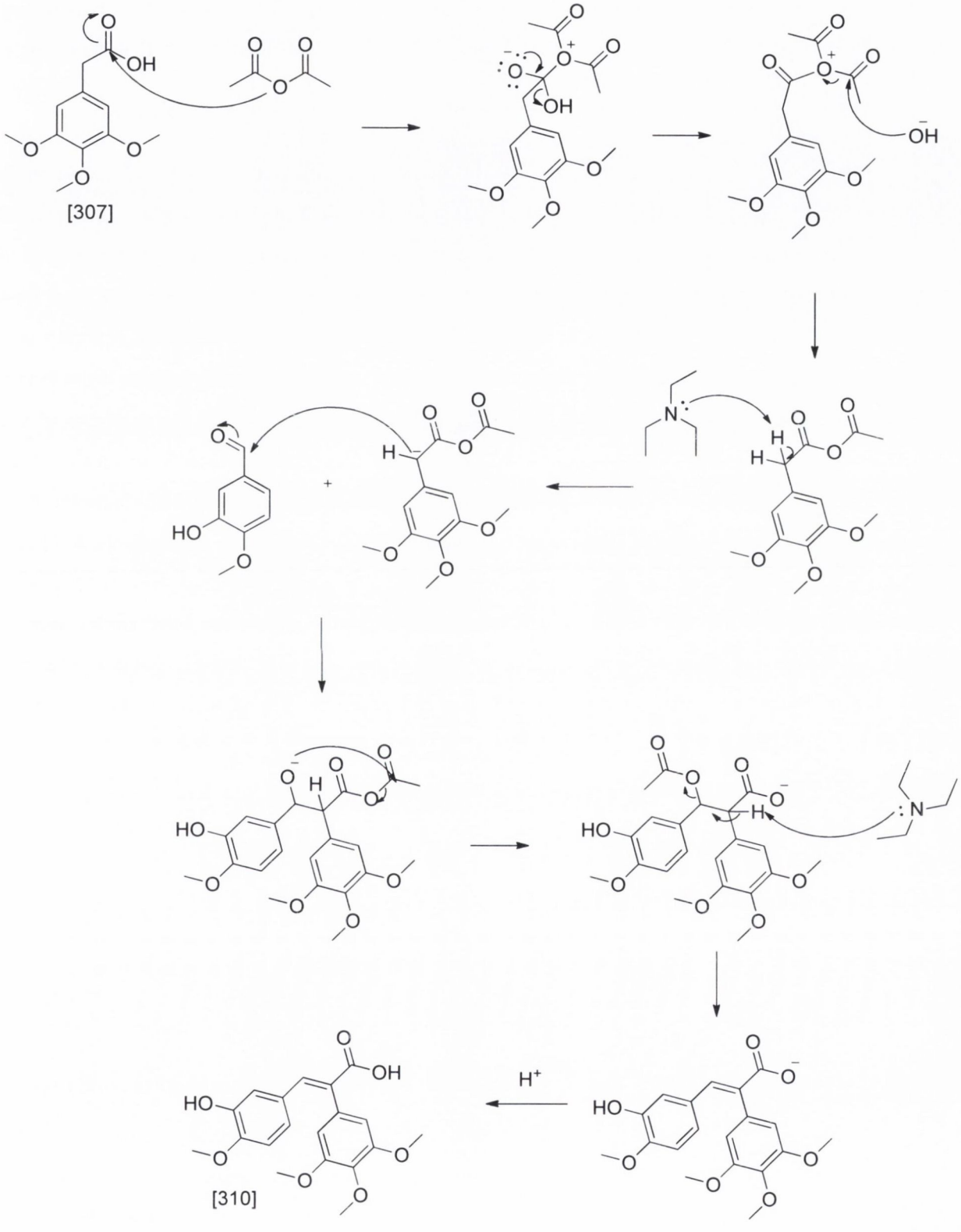

Scheme 3-2 Perkin reaction mechanism (formation of [310])

Modification to the Perkin reaction allows formation of acrylic acid compounds related in structure to the combretastatins. The classical Perkin reaction of the acrylic acids consists of prolonged heating of the phenylacetic acid, benzaldehyde, acetic anhydride and the triethylamine at reflux. In the present work an efficient Perkin reaction was achieved in the microwave synthesiser.

3.3.2 Investigation of microwave irradiation for preparation of the acrylic acid combretastatin analogues.

The objective of this investigation was to successfully synthesise a range of acrylic acids efficiently in a microwave reactor, to obtain a relatively high yield in a reasonably short reaction time. If the reaction time and yield recovered after the microwave synthesis was similar to that of the conventional reflux synthesis, then this method would not have been favourable as a new method for the synthesis of the acrylic acid combretastatin analogues. The Perkin reaction was conventionally carried out under reflux for a minimum 3 h. It was decided to investigate if the Perkin reaction could be achieved *via* microwave irradiation as a feasible option for the synthesis of the acrylic acid combretastatin analogues. A specific Perkin reaction performed previously *via* the reflux method to afford [310] in 40% yield was repeated using the microwave synthesiser (Scheme 3-3). The reactants and equivalents used in the reflux method did not change. The *p*-anisaldehyde (1 eq.) [309] and 3,4,5-trimethoxyphenylacetic acid (1 eq) [307] with acetic anhydride and triethylamine were placed in a 5 mL microwave sealed tube and reacted in the microwave under various conditions. Two parameters in the microwave synthesiser can be easily altered, reaction time and temperature. Therefore it was decided to investigate the effect that changing one or both of these would have on the reaction.

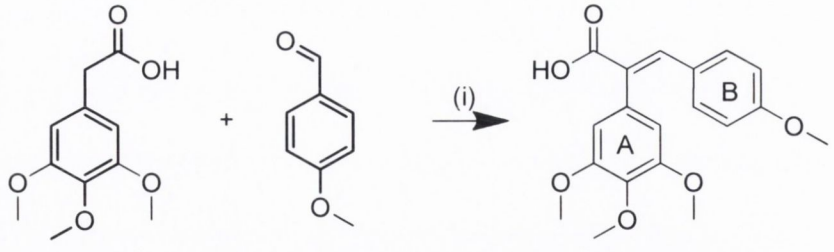

[307] [309] [310]

(i) acetic anhydride, triethylamine, microwave

Scheme 3-3 Synthesis of the acrylic acid combretastatin analogue [310]

Initially it was decided that if one parameter was kept constant then it would be possible to alter the other parameter to see if there was any correlation with reaction yield with the altered condition. Therefore, the investigation into the effect that reaction time had on the reaction yield was undertaken. In doing this it was possible to maintain a constant temperature for the duration of

the reaction. As this was a new reaction method, an initial reaction temperature program sequence would be required. The temperature of 100 °C was decided upon because it was just above boiling point of the lower boiling solvent (acetic anhydride (bp 138-140 °C) and triethylamine (bp 88.8 °C)) to ensure the reaction could be controlled. The investigation began by altering the reaction time from a short time of 1 minute to a maximum reaction time of 3 h, which corresponded to the time required for the reflux method, keeping the temperature constant at 100°C. The results of the investigation are presented in Table 8. All yields are isolated yields on completion of reaction time. Products were isolated by filtration and purified *via* recrystallisation from methanol.

Temp (°C)	Time (min)	Yield (mg)	Yield %
100	1	50	4.7
100	5	200	18.81
100	10	320	30.1
100	30	378	35.56
100	60	467	43.93
100	90	440	41.3
100	120	420	39.5
100	180	0	0
Reflux	240	433	40

Table 8 Effect of reaction time on the isolated yields of compound [310]

When the reaction times were analysed, it was clear that the duration of the reaction had an effect on the isolated yield. After 1 minute, the product had formed, but in a very low yield (4.7%). As the reaction time increased a steady increase in the isolated yield recovered was observed up to 1 h of reaction time. As time increased above 1 hour, a decrease in the isolated yield was observed. It is unclear exactly the reason for this, but energy supplied from microwave irradiation may have caused compound degradation. The TLC plate showed the formation of the product [310] with a Retention Factor (Rf) of 0.35, both *p*-anisaldehyde [309] and 3,4,5-trimethoxyphenylacetic acid [307] starting materials were also visible at Rf of 0.21 and 0.46 respectively. TLC analysis of the reaction mixture with duration of greater than 1 h showed the formation of possible degradation products. After 180 minutes no product was recovered. This analysis was performed *via* TLC for compound [310] with an Rf of 0.35. Only isolated precipitated crystalline product yield was recorded, however it was possible that some further product remained in the mother-liquor. When all the results were compiled (see Table 8) it was apparent that an optimum reaction time was either 30 or 60 minutes.

The yield after 30 minutes was 35.56 % which was lower than that of the 60 minutes (43.93 %). When comparing the yield (mg) per unit time it was clear that the the 30 minute microwave reaction (12.6 mg/min) was more efficient that the 60 minute microwave reaction (7.78 mg/min). It was decided that the reaction time of 30 minutes would be the optimum time from the initial screening of reaction conditions over a range of temperatures.

The second parameter that was examined was the effect of increasing the temperature on the isolated yield with a constant reaction time. A range of temperatures from 100-200 °C was initially screened to determine the impact of increasing temperature on the isolated yield, Table 9.

Time (min)	Temp (°C)	Yield (mg)	Yield %
30	100	378	35.56
30	110	454	42.62
30	120	460	43.19
30	130	285	26.7
30	140	0	0
30	150	0	0
30	200	0	0
240	Reflux	N/A	40

Table 9 Effect of reaction temperature on the isolated yields of [310] in microwave reaction synthesis

Reaction temperature in excess of 120 °C showed degradation occurring. Reactions where the temperatures were in excess of 140 °C did not afford any isolated yield. When the results were compiled it demonstrated that increasing the reaction temperature had a positive effect on the isolated yield. The reaction was increased in 10 °C increments while the reaction time remained constant (30 min). On inspection increasing the temperature to 110 °C gave a significant increase in the isolated yield (~ 7 %) and further more increasing the temperature to 120 °C only improved this yield slightly.

The results (see Table 8 and Table 9) demonstrated that the microwave synthesiser could be used as an efficient method for the preparation of acrylic acid combretastatin analogues *via* the Perkin reaction. After optimising the conditions of the microwave Perkin reaction it was possible to produce a relatively high yielding reaction (43 %) compared to that of the conventional reflux method (40 %). The optimisation of the reaction, gave a 30 minute reaction time although the yield after 60 minutes was greater (44 %) but changing a second parameter (temperature) of the reaction allowed for the increase in isolated yield for the reaction. By increasing the temperature to 120 °C,

this allowed for the isolated yield recovered (43 %) after 30 minutes to be almost identical to that for the 60 minute reaction but in half the reaction time.

This microwave reaction was then used to synthesise a range of acrylic acid combretastatin analogues ([150] and [310]-[327]) *via* the optimum conditions previously found. This new technique was very successful in the synthesis of the desired compounds (Table 10). The isolated product yields for compounds [150] and [310]-[327] from this method were greater than that of the reflux method. The microwave methods also allowed the use of a range of various aldehydes for the formation of the acrylic acid. This enabled the B-ring of the acrylic acids to be changed from the aryl ring to other ring type structures such as thiophene [325], furan [326], etc. In some cases where a phenol was present on the aromatic ring, it was observed that the phenol reacted with the acetic anhydride to form an acetate ester, [318]. Acetylation can occur due to the presence of the acetic anhydride in the presence of an amine base (triethylamine). The acetylation reaction for compound [323] is illustrated in Scheme 3-4. The cleavage of the acetate ester is performed on [323] by stirring in base/MeOH overnight to form the acid salt and acidified to pH4 to from the phenol [318] in an 88% yield (Scheme 3-5).

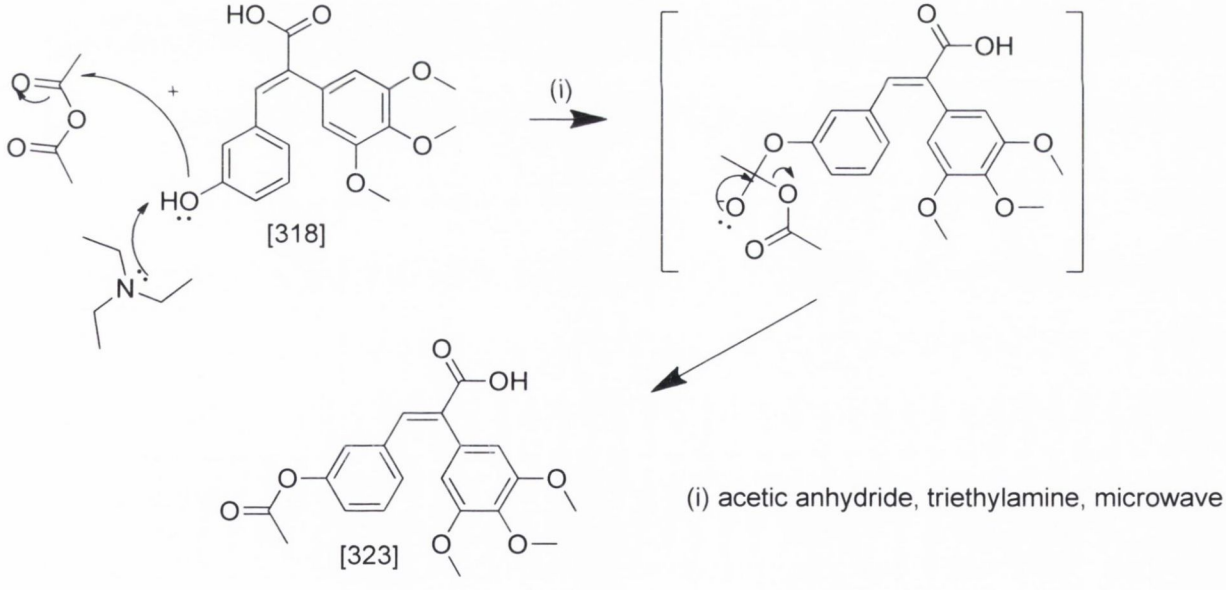

Scheme 3-4 Formation of the acetate ester [323].

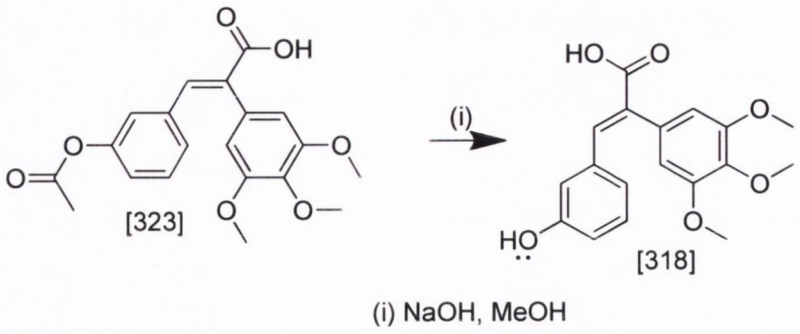

Scheme 3-5 Cleavage of the acetate ester [318]

3.3.3 Synthesised acrylic acid combretastatin analogues

A wide range of novel and previously reported acrylic acid combretastatin analogues were synthesised *via* the Perkin reaction using both the reflux and microwave methods, see Table 10., products [150] and [310]-[327]. The Perkin reaction was a viable and efficient synthetic route to an array of novel combretastatin acrylic acid analogues using a variety of aldehyde starting materials.

Compound ID (* novel)	Structure	Yield % (Reflux)	Yield % (Microwave) # Yield for the cleavage of the acetate ester reaction
[150][504]	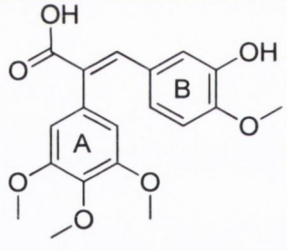	51	64
[311][505]	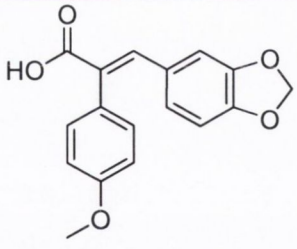	39	47
[312][506]	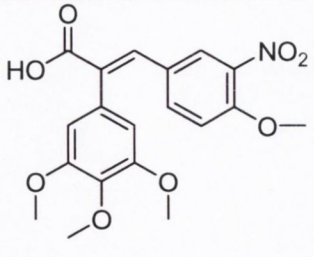	50	65

[313][506]	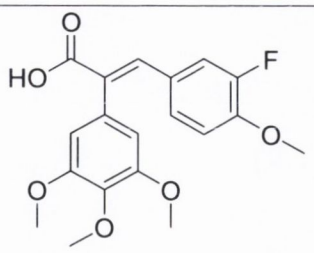	43	65
[310][507]	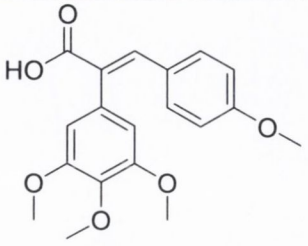	40	45
[314]*	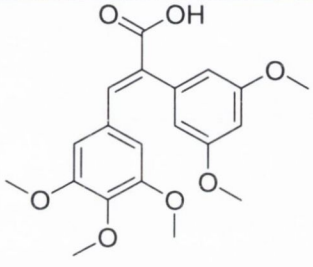	25	35
[315]*	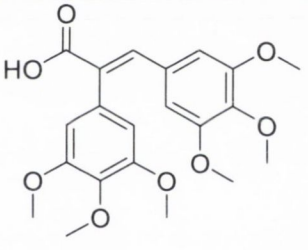	33	96
[316][508]	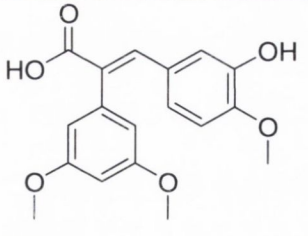	7	N/A
[317][508]	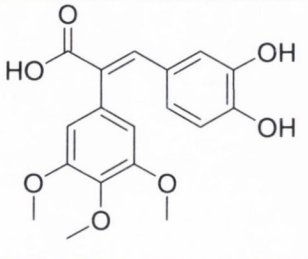	N/A	36

[318]*	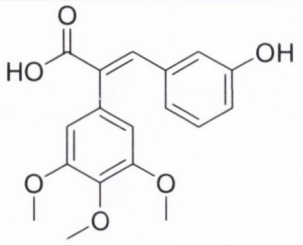	N/A	88#
[319]*	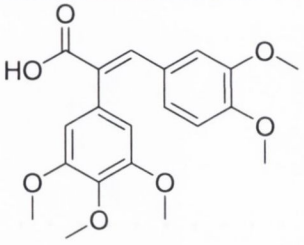	N/A	45
[320]*	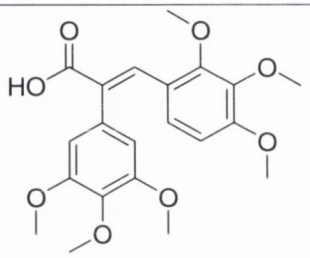	0	30
[321]*	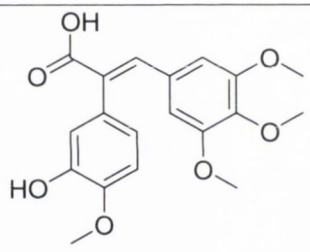	N/A	38
[322]*	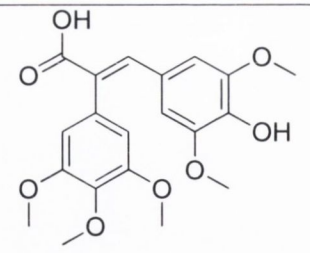	N/A	48
[323]*	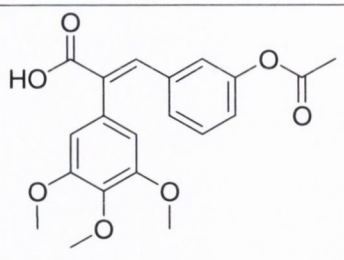	N/A	56

[324]*	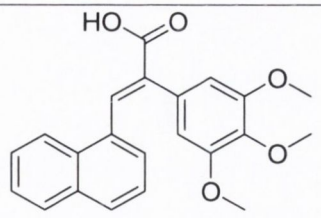	N/A	36
[325]*	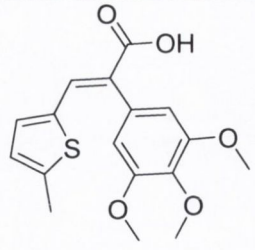	N/A	36
[326]*	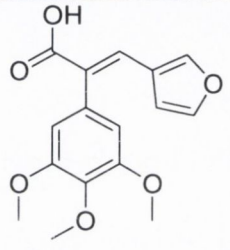	N/A	49
[327]*	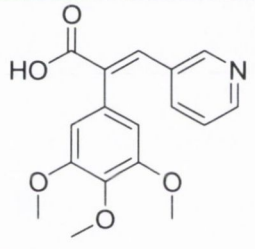	N/A	50

Table 10 Structure and yields of acrylic acids synthesised (* novel compounds)

Compounds [150], [310]-[315] were synthesised *via* the new microwave technique and the conventional reflux methods. Compound [316] was only synthesised *via* the reflux technique due to only having a limited supply of starting material. Compounds [317]-[327] were only synthesised *via* the new microwave method as this technique was optimised and became the preferred route for the efficient synthesis of the acrylic acids. In all cases studied the yields for the microwave method were superior to those of the conventional technique method (Figure 3-2). Not only did the microwave increase the yield but it also reduced the reaction time to 1/6 of the original 3h reaction. The microwave method was a new more productive route in the synthesis of the combretastatin acrylic acid analogues. It is also useful to note that compound [320] was successfully synthesised *via* the microwave method but unsuccessful using the reflux technique.

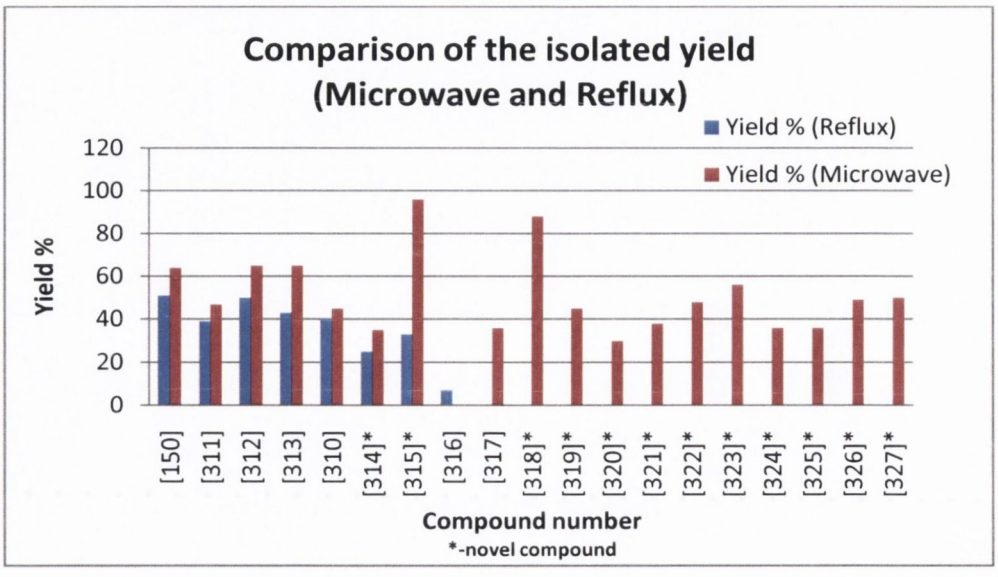

Figure 3-2 Yield comparisons of Microwave and Reflux methods for the acrylic acids synthesised (microwave – 0.5 h, 120 °C; reflux – 3 h, 100 °C)

3.3.3.1 Characterisation of Acrylic acids

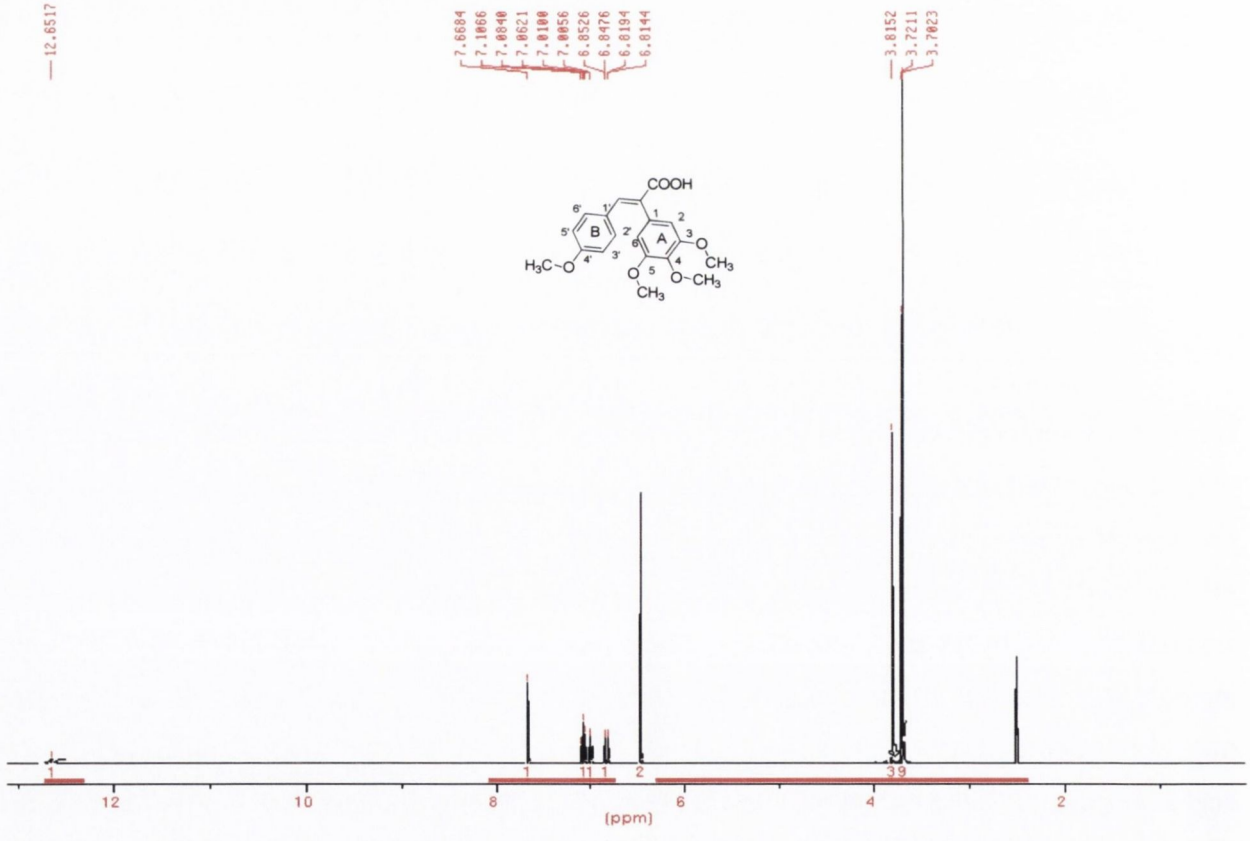

Figure 3-3 ^{1}H-NMR spectrum of [310]

The ^{1}H-NMR spectrum for the acrylic acid analogue [310] is shown in Figure 3-3. The 3-OCH_3 and the 5-OCH_3 protons are both observed as a singlet at 3.70 ppm, the 4-OCH_3 signals are observed as a singlet at 3.72 ppm and the 4'-OCH_3 protons are observed as singlet at 3.81 ppm. The aryl

protons of the trimethoxy-ring (H_2 and H_6) occur as a singlet at 6.45 ppm. The B-ring protons are observed as two doublet at 6.83 ppm (J= 2 Hz) and 6.98 ppm (J= 7 Hz). The alkene bridge proton occurs as a singlet at 7.66 ppm. The proton of the carboxylic group is identified as a broad singlet at 12.65 ppm.

The ^{13}C-NMR spectrum of [310] is shown in Figure 3-4. The 3-OCH_3 and the 5-OCH_3 carbon signals are observed at 56.45 ppm, 4'-OCH_3 (B-ring) carbon at 60.64 and the 4-OCH_3 (A-ring) carbon at 65.40 ppm. The alkene carbon signals are observed at 127.77 ppm and 138.06 ppm. The aromatic carbons of the A-ring are identified at 106.92 ppm (C_2 and C_6), 132.28 ppm (C_1), 137.52 ppm (C_4) and 153.75 ppm (C_3 and C_5) The B-ring aromatic carbons are identified at 113.92 ppm (C_5), 117.34 ppm (C_2), 128.28ppm (C_6), 132.44 ppm (C_1), 148.31 ppm (C_4) and 148.31 ppm(C_3). The carboxylic acid carbon is present at 168.73 ppm.

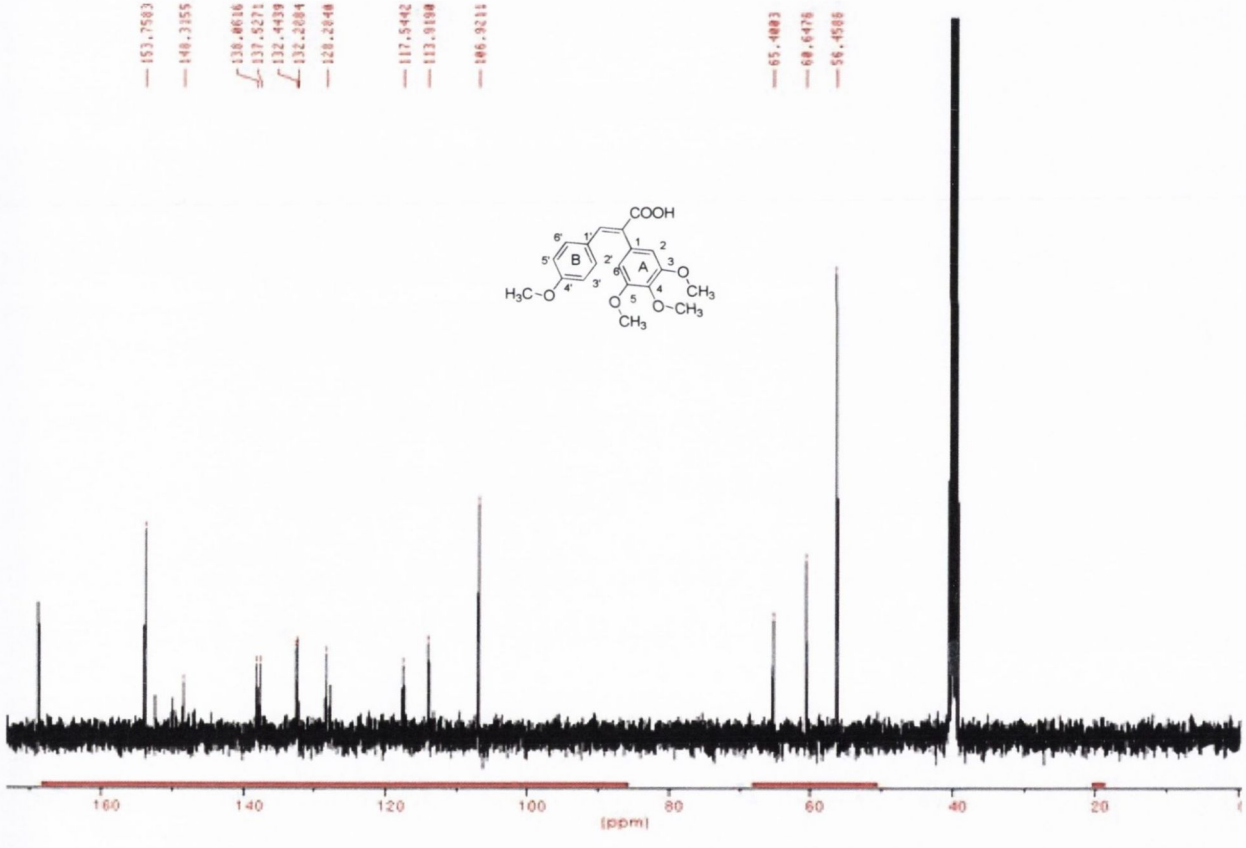

Figure 3-4 ^{13}C-NMR spectrum of [310]

3.3.4 Combretastatin A-4

The synthetic methodologies for preparation of combretastatin A4 [22] are mainly based on Wittig reaction[498, 502], Perkin reaction[500], Suzuki-type reaction[501], Ramberg-Backlund reaction[499], etc. The utilization by our group of the Perkin condensation reaction allowed for the synthesis of a series of acrylic acids [150], [311]-[327] (*cis*-selective) that were required for the synthesis of the

novel conjugates compounds (discussed in Chapter 5). Gaukroger et al. reported the synthesis of CA4 *via* decarboxylation of the Perkin reaction product intermediate [150] shown Figure 3-5.[500, 509] The CA4 was required as a reference compound in this project and was prepared by reaction of compound [150] with copper powder and quinoline at 200 °C for a duration of 2 h to afford the decarboxylated product, CA4 [22], after column chromatography over silica gel and recrystallisation from hexane/ether mix to afford the product [22] in 47% yield as a white crystalline material.

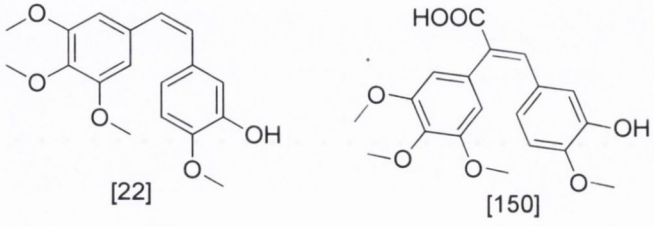

Figure 3-5 Combretastatin A-4 and [150]

3.3.5 Phenylacetic acids

3.3.5.1 Synthetic route for specific phenylacetic acids.

A further extension of this project required the synthesis of specific acrylic acids for conjugation reaction, which were to be obtained *via* the Perkin reaction requiring availability of phenylacetic acids. Some phenylacetic acids required were not commercially available and were synthesised from the corresponding benzaldehyde in a multiple step synthesis illustrated in Scheme 3-6.

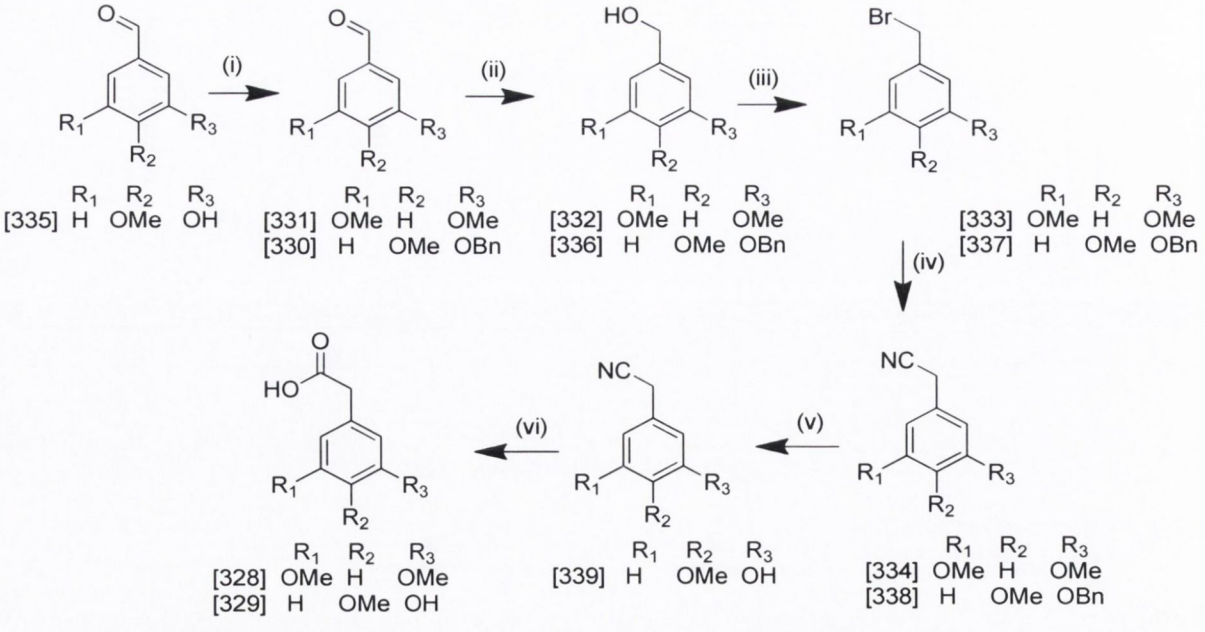

(i) KOH, benzyl bromide, EtOH, 6h, Reflux; (ii) $NaBH_4$, THF, 3h, RT; (iii) PBr_3, DCM, 1h, RT; (iv) Sodium cyanide, DMF, 1h, RT; (v) Pd/C black, EtOAc, H_2, 24 h, Pressure reaction; (vi) conc HCl, 2.5h, Reflux

Scheme 3-6 Synthetic route for the preparation of phenylacetic acid [328] and [329]

The synthetic route for the phenylacetic acids [328] and [329] also required multistep reaction conditions however the compound [329] required two addition steps i.e. the protection of [335] with a benzyl ether to afford [330] and subsequent deprotection to afford [339]. The first step of this synthesis required the reaction of the benzaldehydes [331] and [332] with sodium borohydride to form the corresponding benzylic alcohol. This reduction reaction afforded the benzyl alcohols, [332] and [336] with yields in excess of 95 % and it was possible to proceed to the next step without further purification. The next step in the process was the preparation of the benzylic bromide compounds [333] and [337], and was achieved by the reaction of the alcohols [332] and [336] with phosphorus tribromide at 0 ^{o}C. The mechanism involves initial activation of the alcohol oxygen by the electrophilic phosphorus, followed by an S_N2 substitution at the alcohol carbon.

The nitrile compounds [334] and [338] were obtained by reaction of [333] and [337] with sodium cyanide. The cyanide ion acts as a nucleophile and reacts with benzylic bromide to form the nitrile. This S_N2 mechanism involves an initial ionisation of the bromide, followed by a very rapid attack by the cyanide ion on the carbocation formed. At this stage of the synthesis, removal of the benzyl protecting group was required. The conventional procedure for removal of the benzyl protecting group required a hydrogenation over Pd/C catalyst (as discussed in Section 2.3.5).[483] This reaction for the debenzylation of [338] was tried initially for 3 hours and monitored *via* TLC; after the 3 hours all starting material still remained. This was subsequently repeated with the use of a larger surface area Pd/C catalyst (Palladium black) for the duration of a week constantly monitoring *via* TLC. The TLC showed that all the starting material remained. It was unclear why this reaction was not successful as this is the preferred route for the removal of the benzyl group. It was decided to attempt a pressurised hydrogenation (Parr reactor) over Pd/C.[483] The benzyl protected compound [338] was dissolved in the minimum quantity of ethyl acetate and to this palladium black (large surface area) was added. The reaction vessel was placed under 3 bar of hydrogen gas and was allowed to react for 24 h. After the 24 h the mixture was analysed *via* TLC, it showed the formation of a new product which was subsequently shown to be the deprotected compound [339]. After purification, the yield of the phenol compound [339] recovered was 77%. (Scheme 3-7).

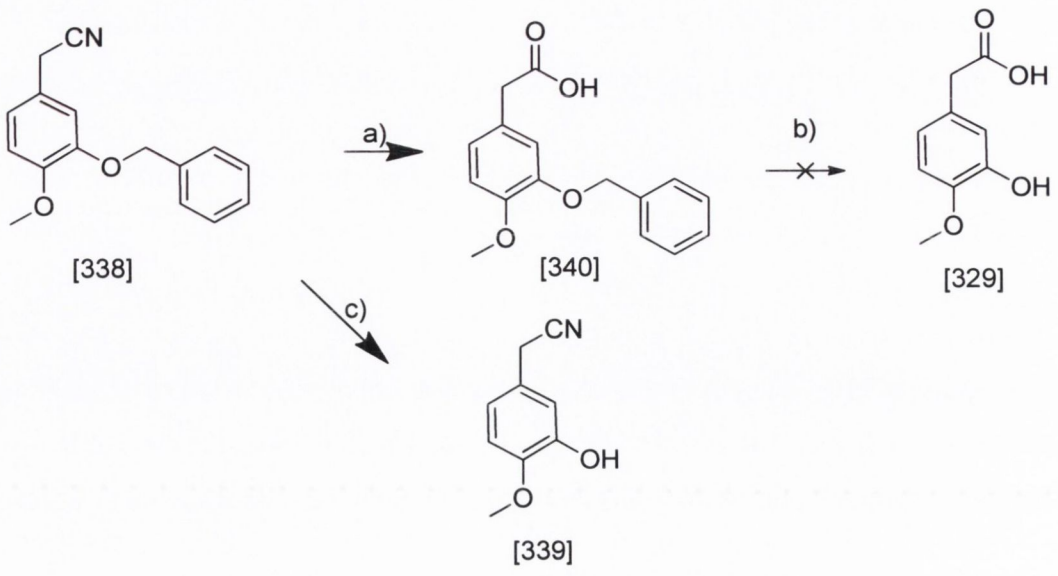

a) HCl, Reflux; b) and c) Pd/C black, EtOAc, H_2, 24 h, 3 barr

Scheme 3-7 Synthesis of benzylic nitrile [339]

It was also investigated whether the deprotection would occur if the protected phenylacetic acid compound [340] was synthesised initially. This reaction was performed under the same condition as for the formation of [339] but the TLC did not show the formation of any new materials indicating the preferred route for the synthesis of the phenylacetic acid [329] was *via* the deprotected benzylic nitrile [339]. The final step in the synthesis of the phenylacetic acids was the hydrolysis of the nitrile compounds [334] and [339] to afford the acid products [328] and [329]. The mechanism of nitrile hydrolysis required the protonation of the amide carbonyl which makes this more electrophilic. The water molecule acts as the nucleophile, attacking the electrophilic carbonyl creating the tetrahedral intermediate. The attached water molecule that loses a proton. Then the NH_2 group becomes protonated and forms a good leaving group. Deprotonation of the oxonium ion gives the carbonyl in the carboxylic acid product and regenerates the acid catalyst, (Scheme 3-7).

Starting material	Yields					
	Benzylation	Benzyl Alcohol	Benzyl Bromide	Benzyl Nitrile	Deprotection	Phenylacetic Acid
[331]	-	[332]– 98%	[333]- 80%	[334]- 74%	-	[328]- 61%
[335]	[330]- 53%	[336]- 95%	[337]- 93%	[338]- 87%	[339]- 77%	[329]- 21%

Table 11 Synthesis of the phenylacetic acids [328] and [329]

The two reaction sequences were successful in producing the desired phenylacetic acid [328] and [329]. The yields throughout were sufficiently high (53-98%) except for the last step in the

formation of the acidic compound [329] which was low (21%) when compared with that of the equivalent step in the formation of [328] (61%), Table 11.

In the ^{1}H-NMR for the phenylacetic acid [329], the CH_2 protons are observed as a singlet at 3.38 ppm and the methoxy protons was found as a singlet at 3.73 ppm. The aromatic protons are seen as a singlet at 6.69 ppm and a doublet at 6.62 ppm, J= 2 Hz. The remaining aromatic proton was observed at 6.62 ppm while the carboxylic acid proton was observed at 12.09 ppm. In ^{13}C-NMR spectrum of [329], the CH_2 carbon signal is identified at 55.61 ppm. The methoxy carbon signal is found at 59.70 ppm. The carboxylic acid carbon is observed at 172.99 ppm. The remaining signals correspond to the aromatic carbons which are identified in the region, 112-146 ppm.

3.3.6 Cinnamic acids and related 3-phenylpropanoic acid

A further objective of this project was to prepare conjugates of endoxifen with cinnamic and phenylpropanoic acids related in structure to A and B rings of CA4. For this modified structure the substituent ring would now be either the 3,4,5-trimethoxy ring (A ring) or the 3-hydroxy-4-methoxy-ring (B ring). Both rings (A and B) have been shown to be essential for the antitubulin combretastatin CA4 activity [22].[497] The investigation was carried out to establish if the dual ring structure and/or the ethylene bridge was essential for biological activity. For this it would be required that all other components of the conjugate molecule to be retained. The appropriate 3,4- and 3,4,5- cinnamic and 3-phenylpropanoic acids were required to afford the desired conjugates for this investigation. The synthesis of compounds [342] and [344] (Scheme 3-8) were performed using microwave methodology. The reaction time was short (8 min). The appropriate aldehyde was reacted with malonic acid in the presence of acetic acid and piperidine. The reaction mechanism is illustrated in Scheme 3-9.

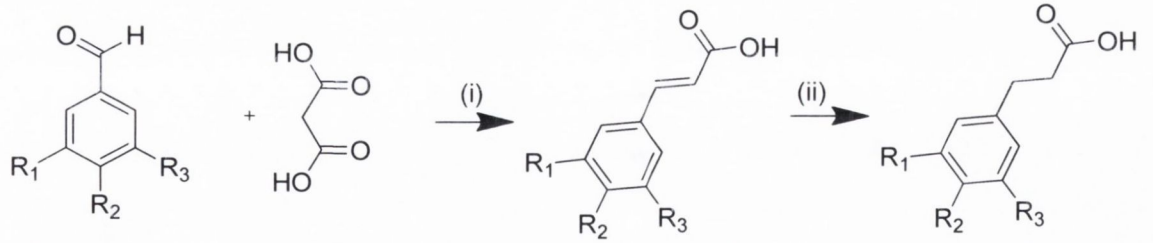

R1	R2	R3
[335]	H	OMe OH
[335a]	OMe	OMe OMe

[341]

	R_1	R_2	R_3
[342]	H	OMe	OH
[344]	OMe	OMe	OMe

	R_1	R_2	R_3
[343]	H	OMe	OH
[345]	OMe	OMe	OMe

(i) piperidine, acetic acid, 8 min, MW; (ii) 12% KOH, Pd/C, H_2, 1h, RT

Scheme 3-8 Synthesis of cinnamic acids and 3-phenylpropanoic acids

Compound	Structure	Yield (%)
[342][510]	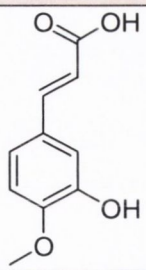	72
[343][510]	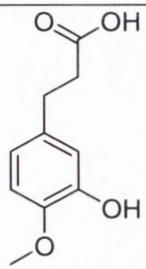	80
[344][511]	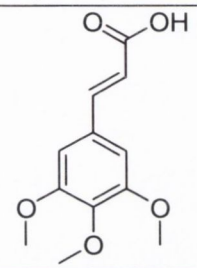	65
[345][511]	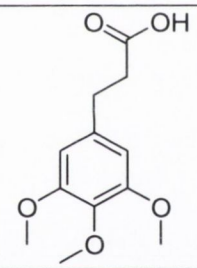	84

Table 12 Synthesised cinnamic acids [342] and [344], and 3-phenylpropanoic acids [343] and [345]

The formation of these single aryl cinnamic acids is achieved *via* the Knoevenagel condensation reaction with the Doebner modification. Conventionally, the Knoevenagel condensation reaction is a reflux reaction of aldehydes/ketones and acids in the presence of pyridine with reaction times of hours, Sinha *et al,* reported that the single cinnamic acids could be formed using microwave irradiation with a short reaction time and higher yields from the corresponding aldehyde.[512] A Knoevenagel condensation is a nucleophilic addition of an active hydrogen compound to a carbonyl group followed by a dehydration reaction in which a molecule of water is eliminated. With malonic acid type compounds the reaction product can lose a molecule of carbon dioxide in a subsequent decarboxylation step in the presence of refluxing pyridine and this is known as the Doebner modification

The condensation of carboxylic acid compounds with aldehydes to afford α,β-unsaturated compounds is known as the Perkin reaction. The Doebner modification, which is possible in the

presence of carboxylic acid groups, includes a piperdine/pyridine-induced decarboxylation. The reaction mechanism of the Knoevenagel condensation can be seen below Scheme 3-9. Firstly the formation of an enol intermediate occurs. This enol reacts with the aldehyde, resulting with an aldol that undergoes subsequent base-induced elimination. The Doebner-modification in refluxing piperidine effects concerted decarboxylation and elimination of CO_2.

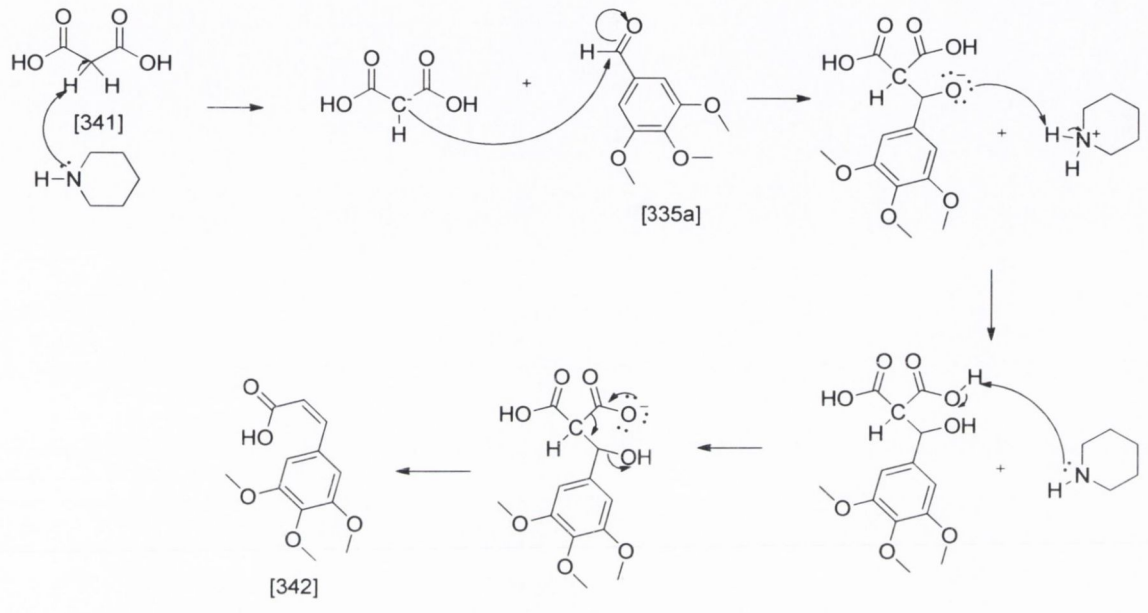

Scheme 3-9 Mechanism for the formation of cinnamic acids [342] and [344] *via* the Doebner modification of the Knoevenagel condensation

3.3.6.1 Spectroscopic characterisation of cinnamic acids

The ^{1}H-NMR spectrum of [342] is shown in Figure 3-6. The methoxy protons are observed as a singlet at 3.80 ppm. The two alkene protons on the ethylene bridge are observed as doublets at 6.25 ppm, *J*= 16Hz and 7.45 ppm, *J*= 16Hz. The aromatic protons are observed as a doublet at 6.94 ppm, *J*= 8Hz and the two remaining aromatic protons appear as a multiplet at 7.08 ppm. The phenolic proton was observed as a broad singlet at 9.19ppm, while the carboxylic acid proton occurs as a broad singlet at 12.20 ppm. The ^{13}C-NMR spectrum of [342] is shown in Figure 3-7. The methoxy carbon signal is observed at 55.59 ppm and the two alkene carbons are observed at 114.06 and 144.2 ppm. The quaternary aromatic carbon were identified at 149.8 ($COCH_3$), 146.6 (C-OH) and 127.0 (ArC-CH_2) ppm. The remaining aromatic carbon signals were observed at 121.0, 116.2 and 111.9 ppm. The carbon of the carboxylic acid group is present at 167.79 ppm.

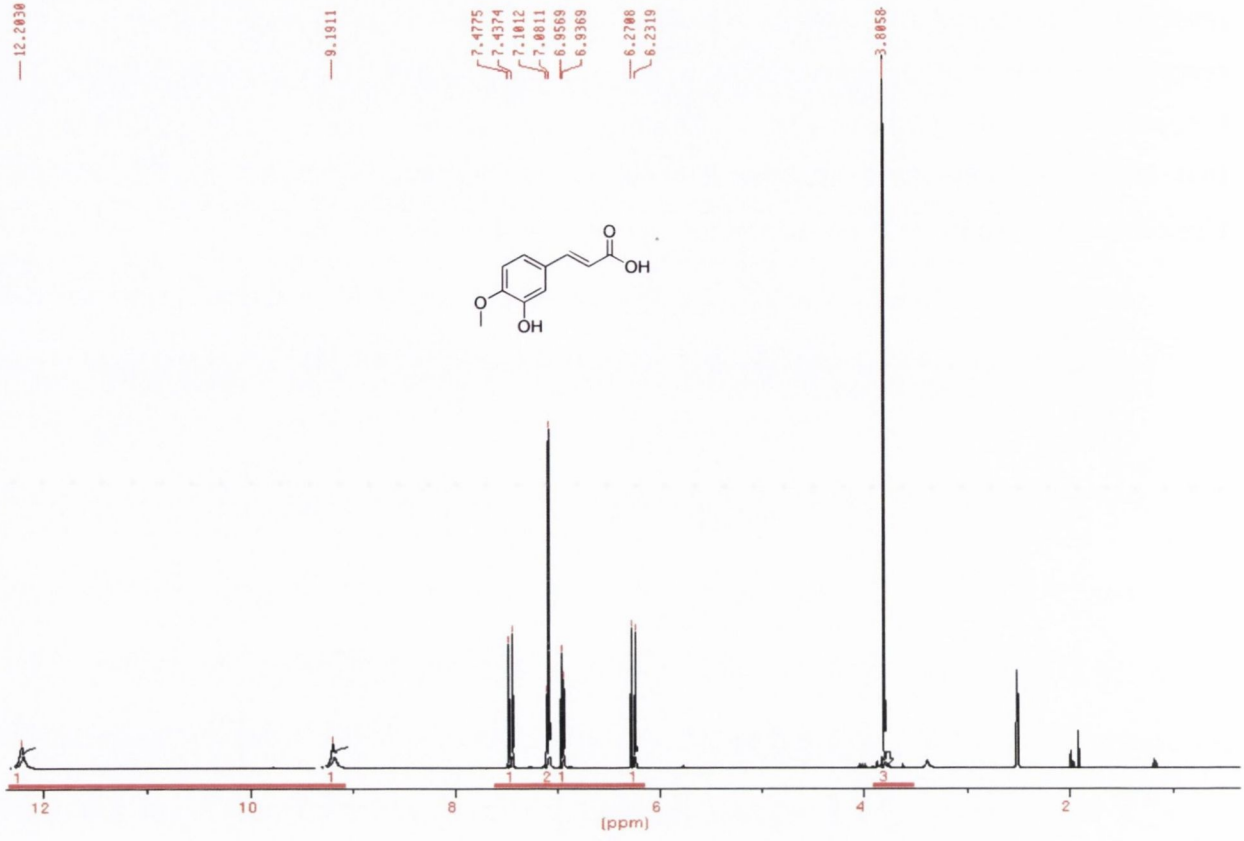

Figure 3-6 ^{1}H-NMR spectrum of [342]

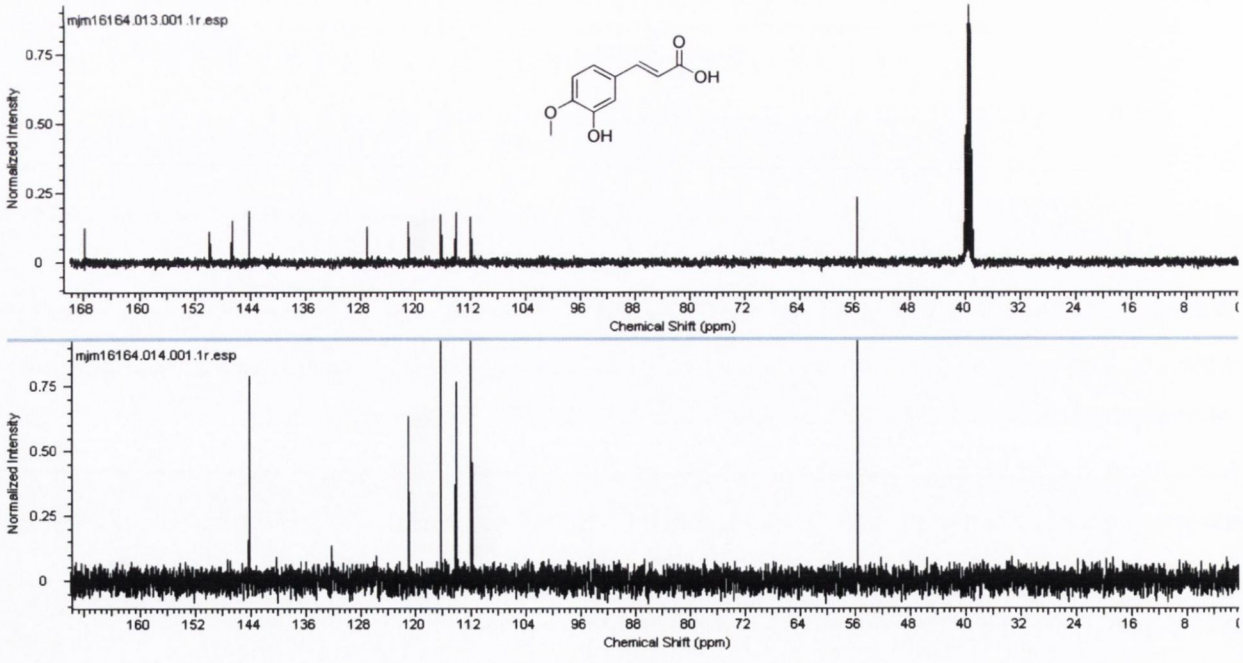

Figure 3-7 ^{13}C-NMR spectrum of [342]

3.3.6.2 Reduction of cinnamic acids

The cinnamic acids [342] and [344] were reduced *via* a palladium/C hydrogenation to produce the corresponding 3-phenylpropanoic acids [343] and [345], with yields in excess of 80 %

(Scheme 3-10). The ^{1}H-NMR spectrum of [343] is shown in Figure 3-8. The CH_2 protons are identified as triplets at 2.44 ppm, *J*= 7.5 Hz and 2.67 ppm, *J*= 7.5 Hz. The methoxy protons are found as a singlet at 3.72 ppm. The aromatic protons are seen as a doublet at 6.58 ppm, *J*= 9 Hz, as a singlet at 6.63 ppm and as a doublet at 6.79 ppm, *J*= 8 Hz. The phenolic proton was noted as a broad singlet at 8.82 ppm. The carboxylic acid proton was observed as a broad singlet at 12.08 ppm. The ^{13}C-NMR spectrum of [343] is shown in Figure 3-9. The two CH_2 carbons are identified at 29.72 and 35.54ppm. The methoxy carbon is seen at 55.64 ppm. The quaternary aromatic carbon were identified at 146.3 ($COCH_3$), 145.9 (C-OH) and 133.5 (ArC-CH_2) ppm. The remaining aromatic carbon signals were observed at 118.6, 115.5 and 112.2 ppm. The carbon of the carboxylic acid group is present at 173.86ppm.

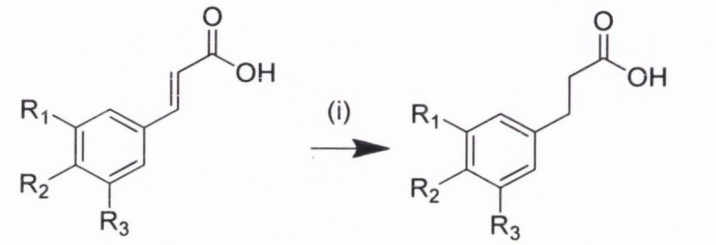

(i) 12% KOH, Pd/C, H_2, 1h, RT

Scheme 3-10 Reduction of the cinnamic acids

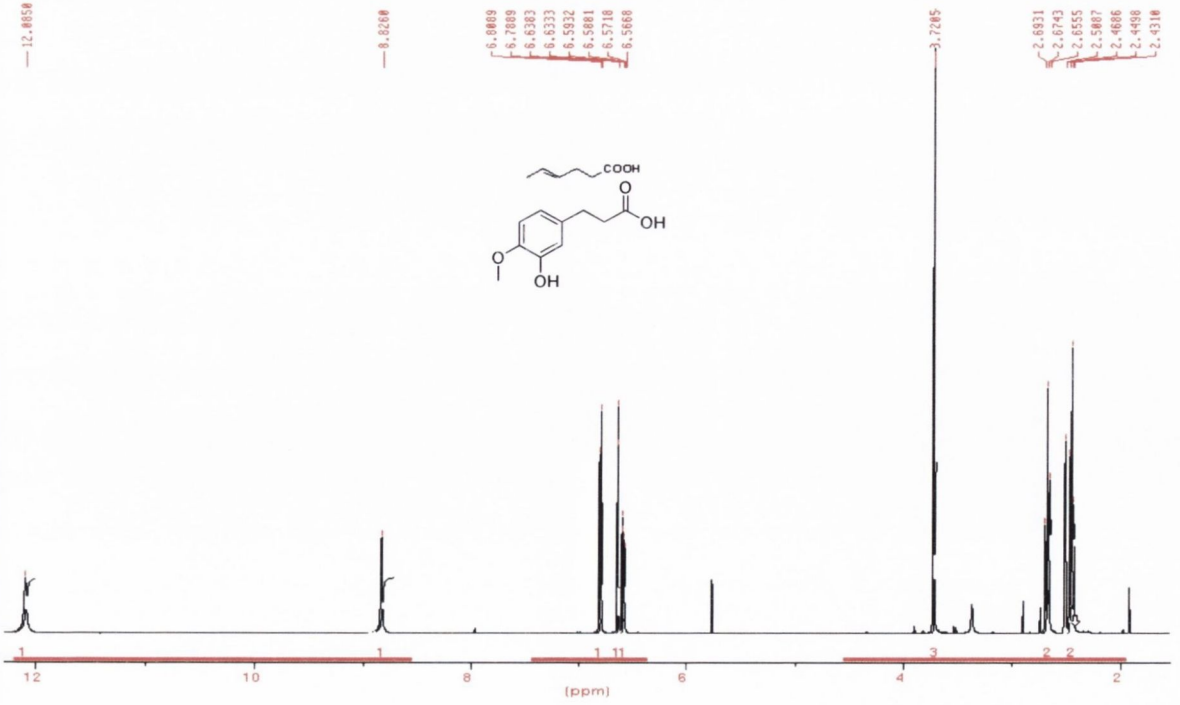

Figure 3-8 ^{1}H-NMR spectrum of [343]

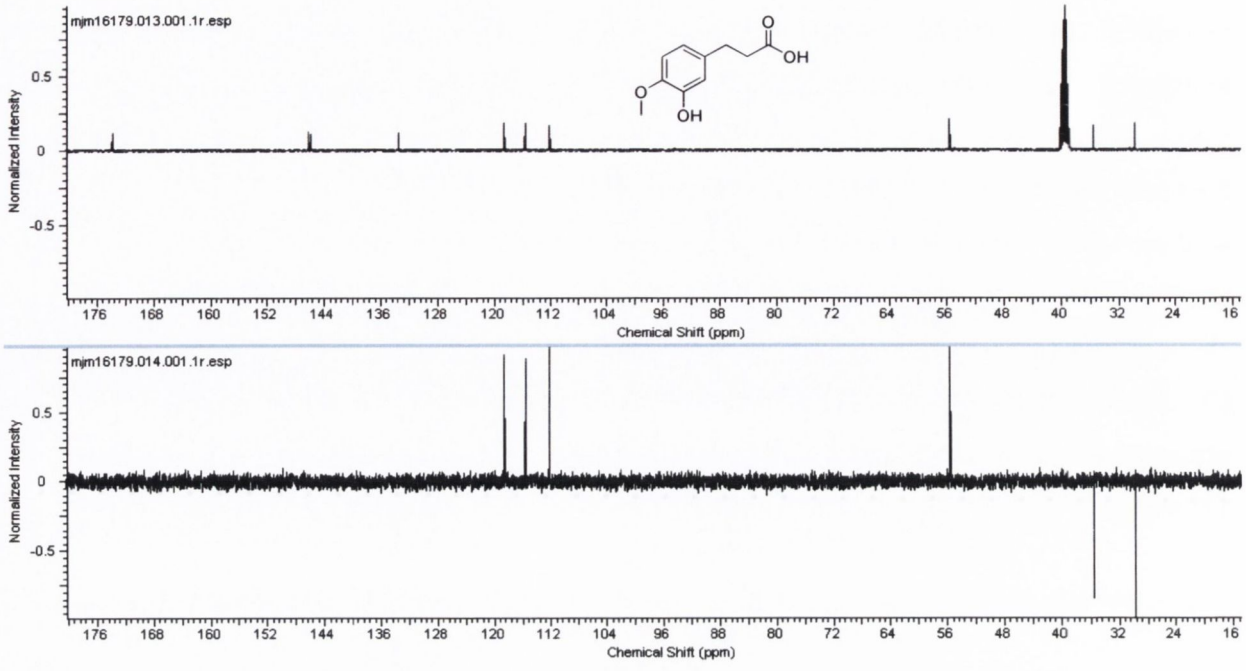

Figure 3-9 ^{13}C-NMR and DEPT-135 spectrums of [343]

3.3.7 Attempted synthesis of Hydroxamic acid derivatives

Hydroxamic acids have received much attention in recent years due to their extensive range of biological activities and low toxicities.[513] Much of the activities of these compounds are due to their chelating properties with metal ions.[514] The utilization of hydroxamic acids is extensively reported; hydroxamic acids and their derivatives are reported as effective antibacterial and antifungal agents[515]. Their ability to coordinate to metal ions is responsible for their antimicrobial action. Some hydroxamic acids are potential antimalarials[516]. The drug ''Desferal'' is used for the elimination of iron from the body.[517] Derivatives of 3,4,5-trimethoxybenzohydroxamic acid act as mental tonic. ''Bufexmac'' is used as an anti-inflammatory agent.[518] Hydroxamic acids have also shown possible therapeutic applications as anticancer[519], antibiotic[520] and antitumor agents[521].

A synthetic route to hydroxamic acid analogues of the CA4 acid [150] was attempted *via* the methyl ester of the acrylic acid, (Scheme 3-11). The esterification reaction was carried out using microwave irradiation for 30 min at 120 °C. These conditions were not optimized but were successful in the formation of the acrylic esters. One benefit of using this method was that the acrylic ester, precipitated out of solution and was filtered. This isolated product required some further purification using column chromatography over silica gel. The synthesis of the hydroxamic acid from the corresponding ester is well documented in the literature.[522-524]

Unfortunately treatment of the acrylic acid ester [363] and [364] with hydroxylamine in the presence of KOH or sodium methoxide did not afford the desired hydroxamic acid derivatives of combretastatin acrylic acid (Scheme 3-11).

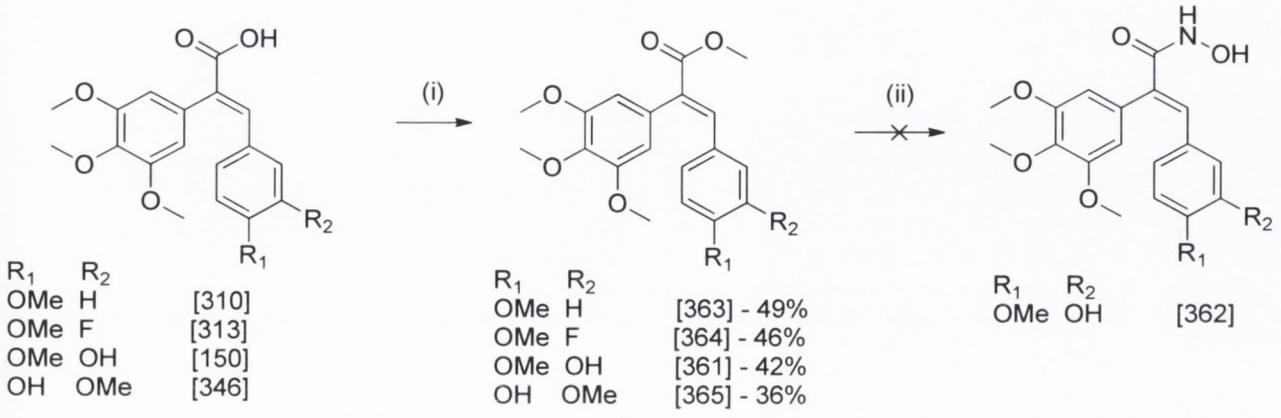

(i) NaOH, MeOH, MW; (ii) a) Hydroxylamine.HCl, NaOMe, MeOH; / b) Hydroxylamine.HCl, KOH, 80 °C, MW

Scheme 3-11 Attempted synthesis of the hydroxamic acid [362] *via* the methyl ester

3.3.7.1 Piperazine derivatives of the acrylic acid scaffold

A series of piperazine amide derivatives of the CA4 acid [22] were prepared for biochemical investigation. Piperazines constitute an attractive pharmacological scaffold and have been exploited for their biological activity. The piperazine ring is found in many drugs, including antianginals, antidepressants, antihistamines and antipsychotics. This small and rigid heterocyclic backbone acts on a various pharmacological targets.[525, 526] The piperazine ring system has been utilized in approximately 7 % of all small molecules that were awarded FDA approval between 1998 and 2009 and is found as phenylpiperazine, benzylpiperazine, diphenylmethylpiperazine (benzhydrylpiperazine), pyridinylpiperazine and pyrimidinylpiperazine.[525] The piperazine ring is used as both a rigid three dimensional diamine core structure and as well as modifying group to introduce an amine residue in molecules. This approach is often taken in order to improve solubility, increase molecular weight or achieve changes in the ionization state of novel drug substances.

The required piperazine amide derivatives [347]-[360] were synthesised from the acrylic acid derivative of combretastatin analogue molecules [150],[310],[313] and [346]. The use of the piperazine derivative was interesting as a small molecule and also had the potential for conjugation to the ER ligand (Scheme 3-12). The novel products [347]-[360] are illustrated in Table 13, together with yields which were in the range 4 - 37%.

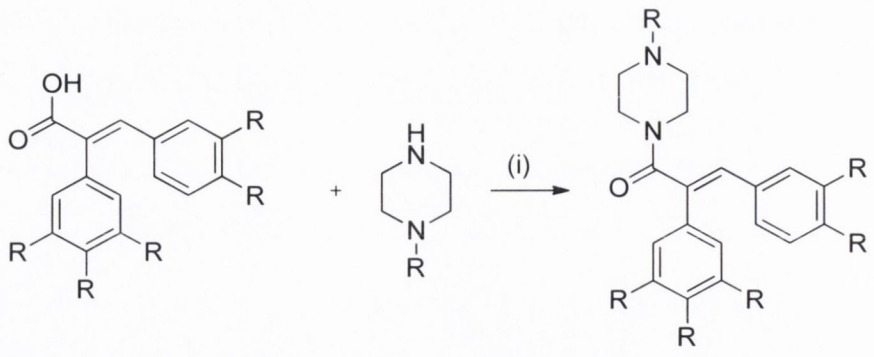

(i) DCC, HOBt, DCM, 16 h, RT

Scheme 3-12 Synthesis of the piperazine derivatives [347]-[360]

DCC (*N,N'*-dicyclohexylcarbodiimide) was successfully used to couple the various piperazine secondary amines with carboxylic functionally on the acrylic acid combretastatin analogues ([150], [310], [313] and [346]) in order to form amide linkages. The DCC acts as a dehydrating condensing agent to activate carboxylic acids for amide formation.[503] When HOBt (Hydroxybenzotriazole) is added to with DCC, it reduces side reactions (intramolecular formations) and increases the yield of coupled product. HOBt reacts with activated acyl groups (carboxylic acid + DCC) to form the activated ester. This ester reacts with amines at ambient temperatures to afford the amide product. The mechanistic detail of the amide formation reaction involving DCC and HOBt is shown in Scheme 3-13. The piperazine analogues have distinctive and characteristic signals observed in the ^{1}H-NMR spectrum (Figure 3-10).

The ^{1}H-NMR spectrum for the piperazine analogue [349] is shown in Figure 3-10. The proton signals for the two CH_2 groups appear as two multiplets at 2.70 - 2.92 ppm and 3.70 -3.80 ppm however they overlap with the methoxy signal at 3.72 ppm having a combined integral of 10 protons (6 H for two methoxy and 4 H for the two CH_2). The 3-OCH_3 and the 5-OCH_3 protons are identified as a singlet at 3.72 ppm. The 4-OCH_3 protons are found as a singlet at 3.78 ppm. The A-ring (or trimethoxy-ring) aromatic protons appear as a singlet at 6.54 ppm. The B-ring protons are observed as a doublet at 6.75 ppm with J= 2 Hz and as a doublet at 7.11 ppm with J= 7 Hz. The alkene proton appears as a singlet at 6.65 ppm. The ^{13}C-NMR spectrum of [349] is shown in Figure 3-11 . The assignment of the acrylic acid portion of the analogue similar to that of [150]. The significant region to note is between 35 – 50 ppm. In this region it was expected to observe the signals for the carbons for the N($\underline{C}H_2$)$_2$ (Figure 3-11). These signals are not observed for both sets carbons of the N(CH_2)$_2$, but with the use of ^{1}H NMR and HRMS (429.2041 required for $C_{23}H_{29}N_2O_6$), and in consultation with Dr. John O'Brien (TCD NMR specialist) it is concluded that [349] was obtained even with the absence of the piperazine CH_2 signals from the ^{13}C NMR spectrum.[527] The carbon signal for the N(CH_2)$_2$

carbons was not present in the ^{13}C NMR spectra for some of the related piperazine analogues synthesised.

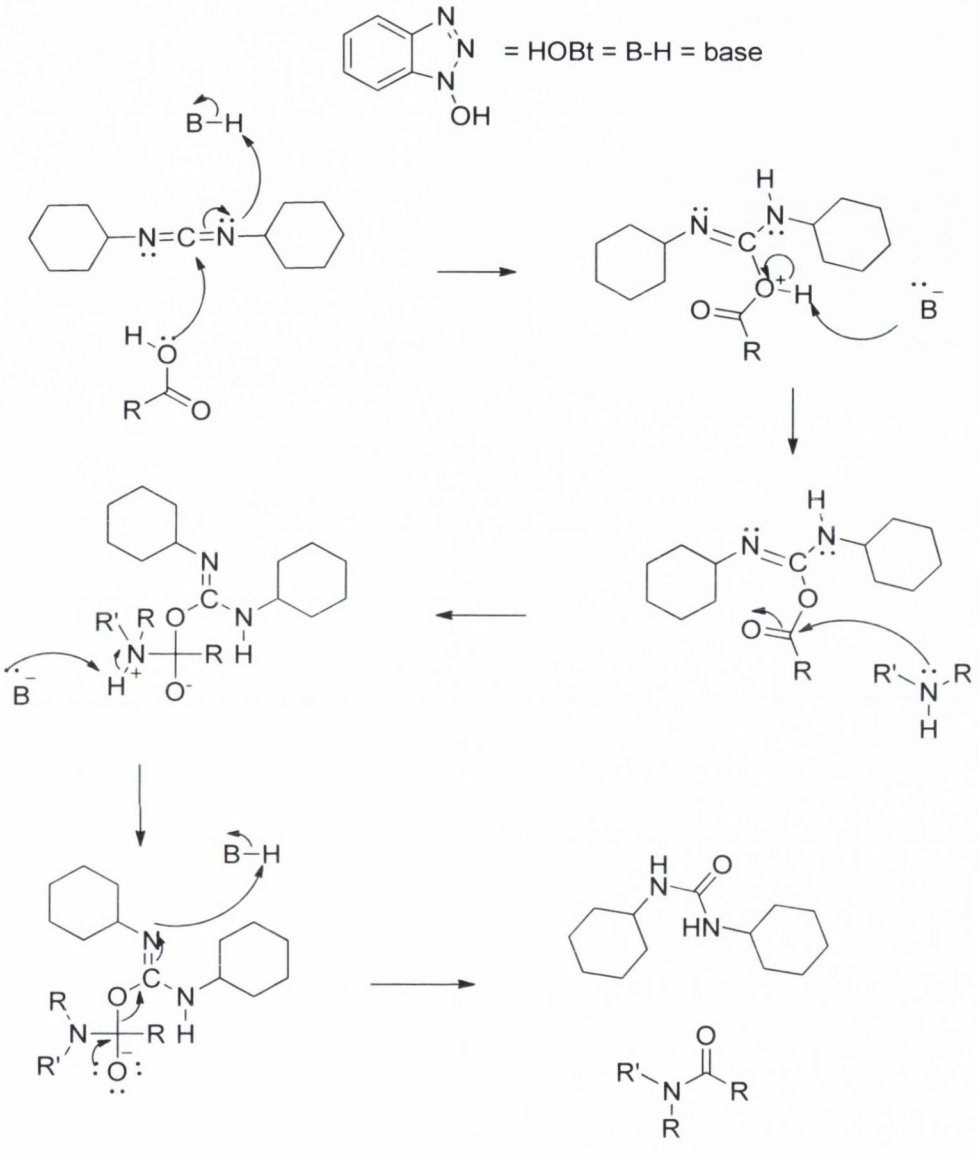

Scheme 3-13 DCC coupling reaction mechanism for amide synthesis

The novel combretastatin-piperazine amide derivatives [347]-[360] will be interesting as a small molecule and also have the potential for conjugation to an ER ligand such as endoxifen. The piperazine amide derivative [347]-[360] will be evaluated as potential small molecule anticancer agents (Chapter 6) and compounds [347]-[340] would potentially be incorporated into the conjugate scaffold.

Starting material	Compound (Novel = *)	Structure	Yield %
[310]	[347]*	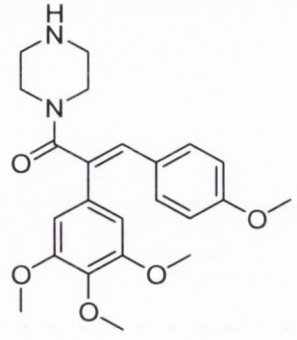	37
[313]	[348]*	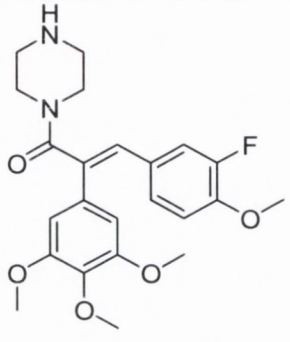	32
[150]	[349]*	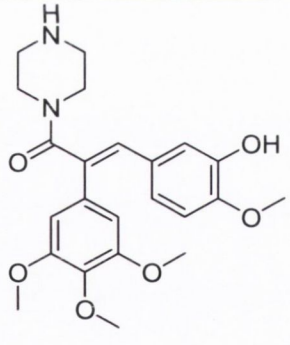	16
[346]	[350]*	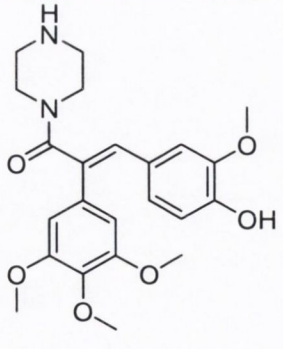	4

[310]	**[351]***	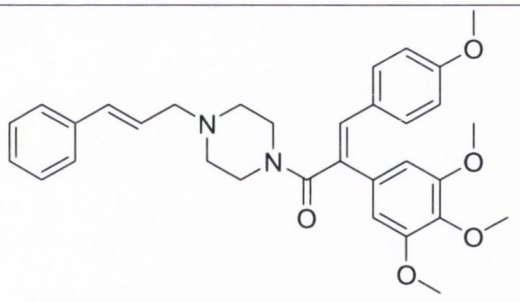	16
[313]	**[352]***	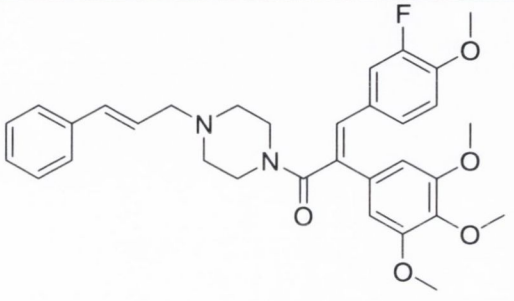	19
[310]	**[353]***	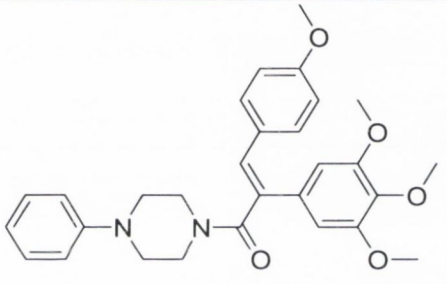	29
[313]	**[354]***	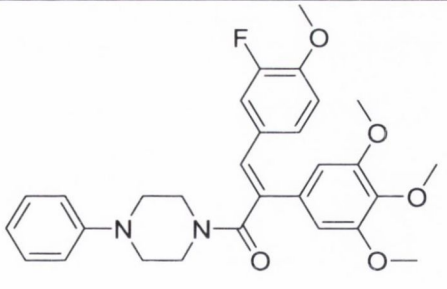	31
[150]	**[355]***	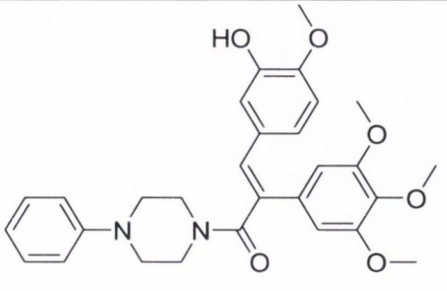	28

[346]	**[356]***	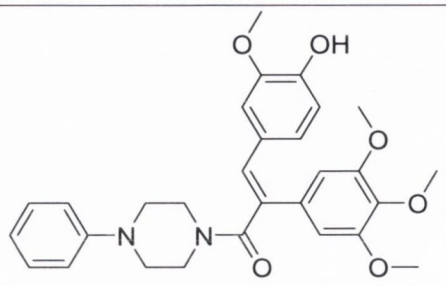	31
[310]	**[357]***	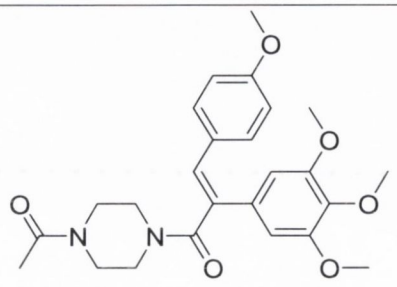	12
[313]	**[358]***	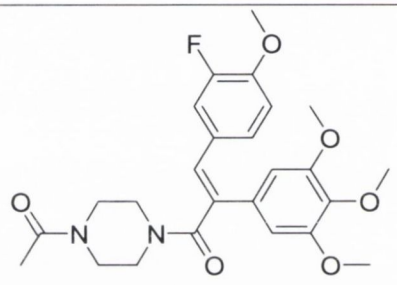	23
[150]	**[359]***	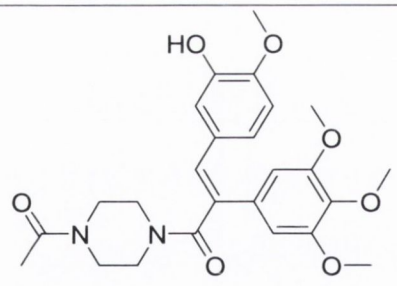	15
[346]	**[360]***	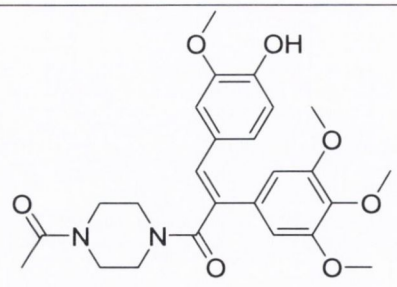	11

Table 13 Piperazine derivatives [347] - [360] (*novel compounds)

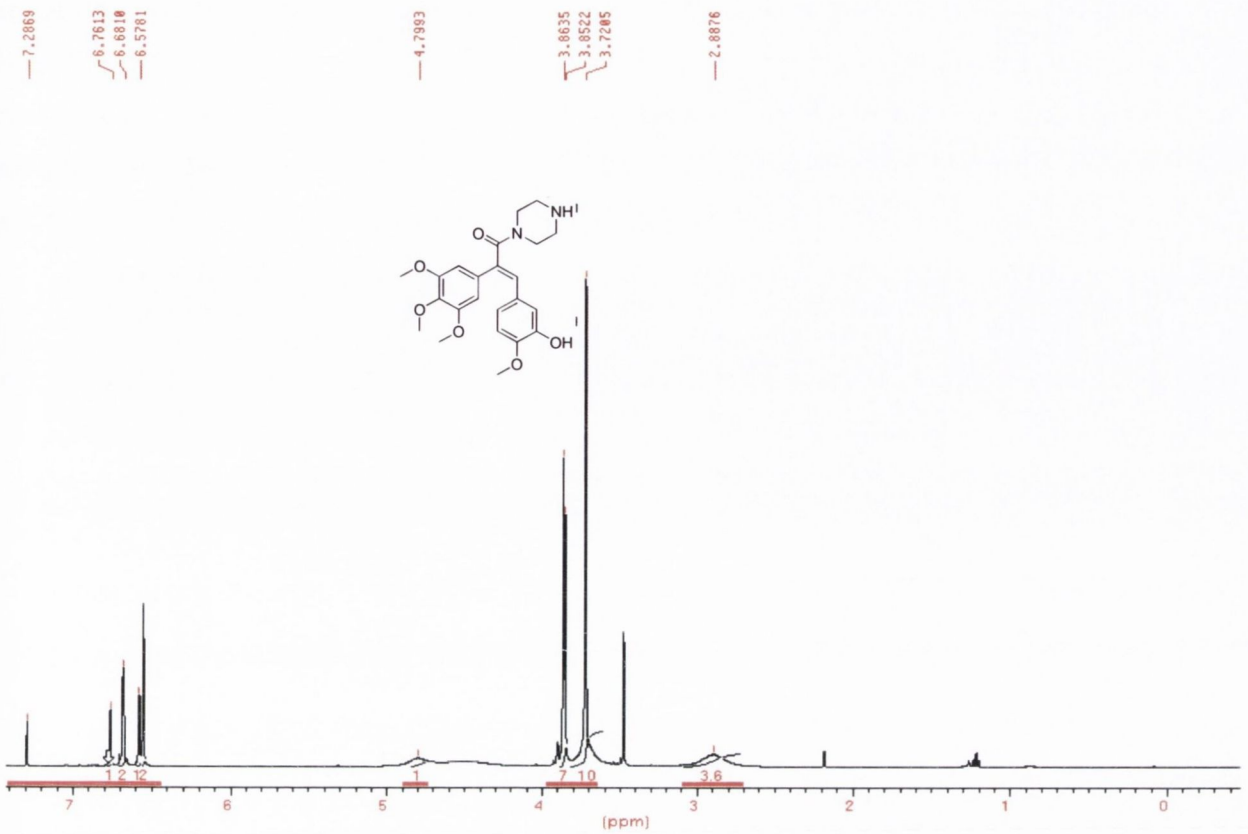

Figure 3-10 ^{1}H-NMR spectrum of [349]

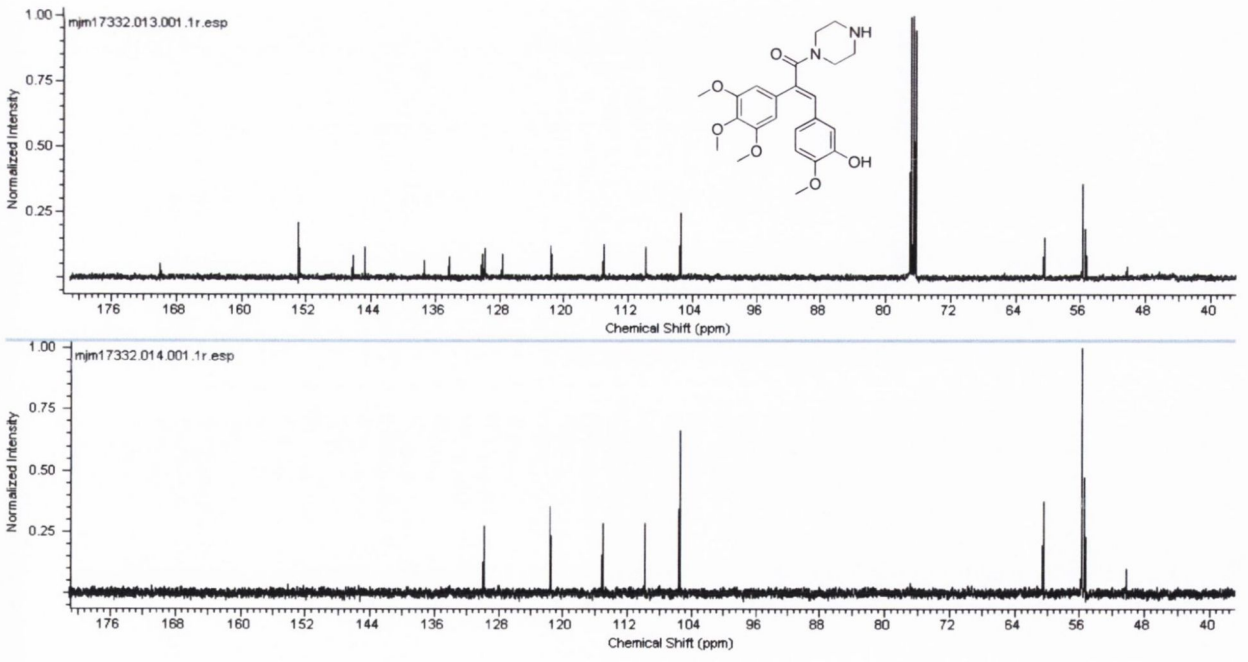

Figure 3-11 ^{13}C-NMR and DEPT-135 spectras of [349]

The synthesis of a series of novel combretastatin based analogues was successful. The investigation of the microwave irradiation induced Perkin reaction for the formation of the acrylic acids found an improved method for the synthesis of these acids with greater yields and reduced

reaction times. The synthesised acrylic acids will be incorporated into the conjugate scaffold as potential cytotoxic agents (Chapter 5). The investigation of the necessity of the bi-aryl pharmacophore of the combretastatin analogues will be investigated by incorporating the cinnamic and propanoic acid of [150] derivatives into the conjugate scaffold and could give valuable information on the role of the acrylic acids bulk within the ER binding pocket. The synthesis of the novel piperazine derivates of the CA4 acrylic acids will be evaluated for antiproliferative activity.

Chapter 4
Aromatase Inhibitors

4.1 Overview

Aromatase inhibiting drugs such as anastrozole and letrozole used in the treatment of hormone dependent breast cancer and have recently replaced tamoxifen as the accepted standard of care in many post menopausal breast cancer patients. The American Society of Clinical Oncology (ASCO) documented that the optimum adjuvant therapy for postmenopausal women should now include the use of an aromatase inhibitor, either as initial treatment or after 2-5 years treatment with tamoxifen, to reduce the risk of tumour recurrence.[528] Aromatase inhibiting drugs act by a different mechanism to than that of tamoxifen. The estrogen in menopausal women is biosynthesised in the adrenal glands rather than the ovaries. The adrenal glands secrete androstenedione which is then converted in fatty areas of the body into estrogen by the enzyme, aromatase. Blocking aromatase activity provides a route to inhibiting estrogen production. Drugs which act as aromatase inhibitors can reduce estrogen production by 90 to 95%.

In the present work, it is proposed that if an aromatase inhibitor pharmacophore could be incorporated into the ER-antagonist conjugate scaffold, the beneficial biological activity of both drugs could be observed. Consequently, the synthesis of a tamoxifen conjugate with an aromatase inhibitor is an interesting target for conjugate drug design. Two design routes are proposed for incorporating the AIs into the conjugate (Scheme 4-1); the first route is to synthesize an anastrozole derivative that could be covalently linked through an amide bond to endoxifen to produce the conjugate [463], Scheme 4-1. The second route is to synthesize a letrozole derivative that would replace the endoxifen ligand and would be linked to the cytotoxic drug to afford the conjugate [464]. It was believed that the second route would lose the ER binding capability of the conjugate however it could show activity *via* restricting the availability of estrogens by interfering with the steroid biosynthetic pathway. The fragments identified for synthesis of [463] and [464] will contain the required structural features of anastrozole and letrozole for aromatase inhibitory activity.

4.2 Synthesis of the anastrozole pharmacophore

Anastrozole [96] is third generation aromatase inhibitors that can selectively binds to, and reversibly inhibit aromatase and has been shown to inhibit tumour growth. An anastrozole pharmacophore was proposed as a novel conjugate ligand. The synthesis of anastrozole has been documented only in the patent literature.[529, 530] The synthetic route proposed in this work is based on a previous route reported to anastrozole-like compounds by Jackson *et al.*[531] in which the synthesis of a series of novel dual aromatase-sulfatase inhibitors (DASIs) incorporated anastrozole derivatives synthesised from 3,5-dimethylbenzoic acid [368]. This route was suitable for the synthesis of anastrozole derivative for the proposed ER-AI conjugate compound but required some modifications as illustrated in Scheme 4-2 for the preparation of [376].

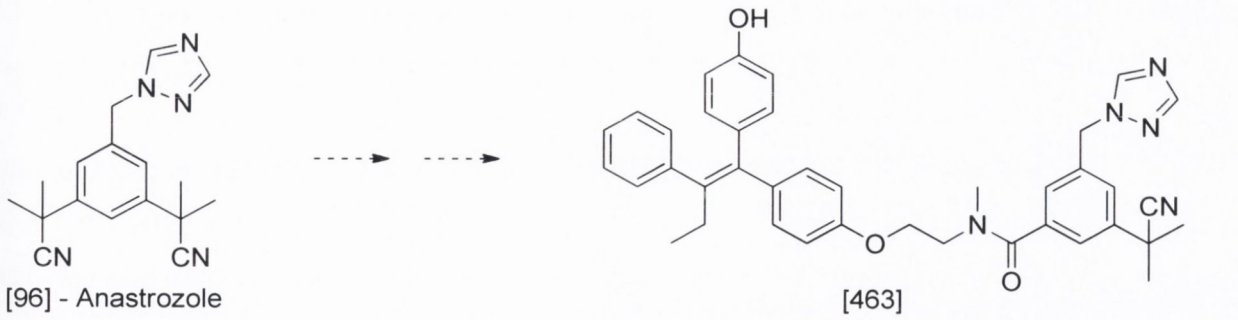

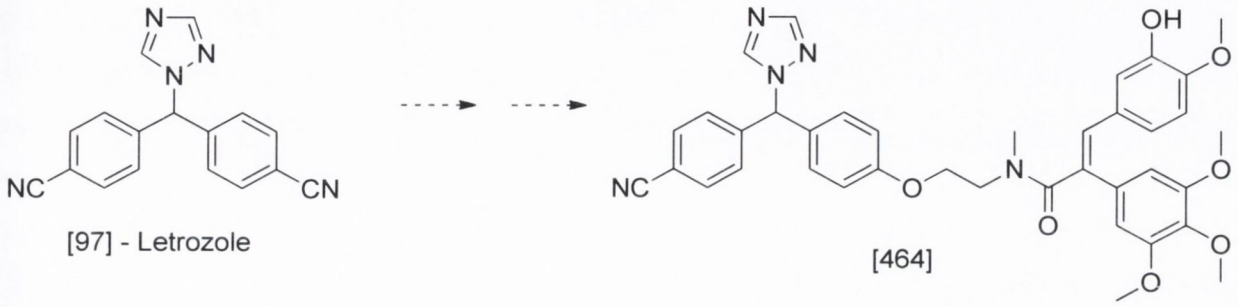

Scheme 4-1 Aromatase inhibitors [96]-[97] and target conjugates [463]-[464]

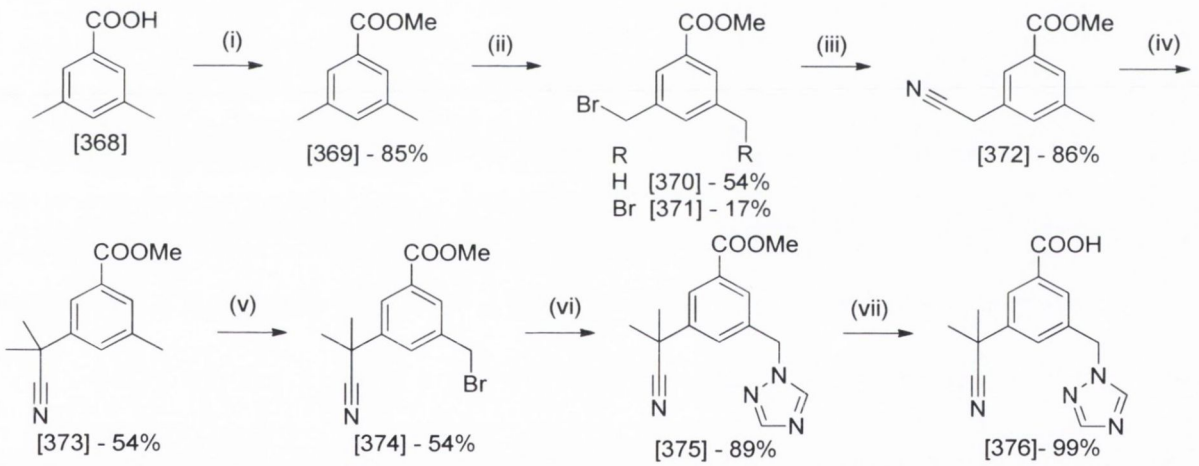

(i) HCl, MeOH, 3 h, reflux; (ii) NBS, Bz_2O_2, CCl_4, reflux; (iii) NaCN, MeOH, H_2O, 16 h, RT; (iv) NaH, MeI, DMF, 16 h, RT; (v) NBS, Bz_2O_2, CCl_4, reflux; (vi) 1,2,4-triazole, K_2CO_3, KI, acetone, 1 h, MW, 120 °C; (vii) NaOH, MeOH, 1 h, reflux.

Scheme 4-2 Route to the anastrozole derivative [376]

The first step in the synthesis of the anastrozole derivate was the esterification of the benzoic acid. The 3,5-dimethylbenzoic acid [368] was refluxed in the presence of concentrated HCl in MeOH for 3 h to afford [396], Scheme 4-2. Following the esterification reaction, mono bromination of one of the methyl substituents was essential for the controlled construction of the desired anastrozole derivative. The bromination method used by Jackson *et al.*[531] to afford the mono-bromination product (instead of the di- bromination required for Anastrozole) was initially described by Kikuchi *et al.*[532] to afford the benzyl bromide. This method was primary investigated to form the

desired mono-bromination product [370], however using the conditions describe by Jackson *et al.*[531] afforded a mixture of mono- (30 %) [370] and di- (29 %) [371] brominated compounds after 4 h. The yield of the mono brominated compound was far inferior to the 85 % previously reported.[531] However, it was possible to perform this bromination using NBS. This reaction was subsequently performed using NBS in the presence of a radical initiator (benzoyl peroxide). The ester [396] was reacted with NBS in the presence of a catalytic amount of benzoyl peroxide in carbon tetrachloride (CCl_4). Examination of the previously reported method verified that mono- and di- bromination had again occurred. Following the work up of the reaction, the crude mixture required column chromatography over silica gel. However due to the structural similarity between the mono- and di-brominated compound (the Rf of the compounds were 0.35 (di-) and 0.3 (mono-)) they were quite difficult to isolate cleanly. It was found that a minimum of 200:1 ratio of silica gel to crude mixture was required to isolate both products without contamination. The isolated mono-brominated compound [370] afforded a yield of 54 %. This product was reported as a clear oil by Jackson *et al.*[531] which was initially the case however when the oil was left stand, it formed a clear crystalline solid.

In the ^{1}H NMR spectrum for [370], the methyl signal appears as a singlet at 2.41 ppm. The ester methyl signal appears as a singlet more downfield at 3.93 ppm. The benzyl bromide CH_2 signal appears as a singlet at 4.49 ppm. The three aromatic protons all appear as singlets and integrate for one proton each at 7.41 (proton on C-4), 7.80 (proton on C-2) and 7.88 ppm (proton on C-6). In the ^{13}C NMR spectrum for [370], the methyl carbon appears at 20.7 ppm. The benzyl CH_2 can be seen at 32.3 ppm and the methyl ester signal appears at 51.8 ppm. The corresponding carbonyl signal for the ester group is located at 166.2 ppm. The three aromatic carbons appear at 126.8 (C-2), 129.8 (C-6) and 133.8 (C-4) ppm. The ^{1}H NMR spectrum for [371] (dibromo compound), the ester methyl signal appears as a singlet more downfield at 3.96 ppm. The two benzyl bromide CH_2 signal appeared as a singlet at 4.53 ppm. The three aromatic protons all appear with two overlapping as singlets at 8.02 ppm and the remaining aromatic proton is observed at 7.46 ppm.

The next step in the synthesis of the anastrozole derivative is the preparation of the phenylacetonitrile [372]. The reaction reported by Jackson *et al.*[531] used potassium cyanide as the source of the nitrile ion. In the present synthesis of the phenylacetonitrile derivative [372] sodium cyanide was used. The benzyl bromide compound was reacted with sodium cyanide in a MeOH : water mixture (3 : 1). Following the work up of the reaction, the crude mixture required column chromatography over silica gel to afford the phenylacetonitrile derivative [372] with a yield of 86 %. The ^{1}H NMR spectrum for [372] is similar to the ^{1}H NMR spectrum for [370]. The key variance to note is that CH_2 signal appears more upfield at 3.78 ppm. In the ^{13}C NMR spectrum, the CH_2 signal appears

more upfield at 22.8 ppm and the presence of the nitrile carbon signal which occurs at 117.1 ppm. The IR spectroscopy also verified the presence of the nitrile group at 2236.7 cm^{-1}.

Gem-dimethylation of the phenylacetonitrile [372] was performed with methyl iodide and NaH in DMF to afford [373] in 54 % yield. Jackson et al.[531] reported the dimethylation reaction in THF with a 78 % yield. However when these condition were performed, it was found that the reaction yield was much lower (54%). Following numerous attempts with THF it was not possible to obtain higher yields. The solvent was then changed to DMF, keeping the other conditions constant to afford the desired compound [373] with a 54 % yield.

The ^{1}H NMR spectrum of [373], shown in Figure 4-1, is similar to that for the ^{1}H NMR spectrum of [372]. The most important feature is the disappearance of the benzyl CH_2 signal and its replacement with the dimethyl signal which integrates for 6 protons and appears as a singlet at 1.76 ppm. The ^{13}C NMR spectrum, shown in Figure 4-2, confirms the formation of the demethylation product. The observed quaternary carbon (36.6 ppm) and methyl carbons (28.6 ppm) confirm that the desired compound [373] was obtained.

Compound [373] afforded the desired moiety for the anastrozole sidechain however incorporation of the haem-ligating heteroaryl unit (1,2,4-triazole) onto the anastrozole derivative was still required. This was achieved *via* bromination of the remaining tolyl functionality of [373] through a similar NBS reaction as previously employed for [370] and then reaction with 1,2,4-triazole to complete the anastrozole type structure [375]. The benzyl bromide [374] was obtained in 54% yield (Scheme 4-2). Following the procedure set out by Jackson *et al.*[531], it was attempted to substitute the 1,2,4-triazole into the anastrozole scaffold of [375]. However, this procedure required a 22 h reflux, undertaken over the course of two days (2 × 11 h refluxes). However only trace amounts of the starting material had reacted to afford the desired product [375]. It was decided to use the same conditions however this time incorporating the efficient heating of the microwave. The microwave reaction of [374] with K_2CO_3 and KI, using acetone (5 mL) as the solvent was attempted. This mixture was placed in a sealed microwave reaction vessel and was heated using microwave energy (120 °C) for 1h (max energy output of 150 W). The substituted triazole compound [375] was successfully isolated in 89 % yield. This reaction was not optimised as the yield was sufficient to move to the next step.

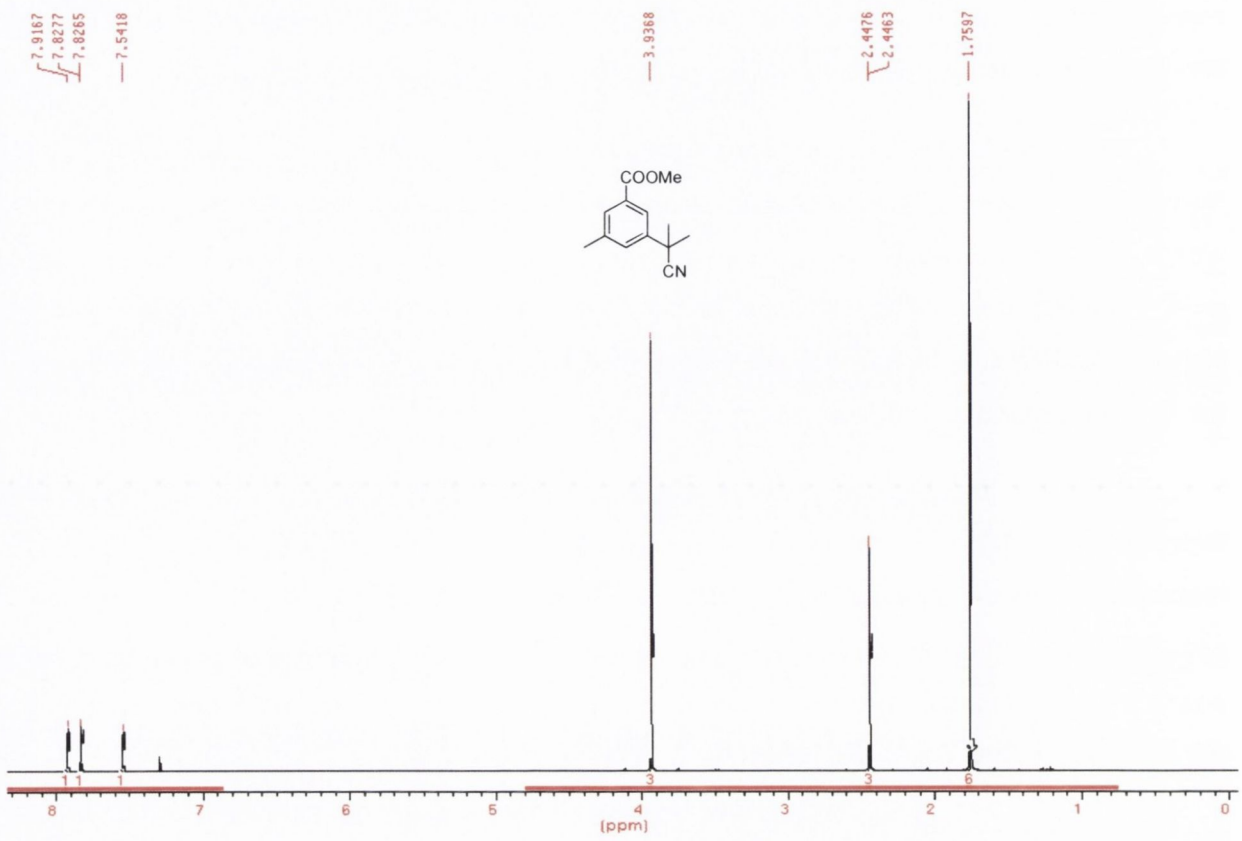

Figure 4-1 ^{1}H NMR spectrum of [373]

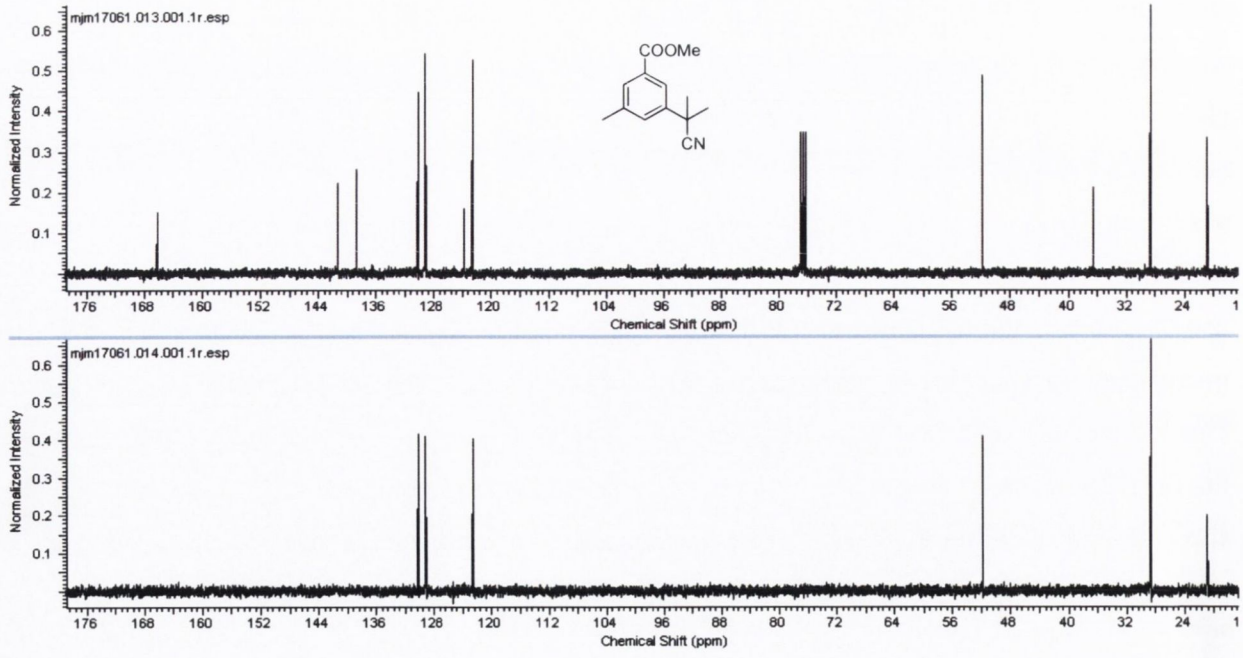

Figure 4-2 ^{13}C NMR and DEPT-135 spectrums of [373]

The mechanism of the reaction is a variation of the Finkelstein reaction in which potassium iodide promotes an S_N2 reaction that results in the exchange of the benzyl bromide to form the benzyl iodide product. The halide exchange is an equilibrium reaction, but the reaction can be driven to completion by taking advantage of the differential solubility of the halide salts. The reaction involves the conversion of the benzyl bromide to the benzyl iodide by the addition of potassium iodide in acetone. Potassium iodide is soluble in acetone and potassium bromide is not. The reaction is driven toward products by mass action due to the precipitation of the insoluble salt, which removes it from the equilibrium reaction. The potassium carbonate can deprotonate the triazole nitrogen. The triazole nitrogen then possesses a negative charge and the electrons attacks the positive dipole in the benzyl iodide compound displacing iodide which acts as a good leaving group. The reaction mechanism for this reaction is illustrated in Scheme 4-3.

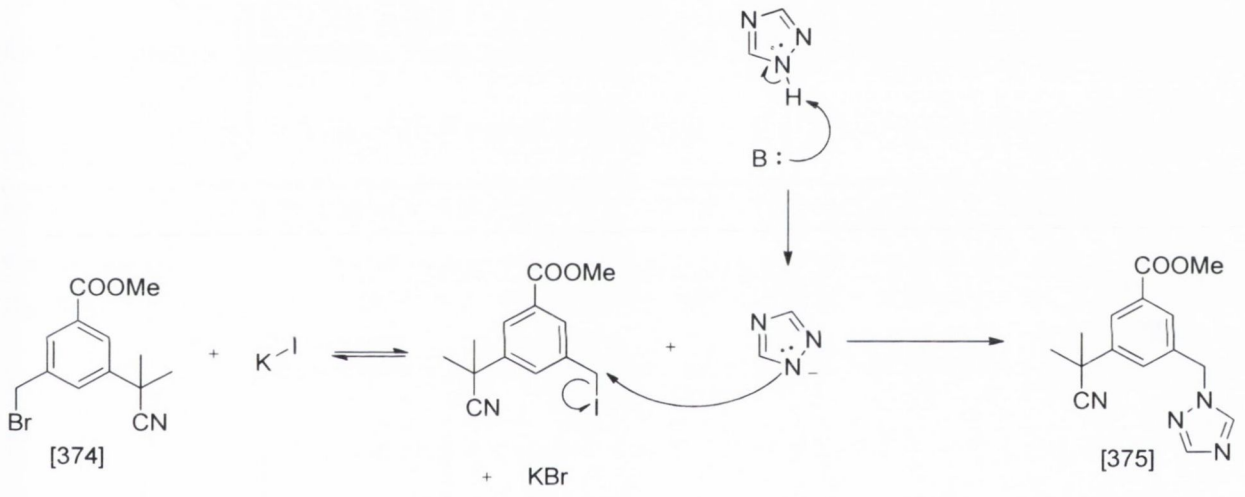

Scheme 4-3 Mechanism for the 1,2,4-triazole substitution

The ^1H NMR spectrum of [375] (Figure 4-3) confirms the synthesis of the triazole product. The signal at 1.76 ppm corresponds to the dimethyl protons on the phenylacetonitrile moiety. The methyl ester is seen at 3.94 ppm and the CH_2 in the triazole moiety is identified at 5.44 ppm. The aromatic protons are observed as singlets at 7.66, 7.90 and 8.03 ppm. The triazole protons occur as the two furthest downfield signals which integrate for one proton each at 8.11 and 8.22 ppm. The ^{13}C NMR spectrum of [375] is shown in Figure 4-4 shows the dimethyl carbons on the phenylacetonitrile moiety at 28.6 ppm. The quaternary carbon in the phenylacetonitrile moiety can be observed at 36.7 ppm. The methyl ester corresponds to the signal at 52.1 ppm. The CH_2 carbon in the triazole moiety is seen at 53.4 ppm, while the nitrile carbon is identified at 123.3 ppm. The signals for the aromatic carbons are found at 125.9, 128.0 and 128.9 ppm. The two pronated triazole carbons can be observed as the two downfield signals at 142.9 and 152.0 ppm. The signal for the methyl ester carbonyl occur at 165.4 ppm.

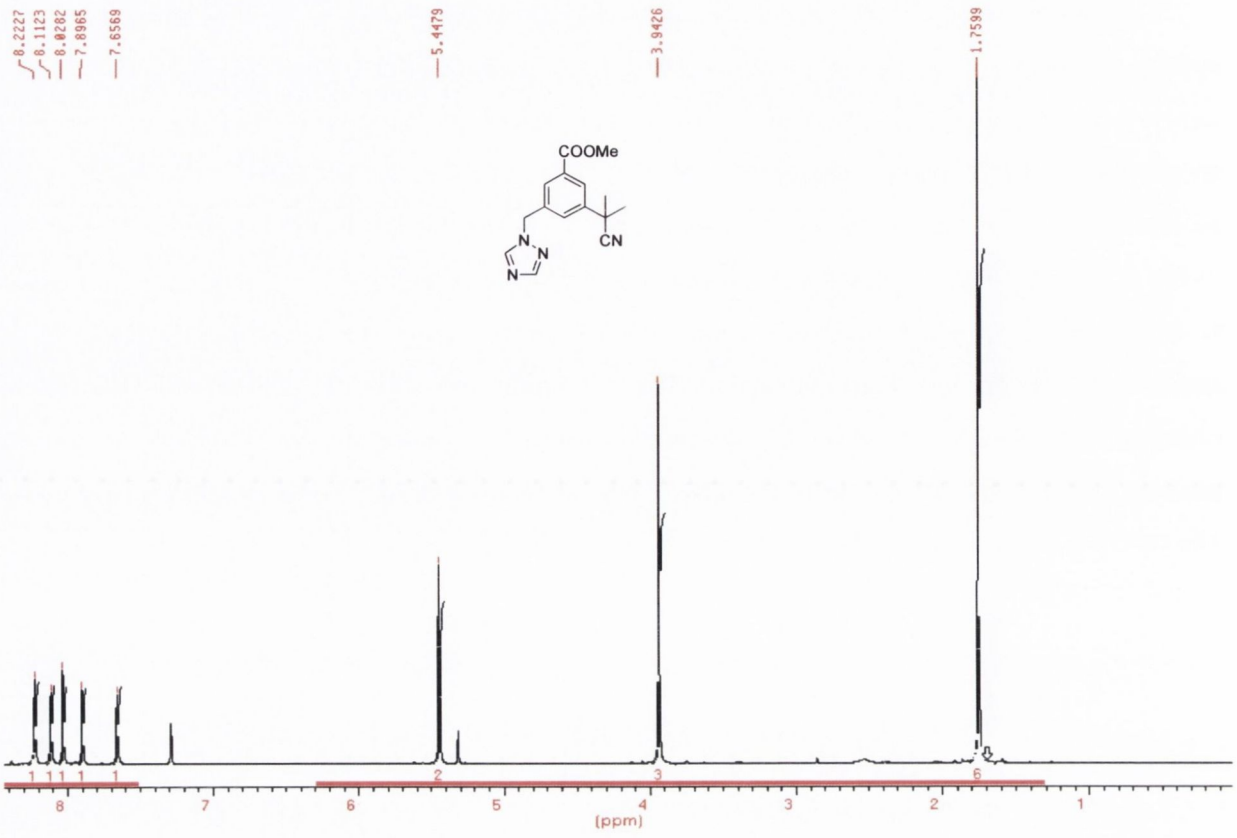

Figure 4-3 ^{1}H NMR spectrum of [375]

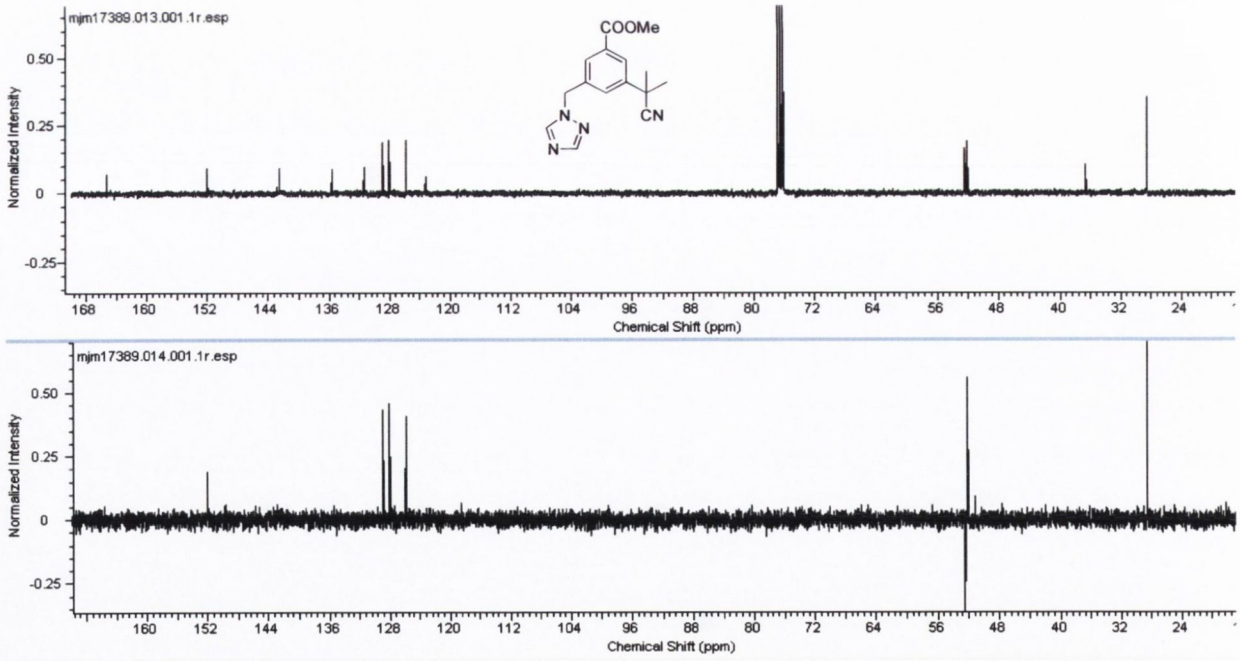

Figure 4-4 ^{13}C NMR and DEPT-135 spectrum of [375]

The final step in the preparation of the anastrozole ligand for conjugation was hydrolysis of [375] to afford the benzoic acid derivative [376], Scheme 4-2. The acid functional group was essential for the conjugate synthesis as it was required for the amide formation *via* a DCC coupling

reaction with endoxifen (discussed later in Chapter 5). The hydrolysis reaction was performed by refluxing [375] in MeOH in the presence of NaOH for 1 h after which all the starting material had reacted. Following an acid workup the product [376] was isolated as a pale yellow solid that did not require further purification.

The hydrolysis of the ester could have also been performed using an acid to afford the benzoic acid product [376]. However, due to the presence of the nitrile functional group, the base method was preferred, to avoid hydrolysis of the nitrile in acid.

After the successful synthesis of [376], it was proposed to attempt the synthesis of a further anastrozole derivative but replacing the 1,2,4-triazole heterocycle with imidazole to determine if this had any effect on the conjugate's activity (Scheme 4-4). The synthesis of the imidazole ester derivative from [374] was performed as per the 1,2,4-triazole substitution method outlined (Scheme 4-4) to afforded [377] as a yellow solid with a yield of 67% after workup (Scheme 4-4). The subsequent step required hydrolysis of the ester to afford [378]. Monitoring of the hydrolysis reaction *via* TLC indicated that all the starting material was reacted. However, on workup of the crude mixture, no product was isolated. It is believed that the water soluble imidazole product was extracted into the water layer during workup. And further attempts to afford [378] were discontinued.

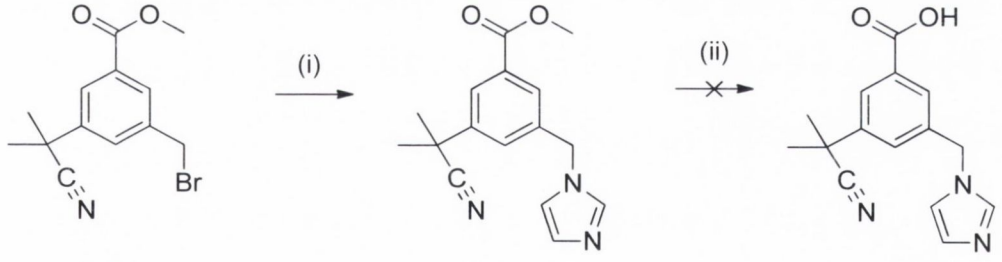

[374] [377] - 67% [378]

(i) imidazole, K_2CO_3, KI, acetone, 1 h, MW @ 120 °C;
(ii) NaOH, MeOH, 1 h, reflux.

Scheme 4-4 Attempted synthesis of [378]

4.3 Letrozole derivative as a conjugate ligand.

Letrozole [97] acts through the aromatase pathway to treat estrogen-sensitive breast cancers by preventing the initial production of estrogen. Unlike tamoxifen, with mixed estrogen agonist and antagonist properties, the aromatase inhibitors have no estrogenic agonist activity.[533] There is now a strong evidence to support the selective inhibition of aromatase to achieve a more effective and selective endocrine therapy for hormone dependent breast cancer. The target

structure for conjugation with a cytotoxic drug was identified as [387]. (see Scheme 4-5 and Scheme 4-6)

4.3.1 Synthesis of letrozole derivatives

The synthesis of letrozole [97] has been documented in the patent literature.[533-537] The predominant route for the synthesis of letrozole is shown in Scheme 4-5. The synthetic route followed in the present work to produce the required aromatase inhibitor pharmacophore [387] follows related chemistry and is illustrated in Scheme 4-6.

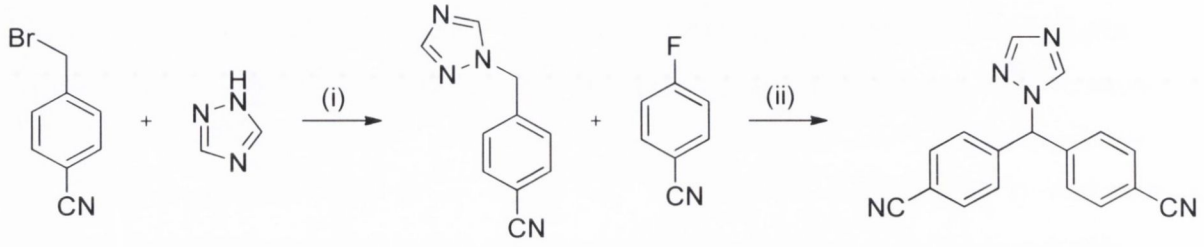

(i) K_2CO_3, KI, Acetone, Reflux; (ii) *t*-BuOK, DMF

Scheme 4-5 Synthesis of letrozole [97]

The first step involves the alkylation of triazole to form [380], followed by nucleophilic aromatic substitution after carbanion generation. This method for the synthesis of letrozole seemed ideal for the synthesis of the letrozole derivatives designed in this project (Scheme 4-5). The required letrozole derivative [387] was intended to become the AI ligand of a conjugate. This conjugate would require that the letrozole derivative contain a moiety which could be used to form a linker to the cytotoxic drug. As the cytotoxic drug that was incorporated in our other conjugate compounds was the acrylic acid derivative of CA4, it was intended that this conjugate also incorporate a similar functional groups. It was proposed that if one of the benzyl nitriles in letrozole was replaced with a phenol this would allow for the addition of an alkyl amine ether moiety similar to that seen in endoxifen. This basic moiety could subsequently be used to generate a direct amide bond with the acrylic acid to produce the novel conjugate. It was proposed that the synthesis of the required letrozole derivative [387] would follow the predominant synthetic route shown in Scheme 4-5. If the nitrile substituent was exchanged for a benzyl protected phenol then this would allow for the subsequent alkylation with alkyl halides for the construction of the basic side chain. The overall synthetic route planned for the letrozole derivate [387] is shown Scheme 4-6.

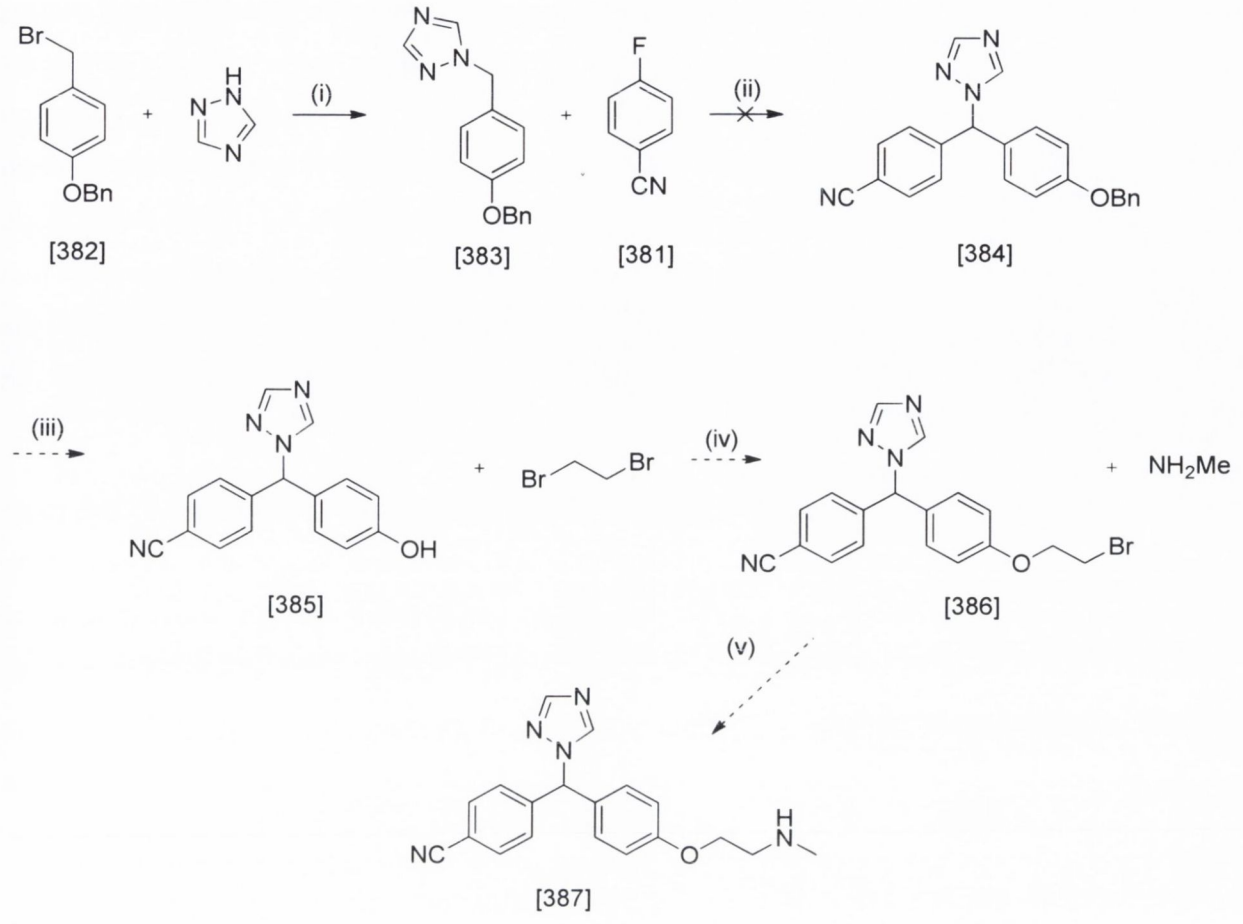

(i) K_2CO_3, KI, Acetone, Reflux; (ii) *t*-BuOK, DMF; (iii) $Pd(OH)_2$, H_2, EtOAc/MeOH;
(iv) NaOH (aq.), $(nBu)_4NHSO_3$; (v) $MeNH_2$, sealed tube, 60 °C;

Scheme 4-6 Proposed synthesis of the letrozole derivative [387]

The benzyl bromide [382] required was obtained by sodium borohydride reduction of [388] to afford the benzyl alcohol [389] as a white solid in 99% yield. Bromination of the benzylic alcohol with phosphorus tribromide afforded the desired benzyl bromide [382] in 98% yield, Scheme 4-7.

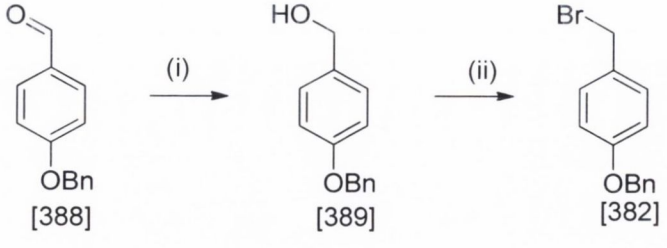

(i) $NaBH_4$, MeOH, 1 h, 0 °C; (ii) PBr_3, DCM, 1 h, 0 °C

Scheme 4-7 Synthesis of [382]

Alkylation of triazole with the benzyl bromide [382] afforded [383] as a white solid in 45% yield. The next step was the addition of the *p*-cyanoaryl fluoride [381] to afford the letrozole scaffold [384]. Compounds [383] and [381] were reacted in DMF in the presence of *t*-BuOK at room

temperature for 2.5 h. After work up of the reaction mixture TLC analysis showed that both starting materials remained. This was unanticipated due to the literature reporting yields of 26 - 66% under the same conditions. Further literature investigation found that for this reaction the substituent on the ring can affect the outcome. In the case of letrozole, the cyano group has an electron withdrawing effect which activates the ring towards nucleophilic attack and the reaction takes place. As this reaction was a nucleophilic aromatic substitution reaction it was possible to rationalise that in this case that the electron donating nature of the benzyl substituent deactivates the ring and the reaction does not proceed. Therefore, this meant that the synthetic route (Scheme 4-6) was not longer possible.

An alternative route proposed for the synthesis of [385] is shown in Scheme 4-8. This route involved the construction of a benzophenone derivative with the desired substituents on each of the aromatic rings. Kim *et al.*[538] documented the preparation of aryl ketones from the aromatic bromide and acid chloride. Ni-catalyzed Negishi-coupling reaction was employed which afforded the required aryl ketones with excellent yields.

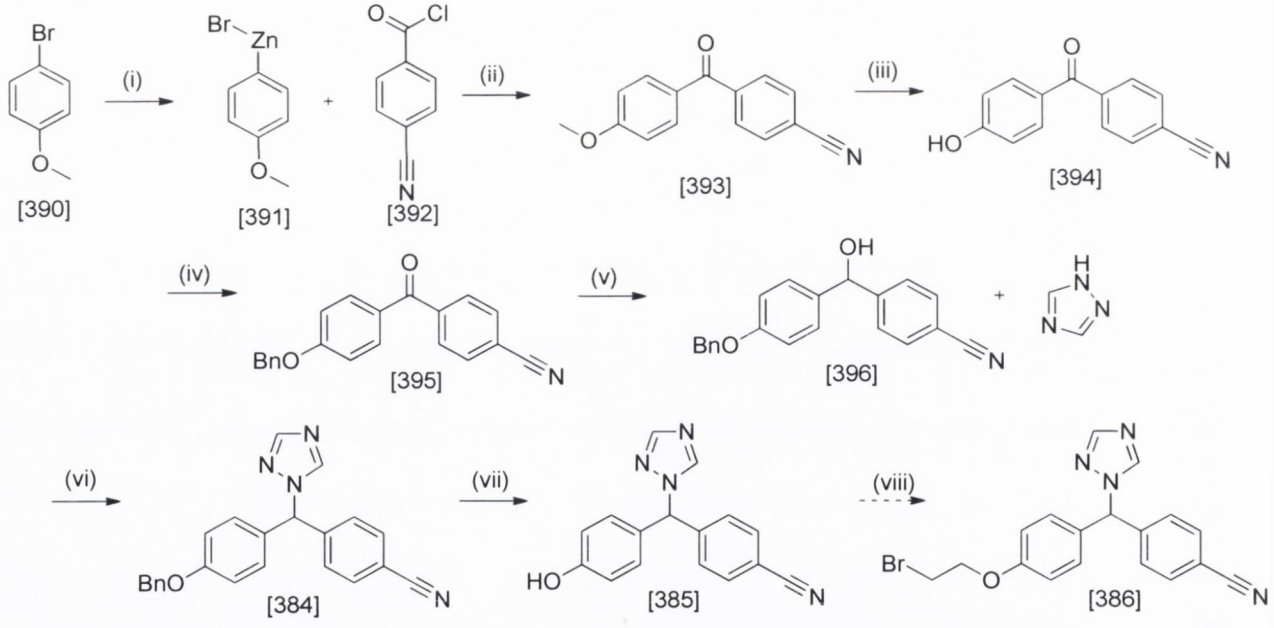

(i)&(ii) $CoBr_2$, ZnBr, bromobenzene, Zn, TFA, ACN, $Ni(acac)_2$, 1 h; (iii) Py.HCl, 20 min, 210 °C; (iv) BnBr, K_2CO_3, ACN, 16 h; (v) $NaBH_4$, MeOH, 15 min; (vi) *p*-TSA, toluene, MW; (vii) $Pd(OH)_2$, EtOAc/MeOH, 30 min; (viii) Br_2CH_2, NaOH (aq.), $(nBu)_4NHSO_3$,

Scheme 4-8 Proposed synthesis of the letrozole derivative [385]

Implementation of the Kim *et al.*[538] method first required the formation of the aryl zinc bromide intermediate from the aryl bromide. 4-Bromoanisole [390] was used as the starting material for the formation of the aryl zinc bromide. It was not the preferred starting material for this

reaction as previous problems had been encountered in the related subsequent demethylation step, see Chapter 2. Despite this it was still seen as a viable option for this synthesis due to the lack of availability of synthesised benzylated starting material. However, the demethylation step would be performed directly after the aryl ketone formation to ensure that similar difficulties in demethylation would not be encountered in the final steps of this synthesis.

The aryl zinc bromide [391] was prepared by following a method reported by Fillion *et al.*[539]. This method allowed for the formation of [391] from the commercially available [390]. The procedure required pre-stirring a mixture of $CoBr_2$, $ZnBr_2$, bromobenzene, Zn dust and TFA, to which [390] was added after 15 min. It must be noted that in the Fillon *et al.*[539] procedure, the reaction was monitored *via* GC for the consumption of aryl bromide. However in our case GC was not used for the determination of starting material present. Fillion *et al.*[539] reported that the reaction time was approximately 15 min, therefore it was decided that a reaction time of 30 min should be adequate to allow the formation of [391]. Compound [391] was not isolated due to its instability but the species was directly used for the Ni-catalyzed Negishi-coupling reaction. The general mechanism of formation for the aryl zinc bromide species is shown in Scheme 4-9.

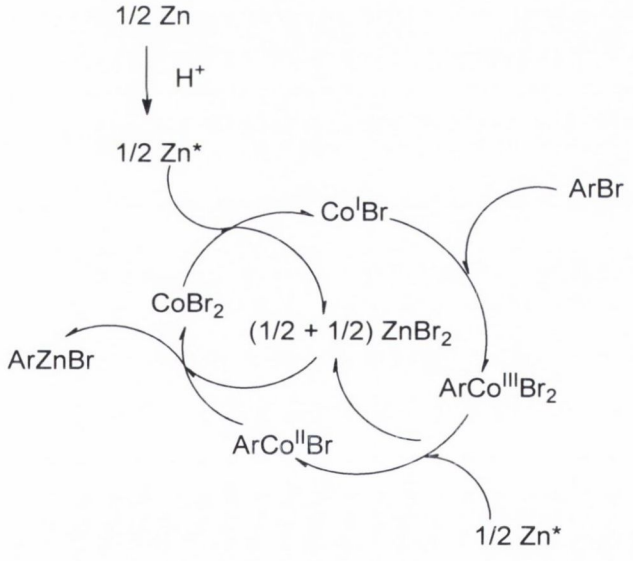

Scheme 4-9 General mechanism of formation of the aryl zinc bromide

The mechanism was reported also by Fillion *et al.*[539] which was based on a mechanism described recently for the electrochemical conversion of aryl halides to aryl zinc compounds by cobalt catalysis in DMF/pyridine.[540] The catalytic cycle is initiated by the reduction of $CoBr_2$ by zinc dust, which needs to be activated previously by acid traces. The resulting Co(I)Br undergoes an oxidative addition with aryl halides to afford the trivalent cobalt complex ArCo(III)Br_2. That latter species is reduced into ArCo(II)Br by the excess of zinc dust. The cycle is completed by a

transmetalation reaction between ArCo(II)Br and $ZnBr_2$ formed in the previous steps, leading to the aryl zinc compound and regenerating divalent cobalt. Compound [391] was not isolated but the species was directly used for the Ni-catalyzed Negishi-coupling reaction. Therefore, it was not possible determine exact molar equivalents to be taken in the next step, however, working on the assumption that 50% conversion of [390] to [391] was sufficient to move directly to the next step. This Ni-catalyzed Negishi-coupling reaction was performed by directly adding $Ni(acas)_2$ to [392] pre-dissolved in THF. The mixture was stirred at RT for 30 min before being filtered through celite. Work up and purification over silica gel afforded the product [393], a yellow solid with overall yield of 25%.

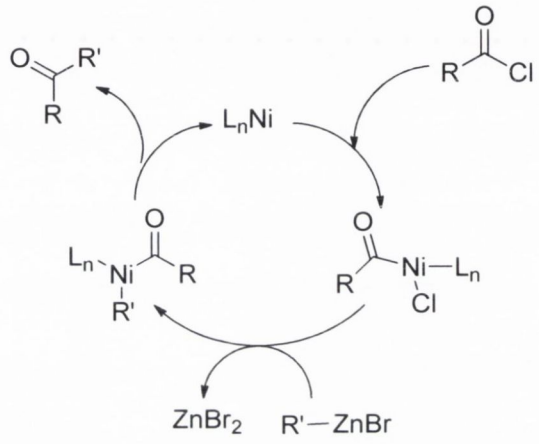

Scheme 4-10 General mechanism of transition metal-catalysed crosscoupling reaction

The general mechanism of transition metal-catalysed cross-coupling reaction involves three key steps (Scheme 4-10). The first consists of oxidative addition of the organohalide to a low valent metal complex to give an organometallic derivative with a higher formal oxidation state on the metal centre. This is followed by transmetalation of the nucleophilic carbon from the nucleophile to the transition metal complex to afford a diorganometal species. Subsequent reductive elimination affords a new C–C bond and generates the catalytically-active species.

The subsequent step in the synthetic scheme involves the demethylation of the methoxy group in [393] to afford the phenol. It was proposed to perform this demethylation step early in the synthesis due to problems encountered in similar demethylation with BBr_3 in the indole synthesis. The free phenol was essential for the construction of the letrozole derivative, in facilitating the addition of the basic side chain moiety. The use of pyridine hydrochloride had been quite successful for similar demethylation of methoxy ethers.[541] This reaction was performed by heating [393] and pyridine hydrochloride at 210 °C for 20 min. Following work up and purification over silica gel the product [394] was isolated as a pale yellow solid with a 53% yield, Scheme 4-8.

The free phenol now contained in compound [394] required protection in subsequent reaction steps. The protection was carried out using a benzyl ether protecting group and afforded [395] in 88% yield, Scheme 4-8. The next step was the reduction of the ketone with sodium borohydride to afford the secondary alcohol [396] with a 95% yield. This secondary alcohol was required for the introduction of the 1,2,4-triazole ring to give the letrozole scaffold. The 1,2,4-triazole substitution reaction was performed in toluene using a Dean stark apparatus. The apparatus allows the water to be separated from the condensed azeotrope preventing it from returning to the reaction mixture. The mechanism for the dehydration reaction followed by the addition of the triazole reaction shown in Scheme 4-11. The *p*-toluene sulfonic acid acts as a strong acid and protonates the oxygen atom of the alcohol, converting it into a good leaving group (H_2O). The heterolysis of the C-O bond forms a carbocation. The *p*-toluene sulfonic acid regenerates itself *via* deprotonating the 1,2,4-triazole proton which in turn reacts with the carbocation to afford [384] in 11% yield.

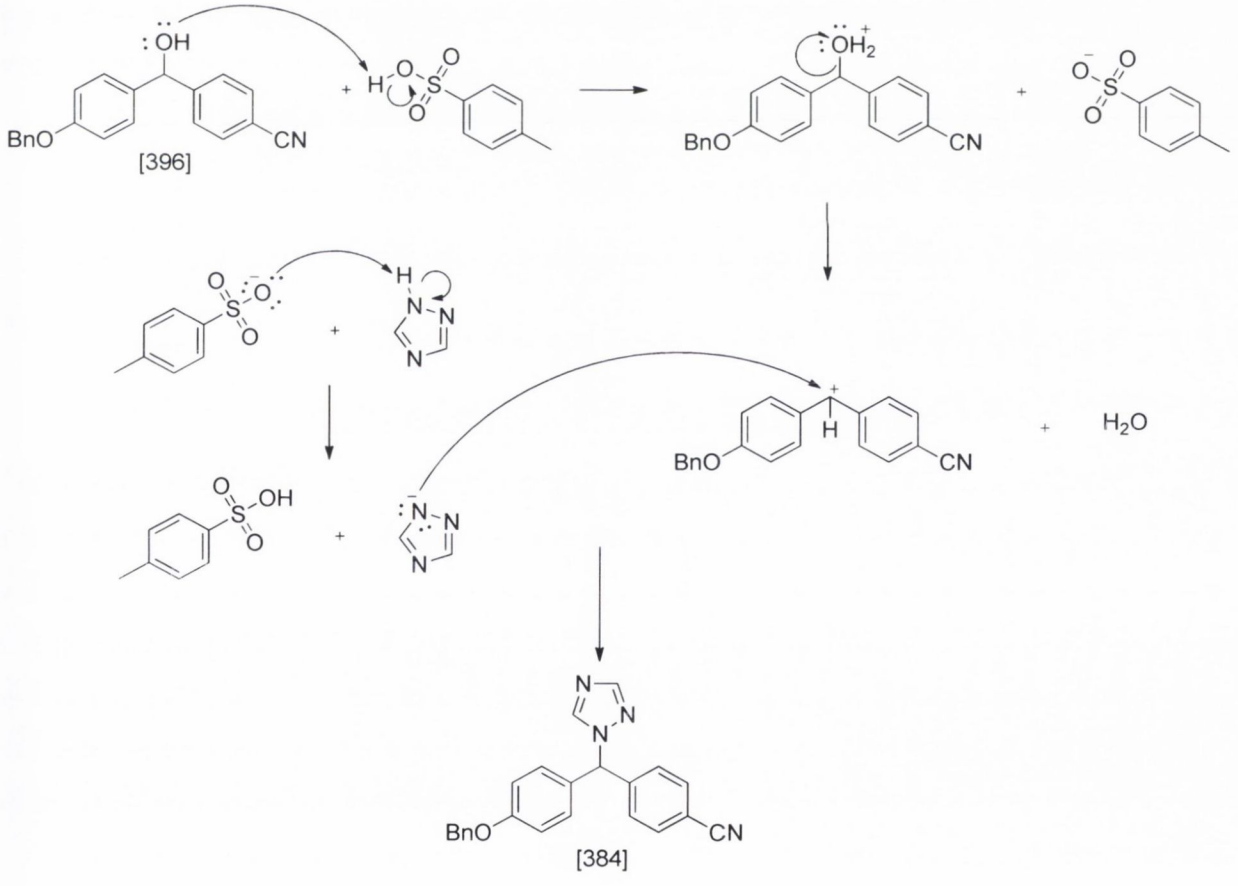

Scheme 4-11 Mechanism for the formation of [384]

Due to the low yield in the synthesis of [393] and feasibility of synthesising [386] because of this low yield it was determined that an alternative route for the synthesis of the letrozole derivative

[396] should be investigated. The synthesis of related secondary alcohols was reported by Misawa *et al.*[542] *via* the aryllithium reagents (generated from aryl bromide by treatment with *n*-butyllithium). Misawa *et al.*[542] documented the synthesis of a series of secondary alcohols through the use of n-butyllithium. The advantage of this method was that variation of either the aldehyde or the aryl bromide would allow the preparation of a series of structurally varied secondary alcohols. This new route is shown in Scheme 4-12.

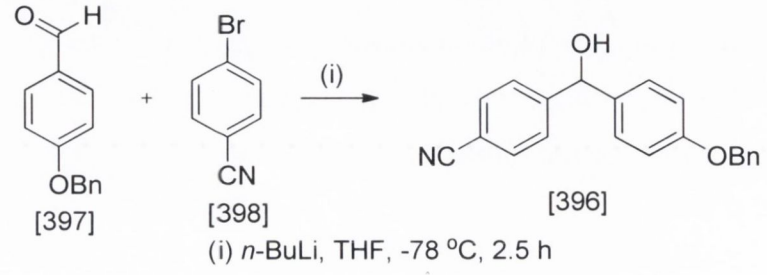

Scheme 4-12 Alternative synthesis route for [396]

n-BuLi is required to convert the aryl bromide to the alkyl lithium reagent. The subsequent step in the reaction is the nucleophilic addition of lithium reagent to the polar multiple bond to give an adduct which upon hydrolytic workup afford the secondary alcohol (Scheme 4-13).

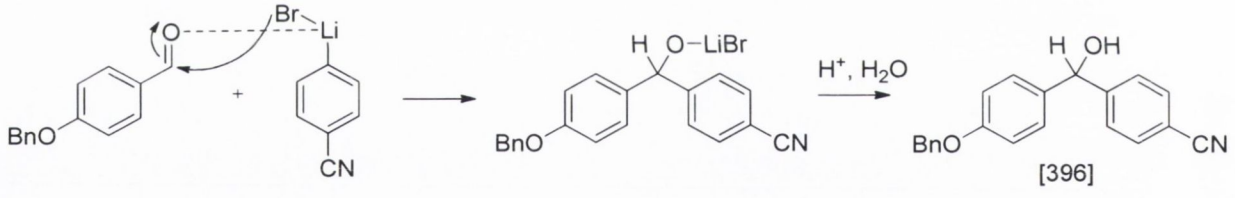

Scheme 4-13 General mechanism for preparation of [396]

The *n*-BuLi reaction was performed by the addition of the aryl-bromide [398] in dry THF at -78 °C. To this stirring mixture was added *n*-BuLi dropwise and the resulting solution was left to stir for 1 h to allow the formation of the alkyl lithium reagent; at which point the aldehyde was added and the reaction mixture was allowed to stir for a further 1.5 h THF at -78 °C. Following work up, the crude mixture was purified *via* column chromatography over silica gel to afford [396] as a yellow solid with a good yield of 88 %. This yield was a considerable improvement when compared to the Ni-catalyzed Negishi-coupling reaction route (25% yield). This method was now a viable route to continue with the synthesis of required letrozole derivative which required reaction with triazole.

The previous attempt at synthesising [384] was hampered by poor reaction yield (Scheme 4-11) and limited starting material. When considering the previous attempt, it was noted that the yield was not sufficient to continue to the next step. One method to increase this yield was to

increase the reaction time. When examining the literature for opportunities to increase the yield for the Dean-Stark method, an interesting paper was found by Veillet *et al.*[543] on microwave accelerated Dean-Stark. The Dean-Stark method was utilised for the removal of water. This method was interesting because of the benefits of microwave heating over conventional heating, and it was also a potentially promising method to increase the yield. This method was different to conventional microwave reactions (sealed tube) performed throughout the previous research as this required an open vessel microwave chamber (Figure 4-5).

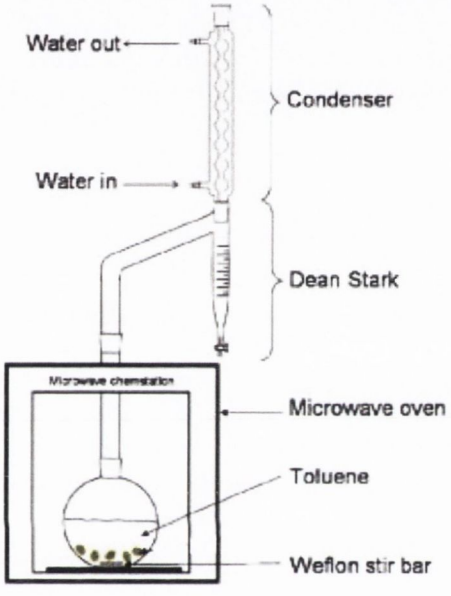

Figure 4-5 Open vessel microwave chamber - Dean-Stark[543]

The CEM microwave reactor had the capability of performing this open vessel microwave chamber reaction. The reaction was performed using toluene as the solvent, compound [396], 1,2,4-triazole and *p*-TSA were added. As the microwave heating has been shown to be more efficient and can reduce reaction times, a reaction time of 4 h was initially decided, with a constant supply of 95 W which was sufficient to allow controlled refluxing. The reaction mixture was worked up, and purification *via* column chromatography over silica gel to afford [384] a yellow solid with a good yield of 67 %. This method was not optimized further as the yield was sufficient to continue to the next step.

The ^{1}H NMR spectrum of [384] (Figure 4-6) confirms the synthesis of the letrozole scaffold. The signal at 5.09 ppm corresponds to the benzyl CH_2 and the proton on the tertiary carbon can be seen at 6.75 ppm. The pair of triazole protons are observed at 7.98 and 8.07 ppm. The remaining signals correspond to the aromatic protons and integrate for 13 protons. The ^{13}C NMR spectrum of [384] is shown in Figure 4-7. The tertiary carbon can be seen at 66.4 ppm and the benzyl CH_2 is

observed at 69.7 ppm. The two tertiary triazole carbons can be observed as the two downfield signals at 143.4 and 152.2 ppm. The carbon of the benzyl ether appears at 159.0 ppm.

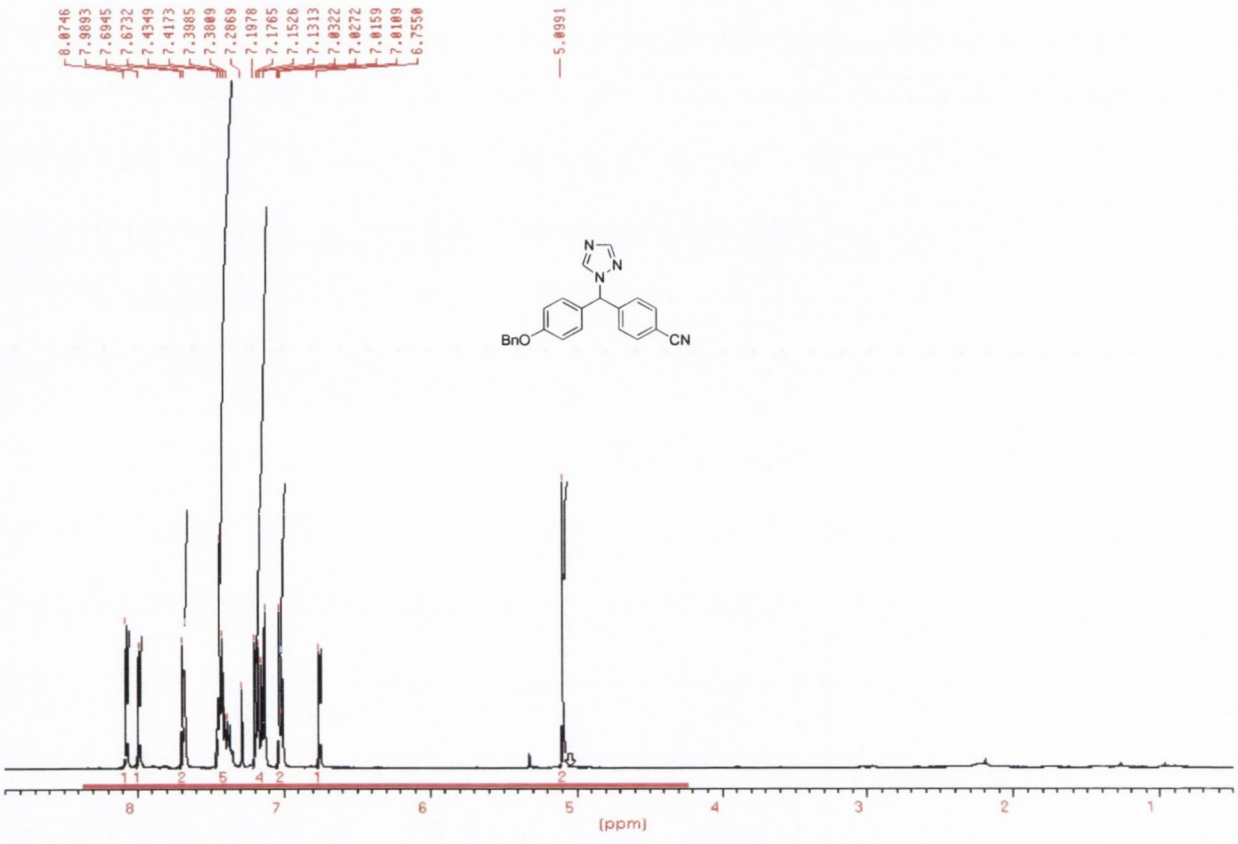

Figure 4-6 ^{1}H NMR spectrum of [384]

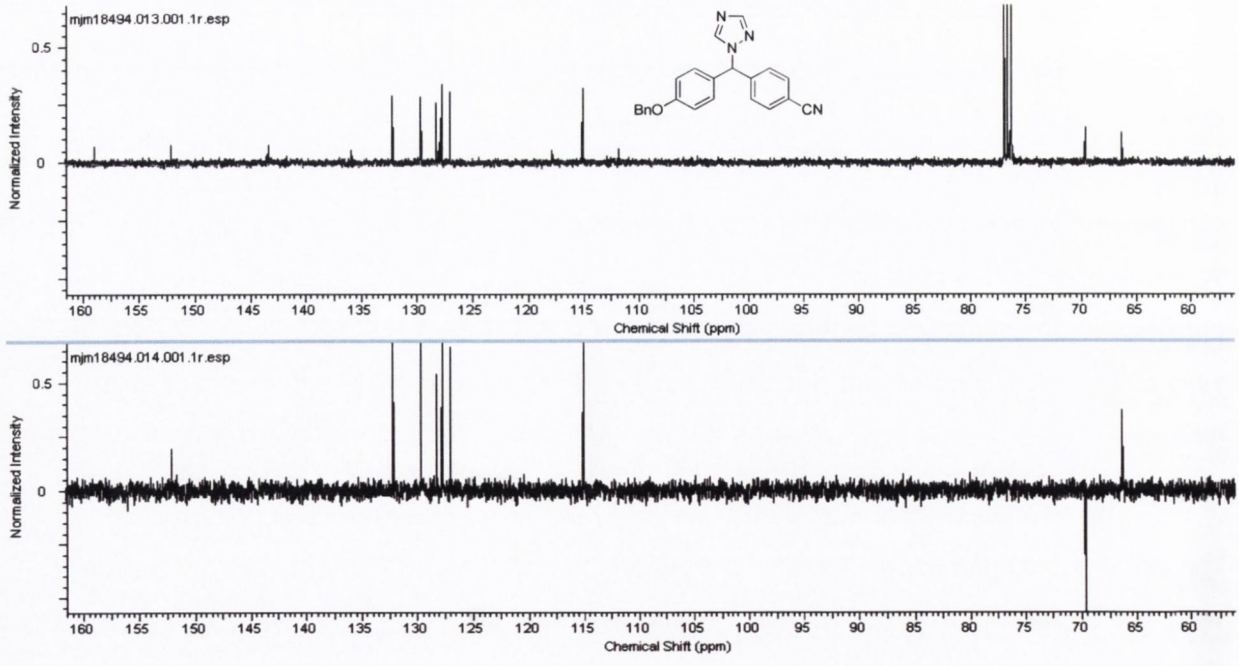

Figure 4-7 ^{13}C NMR and DEPT-135 spectrums of [384]

With the construction of the letrozole scaffold completed, the basic side chain could be introduced. The next step in this synthesis was the debenzylation of [384] (Scheme 4-8). The hydrogenation using $Pd(OH)_2$ of [384] was successful and afforded [385] with a yield of 66 %. The subsequent planned step was the addition of the 1,2-dibromoethane *via* the same conditions employed for the endoxifen synthesis chemistry. However, this reaction was unsuccessful. It was postulated that if the bromo chain was added at the beginning of the synthesis sequence then it would be possible to circumvent this problem.

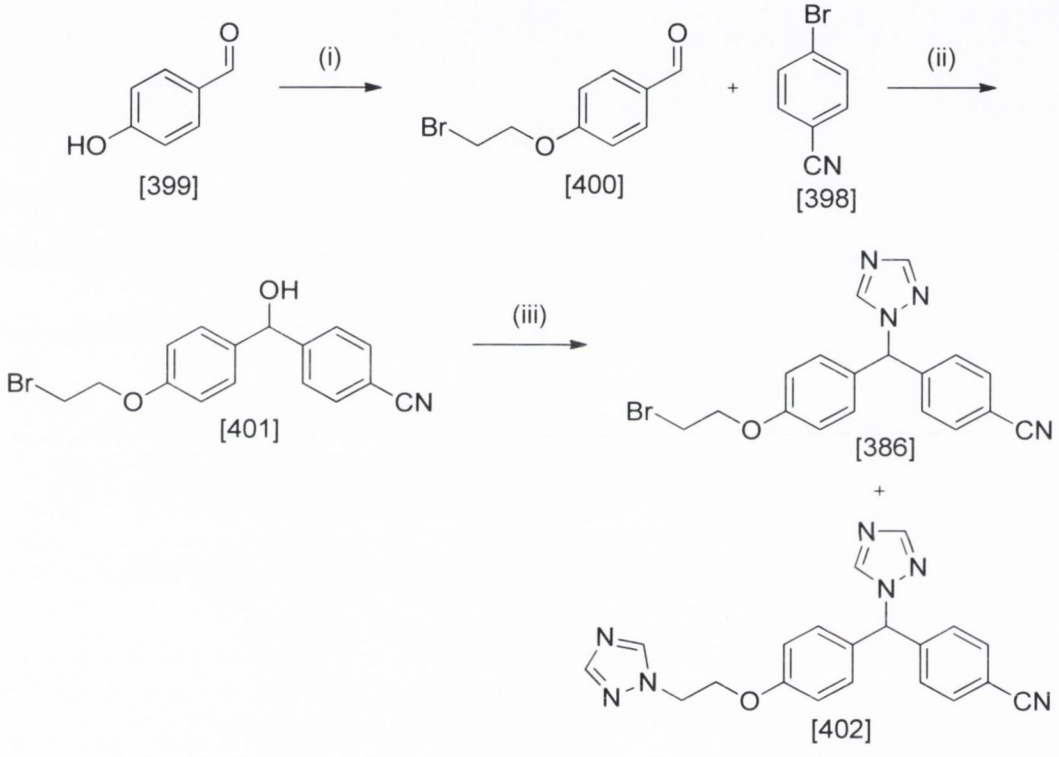

(i) 1,2-dibromoethane, K_2CO_3, DMF, 16 h, RT; (ii) *n*-BuLi, THF, -78 °C, 2.5 h;
(iii) 1,2,4-Triazole, *p*-TSA, toluene, MW, 4 h, 90 W

Scheme 4-14 Altered route for the synthesis of [386]

The altered route involves the presence of ethyl bromine chain at the beginning of the synthetic scheme as illustrated in Scheme 4-14. The synthesis of [400] was achieved with 1,2-dibromoethane and K_2CO_3 in DMF and reacted at RT for 16 h. This step afforded [400] with a 63 % yield. Compound [398] was treated with *n*-BuLi at -78 °C to produce the alkyl lithium reagent at which point compound [400] was added. After work up, purification over silica gel afforded [401] as a yellow solid with 81 % yield. The next step was critical because in the previous synthetic method it was not possible to obtain [386]. Following similar conditions for the previous addition of the 1,2,4-triazole heterocycle, it was possible to obtain the desired product [386] in 51 % yield. The conditions

were similar however the microwave wattage that allowed for safe and controlled refluxing for this reaction was 90 W.

The TLC of [386] crude mixture showed the presence of a second product. Isolation of this unknown material afforded a potentially interesting side product [402] (Scheme 4-14). Compound [402] could be interesting as it contains the letrozole scaffold but it also contains an additional basic triazole moiety and could show potential biochemical activity.

The final step in the synthesis of the letrozole derivative was the amination reaction to afford [387]. Not only was this step important for the synthesis of the proposed letrozole derivate, but it was also key for the synthesis of the conjugate compound discussed later in Chapter 5. The amination reaction was similar to that implemented for the synthesis of all the ER ligands. Compound [386] was added to a sealed pressure tube with an excess of methylamine (1 M in THF) and was stirred at 65 °C for 48 h. Following the workup and purification, compound [387] was obtained as a brown resin with a yield of 88 % (see Scheme 4-15).

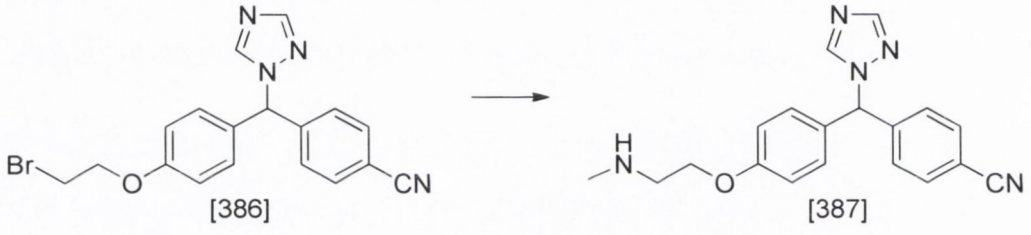

Scheme 4-15 Synthesis of the letrozole derivative [387]

The ^{1}H NMR spectrum of [387] is shown in Figure 4-8. The signal at 2.26 ppm corresponds to the amine proton. The signal at 2.53 ppm corresponds to the methyl group on the amine. The broad singlet at 3.01 ppm is assigned to the CH_2 adjacent to the methyl amine. The signal corresponding to the OCH_2 can be seen as a triplet at 4.10 ppm, J= 5 Hz. The proton on the tertiary carbon can be seen at 6.74 ppm. The pair of triazole protons are observed at 7.95 and 8.05 ppm. The remaining signals correspond to the aromatic protons and integrate for 8 protons. The ^{13}C NMR spectrum of [387] is shown in Figure 4-9. The methyl group attached to the amine is not seen but confirmed in the 2D NMR experiment (Figure 4-10) to be present at 35.7 ppm. This signal is observed at 35.7 ppm on the ^{13}C NMR section of the spectrum with interacts with 2.53 ppm on the ^{1}H NMR portion of the experiment, it was possible deduce from this experiment that the methyl amine signal was located at 35.7 ppm even when it was not observed in the ^{13}C NMR spectrum. The two CH_2 groups on the side chain are observed at 50.0 and 66.6 ppm. The tertiary carbon can be seen at 66.3 ppm. The two protonated triazole carbons can be observed as the two downfield signals at 143.1 and 152.2 ppm. The signal for the carbon attached to the benzyl ether appears at 159.0 ppm.

The synthesis of the letrozole derivative was now complete. This derivative [387] will now be used in the synthesis of the novel conjugate compound discussed later in chapter 5.

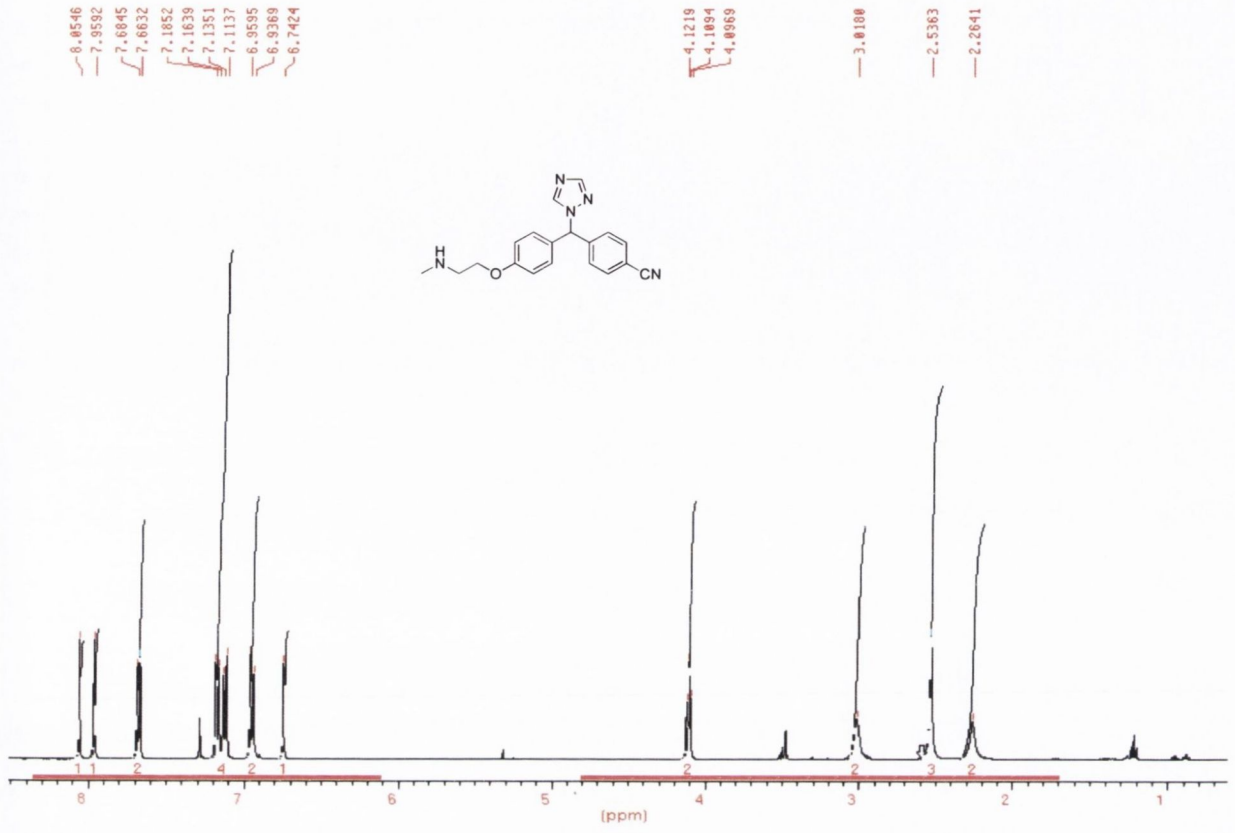

Figure 4-8 ^{1}H NMR spectrum of [387]

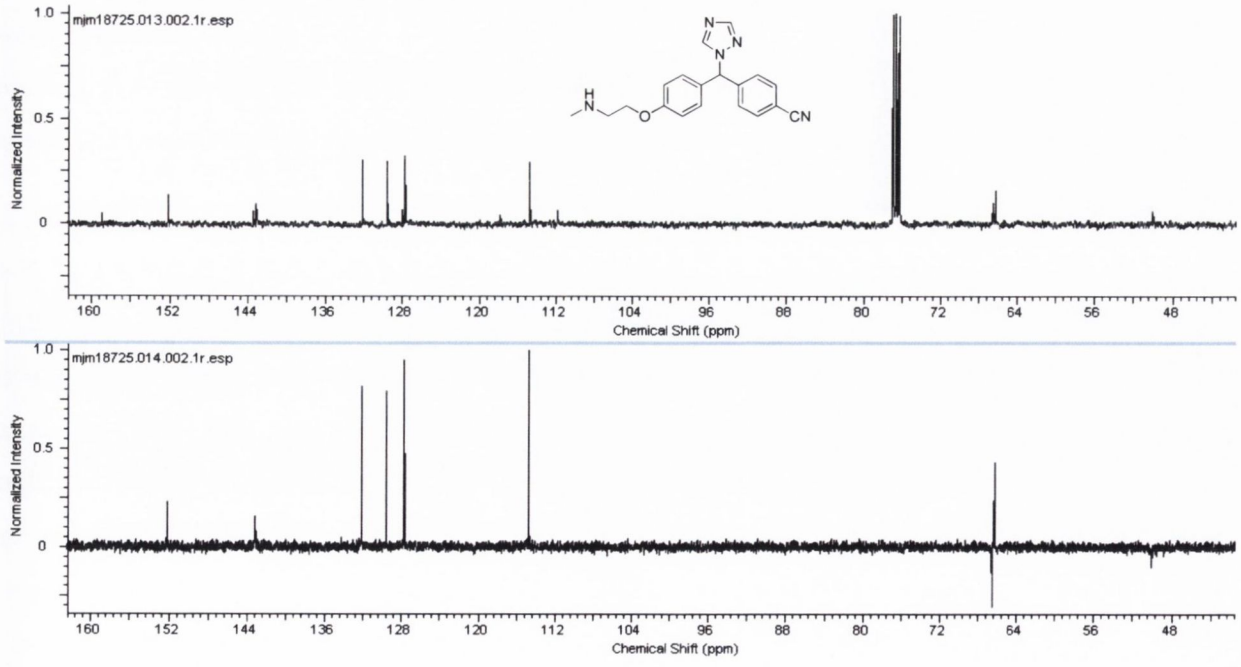

Figure 4-9 ^{13}C NMR and DEPT-135 spectrum of [387]

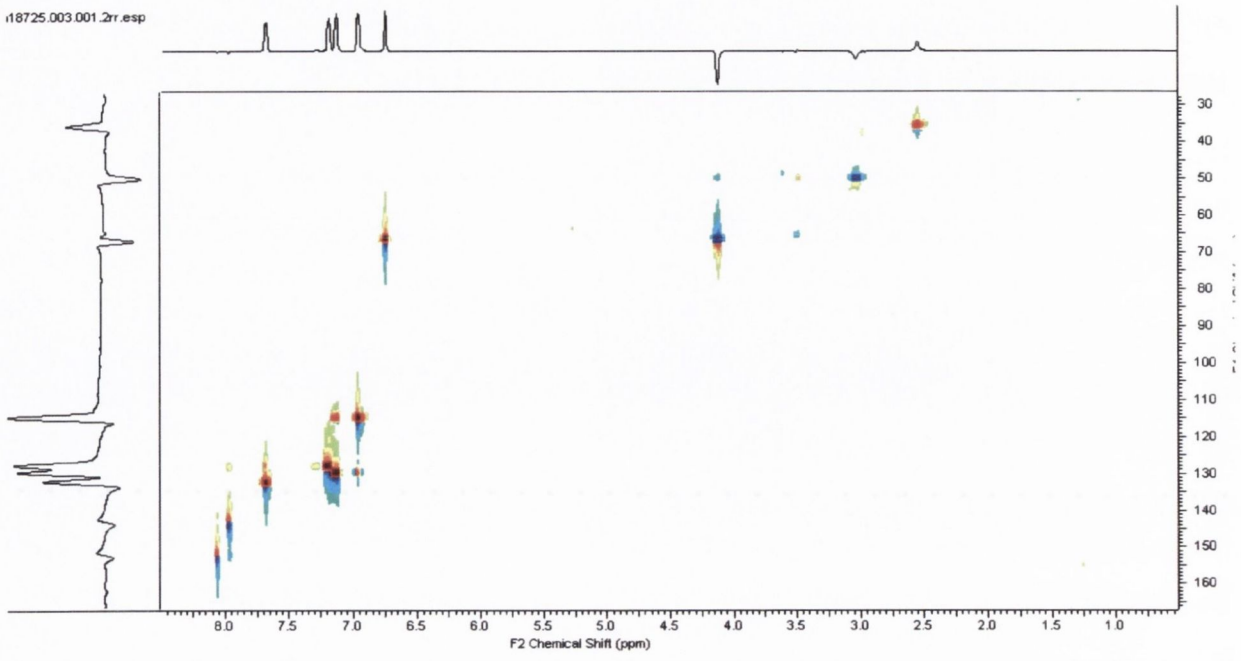

Figure 4-10 ^{1}H-^{13}C COSY experiment of compound [387]

4.4 Aromatase Inhibitor – Combretastatin CA4 hybrid compounds

When synthesising the letrozole scaffold [387] it was proposed that a series of novel molecules that contain the letrozole core, but with modified aryl substituents, be also investigated. The plan was to incorporate the A and/or B ring of CA4 [150] on to the letrozole scaffold. It was proposed that the letrozole scaffold which is essential of AI activity, could be modified to potentially introduce other/dual targets, e.g. AI and tubulin pharmacophore. A series of small molecules were designed and synthesised which contained an aryl ring from letrozole and an aryl ring (A or B) from CA4. The final compound synthesised with the letrozole scaffold contained both type of CA4 aryl rings (rings A and B of CA4) (see Scheme 4-16).

The route for the synthesis of the letrozole derivatives is shown in Scheme 4-16. The synthesis follows the route previously described for the synthesis of the letrozole derivative [387]. The target compounds were obtained *via* the secondary alcohol (Table 14) then further reacted with 1,2,4-triazole to afford the required products. Compounds [409]-[410] and [394] required debenzylation to afford the free phenol compounds. A total of 4 compounds were synthesised that could potentially still retain the AI activity but also could potentially show some cytotoxicity by incorporating the CA4 pharmacophore (Table 14).

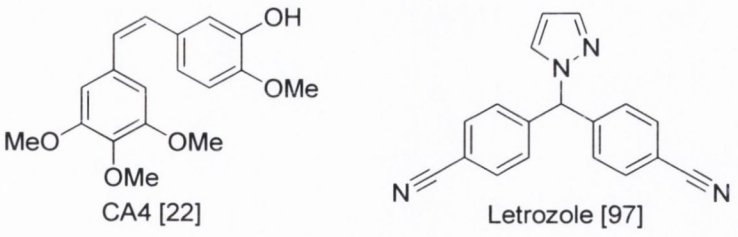

CA4 [22] Letrozole [97]

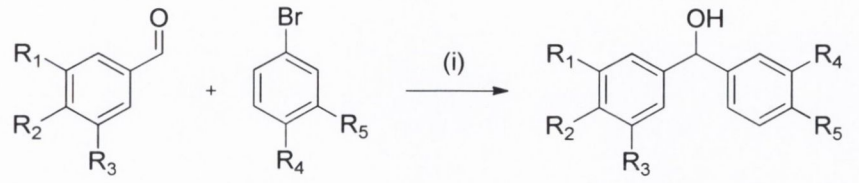

R_1	R_2	R_3	
OMe	OMe	OMe	[403]
OBn	OMe	H	[404]
H	OBn	H	[405]

R_4	R_5	
H	CN	[406]
OMe	OBn	[407]

R_1	R_2	R_3	R_4	R_5	
OMe	OMe	OMe	H	CN	[408] - 92%
OBn	OMe	H	H	CN	[409] - 81%
OMe	OMe	OMe	OMe	OBn	[410] - 85%
H	OBn	H	H	CN	[396] - 88%

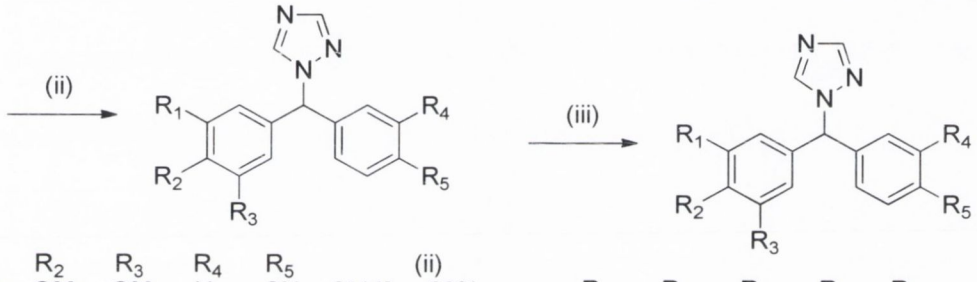

R_1	R_2	R_3	R_4	R_5	(ii)
OMe	OMe	OMe	H	CN	[411] - 63%
OBn	OMe	H	H	CN	[409a] - 74%
OMe	OMe	OMe	OMe	OBn	[410a] - 64%
H	OBn	H	H	CN	[384] - 67%

R_1	R_2	R_3	R_4	R_5	(iii)
OH	OMe	H	H	CN	[412] - 82%
OMe	OMe	OMe	OMe	OH	[413] - 76%
H	OH	H	H	CN	[394] - 66%

(i) *n*-BuLi, THF, -78 °C, 2.5 h; (ii) 1,2,4-Triazole, *p*-TSA, toluene, MW, 4 h, 90-200 W;
(iii) $Pd(OH)_2$, H_2, EtOAc/MeOH, 0.5 h, RT

Scheme 4-16 Synthetic route for the AI-CA4-hybrid compounds

The ^1H NMR spectrum of [413] is shown in Figure 4-11. The methoxy group signals occur at 3.76, 3.85, 3.90 ppm. The proton on the tertiary carbon can be seen at 6.60 ppm. The pair of triazole protons was observed at 7.97 and 8.04 ppm. The remaining signals correspond to the aromatic protons and integrate for 5 protons. The ^{13}C NMR spectrum of [413] is shown in Figure 4-12. The methoxy group carbons correspond to the signals at 55.5, 55.7 and 60.4 ppm. The tertiary carbon can be seen at 67.1 ppm. The two protonated triazole carbons can be observed as the two downfield signals at 143.0 and 151.6 ppm. The signal for the carbon adjacent to the phenol appears at 153.1 ppm. The compounds synthesised in Table 14 will undergo biochemical evaluation for anti-proliferative activity and as potential dual AI and cytotoxic agents, see chapter 6.

Compound	Structure	Debenzylation Yield %
[411]	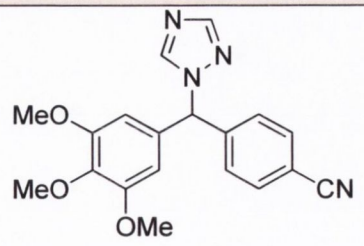	N/A
[412]	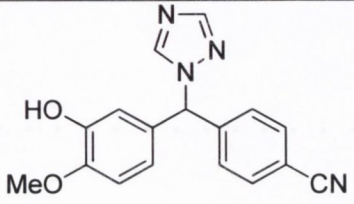	82
[413]	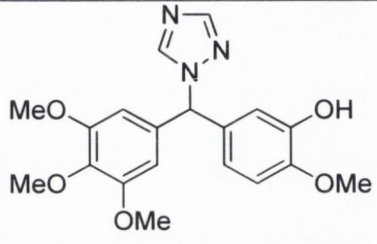	76
[394]	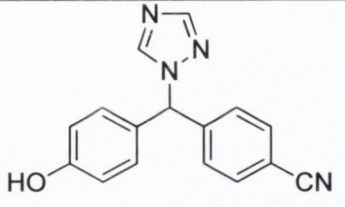	66
[402]	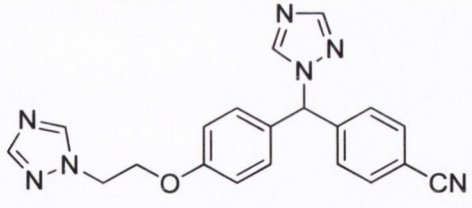	N/A

Table 14 Aromatase inhibitor – combretastatin CA4 hybrid [394], [411]-[413] and [402]

The utilization of the aromatase inhibitor type ligands in the conjugate scaffold should allow for the formation of novel conjugate pharmacophores. The AI ligands will be conjugated to an ER binding ligand and CA-4 type cytotoxic agent for the formation of two prototype/novel conjugates for the treatment of hormone dependent breast cancers. The formation of a series of aromatase inhibitor – combretastatin CA4 hybrid compounds will be evaluated for antiproliferative activity. The hybrid compounds potential mode of action is unknown but it is proposed that due to the structural similarities between letrozole and CA4 that a potential dual action of cytotoxicity on cancer cells and aromatase inhibition may be observed. The hybrid compounds will be initially screened for antiproliferative activity and the lead compound/s will be evaluated for tubulin inhibition.

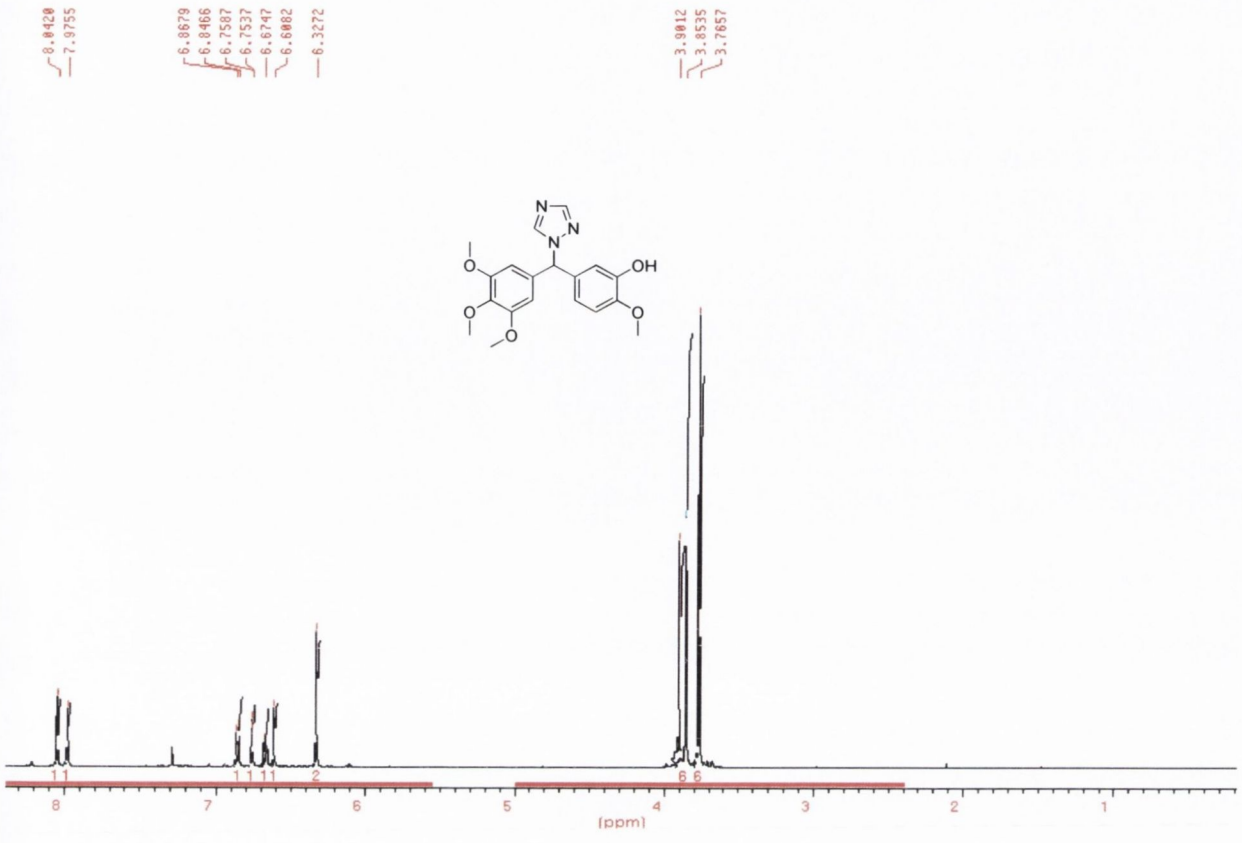

Figure 4-11 ^{1}H NMR spectrum of [413]

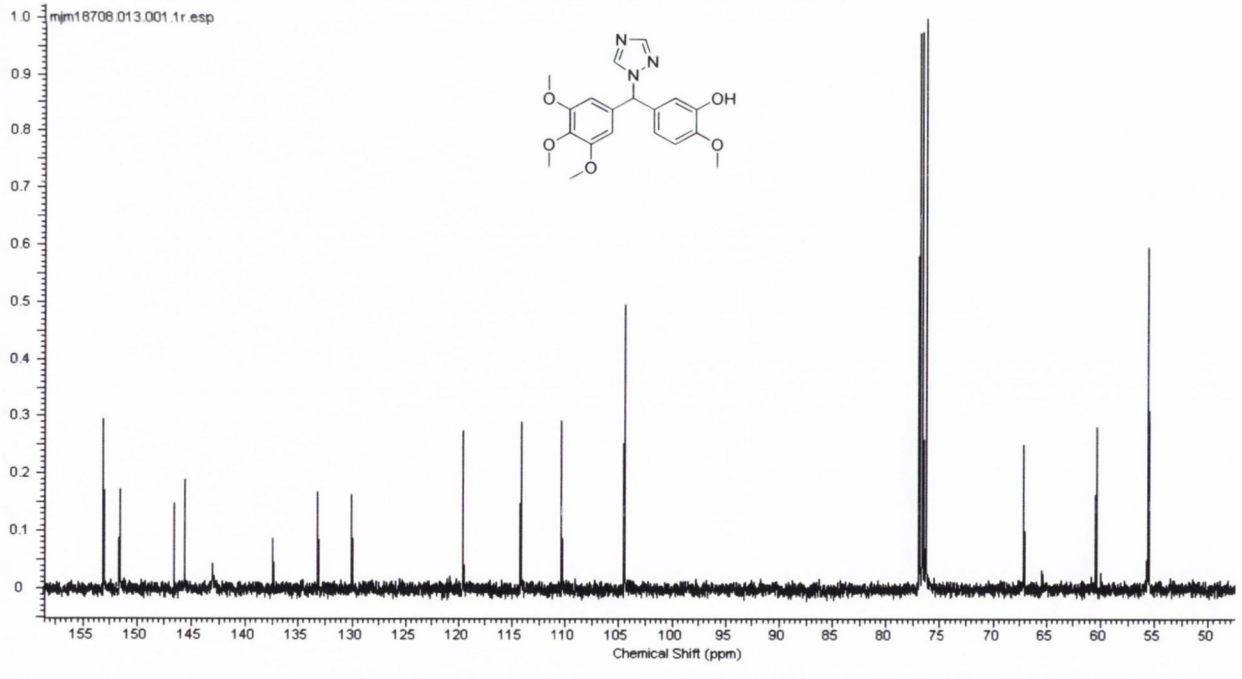

Figure 4-12 ^{13}C NMR spectrum of [413]

Chapter 5
Conjugates

5.1 Overview

The central objective of this research was to synthesise dual-acting, estrogen receptor targeting conjugate products. In the preceding chapters, the syntheses of estrogen receptor (ER) ligands, aromatase inhibitor (AI) ligands and combretastatin analogues were discussed. While these compounds are interesting as new stand-alone active agents, their intended application was directed towards the preparation of conjugated compounds which possessed the combined and possibly enhanced (i.e. dual-action) effects of the individual conjugate moieties. By incorporating an ER-ligand such as endoxifen into the conjugate scaffold, it is envisioned that the conjugate could target breast cancer cells that over-express ER, exerting their antagonist effect while also acting as a carrier to selectively transport the covalently-bound cytotoxic agent to the area of the tumour.

This specific ER-targeting conjugate strategy has been previously investigated for a number of different applications as discussed in the Chapter 1. Burke *et al.* reported the design and synthesis of conjugates which contained the antagonist ER-ligand, 4-hydroxytamoxifen, bound *via* a linker group to the intercalating anticancer agent doxorubicin. The conjugate demonstrated interesting results and showed improved efficacy when compared with the individual conjugate components; 4-fold up to 140-fold enhanced antiproliferative activity relative to doxorubicin and a ER binding affinity of 2.5% relative to *E/Z*-4-hydroxytamoxifen.[417, 419] Keely *et al.* documented that utilization of endoxifen as an ER-ligand covalently bonded to a modified combretastatin cytotoxic agent exhibited potent ER binding affinity with IC_{50} values of 0.9 nM (ERα), 4.7 nM (ERβ) and very potent antiproliferative activity of IC_{50} = 5.1 nM in MCF-7 cell line.[421]

The aims of this project are to expand upon this concept of ER-targeting conjugates by attempting to optimise the antagonistic action and binding affinity of the ER-ligands while conjugated to the cytotoxic agent. The endoxifen ER-ligand conjugates are investigated to optimise the position of attachment of the cytotoxic ligand linking functional group and to identify appropriate cytotoxic agents to be incorporated into the conjugate scaffold.[421] In this project, a selection of cytotoxic agents are incorporated into the conjugate scaffold. Alternative ER-ligands will be evaluated for specific ER-targeting and an aromatase inhibitor will also be incorporated into the conjugate scaffold.

5.2 Conjugate Strategy

A general prototype structure of the conjugates synthesised in the study is shown in Figure 5-1. The prototype contains an ER-ligand, a linker and a cytotoxic agent. The ER-ligand is the core element of the scaffold as it is key to the proposed ER-targeting abilities of the conjugate. The ER-ligands identified for the conjugate study were endoxifen, cyclofenil and 2-phenylindole derivatives

(see Chapter 2). These ligands were chosen due to their antagonist nature and/or impressive ER binding affinities.[114] Non ER-targeting AI ligands letrozole and anastrozole derivatives, was also investigated. These were not envisioned to target the ER but could potentially inhibit estrogen biosynthesis. The linker element acts as an interface between the ER-ligand and the cytotoxic agent. The choice of linker element was previously optimised by Keely in which a direct amide linkage displayed the optimum anti-proliferative activity.[421] The various cytotoxic agents were initially chosen based on literature evidence of activity against breast cancer and assessed for suitability as agents to couple to various ER-ligands. The cytotoxic agents chosen in the present study to undergo conjugation reaction with endoxifen, cyclofenil and 2-phenylindole were combretastatin derivatives [150], [311]-[326], Chapter 3.

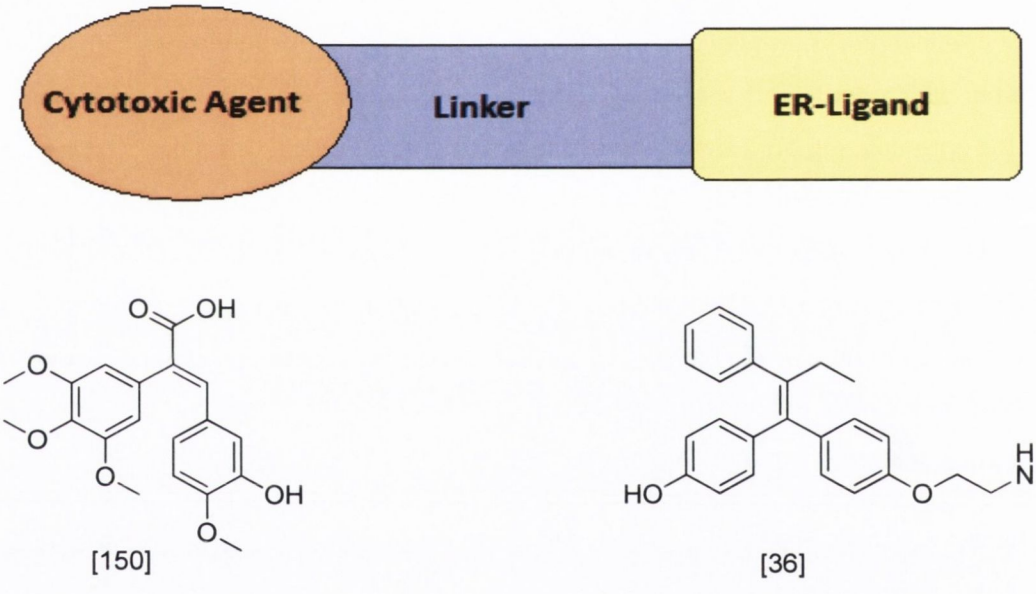

Figure 5-1 General prototype structure and example of CA type cytotoxic agent [150] and ER-ligand endoxifen [36]

Amides are more stable to hydrolysis when compared to esters and are used only to a slight extent as prodrugs due to their relatively high enzymatic stability to hydrolysis *in vivo*. While chemically quite stable, the amide bond can be hydrolysed by amidase, peptidases or proteases.[544, 545] It is proposed that the presence of the amide linkage within the tumour conjugates would be less susceptible to enzymatic hydrolysis and may demonstrate intrinsic antiproliferative action targeting ER/tubulin, AI-tubulin or AI-ER.

5.2.1 Coupling Reactions

The synthesis of the conjugate required a coupling reaction between the carboxylic acid and the amine forming an amide covalent-bond linkage. In this project, the use of DCC (N,N'-dicyclohexylcarbodiimide) and EDC (1-ethyl-3-(3-dimethylaminopropyl)carbodiimide)) was successful

in coupling secondary amines of the ER ligand with the carboxylic acid functionality on the acrylic acid combretastatin analogues in order to form amide linkages.

The conjugate compounds in the project were all synthesised using either DCC or EDC. Carbodiimides, containing a (N=C=N) functionality are dehydration condensing agents often used to activate carboxylic acids towards amide or ester formation.[503] DCC was one of the first developed and is very useful due to its high yielding reactions and relative low cost. DIC (*N,N'*-diisopropylcarbodiimide) and EDC are two other popular carbodiimides, the latter forming water-soluble by-products. In order to reduce side reactions (such as intramolecular *N*-acylureas) and help increase yields, hydrobenzotrizole (HOBt) was added to the coupling reactions performed using DCC and EDC. The use of solvents with low-dielectric constants such as DCM or chloroform can minimise possible side reactions, therefore anhydrous DCM was used for the coupling reactions in this project.

The DCC coupling reagent was successfully used for the formation of the conjugate compounds, however the by-product formed, *N,N'*-dicyclohexylurea, was difficult to remove from the synthesised compound. In the case of EDC on the other hand, the by-product is water soluble and is quite easily removed by an aqueous wash. The coupling reactions discussed later in this chapter were successful using DCC but the NMR spectra showed the presence of *N,N'*-dicyclohexylurea by-product which could not be successfully removed *via* column chromatography. Therefore, it was decided that if the coupling reagent was changed to EDC it could potentially afford a cleaner product. In some cases both reagents were investigated for the formation of the conjugate products. This will be discussed later in this chapter. The mechanism of amide formation reaction *via* the DCC reagent was previously discussed in Section 3.3.7.1 and illustrated for the EDC reagent in Scheme 5-1.

5.3 Direct amide conjugates

5.3.1 Endoxifen conjugates

The combretastatin acrylic acid analogues prepared *via* the Perkin reaction contain the carboxylic acid functional group and allow the formation of the conjugate products. The acrylic acid combretastatin analogues [150], [311]-[327] were directly coupled to the silyl-protected endoxifen analogue [197] (Scheme 5-2). The conjugates were referred to as 'direct amide conjugates' as there is no additional linker moiety required and the carboxylic acid group reacts directly with the secondary amine functionality of the endoxifen analogue to form the amide linkage *via* a DCC/EDC & HOBt coupling (condensation) reaction.

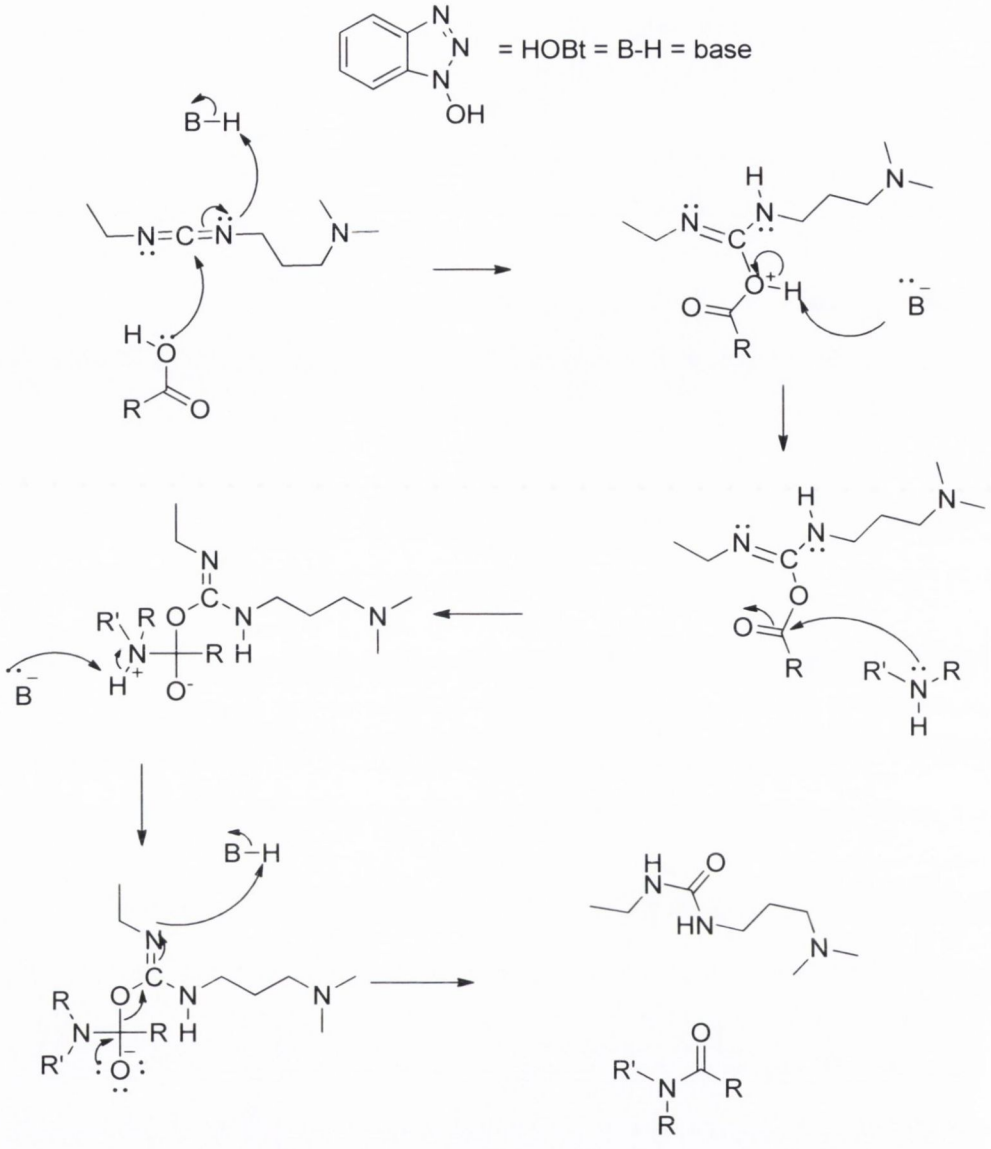

Scheme 5-1 General mechanism for amide synthesis with EDC

The initial procedure investigated DCC as the coupling agent (Scheme 5-2). For the synthesis of this series of conjugates [414]-[430], equimolar amounts of the acrylic acid, amine [197], DCC and HOBt were reacted and the reaction was monitored *via* TLC. The resulting silyl-protected conjugate was not purified and the crude product was carried directly to the next step where an equivalent of 1 M TBAF solution (in THF) was added to deprotect the silyl-protecting group. Upon reaction to afford the direct amide conjugate and following work-up procedure, the mixture was purified *via* flash chromatography to afford the direct amide conjugates [414]-[430] in high yields as ~1:1 (*E/Z*)-isomeric mixtures. The isomeric ratios were calculated based on those of the endoxifen starting material and confirmed by integration of appropriate signals in the ^{1}H NMR spectra.

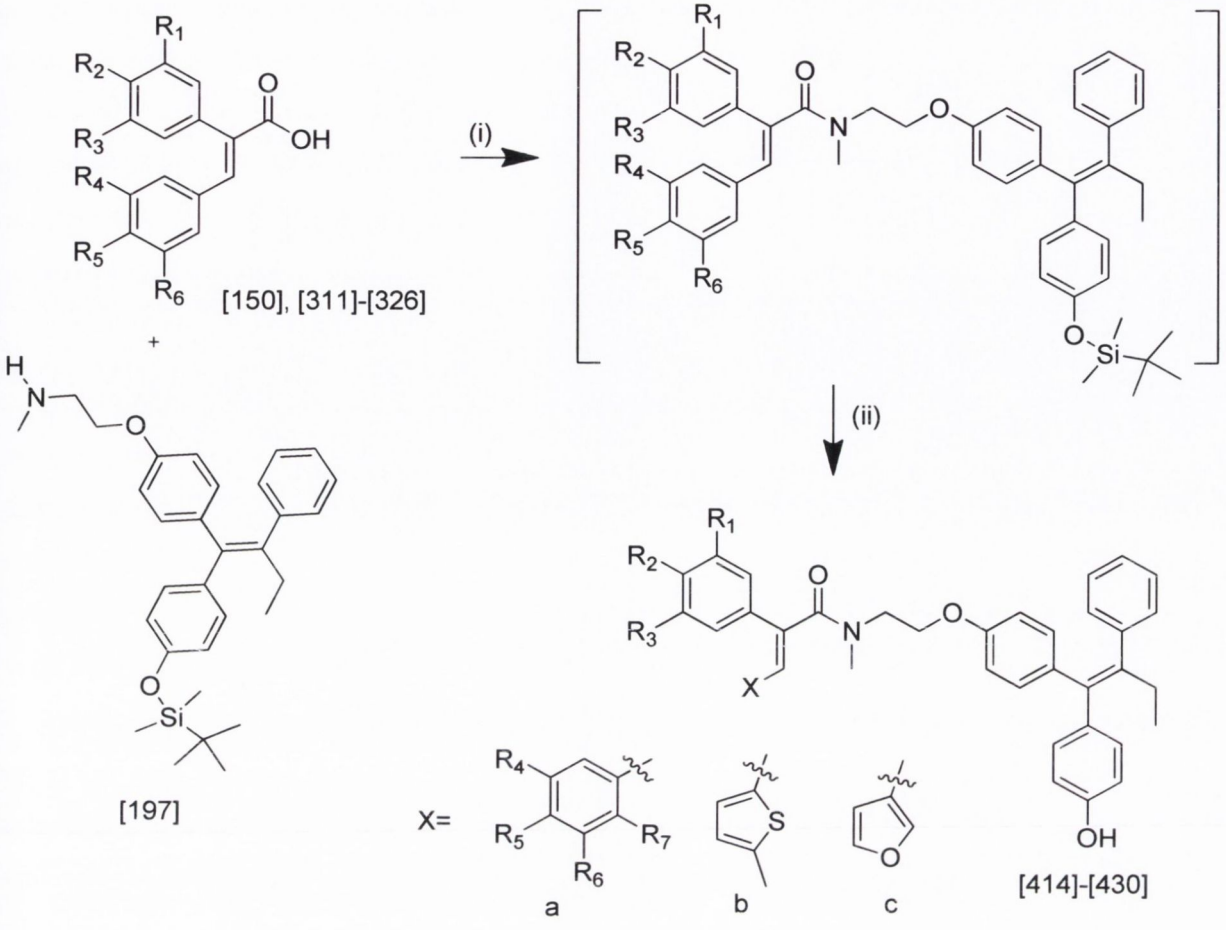

(i) DCC/EDC, HOBt, DCM, 24 h, RT; (ii) TBAF, THF, 0.5 h, RT

Acrylic Acid	X	R_1	R_2	R_3	R_4	R_5	R_6	R_7	Direct Conjugate
[150]	a	OMe	OMe	OMe	H	OMe	OH	H	[414]
[311]	a	H	OMe	H	H	$O(CH_2)O$		H	[415]
[312]	a	OMe	OMe	OMe	H	OMe	NO_2	H	[416]
[313]	a	OMe	OMe	OMe	H	OMe	F	H	[417]
[310]	a	OMe	OMe	OMe	H	OMe	H	H	[418]
[314]	a	OMe	H	OMe	OMe	OMe	OMe	H	[419]
[315]	a	OMe	OMe	OMe	OMe	OMe	OMe	H	[420]
[316]	a	OMe	H	OMe	H	OMe	OH	H	[421]
[317]	a	OMe	OMe	OMe	H	OH	OH	H	[422]
[318]	a	OMe	OMe	OMe	H	H	OH	H	[423]
[319]	a	OMe	OMe	OMe	H	OMe	OMe	H	[424]
[320]	a	OMe	OMe	OMe	H	OMe	OMe	OMe	[425]
[321]	a	H	OMe	OH	OMe	OMe	OMe	H	[426]
[322]	a	OMe	OMe	OMe	OMe	OH	OMe	H	[427]
[324]	a	OMe	OMe	OMe	H	C_4H_4		H	[428]
[325]	b	OMe	OMe	OMe					[429]
[326]	c	OMe	OMe	OMe					[430]

Scheme 5-2 Endoxifen direct-amide conjugates

The second procedure employed EDC as the coupling reagent. For the synthesis of this series of conjugates [414]-[430], the equivalencies were varied to ensure a slight excess of activated ester formed so that when the amine was added a greater yield of amide product was isolated. The ratio of reactants was 1.2 eq of acrylic acid, 1.4 eq EDC, 1.4 eq HOBt and 1 eq of amine and the

reaction was monitored *via* TLC. The silyl-protected conjugate was purified in this procedure but was not fully characterised at this step, but was verified by HRMS. The isolated silyl-protected conjugate was then reacted with an equivalent of 1 M TBAF solution (in THF) to deprotect the silyl-protecting group. Upon reaction to afford the direct amide conjugate and following work-up procedure, the mixture was purified *via* flash chromatography to afford the direct amide conjugates in high yields as ~1:1 (*E/Z*)-isomeric mixtures. The isomeric ratios were again calculated based on the endoxifen starting material.

The use of both coupling reagent agents afforded the desired conjugate compounds Table 15. However compounds [419], [421], [423] and [425] were only successfully produced using the DCC coupling reagent owing to lack of starting material. When DCC was used as a coupling reagent, the *N,N'*-dicyclohexylurea byproduct was found in the isolated products. The products were afforded as brown resins with yields ranging between 7 and 91%. When EDC was used as the coupling reagent, the isolated coupled products were afforded cleanly. The urea by-product which was water soluble and removed by workup and the ^{1}H-NMR product spectra were much cleaner in the 1 - 2 ppm region (region in which the *N,N'*-dicyclohexylurea signal would be observed). It was found that the final deprotection and purification steps were simplified when the clean silyl-protected conjugate was put forward to the next step when compared to the crude mixture. The final deprotected products from the EDC method were isolated as white/off-white solids. The yields for the conjugation-coupling reactions are listed in Table 15.

As an example, the ^{1}H-NMR spectrum of [418] is shown in Figure 5-2. As the product is afforded as an *E/Z* isomeric mixture, many of the signals overlap and appear as multiplets. The protons of the ethyl chain are observed between 0.87-0.92 ppm (CH_3) and 2.40-2.50 ppm (CH_2). The protons for the amine methyl are observed between 3.00-3.20 ppm. This signal pattern which is classified as a multiplet but three overlapping signals are observed suggesting the presence of rotamers which was confirmed from examination of the Variable Temperature NMR Experiments which will be discussed later in this chapter. The proton signals of the methoxy group and the basic side chain methylene (CH_2) are found between 3.55-4.30 ppm and the region between 6.40-7.20 ppm contains signals for the aromatic protons and the ethylene bridge methlyene proton. In the ^{13}C-NMR spectrum of [418] shown in Figure 5-3, ethyl side chain signals are observed at 13.61 ppm (CH_3) and 25.63 ppm (CH_2). The methyl amine carbon is identified as a weak signal at 39.09 ppm, which was confirmed from the ^{13}C-^{1}H COSY spectrum. The basic side chain carbons are identified at 50.78 ppm (NCH_2) and 60.40 ppm (OCH_2). The methoxy signals are observed at 55.22, 55.9 and 60.91 ppm. The remaining aromatic carbons and ethylene carbons are observed between 105.98 and 159.30

ppm. The carbonyl carbon was identified at 173.4 ppm. In the IR spectrum, the hydroxyl group was identified as a broad band at 3426.3 cm^{-1} while the amide carbonyl group is observed as a strong band at 1605.7 cm^{-1}. The characterisation is confirmed through high resolution mass spectrometry where a mass of 722.3102 $(M+Na)^+$ was found for the molecular ion, $C_{44}H_{45}NO_7Na$.

The possible explanation for the complex signal pattern observed for many conjugates in the ^1H and ^{13}C NMR spectra is presented bellow.

Compound no.	DCC coupling Crude yield (%)	Overall DCC coupling & Deprotection yield (%)	EDC coupling Yield (%)	Deprotection yield following EDC coupling (%)	Overall EDC coupling & Deprotection yield (%)
[414]	122	82	85	97	82
[415]	131	91	83	91	76
[416]	93	54	88	93	82
[417]	102	53	77	90	69
[418]	97	55	91	93	84
[419]	84	33	-	-	-
[420]	93	43	88	94	83
[421]	89	54	-	-	-
[422]	77	37	71	84	60
[423]	79	45	-	-	-
[424]	81	31	87	91	79
[425]	63	26	-	-	-
[426]	72	21	85	90	77
[427]	66	35	76	94	71
[428]	61	23	66	84	55
[429]	74	34	56	81	45
[430]	53	7	32	50	16

Table 15 Yields for amide conjugate reaction (DCC and EDC as coupling agent)

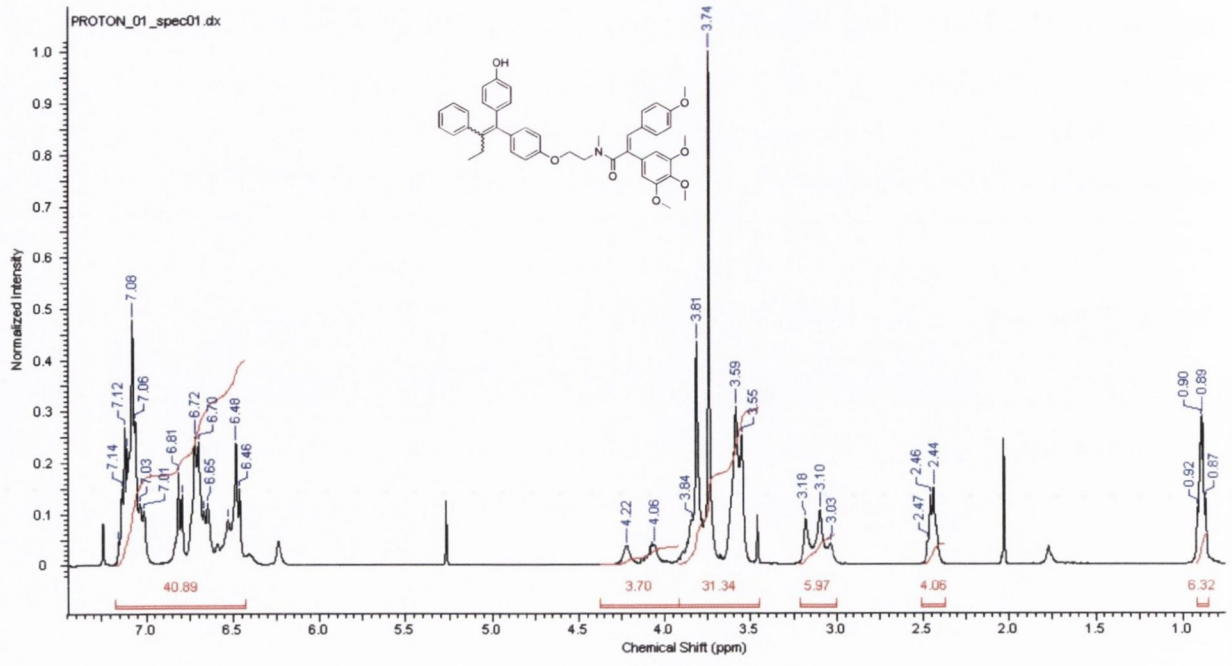

Figure 5-2 ^{1}H-NMR spectrum for [418]

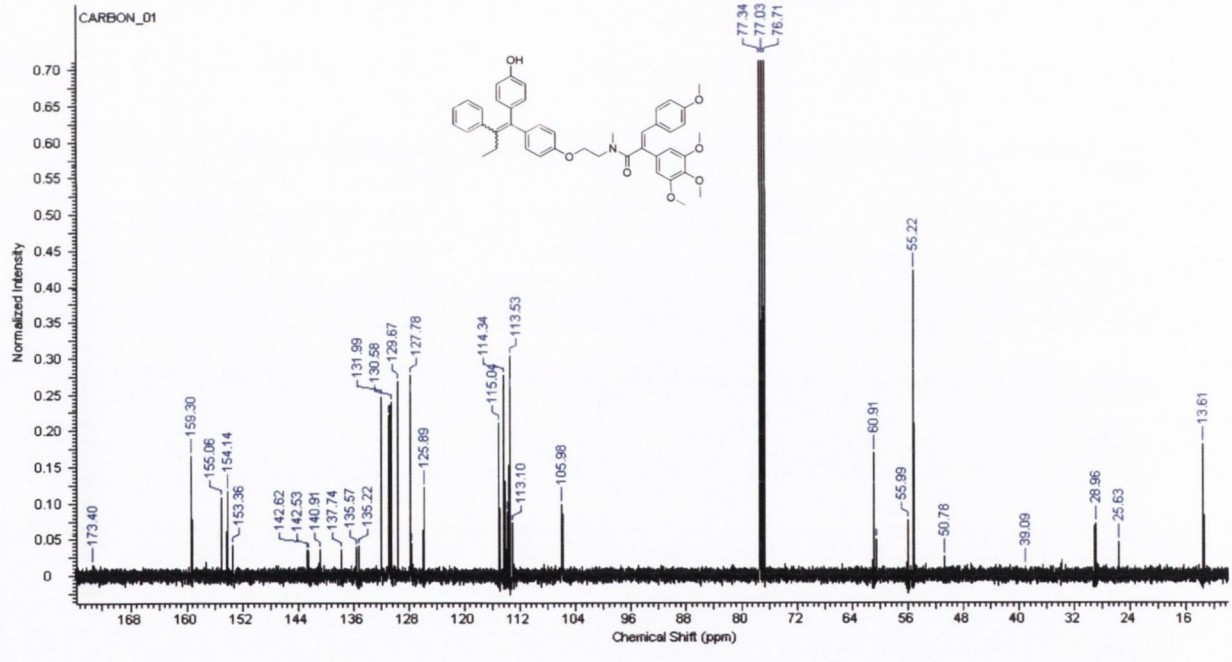

Figure 5-3 ^{13}C-NMR spectrum for [418]

Certain types of bonds, in particular amides, whilst normally considered as 'single', have in fact, sufficient 'double bond character', to render rotation about their axis, 'restricted'. A partial double bond character exists between the carbonyl, and the nitrogen, and may be demonstrated in its resonance structures shown in Scheme 5-3 (amide resonance). The presence of rotamers caused by the hindered rotation around the partial double bond can be witnessed throughout this chapter. Therefore the conjugates in this chapter demonstrated more complicated NMR spectra caused by

peak multiplication. The magnitude of the energy barrier to the rotation determines what the effect on the spectrum. The lower the energy barrier is, then the rotation will be relatively fast on the NMR time scale, causing only slight broadening of signals. Conversely, when the energy barrier is high, rotation will be slow and two distinct sets of signals may be observed.[546]

Scheme 5-3 Amide resonance: partial double bond character

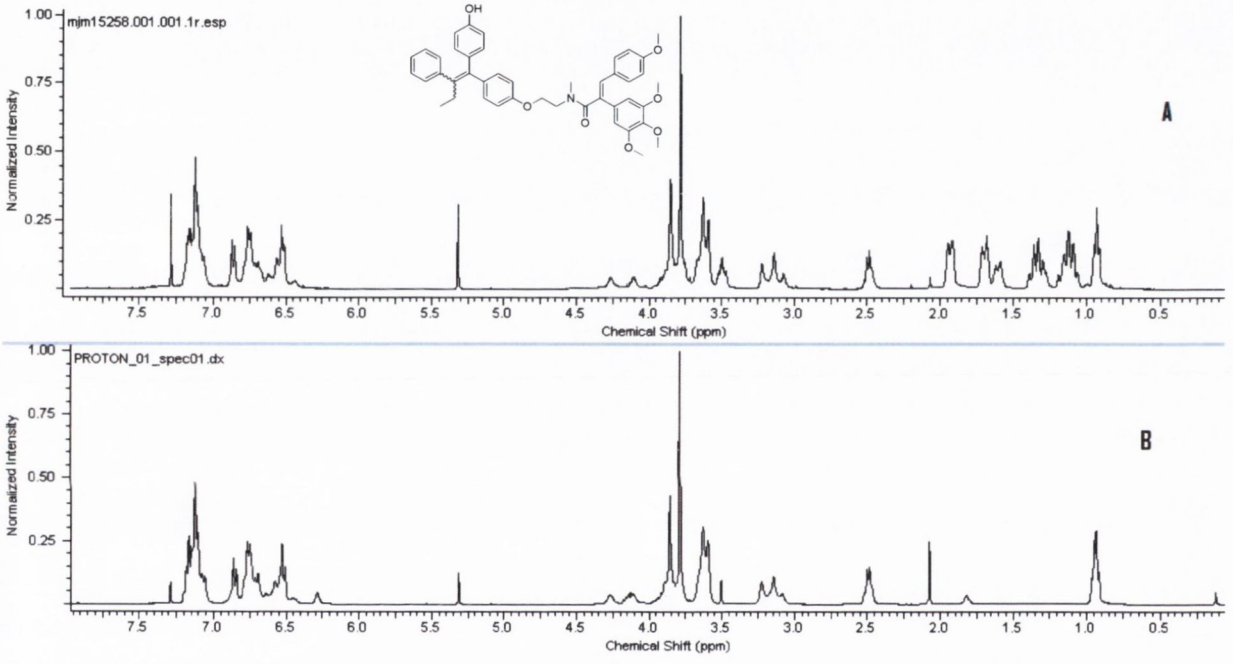

Figure 5-4 ^{1}H NMR spectrum for [418], A - DCC method, B - EDC method

The advantage offered by EDC in isolation of pure product is illustrated for compound [418] (Figure 5-4). The ^{1}H-NMR spectra for [418] are shown in Figure 5-4. Spectrum A shows the ^{1}H NMR spectrum for the isolated DCC coupling synthetic method. Spectrum B is the ^{1}H NMR spectrum for the EDC synthetic method. The signals in spectrum 'A' between 1-2 ppm correspond to the signals expected for the N,N'-dicyclohexylurea by-product (Figure 5-5). This by-product is mostly insoluble but may be present in small quantities and is difficult to observe under UV lamp and separate. Examination of both compounds by TLC shows the presence of a single product and for that reason it was not possible to separate the bi-product from product A *via* column chromatography over silica gel. In spectrum B it should be noted that no urea byproduct is present. Not all the DCC coupled products showed this extent of contamination with the byproduct, in most cases it was possible to detect the presence of this impurity by ^{1}H NMR spectroscopy.

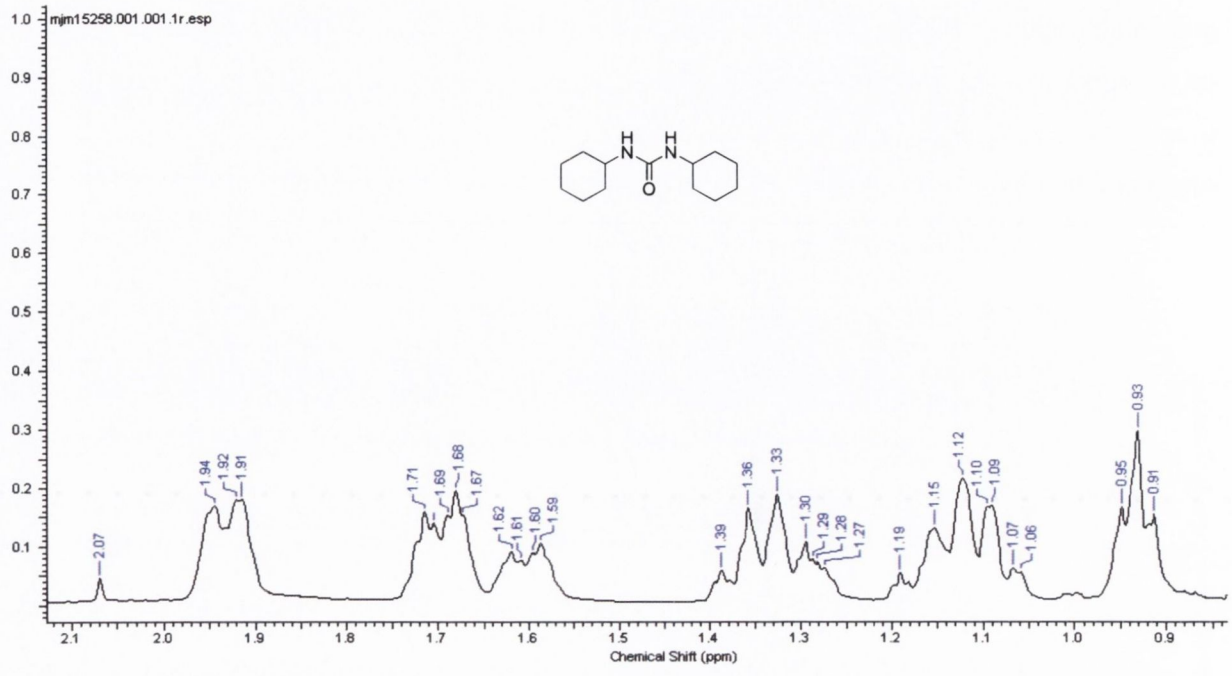

Figure 5-5 Enlarged ^{1}H NMR spectrum between 1-2 ppm for [418], A - DCC method

5.4 Conjugate synthesis with cinnamic and 3-phenylpropanoic acids

A further objective of this project was to prepare conjugates of endoxifen with cinnamic and phenylpropanoic acids related in structure to A and B rings of CA4. For this modified structure the substituent ring would now be either the 3,4,5-trimethoxy-ring (A ring) or the 3-hydroxy-4-methoxy-ring (B ring). Both rings (A and B) have been shown to be essential for the combretastatin CA4 activity [22].[497] This investigation was designed to test if the dual ring structure and/or the ethylene bridge was essential for biological activity. Therefore all other structural features of the conjugate molecule must remain the unchanged. If the other entire ER-ligand component remained structurally identical then it may be possible to deduce that any variation in biological activity could be related to structural modifications. The direct amide linkage required the appropriate cinnamic and 3-phenylpropanoic acids as starting material affording the desired conjugates for this investigation (see Scheme 5-4).

The compounds [342]-[345] prepared in Chapter 3 were used to synthesise the required endoxifen direct-amide conjugates *via* EDC/DCC and HOBt coupling reaction. As with the previous endoxifen conjugates, the first procedure employed DCC as the coupling agent. To synthesise this series of conjugates [431]-[434], equimolar amounts of the acrylic acid, amine [197], DCC and HOBt were reacted and monitored the reaction *via* TLC. The silyl-protected conjugate was not purified and the crude product was used directly in the next reaction step, where an equimolar amount of 1 M TBAF solution (in THF) was added, deprotecting the silyl-protecting group. Upon reaction, the direct amide conjugate, was purified *via* flash column chromatography affording the desired amide

conjugates in high yields as ~1:1 (*E/Z*)-isomeric mixtures. The isomeric ratios were calculated based on the endoxifen starting material and verified by inspection of the integration ratio of the ^{1}H-NMR spectra.

The second procedure employed EDC as the coupling reagent. For the synthesis of this series of conjugates [431]-[434], the molar equivalents were varied to produce a slight excess of active ester, so that when the amine was added it would afford a greater yield of amide product. The ratio of reactant used was; 1.2 eq of acrylic acid, 1.4 eq DCC, 1.4 eq HOBt and 1 eq of amine were reacted and the reaction was monitored *via* TLC. The silyl-protected conjugate was purified during this reaction procedure but was not characterised at this step, however the presence of the coupled product was verified by HRMS. The isolated silyl-protected conjugate was then reacted with an equimolar of 1 M TBAF solution (in THF) to deprotect the silyl-protecting group. Following the work-up procedure and purification *via* flash column chromatography over silica gel, the direct amide conjugates were obtained in high yields (90-95%) as ~1:1 (*E/Z*)-isomeric mixtures. The isomeric ratios were calculated based on the endoxifen starting material [197] and from the integrated signals in the ^{1}H-NMR spectrum. The products obtained [435]-[438] are illustrated in Table 16 together with % yields obtained.

As observed with the previous endoxifen conjugates, when EDC was employed as the coupling reagent, the overall yields were significantly increased and the isolated final conjugates [435]-[438] did not contain any urea byproduct (verified *via* ^{1}H-NMR). The final conjugates were afforded as off-white solids following the EDC coupling reaction and as brown resins after the DCC coupling reaction.

As an example, the ^{1}H-NMR spectrum of [436] shown in Figure 5-6. As the product is afforded as an isomeric mixture many of the signals overlap and appear as multiplets and are quite complex. The protons of the ethyl chain are observed as a triplet at 0.91 ppm with a coupling constant of 6.5 Hz (CH_3) and the CH_2 is observed in a complex region of the spectrum between 2.44-3.07 ppm. In this region the NCH_3 and two CH_2 signals are also observed. The region between 3.62-4.12 ppm shows the methoxy signals and the two CH_2 from the endoxifen basic side chain. The region between 5.60-7.13 ppm certain signals relating to the aromatic protons. The ^{13}C-NMR spectrum of [436] (Figure 5-7) shows a complex pattern of signals. The carbon signals are present as multiple overlapping signals due to the presence of the isomeric mixture and rotamers. This is noticeable in the case of the CH_2 signals which are observed and also with conjugates discussed later in this chapter.

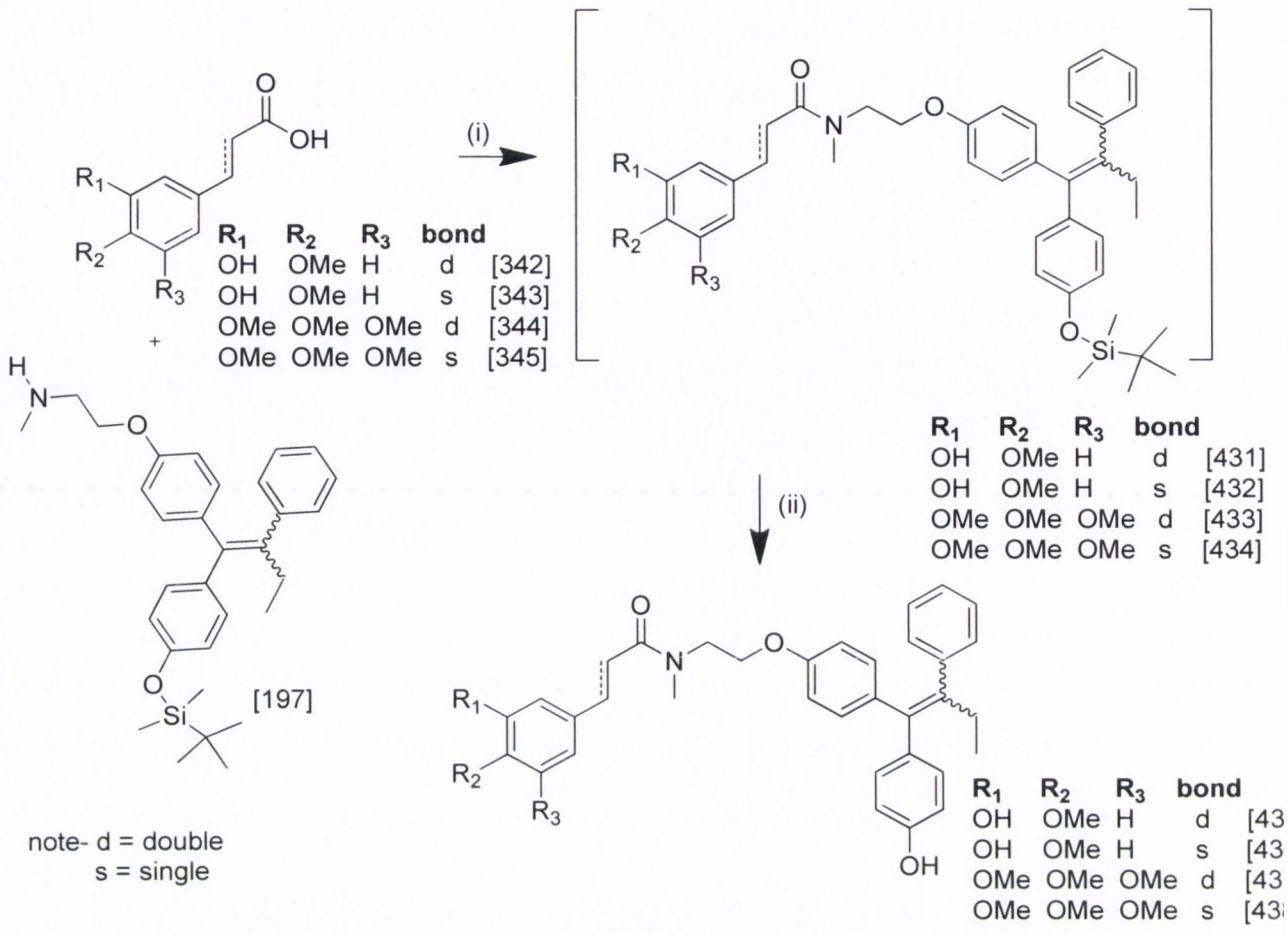

R_1	R_2	R_3	bond	
OH	OMe	H	d	[342]
OH	OMe	H	s	[343]
OMe	OMe	OMe	d	[344]
OMe	OMe	OMe	s	[345]

R_1	R_2	R_3	bond	
OH	OMe	H	d	[431]
OH	OMe	H	s	[432]
OMe	OMe	OMe	d	[433]
OMe	OMe	OMe	s	[434]

R_1	R_2	R_3	bond	
OH	OMe	H	d	[43
OH	OMe	H	s	[43
OMe	OMe	OMe	d	[43
OMe	OMe	OMe	s	[43

(i) DCC/EDC, HOBt, DCM, 24 h, RT; (ii) TBAF, THF, 24 h/0.5 h RT

Scheme 5-4 Synthesis of endoxifen conjugates [435]-[438]

In the ^{13}C NMR spectrum of [436] (Figure 5-7), the ethyl side chain signals are observed at 13.61 ppm (CH_3) and 28.98 ppm and at 28.9 ppm (CH_2). The methyl amine carbon is identified as two signals at 37.5 and 37.6 ppm. The additional CH_2 signals in the conjugate were seen at 30.6, 30.7, 31.0, 35.1, 35.3, 35.6, 48.1, 48.2, 49.1, 60.4, 64.9, 66.3 and 66.6 ppm and verified in the DEPT 135 spectrum. The single methoxy carbon was observed as a signal 37.5 ppm. The remaining aromatic carbons and ethylene bridge are observed between 110.7 and 157.2 ppm. The carbonyl carbon was identified at 172.85 and 172.91 ppm. In the IR spectrum, the hydroxyl group was identified as a broad band at 3444.1 cm^{-1} while the amide carbonyl group is observed as a strong band at 1607.4 cm^{-1}. The characterisation is confirmed by high resolution mass spectrometry where 574.2569 $(M+Na)^+$ was found for the molecular ion $C_{35}H_{37}NO_5Na$.

Compound no.	Structure	DCC coupling & Deprotection yield (%)	EDC coupling Yield (%)	Deprotection yield following EDC coupling (%)	Overall EDC coupling & Deprotection yield (%)
[435]		56	87	95	83
[436]		60	86	90	77
[437]		36	89	95	85
[438]		29	92	93	86

Table 16 Direct amide conjugate reaction yields (DCC and EDC as coupling agent)

Figure 5-6 ^{1}H-NMR spectrum of [436]

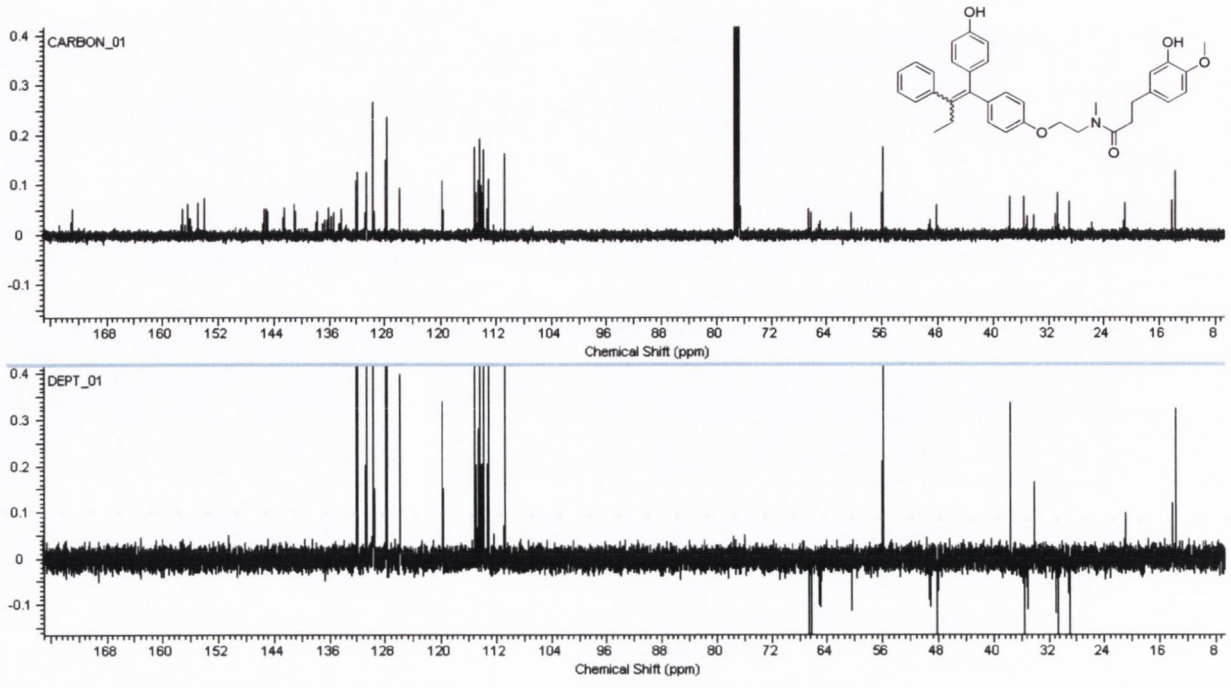

Figure 5-7 ^{13}C-NMR and DEPT-135 spectrums of [436]

5.5 Cyclofenil-based conjugates

The previous section described the preparation of CA4 conjugates with the ER ligand endoxifen as potential anticancer agents. It was now proposed to change the ER ligand from endoxifen to cyclofenil however keeping the cytotoxic agent unchanged.[421] To facilitate direct comparison between the exchanged ER ligands, it is proposed that the linkage should also remain unchanged. The cyclofenil-based ER ligands [216]-[220] were synthesised previously in Section 2.2. Cyclofenil and its derivatives have high binding affinity for ER, often comparable to or greater than that of estradiol and it has mixed agonist-antagonist activity typical for a nonsteroidal selective ER modulator such as tamoxifen or raloxifene.[468, 469] For this reason it was proposed to be a viable ER-ligand for the conjugate scaffold. These novel ER ligands containing a basic side chain ether similar to that of endoxifen, and was now used for the novel linkage to the CA4-type cytotoxic agent.

The formation of the novel conjugates would follow the endoxifen conjugate chemistry (section 5.3) as the secondary amine and the carboxylic acid will be coupled using the EDC & HOBt mediated coupling reaction. This time only EDC was employed as the coupling agent. The EDC coupled products from the endoxifen conjugates were found to be easier to purify and did not contain traces of the urea by-product. The acrylic acid combretastatin analogue [150] was directly coupled to the silyl-protected cyclofenil-based analogues [216]-[220] (Scheme 5-5). The acrylic acid combretastatin analogue [150] showed the best activity when incorporated into the conjugate scaffold[421], therefore for the cyclofenil-based prototype conjugate, [150] was the only cytotoxic agent used in the evaluation of the conjugates. Once again the conjugates were referred as 'direct

amide conjugate' as there is no additional linker moiety required and the carboxylic acid group reacts directly with the secondary amine functionality of the cyclofenil-based analogues to form the amide linkage *via* an EDC & HOBt coupling (condensation) reaction (Scheme 5-5).

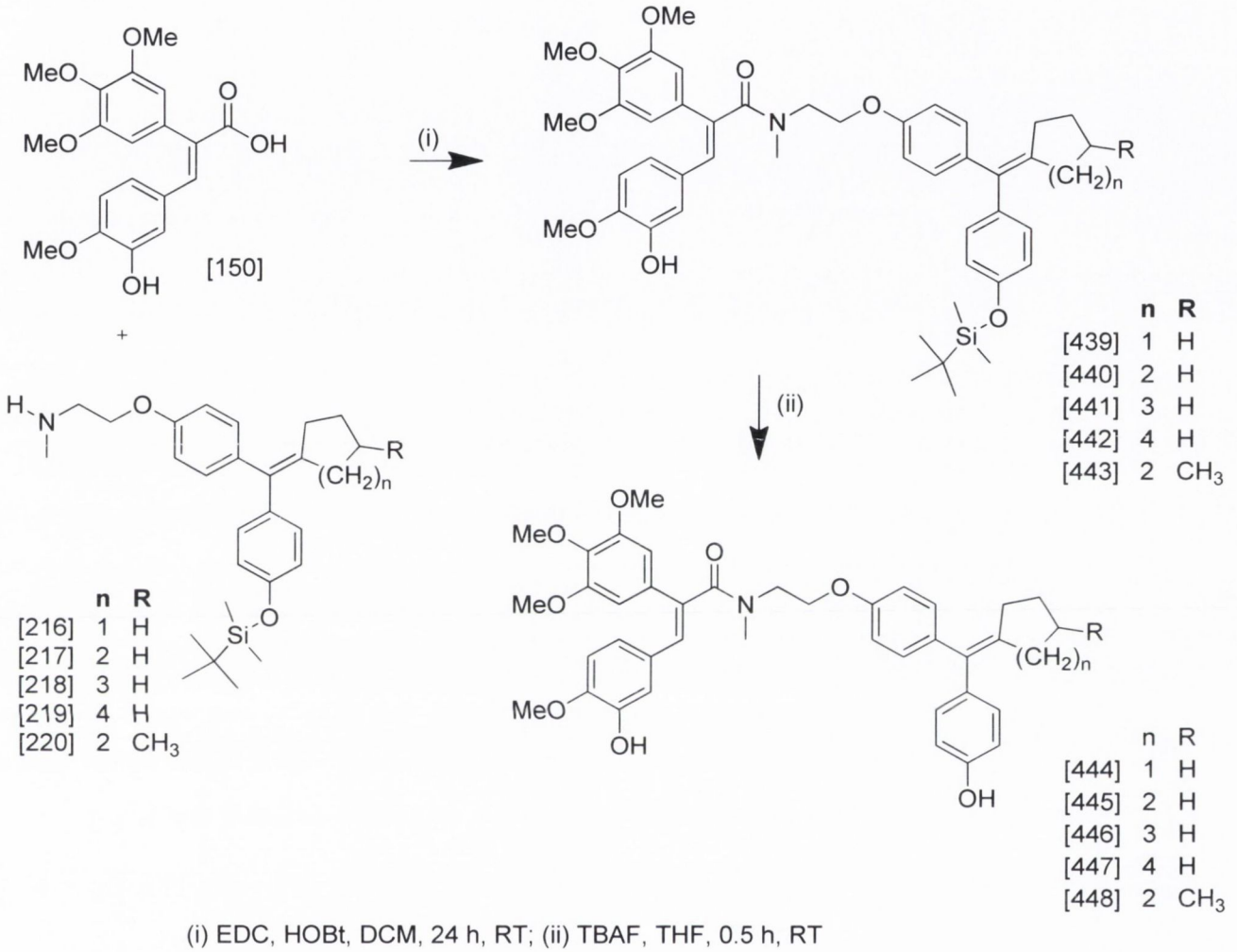

(i) EDC, HOBt, DCM, 24 h, RT; (ii) TBAF, THF, 0.5 h, RT

Scheme 5-5 Cyclofenil-based conjugates

This procedure employed EDC as the coupling reagent. For the synthesis of this series of silyl-protected conjugates [439]-[443], similar to that for the endoxifen conjugates synthesis [414]-[430], the reagent ratio was optimised to allow formation of the activated ester. 1.2 eq of acrylic acid, 1.4 eq. DCC, 1.4 eq. HOBt and 1 eq of amine were reacted and the reaction was monitored *via* TLC. The silyl-protected conjugates were purified in this procedure and was fully characterised at this step. The isolated silyl-protected conjugate was then reacted with an equimolar solution of 1 M TBAF solution (in THF) to deprotect the silyl-protecting group. Upon reaction to afford the direct amide conjugate and following work-up procedure, the mixture was purified *via* flash chromatography to afford the direct amide conjugates [444]-[448] in high yields as yellow solids, Table 17.

Compound no.	EDC coupling Yield (%)	Compound no.	Deprotection yield following EDC coupling (%)
[439]	81	[444]	91
[440]	78	[445]	93
[441]	81	[446]	98
[442]	71	[447]	79
[443]	85	[448]	86

Table 17 Direct amide conjugate reaction yields and deprotection yields

As an example, the ^{1}H-NMR spectrum of [443] is shown in Figure 5-8. Contrasting with the endoxifen conjugates no *E/Z* isomeric mixture is present due to the symmetrical nature of the cyclo alkane rings on the ethylene bridge. However, the presence of rotamers due to the amide bond reduces the resolution of the signals, therefore many signals appear to be duplicated. The methyl protons from the silyl-protecting group are observed at 0.21 ppm ($Si(CH_3)_2$) and at 1.00 ppm ($C(CH_3)_3$). The methyl substituent located on the cycloalkane appears as a multiplet between 0.91 - 0.97 ppm. The CH_2 signals from the cycloalkane ring are observed between 1.05-1.14, 1.72-1.78, 1.79-2.00 and 2.50-2.64 ppm. Protons for the amine methyl are observed between 3.07-3.24 ppm; this signal pattern is classified as a multiplet however the overlapping signals are observed which signifies rotamers. The methoxy signals and the NCH_2 overlap along with the 0.5 × OCH_2 signals are observed in the region between 3.57-3.92 ppm, the remaining 0.5 × OCH_2 signal is seen at 4.23 ppm. The hydroxyl proton is observed as a broad singlet at 5.70 ppm and the signals in the region between 6.57-7.02 ppm relate to the aromatic protons and the ethylene bridge protons.

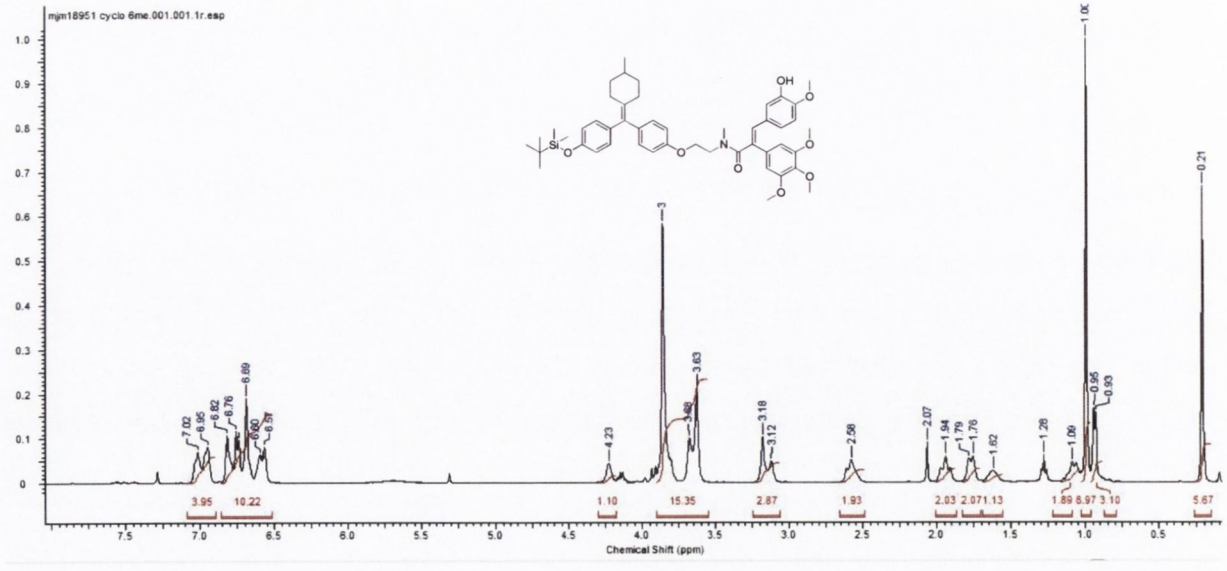

Figure 5-8 ^{1}H-NMR spectrum of [443]

The deprotection of [439]-[443] afforded the novel conjugates [444]-[448]. An example of the ^{1}H-NMR spectrum of [448] is shown in Figure 5-9. The ^{1}H-NMR spectrum for [448] is quite similar to that seen in for [443] in Figure 5-8. The major difference between both is the loss of the silyl protecting methyl substituents which were seen at 0.21 ppm ($Si(CH_3)_2$) and at 1.00 ppm ($C(CH_3)_3$). The ^{13}C-NMR spectrum for [448] is shown in Figure 5-10. The methyl substituent on the cyclo alkane ring can be seen at 21.6 ppm, with the CH signal observed at 32.3 ppm. The CH_2 from the cycloalkane ring is identified at 31.3 and 36.4 ppm. The amine methyl signal is seen at 38.7 ppm. The methoxy signals are observed at 55.4, 55.5, 60.1 and 60.5 ppm. The CH_2 for the basic chain are identified at 47.4 and 65.9 ppm. The remaining aromatic carbons and ethylene bridge are observed between 105.5 and 154.1 ppm. The carbonyl carbon was identified at 172.2 ppm. In the IR spectrum, the hydroxyl group was identified as a broad band at 3421.5 cm^{-1} while the amide group is observed as a strong band at 1605.5 cm^{-1}. The characterisation is confirmed through high resolution mass spectrometry where a mass of 694.3359 $(M+H)^{+}$, was found corresponding to the molecular ion $C_{42}H_{48}NO_8$.

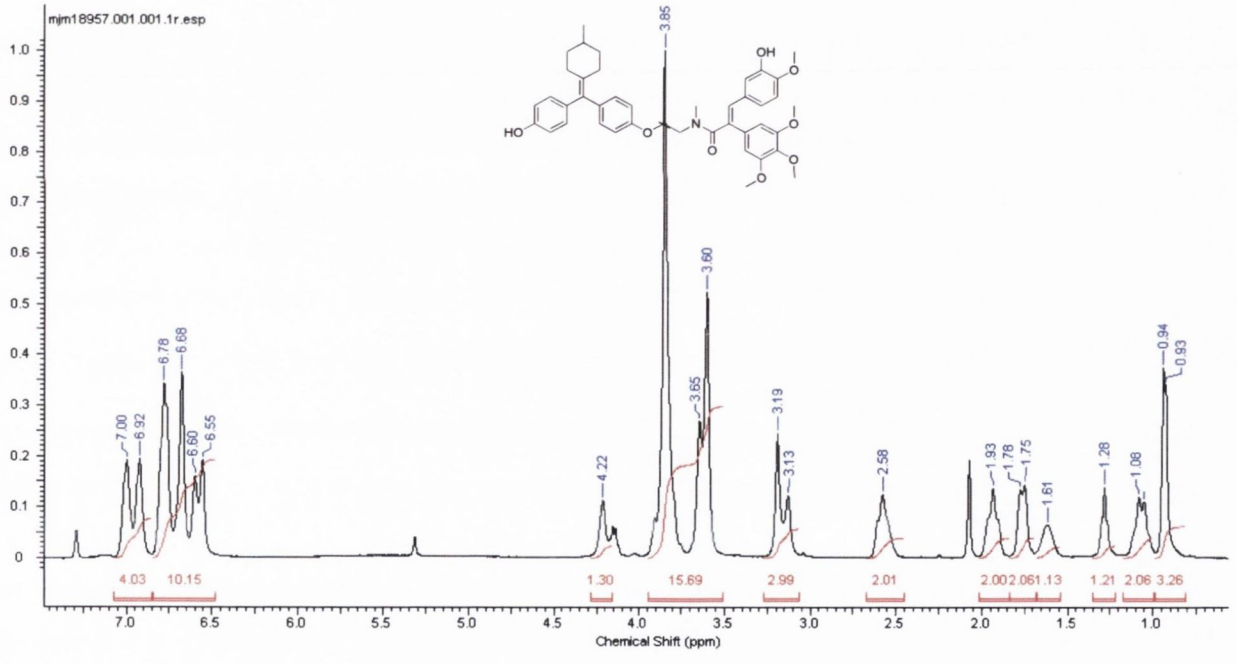

Figure 5-9 ^{1}H-NMR spectrum for [448]

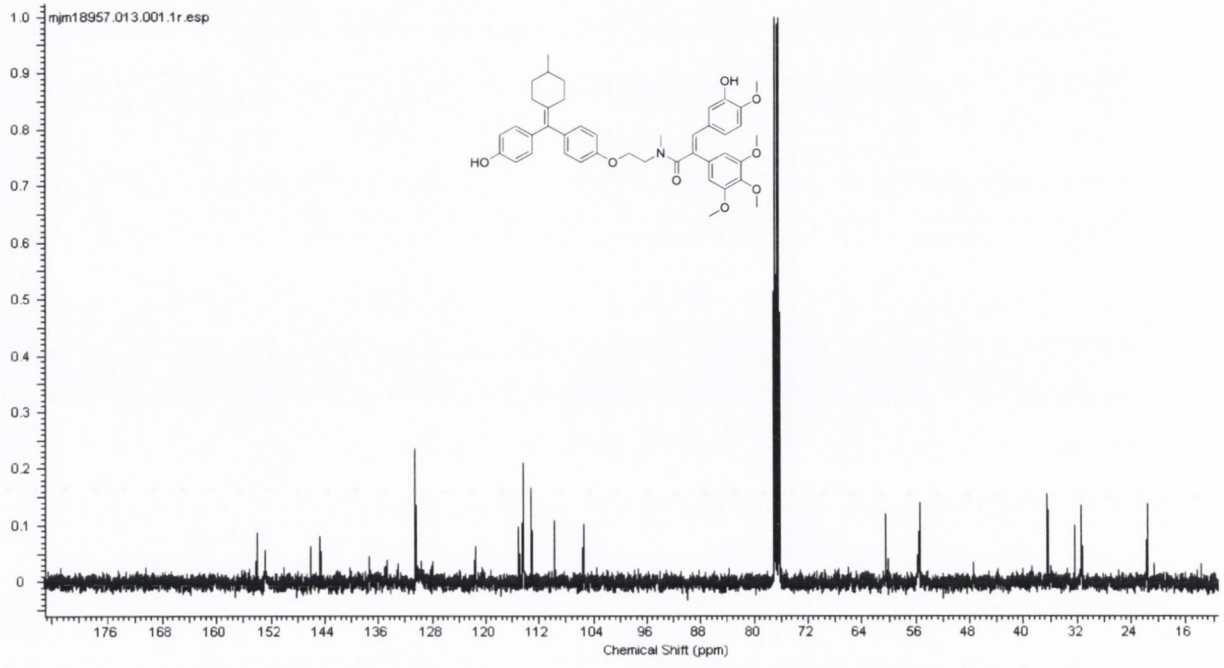

Figure 5-10 ^{13}C-NMR spectrum for [448]

5.6 2-Phenylindole conjugates

The 2-phenylindole core is another known scaffold with excellent ER binding activity.[476] The 2-phenylindole core can be found in bazedoxifene [50], a third generation selective estrogen receptor modulator (SERM). This 2-phenylindole core could now be incorporated into the novel conjugate as the ER-ligand. The new conjugate containing this new ER-ligand should have the potential to bind similarly to that of the endoxifen and cyclofenil conjugates. The novel ER ligand again would contain a basic side chain like that of endoxifen, and would be utilised for the linkage to the cytotoxic agent.

The formation of the novel 2-phenylindole conjugates would follow the endoxifen conjugate chemistry as the secondary amine and the carboxylic acid would be coupled using the EDC and HOBt coupling reaction. Similar to the cyclofenil conjugate synthesis, only EDC was employed as the coupling agent. Once again the acrylic acid combretastatin analogue [150] was directly coupled to the benzyl-protected 2-phenylindole analogues [256]-[260] (Scheme 5-6). As with the cyclofenil conjugates, [150] was the only CA4-type cytotoxic agent used in the evaluation of the conjugates. The conjugates are classified as 'direct amide conjugate' as there is no additional linker moiety required and the carboxylic acid group reacts directly with the secondary amine functionality of the cyclofenil-based analogue to form the amide linkage *via* an EDC and HOBt coupling (condensation) reaction (Scheme 5-6).

This procedure employed EDC as the coupling reagent. For the synthesis of this series of benzyl-protected conjugates [449]-[453], as with the previous conjugates, the equivalents of

reactants were varied to ensure a slight excess of activated ester, so that when the amine was reacted, a greater yield of amide product would be obtained. The ratio of reactants were 1.2 eq of acrylic acid, 1.4 eq DCC, 1.4 eq HOBt and 1 eq of amine. The benzyl-protected conjugates [449]-[453] were purified in this procedure and was fully characterised at this step. The isolated benzyl-protected conjugate was then hydrogenated with $Pd(OH)_2$ under an H_2 atmosphere (in EtOAc/MeOH) to deprotect the benzyl-protecting group. Following work-up, the mixture was purified *via* flash chromatography to afford the direct amide conjugates [454]-[458] in high yields as yellow solids (Table 18).

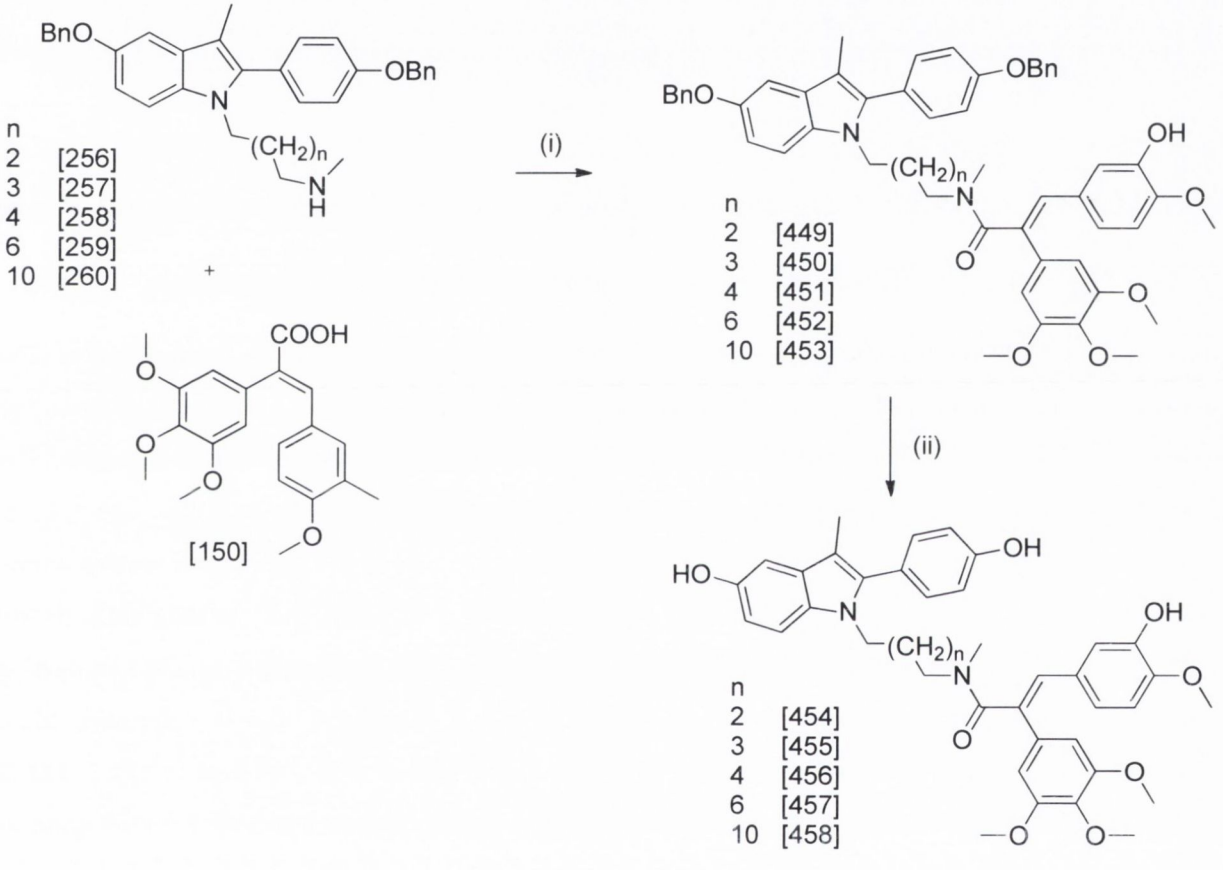

(i) EDC, HOBt, DCM, RT; (ii) $Pd(OH)_2$, H_2, EtOAc/MeOH, 30 min, RT

Scheme 5-6 2-Phenylindole based direct-amide conjugates

As an example of this series of conjugates, the ^{1}H-NMR spectrum of [454] is shown in Figure 5-11. Similar to the cyclofenil based conjugates, no isomeric mixture is present for the 2-phenylindole. However, the presence of 2 rotameric centres (one at the amide bond and at the indole nitrogen) reduces the resolution of the signals significantly, therefore many signals appear as multiplets. The two CH_2 signals from the centre of the basic side chain are observed as multiplets at 1.14-1.51 ppm. The methyl substituent from the indole core can be seen as a singlet at 2.10 ppm.

The signal for the CH_2 located next to the methyl amine appears as 2 multiplets with one visible at 3.10-3.20 ppm and the other masked by the CD_3OD solvent peak at 3.32 ppm. The region between 3.54-4.01 ppm contains the signals for the four methoxy groups and the CH_2 directly attached to the indole nitrogen. The region between 6.41-6.89 ppm, contains signals which relate to the aromatic protons and the ethylene bridge proton.

Compound no.	EDC coupling Yield (%)	Compound no.	Deprotection yield following EDC coupling (%)
[449]	85	[454]	89
[450]	91	[455]	79
[451]	88	[456]	83
[452]	85	[457]	94
[453]	91	[458]	90

Table 18 Direct amide conjugate reaction yields and deprotection yields

The corresponding ^{13}C-NMR spectrum for [454] (Figure 5-12) is quite complex. The presence of the two rotameric centres gives rise to multiplet of signals for some carbons. The corresponding signal for the methyl substituent on the indole ring is observed at 8.5 ppm. The signals for the basic side chain CH_2 (×4) are observed as multiplet signals at 24.0, 24.2, 25.3, 25.5, 26.9, 27.0, 27.1, 27.2, 40.6, 40.9, 43.3, 46.3, 49.3, 50.6, 51.1, 51.3 and 53.8 ppm. The methyl amine signal is seen as four distinct signals at 31.8, 32.9, 34.4 and 35.7 ppm. The methoxy carbons are observed also as a multiplet of signals at 55.5, 55.6, 55.7, 60.1, 60.2 and 60.3 ppm. The remaining tertiary and quaternary aromatic carbons and ethylene bridge carbon are observed between 102.8 and 169.5 ppm. The carbonyl carbon was identified as a multiplet of signals located at 172.9, 173.0, 173.7 and 173.8 ppm. In the IR spectrum, the hydroxyl group was identified as a broad band at 3423.2 cm^{-1} while the amide group is observed as a strong band at 1614.1 cm^{-1}. The characterisation is confirmed through high resolution mass spectrometry where a mass of 667.3016 $(M+H)^+$, was assigned for the molecular ion $C_{39}H_{43}N_2O_8$.

The irregularity of signals seen in the ^{1}H spectra for the conjugates compounds was believed to due to the presence of a rotameric centre(s). This hypothesis of the presence of these rotameric centre(s) can be investigated and verified with the use of high temperature variable Nuclear Magnetic Resonance spectroscopy (VT NMR). At higher temperatures the splitting pattern of the compound changes greatly showing the rotameric behaviour of the compound which was responsible for such complex splitting. Conformational isomerism is a form of stereoisomerism in

which the isomers can be interconverted exclusively by rotations. The verification of rotameric property of compounds can be revealed through VT NMR, although other techniques are also available like Liquid chromatography–mass spectrometry (LCMS) can also be employed. The investigation of the conformation conjugates within the scope of this project were verified by VT NMR.

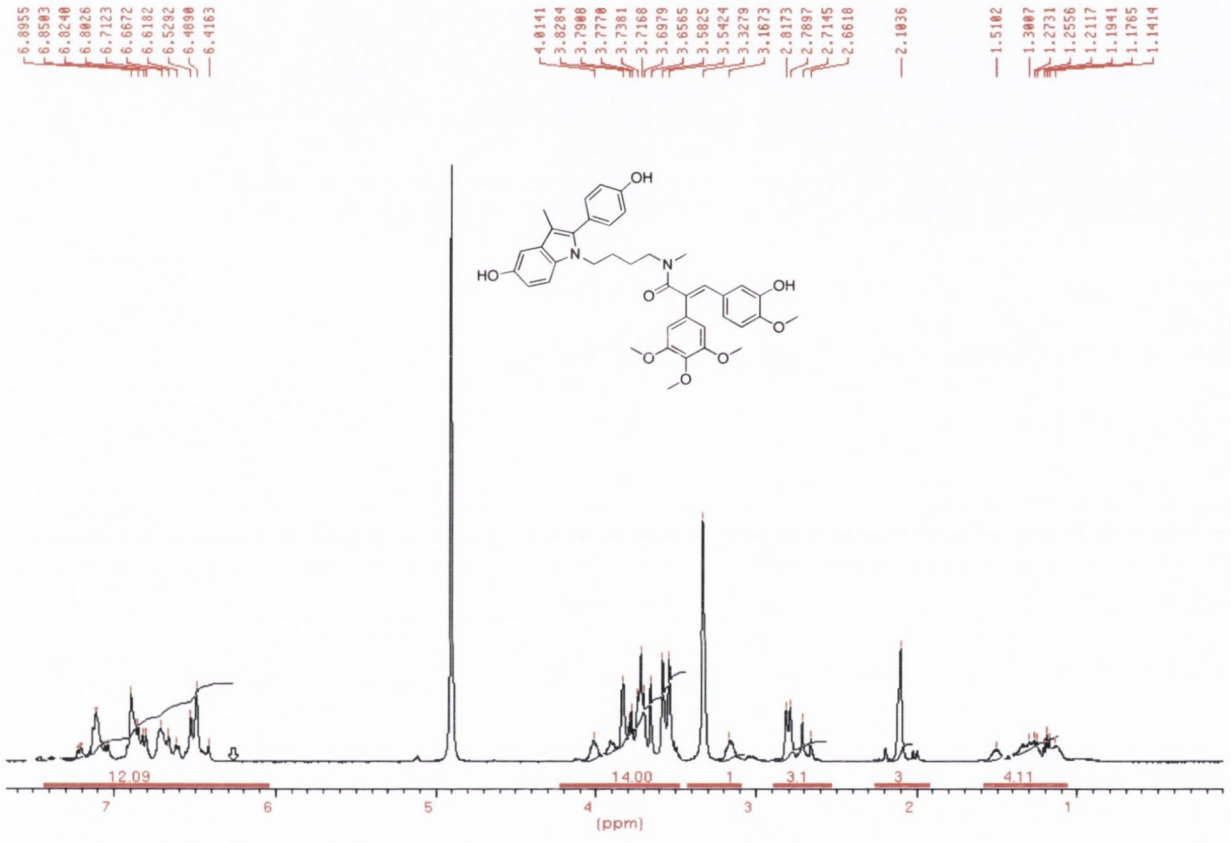

Figure 5-11 ^{1}H-NMR spectrum of [454] - (CD_3OD)

The conjugates synthesised throughout this project all contain a tertiary amide bond which linked the two components (ER ligands, cytotoxic agents and AI ligands) together. Both the ^{1}H and ^{13}C NMR spectra displayed a complex signal pattern that was explained by the presence of a rotameric centre. The verification of the presence of this rotameric centre was investigated and through the use of VT NMR for the examination of compound [458], Figure 5-13. In Figure 5-14 shows the variation of the proton signal with an increase in temperature from 20 °C through to 90 °C, the spectrum was recorded in DMSO-d_6. An important observation shown in Figure 5-14 is the shifting of ppm values at the higher temperature conditions; this is due to the increase in the frequency of rotation on the increase of the temperature. The spectral studies confirm the nature of compound to be rotameric. The region of particular interest is between 2.8-3.0 ppm. In this region we see the N-methyl signal, which at 20 °C appears as two broad singlets. As the temperature is

increased the two broad signals coalesce together and form a broader singlet at 40 °C, and between 60 °C to 90 °C the signal becomes less broad and more defined as singlet. This migration of the two initial broaden signal at 40 °C to the quite defined singlet at 90 °C is a characteristic behaviour of rotamers at higher temperatures. The proton signal pattern for the conjugates compounds display poor resolution due to the rotation of this amide bond but at higher temperature it is possible to see that the resolution of the spectra increase significantly which also can signify the presence of rotamers. This experiment verified the formation of the amide bond rotamers in the conjugate scaffold.

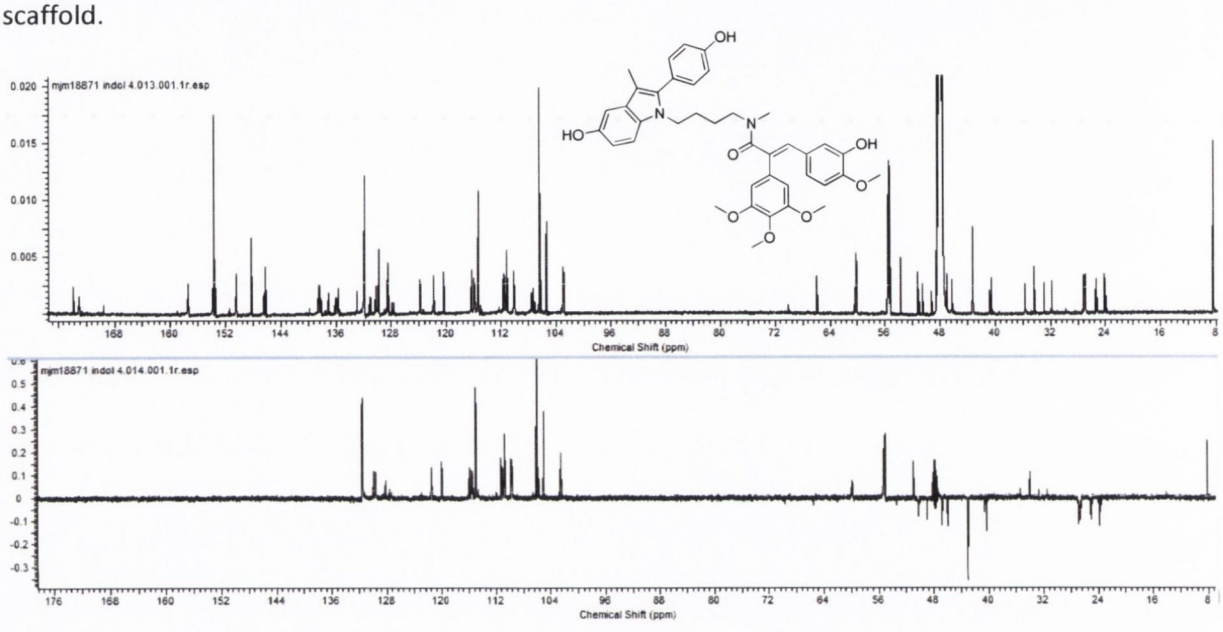

Figure 5-12 ^{13}C-NMR and DEPT-135 spectrums of [454] (CD_3OD)

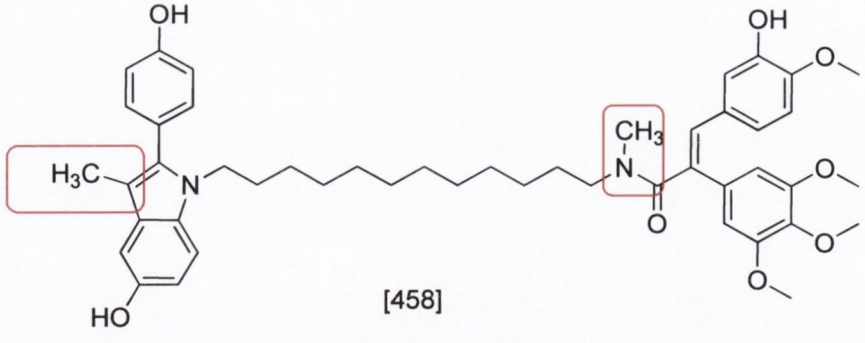

[458]

Figure 5-13 Compound [458]

The 2-phenylindole conjugates displayed this rotameric effect however it was postulated that the nitrogen (indole core)-carbon (moiety) could potentially be displaying an addition rotameric centre. In Figure 5-15, shows for compound [458] the C-3 methyl position on the indole, the signal processed under the standard Window Functions (above) and processed under the Window Functions of Gaussian multiplication (below). The Gaussian multiplication processesed spectrum

treated in this manner tends to show enhanced resolution, at the expense of the signal to noise ratio. The spectra in blue shows an apparent singlet for the methyl however upon closer inspection it is possible to see that this is more likely two overlapping signals than the previously assigned as a singlet. When the processing parameters were changed (in red) it confirmed the presence of two signals. The two signals correspond to two conformational isomers of the methyl substituent. This signifies the presence of another rotameric centre at the indole end of the conjugate. The observation formation of this rotameric centre was not as prevalent as seen for the amide bond (CO-N-CH_3) and was only detected to lesser extent, but provides a rationalisation of the complex signal pattern observed in the ^{1}H and ^{13}C NMR spectra of the indole-acrylic acid conjugate compounds.

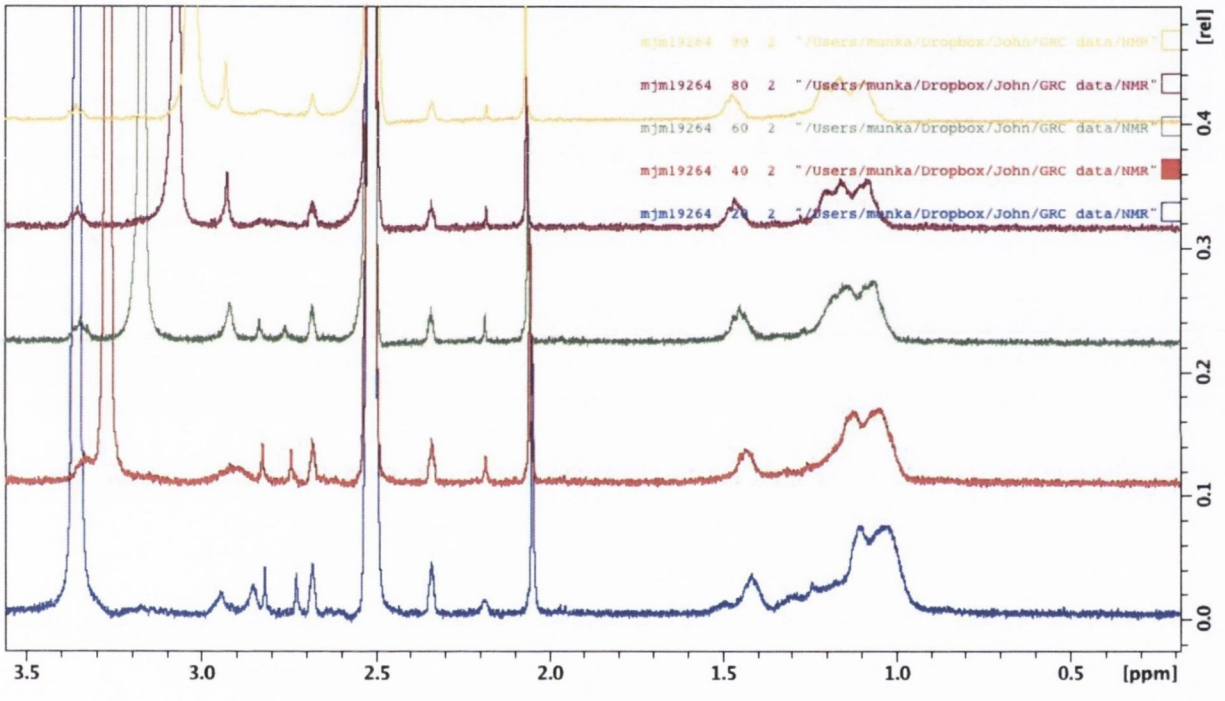

Figure 5-14 ^{1}H-NMR spectrum of [458] as part of VT NMR experiment (blue = 20 °C, red = 40 °C, green = 60 °C, purple = 80 °C, yellow = 90 °C) (DMSO-d_6)

The synthesis of the 5-methoxy-2-phenylindole conjugates with CA4 was also performed. This reaction was carried out as described for the synthesis of [449]-[453]. However, DCC was used as the coupling reagent as this was performed before the benefits of EDC in these reactions were investigated, Figure 5-15. For the synthesis of this series of conjugates [459]-[461], equilmolar amounts of the acrylic acid [150], the appropriate amine [238]-[240], DCC and HOBt were reacted, then monitored *via* TLC. The methoxy conjugate was purified over silica gel to afford the direct amide conjugate in relatively good yields (41-68%). Characterisation of the conjugates was achieved as previously described for conjugate [449]-[453].

Compound [459]-[461] would not be expected to bind in the ER domain as the free hydroxyl groups essential for binding are not present, however, these compounds were evaluated for antiproliferative activity as a direct comparison to the free hydroxyl conjugates synthesised previously.

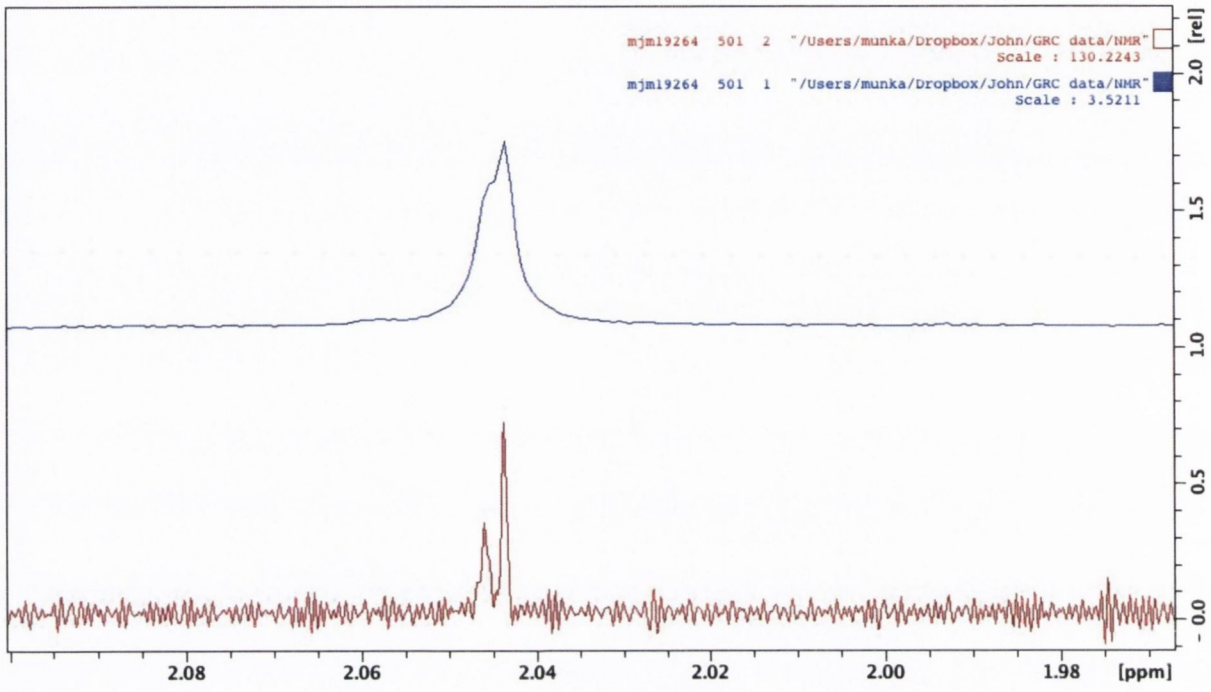

Figure 5-15 Expanded regions of the ^{1}H-NMR spectra of [458], above and the ^{1}H-NMR spectra of [458] processed *via* Gaussian multiplication, below

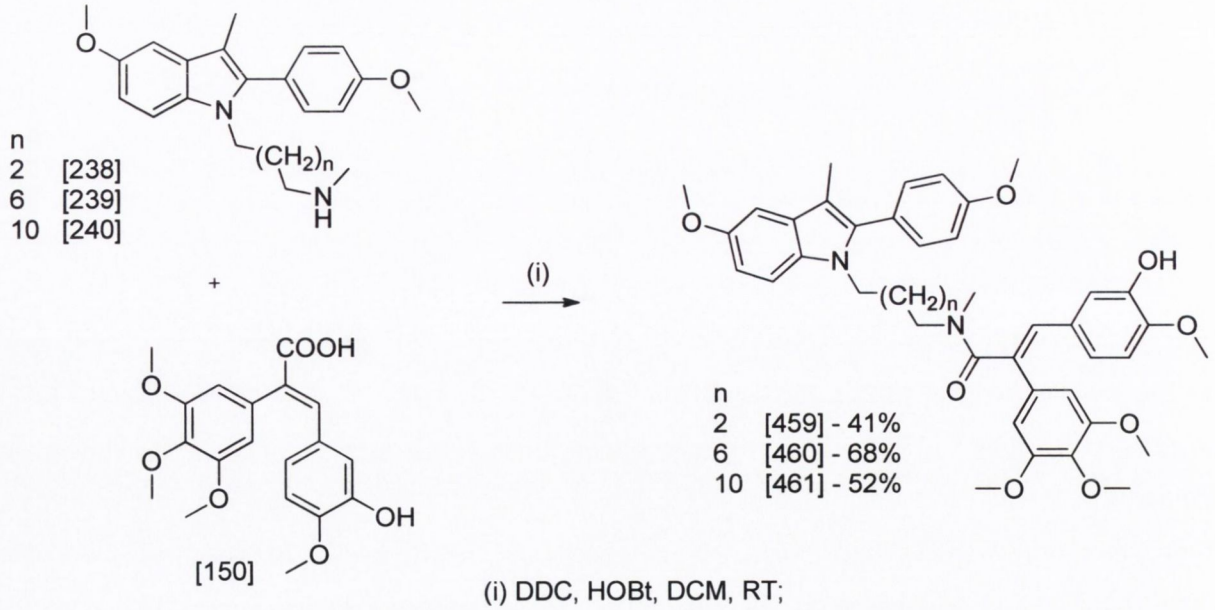

Figure 5-16 Synthesis of the methoxy-2-phenylindole conjugates

5.7 Synthesis of aromatase inhibitor containing conjugate prototype

As a further development of this project it was proposed that incorporating known aromatase inhibitors (AI) analogues into the conjugate scaffold could potentially afford useful anticancer molecules for the treatment of ER positive breast cancers. Two distinct conjugates were proposed. The first conjugate would incorporate an AI scaffold that would be linked to an ER-ligand and the second conjugate would replace the ER-ligand with the AI derivative to design an AI-cytotoxic agent conjugate.

5.7.1 Synthesis of endoxifen-anastrozole conjugate

The conjugate [463] was synthesised by the reaction of the anastrozole fragment [376] with the silyl-protected endoxifen ligand [197] *via* a DCC/HOBt coupling reaction, immediately followed by the TBAF deprotection step (see Scheme 5-7). The reaction was monitored *via* TLC - confirming the formation of the product [463]. The reaction mixture was purified by column chromatography over silica gel to afford a 1:1 *E/Z* isomeric ratio, which was calculated based on the isomeric ratio of the ER-ligand starting material [197] from the integrated signals in the ^{1}H-NMR spectrum. The intermediate [462] was not characterised at this point, however, the presence of [462] was verified using high resolution mass spectrometry, where a mass of 762.3811 $(M+Na)^{+}$ confirmed the required molecular ion $C_{45}H_{53}N_5NaO_3Si$. The two step reaction successfully afforded the conjugate [463] with an overall yield of 49%.

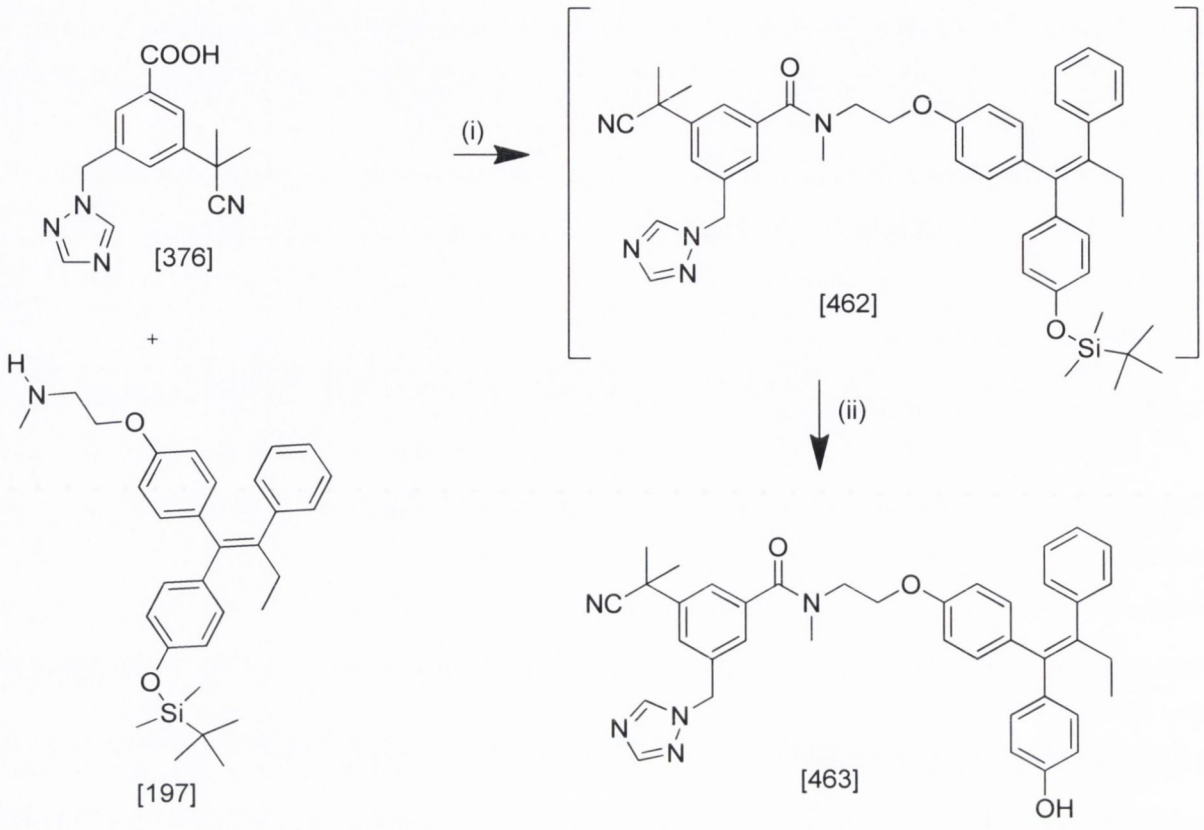

(i) DCC, HOBt, DCM, 24 h, RT; (ii) TBAF, THF, 24 h, RT

Scheme 5-7 Endoxifen-anastrozole conjugate [463]

The ^{1}H-NMR spectrum of [463] is shown in Figure 5-17. As the product is afforded as an isomeric mixture, many of the signals overlap and appear as multiplets. The protons of the ethyl chain are observed between 0.89-0.98 ppm (CH_3) and 2.42-2.56 ppm (CH_2). The two methyl groups located on the anastrozole side chain are seen between 1.64 - 1.77 ppm. The protons for the amine methyl are observed in the region 3.00-3.23 ppm. This signal pattern appears as a multiplet, however three overlapping signals are observed suggesting the presence of rotamers. The proton signal of the basic side chain CH_2s are found between 3.60-4.37 ppm and the protons for the CH_2 linked to the triazole ring appear between 5.28-5.44 ppm. The region between 6.43-7.62 ppm shows signals relating to the aromatic protons. The triazole protons can be observed as a multiplet between 7.85-8.38 ppm.

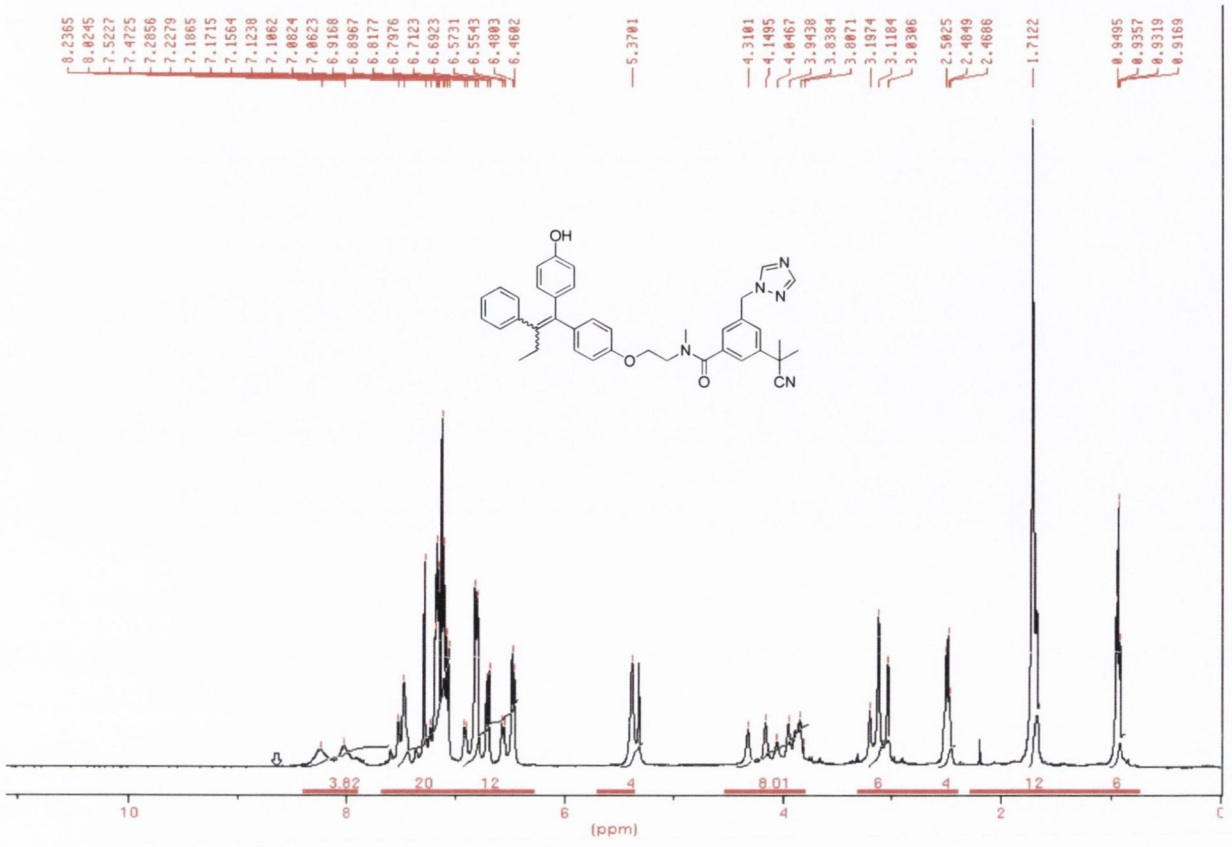

Figure 5-17 ^{1}H-NMR spectrum of [463] ($CDCl_3$)

The corresponding ^{13}C-NMR spectrum for [463] is shown in Figure 5-18. The ethyl side chain signals are observed at 13.2 ppm (CH_3) and 28.6 ppm (CH_2). The quaternary carbon on the anastrozole side chain is observed at 36.7 ppm and the methyl group attached to this carbon is seen at 28.5. The *N*-methyl signal is observed at 39.3 ppm. The CH_2 signals for the linking motif are seen at 47.7 (CH_2N) and 65.9 (CH_2O) ppm. The methylene carbon linking the triazole ring appears at 52.2 ppm. The nitrile carbon signal can be observed at 123.3 ppm. The signals in the region between 112.7-142.2 ppm correspond to the aromatic and ethylene bridge carbons. The triazole carbons are found at 142.5 and 153.9 ppm. The carbonyl carbon signal from the amide is observed at 169.9 ppm. In the IR spectrum, the hydroxyl group was identified as a broad band at 3436.9 cm^{-1}, while the carbonyl group is observed as a strong band at 1628.9 cm^{-1}. The nitrile band is also observed a 2231.5 cm^{-1}. The characterisation is confirmed through high resolution mass spectrometry, where a mass of 648.2921 $(M+Na)^+$, confirmed the required molecular ion $C_{39}H_{39}N_5NaO_3$.

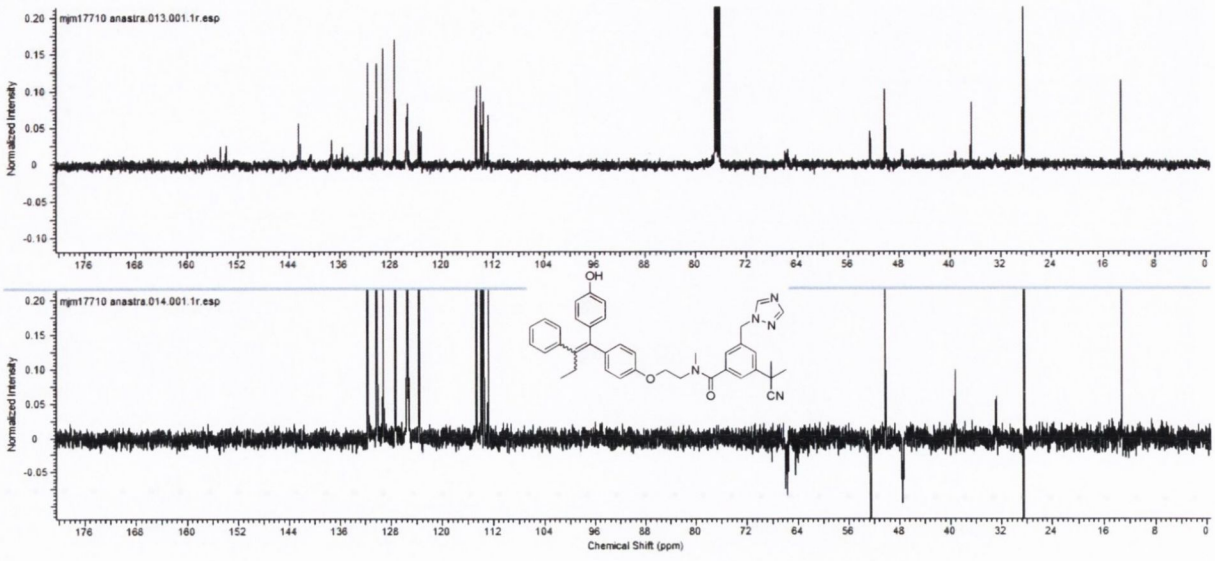

Figure 5-18 ^{13}C-NMR and DEPT-135 spectrums for [463]

This ER-ligand-AI prototype conjugate [463] would be predicted to bind at the ER where the anastrozole ligand moiety would not be expected to have an effect at the ER. The anastrozole ligand moiety itself could still potentially inhibit the production of estrogen, but not when the conjugate is potentially bound to the ER. As the two components are connected *via* a direct amide bond, it is not expected to act as a prodrug and release both agents within the cell. However, this prototype was developed as a potential novel dual-acting conjugate. It will require biochemical evaluation to determine if the concept has any future potential. Also further investigation into the conjugate scaffold, e.g. linking groups, linking position and ER-ligand optimisation will also be required.

5.7.2 Synthesis of letrozole-cytotoxic agent conjugate

The conjugate [464] was synthesised by the reaction of the letrozole fragment [387] with the acrylic acid analogue [150] *via* a EDC/HOBt coupling reaction shown in Scheme 5-8. The reaction was monitored *via* TLC - confirming the formation of the desired product [464]. The reaction mixture was purified by column chromatography over silica gel to afford a yellow solid. This product [464], unlike the previous conjugates, did not require any deprotection after coupling reaction. The coupling reaction successfully afforded [464] with a 78% yield.

The ^{1}H-NMR spectrum of [464] is shown in Figure 5-19. As the product is afforded as a rotameric mixture many of the signals overlap and appear as multiplets. The protons for the *N*-methyl amine are observed as a broad signal between 3.09-3.20 ppm. The methoxy signals appear at 3.67 ppm and between 3.80-3.94 ppm where methoxy signal overlaps with NCH_2 signal. The additional CH_2 from the basic side chain is observed as broad singlet at 4.28 ppm. The proton signal that corresponds to the tertiary CH is observed 6.77 ppm. The signals found in the region, 6.54-7.70

ppm are assigned to the aromatic protons and the alkene bridge proton. The triazole protons can be observed as a two singlets at 8.01 and 8.08 ppm.

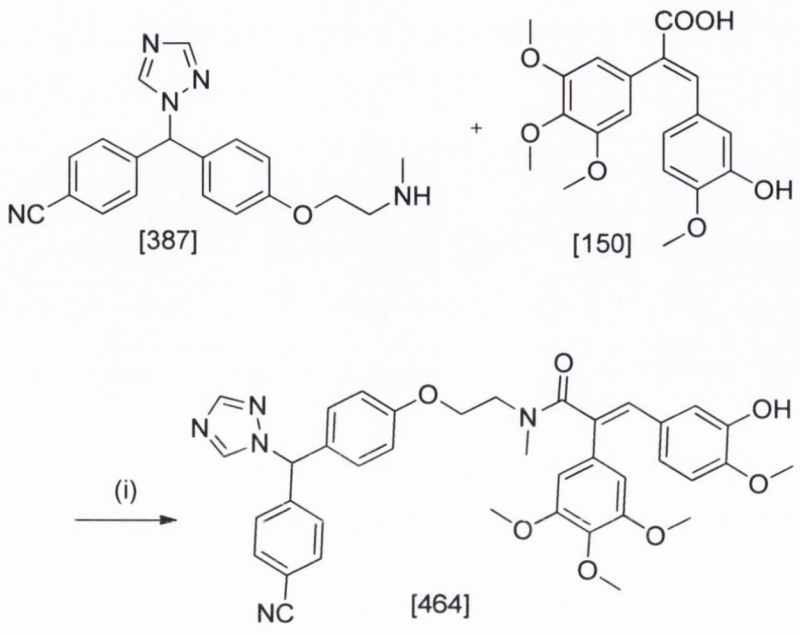

(i) EDC, HOBt, DCM, RT;

Scheme 5-8 Synthesis of letrozole conjugate [464]

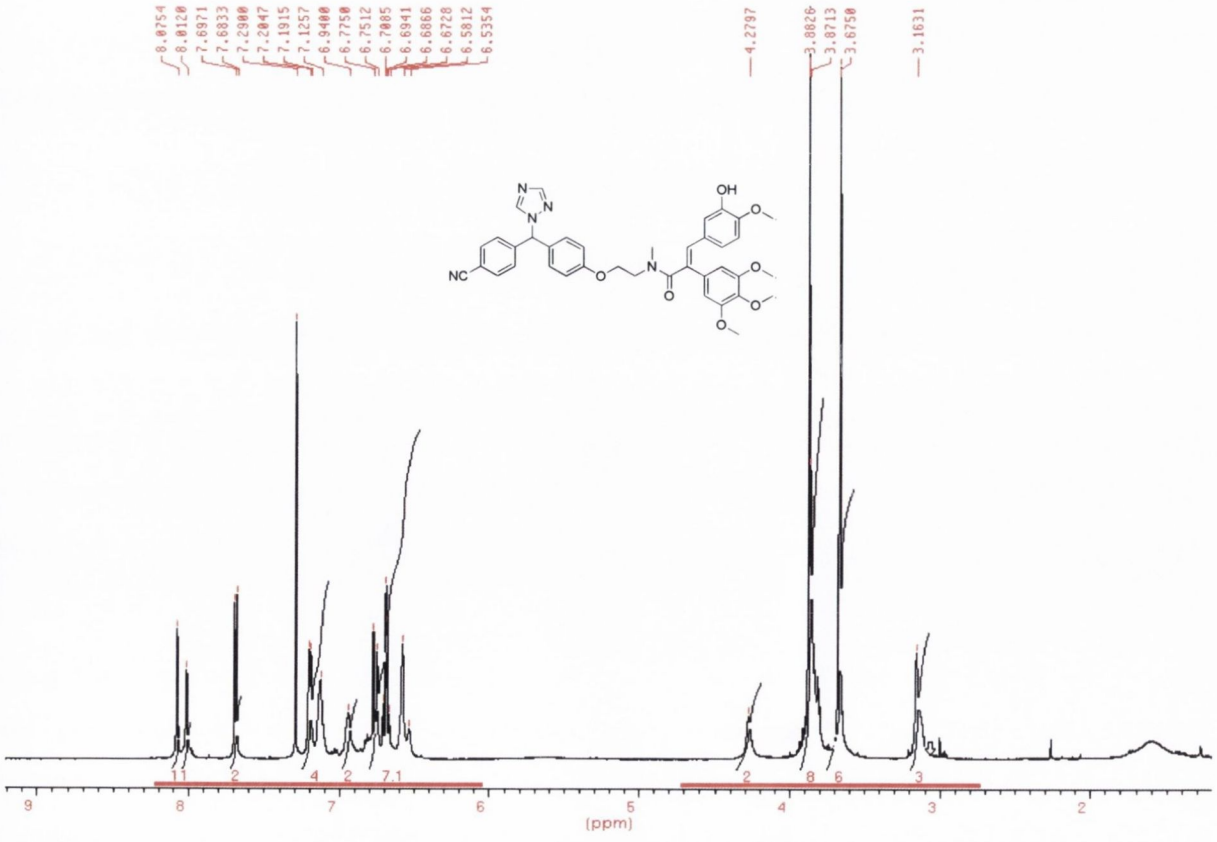

Figure 5-19 ^{1}H-NMR spectrum of [464] ($CDCl_3$)

The ^{13}C-NMR spectrum of [464] is shown in Figure 5-20. The N-CH_3 signal is observed as 38.9 ppm. The CH_2 signals for the linking motif are seen at 53.4 and 65.9 ppm. The methoxy carbons are seen at 55.9, 56.1, 61.0 and 66.9 ppm. The CH signal is identified at 77.2 ppm. The triazole carbons are seen at 143.6 and 152.1 ppm. All other signals in the region between 106.1-153.4 ppm correspond to the nitrile, aromatic and ethylene bridge carbons. The carbonyl carbon signal of the amide is observed at 164.0 ppm. In the IR spectrum, the hydroxyl group was identified as a broad band at 3434.8 cm^{-1} while the carbonyl group is observed as a strong band at 1610.5 cm^{-1}. The nitrile band is also observed a 2230.4 cm^{-1}. The characterisation is confirmed by high resolution mass spectrometry where a mass of 698.2592 $(M+Na)^+$ was found for the molecular ion $C_{38}H_{37}N_5NaO_7$.

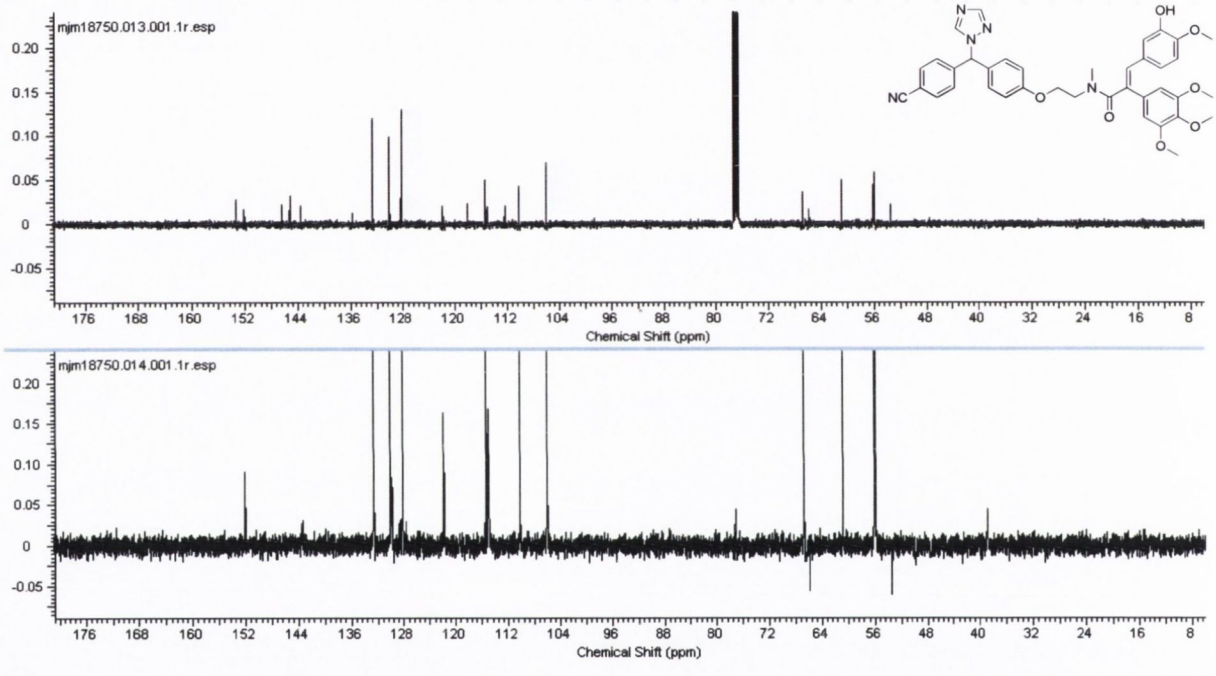

Figure 5-20 ^{13}C-NMR and DEPT-135 spectrums of [464] ($CDCl_3$)

The aromatase inhibitor-cytotoxic agent conjugate [464] could potentially act as an aromatase inhibitor and inhibit the biosynthesis of estradiol but could also act as a potential tubulin targeting cytotoxic agent. Compound [464] will be evaluated initially for biochemical activity as an antiproliferative agent and if the results show potential this prototype could be further explored as a novel dual-acting conjugate. Optimisation of the conjugate scaffold, e.g. linking moiety, linking position and AI activity will also be required.

The objective of this project was to synthesise a series of conjugates that would exert selective antagonistic effect in breast cancer cells while demonstrating good ER-binding affinity. The incorporation of estrogen receptor binding ligands into the conjugate scaffolds, afforded products which would exhibit selectivity for the ER overexpressing breast cancer cells. The conjugates

synthesised in this chapter, utilize an array of estrogen receptor type ligands conjugated to cytotoxic agents. The novel conjugates synthesised in this chapter will be evaluated biochemical for antiproliferative activity and estrogen receptor binding.

Chapter 6

Biochemical evaluation and molecular modelling

6.1 Biochemical evaluation

6.1.1 Overview

The biochemical evaluation of compounds synthesised in the project was carried out routinely throughout the study. The main assays utilised to evaluate the compounds were an AlamarBlue© (viability) assay and a Lanthascreen® ER FRET assay. Compounds were evaluated for antiproliferative activity in the MCF-7 human breast cancer cell-line. MCF-7 is a well-characterized estrogen receptor (ER) positive control cell line (i.e. cells are positive for cytoplasmic estrogen receptors). The ER competitor binding assay was carried out in both ERα and ERβ to determine the binding affinity and possible ER-isoform selectivity of ligands and conjugates synthesised in this study. Using the results obtained from the biochemical evaluations in conjunction with molecular modelling techniques, a structure-activity relationship (SAR) of the ligands and conjugates can be assembled. In this chapter, the details of materials and methods utilised in the different assays is presented followed by a discussion of the biochemical results obtained for the compounds under investigation.

6.1.2 Materials for Biochemical analysis

Materials

Full names and addresses of sources and suppliers are detailed below at the end of the list

AlamarBlue©	Invitrogen
Black-plates, 364-well, low volume	Greiner
DMSO	Sigma
Eagles minimum essential medium	Sigma
Estradiol	Sigma
Foetal bovine serum	Sigma
Lanthascreen® ERα FRET assay	Invitrogen
Lanthascreen® ERβ FRET assay	Invitrogen
L-glutamine	Sigma
Lipofectamine 2000	Invitrogen
Lymphoprep	Axis-shield
MCF-7 cells	E.C.A.C.C
NF-κB luciferase reporter assay	Sabiosciences

Non-essential amino acid medium	Sigma
Phosphate buffered saline	Sigma
Penicillin/Streptomycin	Sigma
Pipettes (sterile)	Greiner
RPMI	Gibco
Tamoxifen	Sigma
Tissue culture flasks	Greiner
Trypsin	Sigma

The tested experimental compounds are obtained from the synthetic studies in this thesis. All other regents were analytical grade and obtained from Sigma whenever possible.

Address of suppliers

Axis-Shield PoC: PO Box 6863 Rodeløkka N0504 Oslo Norway

Biosciences (Invitrogen/Gibco), 3 Charlemont Terrace, Crofton Road, Dun Laoghaire, Co. Dublin, Ireland.

Cruinn Diagnostics Ltd., 5b/6b Hume Centre, Park West Industrial Estate, Navan Road, Dublin 12, Ireland.

European Collection of Animal Cell Cultures (E.C.A.C.C.), PHLS, Centre for Applied British Drug House (BDH) Chemicals Ltd., c/o Lennox Laboratory Supplies Ltd. John F. Kennedy drive, Naas Road, Dublin 12, Ireland.

Greiner GMBH, Maybachstrasse 2, 72636, Frickenhausen, Germany.

Panvera, 501 Charmany Drive, Madison, WI 53719, USA.

Promega Corporation, c/o Medical Supply Co., Santry Hall Industrial Estate, Santry, Dublin 9, Ireland

Sabiosciences c/o QIAGEN Ltd., QIAGEN House, Fleming Way, Crawley, West Sussex, RH10 9NQ, UK

Sigma-Aldrich Ireland Ltd., Vales Road, Arklow, Wicklow, Ireland.

Riedal de Haen, c/o R.B. Chemicals Ltd., Hoechst House, Cookstown Industrial Estate, Tallaght, Dublin 24, Ireland.

6.1.3 Methods for Biochemical analysis

6.1.3.1 Growth and maintenance of human breast carcinoma MCF-7 cell line.

The human breast carcinoma cell line, MCF-7, was purchased from the European Collection of Animal Cell Cultures (E.C.A.C.C.). MCF-7 cells were grown at 37 °C + 5% CO_2 in Eagles Modified Essential Medium (EMEM) containing 10% Foetal Bovine Serum (FBS), 1% Non Essential Amino Acids (NEAA), 2 mM L-glutamine and supplemented with 100 U/mL penicillin and 100 µg/mL streptomycin. All cell culture reagents were supplied by Sigma unless otherwise stated. Cells were passaged after reaching confluency (twice per week). Cells were washed with serum free EMEM (5 mL) and removed from the flask surface by incubating the cells for 2 minutes in 1X trypsin diluted in PBS (2.5 mL). The trypsin was neutralised with 5 mL EMEM and cells were sedimented by centrifugation at 1200 rpm for 5 minutes. The pellet was resuspended in 10 mL complete medium. Cell number was calculated by taking a 10 µL aliquot of cell suspension and counted using a haemocytometer. Cells were reseeded at a density of 2 x 10^4 cells/mL in complete medium.

6.1.3.2 Cryo-preservation of cells

MCF-7 cells were harvested and counted as described previously. The cells were centrifuged and resuspended in a mixture of 60% EMEM/30% FBS/10% DMSO at a density of 5 x 10^6 cells/mL. 1 mL aliquots were transferred to a 1.5 mL cryotube and placed at -20 °C for 24 hours, transferred to -70 °C for 2 hours before being placed in liquid nitrogen at -180 °C. If required, an aliquot of cells was removed from liquid nitrogen and rapidly thawed and resuspended in 10 mL complete medium. The cell suspension was centrifuged at 1200 rpm for 5 minutes and media discarded. The pellet was resuspended in complete medium and cells were seeded in tissue culture flasks (T-25 cm^3).

6.1.3.3 AlamarBlue© Cell viability assay

AlamarBlue© (Invitrogen) is a non-toxic, soluble, REDOX indicator used to quantitatively measure the proliferation of cells in response to toxic agents. Cell viability is assessed by measuring the internal environment of the cell. As proliferating cells have a greater reducing environment then non-proliferating cells, the REDOX indicator AlamarBlue© quantifies viability. It works by accepting electrons from reducing compounds such as FADH and NADH. The initial oxidised, non-fluorescent indigo blue is metabolised to a reduced pink fluorescent state. The observed change is measured by a spectrofluorimetric microtiter well plate reader at excitation and emission wavelengths of 544 and 590 nm. The purpose of an AlamarBlue© viability assay for this project was to assess the effect of tamoxifen and combretastatin related compounds on the proliferation of MCF-7 cells and to calculate the relative IC_{50} values for each compound.

MCF-7 cells were seeded in triplicate in 96-well plates at a density of 2.5 x 10^4 cells/mL in a total volume of 200 µL per well. Cells were treated with varying concentrations of the appropriate compounds to yield the desired final concentration. Ethanol was used as a vehicle and cells were treated with 1% ethanol (v/v) in all experiments. Plates were incubated for 72 hours at 37 °C + 5% CO_2 after which AlamarBlue© was added to each well. The plates were incubated for a further 4 hours without exposure to light. EMEM medium with the addition of AlamarBlue was used as a blank. Vehicle treated cells were considered to be 100% viable and the viabilities of each compound was calculated accordingly. Results were calculated using transformed data [Final Concentration = Log (Final Concentration)] to plot a non-linear, sigmoidal dose response curve from which the relative IC_{50} values were determined.

6.1.3.4 Flow cytometry

MCF-7 cells were seeded at a density of 5 × 10^4 cells/well in a 12-well plate and treated with the indicated compounds for 72 h. Samples were then centrifuged at 650 xg for 5 min and resuspended in 100 µL ice-cold PBS. Ice-cold 70% (v/v) ethanol (1mL) was then added to fix the samples overnight at 4 °C. Samples were subsequently centrifuged at 800 xg for 10 min and resuspended in 200 µL PBS. RNase A (12.5 µL of 10 mg/mL) and propidium iodide (37.5 µL of 1 mg/ mL) were added to samples which were then incubated for 30 min at 37°C. Cell cycle analysis was performed at 488 nm using a Becton Dickinson FACS Calibur flow cytometer. The Macintosh-based application CellQuest was then used to analyse the data of 10,000 gated cells once cell debris had been excluded. Data points represent the mean ± S.E.M. of three independent experiments.

6.1.3.4.1 Generation of human peripheral blood mononuclear cells

Fresh peripheral blood was collected from healthy donors (n = 2) and diluted 1:3 with RPMI medium and added to half the equivalent volume of Lymphoprep. Samples were centrifuged at 750 xg for 30 min to form a Ficoll gradient. The white buffy layer containing the peripheral blood mononuclear cells was removed, diluted to a volume of 50 mL with medium and centrifuged again for 10 min at 650 xg. Cells were then seeded at a density of 1 x 10^6 cells in 1mL of RPMI medium supplemented with 10% FBS, 2 mM L-glutamine and 100 U/mL penicillin and 100 µg/mL streptomycin.

6.1.3.5 ER FRET ligand binding assay

The Lanthascreen® ER FRET assays were purchased from Invitrogen. The protocol follows the suggested method for preparation of buffers and compounds. Nuclear receptor buffer K was prepared by adding DTT to make a final concentration of DTT 5mM. This buffer was used for all other dilutions. A 'no ligand' control was used to show minimum binding. DMSO was added to make a final concentration of 2%. A positive control was also used, in this case estradiol. This served as the 'maximum ligand' control, where estradiol was at a final concentration of 2 µM in each well.

2X dilutions of each ligand were made in buffer. A stock solution of ligand was dissolved in DMSO. From this, 1 µL of 10 mM stock was added to 49 µL buffer. 10 µL of the 2X dilution was added into each well. To make a 4X (12 nM) dilution of Fluoromone ES2 using a stock concentration of 1800 nM, 6.7 µL of fluoromone was added to 993 µL of buffer. 5 µL of this mixture was added to each well.

6.1.3.6 NF-κB luciferase reporter assay

Experiment carried out by Ms Jade Pollock, School of Biochemistry and Immunology, TCD. MCF-7 cells were cultured as previously described. Cells were harvested and re-seeded at a density of 4 x 10^5cells/mL. 100 µL of the cell suspension was seeded in each well in a 96 well plate in complete medium. Cells were left to adhere for 24 hours before being washed with PBS and 100 µL of medium added (Opti-MEM + 5% FBS). The transfection was carried out using the Cignal NF-κB luciferase reporter assay (Sabiosciences).

Tube No.	Cignal reporter (100 ng) (µL)	Negative control (100 ng) (µL)	Positive control construct (100 ng) (µL)	Organic compound	Opti-MEM DNA (µL)	Transfection Reagent (µL)	Opti-MEM + transfection reagent (µL)	Time (hours)
1	0.1				25	0.6	25	30-42
2	0.1			1X	25	0.6	25	30-42
3	0.1			10X	25	0.6	25	30-42
4	0.1			100X	25	0.6	25	30-42
5		0.1			25	0.6	25	30-42
6		0.1		1X	25	0.6	25	30-42
7		0.1		10X	25	0.6	25	30-42
8		0.1		100X	25	0.6	25	30-42
9			0.1		25	0.6	25	30-42

Table 19 Volume of reagents required per well for the NF-κB study

Table 19 represents the volume of reagent in each well. Tubes were prepared as for experimental transfection by diluting 4 µL (400 ng) of reporter in 100 µL Opti-MEM. For control transfections, 4 µL (400 ng) of negative control was diluted in 100 µL Opti-MEM. For the positive control, 1 µL (100 ng) was diluted in 25 µL of Opti-MEM. The transfection cocktails were mixed gently. Specific wells were transfected with 0.6 µL MyD88 (20 ng) to drive NF-κB production.

The transfection reagent dilution was prepared by dispensing 5.4 µL of Lipofectamine 2000 (Invitrogen) in 225 µL Opti-MEM. After 5 minutes incubation period, 100 µL of diluted transfection reagent was added to the reporter and negative control solutions and left for 20 minutes at room temperature to allow the complex to form.

To each well, 50 µL of the specific complexes were aliquoted into the appropriate wells to give a final volume of 150 µL. The plate was incubated at 37 °C + 5% CO_2 for 16 hours. After 16 hours of transfection, the medium was changed to assay medium (Opti-MEM + 0.5% FBS, 1% NEAA, 100U/mL penicillin and 100 µg/mL streptomycin). After 24 hours transfection, the cells were treated with compound, tamoxifen or/and 17β-estradiol.

6.1.4 Antiproliferative assay results

6.1.4.1 Biochemical data for reference compounds

Tamoxifen [34] and combretastatin A-4 [22] were used as reference compounds as the IC_{50} values are in the low micromolar (µM) and low nanomolar range (1-10 nM) range respectively in MCF-7 human cancer cell line consistent with literature values reported.[169, 496, 547-551] These two compounds were tested intermittently and regularly. The compounds synthesised in the thesis have expected values within this range. Endoxifen (potent metabolite of tamoxifen) was included in the table below however was not used as a control in this work. The endoxifen ligand was incorporated in many of synthesised conjugates throughout the thesis it was included for information. Figure 6-1 shows the antiproliferative effects of tamoxifen, endoxifen and combretastatin A4 on MCF-7 cell line, Table 20.

Compound ID	Structure	Name	MCF-7 IC_{50}
[34]	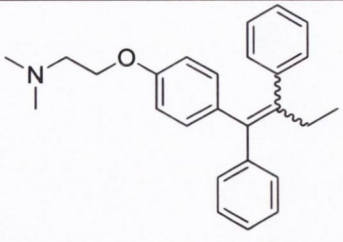	Tamoxifen	2.13 µM (0.19-11.3 µM) lit[169, 547, 548]
[36]	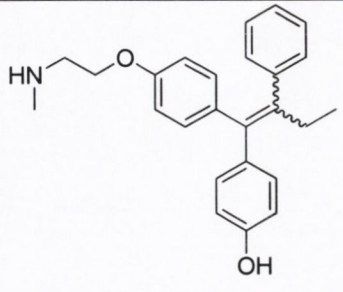	Endoxifen	1.4 nM[552]

[22]	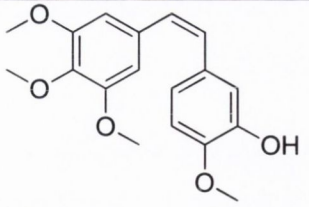	Combretastatin A-4	3.57 nM (3.2-6.9 nM) lit[496, 549-551]

Table 20 Antiproliferative data for reference compounds [22], [34] and [36]

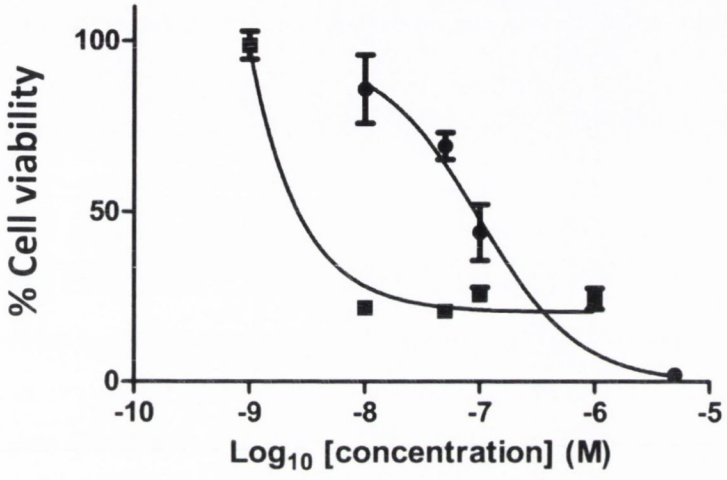

Figure 6-1 Antiproliferative effects of tamoxifen and combretastatin A4 in the MCF-7 human breast cancer cell line. The values represent the mean ± S.E.M. for three independent experiments performed in triplicate

6.1.4.2 Biochemical data of combretastatin direct amide endoxifen conjugates

The antiproliferative activity of this series of conjugates was evaluated using the MCF-7 human breast cancer cell-line. AlamarBlue dye was used to quantify antiproliferative activity. AlamarBlue dye is used to measure cell viability post treatment with a chemotherapeutic agent. Previous research by Keely *et al.*[421] which initially screened a series of combretastatin direct amide conjugates with structural changes on the combretastatin analogue were shown to have good antiproliferative activity. As part of this screen the conjugate compounds were also evaluated in the MDA (ER-negative) human cancer cell line where the ER is underexpressed. Any difference between the biochemical activity between the cell lines could indicate whether the ER plays an important role in the compounds activity. The conjugates demonstrated that the ER does appear to have a key role in determining the activity of the compounds as the activity was more potent in the ER-positive cell-line when compared to the ER-negative cell line. In this study, the viability assay was carried out on MCF-7 cells only as activity is greater in the cells expressing the ER.

The lead compound from previous research was found to be [414] which was the direct amide coupling of endoxifen to the acrylic acid analogue of CA4 [150]. The evaluation of [414] was found to be in the low nanomolar region (33 nM) in the ER-expressing cell line, MCF-7 and low

micromolar region (2.67)[421] in the ER-negative cell line, MDA. This 80-fold difference in activity was rationalised as the conjugate compound working *via* the ER.

In this project, the exploration of different substituents on the acrylic acid analogue was investigated to enhance the activity seen for [414]. A range of acrylic acids were evaluated in the ER expressing cell line, MCF-7. The biochemical data observed is presented in Table 21. Compound [414] when evaluated and was found to have an IC_{50} of 8.51 μM, which a significantly higher value than the IC_{50} value of 33 nM demonstrated by Keely. However, Compound [414] was previously evaluated by an MTT assay in an older MCF-7 cell line and may have been analysed differently which may account for this discrepancy in activity. The most active compound from the present series was [415]. The activity for [415] was in the low micromolar range (IC_{50} = 1.47 μM). Another interesting compound was [426]; this was the opposite substitution pattern on the acrylic acid portion of the conjugate when compared to [414]. Compound [426] showed low micromolar IC_{50} activity of 4.2 μM. Compounds [427] and [430] also displayed low micromolar IC_{50} activity values, 11.75 and 36.5 μM respectively. However, the majority of compounds ([416], [419]-[425] and [428]-[429] did not exhibit any activity below IC_{50} of 100 μM. Therefore, this indicates that the substituent on the acrylic acid analogues play a key role in the activity of these conjugates. The lead compound [414] which incorporated the acrylic acid analogue of CA4 [150] remains the key compound from this series, Table 21. A representative illustration of the antiproliferative effects of compound [427] on MCF-7 cell line is shown in Figure 6-2. Compounds [414]-[430] all have CLogP values greater than 5 and are predicted to have poor oral absorption. (All ClogP values calculated from ChemDraw Ultra, version 12.0)

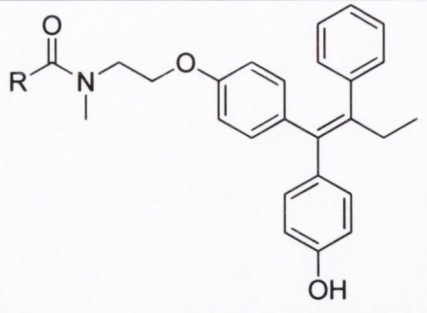

Compound	R	MCF-7 IC_{50} (μM)	CLogP
[414][421]	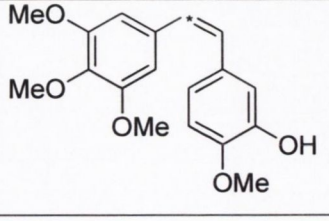	8.51 0.033±2.6[421]	7.69

[415]	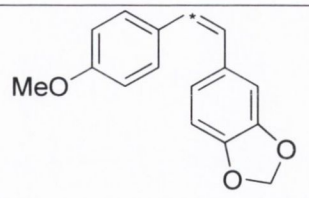	1.47±0.86	9.09
[416]	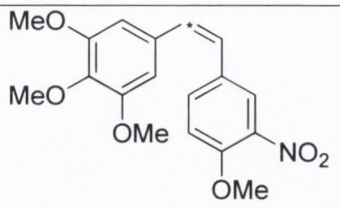	>100	8.19
[419]	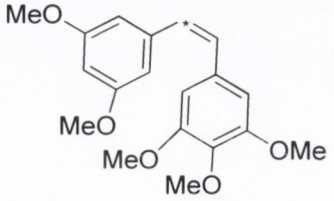	>100	8.02
[420]	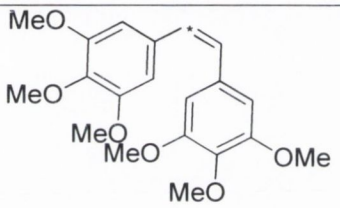	>100	7.61
[421]	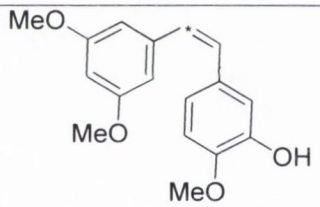	>100	8.40
[422]	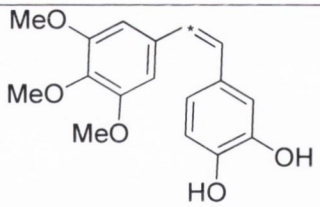	>100	7.24
[423]	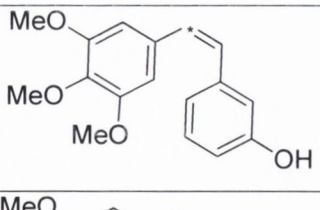	>100	7.84
[424]	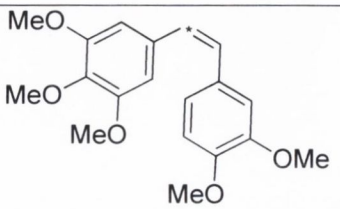	>100	7.62

[425]	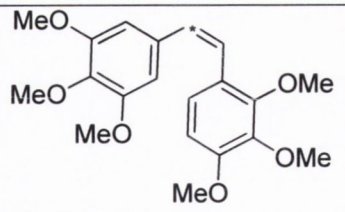	>100	7.63
[426]	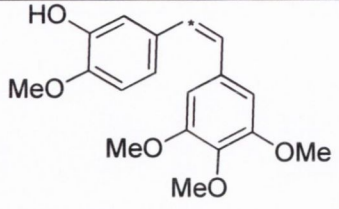	4.2±1.4	7.69
[427]	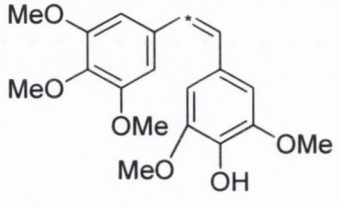	11.75±1.7	7.33
[428]	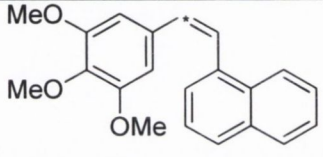	>100	6.82
[429]	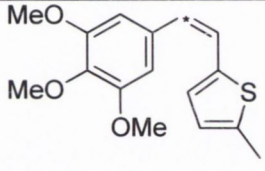	>100	8.65
[430]	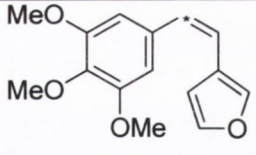	36.5±2.33	7.68

Table 21 Antiproliferative data for novel endoxifen-combretastatin conjugates

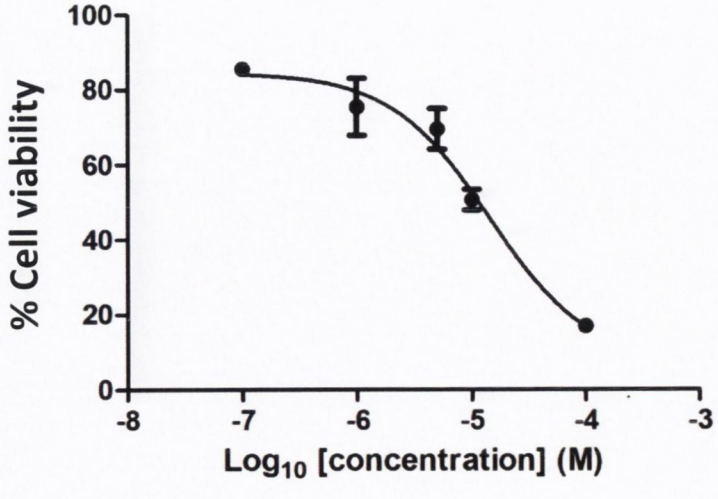

Figure 6-2 The antiproliferative effects of an endoxifen-combretastatin conjugate in the MCF-7 human breast cancer cell line (compound [427]). The values represent the mean ± S.E.M. for three independent experiments performed in triplicate

6.1.4.3 Biochemical data for the structurally modified combretastatin-endoxifen conjugates

Compounds [435]-[438] synthesised in this section were investigated to determine the effect of the core structure of the conjugate scaffold on the antiproliferative activity. The lead compound from previous work was identified as [414]. It was decided to determine if the two aryl rings of combretastatin structure were required for optimum antiproliferative activity. The four compounds [342]-[345] synthesised in chapter 3 were single aryl ring cinnamic acids and 3-phenylpropanoic acids which were subsequently coupled to form the desired conjugates [435]-[438], Chapter 5.

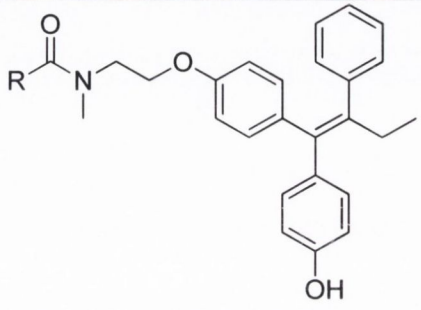

Compound ID	R	MCF-7 IC_{50} (μM)	CLogP
[435]	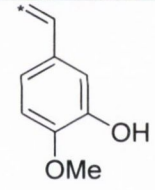	51.3±2.3	7.04
[436]	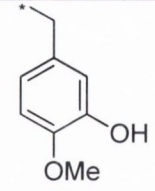	46.77±1.65	6.82
[437]	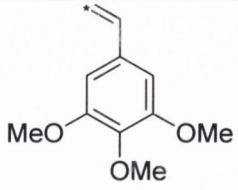	>100	7.16
[438]	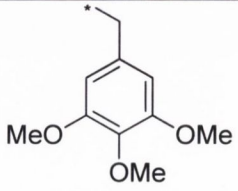	>100	6.94

Table 22 Antiproliferative data for the structurally modified combretastatin-endoxifen conjugates

The biochemical data for compounds [435]-[438] is presented in Table 22. The four compounds evaluated for this investigation showed reduced activity compared with [414].

Compounds [435] and [436] which have the *p*-methoxy and 3-OH substituent showed the greatest activity, with IC_{50} values of 51.3 and 46.7 μM respectively. Compound [436] exhibited slightly greater activity than [435] and this potentially was due to the lack of the double bond which would allow the aryl substituent more freedom to interact within the binding site. Compounds [437]-[438] which contain the 3,4,5-trimethoxy substituent did not show any antiproliferative activity below an IC_{50} value of 100 μM. Therefore from the biochemical data for this series it is apparent that the two aryl rings, A and B, of the combretastatin structure with the CA4 type substituents were essential for optium antiproliferative activity of the compound. Figure 6-3 displays a representative illustration of the antiproliferative effects of [435] and [436] on MCF-7 cells. In this series, the compounds [435]-[438] are predicted to have poor oral absorption with CLogP greater than 5.

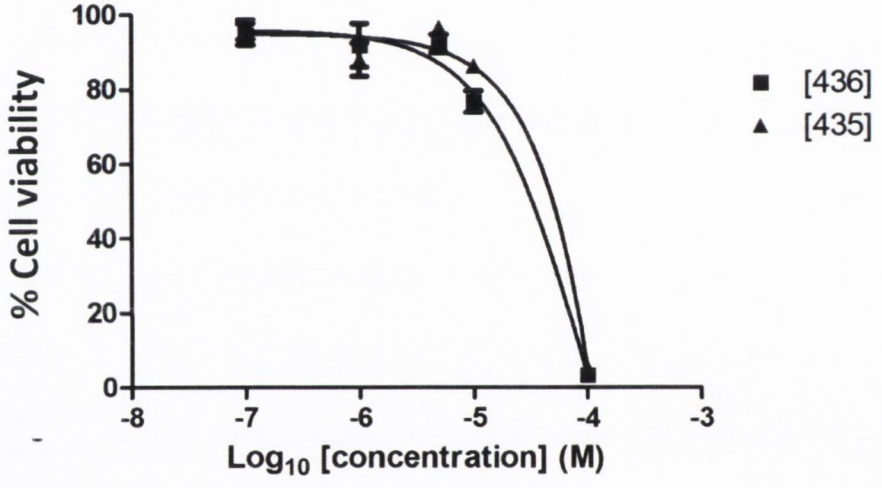

Figure 6-3 Antiproliferative effects of endoxifen-modified combretastatin conjugates [435] and [436] in the MCF-7 human breast cancer cell line (compounds [435] and [436]). The values represent the mean ± S.E.M. for three independent experiments performed in triplicate

6.1.4.4 Biochemical data for cyclofenil-based analogues as potential ER-ligand

The cyclofenil-based analogues [221]-[225] were synthesised based on the reported cyclofenil structure which demonstrated impressive ERα and ERβ binding affinities.[469] It was hypothesised that by incorporating a basic side chain onto the cyclofenil structures that high affinity ER ligands with potential antagonist activity may be achieved. The cyclofenil-based analogues were designed to be used as the potential ER targeting ligands for this series of conjugates. As these cyclofenil-based analogues were novel compounds it was decided that they should be evaluated individually for antiproliferative activity. This data would be beneficial as it would allow the conjugates [444]-[448] to be compared directly to ER-ligands [221]-[225] for reduced/enhanced activity.

The biochemical data for [221]-[225] is presented in Table 23. The cyclofenil-based analogues [221]-[225] all showed low micromolar antiproliferative activity in MCF-7. The antiproliferative activity for these cyclofenil-based analogues [221]-[225] ranged from IC_{50} values

ranging from 1.38 to 4.78 μM.[467] This activity would allow for the rationalization of the next series of conjugates that incorporated the cyclofenil-based analogues. Figure 6-4 shows the antiproliferative effects of compound [223] on MCF-7 breast cancer cells. In this series only [221] had a CLogP less than 5, and this compound would be expected to demonstrate reasonable oral absorption properties.

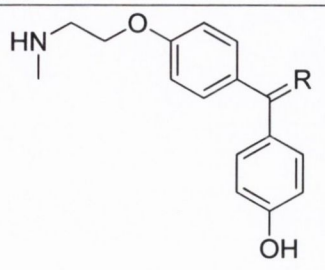

Compound ID	R	MCF-7 IC_{50} (μM)	CLogP
[221]		3.09±0.84	4.62
[222]		4.78±1.3	5.18
[223]		1.38±0.3	5.74
[224]	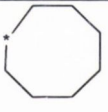	3.23±1.2	6.30
[225]	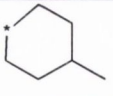	1.77±0.5	5.70

Table 23 Antiproliferative data for cyclofenil-based analogues as potential ER-ligand

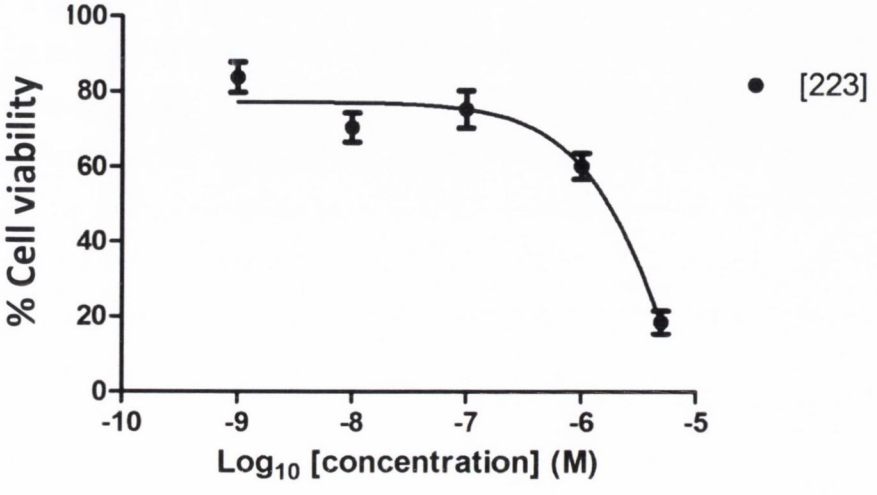

Figure 6-4 A representative graph of the antiproliferative effects of a cyclofenil-based analogue in the MCF-7 human breast cancer cell line (compound [223]). The values represent the mean ± S.E.M. for three independent experiments performed in triplicate

6.1.4.5 Biochemical data of combretastatin-cyclofenil-based conjugates

The conjugates [444]-[448] contained the novel ER-ligands [221]-[225] and were obtained *via* a direct amide linkage to the acrylic acid analogue [150], Chapter 5. The acrylic acid analogue [150] was not varied due to the beneficial enhanced activity seen by the lead compound [414].

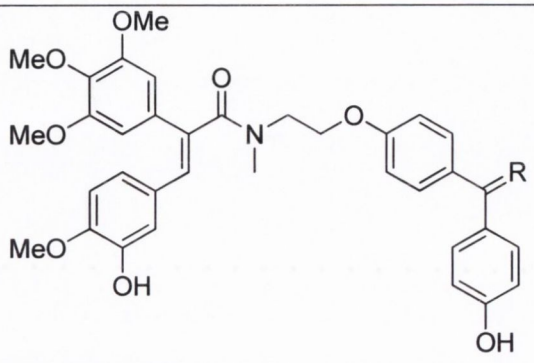

Compound ID	R	MCF-7 IC_{50} (μM)	CLogP
[444]		1.38±0.21	6.75
[445]		2.01±1.1	7.31
[446]		2.50±0.19	7.87
[447]		0.346±0.5	7.83
[448]	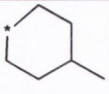	0.182±0.3	7.83

Table 24 Antiproliferative data of combretastatin-cyclofenil based conjugates

The biochemical data for conjugates [444]-[448] is presented in Table 24. The series was evaluated in the ER-positive breast cancer cell line, MCF-7. This series of conjugates [444]-[448] showed mostly low micromolar activity (IC_{50} range of 1.38-2.5 μM) with two compounds exhibiting sub-micromolar activity (IC_{50} values of 0.182 μM [448] and 0.346 μM [447]). The activity of the conjugates varies depending on the structure of the cycloalkane ring attached. However, the biochemical data did not follow any particular trend. However the two most active conjugates, [447] and [448], contain the largest cycloalkane rings which could potentially rationalise the enhanced activity but further investigation of bulkier cycloalkane rings than [447]-[448] would be required to see if this in fact is a trend. In this series, the compounds [444]-[448] are predicted to have poor oral

absorption with CLogP greater than 5. The antiproliferative effects of conjugates [447] and [448] in MCF-7 cells are displayed in Figure 6-5.

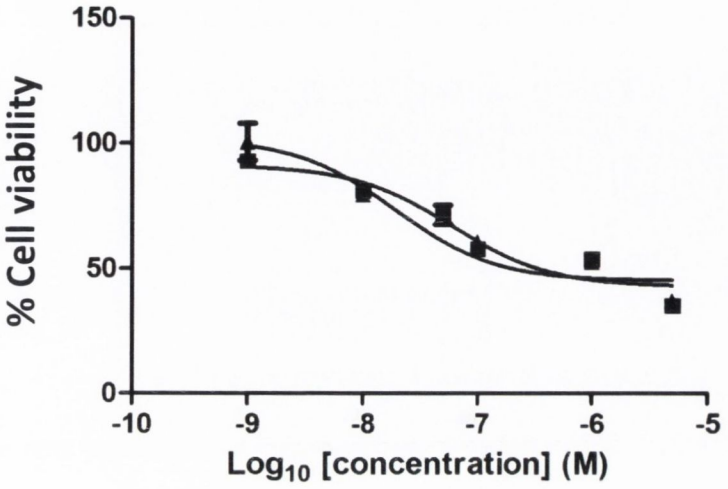

Figure 6-5 A representative graph of the antiproliferative effects of cyclofenil-combretastatin conjugates in the MCF-7 human breast cancer cell line (compounds [447] and [448]). The values represent the mean ± S.E.M. for three independent experiments performed in triplicate

6.1.4.6 Biochemical data for 2-phenylindole-based analogues as potential ER-ligands

The 2-phenylindole-based analogues [241]-[243] and [261]-[262] incorporated the ER-binding indole moiety of the SERM bazedoxifene with various length alkyl amine positioned at the indole nitrogen. The basic side chain substituents were designed to mimic the endoxifen basic side chain terminus. It was hypothesised that by incorporating a basic side chain onto the 2-phenylindole structure that high affinity ER ligands with potential antagonist activity may be achieved. The potential ER binding ligands would then be incorporated into the conjugate scaffold which could potentially give the novel conjugates [454]-[459] affinity for the ER while exerting enhanced anti-proliferative activity in the ER positive MCF-7 cancer cell line. The 2-phenylindole-based analogues are designed to be used as the potential ER targeting ligand for this series of conjugates. As these 2-phenylindole-based analogues were novel compounds it was decided that they should be evaluated individually for activity. This would afford useful data as it would allow the subsequent conjugates [454]-[459] to be compared directly to the ER-ligands [241]-[243] and [261]-[262] for reduced/enhanced antiproliferative activity.

The biochemical data obtained for indoles [241]-[243] and [261]-[262] is presented in Table 25. The 2-phenylindole-based analogues [241]-[243] and [261]-[262] all showed micromolar IC_{50} activity. Interestingly, the 2-phenylindoles generally showed antiproliferative activity ranging from IC_{50} value of 38-49 μM; however when the basic side chain length was increased to 12 carbons, there was a significant >240-fold enhancement of activity (IC_{50} = 158 nM). This activity would allow for the rationalization of the subsequent series of conjugates that incorporated the cyclofenil-based

analogues. Figure 6-6 shows the antiproliferative effects of compound [243] on MCF-7 breast cancer cells. The ER ligands with an alkyl chain length <6 carbons would be expected to have good oral bioavailability as the CLogP values are less than 5 but the longer non-polar chain length >6 carbons would be expected be more lipophilic and display poorer oral absorption properties.

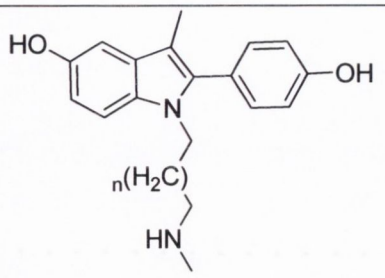

Compound	n	MCF-7 IC_{50} (μM)	CLogP
[241]	2	40.7±1.5	3.66
[261]	3	48.97±8.1	4.19
[262]	4	41.68±4.8	4.72
[242]	6	38.90±1.8	5.78
[243]	10	0.158±0.14	7.89

Table 25 Antiproliferative data for 2-phenylindole-based analogues as potential ER-ligands

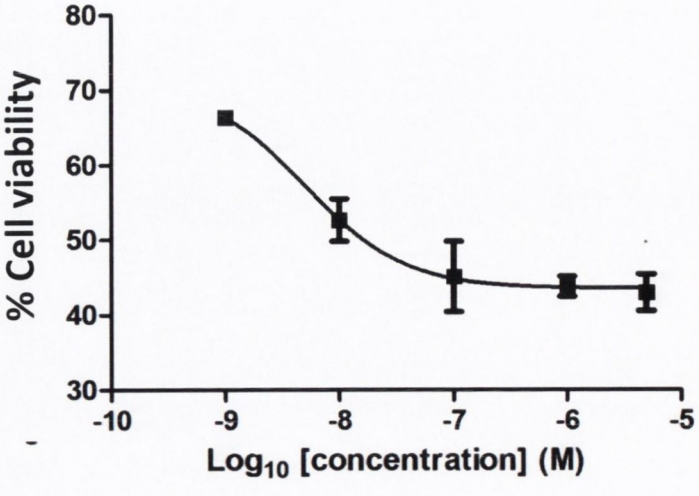

Figure 6-6 The antiproliferative effects of a 2-phenylindole analogue in the MCF-7 human breast cancer cell line (compound [243]). The values represent the mean ± S.E.M. for three independent experiments performed in triplicate

6.1.4.7 Biochemical data of combretastatin-2-phenylindole-based conjugates

The novel ER-ligands [241]-[243] and [261]-[262] evaluated showed micromolar activity with the 12 carbon analogue [243] exhibiting sub-micromolar IC_{50} antiproliferative activity. These novel ER-ligands [241]-[243] and [261]-[262] were incorporated into the conjugates scaffold as the ER-targeting ligand. The conjugate [454]-[459] contained the novel ER-ligands [241]-[243] and [261]-[262] *via* a direct amide linkage to the acrylic acid CA4 analogue [150]. The acrylic acid CA4 analogue [150] was not varied due to the beneficial enhanced activity established in the lead compound [414].

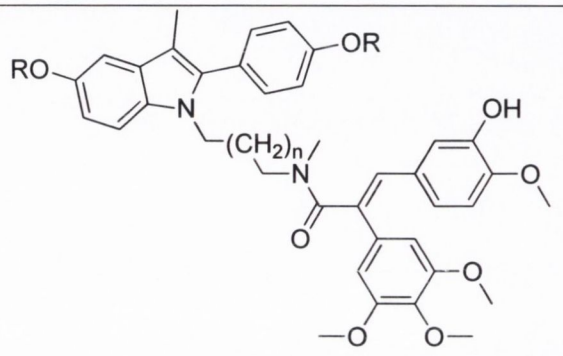

Compound ID	R	n	MCF-7 IC_{50} (μM)	CLogP
[454]	H	2	1.99±1.1	5.81
[455]	H	3	2.93±1.2	6.24
[456]	H	4	2.34±0.44	6.87
[457]	H	6	2.95±0.91	7.86
[458]	H	10	1.86±0.8	9.27
[459]	Me	4	81.28±7.3	6.91

Table 26 Antiproliferative data of combretastatin-2-phenylindole-based conjugates

The biochemical data for conjugates [454]-[459] is presented in Table 26. The series was evaluated in the ER-positive breast cancer cell line, MCF-7. This series of conjugates [454]-[458] showed mostly low micromolar activity (IC_{50} in the range of 1.86-2.95 μM) with the methoxy substituted compound [459] exhibiting reduced activity (IC_{50} = 81 μM) which was a 27-fold reduction. When the results of free hydroxyl compounds [454]-[458] are compared with the

methoxy compound [459] it was clear that the presence of the hydroxyl groups was essential for the enhanced activity of the conjugate compounds. However, the biochemical data for the series showed that the 12 carbon conjugate compound [458] exhibited the highest potency (IC_{50} = 1.86 μM) as was seen with the ER-ligand analogue [243] itself when compared with the other analogues in this series. However all the compounds [454]-[458] exhibited activity in the range of IC_{50} = 1.86-2.95 μM. Figure 6-7 displays a representative illustration of the antiproliferative effects of [458] on MCF-7 cells. In this series, the compounds [454]-[458] and [459] are predicted to have poor oral absorption with CLogP greater than 5. The antiproliferative effect of conjugate [458] is displayed in Figure 6-7.

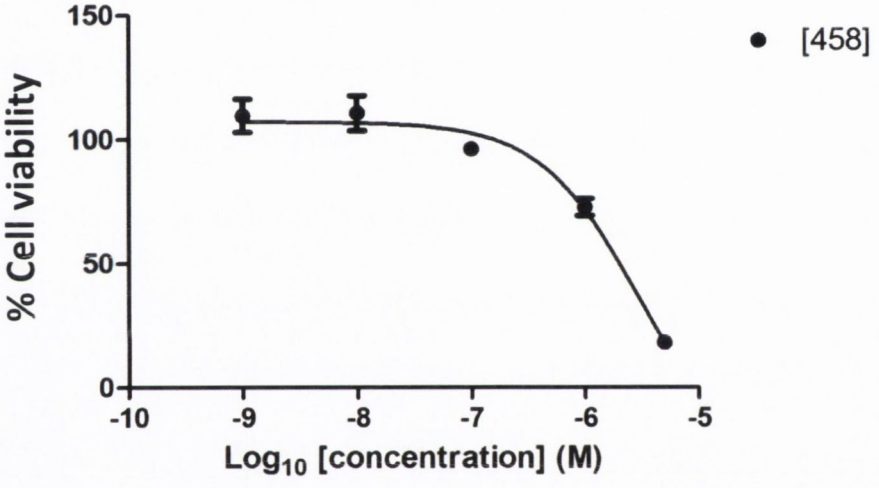

Figure 6-7 A representative graph of the antiproliferative effects of a 2-phenylindole-combretastatin conjugate in the MCF-7 human breast cancer cell line (compound [458]). The values represent the mean ± S.E.M. for three independent experiments performed in triplicate

6.1.4.8 Biochemical data for bis-2-phenylindole-based analogues as potential ER-ligands

The 2-phenylindole-based analogues [241]-[243] and [261]-[262] containing the ER-binding 2-phenylindole component of the SERM bazedoxifene where shown to have moderate micromolar antiproliferative activity. During the synthesis of the 2-phenylindole-based analogues [241]-[243] and [261]-[262] at the bromoalkylation step, the formation of the *bis*-2-phenylindoles by-products [268]-[272] was observed. It was postulated that these by-product which contained two of the ER-ligands separated *via* the alkyl chain as they could potentially show ER related activity. As they contain two ER-targeting ligands and could potentially bind to the ER-LBD at either end of the analogue.

The biochemical data of compounds [268]-[272] is presented in Table 27. The *bis*-2-phenylindole-based analogues [268]-[272] showed low micromolar activity (IC_{50} = 2.75-8.16 μM). However, the biochemical data did not follow any particular trend. The two most active conjugates,

[468] and [472], contained the shortest (4 carbon) and the longest (12 carbon) chains respectively. The antiproliferative effects of compound [268] are displayed in Figure 6-8. The oral absorption of this series is predicted to be very poor as the CLogP value increases from 8.00 to 12.23 as the chain length is increased from n=2 [268] to n=10 [272].

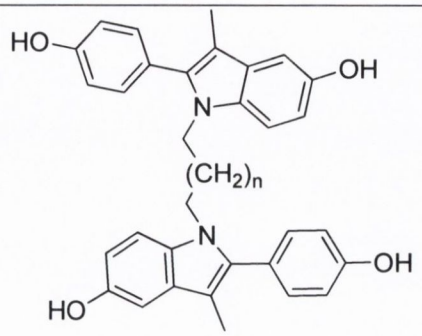

Compound ID	n	MCF-7 IC_{50} (μM)	CLogP
[268]	2	2.75±1.2	8.00
[269]	3	4.16±2.1	8.53
[270]	4	8.16±1.3	9.06
[271]	6	6.6±4.4	10.11
[272]	10	5.24±2.1	12.23

Table 27 Antiproliferative data of for bis-2-phenylindole-based analogues as potential ER-ligand

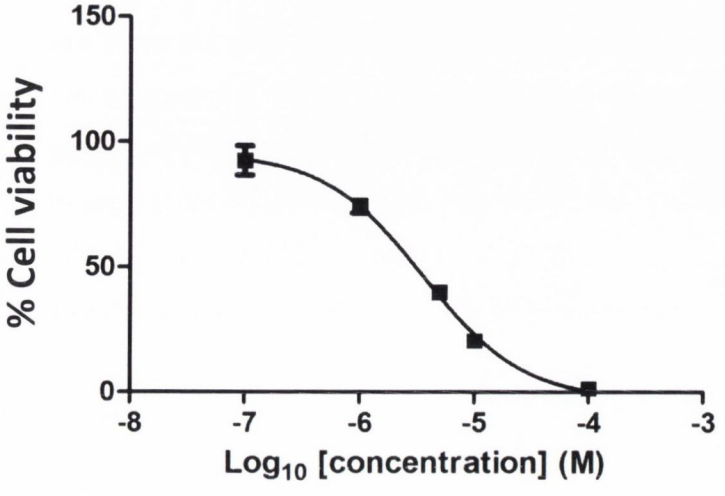

Figure 6-8 A representative graph of the antiproliferative effects of a bis-2-phenylindole analogue in the MCF-7 human breast cancer cell line (compound [268]). The values represent the mean ± S.E.M. for three independent experiments performed in triplicate

6.1.4.9 Biochemical data of the aromatase inhibitor (AI) containing conjugates

The two aromatase inhibitor containing conjugates, [463] and [464], evaluated in this section differ from the general conjugate prototype that was employed previously for conjugate design. The previously synthesised products incorporated a range of ER-ligands conjugated with cytotoxic agents. The two AI containing compounds that were evaluated in this section either contain an ER-ligand or a cytotoxic agent covalently bonded *via* a direct amide linkage to an aromatase inhibitor. As these types of compounds had not been reported in the literature, it was decided to validate the concept that a conjugate consisting of (i) an ER-ligand with an AI [463] and (ii) a cytotoxic agent with an AI [464], could be successfully synthesised and evaluated.

The first AI containing compound to be evaluated was [463] which was the anastrozole derivative linked *via* a direct amide linkage to endoxifen. It was proposed that compound [463] would still exhibit selectivity for the ER but potentially interrupt the biosynthesis of estradiol due to the presence of the AI part of the conjugate. The novel conjugate [463] was evaluated in the ER-positive breast cancer cell line, MCF-7, and exhibited sub-micromolar activity (IC_{50} = 316 nM). This result shown in Table 28, validates the concept of ER-AI conjugates and would justify further investigation of these type conjugates. However, similarly with the endoxifen-cytotoxic conjugates, the sub-micromolar activity of [463] could potentially be attributed to the AI portion of the molecule acting as a bulky substituent on the basic side chain which inhibited the ER mediated action of Helix-12 and may not exert any AI action. Figure 6-9 shows the antiproliferative effects of compound [463] on MCF-7 breast cancer cells. This ER ligand-AI conjugate was predicted to have decreased oral absorption as it CLogP was calculated in excess of 5. Further biochemical evaluation of the AI activity of [463] is required.

The AI containing compound [464] contains the letrozole derivative [387] linked *via* a direct amide linkage to [150]. As this conjugate did not contain any ER-ligand it was not expected to show any selectivity towards the ER. The concept of this design was to determine for a conjugate [464] lacking ER targeting selectivity, would show any effects on the ER-positive breast cancer cell line, MCF-7. The conjugate [464] exhibited low micromolar activity (IC_{50} = 1.14 μM) (Table 28) which was surprising as this conjugate would not be expected to show selectivity for the ER containing tumour cells. This conjugate exhibited an interesting result and should be evaluated in a tubulin binding assay and aromatase inhibition assay to obtain a greater understanding of compound [464] mode of action. Figure 6-9 displays a representative of the antiproliferative effects of [464] on MCF-7 cells. Unlike compound [463] this AI containing conjugate [464] would be predicted to have good oral absorption (CLogP = 3.66).

Compound	Compound	MCF-7 IC_{50} (μM)	CLogP
[463]	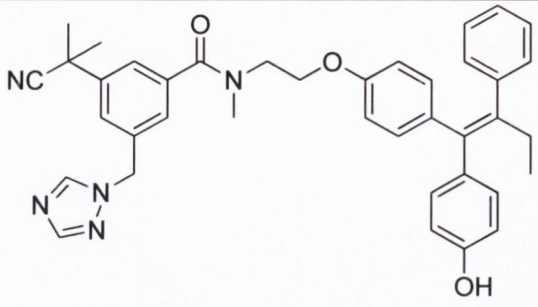	0.316±0.3	5.87
[464]	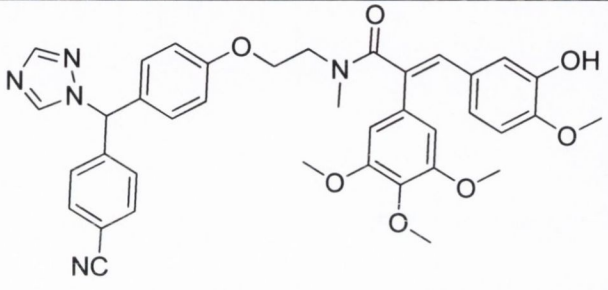	1.14±0.41	3.66

Table 28 Antiproliferative data of for the Aromatase inhibitor containing conjugates

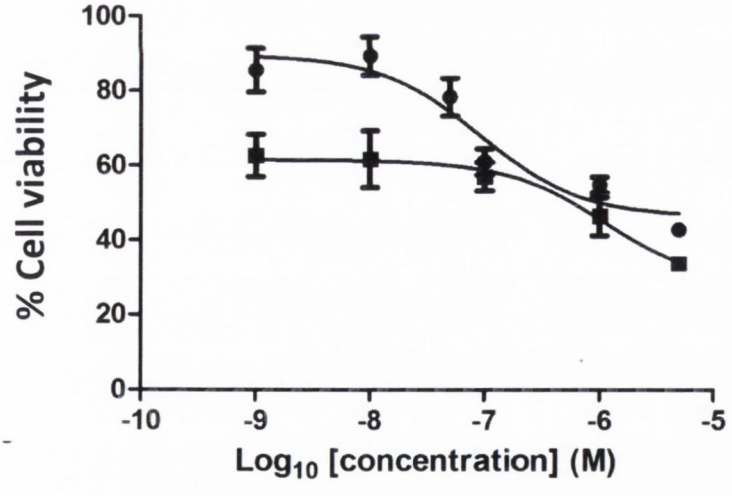

Figure 6-9 Antiproliferative effects of the aromatase inhibitor containing conjugates ([464] & [463]) in the MCF-7 human breast cancer cell line. The values represent the mean ± S.E.M. for three independent experiments performed in triplicate

6.1.4.10 Biochemical data for the letrozole analogues

The letrozole-CA4 hybrid type compounds derivatives [394] and [411]-[413] were synthesised to investigate the effects of introducing CA4 type substitution on the letrozole scaffold. This investigation led to the development of 4 compounds based on the benzhydryl-1*H*-1,2,4-triazole scaffold. It was postulated that by modifying one/both rings of the letrozole scaffold that it was potentially possible to design a dual acting aromatase inhibitor and VTA compound. In addition, compound [402] was screened in this class as it was an interesting by-product in the synthesis of [387]. Compound [402] contained the scaffold of letrozole but also contained a basic ether side

chain in place of the nitrile substituent on one of the rings. This type of substitution is commonly associated with ER antagonist activity.

Compound ID	Structure	MCF-7 IC_{50} (μM)	CLogP
[411]	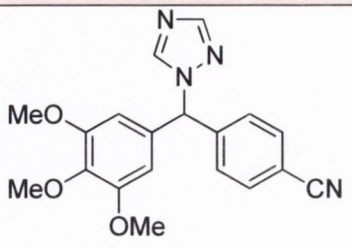	>100	1.58
[412]	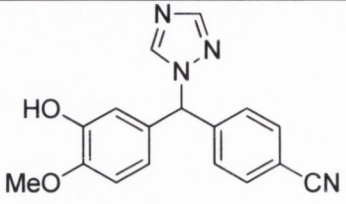	>100	1.13
[413]	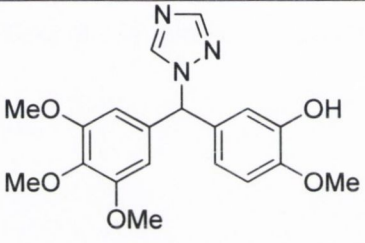	0.295	0.85
[394]	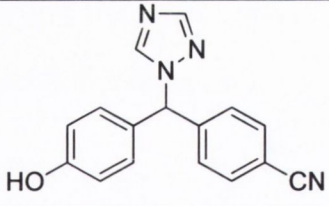	>100	0.98
[402]	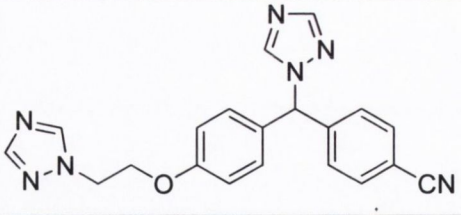	>100	0.817

Table 29 Antiproliferative data for the letrozole derivatives

The letrozole derivatives [394], [402] and [411]-[413] were evaluated on ER-positive breast cancer cell line, MCF-7. The evaluation showed that replacing one of the nitrile substituents with either A/B ring of CA4, phenol [394] or the basic side chain [402] did not result in any significant antiproliferative activity below 100 μM. However, when both rings of the letrozole compound were exchanged with the A and B ring of CA4, sub-micromolar activity (IC_{50} = 295 nM) was observed in compound [413]. The antiproliferative effects of compound [413] are displayed in Figure 6-10. This result was very interesting and for a greater understanding [413] mode of action it was subsequently

evaluated in a tubulin binding assay. The compound of interest [413] show a low CLogP value (0.85) which predicts it to have good oral bioavailability and the CLogP values for this series are less than 5. Compound [413] has structural features of both letrozole and CA4 and also shows much lower CLogP value when compared to the two individual compounds, calculated as 3.31 [150] and 1.23 [97] respectively.

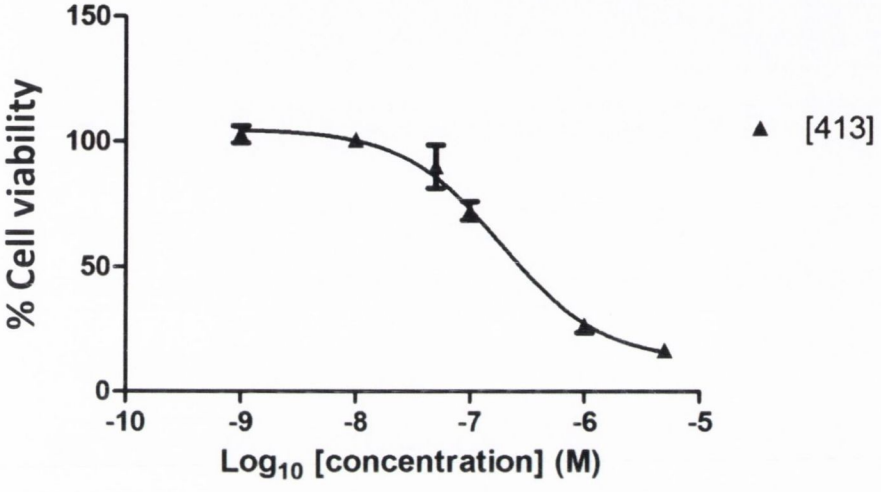

Figure 6-10 Antiproliferative effects of the letrozole derivative [413] in the MCF-7 human breast cancer cell line. The values represent the mean ± S.E.M. for three independent experiments performed in triplicate

6.1.4.11 Evaluation of tubulin binding activity of compound [413]

Compound [413] was chosen to be investigated for tubulin binding activity due to its notable antiproliferative activity (IC_{50} = 295 nM). It was proposed that compound [413] would exert its activity on tubulin because of the similarity in structure (A and B rings) to CA4. In addition it could also exert aromatase inhibition activity due to its structural similarity with letrozole. The tubulin binding activity of [413] was determined by Dr. Seema Nathwani (School of Biochemistry and Immunology, Trinity College Dublin) using a tubulin polymerization assay kit from Cytoskeleton (BK006P)[553]. This assay is based on an adaptation of the original method of Shelanski *et al*[554] and Lee *et al*[555] which demonstrated that light is scattered by microtubules to an extent that is proportional to the concentration of microtubule polymer. Final concentration of porcine tubulin was 3mg/mL and glycerol was 10%. The tested compounds at 10 μM concentration were first mixed with purified bovine tubulin in 96-well plate on ice. After placing the plate into a 37 °C incubator, the effects on tubulin assembly were monitored in a spectrometer at 340 nm at 30 s intervals for 30 or 60 min at 37 °C. Percentage inhibition of polymerization was recorded for each reaction. Time-optical density curves at 340 nm of compound [413] are illustrated in Figure 6-11. The V_{max} is the maximum velocity or rate at which the enzyme catalysed a reaction, which is obtained *via* the software softMax. This will be reduced in the presence of an inhibitor of the enzyme[553]. The V_{max} for [413] was calculated to

be 3.582 mOD/min. This V_{max} for [413] can be compared to the vehicle V_{max} which in this case is EtOH that has a V_{max} of 7.378 mOD/min. At 10 μM final concentration, [413] causes a twofold reduction in polymer mass.

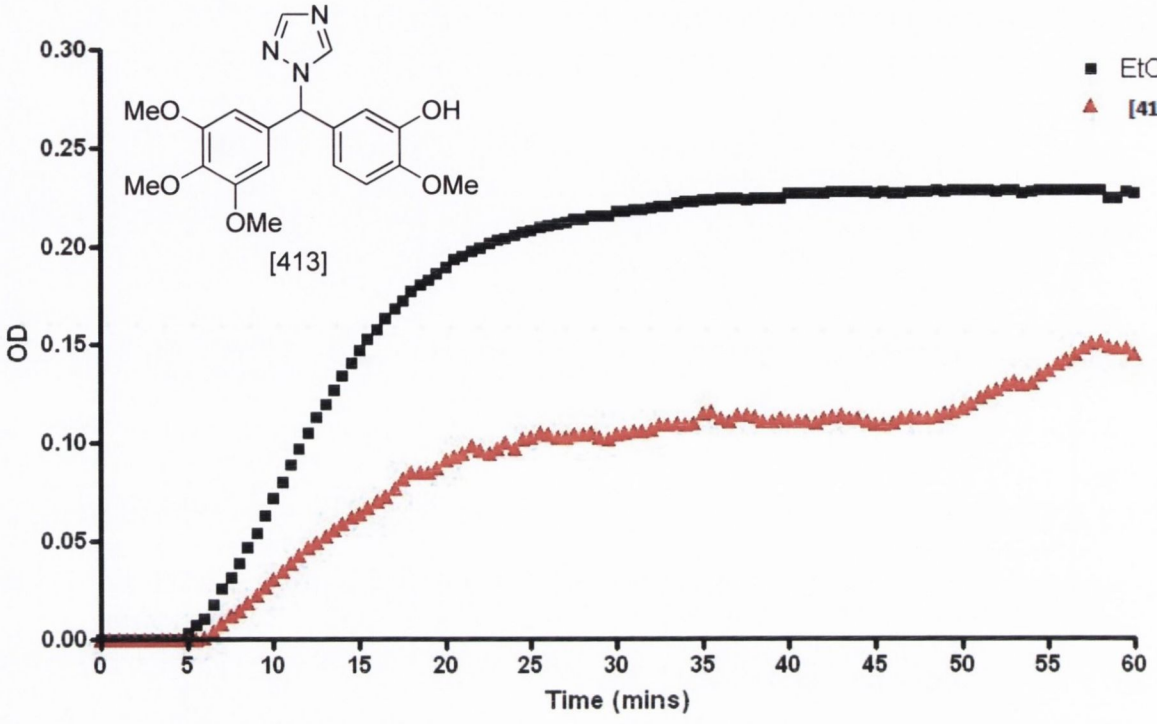

Figure 6-11 Tubulin polymerization assay for compound [413] (10 μM) with EtOH

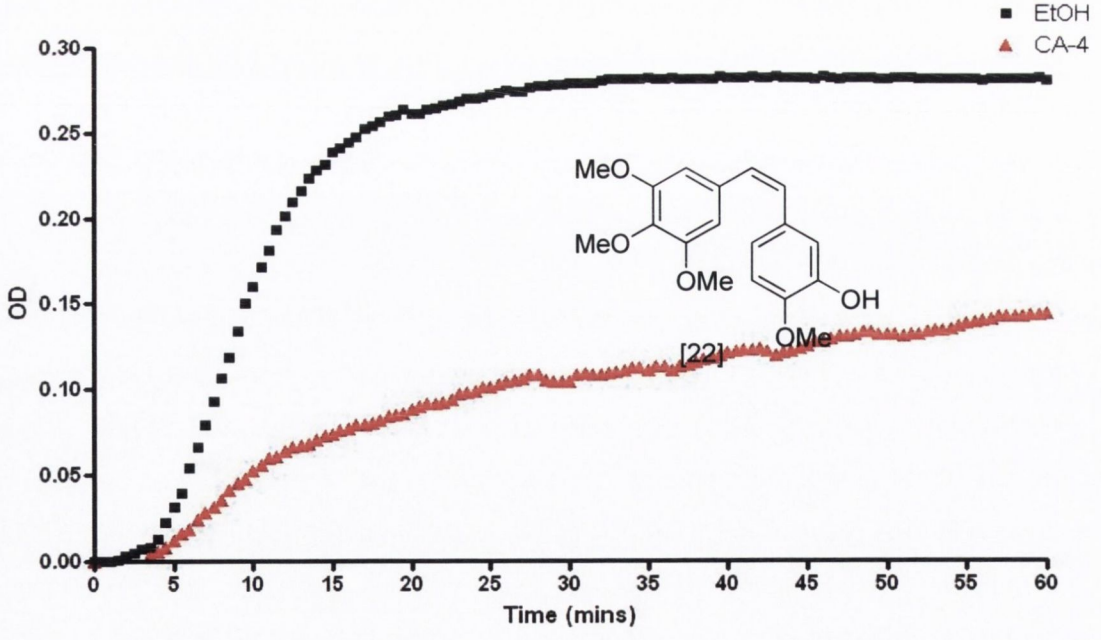

Figure 6-12 Tubulin polymerization assay for CA4 (10 μM) with EtOH

In Figure 6-12, the tubulin polymerization of the control compound CA4 with EtOH is displayed. The V_{max} for CA4 was calculated to be 3.245 mOD/min. This V_{max} for CA4 can be compared to the

vehicle V_{max} which in this case is EtOH that has a V_{max} of 10.996 mOD/min. At 10 μM final concentration, CA4 causes a 3.4-fold reduction in polymer mass. However compound [413] demonstrated a twofold reduction in polymer mass and is shown to exhibit the characteristic action of a tubulin binding agent such as CA4. Compound [413] a novel hybrid CA4-AI type scaffold displayed the desired tubulin polymerisation inhibitory activity.

6.1.4.12 Biochemical data for piperazine derivative of the acrylic acid scaffold

This piperazine derivatives of the acrylic acid scaffold [349] were synthesised to produce a range of piperazine containing amide derivatives of the acrylic acids. The antiproliferative evaluation was performed on one of the derivatives, [349] (shown in Table 30). This derivative exhibited low micromolar activity (4.57 μM) in MCF-7 cells and was chosen as it contained the CA4 scaffold with the covalently bonded piperazine ring substituent. Figure 6-13 displays a representative of the antiproliferative effects of [349] on MCF-7 cells. The piperazine derivative of [150] was predicted to have good oral absorption as it CLogP value was 1.58. The piperazine are sometimes used to increase the solubility of a drug; in this case the piperazine decreased the CLogP value from 2.07 for [150] hence decreasing the lipophilicity of the drug.

Compound ID	Structure	MCF-7 IC_{50} (μM)	CLogP
[349]	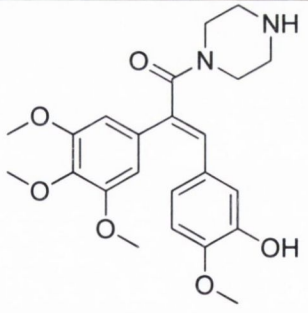	4.57±3.1	1.58

Table 30 Antiproliferative data for selected piperazine acrylic acid derivative

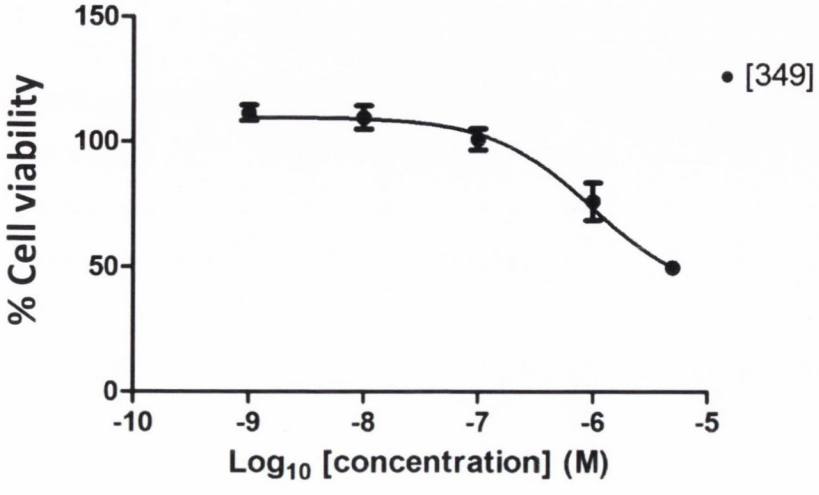

Figure 6-13 Antiproliferative effects of the selected piperazine acrylic acid derivative [349] in the MCF-7 human breast cancer cell line. The values represent the mean ± S.E.M. for three independent experiments performed in triplicate

6.1.4.13 ER binding assay of selective active compounds

It is necessary to test the binding efficiency of each compound for both estrogen receptor (ER) isoforms (ERα and ERβ), to determine how effectively the ligand binds to the receptor and whether the compound is acting as an antagonist or agonist. The Lanthascreen® FRET kit contains a terbium labelled antibody which is attached to the nuclear receptor, in this case the ERα and ERβ, and a fluoromone which is found in the binding site of the receptor. If the ligand displaces the fluoromone, fluorescence decreases, determining the efficiency of the ligand to bind to the receptor.

The most active SERM type compounds and conjugate from the antiproliferative assay were now selected for ER binding study. In Table 31, the ER binding IC_{50} values for both ER isoforms are displayed for the selected compounds for the most active ER type ligands and conjugate compounds incorporating an ER type in the conjugate scaffold. The selectivity value is reported as the ratio of RBA values or binding affinities, ERα relative to ERβ, for each of the compounds (see Table 31) (single experiment carried out in triplicate). For selectivity values greater than 1, the compounds have a more pronounced affinity for ERα binding site, while for values less than 1, the compounds have a more pronounced affinity for the ERβ binding site.

Compound no.	ER α IC_{50} (nM)	ER β IC_{50} (nM)	ERα/ERβ Selectivity
[426]	182	436	2.40
[223]	1738	199	0.11
[447]	170	112	0.66
[225]	3162	67	0.02
[448]	19	229	12.05
[463]	2239	245	0.11
[458]	574	155	0.27
[243]	380	1660	4.37
[268]	436	41	0.09
Estradiol	1.7	3	-

Table 31 ERα and ERβ binding data for the most active novel compounds

The cohort of compounds evaluated for both estrogen receptor (ER) isoforms (ERα and ERβ) exhibit good binding activity (see Figure 6-14). Compounds [426], [447], [448], [458] and [268] display ER binding activity in the nanomolar region for both ER isoforms, while compounds [223], [225] and [468] display nanomolar activity in ERβ and low micromolar activity in ERα and compound [243] exhibits nanomolar activity in ERα and low micromolar activity in ERβ. The selective of ERβ binding was exhibited by compounds [223], [447], [225], [468], [458] and [268] with selectivity in the

range of 0.02-0.66. Compound [225] which was a cyclofenil type ligand exhibited the greatest selectivity (0.02) towards the ERβ isoform while compound [448] which was a direct conjugate of [225] displayed the greatest selectivity (12.05) towards ERα. Low nanomolar binding activity was seen for [448] in ERα and, [225] and [268] in ERβ.

6.1.4.1 Effects of selective active compounds on cell cycle and cell death.

Based on the cell viability assay results, a selected cohort of the most active compounds from each set synthesised series of compounds (IC_{50} values 0.182 – 4.57 μM) shown in Figure 6-14 were subjected to cell cycle analysis. Flow cytometry using with propidium iodide stained cells was carried out to analyse the percentage of cells in each stage of the cell cycle and the number of apoptotic or dead cells. Samples were treated for 72h at 10μM. Experiments carried out by Dr. Sandra Bright, School of Biochemistry and Immunology, TCD. Results showed that all compounds tested increased apoptosis when compared to vehicle-treated cells, with the exception of compounds [464] and [243]. Of the active compounds, the cyclofenil based analogues [223] and [225] proved significantly more active than the positive control tamoxifen (p value < 0.001). The most potent compound tested, [223], induced 79.7 ± 5.2% apoptosis at 10μM and should be selected as a lead compound for future biological studies (Figure 6-15A).

Interestingly, in addition to inducing apoptosis, the CA4-AI compounds [349] and [413] (p value < 0.001) and the CA4 direct amide cyclofenil based conjugate [447] (p value < 0.01) also induced a significant G2/M-arrest in MCF-7 cells when compared to vehicle-treated cells. A G2/M arrest typically, though not necessarily always, precedes apoptosis. Future studies at earlier time-points (24h and 48h) could be undertaken to establish if the other active compounds in this cohort also induce a G2/M arrest preceding apoptosis. A G2/M arrest is commonly observed with tubulin-targeting compounds and so this data suggests that the tubulin-targeting ability of combretastatins is maintained when complexed to various ligands.

Next, the same cohort of compounds (Figure 6-14) was tested on peripheral blood mononuclear cells isolated from the blood of healthy donors. Cells were treated with 10μM of each compound for 72 hrs and subjected to flow cytometry. Results showed that only two of the compounds, ([223] and [225], the most active compounds in the MCF-7 cells), induced apoptosis in these normal blood cells, with no toxic effects observed with the other compounds (Figure 6-16). None of the compounds caused a G2/M arrest in the normal blood cells (Figure 6-16). The potent activity of several members of this cohort of compounds in MCF-7 breast cancer cells and their lack of toxicity in normal blood cells make them ideal candidates for further anti-cancer studies.

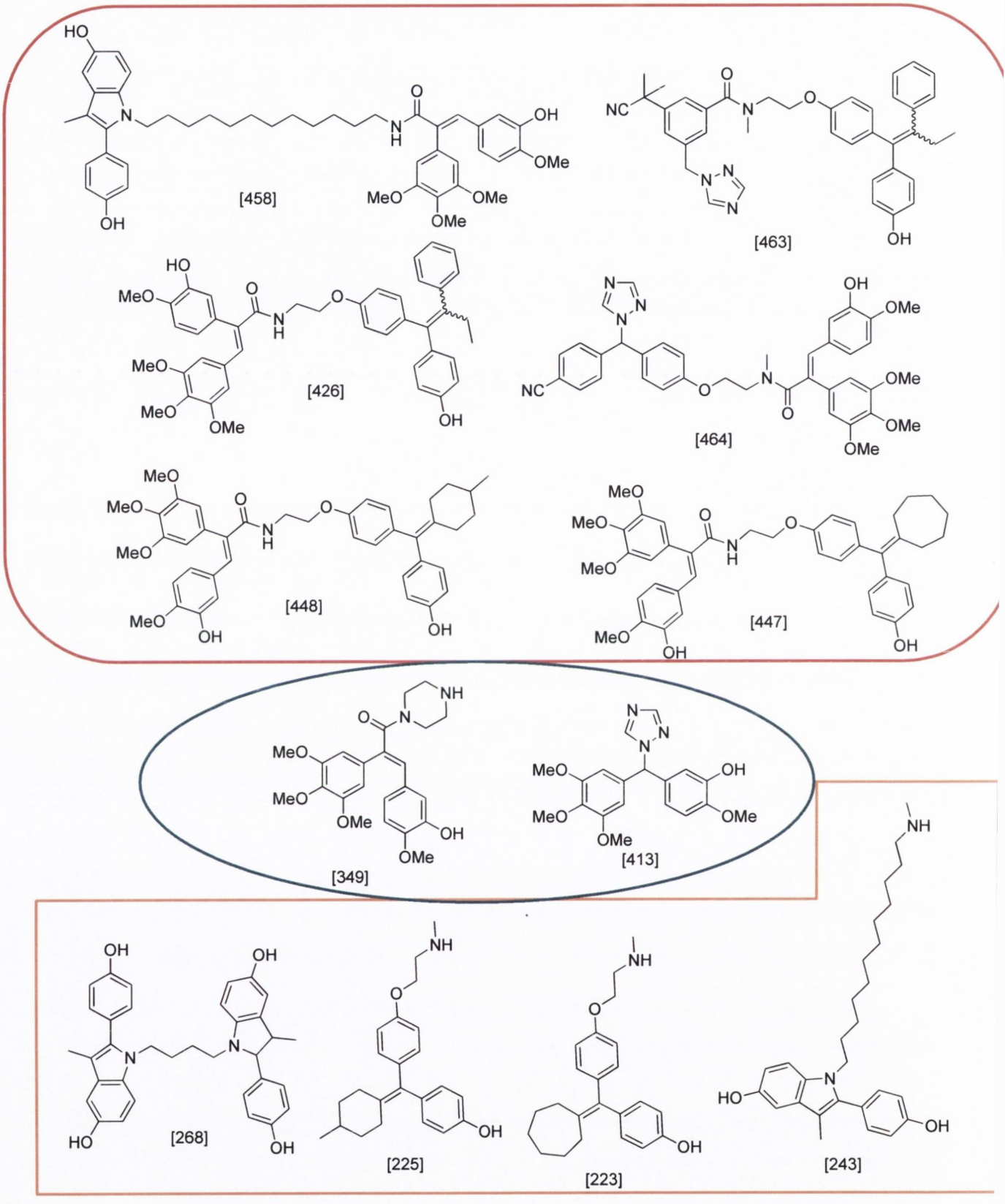

Figure 6-14 Selected cohort of the most active compounds from each set of synthesised compounds, Conjugate (Red), ER type ligands (orange) and VTA/ letrozole-CA4 (blue)

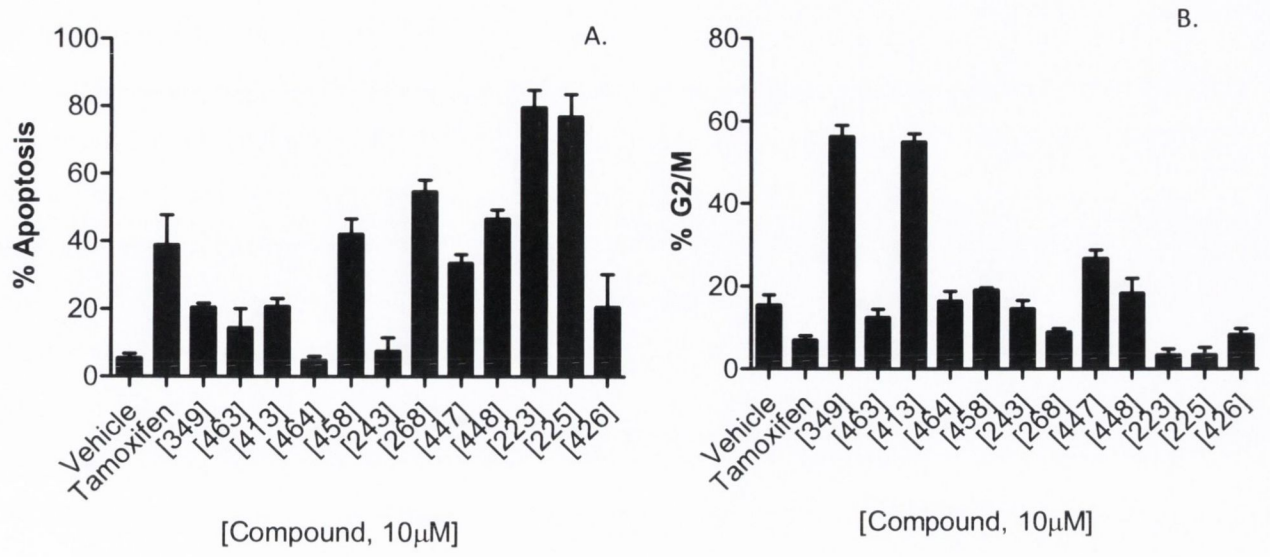

Figure 6-15 Compounds potently induce apoptosis in MCF-7 cells. MCF-7 cells were treated for 72 h with a vehicle or the indicated compounds. After the required incubation period, cells were fixed in 1 mL ethanol and 100 µL PBS and stained with propidium iodide. Cells were subsequently analysed by flow cytometry to determine the percentage of (**A.**) apoptosis, as assessed by quantification of the pre-G1 peak and (**B.**) G2/M-arrested cells. Values represent the mean ± S.E.M. of three independent experiments.

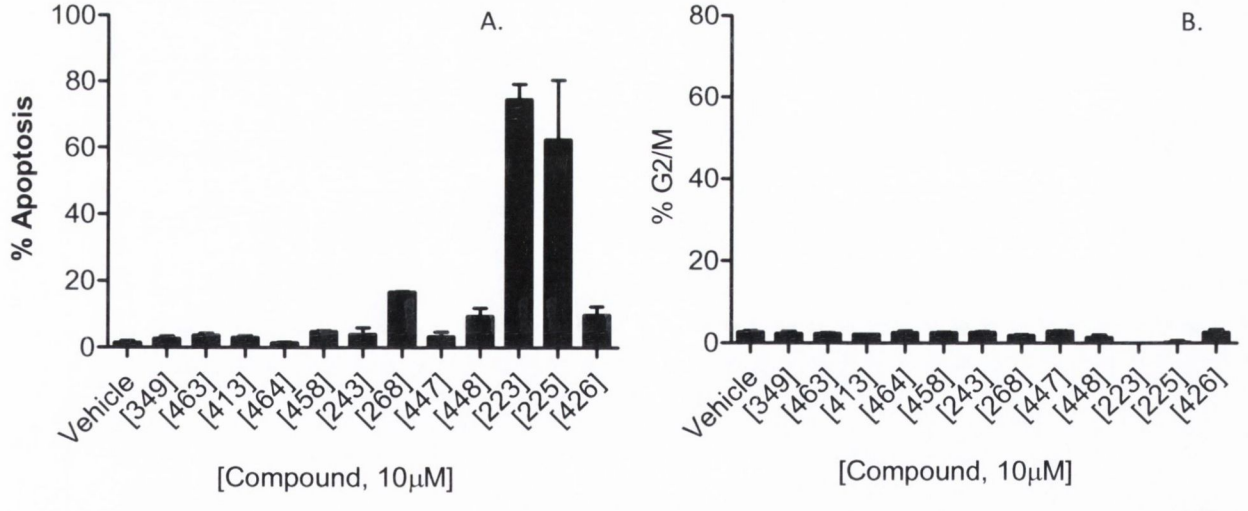

Figure 6-16 The majority of tested compounds do not induce apoptosis in blood cells from healthy donors. Peripheral blood mononuclear cells from healthy donors (n=2) were treated for 72 h with a vehicle or the indicated compounds. After the required incubation period, cells were fixed in 1 mL ethanol and 100 µL PBS and stained with propidium iodide. Cells were subsequently analysed by flow cytometry to determine the percentage of (**A.**) apoptosis, as assessed by quantification of the pre-G1 peak and (**B.**) G2/M-arrested cells.

6.1.5 Biochemical data for the NF-κB study

In the antiproliferative assay for indole based compounds, the compounds synthesised for this study all contained the 2-phenylindole ER type structure ligand. However, as these novel ligands were designed as anti-inflammatory compounds, it was not expected that they would display high levels of anti-proliferative activity. An addition compound [271] which was evaluated in previous section (IC_{50} = 6.6 μM) was also used for this study. The antiproliferative activity for the compounds tested in this series were generally in the low to moderate micromolar region (IC_{50} = 3.5 – 41.0 μM) with the exception of [296] which displayed much lower antiproliferative activity (IC_{50} = 332 μM). From the compounds screened, the two *bis*-indole compounds displayed the greatest activity ([271] with an IC_{50} = 6.6 μM, and [297] with an IC_{50} = 3.5 μM) in MCF-7 cell line with the most active compound, [297], exhibiting slightly lower potency than tamoxifen (IC_{50} = 2.13 μM). Overall, the compounds had a varying effect on cell viability although none of the compounds displayed high levels of cyctoxicity, this is not unexpected as the compounds are designed as potential anti-inflammatory agents and are not required to be highly cytotoxic to cells.

Compound	Structure	MCF-7 IC_{50} (μM)	CLogP
[292]	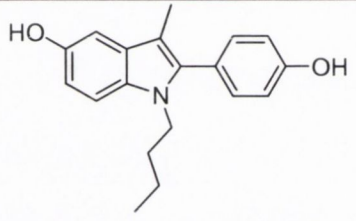	34.0	5.40
[293]	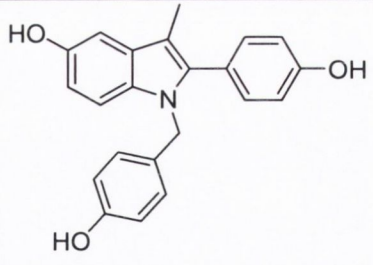	38.9	4.91
[294]	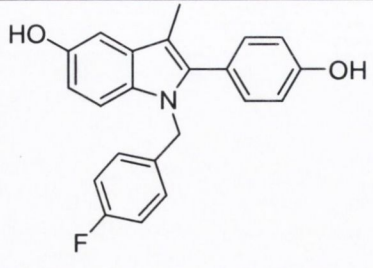	41.0	5.73

[295]	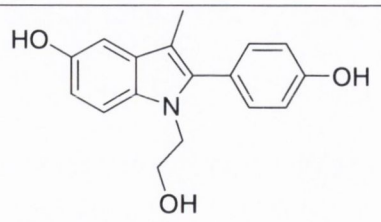	17.7	2.98
[296]	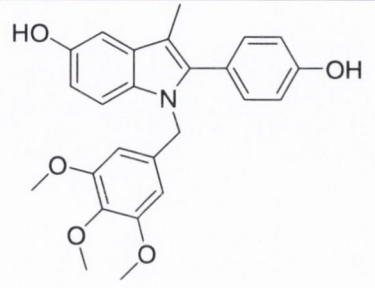	332	4.88
[297]	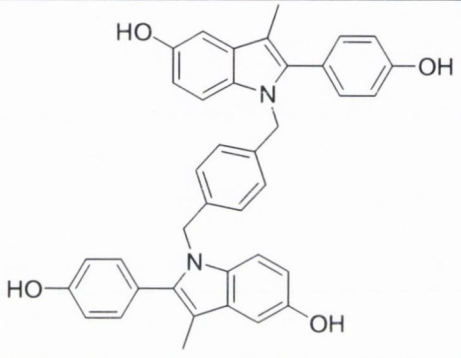	3.5	9.03

Table 32 Antiproliferative data for the selected compounds synthesised for the NF-κB study

6.1.5.1 ER-binding assay

In Table 33, the ER binding IC_{50} values for both ER isoforms (ERα and ERβ) are displayed for the selected compounds for the NF-κB study. The selectivity value is reported as the ratio of RBA values or binding affinities, ERα relative to ERβ, for each of the compounds (see Table 33). For selectivity values greater than 1, the compounds have a more pronounced affinity for ERα binding site, while for values less than 1, the compounds have a more pronounced affinity for the ERβ binding site.

All the compounds screened exhibited low nanomolar binding activity in both ER isoforms with the exception of [296] and [297] which displayed strong selectivity towards ERβ. Compound [294] exhibited the highest affinity for binding to both ERα (IC_{50} = 15 nM) and ERβ (IC_{50} = 58 nM) with slight selectivity towards ERα. Compound [297] displayed the most pronounced selectivity towards ERβ (RBA = 0.01) between the two ER isoforms.

Compound	ER α IC_{50} (nM)	ER β IC_{50} (nM)	ERα/ERβ Selectivity
[292]	18	44	2.44
[293]	24	35	1.46
[294]	15	58	3.86
[295]	19	50	2.63
[296]	1224	40	0.03
[297]	8900	115	0.01
[271]	65	302	4.65
Estradiol	1.7	3	1.76

Table 33 ERα and ERβ binding data for the novel compounds selected for the NF-κB study

6.1.6 NF-κB assay

Experiments were carried out by Jade Pollock, School of Biochemistry and Immunology, TCD. Chronic inflammation is linked to the progression of many diseases including IBD and cancer. Cellular events associated with this inflammation include the infiltration of immune cells which increases the inflammatory response. The transcription factor NF-κB is a key player in mediating the inflammatory response. Genes encoding cytokines, chemokines and acute phase proteins are regulated by NF-κB. This important transcription factor can be activated in the cell by a variety of extracellular signals such as oxidative stress and cytokines. NF-κB is composed of homodimeric and heterodimeric complexes of the Rel family of proteins p65 (Rel A), p50/105, c-Rel, p52/100 and Rel B. It is found in a non-active state in the cytoplasm of the cell, where is it bound by IκB. IκB is degraded in response to extracellular inflammatory signals, allowing the translocation of NF-κB to the nucleus of the cell. Non-selective estrogens such as E2 are known to have anti-inflammatory activity, which has been linked to the inhibition of NF-κB activity.

To explore a potential role for these novel ER ligands in the inhibition of NF-κB MCF-7 breast cancer cells were transfected with an NFκB reporter gene. Following transfection cells were treated with a range of concentrations of [297] for 6 hours at 37°C. After treatment, cells were lysed for 15 minutes and the resulting supernatants were analysed for renilla (a control to show cell viability) and luciferase (showing NF-κB activity) levels.

Figure 6-17 shows that after treatment with the novel ER ligand [297], there was a decrease in NF-κB activity above 10 μM. This decrease can be attributed to the treatment with the ligand as

renilla values remained the same for all treatments, showing cell viability was not affected. The increase in concentration from 1 to 100 μM shows an 87% decrease in the NF-κB activity. It would be necessary to extend the range of concentrations of ER ligand to investigate the effect of lower concentrations of the ligand on NF-κB activity. This result seems promising but there is still much to investigate.

The other compounds [271] and [292]-[296] that were also evaluated for inhibition of NF-κB activity however the results from this assay exhibited conflicting results and did not give a clear indication of the activity of the compounds. These compounds are to be re-evaluated to get a true determination to what extent these compounds are affecting the NF-κB activity.

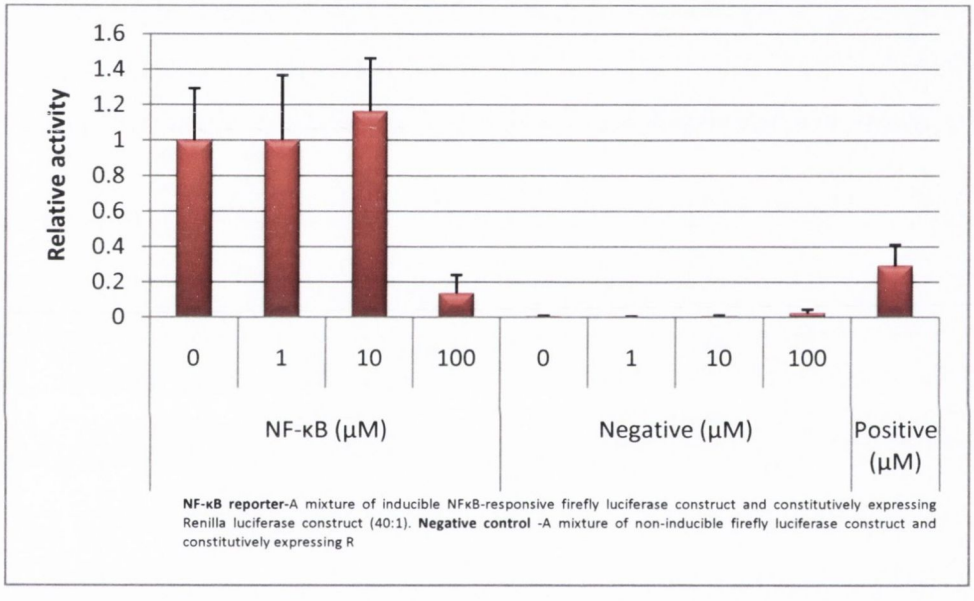

Figure 6-17 Inhibition of NF-κB activity after treatment with novel ER ligand [297]. MCF-7 breast cancer cells cultured as previously described and transfected with NF-κB reporter for 24 hours, after which the cells were treated with compound [297] for a further 6 hours. Cells were treated in triplicate with three concentrations of the compound (1, 10 and 100 μM). n=1.

The inhibition of NF-kB transcriptional activity by estradiol bound to the nuclear receptors ERα or ERβ has been well documented. Effects on selective expression of NF-κB have been reported for some ER ligands. NF-κB can function as a tumour promoter in inflammation associated cancer. Therefore the identification of selective ligands for the ER has been sought, which would retain the beneficial outcomes of estrogen therapy, while eliminating the unwanted side effects. This nonclassical anti-inflammatory activity of estrogen has been attributed to interference of NF-κB activity. Chadwick *et al.* reported that a known pathway-selective estrogen receptor (ER) ligand, WAY-169916 [465] does not promote the classic actions of estrogens such as stimulation of uterine proliferation or ER-mediated gene expression, but is a potent anti-inflammatory agent.[488] The

selective inhibition of NF-κB activity by the [297] may have potential therapeutic uses in the treatment of inflammatory diseases.

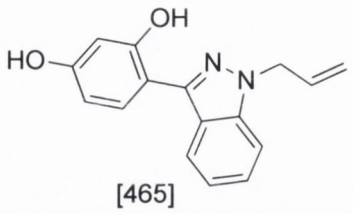

[465]

Figure 6-18 WAY-169916 [465]

6.2 Molecular modelling studies

6.2.1 Modelling method

Molecular modelling studies were a fundamental part of the project from preliminary design work to retrospective study. In recent years, research on the estrogen receptor, has provided a diverse variety of crystal structure determinations of both agonists and antagonists bound to both ERα and ERβ.[81] The interaction of SERMs within the estrogen receptor is highly complex. Research involving molecular modelling studies help approach a solution to the 'puzzle' of the SERMs (and SERM subtype) molecular mode of action.[97] This section outlines some of the modelling techniques used to obtain structural information at a molecular level and allow for correlation and explanation of the relationship between structure and activity of the compounds studied in this thesis.

In this study, when modelling the compounds synthesised in the project, consistent molecular modelling strategies were used. The lowest energy conformer of a compound was created and a set of conformers were generated and then this set of conformers was docked and scored to determine the highest ranking docked solution. The software package MOE (Molecular Operating Environment)[556] is used for docking. MOE is a software system designed by the Chemical Computing Group to support Cheminformatics, Molecular Modelling, Bioinformatics, Virtual Screening and Structure-based-design.

6.2.2 Ligand binding site

The molecular basis of estrogen receptor agonism and antagonism has been well reported.[81, 97, 557] Within the binding site of ERα and ERβ, ligand recognition is achieved through a combination of specific hydrogen bonds and Van der Waals interaction together with the complementarily non polar character of the binding cavity amino acid residues with the relevant ligand. To date, different agonists and antagonists have been co-crystallised with 34 human ERα isoforms, 15 human ERβ isoforms and 2 rat ER isoforms[81, 97] (see table Table 34).

Estradiol, the main endogenous ER ligand, possesses a phenolic hydrogen on the A-ring of its structure which interacts in the human ERα isoform through direct hydrogen bonds to the carboxylate of Glu 353, the guanidinium group of Arg394, and a water molecule. The 17-β hydroxyl of the D-ring makes a single hydrogen bond interaction with His 524 in the LBD. The remainder of the molecule participates in hydrophobic contacts that are concentrated over the A, A/B interface and D-rings. A mixture of the specific polar and non-polar interactions within the LBD allow the ER to selectively recognize and bind estradiol with sub-nanomolar affinity over the large and varied range of endogenous steroids.[100] The ER's ability to bind an array of ligands can be attributed to the size of the cavity, which has a probe accessible volume of 450A°^{3} which is nearly twice that of estradiol's molecular volume (245 A°^{3}). Other ligands that can mimic these characteristic attributes of estradiol tend to bind favourably to the ER (Figure 6-19).

PDB code	Ligand	Protein
1ERE.pdb[100]	Estradiol	hERα
3ERT.pdb[102]	4-hydroxytamoxifen	hERα
1QKN.pdb[558]	Raloxifene	rERβ
1HJ1.pdb[104]	ICI 164,384	hERβ
1ERR.pdb[100]	Raloxifene	hERα
1SA0.pdb[559]	Colchicine	Tubulin
3EQM.pdb[560]	4-Androstene-3-17-dione	Aromatase

Table 34 Crystal structure codes with corresponding ligand and protein

Antagonistic ligands, such as 4-hydroxytamoxifen and raloxifene, have molecular characteristics similar to estradiol such as the phenolic groups which partake in direct hydrogen bonding with the same key residues in the ER (i.e. Glu353, Arg394 and His524 in human ERα). In addition, antagonists commonly contain a side chain amine ether which is too large to be accommodated in the binding cavity which causes a displacement of the Helix-12 in the protein structure. The nature of the ligand effects can be determined by the ability to displace the Helix-12 positioning. When the estradiol ligand is bound within the LBD, the Helix-12 sits snugly over the LBD. The estradiol does not interact with the Helix-12 allowing for formation of a complete AF-2 region that facilitates the recruitment of coactivators and precedes to transcriptional activation which results in ER agonism. However, in the case of the antagonists, the Helix-12 is displaced by the amine side chain, stopping the formation of a complete AF-2 region, hence disrupting the coactivator recruitment and leading to corepressor recruitment resulting in ER antagonism.

In Figure 6-19 and Figure 6-20, the important binding residues are shown for agonist (estradiol: 1ERE.pdb)[100] and antagonist (4-hydroxytamoxifen: 3ERT.pdb)[102] ligands in their respective human ERα binding pocket.

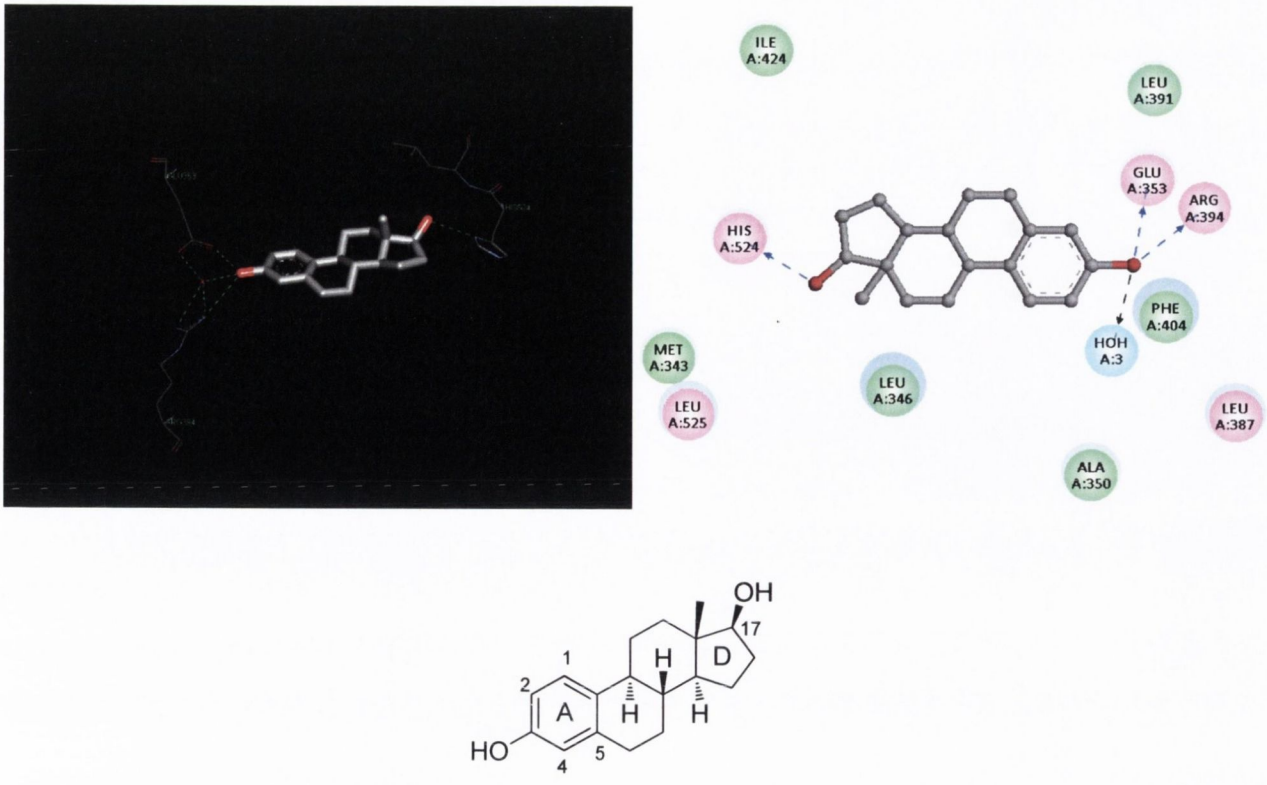

Figure 6-19 Estradiol agonist in the human ERα ligand binding domain, 1ERE.pdb. Images rendered using Discovery Studio® visualizer software

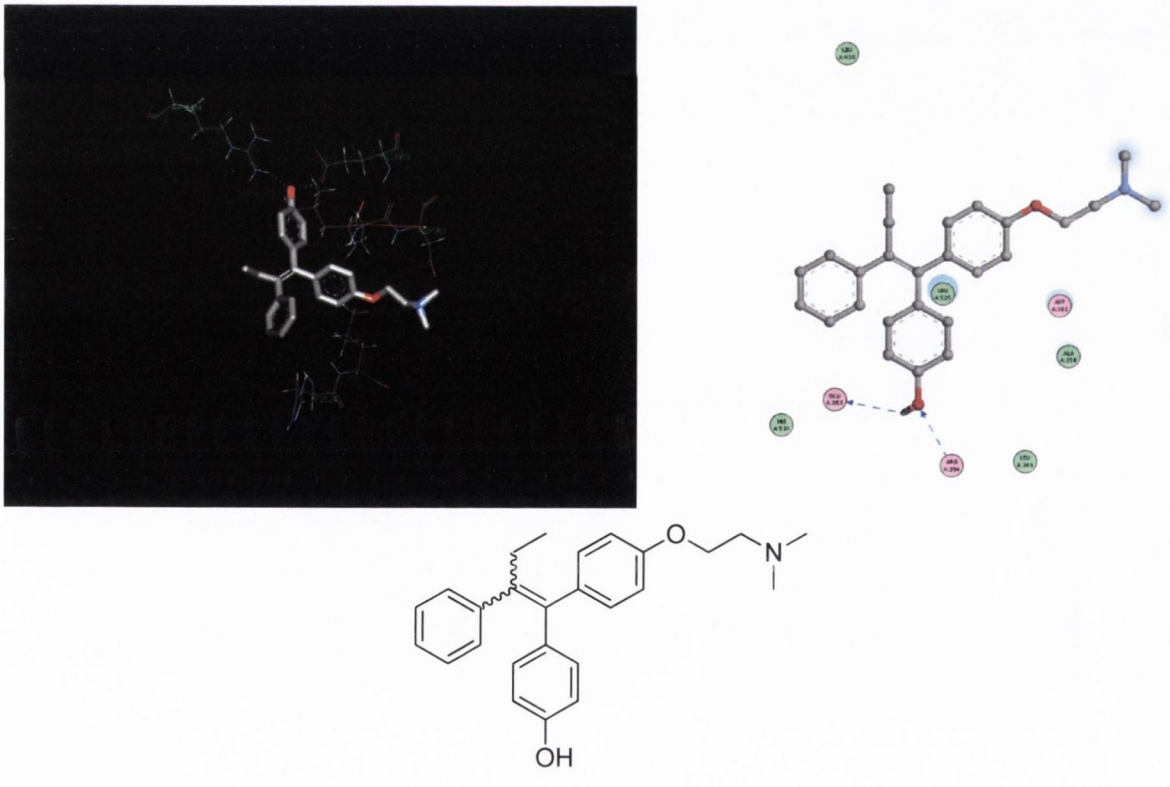

Figure 6-20 4-Hydroxytamoxifen antagonist in the human ERα ligand binding domain, 3ERT.pdb. Images rendered using Discovery Studio® visualizer software

The interaction of the antagonist side chain with Asp351 residue varies amongst ligands. Raloxifene displays (Figure 6-21) a tight interaction between the Asp351 residue and piperidine ring nitrogen through hydrogen bonding (2.66 Å) (1ERR.pdb[100] and 1QKN.pdb[558]) The interaction between the nitrogen of 4-hydroxytamoxifen and Asp351 is not direct but can be facilitated through a salt bridge between the dimethylamino group of the side chain and the β-carboxylate of Asp-351, which lies at a distance of 3.8 Å away.[102] The ICI 164,384 side chain, unlike the corresponding regions of raloxifene and 4-hydroxytamoxifen, is not tethered to the LBD through an interaction with Asp258 (1HJ1.pdb[104], Figure 6-22). With ICI 164,384, the increased length and resultant positioning of the bulky side chain extension compared to AF2 antagonists such as raloxifene, is probably responsible for the displacement of H12.[104] Co-crystallised ICI 164,384 and ERβ have been produced with rat ERβ-LBD (rERβ-LBD) however no crystal structure has been solved in hERβ-LBD. The Asp258 residue in rERβ corresponds with Asp351 in hERβ-LBD, this is discussed later in this chapter. A crystal structure of rat ERβ-LBD (rERβ-LBD) complexed with ICI 164,384 is shown to represent the interaction expected with the hERβ.

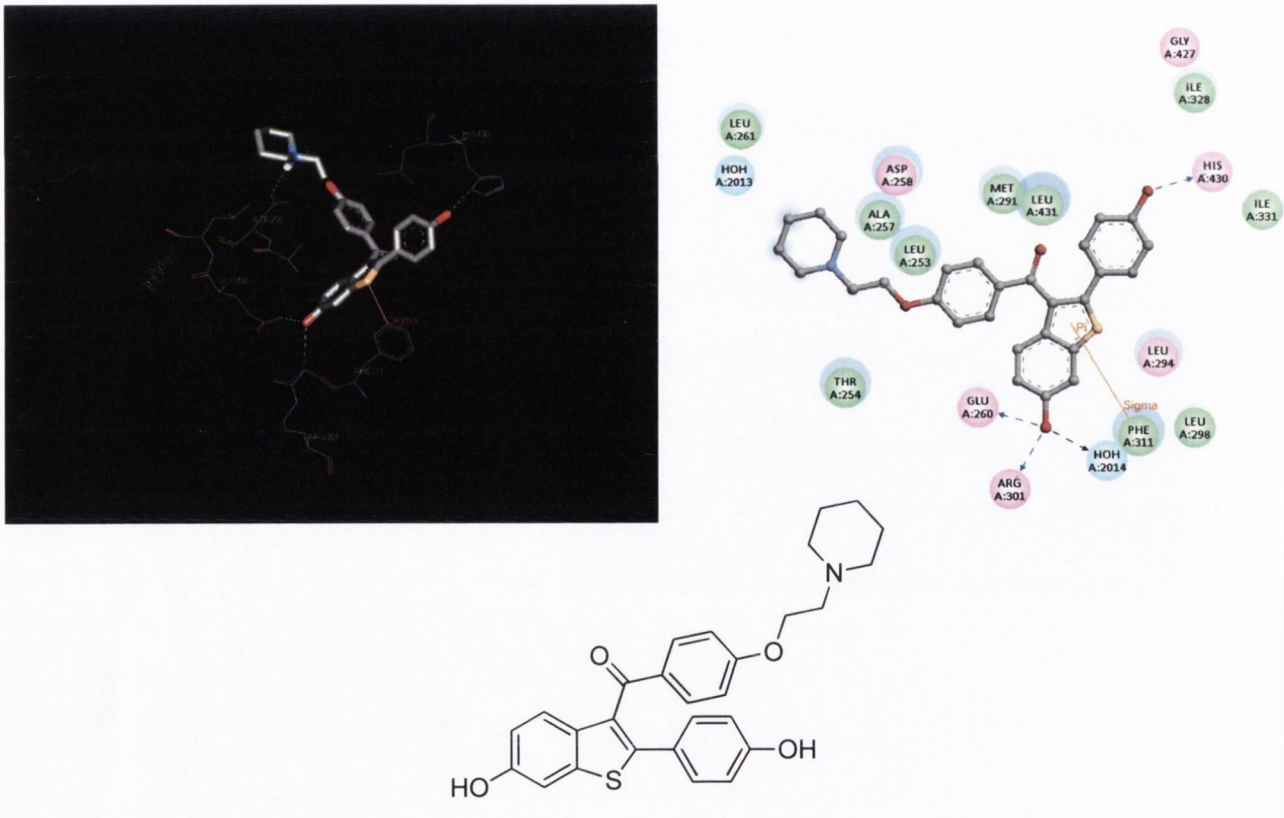

Figure 6-21 Antagonistic side chain interaction of raloxifene in rERβ (1QKN.pdb)

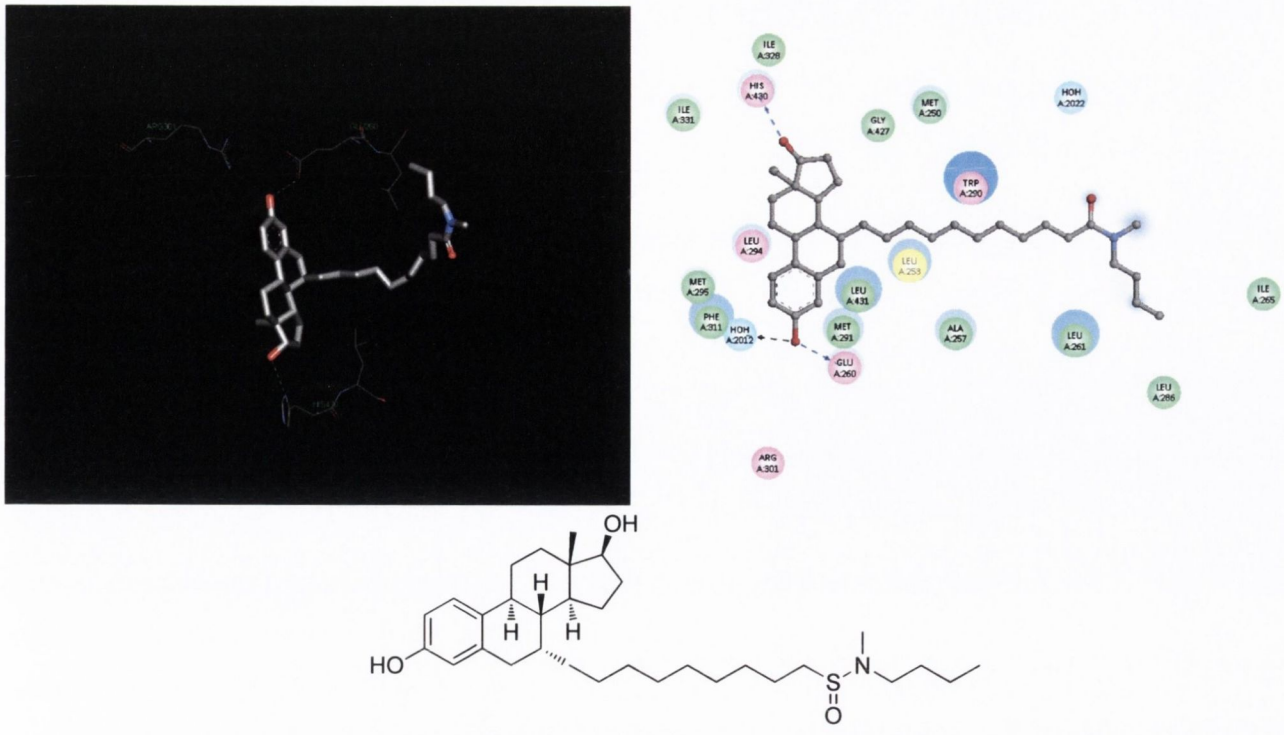

Figure 6-22 Antagonistic side chain interaction of ICI 164,384 (B) within the rERβ LBD (1HJ1.pdb)

ERα and ERβ exhibit a high degree of sequence identity (56%) in the LBD and adopt very similar 3D structures.[81, 97] The residues that directly surround the ligand are quite similar with only two conservative changes among the approximately 20 residues. In ERα where Leu384 and Met421 resides, Met336 and Ile373 are present in ERβ respectively. As the ligand cavity homologies are very similar, both ERα and ERβ have a tendency to bind compounds with similar affinities. However, these two slight changes with the cavity together with differences in distant regions of the LBD allow for ligand selectivity.

Compared with agonists, there is a lack of antagonistic ligands co-crystallised in any human, rat or any other species of the ERβ ligand binding site. Two antagonists – raloxifene (1QKN.pdb)[558] and ICI-164,384 (1HJ1.pdb)[104] have been co-crystallised in rat ERβ LBD. The LBD of the rat and human ERβ are highly conserved. Five key ERβ residues of the human ERβ isoform found in the rat isoform (see Table 35).

Residue in human	Residue in rat
Glu305	Glu260
Arg346	Arg301
His475	His430
Met336	Met291
Ile373	Ile328

Table 35 Correlation of key binding residues in human and rat ERβ isoforms

6.2.3 Docking studies

An example of each of the analogues synthesised in this project were modelled *in silico* in order to gain an insight into the most probable binding orientation within the human ERα and human/rat ERβ isoforms and to rationalise findings from the biochemistry assays. All of the analogue ligands were docked in one of the following crystal structures, 3ERT.pdb (4-OHT bound in hERα), 1ERR.pdb (RAL bound in hERα), 1HJ1.pdb (ICI 164,368 bound in rERβ) or 1QKN.pdb (RAL bound in rERβ). The crystal structure that was used depended on the conjugate that was been modelled. For example, the endoxifen analogue ligands were docked using 3ERT.pdb as the 4-OHT ligand would allow for the accurate comparison in docking study.

The dockings was performed using MOE 2012.10 software.[556] All parameters were kept at default unless stated otherwise. The initial and final energy of protein were calculated (in kcal/mol) by GizMOE using MMFF94X force field with conjugant gradient method. The docked ligands were drawn in MOE and conformers were not created as the ligands were not docked as rigid molecules. The docking protocol was set as 'Rigid Receptor' and a pharmacophore was used in most cases. The placement method used was Triangle Matcher with the rescoring function of London dG. This was subsequently refined using the refinement of Forcefield with a rescoring function of GBVI/WSA dG. The docking protocol was set to keep 30 docking poses only. The resulting docked compounds were then visualised using Discovery Studio Visulizer.[561]

6.2.3.1 Molecular docking results for the combretastatin -endoxifen conjugate [414]

Compound [414] was docked in 3ERT.pdb[102] and the top ranking docked conformation is shown in Figure 6-23. The Glu353 and Arg394 residues form hydrogen bond interaction *via* a water bridge to the phenol on the endoxifen ligand part of the conjugates. This interaction is key to the binding in the estrogen receptor and is seen with 4-OHT and estradiol. The orientation of the ER ligand part of the molecule [414] overlaps very well the 4-OHT ligand in ERα LBD (Figure 6-24) which indicates that the conjugates still posses the ability to bind in the ER. The combretastatin fragment occupies the vacant space left by the displaced Helix-12 snugly, however, no interaction is observed with Asp351. Within the space occupied by the combretastatin fragment there are a network of nitrogen containing residues. The presence of water molecules could allow for a network of H-bonding to extend within this LBD area and lead to favourable interaction. When this docking is used to rationalise the ER binding activity (ERα IC_{50} =282 nM and ERβ IC_{50} = 436 nM) seen by another compound [426] within this family it is possible to see that this type compound can comfortably occupy the ER binding site. The interactions observed from the molecular modelling could potentially rationalise the low nanomolar ER binding activity.

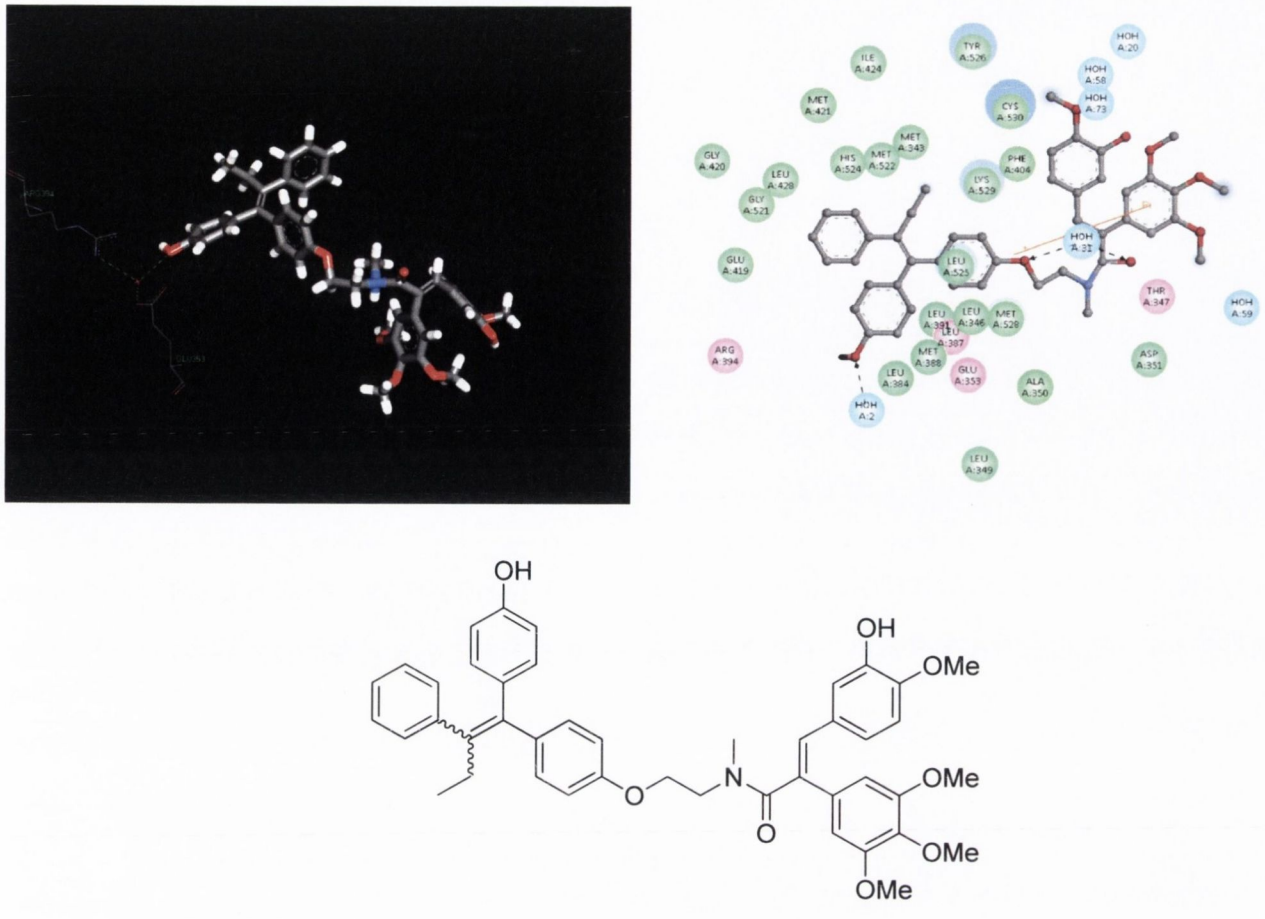

Figure 6-23 Top-ranking docked conformation of [414] in ERα, 3ERT.pdb. The docked confirmation is coloured by element type (carbon = grey, hydrogen = white, oxygen = red, nitrogen = blue)

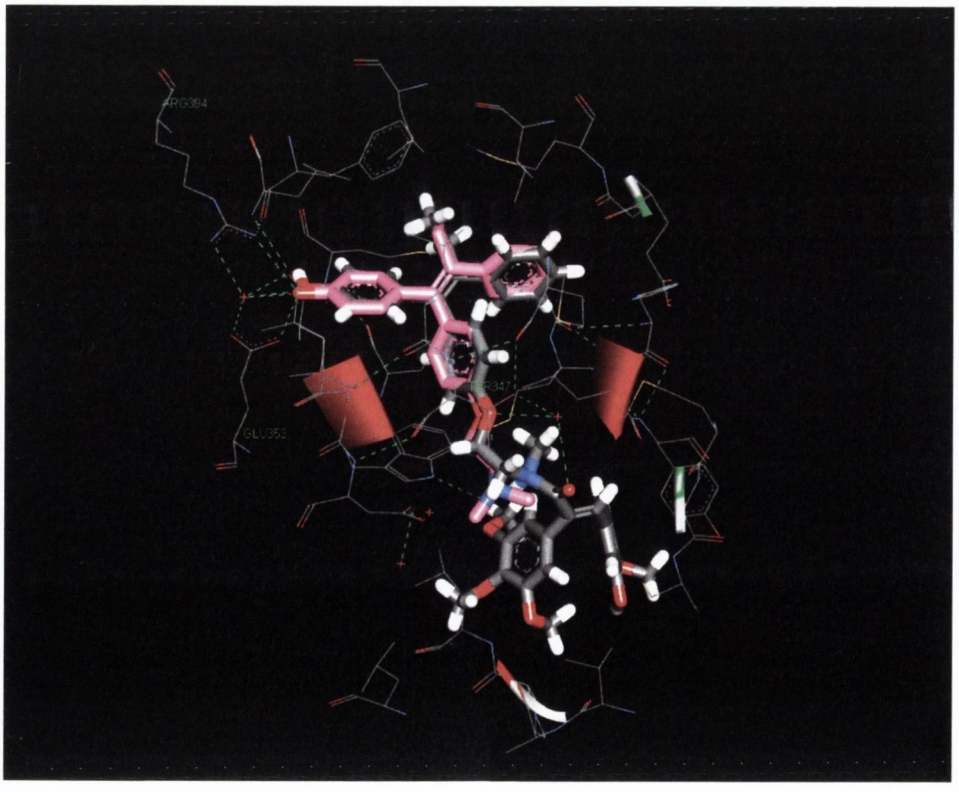

Figure 6-24 Superposition of 4-OHT (pink) and [414] (grey) docked conformations in ERα (3ERT.pdb)

6.2.3.2 *Molecular docking results for the structurally modified combretastatin-endoxifen conjugate [436]*

Compound [436] was docked in the LBD of ERα, 3ERT.pdb[102] and the top ranking docked conformation is shown in Figure 6-25, the Glu353 and Arg394 ER residues form hydrogen bond interactions to the phenol on the endoxifen ligand part of the conjugate. Compound [436] was observed to dock in a similar orientation to that for [414]. The structurally modified combretastatin fragment occupies the vacant space left by the displaced Helix-12 and due to the lack of steric hindrance has the potential to reorient itself so that the phenol can form a hydrogen bond with the Asp351. This interaction could rationalise why [435] and [436] exhibited more potent antiproliferative activity when compared to the two trimethoxy conjugates [437] and [438]. Compound [436] can be seen in Figure 6-26 to bind in a similar manner to that of 4-OHT in the LBD of the ERα. The structurally modified combretastatin fragment seem to act as an extension of the side chain and potentially inhibits the Helix-12 from completing the AF-2 region, disrupting the coactivator recruitment and appears to lead to co-repressor recruitment resulting in ER antagonism effect. However for this series of compounds the antiproliferative activity (IC_{50} = 46 - >100 μM) was inferior than that seen by lead compound [414] (IC_{50} = 8.51 μM) and it suggests that the large CA4 type structure is required for the greater antiproliferative activity.

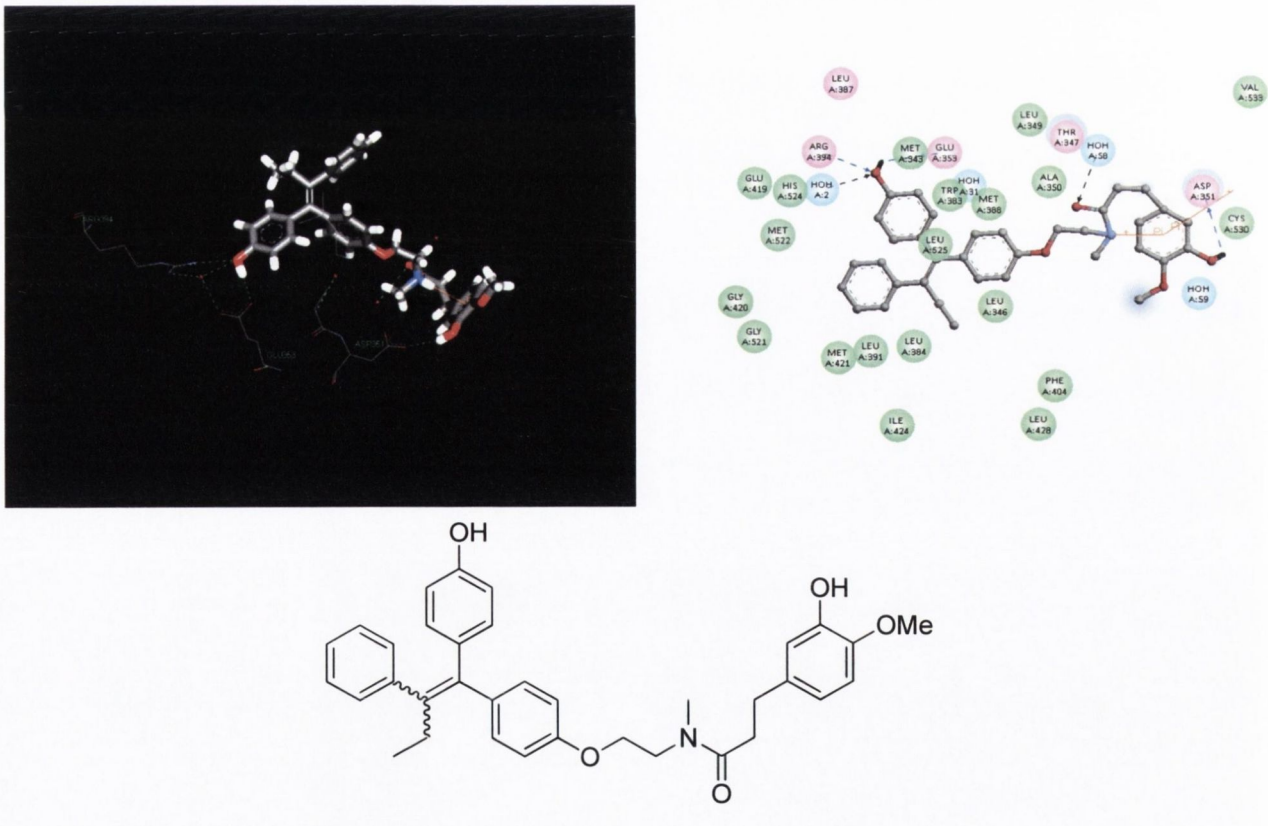

Figure 6-25 Top-ranking docked conformation of [435] in the LBD of ERα, 3ERT.pdb. The docked confirmation is coloured by element type (carbon = grey, hydrogen = white, oxygen = red, nitrogen = blue)

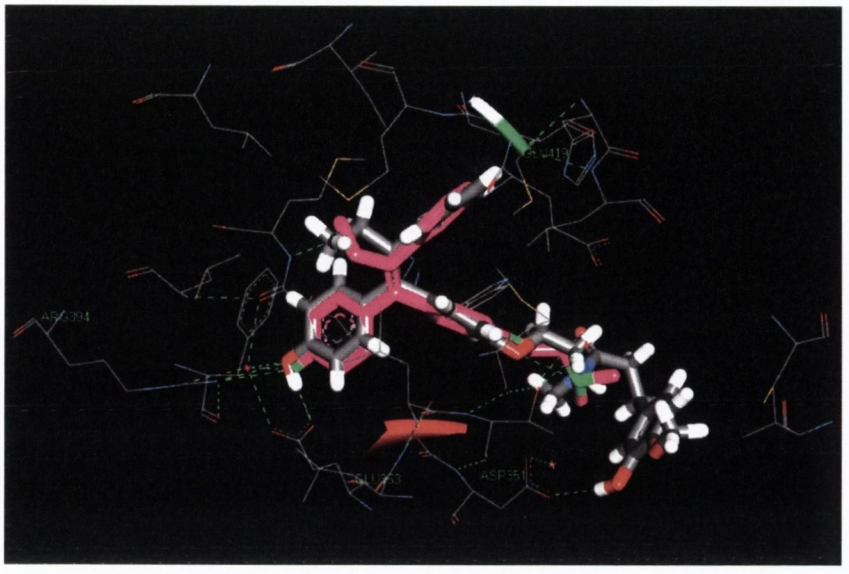

Figure 6-26 Superimposition of 4-OHT (pink) and [436] (grey) docked conformations in ERα, 3ERT.pdb

6.2.3.3 Molecular docking for the combretastatin-cyclofenil-based conjugates

The cyclofenil-CA4 conjugate [448] was docked in the ERα-LBD using 3ERT.pdb[102], as the orientation of its binding with the LBD of the ER was expected to be quite similar to that of 4-OHT. In Figure 6-27, the conjugate [448] shows hydrogen bond interaction with the Arg394 and Glu353 residues which are key for binding with the LBD of the ER. There is also additional interaction seen between the Asp351 *via* a water bridge to the carbonyl of the amide bond. This interaction with the Asp351 is known to disrupt the Helix-12 and could explain the antiproliferative activity of 182 nM seen for this conjugate. The most potent compounds [447] and [448] in this series both contained the bulkiest cycloalkane group. When examining the orientation of the docked [448], the cycloalkane is orientated to fill the free space close to the residues of Gly531, Met421, Ile424 and Met338 as shown in Figure 6-28. In this case the larger/bulkier the cycloalkane group, are the tighter it can bind within the area of free space and this could be why the two bulkier substituents exhibits more potent antiproliferative activity. The cyclofenil conjugates [447] and [448] exhibited very impressive ER binding activity with ERα IC_{50} =170 nM and ERβ IC_{50} = 112 nM for [447] and ERα IC_{50} =19 nM and ERβ IC_{50} = 229 nM) for [448]. The ER binding results observed would complement with the molecular modelling study. That this type of conjugate could occupy the binding of site and interact with the key residues essential for ER binding activity.

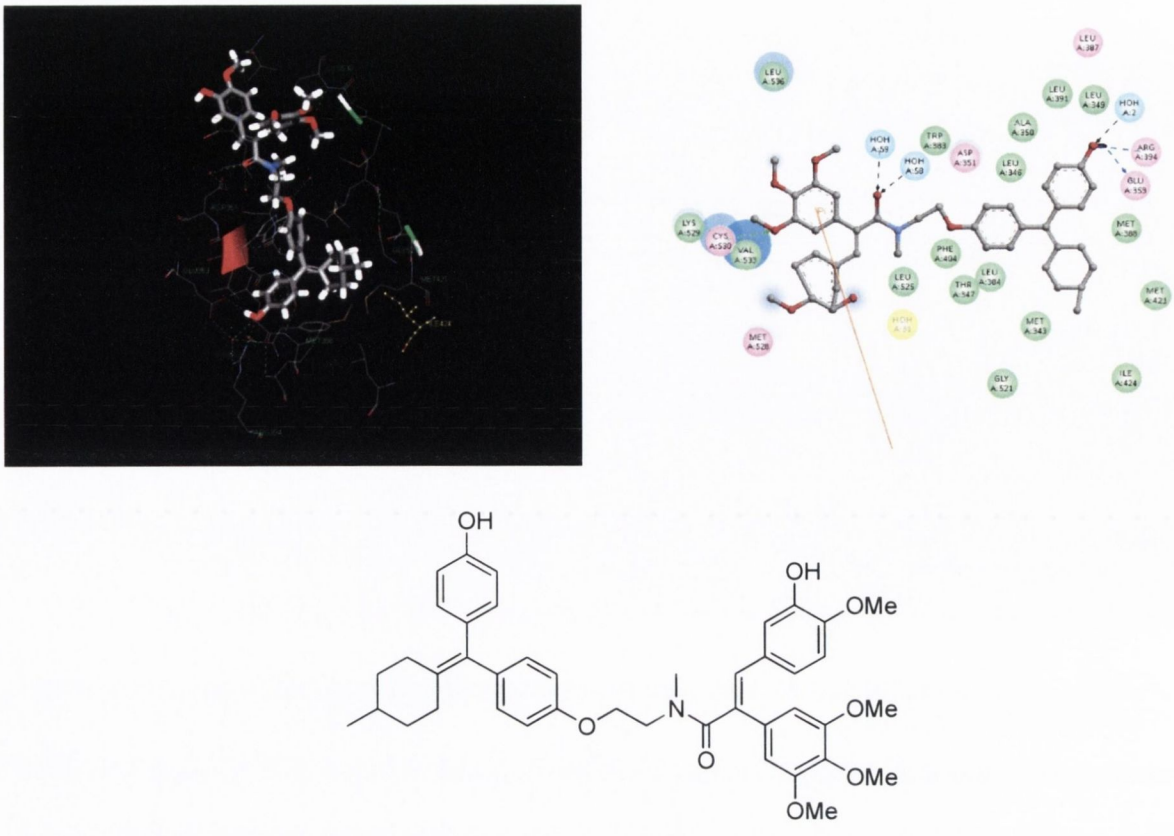

Figure 6-27 Top-ranking docked conformation of [448] in 3ERT (ERα). The docked confirmation is coloured by element type (carbon = grey, hydrogen = white, oxygen = red, nitrogen = blue)

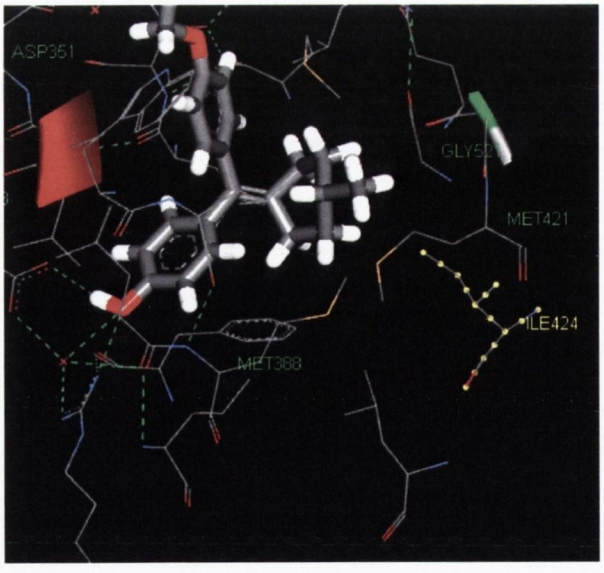

Figure 6-28 Orientation of [448] cyclofenil ligand fragment docked within the ERα

6.2.3.4 Molecular docking for the 2-phenylindole-based analogues

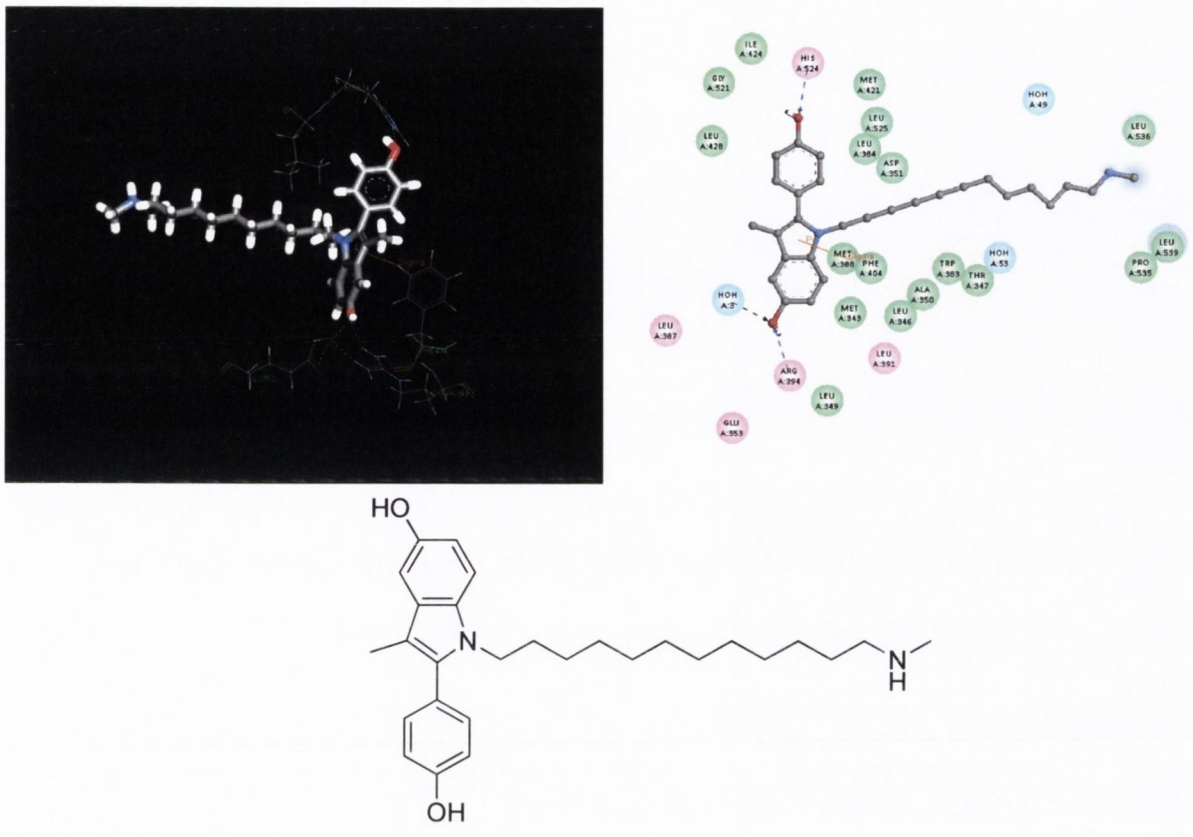

Figure 6-29 Top-ranking docked conformation of [243] in 1ERR, (ERα). The docked confirmation is coloured by element type (carbon = grey, hydrogen = white, oxygen = red, nitrogen = blue)

The ER ligand [243] containing the 2-phenylindole core was docked using in hERα cocrystallised with raloxifene (1ERR.pdb[100]). The 2-phenylindoles have more structural similarity with raloxifene that 4-OHT. It was also proposed that compound [243] should exhibit similar interaction seen for raloxifene. In Figure 6-29, the two phenols on the 2-phenylindole core form hydrogen bond interaction, one phenol interacting with Arg394 directly and to Glu353 *via* a water bridge interaction, and the other phenol seen to directly interact with the His524. These three interactions are also seen for raloxifene so it is proposed that [243] should bind within the LBD of the ER similarly. However, raloxifene also interacts with Asp351 which displaces the Helix-12, but this is not observed with [243]. The long chain of [243] should remain relatively straight with the LBD and the nitrogen is potentially too far away to allow this interaction. For this reason it was proposed that the side chain could potentially be acting similarly to that of ICI 164,384 which is a known full antagonist of the ER. Compound [243] was also docked with the cocrystalised ICI 164,384 with rERβ (1HJ1.pdb) to examine if the two long side chains would have similar positioning in the LBD. In Figure 6-30, the two ligands overlap very well and most importantly the two side chains are positioned in the same

region of the LBD. The long side chain of [243] could act in a similar mode to that of ICI 164,384 and distort the Helix-12. The similar bind and potential mode of action of [243] and ICI 164,384 may explain the large difference in activity between the 12 chain analogue [243] (IC_{50} = 158 nM) and the shorter chains analogues [241]-[242] and [261]-[262] (IC_{50} = 38-48 μM) of this series. The 2-phenylindole type ligands exhibited good ER binding activity with ERα IC_{50} = 380 nM and ERβ IC_{50} = 1660 nM for [243]. The 2-phenylindole core that is part of the ER type ligand scaffold and which is also contained within the bazedoxifene core structure can show selectivity towards the ER. The molecular modelling shows that the 2-phenylindole core interacts with the key residues required for binding and this could rationalise the good ER binding activity observed for [243].

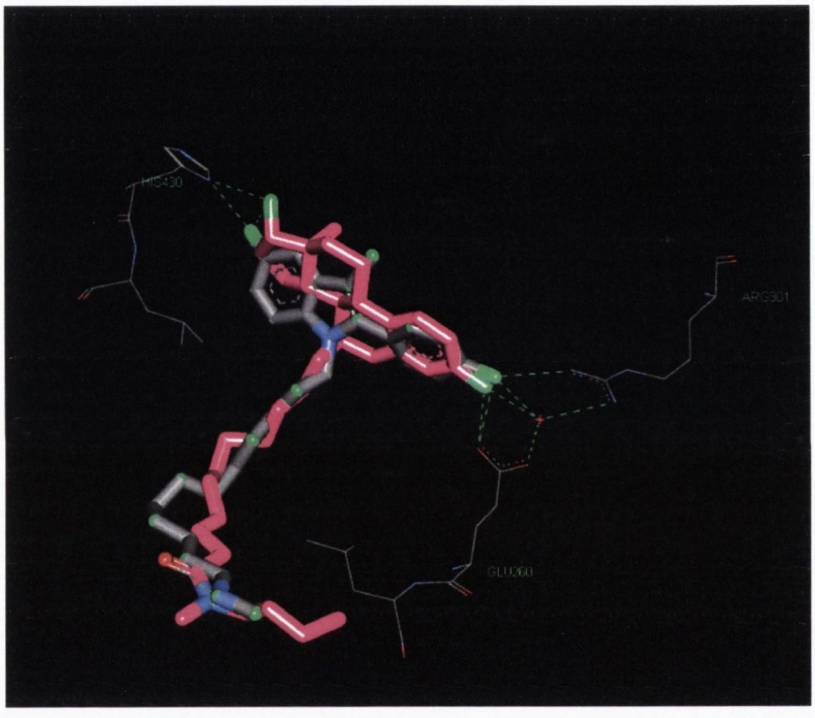

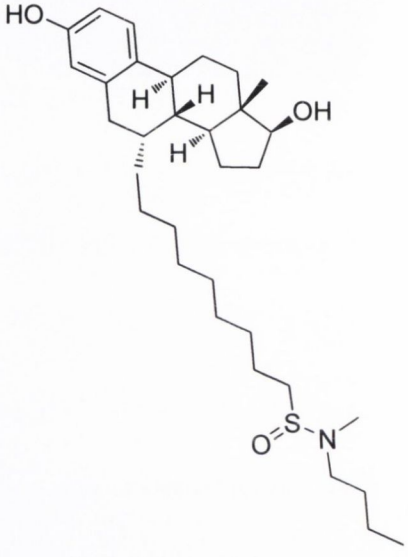

Figure 6-30 Superposition of ICI 164,384 (pink) and [243] (grey) docked conformations in ERβ 1HJ1.pdb

6.2.3.5 Molecular docking for the combretastatin-2-phenylindole-based conjugates

The top-ranked docked conformation for [458] exhibits the same characteristic binding in the LBD of ER as was seen for the compound [243] in 1ERR[100] and is shown in Figure 6-31. The 2-phenylindole core displays the same hydrogen bond interaction seen for raloxifene and [243] with the His524, Arg394 and Glu353 residues. In this case, the combretastatin fragment of the conjugates exhibits two addition π bond interactions with Tyr526 and Pro535. The hydrogen bond interaction can also be seen in the rERβ (1QKN.pdb[558], Figure 6-30) however in the ERβ LBD, no π-bond interactions were observed but an addition hydrogen bond interaction with Asp444 can be seen in Figure 6-32. The additional interactions seen with the combretastatin fragment in both ER isoforms suggests that the long chain with the bulky substituent would allow for strong binding interaction in the LBD. The ER binding results for [458] support this hypothesis with ERα IC_{50} = 574 nM and ERβ IC_{50} = 155 nM

observed. The good ER binding observed suggests that the 2-phenylindole core can interact with the required residues for strong ER binding activity.

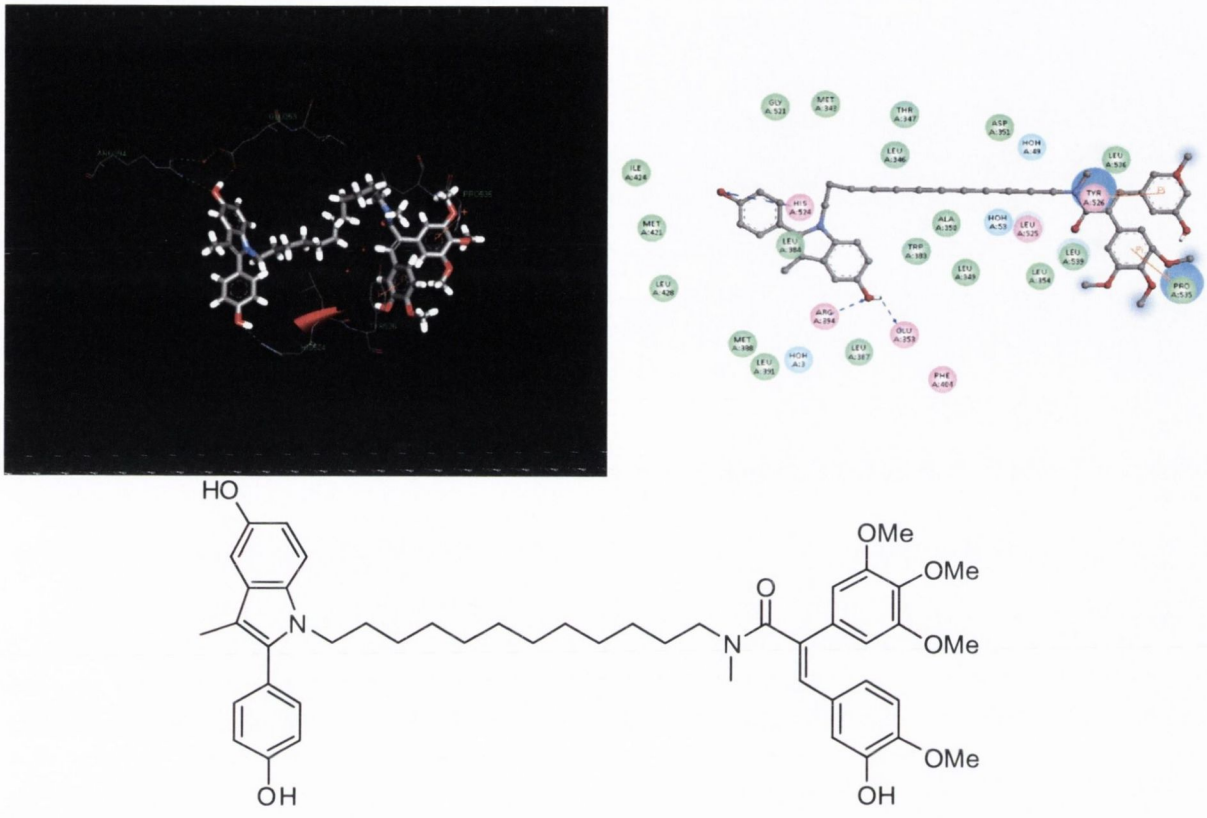

Figure 6-31 Top-ranking docked conformation of [458] in ERα, 1ERR.pdb. The docked confirmation is coloured by element type (carbon = grey, hydrogen = white, oxygen = red, nitrogen = blue)

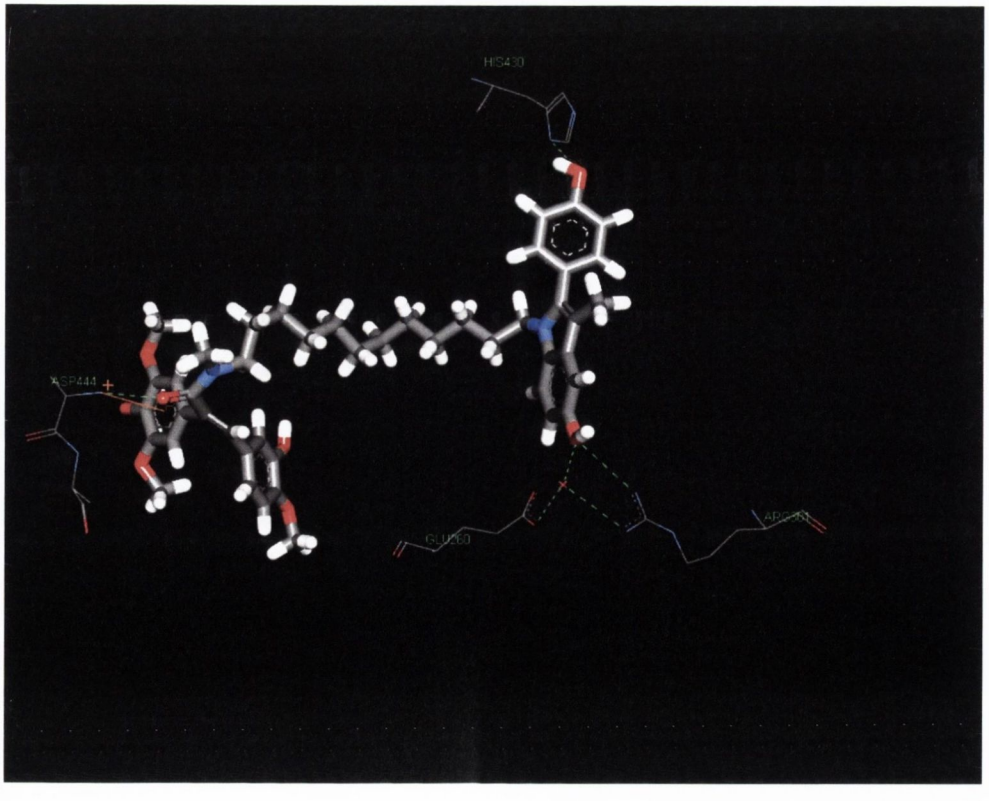

Figure 6-32 Top-ranking docked conformation of [458] in 1QKN (rERβ). The docked confirmation is coloured by element type (carbon = grey, hydrogen = white, oxygen = red, nitrogen = blue)

6.2.3.6 Molecular docking for bis-2-phenylindole-based analogues

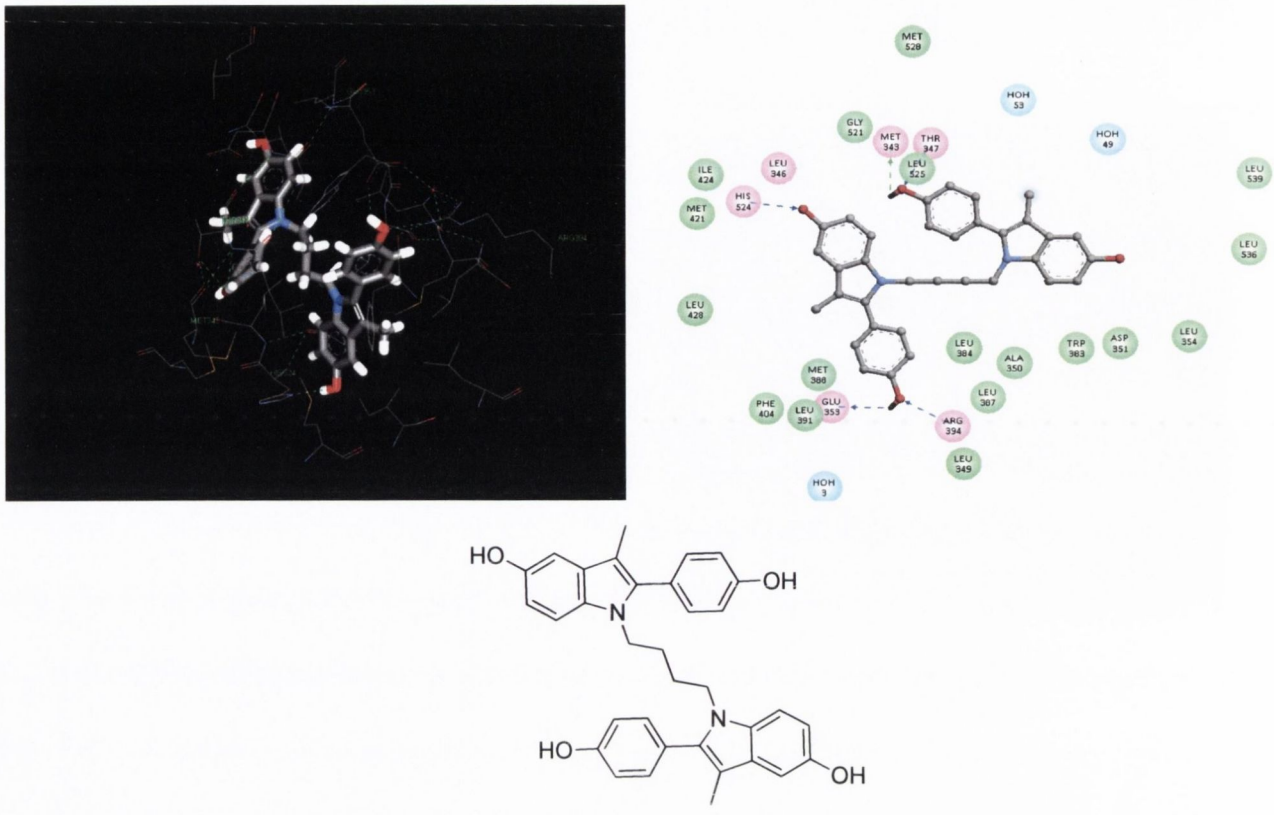

Figure 6-33 Top-ranking docked conformation of [268] in ERα, 1ERR.pdb. The docked confirmation is coloured by element type (carbon = grey, hydrogen = white, oxygen = red, nitrogen = blue)

For the docking studies of the bis-2-phenylindole analogue [268], the X-ray structure of the ERα (1ERR.pdb)[100] cocrystallised with the raloxifene was used. It was proposed that the bis-2-phenylindole analogues would bind with one of the 2-phenylindole with similar interaction as seen with raloxifene, anchoring the bis-compound in place with the linking chain having a close orientation to that seen by raloxifene. The other 2-phenylindole part of the molecule that was not involved in the binding to the Glu353, Arg394 and His524 was expected to potentially act as a large bulky group that could disrupt the Helix-12. When [268] was docked with raloxifene (shown in Figure 6-33), key binding interactions were observed with the Glu353, Arg394 and His524 residue. In addition interaction, to this the analogue was seen to form two additional hydrogen bonds with Met343 and Thr347 to the phenol on the second 2-phenyindole fragment. The additional hydrogen bonds should stabilise the analogue in the LBD of the ER. The compound was evaluated and was found to bind in the nanomolar region (ERα IC_{50} = 436 nM and ERβ IC_{50} = 41 nM) and the low micromolar antiproliferative activity (IC_{50} = 2.75 μM) observed.

6.2.3.7 *Molecular docking for the aromatase inhibitor (AI) containing conjugates*

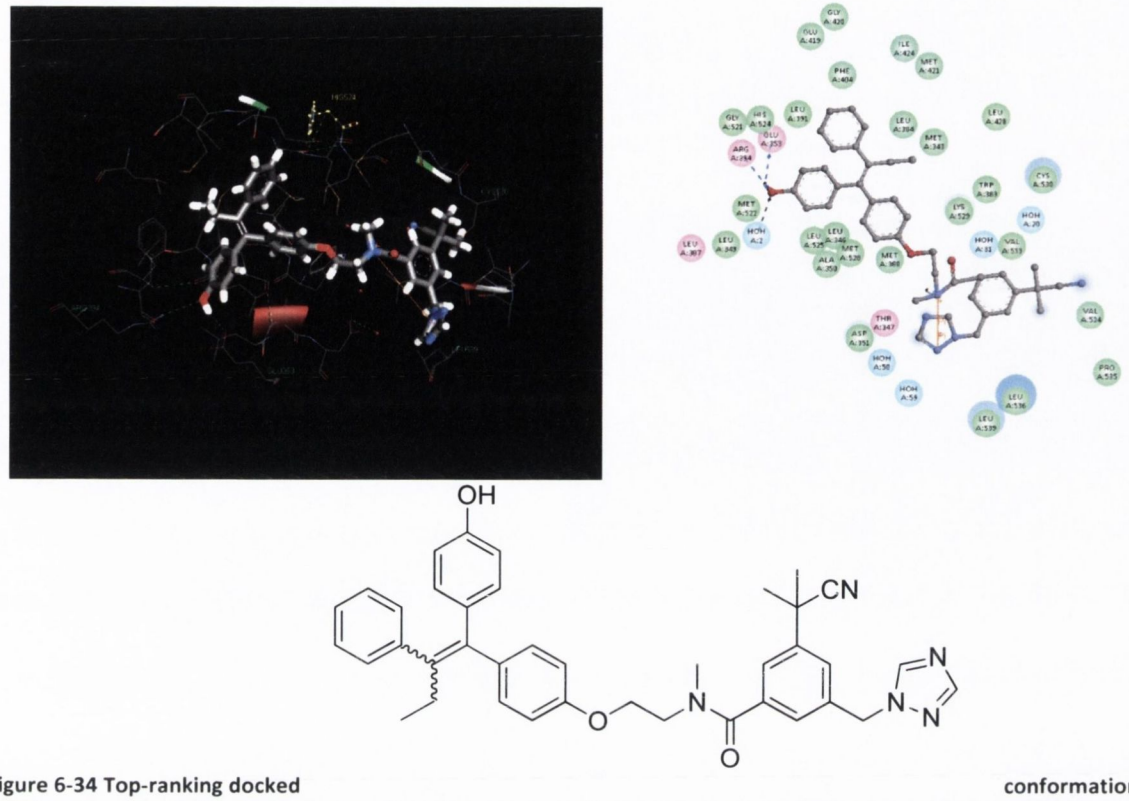

Figure 6-34 Top-ranking docked conformation of [463] in ERα, 3ERT.pdb. The docked confirmation is coloured by element type (carbon = grey, hydrogen = white, oxygen = red, nitrogen = blue)

The conjugate [463] was docked in ERα LBD using the 3ERT.pdb[102] as the orientation of its binding with the LBD of the ER was expected to be quite similar to that of 4-OHT (Figure 6-34). As seen with the previous endoxifen containing conjugates, the key interactions are also observed with [463]. The hydrogen bond interaction with the Glu353 and Arg394 are essential of the binding within the LBD of the ER. The anastrozole fragment does not exhibit any addition interaction within the LBD however and may act as a bulky group at the end of the side chain which protrudes out of the LBD and disrupts the Helix-12 and inhibits the cell proliferation. Compound [463] exhibited good ER binding activity with ERα IC_{50} = 2239 nM and ERβ IC_{50} = 245 nM and showed selectivity for ERβ of 0.11. The ER binding result could be rationalised with the molecular modelling study and confirms the molecular basis for the strong ER binding capability.

6.2.3.8 *Molecular docking results for the piperazine-acrylic acid scaffold*

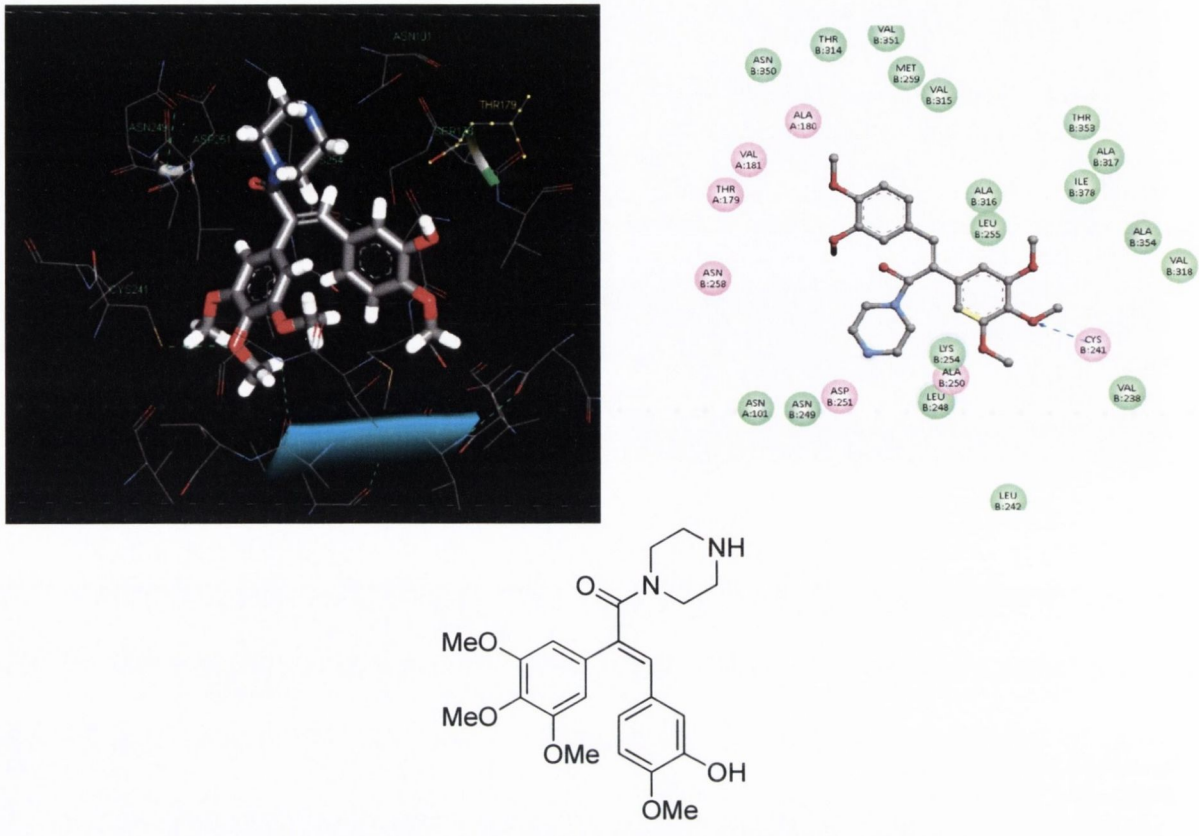

Figure 6-35 Top-ranking docked conformation of [349] in colchicine binding site of tubulin (1SA0.pdb). The docked confirmation is coloured by element type (carbon = grey, hydrogen = white, oxygen = red, nitrogen = blue)

In Figure 6-35, the binding orientation of [349] in the colchicine binding site of tubulin is illustrated. The 2D image displays the two phenyl ring in *trans* orientation but from the 3D structure on the left shows [349] docked in the *cis* orientation from which the 2D image was created. Compound [349] shows an interaction with the Cys241 residue which is a key hydrogen bond interaction for binding within the LBD. The hydrogen bond interaction was possible due to the near perfect overlap of the A-ring of colchicine and the A-ring of [349] shown in Figure 6-36. The B-ring of [349] can be seen to sit quite well where the methoxy and phenol substituents overlap with the methoxy and carbonyl substituents on the C-ring of colchicine. The piperazine rings is positioned in the free space between the Leu248, Asn101 and Ser178. The similarity of the docking pose of [349] to colchicine could rationalize the inhibition of tubulin polymerisation and the low micromolar activity seen for the antiproliferative activity of this compound.

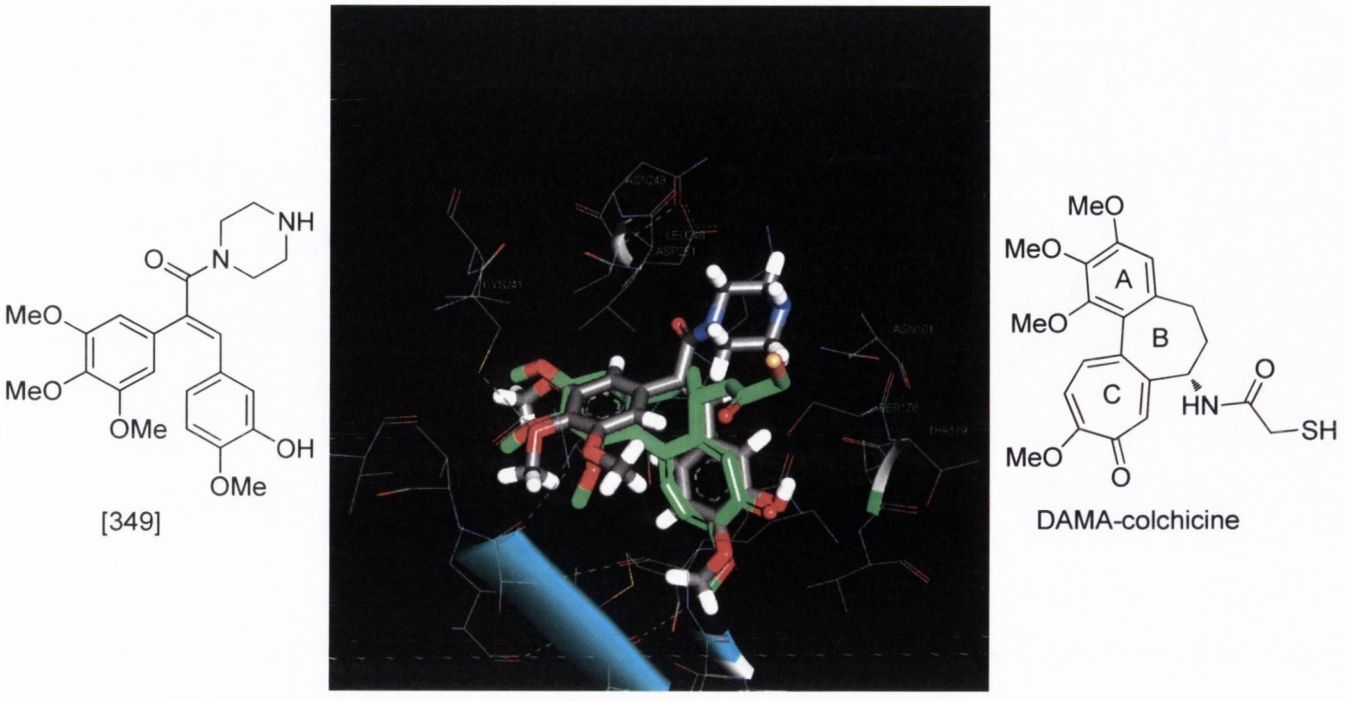

Figure 6-36 Superposition of DAMA Colchicine (green) and [349] (grey) docked conformations in tubulin (1SA0)

6.2.3.9 Molecular docking for the letrozole analogue

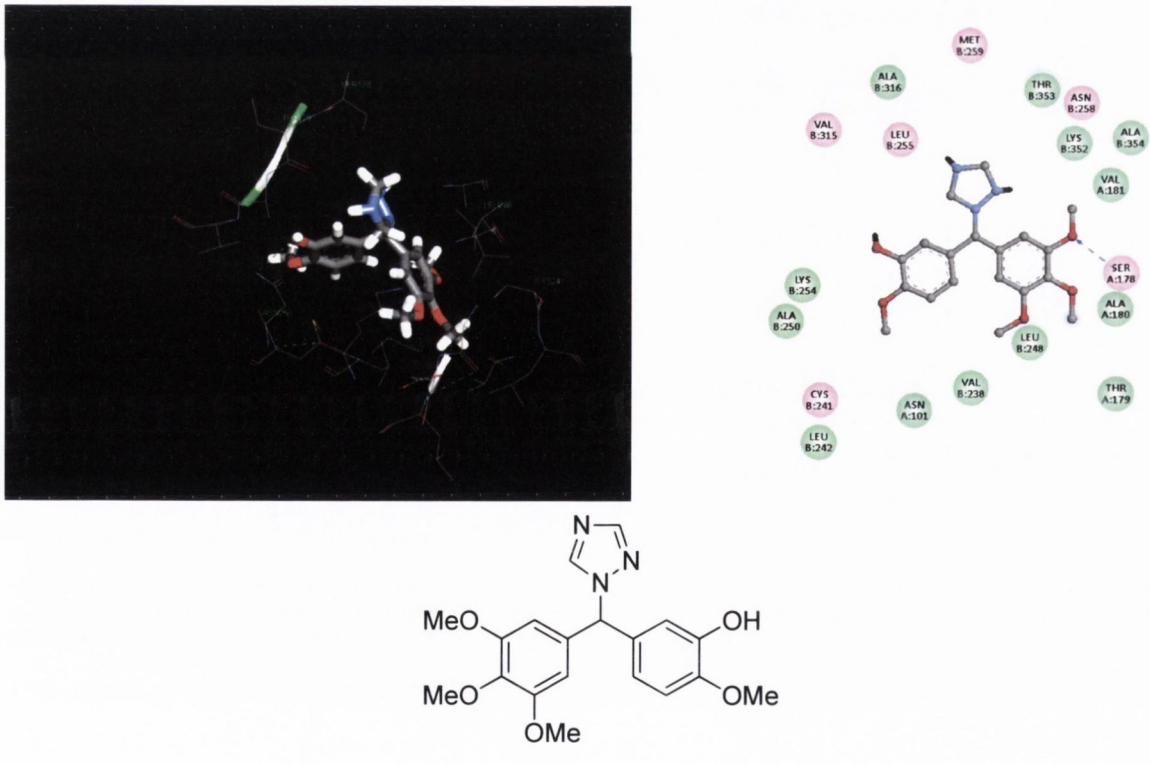

Figure 6-37 Top-ranking docked conformation of [413] in colchicine binding site of tubulin (1SA0,pdb). The docked confirmation is coloured by element type (carbon = grey, hydrogen = white, oxygen = red, nitrogen = blue)

For the docking studies of the letrozole analogue, the X-ray structure of the tubulin protein (1SA0.pdb)[562] cocrystallised with the ligand DAMA-colchicine was used. In Figure 6-37, compound [413] can be observed in the colchicine binding site of tubulin. The orientation of [413] gives good overlap with the trimethoxy ring 'A' but the trimethoxy substituents do not directly overlap but are in the same region of space (Figure 6-38). Compound [413] has similar orientation to the docked colchicine but no interaction was observed between the Cys241B residue and the methoxy substituent of [413] which is a known interaction that is seen with colchicine. There is a hydrogen bond interaction observed between one of the methoxy substituent of the A ring and Ser178. The similarity of the binding orientation of [413] and colchicine along with the common overlap in the structural features potentially could rationalise the potent antiproliferative activity (IC_{50} = 295 nM) and the two-fold reduction in tubulin polymerization exhibited by [413].

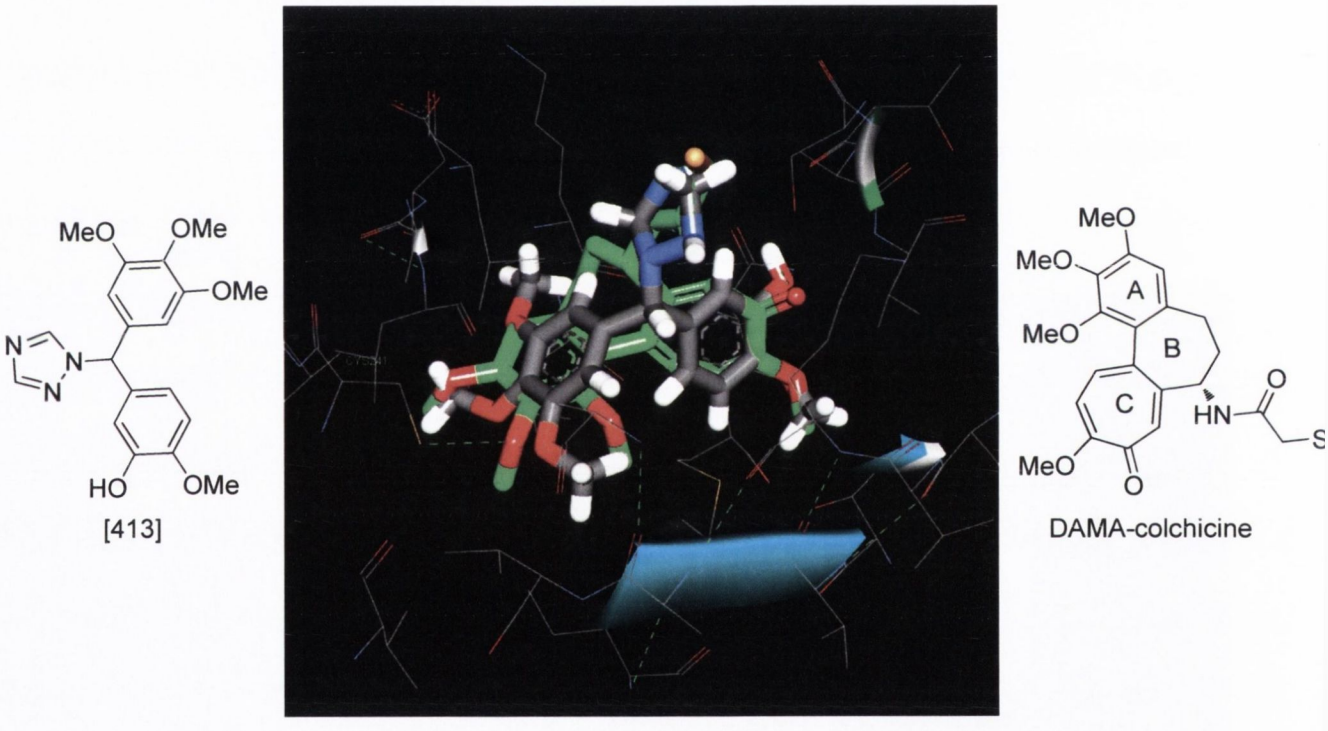

Figure 6-38 Superposition of DAMA Colchicine (green) and [413] (grey) docked conformations in 1SA0

Compound [413] is structurally similar to CA4 and letrozole, therefore it is proposed that this molecule could potentially act as a hybrid compound in tubulin (discussed earlier) and aromatase. However, compound [413] was not evaluated in a tubulin binding assay, but not for in aromatase activity. In the absence of biochemical evaluation, the use of molecular modelling was employed to substantiate the claim that compound [413] could infact inhibit aromatase. In Figure 6-39 illustrates compound [413] docked with androstenedione (aromatase converts androstenedione to estrone). The key interaction that is observed is a hydrogen bond interaction between the Met174 and the phenol from [413] a similar interaction is seen with the ketone at 17β position of androstenedione.

An additional interaction is observed between the triazole ring and Arg135 which should increase the binding affinity of compound [413] within the LBD of aromatase.

The docking study performed on compound [413] does not prove that it can inhibit aromatase however does suggest that it has the required structural features to bind and potentially act as an aromatase inhibitor type compound. This would suggest that compound [413] has the potential of being a CA4-AI hybrid.

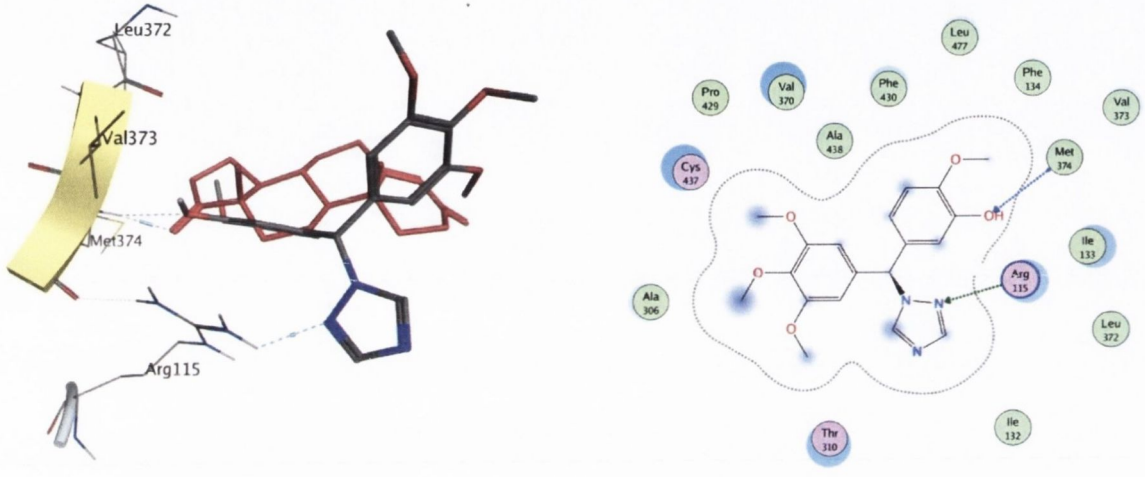

Figure 6-39 Top-ranking [413] docked conformation in 3EQM with androstenedione (ligand). The docked confirmation is coloured by element type (carbon = grey, hydrogen = white, oxygen = red, nitrogen = blue)

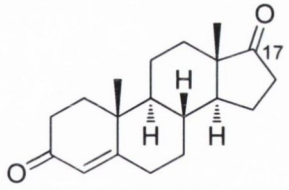

[466]

Figure 6-40 Androstenedione [466]

Chapter 7
Conclusion

7.1 Summary and Conclusion

Many approaches have been reported for the design and evaluation of novel molecules which target the proliferation of human breast cancer cells. The objective of this project was to synthesise a range of novel conjugate compounds for the treatment of estrogen receptor positive breast cancer. The strategy required the selection of ER binding ligands which could be incorporated into the conjugate scaffold comprising ER ligand - cytotoxic agent conjugate structure. The cytotoxic agent chosen was the acrylic acid derivative of the combretastatin CA4 compound [22]. A further strategy was to incorporate aromatase inhibitor type compounds into the conjugate scaffold in the design ER ligand – aromatase inhibitor and aromatase inhibitor - cytotoxic agent.

The convergent synthesis of the conjugate compounds required the preparation of the component parts of the conjugate separately and then the appropriate chemistry to link them together to afford the novel conjugate compounds. This convergent approach required the successful synthesis of the ER type ligands endoxifen [36], cyclofenil [198] and the bazedoxifene related 2-phenylindole [50]. The synthesis of the endoxifen and cyclofenil ligands required a McMurry coupling reaction to afford the triarylene/tricyclic core in good yield (88%/86-97%), followed by alkylation and subsequent amination reaction to give the endoxifen and cyclofenil ligands. The modification to the cycloalkane group on the cyclofenil core was possible by introduction of a variety of cycloketones in the McMurry reaction. The synthesis of the 2-phenylindole ligand provided some difficulties and also resulted in the isolation interesting of side products. The initial synthesis of the 4',5-dimethoxy 2-phenylindole *via* the Fisher indole synthesis reaction was very successful (75%). Subsequent *N*-alkylation of the indole with various dibromoalkanes, followed by amination reaction all afforded a series of 4',5-dimethoxy 2-phenylindole products. However the 4',5-dihydroxy-2-phenylindole scaffold was required for the conjugate products as the phenolic hydroxyl groups were essential for optimum ER binding activity. Initial demethylation reaction of the 4',5-dimethoxy 2-phenylindole scaffold was unsuccessful, and afforded the required products in trace amounts. Alternative protection of the phenolic group was required. This led to the use of benzyl ether protecting groups which on selection of the correct catalyst (palladium hydroxide) were easily removed. Interestingly, the alkylation step in the synthesis of the required *N*-alkyl-2-phenylindole ligands afforded an unexpected by-product. In each case, this by-product was found to be a rearranged alkylated product (e.g. the 2-phenyl-3*H*-indole [273]) and was isolated in moderate yield. This rearrangement for the alkylation reaction was previously unreported under these conditions. The successful synthesis of the ER ligands provided 12 ER targeting compound ligands ([197], [221]-[225] and [241]-[243],[261]-[262]) for screening

individually for antiproliferative activity in MCF-7 breast cancer cell line, ER binding activity and for incorporation into the conjugate scaffold.

The components of the conjugate compounds would be synthesised individually and subsequently combined to afford the target conjugate products. The next step was the preparation of the cytotoxic agents that were to be incorporated into the conjugate compounds. The cytotoxic agents that were used within this project were the acrylic acid derivatives of combretastatin CA4. The successful synthesis of the acrylic acids [150], [311]-[327] was performed using the Perkin reaction which affords the desired compounds in good yields. An investigation into the use of microwave assisted organic synthesis (MAOS) on the Perkin reaction afforded the desired acrylic acids with improved yields with a 1/6 reduction in time. This MAOS method gave a viable and more productive method for the synthesis of acrylic acids. The 21 synthesised acrylic acid [150], [311]-[327] were to be incorporated into the conjugate scaffold. Another investigation on the importance of the acrylic acid structure on antiproliferative activity led to the preparation of a series of cinnamic ([342],[344]) and propanoic ([343],[345]) acids. The synthesis of a series of piperizine derivatives of the acrylic acid combretastatin CA4 led to the isolation of amide compounds [347]-[360] that have the potential to act as potent cytotoxic agents.

The inclusion of aromatase inhibitor (AI) ligands into the conjugate scaffold was next explored. The synthesis of two AI type compounds containing the required letrozole and anastrozole pharmacophores was designed. The anastrozole based ligand which was the benzoic acid derivative, was successfully prepared in a 6 step procedure. The synthesis of letrozole ligand [387] was less than straightforward. A variety of routes where employed in designing a successful synthesis of the desired [387]. In the initial approach to the synthesis of [387], the modified substituents required on the aryl rings (including the nitrile and phenol) inhibited the *p*-cyanoaryl fluoride [381] reacting with [383] (Scheme 4-6) due to increased electron density (reaction required electron withdrawing group and the phenol which was an electron donating group). Another approach explored for the synthesise the letrozole type ligand [387] was *via* the Ni-catalyzed Negishi-coupling reaction, however because of low yield this route was discontinued. The letrozole ligand was successfully synthesised *via* the *n*-BuLi mediated reaction of [397] with [398] which afford the desired secondary alcohol in good yield. Subsequent addition of 1,2,4-triazole gave the letrozole scaffold. This *n*-BuLi mediated reaction provided access to a series of novel aromatase inhibitor– CA4 hybrid type compounds [394], [402] and [411]-[413].

Following the synthesis of the components of the conjugates , the next step was to combine the estrogen receptor (ER) antagonist ligands and the aromatase inhibitor(AI) ligands with the

required cytotoxic agents or AI ligand as appropriate. The synthesis of conjugates was facilitated by a carbodiimide coupling reaction between the carboxylic acid functional groups of the acrylic acid and/or anastrozole (AI) ligand with the secondary amine of the ER ligands and/or the letrozole (AI) ligand. The carbodiimide mediated coupling reaction was investigated and for the purpose of this project. EDC was preferred to DCC based on ease of removal of the urea byproduct and increased yields. This EDC coupling reaction led to the successful synthesis of 33 novel conjugates (16 endoxifen-cytotoxic agent conjugates [414]-[430], 4 endoxifen-modified cytotoxic agent conjugates [435]-[438], 5 cyclofenil-cytotoxic agent conjugates [444]-[448], 6 of the 2-phenylindole-cytotoxic agent conjugates [454]-[459], together with the endoxifen-AI conjugate [463] and the AI-cytotoxic agent [464]). These products were to be examined for antiproliferative activity in MCF-7 hormone dependent breast cancer cells and also examined for ER binding activity.

The ER ligands and the novel conjugate compounds synthesised were tested for antiproliferative activity in MCF-7 ER-overexpressing cell line. The cyclofenil ER ligands were evaluated and exhibited low micromolar activity (IC_{50} values 1-5 μM) in the MCF-7 cell line. The 2-phenylindole ER ligands displayed micromolar activity with one compound [243] in the series exhibiting sub nanomolar activity (IC_{50} = 0.158 μM). The potent activity of [243] could be attributed to the length of the aliphatic chain located at the N-1 position. In the molecular modelling studies it is apparent that this lipophilic aliphatic substituent has the potential to mimic the lipophilic substituent of the ER steroid ligand fulvestrant, and possibly exhibits a mechanism of action similar to fulvestrant. These results indicate that the direct conjugate formed from two ER targeting ligands could exhibit similar activity.

The endoxifen-cytotoxic agents [414]-[430] were evaluated for antiproliferative activity and the results varied considerably. The most potent compound from this series was [415] with an IC_{50} value of 1 μM, with two other compound ([414] and [426]) exhibiting similar activity. The majority of rest of this series had an IC_{50} of >100 μM. Further conjugates were synthesized to investigate the contribution of each element of the CA4 structure for antiproliferative activity, and it was concluded that the biaryl structure was essential for the desired low micromolar activity. The cyclofenil-cytotoxic agent conjugates [444]-[448] demonstrated lower antiproliferative activity when compared to the ER ligand alone, with two of the novel conjugate compounds ([447] and [448]) exhibiting sub - micromolar activity. From molecular modelling studies it was rationalized that the more potent activity observed for [447] and [448] could be attributed to the fact that they both contained the bulkiest cycloalkane ring substituents which could occupy the free space in the LBD and form interactions to a greater extent than the other conjugates in this series. The 2-phenylindole-

cytotoxic agent conjugates [454]-[459] also displayed very potent antiproliferative activity with the longest chain derivative [458] exhibiting an IC_{50} value of 1.86 μM. Similar to the direct ER ligand conjugate [243], from the molecular modelling study is believed to follow a similar mode of action to fulvestrant. The aromatase inhibitor conjugates were of particular interest due to their novel nature. The endoxifen-AI conjugate [463] exhibited potent activity (IC_{50} = 0.316 μM) in MCF-7 and similarly too did the AI-cytotoxic agent conjugate [464] (IC_{50} = 1.14 μM). The exact mechanism of action is not clear as they potentially have two modes of action possible in each case:, compound [463] can act *via* both estrogen receptor antagonism and aromatase inhibition, while it is possible for compound [464] to act by either aromatase inhibition or tubulin polymerization inhibition mechanisms.

The lead compounds ([223], [225], [243], [268], [468], [464], [458], [426], [447] and [448]) were identified from each series and evaluated for ER binding activity *via* a Lanthascreen® FRET kit. The compounds exhibited low micromolar to low nanomolar activity for binding to ERα and ERβ. Compound [448] exhibited the highest activity for ERα with IC_{50} of 19 nm and a selectivity for ERα/ERβ. of 12 fold. Compound [268] exhibited the highest activity for ERβ when compared to ERα of IC_{50} of 41 nm and a selectivity for ERα/ERβ of 0.09.

To investigate the mechanism of action of the compound in more detail, the lead compounds ([223], [225], [243], [268], [349], [413], [468], [464], [458], [426], [447] and [448]) from each series were subjected to cell cycle analysis. All compounds tested increased apoptosis when compared to vehicle-treated cells, with the exception of compounds [464] and [243] which was not expected due to their *in vitro* activity. The cyclofenil based analogues [223] and [225] proved significantly more active than the positive control tamoxifen. The potent activity of several members of this cohort of compounds in MCF-7 breast cancer cells and their lack of toxicity in normal blood cells make them ideal candidates for further anti-cancer studies.

The synthesis of the AI-CA4 hybrid compounds [394], [402] and [411]-[413] were interesting as it was the first time such compounds had been reported. This series of compounds [394], [402] and [411]-[413] exhibited no antiproliferative activity below 100 μM in MCF-7 cells, except for the compound [413] which exhibited a sub micromolar activity (IC_{50} = 0.295 μM). This result was extremely interesting and it was then evaluated for tubulin inhibition. Compound [413] induced a twofold reduction in polymer mass. This result proved that the hybrid compound was targeting tubulin but it was not possible to evaluate [413] on aromatase to determine if the molecule exhibited two modes of action, or was functioning solely as a tubulin polymerisation inhibitor. Compound [413] was also shown to cause G2M arrest which is expected for tubulin binding agents and was demonstrated to be non toxic in peripheral blood mononuclear cells.

In summary, a library of novel estrogen receptor (ER) ligands, combretastatin analogues, aromatase inhibitor (AI) ligands, conjugates [444] and [458] and aromatase inhibitor-combretastatin CA4 hybrid compound [413] have been successfully synthesised and biochemically evaluated for antiproliferative activity, tubulin inhibition ([413]), cell cycle analysis, ER binding and toxicity. The potent activity of several members of this cohort of compounds in MCF-7 breast cancer cells and their lack of toxicity in normal blood cells make them ideal candidates for further anti-cancer studies and drug development, Figure 7-1.

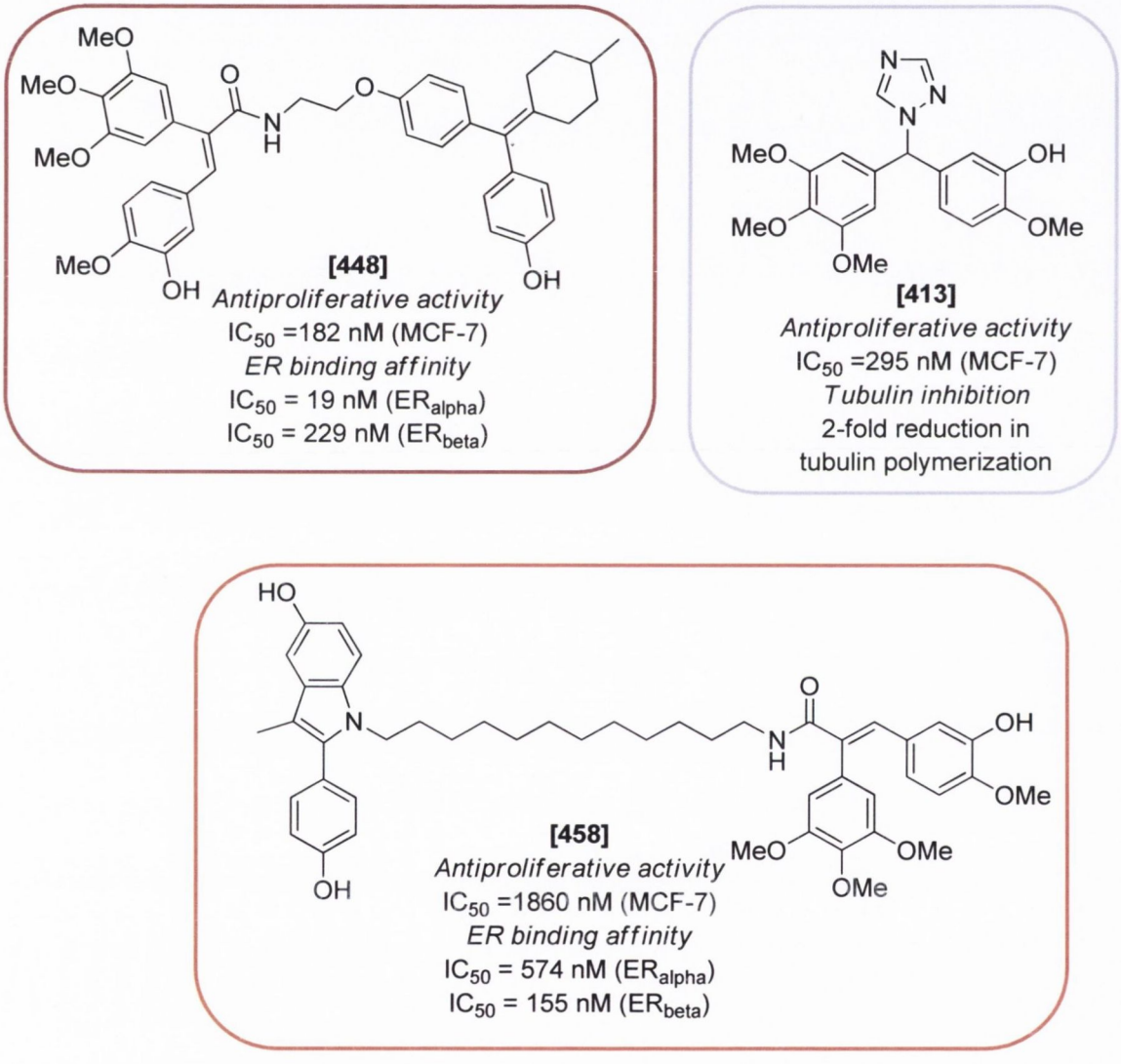

Figure 7-1 Example of synthesised compounds which would be ideal candidates for further anti-cancer studies

Chapter 8
Experimental

8.1 General experimental details

Uncorrected melting points were measured on a Gallenkamp apparatus. Infra-red (IR) spectra were recorded on a Perkin Elmer FT-IR Paragon 1000 spectrometer. ^{1}H, ^{13}C and ^{19}F nuclear magnetic resonance (NMR) spectra were recorded at 27 °C on a Brucker DPX 400 spectrometer (400.13 MHz, ^{1}H; 100.61 MHz, ^{13}C; 376.47 MHz, ^{19}F) in either $CDCl_3$ (internal standard tetramethylsilane (TMS)) or CD_3OD. For $CDCl_3$, ^{1}H-NMR spectra were assigned relative to the TMS peak at 0.00 δ and ^{13}C-NMR spectra were assigned relative to the middle $CDCl_3$ triplet at 77.00 ppm. For CD_3OD, ^{1}H and ^{13}C-NMR spectra were assigned relative to the center peaks of the CD_3OD multiplets at 3.30 δ and 49.00 ppm respectively. ^{19}F-NMR spectra were not calibrated. Coupling constants are reported in Hertz. For ^{1}H-NMR assignments, chemical shifts are reported: shift value (number of protons, description of absorption, coupling constant(s) where applicable). Electrospray ionisation mass spectrometry (ESI-MS) was performed in the positive ion mode on a liquid chromatography time-of-flight mass spectrometer (Micromass LCT, Waters Ltd., Manchester, UK). The samples were introduced into the ion source by an LC system (Waters Alliance 2795, Waters Corporation, USA) in acetonitrile : water (60:40 %v/v) at 200 µL/min. The capillary voltage of the mass spectrometer was at 3 kV. The sample cone (de-clustering) voltage was set at 40 V. For exact mass determination, the instrument was externally calibrated for the mass range m/z 100 to m/z 1000. A lock (reference) mass (m/z 556.2771) was used. Mass measurement accuracies of < ±5 ppm were obtained. Low resolution mass spectra (LRMS) were acquired on a Hewlett-Packard 5973 MSD GC-MS system in electron impact (EI) mode. Elemental analyses were performed on an Exetor Analytical CE4400 CHN analyser in the microanalysis laboratory, Department of Chemistry, University College Dublin. R_f values are quoted for thin layer chromatography on silica gel Merck F-254 plates, unless otherwise stated. Flash column chromatography was carried out on Merck Kieselgel 60 (particle size 0.040-0.063mm), Aldrich aluminium oxide, (activated, neutral, Brockmann I, 50 mesh) or Aldrich aluminium oxide, (activated, acidic, Brockmann I, 50 mesh). Chromatograpic separations were also carried out on Biotage SP4 instrument. Microwave experiments were carried out with in the Biotage initiator and Discover CEM microwave synthesisers.

8.1.1 Combretastatin A-4 [22][281]

To a suspension of Cu powder (0.915 g, 14.4 mmol) in quinoline (10 mL) was added [150] (1.0 g, 2.78 mmol) and the resulting mixture was stirred under N_2 at 200 °C for 3 h. Upon cooling, the mixture was diluted with EtOAc (50 mL), and the Cu was filtered off. The filtrate was washed with *aq.* 1 M HCl (3 × 20 mL), and the aqueous layer was separated and extracted with EtOAc (3 × 10 mL). The combined organic layers were washed with brine (2 × 10 mL), dried ($MgSO_4$), and concentrated under reduced pressure to afford a brown viscous solid. The material was purified *via* flash chromatography on silica gel (*n*-Hexane:DCM, 2:1) to afford the product as a light yellow oil and subsequent recrystallization from *n*-Hexane–diethyl ether to give [22] as colorless crystals (413 mg, 47%).

^{1}H-NMR 400MHz ($CDCl_3$): δ 3.68 (s, 6 H, OCH_3), 3.84 (s, 3 H, OCH_3), 3.89 (s, 3 H, OCH_3), 5.49 (br. s, 1 H, OH), 6.42 (d, 1H, *J* = 12.4 Hz, C=CH), 6.45 (d, 1 H, *J* = 12.4 Hz, C=CH), 6.51 (s, 2 H, Ar-H), 6.71 (d, 1 H, J =8.0 Hz, Ar-H), 6.79 (dd, 1 H, *J*= 8.0, 2.0 Hz, Ar-H), 6.91 (d, 1 H, *J*= 2.0 Hz, Ar-H) **^{13}C-NMR 100MHz** ($CDCl_3$): δ 152.85 (C-OCH_3), 145.78 (C-OCH_3), 145.26 (C-OCH_3), 137.17 (C-OH), 132.68, 130.63, 129.47, 129.01, 121.08, 115.04, 110.32, 106.07, 60.90 (OCH_3), 55.93 (OCH_3), 55.92 (OCH_3) **IR:** ν_{max} (KBr) cm^{-1}: 3424.2, 3002.0, 2938.8, 2836.5, 1610.4, 1579.2, 1508.9, 1459.1, 1419.4, 1328.0, 1182.3, 1025.3, 1004.1, 944.8, 881.1, 854.7, 796.6 **HRMS** (EI): Found 339.1220 $(M+Na)^+$, $C_{18}H_{20}O_5Na$ requires 339.1208. **M.P.** 116-117 °C

8.2 Synthesis of protected endoxifen

8.2.1 (4-((*E/Z*)-1-(4-(2-Hydroxy)phenyl)-2-phenylbut-1-enyl)phenoxy)(*tert*-butyl)dimethylsilane [193][421]

Zinc dust (5.254 g, 80.37 mmol) was weighed out and transferred to a three-necked round bottomed flask containing 50 mL of dry THF. Titanium tetrachloride was added (7.623 g, 4.4 mL, 40.185 mmol) *via* syringe to the mixture and then refluxed for 2 h under darkness and a N_2 environment. [194] (2.93 g, 8.93 mmol) and propiophenone [195] (3.59 g, 3.6 mL, 26.79 mmol) were dissolved in 40 mL of dry THF. This mixture was added to the mixture in the round-bottomed flask carefully *via* syringe. The mixture was then refluxed for a further 3 h. Afterwards, the mixture was allowed to cool then diluted with 150 mL ethyl acetate and washed with 10 % potassium carbonate solution (60 mL). After filtration, the organic layer was separated out and the aqueous layer was extracted with ethyl acetate (100 mL x 3). The combined organic layers were dried over anhydrous sodium sulfate, filtered and evaporated to dryness *in vacuo* to yield crude product. The material was purified *via* flash chromatography on silica gel (*n*-Hexane:EtOAc, 4:1) to afford the product as a brown resin. (3.4 g, 88 %)

^{1}H-NMR 400MHz ($CDCl_3$): δ 0.13 (s, 0.25 × 12 H, $SiCH_3$), 0.25 (s, 0.75 × 12 H, $SiCH_3$), 0.94-1.03 (m, 24 H, $SiC(CH_3)_3$,CH_3), 2.48-2.53 (q, 4H, *J*= 7.5 Hz, CH_2) 6.49-6.52 (m, 4 H, Ar-H), 6.68 (t, 4 H, J= 8.5 Hz, Ar-H), 6.83-6.85 (m, 4 H, Ar-H), 7.11-7.19 (m, 14 H, Ar-H) **^{13}C-NMR 100MHz** ($CDCl_3$): δ 153.68, 153.05, 152.84, 142.11, 140.64, 135.94, 135.62, 131.70, 131.38, 130.35, 130.08, 129.26, 127.37, 127.29, 127.19, 126.93, 126.68, 126.41, 126.21, 125.40, 119.08, 118.15, 114.44, 113.74, 27.21, 25.23, 17.74, 13.20, 13.17, -4.80, -4.82, -4.92 **IR:** ν_{max} (KBr) cm^{-1}: 3560.4, 2967.6, 1738.9, 1598.4, 1463.1, 1445.1, 1251.1, 1115.8, 1072.3, 896.1, 739.1, 703.2, 655.0 **HRMS** (EI): Found 453.2220 $(M+Na)^+$, $C_{28}H_{34}O_2NaSi$ requires 453.2226.

8.2.2 [4-(*tert*-Butyldimethylsilanyloxy)phenyl]-(4-hydroxyphenyl)methanone [194][421]

4,4'-Dihydroxybenzophenone [192] (6.00 g, 28 mmol) and imidazole (2.094 g, 31 mmol) were dissolved in DMF (20 mL) with stirring. A solution of *tert*-butyldimethylsilyl chloride (4.22 g, 28 mmol) in DMF (20 mL) was added to the mixture slowly over the course of 1 h. Reaction mixture was allowed to stir at room temperature for 16 h. The reaction was worked up *via* the addition of ethyl acetate (100 mL) and 10% hydrochloric acid (50 mL). The organic layer was washed with water (100 mL), brine (100 mL), dried over sodium sulphate and evaporated to dryness in vacuo to yield crude product. The material was purified *via* flash chromatography on silica gel (*n*-Hexane:DCM, 5:1) to afford the product as a light yellow oil. (3.34 g, 27 %)
Mono-protected protected [194]

^{1}H-NMR 400MHz ($CDCl_3$): δ 7.76 (dd, 4H, *J*= 6.5Hz, Ar-H), 6.94 (dd, 4H, *J*= 7.5Hz, Ar-H), 1.02 (s, 9H, CH_3), 0.27 (s, 6H, CH_3) **^{13}C-NMR 100MHz** ($CDCl_3$): δ 195.66(C=O), 160.25, 159.47, 132.41, 132.02, 130.50, 129.37, 119.30, 114.90, 25.16 (CH_3), 17.80, -4.78 (SiC) **IR:** ν_{max} (KBr) cm^{-1}: 3362.6, 295.9, 2930.0, 2856.9, 1641.6, 1602.3, 1580.3, 1508.1, 1470.5, 1313.0, 1278.1, 1161.1, 913.4, 839.1, 771.9 **HRMS** (EI): Found 329.1579 $(M+H)^+$, $C_{19}H_{25}O_3Si$ requires 329.1595.

8.2.2.1 (4-((tert-Butyldimethylsilyl)oxy)phenyl)(4-((ethyldimethylsilyl)oxy)phenyl) methanone [194a]

The material was purified *via* flash chromatography on silica gel (*n*-Hexane:DCM, 5:1) to afford the product as a colourless oil. (34 %)

^{1}H-NMR 400MHz ($CDCl_3$): δ 7.75 (d, 4 H, *J*= 8.5 Hz, Ar-H), 6.91 (d, 4H, *J*= 8.5 Hz, Ar-H), 1.02 (s, 18 H, CH_3), 0.26 (s, 12 H, CH_3) **^{13}C-NMR 100MHz** ($CDCl_3$): δ 194.1 (C=O), 159.0, 131.7, 130.8, 119.2, 119.1, 25.2 (CH_2), 17.8, -4.79 (SiC) **IR:** ν_{max} (Neat) cm^{-1}: 2956.0, 2930.8, 2886.7, 2858.8, 1653.1, 1599.1, 1508.0, 1267.5, 1161.2, 1006.4, 909.2 **HRMS** (EI): Found 437.1937 $(M+Na)^+$, $C_{23}H_{34}O_3Si_2Na$ requires 437.1944.

8.2.3 (4-((*E/Z*)-1-(4-(2-Bromoethoxy)phenyl)-2-phenylbut-1-enyl)phenoxy)(*tert*-butyl)dimethylsilane [196][421]

(4-((*E/Z*)-1-(4-(2-Hydroxy)phenyl)-2-phenylbut-1-enyl)phenoxy)(*tert*-butyl)dimethylsilane [193] (3.28 g, 7.63 mmol) was dissolved in 1,2-dibromoethane (71.69 g, 33 mL, 381.6 mmol) with stirring. Tetrabutylammonium hydrogen sulfate (2.59 g, 7.63 mmol) was added, followed by 1 M sodium hydroxide solution (35 mL). The biphasic mixture was stirred vigorously at room temperature for 16 h. The reaction mixture was worked up *via* the addition of dichloromethane (100 mL) and sodium bicarbonate solution (100 mL). The aqueous layer was extracted with dichloromethane (100 mL). The organic layers were combined, dried over sodium sulfate and concentrated *in vacuo* to yield crude product. The material was purified *via* flash chromatography on silica gel (*n*-Hexane:EtOAc, 6:1) to afford the product as a brown resin. (3.2 g, 78 %)
^{1}H-NMR 400MHz ($CDCl_3$): δ 0.12 (s, 0.54 × 12H, $SiCH_3$), 0.24 (s, 0.46 × 12 H, $SiCH_3$), 0.92-1.03 (m, 24 H, $SiC(CH_3)_3$), 2.50 (q, 4 H, J= 7.5 Hz, CH_2), 3.58 (t, 0.54 × 4H, J= 6.5 Hz, CH_2), 3.69 (t, 0.46 × 4 H, J=6.5 Hz, CH_2), 4.18 (t, 0.46 × 4H, J= 6.5 Hz, CH_2), 4.34 (t, 0.54 × 4 H, J= 6.5 Hz, CH_2), 6.45-6.6 (m, 4 H, Ar-H), 6.7-6.95 (m, 8 H, Ar-H), 7.08-7.22 (m, 14 H, Ar-H) **^{13}C-NMR 100MHz** ($CDCl_3$): δ 156.28, 155.45, 142.04, 140.74, 136.56, 135.88, 131.61, 131.37, 130.26, 130.09, 129.25, 127.40, 127.30, 125.48, 119.10, 118.52, 113.78, 113.00, 67.35, 31.15, 28.79, 28.73, 28.45, 25.23, 25.21, 13.70, 13.21, 13.16, -4.81, -4.92 **IR:** ν_{max} (KBr) cm^{-1}: 3436.4 (OH), 2957.9, 2930.4, 2858.5, 1604.9, 1507.3, 1472.3, 1254.7,

1168.3, 916.2, 838.8, 804.2, 780.3 **HRMS** (EI): Found 559.1630 $(M+Na)^+$, $C_{30}H_{37}O_2BrSiNa$ requires 559.1644.

8.2.4 (4-((*E/Z*)-1-(4-(2-methylaminoethoxy)phenyl)-2-phenylbut-1-enyl)phenoxy)(*tert*-butyl)dimethylsilane [197][421]

(4-((*E/Z*)-1-(4-(2-Bromoethoxy)phenyl)-2-phenylbut-1-enyl)phenoxy)(*tert*-butyl)dimethylsilane [196] (1.457 g, 2.69 mmol) was dissolved in a 2 M solution of methylamine in THF (1.678 g, 26.99 mL, 54 mmol). The reaction mixture was stirred in a sealed pressure tube for 48 h at 60 °C. The reaction was worked up *via* the addition of 100 mL of dichloromethane. The organic phase was washed with a sodium bicarbonate / sodium carbonate ~pH 10 aqueous buffer (50 mL). The aqueous phase was then extracted with 3 x 50 mL dichloromethane. The organic layers were combined, dried over sodium sulfate and concentrated *in vacuo* to yield crude product. The material was purified *via* flash chromatography on silica gel (DCM:EtOAc 3:1) to afford the product as a brown resin. (1.24 g, 94 %) **^{1}H-NMR 400MHz** ($CDCl_3$): δ 7.20-6.50 (m, 26H, Ar-H), 4.11 (t, 0.43 x 4H, *J*= 5.0 Hz, CH_2), 3.95 (t, 0.43 x 4H *J*= 5.0 Hz, CH_2), 3.36 (s, 2H, NH), 2.99 (s, 0.57 x 4H, CH_2), 2.89 (s, 0.43 x 4H, CH_2) 2.53 (m, 10H, NCH_3, CH_2), 1.01-0.92 (m, 24H, CH_3, $(CH_3)_3$), 0.26 (s, 0.43 x 12H, $Si(CH_3)_2$)), 0.13 (s, 0.57 x 12H, $Si(CH_3)_2$) **^{13}C-NMR 100MHz** ($CDCl_3$): δ 156.94, 156.10, 153.84, 153.06, 142.19, 142.11, 140.65, 140.59, 137.53, 137.44, 136.35, 136.06, 136.02, 135.68, 131.57, 131.43, 130.20, 130.12, 129.25, 127.41, 127.33, 125.48, 125.44, 119.12, 118.54, 113.54, 112.80, 65.99, 65.73, 50.12, 50.03, 49.47, 35.39, 35.26, 28.60, 28.47, 25.26, 25.24, 17.75, 13.24, 13.21, -4.80, -4.91 **IR:** ν_{max} (KBr) cm^{-1}: 3431.2, 1606.0, 1508.0, 1241.3, 1173.2, 1099.5, 1078.8, 1036.9, 938.9, 846.8 **HRMS** (EI): Found 488.3088 $(M+H)^+$, $C_{31}H_{41}NO_2Si$ requires 488.2907.

8.3 Synthesis of cyclofenil derivatives

8.3.1 General method for the synthesis of Cyclofenil derivatives *via* McMurry coupling.

Zinc dust (9 eq., 3.58 g, 54.81 mmol) was transferred to a three neck round bottom flask containing dry THF (50 mL). Titanium tetrachloride (4.5 eq., 5.2 g, 37.4 mmol, 3 mL) was added *via* a syringe dropwise to the mixture and refluxed for 2 h in darkness and under a N_2 atmosphere. The appropriate phenolic ketone [194] (1 eq.) and relevant cyclic-ketone [201]-[205] (3 eq.) were dissolved in dry THF (40 mL). This mixture was added to the three-neck round bottom flask carefully *via* syringe dropwise. The mixture was then refluxed for a further 3 h. The mixture was allowed to cool and then diluted with EtOAc (75 mL) and 10 % K_2CO_3 solution. The mixture was filtered under vacuum to remove the dark blue metal complex. The filtrate was then separated and the aq. layer was extracted with EtOAc (3 × 50 mL). The combined organic layers were washed with 10 % K_2CO_3 solution (20 mL), water (50 mL) and brine (50 mL) then dried over Na_2SO_4, filtered and the solvent was evaporated under reduced pressure to afford the crude product. The material was purified *via* flash chromatography over silica gel to afford the product.

8.3.2 4-((4-((*tert*-Butyldimethylsilyl)oxy)phenyl)(cyclopentylidene)methyl)phenol [206]

As per general method 8.3.1, $TiCl_4$ (4.5 eq., 5.2 g, 27.4 mmol, 3 mL), Zn dust (9 eq., 3.58 g, 54.81 mmol), [194] (1 eq., 2 g, 6.09 mmol) and cyclopentanone [201] (3 eq., 1.54 g, 18.26 mmol, 1.88 mL) were reacted. The crude material was purified *via* flash chromatography over silica gel (*n*-Hexane:DCM, 3:1) to afford the product as an orange resin (2.25 g, 97%)

^{1}H NMR ($CDCl_3$, 400 MHz) δ 7.01 - 7.11 (m, 4H, (Ar-H)), 6.74 - 6.82 (m, 4H, (Ar-H)), 2.40 (t, *J* = 7.00 Hz, 4H, (2 × CH_2)), 1.69 (quin, *J* = 3.50 Hz, 4H, (2 × CH_2)), 1.01 (s, 9H, (3 × CH_3)), 0.22 (s, 6H, (2 × CH_3)) **^{13}C NMR ($CDCl_3$, 100 MHz)** δ 153.4 (C-OH), 153.1 (C-O-Si), 141.6 (C=C), 136.4 (C=C), 135.7 (C_q), 131.5 (C_q), 130.0 (ArC), 129.7 (ArC), 118.9 (ArC), 114.3 (ArC), 32.8 (CH_2), 26.5 (CH_2), 25.2 (CH_3), 17.7 ($\underline{C}(CH_3)_3$), -4.8 (CH_3) **HRMS (EI):** Found 379.2101 $(M-H)^-$, $C_{24}H_{31}O_2Si$ requires 379.2099. **IR :** ν_{max} (KBr) cm^{-1}: 3400.5 (br.), 2955.5, 2930.6, 2358.3, 1635.33, 1598.3, 1507.4, 1270.0 (br.), 1163.4, 911.7

8.3.3 4-((4-((*tert*-Butyldimethylsilyl)oxy)phenyl)(cyclon-hexaneylidene)methyl)phenol [207]

As per general method 8.3.1, $TiCl_4$ (4.5 eq., 5.2 g, 27.4 mmol, 3 mL), Zn dust (9 eq., 3.58 g, 54.81 mmol), [194] (1 eq., 2 g, 6.09 mmol) and cyclohexaneanone [202] (3 eq., 1.79 g, 18.26 mmol, 1.9 mL) were reacted. The crude material was purified *via* flash chromatography over silica gel (*n*-Hexane:DCM, 3:1) to afford the product as an orange resin (2.1 g, 87%)

^{1}H NMR ($CDCl_3$, 400 MHz) δ 6.95 - 7.04 (m, 4H, Ar-H), 6.74 - 6.79 (m, 4H, Ar-H), 2.23 - 2.31 (m, 4H, 2 × CH_2), 1.55 - 1.69 (m, 6H, 3 × CH_2), 1.02 (s, 9H, 3 × CH_3), 0.24 (s, 6H, 2 × CH_3) **^{13}C NMR ($CDCl_3$, 100 MHz)** δ 153.3 (C-OH), 153.2 (C-O-Si), 137.8 (C=C), 136.0 (C=C), 135.6 (C_q), 133.1 (C_q), 130.7 (ArC), 130.4 (ArC), 118.8 (ArC), 114.2 (ArC), 32.1 (CH_2), 28.2 (CH_2), 26.4 (CH_2), 25.2 (CH_3), 17.7 ($\underline{C}(CH_3)_3$), -4.8 (CH_3) **HRMS (EI):** Found 395.2405 $(M+H)^+$, $C_{25}H_{35}O_2Si$ requires 395.2406. **IR :** ν_{max} (KBr) cm^{-1}:3390.8, 2928.4, 2855.8, 1698.7, 1604.9, 1505.7, 1471, 1463.2, 1447.1, 1258.7, 1167.1, 1099.0, 915.8, 802.1

8.3.4 4-((4-((*tert*-Butyldimethylsilyl)oxy)phenyl)(cycloheptylidene)methyl)phenol [208]

As per general method 8.3.1, $TiCl_4$ (4.5 eq., 5.2 g, 27.4 mmol, 3 mL), Zn dust (9 eq., 3.58 g, 54.81 mmol), [194] (1 eq., 2 g, 6.09 mmol) and cycloheptanone [203] (3 eq., 2.04 g, 18.26 mmol, 2.15 mL) were reacted. The crude material was purified *via* flash chromatography over silica gel (*n*-Hexane:DCM, 3:1) to afford the product as an orange resin (2.1 g, 84%)

^{1}H NMR ($CDCl_3$, 400 MHz) δ 6.99 - 7.06 (m, 4H, Ar-H), 6.73 - 6.79 (m, 4H, Ar-H), 2.33 (s, 4H, 2 × CH_2), 1.59 (s, 8H, 4 × CH_2), 1.00 (s, 9H, 3 × CH_3), 0.21 (s, 6H, 2 × CH_3) **^{13}C NMR ($CDCl_3$, 100 MHz)** δ 153.1 (C-OH, C-O-Si), 139.1 (C=C), 136.4 (C=C), 136.1 (C_q), 135.8 (C_q), 130.1 (ArC), 129.9 (ArC), 118.9 (ArC), 114.3 (ArC), 33.0 (CH_2), 32.96 (CH_2), 29.0 (CH_2), 27.7 (CH_2), 25.2 (CH_3), 17.7 ($\underline{C}(CH_3)_3$), -4.8 (CH_3) **HRMS (EI):** Found 409.2574 $(M+H)^+$, $C_{26}H_{37}O_2Si$ requires 409.2563. **IR :** ν_{max} (KBr) cm^{-1}: 3401.2, 2929.5, 2857.5, 1647.7, 1599.7, 1507.2, 1462.9, 1268.2, 1163.6, 1013.5, 912.9, 840.0, 805.4, 781.4

8.3.5 4-((4-((*tert*-Butyldimethylsilyl)oxy)phenyl)(cyclooctylidene)methyl)phenol [209]

As per general method 8.3.1, $TiCl_4$ (4.5 eq., 5.2 g, 27.4 mmol, 3 mL), Zn dust (9 eq., 3.58 g, 54.81 mmol), [194] (1 eq., 2 g, 6.09 mmol) and cyclooctanone [204] (3 eq., 2.30 g, 18.26 mmol, 2.4 mL) were reacted. The crude material was purified *via* flash chromatography over silica gel (*n*-Hexane:DCM, 3:1) to afford the product as an orange resign (2.3 g, 89%)

^{1}H NMR ($CDCl_3$, 400 MHz) δ 6.99 - 7.11 (m, 4H, Ar-H), 6.73 - 6.80 (m, 4H, Ar-H), 2.28 (t, *J* = 6.50 Hz, 4H, 2 × CH_2), 1.63 - 1.71 (m, 2H, CH_2), 1.47 - 1.62 (m, 8H, 4 × CH_2), 0.99 (s, 9H, 3 × CH_3), 0.21 (s, 6H, 2 × CH_3) **^{13}C NMR ($CDCl_3$, 100 MHz)** δ 153.1 (C-OH, C-O-Si), 139.4 (C=C), 136.7 (C=C), 136.3 (C_q), 135.8 (C_q), 129.8 (ArC), 129.5 (ArC), 119.1 (ArC), 114.4 (ArC), 32.0 (CH_2), 26.1 (CH_2), 25.9 (CH_2), 25.8 (CH_2), 25.2 (CH_3), 17.7 ($\underline{C}(CH_3)_3$), -4.9 (CH_3) **HRMS (EI):** Found 445.2519 $(M+Na)^+$, $C_{27}H_{38}NaO_2Si$ requires 455.2539. **IR:** ν_{max} (KBr) cm^{-1}: 3345.2 (br.), 2928.7, 2856.5, 1603.4, 1503.5, 1253.8 (br.), 1166.7, 917.0

8.3.6 4-((4-((*tert*-Butyldimethylsilyl)oxy)phenyl)(4-methylcyclon-hexaneylidene)methyl)phenol [210]

As per general method 8.3.1, $TiCl_4$ (4.5 eq., 5.2 g, 27.4 mmol, 3 mL), Zn dust (9 eq., 3.58 g, 54.81 mmol), [194] (1 eq., 2 g, 6.09 mmol) and 4-methylcyclon-hexaneanone [205] (3 eq., 2.05 g, 18.27 mmol, 2.24 mL) were reacted. The crude material was purified *via* flash chromatography over silica gel (*n*-Hexane:DCM, 3:1) to afford the product as an orange resin (2.15 g, 86%)

^{1}H NMR ($CDCl_3$, 400 MHz) δ 7.04 -7.08 (m, 4H, Ar-H), 6.80 – 6.86 (m, 4H, Ar-H), 2.69 (d, *J* = 13.1 Hz, 4H, 2 × CH_2), 2.05 (m, 5H, CH, 2 × CH_2), 1.09 (s, 9H, 3 × CH_3), 1.02 (d, 3H, J=6.5 Hz, CH_3), 0.30 (s, 6H, 2 × CH_3) **^{13}C NMR ($CDCl_3$, 100 MHz)** δ 153.4 (C-OH), 153.3 (C-OSi), 137.4 (C_q), 136.2 (C_q), 135.6 (C_q), 133.3 (C_q), 130.7, 130.5, 118.9, 114.4, 32.4 (CH), 29.0 (CH_2), 26.6 (CH_2), 25.2 (CH_3), 17.8 ($\underline{C}(CH_3)_3$), -4.7 (CH_3) **HRMS (EI):** Found 409.2570 $(M+H)^+$, $C_{26}H_{37}O_2Si$ requires 409.2563. **IR :** ν_{max} (KBr) cm^{-1}: 3369.1, 3031.2, 2919.0, 2855.1, 1704.1, 1603.2. 1505.4, 1471.7, 1362.1, 1253.0, 1167.5, 1099.6, 1007.4, 916.0839, 780.7, 734.2

8.3.7 General method for the bromoalkylation of phenol

The appropriate phenol [206]-[210] (1 eq.) was dissolved in 1,2-dibromoethane (~50 eq.) with stirring. Tetrabutylammonium hydrogen sulfate (5 mmol) was added followed by 1 M NaOH solution (50 mL). The biphasic mixture was stirred vigorously at RT for 16 h. The reaction mixture was worked up *via* the addition of DCM (100 mL) and $NaHCO_3$ solution (100 mL). The aq. layer was extracted with DCM (100 mL) and the organic layer were combined and washed with water (50 mL), brine (50 mL) and dried over Na_2SO_4 after filtration the solvent was evaporated under reduced pressure. The material was purified *via* flash chromatography over silica gel to afford the product. (DCM : *n*-Hexane)

8.3.8 (4-((4-(2-Bromoethoxy)phenyl)(cyclopentylidene)methyl)phenoxy)(*tert*-butyl)dimethylsilane [211]

As per general method 8.3.7, phenol [206] (1 eq., 2.1 g, 5.52 mmol), 1,2-dibromoethane (~50 eq. 52.29 g, 275.8 mmol, 24 mL) and tetrabutylammonium hydrogen sulfate (1.7 g, 5 mmol) were reacted together. The crude product was purified *via* flash chromatography over silica gel (*n*-Hexane:DCM, 4:1) to afford the product as a clear resin (2.5 g, 93%)

^{1}H NMR ($CDCl_3$, 400 MHz) δ 6.67 - 7.46 (m, 8H, Ar-H), 4.23 - 4.39 (m, 2H, CH_2), 3.59 - 3.75 (m, 2H, CH_2), 1.46 - 1.78 (m, 4H, 2 × CH_2), 1.01 (s, 9H, 3 × CH_3), 0.23 (s, 6H, 2 × CH_3) **^{13}C NMR ($CDCl_3$, 100 MHz)** δ 156.9 (C-OSi), 154.6 (C-OCH_2), 130.0, 129.7, 128.9, 128.8, 128.6, 120.1, 118.9, 113.6, 113.6, 113.5, 67.3 (CH_2), 32.8 (CH_2), 28.7 (CH_2), 26.6 (CH_2), 25.2 (CH_3), 17.7 ($\underline{C}(CH_3)_3$), -4.8 (CH_3) **HRMS (EI):** Found 487.1666 $(M+H)^+$, $C_{26}H_{36}BrO_2Si$ requires 487.1662 **IR :** ν_{max} (KBr) cm^{-1}: 2955.0, 2858.7, 1651.1, 1597.8, 1508.3, 1255.3 (br.), 1169.7, 913.6

8.3.9 (4-((4-(2-Bromoethoxy)phenyl)(cyclon-hexaneylidene)methyl)phenoxy)(*tert*-butyl)dimethylsilane [212]

As per general method 8.3.7, phenol [207] (1 eq., 2.1 g, 5.32 mmol), 1,2-dibromoethane (~50 eq. 52.29 g, 275.8 mmol, 24 mL) and tetrabutylammonium hydrogen sulfate (1.7 g, 5 mmol) were reacted together. The crude product was purified *via* flash chromatography over silica gel (*n*-Hexane:DCM, 4:1) to afford the product as a clear resin (2.44 g, 91%)

^{1}H NMR ($CDCl_3$, 400 MHz) δ 7.06 (d, *J* = 8.53 Hz, 2H, Ar-H), 6.98 (d, *J* = 8.28 Hz, 2H, Ar-H), 6.85 (d, *J* = 8.78 Hz, 2H, Ar-H), 6.76 (d, *J* = 8.78 Hz, 2H, Ar-H), 4.30 (t, *J* = 6.27 Hz, 2H, CH_2), 3.66 (t, *J* = 6.27 Hz, 2H, CH_2), 2.23 - 2.31 (m, 4H, 2 × CH_2), 1.59 - 1.68 (m, 6H, 3 × CH_2), 1.01 (s, 9H, 3 × CH_3), 0.23 (s, 6H, 2 × CH_3) **^{13}C NMR ($CDCl_3$, 100 MHz)** δ 156.3 (C-O-CH_2), 153.8 (C-O-Si), 138.4 (C=C), 136.8 (C=C), 136.3 (C_q), 133.5 (C_q), 131.0 (ArC), 130.8 (ArC), 119.3 (ArC), 114.1 (ArC), 67.8 (CH_2), 32.5 (CH_2), 29.2 (CH_2), 28.7 (CH_2), 26.9 (CH_2), 25.7 (CH_3), 18.2 ($\underline{C}(CH_3)_3$), -4.4 (CH_3) **HRMS (EI):** Found 501.1827 $(M+H)^+$, $C_{27}H_{38}BrO_2Si$ requires 501.1819. **IR :** ν_{max} (KBr) cm^{-1}: 2930.1, 2857.5, 1654.4, 1600.6, 1508.2, 1471.9, 1254.5, 1168.0, 913.8, 838.9, 804.6, 781.1

8.3.10 (4-((4-(2-Bromoethoxy)phenyl)(cycloheptylidene)methyl)phenoxy)(*tert*-butyl)dimethylsilane [213]

As per general method 8.3.7, phenol [208] (1 eq., 2.35 g, 5.70 mmol), 1,2-dibromoethane (~50 eq. 56.64 g, 298.8 mmol, 26 mL) and tetrabutylammonium hydrogen sulfate (1.7 g, 5 mmol) were reacted together. The crude product was purified *via* flash chromatography over silica gel (*n*-Hexane:DCM, 4:1) to afford the product as a clear resin (2.76 g, 94%)

^{1}H NMR ($CDCl_3$, 400 MHz) δ 7.09 (d, *J* = 8.53 Hz, 2H, Ar-H), 7.00 (d, *J* = 8.53 Hz, 2H, Ar-H), 6.84 (d, *J* = 8.53 Hz, 2H, Ar-H), 6.75 (d, *J* = 8.53 Hz, 2H, Ar-H), 4.29 (t, *J* = 6.27 Hz, 2H, CH_2), 3.65 (t, *J* = 6.27 Hz, 2H, CH_2), 2.32 (s, 4H, 2 × CH_2), 1.59 (s, 8H, 4 × CH_2), 0.99 (s, 9H, 3 × CH_3), 0.20 (s, 6H, 2 × CH_3) **^{13}C NMR ($CDCl_3$, 100 MHz)** δ 155.7 (C-O-CH_2), 153.2 (C-O-Si), 139.2 (C=C), 136.7 (C=C), 136.3 (C_q), 135.8 (C_q), 130.1 (ArC), 129.8 (ArC), 118.9 (ArC), 113.6 (ArC), 67.3 (CH_2), 32.9 (CH_2), 29.0 (CH_2), 28.8 (CH_2), 27.7 (CH_2), 25.2 (CH_3), 17.7 ($\underline{C}(CH_3)_3$), -4.9 (CH_3) **HRMS (TOF-MS):** Found 514.1895 $(M+H)^+$, $C_{28}H_{39}O_2BrSi$ requires 514.1903. **IR :** ν_{max} (KBr) cm^{-1}: 2929.0, 2856.8, 1602.8, 1507.6, 1471.7, 1254.1, 1168.0, 1016.7, 913.9, 839.4, 781.0

8.3.11 (4-((4-(2-Bromoethoxy)phenyl)(cyclooctylidene)methyl)phenoxy)(*tert*-butyl)dimethylsilane [214]

As per general method 8.3.7, phenol [209] (1 eq., 2.33 g, 5.70 mmol), 1,2-dibromoethane (~50 eq. 56.64 g, 298.8 mmol, 26 mL) and tetrabutylammonium hydrogen sulfate (1.7 g, 5 mmol) were reacted together. The crude product was purified *via* flash chromatography over silica gel (*n*-Hexane:DCM, 4:1) to afford the product as a clear resin (2.83 g, 94%)

^{1}H NMR ($CDCl_3$, 400 MHz) δ 7.12 (d, *J* = 8.53 Hz, 2H, Ar-H), 7.03 (d, *J* = 8.03 Hz, 2H, Ar-H), 6.85 (d, *J* = 8.53 Hz, 2H, Ar-H), 6.76 (d, *J* = 8.53 Hz, 2H, Ar-H), 4.28 (t, *J* = 6.27 Hz, 2H, CH_2), 3.65 (t, *J* = 6.27 Hz, 2H, CH_2), 2.24 - 2.32 (m, 4H, 2 × CH_2), 1.63 - 1.71 (m, 2H, CH_2), 1.48 - 1.63 (m, 8H, 4 × CH_2), 0.99 (s, 9H, 3 × CH_3), 0.20 (s, 6H, 2 × CH_3) **^{13}C NMR ($CDCl_3$, 100 MHz)** δ 155.6 (C-O-CH_2), 153.1 (C-O-Si), 139.6 (C=C), 137.0 (C=C), 136.5 (C_q), 135.7 (C_q), 129.7 (ArC), 129.5 (ArC), 119.1 (ArC), 113.8 (ArC), 67.3 (CH_2), 32.0 (CH_2), 28.8 (CH_2), 26.1 (CH_2), 26.0 (CH_2), 25.8 (CH_2), 25.2 (CH_3), 17.7 ($\underline{C}(CH_3)_3$), -4.8 (CH_3) **HRMS (EI):** Found 529.2139 $(M+H)^+$, $C_{29}H_{42}BrO_2Si$ requires 529.2132 **IR :** ν_{max} (KBr) cm^{-1}: 2929.6, 2857.7, 1651.2, 1598.9, 1508.5, 1255.3 (br.), 1168.2, 912.8

8.3.12 (4-((4-(2-Bromoethoxy)phenyl)(4-methylcyclon-hexaneylidene)methyl)phenoxy)(*tert*-butyl)dimethylsilane [215]

As per general method 8.3.7, phenol [210] (1 eq., 2.3 g, 5.63 mmol), 1,2-dibromoethane (~50 eq. 56.64 g, 298.8 mmol, 26 mL) and tetrabutylammonium hydrogen sulfate (1.7 g, 5 mmol) were reacted together. The crude product was purified *via* flash chromatography over silica gel (*n*-Hexane:DCM, 4:1) to afford the product as a clear resin (2.61 g, 90%)

^{1}H NMR ($CDCl_3$, 400 MHz) δ 7.09 (d, J = 8.5 Hz, 2H, Ar-H), 7.02 (d, *J* = 8.0 Hz, 2H, Ar-H), 6.87 (d, *J* = 8.5 Hz, 2H, Ar-H), 6.80 (d, *J* = 8.0 Hz, 2H, Ar-H), 4.31 (t, *J* = 6.3 Hz, 2H, CH_2), 3.67 (t, *J* = 6.3 Hz, 2H, CH_2), 2.64 (t, *J* = 11.5 Hz, 2H, CH_2), 1.96 – 2.03 (m, 2H, CH_2), 1.82 (d, *J* = 12.0 Hz, 2H, CH_2), 1.61 – 1.72 (m, 1H, CH), 1.08 – 1.18 (m, 2H, CH_2), 1.04 (s, 9H, CH_3), 0.98 (d, *J* = 6.5 Hz, 3H, CH_3), 0.21 (s, 6H, 2 × CH_3) **^{13}C NMR ($CDCl_3$, 100 MHz)** δ 155.9 (C-OC), 153.4 (C-OSi), 137.6 (C_q), 136.3 (C_q), 135.9 (C_q), 133.2 (C_q), 130.6 (C_q), 130.4, 118.8, 118.8, 113.6, 69.3 (CH_2), 36.5 (CH_2), 32.4 (CH), 31.4 (CH_2), 28.8 (CH_2), 25.3 (CH_3), 17.77 ($\underline{C}(CH_3)_3$), -4.8 (CH_3) **HRMS (EI):** Found 515.2006 $(M+H)^+$, $C_{28}H_{40}O_2SiBr$ requires 515.1981. **IR :** ν_{max} (KBr) cm^{-1}: 2951.7, 2927.8, 2857.0, 1604.5, 1507.3, 1472.0, 1457.4, 1254.1, 1168.2, 1017.15, 914.7, 839.7, 804.7, 780.5

8.3.13 General method for the amination of bromoalkyl ketones.

Methylamine (2 M in THF) (~20 eq.) was added to the alkyl bromide compound [211]-[215] and sealed in a high pressure tube. The reaction mixture was heated to 60 °C while stirring for 48 h. The reaction mixture was allowed sufficient time to cool, allowing the internal pressure to decrease prior to opening the pressure tube. The solvent was evaporated under reduced pressure. The oil was dissolved in DCM (30 mL) and was washed with a pH10 aq. Solution* (30 mL). The pH 10 aq. Solution* was extracted with DCM (2 × 30 mL). The organic layers were combined and washed with water (50 mL), brine (50 mL) and dried over Na_2SO_4. The solvent was evaporated under reduced pressure to obtain a brown oil. The crude material was purified *via* flash chromatography on silica gel. (DCM : EtOAc)

* pH10 aq. Solution = 6 g of $NaHCO_3$ and 6 g of Na_2CO_3 per 100 mL of water

8.3.14 2-(4-((4-((*tert*-Butyldimethylsilyl)oxy)phenyl)(cyclopentylidene)methyl) phenoxy)-N-methylethanamine [216]

As per general method 8.3.13, [211] (1 g, 2.05 mmol) and methylamine (~20 eq, 41.02 mmol, 20 mL) were reacted together. The crude material was purified *via* flash chromatography on silica gel (DCM:EtOAc, 2:1) to afford a brown resin (737 mg, 82%)

^{1}H NMR ($CDCl_3$, 400 MHz) δ 7.10 (d, *J* = 8.53 Hz, 2H, Ar-H), 7.03 (d, *J* = 8.53 Hz, 2H, Ar-H), 6.86 (d, *J* = 8.53 Hz, 2H, Ar-H), 6.76 (d, *J* = 8.03 Hz, 2H, Ar-H), 4.12 - 4.19 (m, 2H, CH_2), 3.03 - 3.16 (m, 2H, CH_2), 2.58 (s, 3H, CH_3), 2.34 - 2.44 (m, 4H, 2 × CH_2), 1.63 - 1.73 (m, 4H, 2 × CH_2), 1.00 (s, 9H, 3 × CH_3), 0.20 (s, 6H, 2 × CH_3) **^{13}C NMR ($CDCl_3$, 100 MHz)** δ 156.0 (C-O-CH_2), 153.2 (C-O-Si), 141.8 (C=C), 136.4 (C=C), 136.3(C_q), 131.4 (C_q), 129.9 (ArC), 129.7 (ArC), 118.9 (ArC), 113.4 (ArC), 65.1 (CH_2), 49.5 (CH_2), 32.8 (CH_3), 26.49 (CH_2), 26.47 (CH_2), 25.2 (CH_3), 17.7 ($\underline{C}(CH_3)_3$), -4.8 (CH_3) **HRMS (EI):** Found 438.2838 $(M+H)^+$, $C_{27}H_{40}NO_2Si$ requires 438.2823. **IR :** ν_{max} (KBr) cm^{-1}: 3343.1 (br.), 2955.1, 2930.6, 2857.7, 1660.9, 1604.1, 1508.4, 1254.1 (br.), 1168.9, 915.4

8.3.15 2-(4-((4-((*tert*-Butyldimethylsilyl)oxy)phenyl)(cyclon-hexaneylidene)methyl) phenoxy)-N-methylethanamine [217]

As per general method 8.3.13, [212] (1 g, 2.0 mmol) and methylamine (~20 eq, 41.02 mmol, 20 mL) were reacted together. The crude material was purified *via* flash chromatography on silica gel (DCM:EtOAc, 2:1) to afford a brown resin (781 mg, 86%)

^{1}H NMR ($CDCl_3$, 400 MHz) δ 7.03 (d, *J* = 8.5 Hz, 2H, Ar-H), 6.96 (d, *J* = 8.5 Hz, 2H, Ar-H), 6.84 (d, *J* = 8.5 Hz, 2H, Ar-H), 6.74 (d, *J* = 8.5 Hz, 2H, Ar-H), 4.13-4.17 (m, 2H, CH_2), 3.08 (d, *J* = 6.5 Hz, 2H, CH_2), 2.58 (s, 3H, CH_3), 2.24 (d, *J* = 5.0 Hz, 4H, 2 × CH_2), 1.56-1.63 (m, 6H, 3 × CH_2), 0.99 (s, 9H, CH_3), 0.21 (s, 6H,

CH_3) **^{13}C NMR ($CDCl_3$, 100 Hz)** δ 156.1 (C-O-CH_2), 153.3 (C-OSi), 137.9 (C_q), 136.0 (C_q), 135.8 (C_q), 133.0 (C_q), 130.5, 130.3, 118.8, 113.4, 65.1 (CH_2), 49.5 (CH_2), 34.7 (NCH_3), 32.1 (CH_2), 32.0 (CH_2), 28.2 (CH_2), 26.4 (CH_3), 17.71 ($\underline{C}(CH_3)_3$), -4.83 (CH_3) **HRMS (EI):** Found 452.2982 $(M+H)^+$, $C_{28}H_{42}NO_2Si$ requires 452.2985. **IR :** ν_{max} (KBr) cm^{-1}: 3435.1, 2928.5, 2854.3, 1606.2, 1507.9, 1471.3, 1255.0, 1168.7, 915.1, 835.8, 778.9

8.3.16 2-(4-((4-((*tert*-Butyldimethylsilyl)oxy)phenyl)(cycloheptylidene)methyl) phenoxy)-N-methylethanamine [218]

As per general method 8.3.13, [213] (1 g, 1.94 mmol) and methylamine (~20 eq, 41.02 mmol, 20 mL) were reacted together. The crude material was purified *via* flash chromatography over silica gel (DCM:EtOAc, 2:1) to afford a brown resin (813 mg, 90%)

^{1}H NMR ($CDCl_3$, 400 MHz) δ 7.07 (d, *J* = 8.8 Hz, 2H, Ar-H), 7.00 (d, *J* = 8.3 Hz, 2H, Ar-H), 6.83 (d, *J* = 8.3 Hz, 2H, Ar-H), 6.74 (d, *J* = 8.3 Hz, 2H, Ar-H), 4.08 (d, *J* = 6.5 Hz, 2H, CH_2), 3.61 (d, *J* = 6.5 Hz, 2H, CH_2), 2.99 (s, 1H, NH), 2.52 (s, 3H, CH_3), 2.29-2.33 (m, 4H, 2 × CH_2), 1.55-1.64 (m, 8H, 4 × CH_2), 0.99 (s, 9H, CH_3), 0.20 (s, 6H, CH_3) **^{13}C NMR ($CDCl_3$, 100 MHz)** δ 156.7 (C-O-CH_2), 153.6 (C-OSi), 139.5 (C_q), 136.8 (C_q), 136.7 (C_q), 136.4 (C_q), 132.0 (C_q), 130.4, 130.3, 128.5, 120.0, 119.3, 113.8, 113.6, 65.1 (CH_2), 49.5 (CH_2), 33.5 (NCH_3), 33.4 (CH_2), 29.4 (CH_2), 28.2 (CH_2), 28.1 (CH_2), 25.7 (CH_3), 18.1 ($\underline{C}(CH_3)_3$), -4.8 (CH_3) **HRMS (EI):** Found 446.3152 $(M+H)^+$, $C_{29}H_{44}NO_2Si$ requires 446.3141 . **IR :** ν_{max} (KBr) cm^{-1}: 3436.1, 2928.1, 2855.9, 1604.3, 1507.1, 1471.7, 1253.4, 1171.7, 1045.2, 914.6, 839.2, 805.0, 780.6

8.3.17 2-(4-((4-((*tert*-Butyldimethylsilyl)oxy)phenyl)(cyclooctylidene)methyl)phenoxy)-N-methylethanamine [219]

As per general method 8.3.13, [214] (1 g, 1.89 mmol) and methylamine (~20 eq, 41.02 mmol, 20 mL) were reacted together. The crude material was purified *via* flash chromatography over silica gel (DCM:EtOAc, 2:1) to afford a brown resin (761 mg, 84%).

^{1}H NMR ($CDCl_3$, 400 MHz) δ 7.06 - 7.15 (m, 2H, Ar-H), 6.98 - 7.06 (m, 2H, Ar-H), 6.85 - 6.93 (m, 2H, Ar-H), 6.71 - 6.79 (m, 2H, Ar-H), 4.16 - 4.26 (m, 2H, CH_2), 3.10 - 3.24 (m, 2H, CH_2), 2.60 (s, 3H, CH_3), 2.20 - 2.32 (m, 4H, 2 × CH_2), 1.62 - 1.73 (m, 2H, CH_2), 1.45 - 1.62 (m, 8H, 4 × CH_2), 0.99 (s, 9H, 3 × CH_3), 0.19 (s, 6H, 2 × CH_3) **^{13}C NMR ($CDCl_3$, 100 MHz)** δ 155.4 (C-O-CH_2), 153.1 (C-O-Si), 139.6 (C=C), 137.1 (C=C), 136.5 (C_q), 135.6 (C_q), 129.6 (ArC), 129.4 (ArC), 119.1 (ArC), 113.8 (ArC), 63.3 (CH_2), 48.5 (CH_2), 33.6 (CH_3), 32.0 (CH_2), 26.0 (CH_2), 25.9 (CH_2), 25.7 (CH_2), 25.2 (CH_3), 17.7 ($\underline{C}(CH_3)_3$), -4.8 (CH_3) **HRMS (EI):** Found 480.3301 $(M+H)^+$, $C_{30}H_{46}NO_2Si$ requires 480.3292. **IR :** ν_{max} (KBr) cm^{-1}: 3413.8 (br.), 2927.7, 2856.0, 1643.2, 1605.9, 1506.7, 1241.1 (br.), 1168.5, 835.8

8.3.18 2-(4-((4-((*tert*-Butyldimethylsilyl)oxy)phenyl)(4-methylcyclon-hexaneylidene)methyl)phenoxy)-N-methylethanamine [220]

As per general method 8.3.13, [215] (1 g, 1.94 mmol) and methylamine (~20 eq, 41.02 mmol, 20 mL) were reacted together. The crude material was purified *via* flash chromatography on silica gel (DCM:EtOAc, 2:1) to afford brown resin (722 mg, 80%)

^{1}H NMR ($CDCl_3$, 400 MHz) δ 7.04 (d, *J* = 7.0 Hz, 2H, Ar-H), 6.97 (d, *J* = 8.5 Hz, 2H, Ar-H), 6.84 (d, *J* = 8.5 Hz, 2H, Ar-H), 6.75 (d, *J* = 8.5 Hz, 2H, Ar-H), 4.09 (t, *J* = 4.5 Hz, 2H, CH_2), 3.01 (s, 2H, CH_2), 2.75 (s, 1H, NH), 2.54 – 2.62 (m, 5H, CH_3, CH_2), 1.95 (t, *J* = 12.5 Hz, 2H, CH_2), 1.78 (d, 2H, CH_2), 1.60-1.64 (m, 1H, CH), 1.09 (q, *J* = 12.0 Hz, 2H, CH_2), 1.00 (s, 9H, CH_3), 0.94 (d, *J* = 6.6 Hz, 3H, CH_3), 0.22 (s, 6H, CH_3) **^{13}C NMR ($CDCl_3$, 100 MHz)** δ 156.5 (C-O-CH_2), 153.3 (C-OSi), 137.4 (C_q), 135.9 (C_q), 135.8 (C_q), 133.2 (C_q),

130.5, 130.4, 130.4, 118.8, 113.3, 66.1 (CH_2), 50.2 (CH_2), 36.4 (CH_2), 35.6 (NCH_3), 32.4 (CH), 31.3 (CH_2), 25.2 (CH_3), 17.7 ($\underline{C}(CH_3)_3$), -4.8 (CH_3) **HRMS (EI):** Found 466.3156 $(M+H)^+$, $C_{29}H_{44}NO_2Si$ requires 466.3141. **IR :** ν_{max} (KBr) cm^{-1}: 3435.6, 2946.9, 2927.7, 2856.3, 1605.4, 1507.9, 1457.6, 1471.9, 1253.3, 1168.5, 1045.1, 915.2, 838.1, 805.0, 780.0

8.3.19 General method for deprotection of *tert*-butyldimethylsilyl (TBDMS) ether group

The appropriate silyl ether [216]-[220] was dissolved in a minimum amount of THF (~3 mL) while stirring under N_2. An equimolar quantity of TBAF (1 M in THF) was added and the mixture was allowed to stir for 30 min. The reaction was monitored *via* TLC. The solvent was evaporated to dryness. The residue was redissolved in DCM (20 mL) and washed with a 10% HCl solution (10 mL). The organic phase was dried over Na_2SO_4 and evaporated to dryness in *vacuo*. The residue is purified *via* flash chromatography on silica gel to afford the products.

8.3.20 4-(Cyclopentylidene(4-(2-(methylamino)ethoxy)phenyl)methyl)phenol [221]

As per general deprotection method 8.3.19, protected cyclofenil derivative [216] (200 mg, 0.457 mmol) and TBAF (1 M in THF) (0.457 mmol, 0.457 ml) were reacted together in THF (3 mL). The residue was purified *via* flash chromatography on silica gel (DCM:MeOH, gradient 50:1 to 40:1) to afford the product as a pale pink solid (107 mg, 73%).

^{1}H NMR ($CDCl_3$, 400 MHz) δ 9.23 - 9.42 (m, 1H, OH), 7.03 (d, *J* = 8.53 Hz, 2H, Ar-H), 6.92 (d, *J* = 8.53 Hz, 2H, Ar-H), 6.86 (d, *J* = 8.53 Hz, 2H, Ar-H), 6.68 (d, *J* = 8.53 Hz, 2H, Ar-H), 4.00 (t, *J* = 5.52 Hz, 2H, CH_2), 2.84 (t, *J* = 5.27 Hz, 2H, CH_2), 2.35 (s, 3H, NCH_3), 2.26 - 2.34 (m, 4H, 2 × CH_2), 1.54 - 1.69 (m, 4H, 2 ×CH_2) **^{13}C NMR ($CDCl_3$, 100 MHz)** δ 157.1 (C-OH), 155.9 (C-O-CH_2), 140.9 (C=C), 136.3 (C=C), 134.5 (C_q), 132.4 (C_q), 130.3 (ArC), 115.2 (ArC), 114.3 (ArC), 67.2 (CH_2), 50.6 (CH_2), 36.4 (NCH_3), 33.2 (CH_2), 26.9 (CH_2) **HRMS (EI):** Found 324.1950 $(M+H)^+$, $C_{21}H_{26}NO_2$ requires 324.1958. **IR :** ν_{max} (KBr) cm^{-1}: 3438.3 (br.), 2952.55, 2864.3, 2591.1, 1608.2, 1507.1, 1268.9, 1235.6, 1053.8, 834.8 **MP:** 160-163 °C

8.3.21 4-(Cyclonhexaneylidene(4-(2-(methylamino)ethoxy)phenyl)methyl)phenol [222]

As per general deprotection method 8.3.19, protected cyclofenil derivative [217] (200 mg, 0.442 mmol) and TBAF (1 M in THF) (0.442 mmol, 0.442 ml) were reacted together in THF (3 mL). The residue was purified *via* flash chromatography on silica gel (DCM:MeOH, gradient 50:1 to 40:1) to afford the product as a white solid (116 mg, 78%).

^{1}H NMR (DMSO-d_6, 400 MHz) δ 6.95 (d, *J* = 8.53 Hz, 2H, Ar-H), 6.77 - 6.88 (m, 4H, Ar-H), 6.67 (d, *J* = 8.53 Hz, 2H, Ar-H), 3.98 (t, *J* = 5.52 Hz, 2H, CH_2), 2.80 (t, *J* = 5.65 Hz, 2H, CH_2), 2.33 (s, 3H, NCH_3), 2.09 - 2.23 (m, 4H, 2 × CH_2), 1.46 - 1.64 (m, 6H, 3 × CH_2) (OH not present) **^{13}C NMR (DMSO-d_6, 100 MHz)** δ 157.3 (C-OH), 157.0 (C-OCH_2), 137.0 (C_q), 135.9 (C_q), 134.2 (C_q), 133.2 (C_q), 130.9, 130.8, 115.3, 114.3, 67.5 (CH_2), 50.8 (CH_2), 36.6 (NCH_3), 32.4 (CH_2), 28.6 (CH_2), 23.5 (CH_2) **HRMS (EI):** Found 338.2104 $(M+H)^+$, $C_{22}H_{28}NO_2$ requires 338.2115 **IR :** ν_{max} (KBr) cm^{-1}: 3438.2 (br.), 2930.0, 2847.3, 2660.1, 2591.11, 1607.8, 1508.4, 1465.7, 1302.6, 1273.0, 1168.4, 1041.8, 833.7 **MP:** 169-170 °C

8.3.22 4-(Cycloheptylidene(4-(2-(methylamino)ethoxy)phenyl)methyl)phenol [223]

As per general deprotection method 8.3.19, protected cyclofenil derivative [218] (200 mg, 0.429 mmol) and TBAF (1 M in THF) (0.429 mmol, 0.429 ml) were reacted together in THF (3 mL). The residue was purified *via* flash chromatography on silica gel (DCM:MeOH, gradient 50:1 to 40:1) to afford the product as a pale pink solid (122 mg, 81%).

^{1}H NMR (DMSO-d_6, 400 MHz) δ 7.00 (d, *J* = 8.78 Hz, 2H, Ar-H), 6.80 - 6.95 (m, 4H, Ar-H), 6.67 (d, *J* = 8.53 Hz, 2H, Ar-H), 3.97 (t, *J* = 5.65 Hz, 2H, CH_2), 2.80 (t, *J* = 5.52 Hz, 2H, CH_2), 2.33 (s, 3H, NCH_3), 2.18 - 2.27 (m, 4H, 2 × CH_2), 1.46 - 1.63 (m, 8H, 4 × CH_2) **^{13}C NMR (DMSO-d_6, 100 MHz)** δ 157.2 (C-OH), 156.0 (C-OCH_2), 138.4 (C_q), 137.1 (C_q), 136.4 (C_q), 134.5 (C_q), 130.3, 130.3, 115.2, 114.3, 67.5 (CH_2), 50.8 (CH_2), 36.6 (NCH_3), 33.3 (CH_2), 29.2 (CH_2), 28.0 (CH_2), 23.5 (CH_2) **HRMS (EI):** Found 352.2261 $(M+H)^+$, $C_{23}H_{30}NO_2$ requires 352.2271 **IR :** ν_{max} (KBr) cm^{-1}: 3440.6 (br.), 2929.7, 2849.4, 2575.8, 1607.4, 1505.9, 1463.3, 1274.6, 1240.8, 1168.6, 1045.2, 828.8 **MP:** 169-171 °C

8.3.23 4-(Cyclooctylidene(4-(2-(methylamino)ethoxy)phenyl)methyl)phenol [224]

As per general deprotection method 8.3.19, protected cyclofenil derivative [219] (200 mg, 0.417 mmol) and TBAF (1 M in THF) (0.417 mmol, 0.417 ml) were reacted together in THF (3 mL). The residue was purified *via* flash chromatography on silica gel (DCM:MeOH, gradient 50:1 to 40:1) to afford the product as a clear oil (119 mg, 78%).

^{1}H NMR (DMSO-d_6, 400 MHz) δ 7.02 (d, *J* = 8.53 Hz, 2H, Ar-H), 6.80 - 6.93 (m, 4H, Ar-H), 6.68 (d, *J* = 8.53 Hz, 2H, Ar-H), 3.96 (t, *J* = 5.65 Hz, 2H, CH_2), 2.80 (t, *J* = 5.77 Hz, 2H, CH_2), 2.32 (s, 3H, NCH_3), 2.13 - 2.26 (m, 4H, 2 × CH_2), 1.40 - 1.68 (m, 10H, 5 × CH_2) **^{13}C NMR (DMSO-d_6, 100 MHz)** δ 157.1 (C-OH), 156.8 (C-OCH_2), 138.5 (C_q), 137.2 (C_q), 136.8 (C_q), 134.1 (C_q), 130.0, 129.8, 115.5, 114.5, 67.5 (CH_2), 50.8 (CH_2), 36.6 (NCH_3), 32.4 (CH_2), 26.4 (CH_2), 26.2 (CH_2), 23.5 (CH_2) **HRMS (EI):** Found 366.2414 $(M+H)^+$, $C_{24}H_{32}NO_2$ requires 366.2428 **IR :** ν_{max} (KBr) cm^{-1}: 3438.1 (br.), 2932.3, 2871.9, 2852.2, 2640.4, 2566.5, 1607.9, 1587.1, 1505.9, 1455.8, 1274.9, 1239.5, 1168.1, 1046.6, 838.9

8.3.24 4-((4-(2-(Methylamino)ethoxy)phenyl)(4-methylcyclonhexaneylidene)methyl)phenol [225]

As per general deprotection method 8.3.19, protected cyclofenil derivative [220] (200 mg, 0.429 mmol) and TBAF (1 M in THF) (0.429 mmol, 0.429 ml) were reacted together in THF (3 mL). The residue was purified *via* flash chromatography on silica gel (DCM:MeOH, gradient 50:1 to 40:1) to afford the product as a pale pink solid (124 mg, 82%).

^{1}H NMR (DMSO-d_6, 400 MHz) δ 6.94 (d, *J* = 8.50 Hz, 2H, Ar-H), 6.78 - 6.88 (m, 4H, Ar-H), 6.68 (d, *J* = 8.53 Hz, 2H, Ar-H), 3.98 (t, *J* = 5.52 Hz, 2H, CH_2), 2.80 (t, *J* = 5.40 Hz, 2H, CH_2), 2.48 (t, *J* = 16.10 Hz, 2H, CH_2), 2.33 (s, 3H, NCH_3), 1.90 (dt, *J* = 3.14, 12.86 Hz, 2H, CH_2), 1.72 (d, *J* = 11.80 Hz, 2H, CH_2), 1.51 - 1.63 (m, 3H, CH_2, CH), 0.90 (d, *J* = 6.27 Hz, 3H, CH_3) **^{13}C NMR (DMSO-d_6, 100 MHz)** δ 157.3 (C-OH), 156.6 (C-OCH_2), 136.7 (C_q), 135.9 (C_q), 134.3 (C_q), 133.6 (C_q), 130.9, 130.8, 115.2, 114.3, 67.5 (CH_2), 50.8 (CH_2), 36.6 (NCH_3), 32.7 (CH), 31.7 (CH_2), 23.5 (CH_2), 22.4 (CH_3) **HRMS (EI):** Found 352.2264 $(M+H)^+$, $C_{23}H_{30}NO_2$ requires 352.2271 **IR :** ν_{max} (KBr) cm^{-1}: 3439.7 (br.), 2945.8, 2913.1, 2887.4, 2866.9, 1607.06, 1505.9, 1456.2, 1270.3, 1234.5, 1168.2, 1043.6, 830.4 **MP:** 74-76 °C

8.4 Synthesis of 2-phenylindole derivatives

8.4.1 5-Methoxy-2-(4-methoxyphenyl)-3-methyl-1*H*-indole [231][563]

A mixture of 4-methoxyphenylhydrazine [230] (2g, 11.44 mmol) and 4-methoxypropiophenone [229] (2.06 g, 12.58 mmol) was dissolved in EtOH (50 mL). To this solution, 10 drops of concentrated HCl was added. The solution was heated at reflux at 80 °C for 6 hrs. The resulting solution was allowed to cool and a precipitate formed. This solution was filtered using vacuum filtration. The filtrate was washed with cold EtOH (5 mL) to afford the product as a pale pink solid (2.3 g, 75.3 %), which was recrystallised from EtOH.

^{1}H NMR ($CDCl_3$, 400 MHz) δ 7.88 (br s, 1H, NH), 7.53 (d, *J*= 8.8 Hz, 2H, Ar-H), 7.26 (d, *J*= 8.5Hz, 1H, Ar-H), 7.04 (s, 2H, Ar-H), 7.02 (s, 1H, Ar-H), 6.88 (dd, *J*=8.5Hz, J=2Hz, 1H, Ar-H), 3.92 (s, 3H, OCH_3), 3.89 (s, 3H, OCH_3), 2.44 (s, 3H, CH_3) **^{13}C NMR ($CDCl_3$, 400 MHz)** δ 158.47 (C-OCH_3), 153.63 (C-OCH_3), 134.55 (C_q), 130.37 (C_q), 130.03 (C_q), 128.48 (C=C), 113.80 (Ar-C), 111.48 (Ar-C), 110.88 (Ar-C), 107.09 (C=C), 100.27 (Ar-C), 55.53 (OCH_3), 54.91 (OCH_3), 9.26 (CH_3) **HRMS (EI):** Found 268.1335 $(M+H)^+$, $C_{17}H_{18}NO_2$ requires 268.1338 **IR:** ν_{max} (KBr) cm^{-1}: 3382.0 (NH), 2933.2, 2833.0 (C-H), 1610.3, 1572.1, 1557.5, 1509.6, 1487.1, 1451.6, 1435.5, 1409.2, 1287.8, 1247.8, 1179.8, 1111.0, 1063.4, 1031.9, 1012.0, 995.9, 933.1, 840.4, 826.7, 803.9, 622.7, 570.7, 520.1, 503.2 **MP:** 142-146 °C

8.4.2 General method for alkylation of 5-Methoxy-2-(4-methoxyphenyl)-3-methyl-1*H*-indole

To a round bottomed flask was added sodium hydride (60 % in mineral oil, 10eq). The sodium hydride was washed 3 times with *n*-hexane (5 mL) to remove the mineral oil. The sodium hydride was then placed under nitrogen and to this was added dry THF (5 mL) at 0 °C. To this was added the phenylindole [231] (1 eq) and the mixture was allowed to stir for 15 min at 0 °C. The dibromoalkane [232]-[234] (5 eq) was then added and the mixture was allowed to stir for 15 min at 0 °C. The reaction was then put to reflux for 2 hours. To the resulting mixture was added water dropwise (5 mL) and then evaporated to dryness to afford a crude oil. The resulting crude mixture was re-dissolved in DCM (30 mL) and washed with water (3 × 30 mL), brine (30 mL) and dried over Na_2SO_4. The solvent was evaporated to dryness to yield crude product. The residue was purified *via* flash chromatography over silica gel (*n*-hexane: DCM) to afford the product.

8.4.3 1-(4-Bromobutyl)-5-methoxy-2-(4-methoxyphenyl)-3-methyl-1*H*-indole [235]

As per general method 8.4.2, indole [231] (0.5g, 1.5 mmol) and 1,4-dibromobutane [232] (1.87 mmol, 0.4g, 0.22 mL) were reacted together in dry THF (5 mL). The resulting oil was purified using flash chromatography over silicia gel to (*n*-Hexane:DCM, gradient 4:1 to 2:1) to afford the product as a yellow oil (0.35 g, 47%).

^{1}H NMR ($CDCl_3$, 400 MHz) δ 7.32 (d, *J*=8.8Hz, 2H, Ar-H), 7.26 (t, *J*= 8.8Hz, 1H, Ar-H), 7.07 (s, 2H, Ar-H), 7.04 (s, 1H, Ar-H), 6.92 (dd, *J*= 8.8Hz, 1H, Ar-H), 4.05 (t, J= 6.5 Hz, 2H, CH_2=N), 3.92 (s, 6H, OCH_3), 3.20 (t, 2H, J= 6.8, CH_2-Br), 2.23 (s, 3H, CH_3), 1.76 (quin, *J*= 7 Hz, 2H, CH_2), 1.63 (quin, *J*= 7 Hz, 2H, CH_2) **^{13}C NMR ($CDCl_3$, 400 MHz)** δ 158.83 (C-OCH_3), 153.47 (C-OCH_3), 137.49, 131.27 (Ar-C), 130.94 (Ar-C), 128.48, 124.10, 113.49 (Ar-C), 111.09 (Ar-C), 109.81(Ar-C), 107.93 (C=C), 100.33 (Ar-C), 55.57 (OCH_3), 54.89 (OCH_3), 42.42 (CH_2N), 32.61 (CH_2), 29.33 (CH_2), 28.09 (CH_2), 8.90 (CH_3), **HRMS (EI):** Found 402.1081 $(M+H)^+$, $C_{21}H_{25}{}^{79}BrNO_2$ requires 402.1069 **IR:** ν_{max} (KBr) cm^{-1}: 2934.18 (N-C), 2067.46, 1613.94,1560.12, 1507.89, 1482.65, 1459.30, 1438.68, 1417.92, 1383.68, 1353.06, 1289.79, 1248.47, 1228.33, 1209.44, 1174.27, 1152.85, 1107.69, 1036.51, 906.03, 836.53, 795.70, 737.85, 708.46, 632.56, 608.89.

8.4.4 1-(8-Bromooctyl)-5-methoxy-2-(4-methoxyphenyl)-3-methyl-1*H*-indole [236]

As per general method 8.4.2, indole [231] (1.5 g, 5.61 mmol) and 1,8-dibromooctane [233] (28.05 mmol, 7.63 g, 5.17 mL) were reacted together in THF (5 mL). The resulting oil was purified by flash chromatography over silica gel (*n*-Hexane:DCM, gradient 4:1 to 2:1) to afford the product as a yellow oil (1.34 g, 52%).

^{1}H NMR ($CDCl_3$, 400 MHz) δ 7.33 (d, *J*= 8.2 Hz, 2H, Ar-H), 7.27 (d, *J*= 8.8 Hz, 1H, Ar-H), 7.06 (s, 2H, Ar-H), 7.04 (s, 1H, Ar-H), 6.90 (dd, *J*= 2 Hz, *J*= 8.8 Hz, 1H, Ar-H), 4.00 (t, *J*= 6.8 Hz, 2H, CH_2N), 3.93 (s, 3H,

OCH_3), 3.92 (s, 3H, OCH_3), 3.40 (t, *J*= 6.8 Hz, 2H, CH_2), 2.24 (s, 3H, CH_3), 1.82(t, *J*= 8 Hz, 2H, CH_2), 1.60 (t, *J*= 7 Hz, 2H, CH_2), 1.36 (t, *J*= 7 Hz, 2H, CH_2), 1.17 (s, 4H, 2 × CH_2) **^{13}C NMR ($CDCl_3$, 400 MHz)** δ 158.73 ($COCH_3$), 153.35 ($COCH_3$), 137.57, 131.29 (Ar-C), 131.01 (Ar-C), 128.34, 124.36, 113.35 (Ar-C), 110.93 (Ar-C), 109.90 (Ar-C), 107.55, 100.21 (Ar-C), 55.39 (OCH_3), 54.89 (OCH_3), 43.38 (CH_2-N), 33.60 (CH_2-Br), 32.26 (CH_2), 29.51 (CH_2), 28.43 (CH_2), 28.04 (CH_2), 27.55 (CH_2), 26.17 (CH_2), 8.93 (CH_3) **HRMS (EI):** Found 458.1711 $(M+H)^+$, $C_{25}H_{33}{}^{79}BrNO_2$ requires 458.1695 **IR:** ν_{max} (KBr) cm^{-1}: 2931.06, 2855.84, 1614.40, 1560.01, 1507.91, 1483.03, 1460.31, 1438.57, 1383.12, 1353.00, 1289.51, 1247.72, 1217.84, 1173.91, 1107.09, 1076.80, 1037.71, 906.34, 834.86, 794.32, 723.88, 708.45, 632.84, 609.01

8.4.5 1-(12-Bromododecyl)-5-methoxy-2-(4-methoxyphenyl)-3-methyl-1*H*-indole [237]

As per general method 8.4.2, indole [231] (1 g, 3.74 mmol) and 1,12-dibromododecanane [234] (1.84 g, 5.61 mmol, 1.5 eq) were reacted together in THF (5 mL). The resulting oil was purified by flash chromatography over silica gel (*n*-Hexane:DCM, gradient 4:1 to 2:1) to afford the product as a yellow oil (1.08 g, 56%).

^{1}H NMR ($CDCl_3$, 400 MHz) δ 7.34 (d, *J*= 9 Hz, 2H, Ar-H), 7.27 (d, *J*= 9 Hz, 1H, Ar-H), 7.07 (s, 2H, Ar-H), 7.05 (s, 1H, Ar-H), 6.92 (dd, *J*= 7.5 Hz, *J*= 2.5 Hz, 1H, Ar-H), 4.01 (t, 2H, J=6.8Hz, CH_2-N), 3.94 (s, 3H, OCH_3), 3.92 (s, 3H, OCH_3), 3.45 (t, *J*= 6.8 Hz, 2H, CH_2-Br), 2.25 (s, 3H, CH_3), 1.89 (quin, *J*= 7.5 Hz, 2H, CH_2), 1.62 (d, J=6.5Hz, 2H, CH_2), 1.42 -1.45 (m, 2H, CH_2), 1.26 (m, 14H, CH_2) **^{13}C NMR ($CDCl_3$, 400 MHz)** δ 158.74 ($COCH_3$), 153.35 ($COCH_3$), 137.59, 131.30 (Ar-C), 131.05, 128.34, 124.40, 113.34 (Ar-C), 110.92 (Ar-C), 109.92 (Ar-C), 107.51, 100.21 (Ar-C), 55.59 (OCH_3), 54.86 (OCH_3), 43.48 (CH_2-N), 34.26 (CH_2-Br), 32.41 (CH_2), 29.65 (CH_2), 29.25 (CH_2), 29.00 (CH_2), 28.97 (CH_2), 28.68 (CH_2), 28.33 (CH_2), 27.74 (CH_2), 26.50 (CH_2), 26.35 (CH_2), 8.94 (CH_3) **HRMS (EI):** Found 514.2333 $(M+H)^+$ $C_{29}H_{41}{}^{79}BrNO_2$ requires 514.2321. **IR:** ν_{max} (KBr) cm^{-1}: 2926.84, 2853.74, 1614.47, 1560.15, 1507.91, 1483.01, 1459.86, 1438.38, 1383.02, 1353.33, 1289.46, 1219.21, 1173.66, 1106.96, 1079.48, 1038.29, 906.66, 834.06, 793.86

8.4.6 General method for synthesis of aminated derivatives of phenylindoles

The methylamine solution (2 M solution in THF, 20 eq) was added to the bromoalkyl phenylindole [235]-[237] and sealed in a high pressure tube. The reaction was heated to 65 °C while stirring for 48 hours. The reaction mixture was allowed sufficient time to cool, allowing any internal pressure to clear prior to carefully opening the reaction tube. The reaction was worked up *via* the addition of pH 10 buffer solution* (50 mL). The organic layers were combined, dried over sodium sulphate and the solvent evaporated in *vacuo* to afford a crude product which was then purified *via* flash chromatography over silica gel to afford product.

* pH10 aq. Solution = 6 g of $NaHCO_3$ and 6 g of Na_2CO_3 per 100 mL of water

8.4.7 4-(5-Methoxy-2-(4-methoxyphenyl)-3-methyl-1*H*-indol-1-yl)-*N*-methylbutan-1-amine [238]

As per general method 8.4.6, [235] (500 mg, 1.25 mmol) and methylamine (20 eq, 25 mmol, 12.5 mL) were reacted in THF (12 mL). The material was purified *via* flash chromatography on silica gel (DCM:EtOAc, gradient 4:1 to 2:1) to afford the product as a light brown oil (330 mg, 75 %)

^{1}H NMR ($CDCl_3$, 400 MHz) δ 7.32 (d, *J*= 8.5 Hz, 2H, Ar-H), 7.27 (d, *J*= 8.5 Hz, 1H, Ar-H), 7.05 (s, 2H, Ar-H), 7.03 (s, 1H, Ar-H), 6.90 (d, *J*= 9 Hz, 1H Ar-H), 4.03 (t, *J*= 7.5Hz, 2H, CH_2-N), 3.91 (s, 3H, OCH_3), 3.90 (s, 3H, OCH_3), 2.42 (t, 2H, CH_2), 2.35 (s, 3H, NCH_3), 2.22 (s, 3H, CH_3), 1.62 (quin, 2H, *J*= 7Hz, CH_2), 1.31 (quin, 2H, *J*= 7.5Hz, CH_2) **^{13}C NMR ($CDCl_3$, 400 MHz)** δ 158.78 (C-OCH_3), 153.40 (C-OCH_3), 137.49, 131.26 (Ar-C), 130.99, 128.43, 124.22, 113.44 (Ar-C), 110.99 (Ar-C), 109.85 (Ar-C), 107.78, 100.29 (Ar-C), 55.60 (OCH_3) 54.87 (OCH_3), 50.53 (OCH_2), 43.08 (CH_2-N), 35.30 (NCH_3), 27.23 (CH_2), 25.91 (CH_2), 8.89 (CH_3) **HRMS:** Found 353.2232 (M+H) + $C_{22}H_{29}N_2O_2$ requires 353.2229 **IR:** ν_{max} (KBr) cm^{-1}: 2932.54, 2834.91, 2791.39, 1613.87, 1507.83, 1482.73, 1460.05, 1439.60, 1355.29, 1289.37, 1216.53, 1174.35, 1037.04, 906.62, 835.00, 794.08.

8.4.8 8-(5-Methoxy-2-(4-methoxyphenyl)-3-methyl-1*H*-indol-1-yl)-*N*-methyloctan-1-amine [239]

As per general method 8.4.6, [236] (750 mg, 1.63 mmol) and methylamine (20 eq, 32.6 mmol, 16.3 mL) were reacted in THF (12 mL). The material was purified *via* flash chromatography over silica gel (DCM:EtOAc, gradient 4:1 to 2:1) to afford the product as a light brown oil (440 mg, 66 %)

^{1}H NMR ($CDCl_3$, 400 MHz) δ 7.31 (d, *J*= 8.5 Hz, 2H, Ar-H), 7.27 (d, *J*= 8.5 Hz, 1H, Ar-H), 7.05 (s, 2H, Ar-H), 7.03 (s, 1H, Ar-H), 6.90 (d, *J*= 8.5Hz, 1H, Ar-H), 3.98 (t, 2H, *J*= 7.5 Hz, CH_2-N), 3.92 (s, 3H, OCH_3), 3.91 (s, 3H, OCH_3), 2.58 (t, *J*= 7.5 Hz, 2H, CH_2-N), 2.46 (s, 3H, NCH_3), 2.22 (s, 3H, CH_3), 1.59 (quin, *J*= 7 Hz, 2H, CH_2), 1.47 (quin, *J*= 7 Hz, 2H, CH_2), 1.15 (m, 8H, 4 × CH_2) **^{13}C NMR ($CDCl_3$, 400 MHz)** δ158.71(C-OCH_3), 153.32 (C-OCH_3), 137.57 (Ar-C), 131.27 (Ar-C), 131.01, 128.32, 124.36, 113.34 (Ar-C), 110.91 (Ar-C), 109.90 (Ar-C), 107.51, 100.20 (Ar-C), 55.58 (OCH_3), 54.86 (OCH_3), 51.52 (CH_2), 43.42 (CH_2), 35.52 (NCH_3), 29.59 (CH_2), 28.81 (CH_2), 28.58 (CH_2), 26.66(CH_2), 26.26 (CH_2), 8.92 (CH_3) **HRMS (EI):** Found 409.2866 $(M+H)^+$, $C_{26}H_{37}N_2O_2$ requires 409.2855 **IR:** ν_{max} (KBr) cm^{-1}: 2929.02, 2855.08, 1614.09, 1558.24, 1507.71, 1482.90, 1460.78, 1383.03, 1289.47, 1247.27, 1173.77, 1107.03, 1077.98, 1036.73, 906.51, 834.95, 793.94, 708.11

8.4.9 12-(5-Methoxy-2-(4-methoxyphenyl)-3-methyl-1*H*-indol-1-yl)-*N*-methyldodec-1-amine [240]

As per general method 8.4.6, [237] (500 mg, 0.97 mmol) and methylamine (20 eq, 19.4 mmol, 9.7 mL) were reacted in THF (12 mL). The material was purified *via* flash chromatography on silica gel (DCM:EtOAc, gradient 4:1 to 2:1) to afford the product as a light brown oil (350 mg, 78 %)

^{1}H NMR ($CDCl_3$, 400 MHz) δ 7.31 (d, *J*= 8.5 Hz, 2H, Ar-H), 7.27 (d, *J*= 8.5 Hz, 1H, Ar-H), 7.05 (s, 2H, Ar-H), 7.02 (s, 1H, Ar-H), 6.90, (dd, *J*=2.5Hz, *J*= 9 Hz, 1H, Ar-H), 3.98 (t, *J*= 7.5 Hz, 2H, CH_2-N), 3.92 (s, 3H, OCH_3), 3.91 (s, 3H, OCH_3), 2.62 (t, *J*= 7.5 Hz, 2H, CH_2-NCH_3), 2.49 (s, 3H, NCH_3) 2.22 (s, 3H, CH_3), 1.56 (quin, *J*= 7 Hz, 4H, 2 × CH_2), 1.05-1.25 (m, 16H, 8CH_2)**^{13}C NMR ($CDCl_3$, 400 MHz)** δ 158.71 (C-OCH_3), 153.31 ($COCH_3$), 137.58, 131.27 (Ar-C), 131.01, 128.30, 124.37, 113.31 (Ar-C), 110.89 (Ar-C), 109.90 (Ar-C), 107.47, 100.19 (Ar-C), 55.58 (OCH_3), 54.85 (OCH_3), 51.19 (CH_2), 43.47 (CH_2), 35.33 (NCH_3), 29.64 (CH_2), 29.11 (CH_2), 29.09 (CH_2), 29.03 (CH_2), 28.97 (CH_2), 28.67 (CH_2), 26.67 (CH_2), 26.34 (CH_2), 8.91 (CH_3) **HRMS (EI):** Found 465.3501 $(M+H)^+$ $C_{30}H_{45}N_2O_2$ requires 465.3481 **IR:** ν_{max} (KBr) cm^{-1}: 2927.36, 2853.06, 1614.12, 1507.99, 1482.90, 1459.47, 1353.85, 1289.30, 1247.27, 1173.46, 1037.73, 906.25, 833.82, 793.27

8.4.10 1-(4-(Benzyloxy)phenyl)propan-1-one [246]

4-Hydroxypropiophenone [244] (5 g, 33.3 mmol) was dissolved in ACN (50 mL) under N_2, to the solution was added K_2CO_3 (3 g, 21.64 mmol) and benzyl bromide (5.7 g, 3.95 mL, 33.3 mmol). The mixture was stirred at RT for 16 h. The mixture was filtered and the solvent was evaporated under reduced pressure. The resulting oil was dissolved in DCM (100 mL) and the mixture was extracted with 1M HCL (50 mL), water (2 × 50 mL), brine (50 mL) and dried over Na_2SO_4. The solvent was evaporated under reduced pressure to obtain a pale yellow resin. The material was purified *via* flash chromatography on silica gel (DCM) to afford the product as a white solid. (7.5 g, 93%)

^{1}H NMR ($CDCl_3$, 400 MHz) δ 7.97 (d, *J* = 9.35 Hz, 2H, Ar-H), 7.34 - 7.51 (m, 5H, Ar-H), 7.04 (d, *J* = 9.35 Hz, 2H, Ar-H), 5.15 (s, 2H, CH_2), 2.98 (q, *J* = 7.02 Hz, 2H, CH_2), 1.24 (t, *J* = 7.31 Hz, 3H, CH_3) **^{13}C NMR ($CDCl_3$, 100 MHz)** δ 199.0 (C=O), 162.0 (ArC), 135.8 (ArC), 129.8 (ArC), 129.8 (ArC), 128.3 (ArC), 127.8 (ArC), 127.1 (ArC), 114.1 (ArC), 69.7 (CH_2), 31.0 (CH_2), 8.0 (CH_3) **HRMS** (EI): Found 263.1052 $(M+Na)^+$, $C_{16}H_{16}NaO_2$ requires 152.1048 **IR :** ν_{max} (KBr) cm^{-1}: 2938, 1680 (C=O), 1599, 1224, 1012 **MP:** 100-102 °C

8.4.11 1-(4-(Benzyloxy)phenyl)hydrazine hydrochloride [247]

Note: The reaction mixture and all added solutions were maintained at 0 °C during this procedure. 4-Benzyloxyaniline hydrochloride [245] (3 g, 12.5 mmol) was added to conc. aq. HCl (25 mL) and stirred for 10 min at 0 °C, followed by dropwise addition of $NaNO_2$ (852 mg, 12.3 mmol) in water (6 mL) over the course of 15 min. The mixture was stirred for additional 15 min and then a solution of $SnCl_2$ (6.4 g, 33.1 mmol) in conc. aq. HCl (7.5 mL) was added dropwise. The reaction mixture was stirred for 1 h and filtered to yield an off-white precipitate, which was washed with water and triturated with Et_2O, to afford an off-white solid (2.9 g, 92.5 %).

^{1}H NMR (DMSO-d_6, 400 MHz) δ 10.14 (br s, 3H, NH-NH_2), 7.35 - 7.48 (m, 4H, Ar-H), 7.27 - 7.35 (m, 1H, Ar-H), 6.92 - 7.05 (m, 4H, Ar-H), 5.06 (s, 2H, CH_2) **^{13}C NMR (DMSO-d_6, 100 MHz)** δ 153.7 (ArC-O), 139.1 (ArC-N), 137.3 (ArC), 128.5 (ArC), 128.4 (ArC), 128.3 (ArC), 127.9 (ArC), 127.7 (ArC), 117.1 (ArC), 116.9 (ArC), 115.5 (ArC), 115.3 (ArC), 69.5 (CH_2) **HRMS (EI):** Found 215.1180 $(M+H)^+$, $C_{13}H_{15}N_2O$ requires 215.1179. **IR :** vmax (KBr) cm^{-1}: 3232, 2907 (br), 1638, 1618, 1511, 1246, 1178 **MP:** 179-181 °C

8.4.12 5-(Benzyloxy)-2-(4-(benzyloxy)phenyl)-3-methyl-1*H*-indole [248]

1-(4-(Benzyloxy)phenyl)propan-1-one [246] (1.91 g, 7.97 mmol) and 1-(4-(benzyloxy)phenyl) hydrazine hydrochloride [247] (2 g, 7.97 mmol) were dissolved in EtOH (50 mL) and 5 drops of conc. HCl was added and the mixture was refluxed for 2 h. The reaction mixture was then allowed to cool and was stirred for 1 h. The mixture was filtered to afford an pale pink solid. The solid was washed with cold EtOH (10 mL) followed by *n*-hexane (20 mL). (2.8 g, 84%)

^{1}H NMR ($CDCl_3$, 400 MHz) δ 7.86 (br s, 1H, NH), 7.48 - 7.58 (m, 6H, Ar-H), 7.33 - 7.47 (m, 6H, Ar-H), 7.25 - 7.31 (m, 1H, Ar-H), 7.14 - 7.18 (m, 1H, Ar-H), 7.07 - 7.13 (m, 2H, Ar-H), 6.97 (d, *J* = 7.53 Hz, 1H, Ar-H), 5.18 (s, 2H, CH_2), 5.15 (s, 2H CH_2), 2.43 (s, 3H, CH_3) **^{13}C NMR ($CDCl_3$, 100 MHz)** δ 157.7 (BnO-C), 157.3 (BnO-C), 143.6 (Ar-C-CH_2), 137.3 (C_q), 136.3 (C_q), 136.0 (C_q), 129.9 (ArC), 128.5 (ArC), 128.2 (ArC), 128.2 (ArC), 127.7 (ArC), 127.6 (Ar-C), 127.1 (ArC), 120.4 (ArC), 114.7 (ArC), 114.6 (ArC), 114.3 (ArC), 112.2 (C_q), 110.8 (C=C), 108.8 (ArC), 102.0 (ArC), 70.0 (CH_2), 69.6 (CH_2), 9.3 (CH_3) **HRMS** (EI): Found 442.1797 $(M+Na)^+$, $C_{29}H_{25}NNaO_2$ requires 442.1783 **IR :** ν_{max} (KBr) cm^{-1}: 3470 (N-H), 2880, 2820, 1620 (C=C) **MP :** 149-152 °C

8.4.13 General method for the alkylation of Indoles.

The indole [248] dissolved in THF (10 mL) was added dropwise to a stirring mixture of NaH in THF (10 mL) at 0 °C under N_2 atmosphere. The mixture was stirred for 10 min, at which point the appropriate dibromoalkane [232]-[234] and [249]-[250] was added and the mixture was stirred for 30 min at 0 °C. The reaction was refluxed for a further 30 min under N_2 atmosphere, the mixture was allowed to cool at which point water was added dropwise until the solution became clear. The solvent was then evaporated under reduced pressure to obtain a brown oil. The resin was dissolved in DCM (50 mL) and washed with water (3 × 50 mL), brine (50 mL) and dried over Na_2SO_4. The solvent was evaporated under reduced pressure to obtain a brown oil. The material was purified *via* flash chromatography over silica gel.

8.4.14 5-(Benzyloxy)-2-(4-(benzyloxy)phenyl)-1-(4-bromobutyl)-3-methyl-1*H*-indole [251]

As per general method 8.4.13, indole [248] (800 mg, 1.9 mmol), NaH (5 eq, 228 mg, 9.5 mmol) and 1,4-dibromobutane [232] (1 eq, 1.9 mmol, 411 mg, 0.227 mL) were reacted. The material was purified *via* flash chromatography over silica gel (*n*-Hexane:DCM, gradient 4:1 to 2:1) to afford the product as a white solid (658 mg, 63%).

^{1}H NMR ($CDCl_3$, 400 MHz) δ 7.50 - 7.57 (m, 4H, Ar-H), 7.39 - 7.50 (m, 5H, Ar-H), 7.36 - 7.39 (m, 1H, Ar-H), 7.33 (d, *J* = 8.18 Hz, 2H, Ar-H), 7.27 (d, *J* = 9.35 Hz, 1H, Ar-H), 7.17 (d, *J* = 2.34 Hz, 1H, Ar-H), 7.10 - 7.15 (m, 2H, Ar-H), 7.01 (dd, *J* = 2.34, 8.77 Hz, 1H, Ar-H), 5.19 (s, 2H, CH_2), 5.17 (s, 2H, CH_2), 4.07 (t, *J* = 7.02 Hz, 2H, CH_2), 3.21 (t, *J* = 6.43 Hz, 2H, CH_2), 2.23 (s, 3H, CH_3), 1.77 (quin, *J* = 7.02 Hz, 2H, CH_2), 1.65 (quin, *J* = 6.40 Hz, 2H, CH_2) **^{13}C NMR ($CDCl_3$, 100 MHz)** δ 158.1 (BnO-C), 152.7 (BnO-C), 137.5 (Ar-C-CH_2), 137.4 (C_q), 136.3 (C_q), 131.3 (ArC), 131.2 (ArC), 128.2 (ArC), 128.1 (ArC), 127.7 (ArC), 127.3 (ArC), 127.2 (ArC), 124.4 (C=C), 115.3 (C_q), 114.4 (ArC), 111.8 (ArC), 109.8 (ArC), 108.0 (C=C), 102.0 (ArC), 69.7 (CH_2), 43.2 (CH_2), 42.4 (CH_2), 32.6 (CH_2), 29.3 (CH_2), 28.1 (CH_2), 8.9 (CH_3) **HRMS** (EI): Found 554.1688 $(M+H)^+$, $C_{33}H_{33}{}^{79}BrNO_2$ requires 554.1689 **IR :** ν_{max} (KBr) cm^{-1}: 3062.1, 3232.52, 3086.0, 2927. 50, 1613.8, 1506.0, 1478.9, 1454.2, 1242.7, 1223.6, 1026.0, 736.1, 696.7 **MP :** 101-102 °C

8.4.15 5-(Benzyloxy)-2-(4-(benzyloxy)phenyl)-1-(5-bromopentyl)-3-methyl-1*H*-indole [252]

As per general method 8.4.13, indole [248] (800 mg, 1.9 mmol), NaH (5 eq, 228 mg, 9.5 mmol) and 1,5-dibromopentane [249] (1 eq, 1.9 mmol, 437 mg, 0.260 mL) were reacted. The material was purified *via* flash chromatography over silica gel (*n*-Hexane:DCM, gradient 4:1 to 2:1) to afford the product as a white solid (701 mg, 65%)

^{1}H NMR ($CDCl_3$, 400 MHz) δ 7.50 - 7.58 (m, 4H, Ar-H), 7.36 - 7.50 (m, 6H, Ar-H), 7.33 (d, *J* = 8.77 Hz, 2H, Ar-H), 7.24 - 7.28 (m, 1H, Ar-H), 7.11 - 7.19 (m, 3H, Ar-H), 7.01 (dd, *J* = 2.34, 8.77 Hz, 1H, Ar-H), 5.19 (s, 2H, CH_2), 5.18 (s, 2H, CH_2), 4.04 (t, *J* = 7.31 Hz, 2H, CH_2), 3.28 (t, *J* = 6.72 Hz, 2H, CH_2), 2.23 (s, 3H, CH_3), 1.58 - 1.75 (m, 4H, 2 × CH_2), 1.27 (quin, *J* = 7.60 Hz, 2H, CH_2) **^{13}C NMR ($CDCl_3$, 100 MHz)** δ 158.1 (BnO-C), 152.7 (BnO-C), 137.5 (Ar-C-CH_2), 137.4 (C_q), 136.4 (C_q), 131.3 (ArC), 131.2 (ArC), 128.4 (ArC), 128.2 (ArC), 128.1 (ArC), 127.7 (ArC), 127.3 (ArC), 127.2 (ArC), 124.5 (C=C), 114.3 (ArC), 111.7 (ArC), 109.8 (ArC), 107.8 (C=C), 102.0 (ArC), 70.6 (CH_2), 69.7 (CH_2), 43.1 (CH_2), 33.0 (CH_2), 31.7 (CH_2), 28.7 (CH_2), 24.9 (CH_2), 8.9 (CH_3) **HRMS** (EI): Found 568.1848 $(M+H)^+$, $C_{34}H_{35}{}^{79}BrNO_2$ requires 568.1848

IR : ν_{max} (KBr) cm^{-1}: 3031.0, 2947.5, 2911.3, 2866.2, 1610.6, 1480.6, 1455.0, 1378.5, m1230.7, 1020.6, 704.6 **MP :** 98-101 °C

8.4.16 5-(Benzyloxy)-2-(4-(benzyloxy)phenyl)-1-(6-bromohexanoyl)-3-methyl-1*H*-indole [253]

As per general method 8.4.13, Indole [248] (800 mg, 1.9 mmol), NaH (5 eq, 228 mg, 9.5 mmol) and 1,6-dibromohexaneane [250] (1 *eq*, 1.9 mmol, 460 mg, 0.290 mL) were reacted. The material was purified *via* flash chromatography on silica gel (*n*-Hexane:DCM, gradient 4:1 to 2:1) to afford the product as a white solid (730 mg, 66%)

^{1}H NMR ($CDCl_3$, 400 MHz) δ 7.51 - 7.58 (m, 4H, Ar-H), 7.40 - 7.50 (m, 5H, Ar-H), 7.36 - 7.39 (m, 1H, Ar-H), 7.30 - 7.35 (m, 2H, Ar-H), 7.24 - 7.30 (m, 1H, Ar-H), 7.10 - 7.18 (m, 3H, Ar-H), 7.01 (dd, *J* = 2.01, 8.53 Hz, 1H, Ar-H), 5.19 (s, 2H, CH_2), 5.18 (s, 2H, CH_2), 4.03 (t, *J* = 7.28 Hz, 2H, CH_2), 3.33 (t, *J* = 6.78 Hz, 2H, CH_2), 2.23 (s, 3H, CH_3), 1.74 (quin, *J* = 7.15 Hz, 2H, CH_2), 1.56 - 1.67 (m, 2H, CH_2), 1.24 - 1.35 (m, 2H, CH_2), 1.10 - 1.21 (m, 2H, CH_2) **^{13}C NMR ($CDCl_3$, 100 MHz)** δ 158.1 (BnO-C), 152.6 (BnO-C), 137.5 (Ar-C-CH_2), 137.4 (C_q), 136.4 (C_q), 131.3 (ArC), 131.2 (ArC), 128.4 (ArC), 128.2 (ArC), 128.1 (ArC), 127.7 (ArC), 127.3 (ArC), 127.2 (ArC), 124.6 (C=C), 114.3 (ArC), 111.7 (ArC), 109.8 (ArC), 107.7 (C=C), 102.0 (ArC), 70.6 (CH_2), 69.7 (CH_2), 43.2 (CH_2), 33.3 (CH_2), 32.1 (CH_2), 29.3 (CH_2), 27.2 (CH_2), 25.4 (CH_2), 8.9 (CH_3) **HRMS** (EI): Found 582.1999 $(M+H)^+$, $C_{35}H_{37}{}^{79}BrNO_2$ requires 582.2002 **IR :** ν_{max} (KBr) cm^{-1}: 3063.1, 3032.7, 1932.3, 1931.4, 1612.9, 1506.0, 1479.6, 1454.9, 1238.2, 1174.5, 1026.18, 735.94, 696.79 **MP :** 101-102 °C

8.4.17 5-(Benzyloxy)-2-(4-(benzyloxy)phenyl)-1-(8-bromooctyl)-3-methyl-1*H*-indole [254]

As per general method 8.4.13, indole [248] (800 mg, 1.9 mmol), NaH (5 eq, 228 mg, 9.5 mmol) and 1,8- dibromooctane [233] (1 *eq*, 1.9 mmol, 516 mg, 0.35 mL) were reacted. The material was purified *via* flash chromatography on silica gel (*n*-Hexane:DCM, gradient 4:1 to 2:1) to afford the product as a white solid (700 mg, 60%)

^{1}H NMR ($CDCl_3$, 400 MHz) δ 7.50 - 7.59 (m, 4H, Ar-H), 7.39 - 7.50 (m, 5H, Ar-H), 7.35 - 7.39 (m, 1H, Ar-H), 7.31 - 7.35 (m, 2H, Ar-H), 7.24 - 7.28 (m, 1H, Ar-H), 7.15 - 7.19 (m, 1H, Ar-H), 7.10 - 7.15 (m, 2H, Ar-H), 7.00 (dd, *J* = 2.26, 8.78 Hz, 1H, Ar-H), 5.18 (s, 2H, CH_2), 5.17 (s, 2H, CH_2), 4.00 (t, *J* = 7.53 Hz, 2H, CH_2), 3.40 (t, *J* = 7.03 Hz, 2H, CH_2), 2.23 (s, 3H, CH_3), 1.82 (quin, *J* = 7.15 Hz, 2H, CH_2), 1.56 - 1.66 (m, 2H, CH_2), 1.36 (quin, *J* = 7.15 Hz, 2H, CH_2), 1.09 - 1.26 (m, 6H, 3 × CH_2) **^{13}C NMR ($CDCl_3$, 100 MHz)** δ 158.0 (BnO-C), 152.6 (BnO-C), 137.6 (Ar-C-CH_2), 137.4 (C_q), 136.4 (C_q), 131.3 (ArC), 131.2 (ArC), 128.4 (ArC), 128.2 (ArC), 128.1 (ArC), 127.7 (ArC), 127.3 (ArC), 127.2 (ArC), 124.6 (C=C), 114.2 (ArC), 111.6 (ArC), 109.9 (ArC), 107.6 (C=C), 101.9 (ArC), 70.6 (CH_2), 69.7 (CH_2), 43.4 (CH_2), 33.6 (CH_2), 32.3 (CH_2), 29.5 (CH_2), 28.4 (CH_2), 28.1 (CH_2), 27.5 (CH_2), 26.2 (CH_2), 8.9 (CH_3) **HRMS** (EI): Found 610.2301 (M+H)+, $C_{37}H_{41}{}^{79}BrNO_2$ requires 610.2321 **IR :** ν_{max} (KBr) cm^{-1}: 3062.9, 3032.5, 2929.4, 1612.8, 1505.9, 1476.9, 1454.1, 1287.4, 1241.7, 1025.8, 735.6, 696.3 **MP :** 104-106 °C

8.4.18 5-(Benzyloxy)-2-(4-(benzyloxy)phenyl)-1-(12-bromododecyl)-3-methyl-1*H*-indole [255]

As per general method 8.4.13, indole [248] (800 mg, 1.9 mmol), NaH (5 eq, 228 mg, 9.5 mmol) and 1,12- dibromododecane [234] (1 *eq*, 1.9 mmol, 623 mg) were reacted. The material was purified *via* flash chromatography on silica gel (*n*-Hexane:DCM, gradient 4:1 to 2:1) to afford the product as a white solid (750 mg, 59%)

^{1}H NMR ($CDCl_3$, 400 MHz) δ 7.50 - 7.57 (m, 4H, Ar-H), 7.30 - 7.49 (m, 8H, Ar-H), 7.24 - 7.28 (m, 1H, Ar-H), 7.14 - 7.17 (m, 1H, Ar-H), 7.12 (s, 2H, Ar-H), 6.99 (dd, *J* = 2.51, 9.03 Hz, 1H, Ar-H), 5.18 (s, 2H, CH_2), 5.16 (s, 2H, CH_2), 3.99 (t, *J* = 7.53 Hz, 2H, CH_2), 3.44 (t, *J* = 7.03 Hz, 2H, CH_2), 2.22 (s, 3H, CH_3), 1.59 (m, 4H, 2 × CH_2), 1.39 - 1.51 (m, 8H, 4 × CH_2), 1.09 - 1.37 (m, 8H, 4 × CH_2) **^{13}C NMR ($CDCl_3$, 100 MHz)** δ 158.0 (BnO-C), 152.6 (BnO-C), 137.6 (Ar-C-CH_2), 137.4 (C_q), 136.4 (C_q), 131.3 (ArC), 128.3 (Ar-C), 128.2 (ArC), 128.1 (ArC), 127.7 (ArC), 127.3 (ArC), 127.1 (ArC), 124.6 (C=C), 114.2 (ArC), 111.6 (ArC), 109.9 (ArC), 107.6 (C=C), 101.9 (ArC), 70.6 (CH_2), 69.6 (CH_2), 43.5 (CH_2), 33.7 (CH_2), 32.4 (CH_2), 29.6 (CH_2), 29.3 (CH_2), 29.04 (CH_2), 29.01 (CH_2), 28.7 (CH_2), 28.5 (CH_2), 28.4 (CH_2), 28.3 (CH_2), 27.7 (CH_2), 26.3 (CH_2), 8.9 (CH_3) **HRMS** (EI): Found 666.2941 $(M+H)^+$, $C_{41}H_{49}{}^{79}BrNO_2$ requires 666.2941 **IR :** ν_{max} (KBr) cm^{-1}: 3062.8, 3032.8, 2922.7, 2853.7, 1613.0, 1505.9, 1479.6, 1287.2, 1241.7, 1025.9, 735.8, 696.12 **MP :** 71-73 °C

8.4.19 General method for the amination of bromoalkyl indoles

The appropriate brominated indole was dissolved in dry THF (10 mL) and transferred to a pressure tube. To this solution was added a solution of methylamine (2 M in THF) and the mixture was flushed with N_2 before sealing the tube. The tube was left stir at 65 °C for 48 h. The tube was then allowed to cool to reduce the internal pressure, then opened carefully and the solvent was evaporated under reduced pressure to obtain a brown oil. The oil was dissolved in DCM (30 mL) and was washed with an pH 10 aq. solution* (30 mL); the pH 10 aq. solution* was extracted with DCM (2 × 30 mL). The organic layers were combined and washed with water (50 mL), brine (50 mL) and dried over Na_2SO_4. The solvent was evaporated under reduced pressure to obtain a brown oil. The material was purified *via* flash chromatography over silica gel (DCM : MeOH).

* pH10 aq. Solution = 6 g of $NaHCO_3$ and 6 g of Na_2CO_3 per 100 mL of water

8.4.20 4-(5-(Benzyloxy)-2-(4-(benzyloxy)phenyl)-3-methyl-1*H*-indol-1-yl)-N-methylbutan-1-amine [256]

As per general method 8.4.19, [251] (440 mg, 0.79 mmol) and methylamine (20 eq, 15.86 mmol, 8 mL) were reacted. The material was purified *via* flash chromatography on silica gel (DCM:EtOAc, gradient 4:1 to 2:1) to afford the product as a brown resin (365 mg, 92 %)

^{1}H NMR ($CDCl_3$, 400 MHz) δ 7.49 - 7.58 (m, 4H, Ar-H), 7.38 - 7.49 (m, 5H, Ar-H), 7.35 - 7.38 (m, 1H, Ar-H), 7.30 - 7.34 (m, 2H, Ar-H), 7.26 (d, *J* = 8.53 Hz, 1H, Ar-H), 7.08 - 7.18 (m, 3H, Ar-H), 6.99 (dd, *J* = 2.26, 8.78 Hz, 1H, Ar-H), 5.17 (s, 2H, CH_2), 5.16 (s, 2H, CH_2), 4.03 (t, *J* = 7.28 Hz, 2H, CH_2), 2.39-2.51 (m, 3H, N-H, CH_2), 2.36 (s, 3H, CH_3), 2.21 (s, 3H, CH_3), 1.57 - 1.69 (m, 2H, CH_2), 1.31 - 1.42 (m, 2H, CH_2) **^{13}C NMR ($CDCl_3$, 100 MHz)** δ 158.1 (BnO-C), 152.6 (BnO-C), 137.5 (Ar-C-CH_2), 137.4 (C_q), 136.4 (C_q), 131.3 (ArC), 128.2 (ArC), 128.1 (ArC), 127.7 (ArC), 127.3 (ArC), 127.2 (ArC), 124.5 (C=C), 114.3 (ArC), 111.7 (ArC), 109.8 (ArC), 107.9 (C=C), 102.0 (ArC), 70.6 (CH_2), 69.7 (CH_2), 50.5 (CH_2), 43.1 (CH_2), 35.2 (CH_3), 27.2 (CH_2), 25.8 (CH_2), 8.9 (CH_3) **HRMS** (EI): Found 505.2852 $(M+H)^+$, $C_{34}H_{37}N_2O_2$ requires 505.2855 **IR :** ν_{max} (KBr) cm^{-1}: 3333.3, 3032,7, 2928.0, 2860.2, 2790.8, 1612.4, 1505.8, 1476.9, 1454.3, 1287.0, 1241.2, 1025.8, 736.2, 696.7 **MP :** 79-82 °C

8.4.21 5-(5-(Benzyloxy)-2-(4-(benzyloxy)phenyl)-3-methyl-1*H*-indol-1-yl)-N-methylpentan-1-amine [257]

As per general method 8.4.19, [252] (450 mg, 0.791 mmol)and methylamine (20 eq, 15.86 mmol, 8 mL) were reacted. The material was purified *via* flash chromatography on silica gel (DCM:EtOAc, gradient 4:1 to 2:1) to afford the product as a brown resin (381 mg, 93%).

^{1}H NMR ($CDCl_3$, 400 MHz) δ 7.49 - 7.57 (m, 4H, Ar-H), 7.38 - 7.49 (m, 5H, Ar-H), 7.34 - 7.38 (m, 1H, Ar-H), 7.29 - 7.34 (m, 2H, Ar-H), 7.23 - 7.27 (m, 1H, Ar-H), 7.08 - 7.17 (m, 3H, Ar-H), 6.99 (dd, *J* = 2.26, 8.78 Hz, 1H, Ar-H), 5.17 (s, 2H, CH_2), 5.16 (s, 2H, CH_2), 4.01 (t, *J* = 7.28 Hz, 2H, CH_2), 2.45 - 2.54 (m, 2H, CH_2), 2.41 (s, 3H, CH_3), 2.21 (s, 4H, N-H, CH_3), 1.60 (quin, *J* = 7.30 Hz, 2H, CH_2), 1.40 (quin, *J* = 7.28 Hz, 2H, CH_2), 1.16 (quin, *J* = 7.40 Hz, 2H, CH_2) **^{13}C NMR ($CDCl_3$, 100 MHz)** δ 158.0 (BnO-C), 152.6 (BnO-C), 137.5 (Ar-C-CH_2), 137.4 (C_q), 136.4 (C_q), 131.3 (ArC), 128.4 (ArC), 128.2 (ArC), 128.1 (ArC), 127.7 (ArC), 127.3 (ArC), 127.2 (ArC), 124.5 (C=C), 114.3 (ArC), 111.7 (ArC), 109.8 (ArC), 107.8 (C=C), 102.0 (ArC), 70.6 (CH_2), 69.7 (CH_2), 50.9 (CH_2), 50.3 (CH_2), 43.3 (CH_2), 35.4 (CH_3), 29.4 (CH_2), 28.3 (CH_2), 8.9 (CH_3) **HRMS** (EI): Found 519.3033 $(M+H)^+$, $C_{35}H_{39}N_2O_2$ requires 519.3012 **IR :** ν_{max} (KBr) cm^{-1}: 3327.0, 3032.7, 2930.2, 2859.8, 2790.5, 1612.6, 1505.9, 1476.9, 1454.3, 1287.58, 1243.51, 1174.9, 1025.9, 736.25, 696.8 **MP :** 81-83 °C

8.4.22 6-(5-(Benzyloxy)-2-(4-(benzyloxy)phenyl)-3-methyl-1*H*-indol-1-yl)-N-methyl hexan-1-amine [258]

As per general method 8.4.19, [253] (540 mg, 0.927 mmol)and methylamine (20 eq, 18.54 mmol, 10 mL) were reacted. The material was purified *via* flash chromatography on silica gel (DCM:EtOAc, gradient 4:1 to 2:1) to afford the product as a brown resin (470 mg, 95%)

^{1}H NMR ($CDCl_3$, 400 MHz) δ 7.49 - 7.58 (m, 4H, Ar-H), 7.39 - 7.49 (m, 5H, Ar-H), 7.35 - 7.39 (m, 1H, Ar-H), 7.30 - 7.35 (m, 2H, Ar-H), 7.23 - 7.28 (m, 1H, Ar-H), 7.09 - 7.18 (m, 3H, Ar-H), 7.00 (dd, *J* = 2.01, 8.53 Hz, 1H, Ar-H), 5.18 (s, 2H, CH_2), 5.16 (s, 2H, CH_2), 4.00 (t, *J* = 7.28 Hz, 2H, CH_2), 2.61 (br s, 1H, N-H) 2.49 - 2.58 (m, 2H, CH_2), 2.45 (s, 3H, CH_3), 2.22 (s, 3H, CH_3), 1.55 - 1.67 (m, 2H, CH_2), 1.38 - 1.49 (m, 2H, CH_2), 1.09 - 1.25 (m, 4H, 2 × CH_2) **^{13}C NMR ($CDCl_3$, 100 MHz)** δ 158.0 (BnO-C), 152.6 (BnO-C), 137.6 (Ar-C-CH_2), 137.4 (C_q), 136.4 (C_q), 131.3 (ArC), 131.2 (ArC), 128.4 (ArC), 128.2 (ArC), 128.1 (ArC), 127.7 (ArC), 127.3 (ArC), 127.2 (ArC), 124.6 (C=C), 114.2 (ArC), 111.6 (ArC), 109.9 (ArC), 107.7 (C=C), 101.9 (ArC), 70.6 (CH_2), 69.7 (CH_2), 51.0 (CH_2), 43.3 (CH_2), 35.4 (CH_3), 29.5 (CH_2), 28.6 (CH_2), 26.3 (CH_2), 26.2 (CH_2), 8.9 (CH_3) **HRMS** (EI): Found 533.3162 $(M+H)^+$, $C_{36}H_{41}N_2O_2$ requires 533.3168 **IR :** ν_{max} (KBr) cm^{-1}: 3324.6, 3033.3, 2929.5, 2858.1, 2790.9, 1613.49, 1515.8, 1479.3, 1454.23, 1380.7, 1287.2, 1241.3, 1174.7, 1025.9, 735.5, 696.8 **MP :** 79-82 °C

8.4.23 Synthesis of 8-(5-(benzyloxy)-2-(4-(benzyloxy)phenyl)-3-methyl-1*H*-indol-1-yl)-N-methyloctan-1-amine [259]

As per general method 8.4.19, [254] (400 mg, 0.686 mmol)and methylamine (20 eq, 13.73 mmol, 7 mL) were reacted. The material was purified *via* flash chromatography on silica gel (DCM:EtOAc, gradient 4:1 to 2:1) to afford the product as a brown resin (351 mg, 91%)

^{1}H NMR ($CDCl_3$, 400 MHz) δ 7.49 - 7.58 (m, 4H, Ar-H), 7.39 - 7.49 (m, 5H, Ar-H), 7.35 - 7.38 (m, 1H, Ar-H), 7.30 - 7.34 (m, 2H, Ar-H), 7.23 - 7.28 (m, 1H, Ar-H), 7.09 - 7.17 (m, 3H, Ar-H), 6.99 (d, *J* = 8.53 Hz, 1H, Ar-H), 5.18 (s, 2H, CH_2), 5.16 (s, 2H, CH_2), 3.99 (t, *J* = 7.28 Hz, 2H, CH_2), 2.58 (t, *J* = 7.03 Hz, 2H, CH_2), 2.45 (s, 3H, CH_3), 2.22 (s, 3H, CH_3), 2.09 (br s, 1H, N-H), 1.61 (d, *J* = 6.53 Hz, 2H, CH_2), 1.43 - 1.52 (m, 2H, CH_2), 1.07 - 1.30 (m, 8H, 4 × CH_2) **^{13}C NMR ($CDCl_3$, 100 MHz)** δ 158.0 (BnO-C), 152.6 (BnO-C), 137.6 (Ar-C-CH_2), 137.4 (C_q), 136.4 (C_q), 131.3 (ArC), 128.3 (ArC), 128.2 (ArC), 128.1 (ArC), 127.7 (ArC), 127.3 (ArC), 127.2 (ArC), 124.6 (C=C), 114.2 (ArC), 111.6 (ArC), 109.9 (ArC), 107.6 (C=C), 101.9 (ArC), 70.6 (CH_2), 69.7 (CH_2), 51.3 (CH_2), 43.5 (CH_2), 35.6 (CH_3), 29.6 (CH_2), 28.8 (CH_2), 28.6 (CH_2), 26.7 (CH_2), 26.3 (CH_2), 8.9 (CH_3) **HRMS** (EI): Found 561.3469 $(M+H)^+$, $C_{38}H_{45}N_2O_2$ requires 561.3481 **IR :**

ν_{max} (KBr) cm^{-1}: 3327.5, 3062.7, 3032.9, 2927.5, 2855.2, 2790.0, 1612.9, 1506.1, 1479.3, 1454.3, 1380.6, 1287.5, 1241.8, 1174.3, 1025.9, 735.9, 696.6 **MP :** 81-84 °C

8.4.24 12-(5-(Benzyloxy)-2-(4-(benzyloxy)phenyl)-3-methyl-1*H*-indol-1-yl)-N-methyldodecan-1-amine [260]

As per general method 8.4.19, [255] (357 mg, 0.535 mmol) and methylamine (20 eq, 13.73 mmol, 7 mL) were reacted. The material was purified *via* flash chromatography on silica gel (DCM:EtOAc, gradient 4:1 to 2:1) to afford the product as a brown resin (287 mg, 87%)

^{1}H NMR ($CDCl_3$, 400 MHz) δ 7.49 - 7.58 (m, 4H, Ar-H), 7.39 - 7.49 (m, 5H, Ar-H), 7.35 - 7.38 (m, 1H, Ar-H), 7.30 - 7.34 (m, 2H, Ar-H), 7.24 - 7.28 (m, 1H, Ar-H), 7.08 - 7.18 (m, 3H, Ar-H), 6.99 (dd, *J* = 2.01, 8.53 Hz, 1H, Ar-H), 5.18 (s, 2H, CH_2), 5.16 (s, 2H, CH_2), 3.99 (t, *J* = 7.28 Hz, 2H, CH_2), 2.60 (t, *J* = 7.03 Hz, 2H, CH_2), 2.46 (s, 3H, CH_3), 2.22 (s, 3H, CH_3), 2.02 (br. s., 1H, N-H), 1.56 - 1.66 (m, 2H, CH_2), 1.51 (s, 2H, CH_2), 1.08 - 1.36 (m, 16H, 8 × CH_2) **^{13}C NMR ($CDCl_3$, 100 MHz)** δ 158.4 (BnO-C), 153.0 (BnO-C), 138.0 (Ar-C-CH_2), 137.8 (C_q), 136.8(C_q), 131.7 (ArC), 131.6 (ArC), 128.7 (ArC), 128.6 (ArC), 128.5 (ArC), 128.1 (ArC), 127.7 (ArC), 127.6 (ArC), 125.0 (C=C), 114.6 (ArC), 112.0 (ArC), 110.3 (ArC), 108.0 (C=C), 102.3 (ArC), 71.0 (CH_2), 70.0 (CH_2), 51.9 (CH_2), 43.9 (CH_2), 36.1 (CH_3), 30.1 (CH_2), 29.5 (CH_2), 29.4 (CH_2), 29.1 (CH_2), 28.8 (CH_2), 28.6 (CH_2), 27.6 (CH_2), 27.3 (CH_2), 26.8 (CH_2), 26.6 (CH_2), 9.3 (CH_3) **HRMS** (EI): Found 617.4100 $(M+H)^+$, $C_{42}H_{53}N_2O_2$ requires 617.4107 **IR :** ν_{max} (KBr) cm^{-1}: 3326.9, 3063.3, 3033.2, 2927.5, 2853.4, 2790.1, 1613.5, 1506.1, 1479.5, 1454.7, 1287.2, 1242.0, 1174.2, 1026.4, 735.2, 696.4 **MP :** 66-69 °C

8.4.25 General method for the debenzylation of indoles

The protected aminated indole [256]-[260] was dissolved in MeOH:EtOAc (1:4) (20 mL) and transferred to a 3-neck flask. To the flask was added 20% $Pd(OH)_2$ and the mixture was placed under a H_2 atmosphere. The hydrogenation reaction was monitored *via* TLC until the starting material had disappeared (10 – 60 min). The reaction mixture was filtered through celite and the solvent was evaporated under reduced pressure to obtain a brown oil. The material was purified *via* flash chromatography.

8.4.26 2-(4-Hydroxyphenyl)-3-methyl-1-(4-(methylamino)butyl)-1*H*-indol-5-ol [241]

As per general method 8.4.25, the protected aminated indole [256] (150 mg, 0.297 mmol) and a small tipful of spatula of $Pd(OH)_2$ (~20 mg) were reacted under a hydrogenation atmosphere for 30 min. The material was purified *via* flash chromatography on silica gel (DCM:MeOH, gradient 40:1 to 30:1) to afford the product as an off white solid (77 mg, 80%)

^{1}H NMR (CD_3OD, 400 MHz) δ 7.20 - 7.27 (m, 3H, Ar-H), 6.91 - 6.97 (m, 2H, Ar-H), 6.89 (s, 1H, Ar-H), 6.74 (dd, *J* = 2.51, 8.53 Hz, 1H, Ar-H), 4.12 (t, *J* = 6.53 Hz, 2H, CH_2), 2.70 (t, *J* = 7.53 Hz, 2H, CH_2), 2.54 (s, 3H, NCH_3), 2.13 (s, 3H, CH_3), 1.54 - 1.65 (m, 2H, CH_2), 1.29 - 1.40 (m, 2H, CH_2), (N-H and OH - not seen) **^{13}C NMR (CD_3OD, 100 MHz)** δ 156.7 (C-OH), 149.7 (C-OH), 137.6 (C_q), 131.0 (C_q), 130.9 (ArC), 130.8 (ArC), 129.1 (C_q), 122.8 (C=C), 114.6 (ArC), 110.3 (ArC), 109.2 (ArC), 106.8 (C=C), 102.0 (ArC), 48.0 (CH_2) 41.9 (CH_2), 31.5 (CH_3), 26.0 (CH_2), 22.6 (CH_2), 7.6 (CH_3) **HRMS** (EI): Found 325.1916 $(M+H)^+$, $C_{20}H_{25}N_2O_2$ requires 325.1911 **IR :** ν_{max} (KBr) cm^{-1}: 3433.5 (br), 3246.3, 2931.6, 2852.2, 1613.1, 1508.2, 1462.8, 1361.2, 1262.7, 1268.0, 1098.0, 841.4 **MP :** 61-63 °C

8.4.27 2-(4-Hydroxyphenyl)-3-methyl-1-(8-(methylamino)octyl)-1*H*-indol-5-ol [242]

As per general method 8.4.25, the protected aminated indole [259] (150 mg, 0.267 mmol) and a small tipful of spatula of $Pd(OH)_2$ (~20 mg) were reacted under a hydrogen atmosphere for 30 min. The material was purified *via* flash chromatography over silica gel (DCM:MeOH, gradient 40:1 to 30:1) to afford the product as an off white solid (92 mg, 91%)

^{1}H NMR (CD_3OD, 400 MHz) δ 7.12 - 7.24 (m, 3H, Ar-H), 6.90 - 6.98 (m, 2H, Ar-H), 6.89 (s, 1H, Ar-H), 6.68 - 6.75 (m, 1H, Ar-H), 4.01 (t, *J* = 7.03 Hz, 2H, CH_2), 2.91 (t, *J* = 7.53 Hz, 2H, CH_2), 2.68 (s, 3H, CH_3), 2.13 (s, 3H, CH_3), 1.44 - 1.64 (m, 4H, 2 × CH_2), 1.01 - 1.28 (m, 8H, 4 × CH_2) **^{13}C NMR (CD_3OD, 100 MHz)** δ 158.6 (C-OH), 151.4 (C-OH), 139.8 (C_q), 133.0 (ArC), 130.9 (C_q), 125.1 (C=C), 116.4 (ArC), 112.0 (ArC), 111.2 (ArC), 108.2 (C=C), 103.9 (ArC), 50.6 (CH_2), 44.5 (CH_2), 33.8 (CH_3), 30.7 (CH_2), 30.0 (CH_2), 29.9 (CH_2), 27.5 (CH_2), 27.4 (CH_2), 27.3 (CH_2), 9.6 (CH_3) HRMS (EI): Found 381.2557 $(M+H)^+$, $C_{24}H_{33}N_2O_2$ requires 381.2537 **IR :** ν_{max} (KBr) cm^{-1}: 3428.6 (br.), 3241.4, 2931.0, 2852.2, 1614.2, 1508.4, 1462.8, 1380.6, 1260.2, 1147.4, 1093.0, 839.0 **MP :** 71-72 °C

8.4.28 2-(4-Hydroxyphenyl)-3-methyl-1-(12-(methylamino)dodecyl)-1*H*-indol-5-ol [243]

As per general method 8.4.25, the protected aminated indole [260] (150 mg, 0.243 mmol) and a small tipful of spatula of $Pd(OH)_2$ (20 mg) were reacted under a hydrogen atmosphere for 30 min. The material was purified *via* flash chromatography over silica gel (DCM:MeOH, gradient 40:1 to 30:1) to afford the product as an off white solid (93 mg, 88%)

^{1}H NMR (CD_3OD, 400 MHz) δ 7.09 - 7.22 (m, 3H, Ar-H), 6.87 - 6.96 (m, 3H, Ar-H), 6.67 - 6.74 (m, 1H, Ar-H), 3.94 - 4.03 (m, 2H, CH_2), 2.25 - 2.33 (m, 2H, CH_2), 2.13 (s, 3H, CH_3), 2.03 (s, 3H, CH_3), 1.61 - 1.76 (m, 4H, 2 × CH_2), 1.44 - 1.55 (m, 4H, 2 × CH_2), 0.98 - 1.41 (m, 12H, 6 × CH_2) **^{13}C NMR (CD_3OD, 100 MHz)** δ 158.9 (C-OH), 151.8 (C-OH), 140.1 (C_q), 133.7 (ArC), 133.3, 131.3, 125.4 (C=C), 116.8 (ArC), 116.7 (ArC), 112.3 (ArC), 111.5 (ArC), 108.5 (C=C), 104.3 (ArC), 51.0 (CH_2), 44.9 (CH_2), 34.1 (NCH_3), 31.2 (CH_2), 31.1 (CH_2), 31.0 (CH_2), 30.9 (CH_2), 30.8 (CH_2), 30.7 (CH_2), 30.5 (CH_2), 28.3 (CH_2), 28.0 (CH_2), 27.8 (CH_2), 10.0 (CH_3) **HRMS** (EI): Found 437.3170 $(M+H)^+$, $C_{28}H_{41}N_2O_2$ requires 437.3163 **IR :** ν_{max} (KBr) cm^{-1}: 3433.5 (br.), 3251.2, 2922.1, 2847.3, 1639.5, 1616.5, 1505.9, 1437.2, 1380.6, 1267.5, 1148.6, 1088.1, 839.1 **MP :** 91-93 °C

8.4.29 2-(4-Hydroxyphenyl)-3-methyl-1-(5-(methylamino)pentyl)-1*H*-indol-5-ol [261]

As per general method 8.4.25, the protected aminated indole [257] (150 mg, 0.289 mmol) and a small tipful of spatula of $Pd(OH)_2$ (~20 mg) were reacted under a hydrogen atmosphere for 30 min. The material was purified *via* flash chromatography over silica gel (DCM:MeOH, gradient 40:1 to 30:1) to afford the product as an off white solid (69 mg, 71%)

^{1}H NMR (CD_3OD, 400 MHz) δ 7.17 - 7.26 (m, 3H, Ar-H), 6.85 - 6.97 (m, 3H, Ar-H), 6.69 - 6.75 (m, 1H, Ar-H), 4.06 (t, *J* = 7.00 Hz, 2H, CH_2), 2.79 (t, *J* = 7.00 Hz, 2H, CH_2), 2.61 (s, 3H, NCH_3), 2.13 (s, 3H, CH_3), 1.52 - 1.62 (m, 2H, CH_2), 1.41 - 1.51 (m, 2H, CH_2), 1.09 - 1.17 (m, 2H, CH_2), (N-H and O-H - not seen) **^{13}C NMR (CD_3OD, 100 MHz)** δ 156.6 (C-OH), 149.6 (C-OH), 137.6, 131.0 (ArC), 128.9(C_q), 123.0 (C=C), 114.5 (ArC), 110.1 (ArC), 109.1 (ArC), 106.5 (C=C), 102.0 (ArC), 65.0 (CH_2), 31.6 (CH_3), 28.9 (CH_2), 28.5 (CH_2), 24.8 (CH_2), 22.6 (CH_2), 7.6 (CH_3) **HRMS** (EI): Found 339.2069 $(M+H)^+$, $C_{21}H_{27}N_2O_2$ requires 339.2067 **IR :** ν_{max} (KBr) cm^{-1}: 3433.5 (br.), 2925.5, 2852.2, 1615.6, 1507.5, 1461.9, 1365.9, 1199.8, 1695.5, 838.29 **MP :** 63-65 °C

8.4.30 2-(4-Hydroxyphenyl)-3-methyl-1-(6-(methylamino)n-hexanoyl)-1*H*-indol-5-ol [262]

As per general method 8.4.25, the protected aminated indole [258] (150 mg, 0.281 mmol) and a small tipful of spatula of $Pd(OH)_2$ (~20 mg) were reacted under a hydrogen atmosphere for 30 min. The material was purified *via* flash chromatography over silica gel (DCM:MeOH, gradient 40:1 to 30:1) to afford the product as an off white solid (75 mg, 76%).

^{1}H NMR (CD_3OD, 400 MHz) δ 7.13 - 7.22 (m, 3H, Ar-H), 6.89 - 6.96 (m, 2H, Ar-H), 6.87 (s, 1H, Ar-H), 6.67 - 6.73 (m, 1H, Ar-H), 4.03 (t, *J* = 6.78 Hz, 2H, CH_2), 2.79 (t, *J* = 7.53 Hz, 2H, CH_2), 2.62 (s, 3H, CH_3), 2.11 (s, 3H, CH_3), 1.42 - 1.58 (m, 4H, 2 × CH_2), 1.01 - 1.21 (m, 4H, 2 × CH_2) **^{13}C NMR (CD_3OD, 100 MHz)** δ 158.6 (C-OH), 151.5 (C-OH), 139.7 (C_q), 133.0 (ArC), 130.9 (C_q), 125.1 (C=C), 116.4 (ArC), 112.1 (ArC), 111.3 (ArC), 108.4 (C=C), 104.0 (ArC), 50.4 (CH_2), 44.4 (CH_2), 33.7 (CH_3), 30.7 (CH_2), 27.2 (CH_2), 27.1 (CH_2), 27.0 (CH_2), 9.6 (CH_3) **HRMS** (EI): Found 353.3327 $(M+H)^+$, $C_{22}H_{29}N_2O_2$ requires 353.3334 **IR :** ν_{max} (KBr) cm^{-1}: 3433.5 (br), 2927.1, 2852.2, 1613.8, 1560.0, 1508.1, 1461.4, 1366.7, 1168.8, 1100.4, 840.8 **MP :** 75-76 °C

8.4.31 1,4-bis(5-(Benzyloxy)-2-(4-(benzyloxy)phenyl)-3-methyl-1*H*-indol-1-yl)butane [263]

Column chromatography of [251] afforded a by-product as a white solid (169 mg, 20%).

^{1}H NMR ($CDCl_3$, 400 MHz) δ 7.51 (m, 8H, Ar-H), 7.38 - 7.45 (m, 8H, Ar-H), 7.32 - 7.38 (m, 4H, Ar-H), 7.06 - 7.16 (m, 7H, Ar-H), 7.03 (m, 5H, Ar-H), 6.95 (dd, *J* = 1.76, 8.78 Hz, 2H, Ar-H), 5.17 (s, 4H, 2 × CH_2), 5.13 (s, 4H, 2 × CH_2), 3.70- 3.86 (m, 4H, 2 × CH_2), 2.18 (s, 6H, 2 × CH_3), 1.24 - 1.37 (m, 4H, 2 × CH_2) **^{13}C NMR ($CDCl_3$, 100 MHz)** δ 157.9 (BnO-C), 152.6 (BnO-C), 137.4 (C_q), 137.3 (C_q), 136.3 (C_q), 131.2 (ArC), 128.2 (ArC), 128.1 (ArC), 127.7 (ArC), 127.3 (ArC), 127.2 (ArC), 127.1 (ArC), 124.4 (C=C), 114.2 (ArC), 111.6 (ArC), 109.8 (ArC), 107.8 (C=C), 101.9 (ArC), 70.6 (CH_2), 69.6 (CH_2), 42.6 (CH_2), 26.5 (CH_2), 8.9 (CH_3) **HRMS** (EI): Found 893.4332 $(M+H)^+$, $C_{62}H_{57}N_2O_4$ requires 893.4313 **IR :** ν_{max} (KBr) cm^{-1}: 3021.8, 2922.9, 2858.2, 1610.6, 1504.4, 1478.9, 1454.4, 1378.3, 1289.8, 1241.9, 1198.7, 1167.7, 1025.4, 833.3 **MP :** 201-203 °C

8.4.32 1,5-bis(5-(Benzyloxy)-2-(4-(benzyloxy)phenyl)-3-methyl-1*H*-indol-1-yl)pentane [264]

Column chromatography of [252] afforded a by-product as a white solid (192 mg, 22%)

^{1}H NMR ($CDCl_3$, 400 MHz) δ 7.32 - 7.57 (m, 18H, Ar-H), 7.06 - 7.20 (m, 8H, Ar-H), 6.94 - 7.06 (m, 8H, Ar-H), 5.17 (s, 4H, CH_2), 5.10 (s, 4H, CH_2), 3.79 - 3.94 (m, 4H, CH_2), 2.18 (s, 6H, CH_3), 1.53 - 1.68 (m, 2H, CH_2), 1.34 - 1.46 (m, 2H, CH_2), 0.74 - 0.89 (m, 2H, CH_2) **^{13}C NMR ($CDCl_3$, 100 MHz)** δ 158.0 (C-OBn), 152.6 (C-OBn), 137.5 (C_q), 137.4 (C_q), 136.3 (C_q), 131.2, 128.2, 128.1, 127.7, 127.3, 127.2, 124.5 (C_q), 114.2, 111.6, 109.8, 107.7 (C_q), 103.2, 101.9, 97.4, 70.6 (CH_2), 69.6 (CH_2), 43.1 (CH_2), 29.1 (CH_2), 23.1 (CH_2), 8.9 (CH_3) **HRMS** (EI): Found 929.4296 $(M+Na)^+$, $C_{63}H_{58}N_2NaO_4$ requires 929.4296 **IR :** ν_{max} (KBr) cm^{-1}: 3059.1, 3032.8, 2910.2, 2857.3, 1609.9, 1476.5, 1452.9, 1382.5, 1234.7, 1174.3, 1018.5, 837.8 **MP :** 169-171 °C

8.4.33 1,6-bis(5-(Benzyloxy)-2-(4-(benzyloxy)phenyl)-3-methyl-1*H*-indol-1-yl)hexane [265]

Column chromatography of [253] afforded a by-product as a white solid (224 mg, 26%)

^{1}H NMR ($CDCl_3$, 400 MHz) δ 7.48 - 7.58 (m, 8H, Ar-H), 7.33 - 7.47 (m, 8H, Ar-H), 7.24 - 7.30 (m, 4H, Ar-H), 7.18 - 7.23 (m, 2H, Ar-H), 7.16 (s, 2H, Ar-H), 7.05 - 7.11 (m, 6H, Ar-H), 7.00 (dd, *J* = 1.76, 8.78 Hz, 2H, Ar-H), 5.18 (s, 4H, 2 × CH_2), 5.13 (s, 4H, 2 × CH_2), 3.92 (t, *J* = 7.03 Hz, 4H, 2 × CH_2), 2.21 (s, 6H, 2 × CH_3), 1.45 - 1.56 (m, 4H, 2 × CH_2), 0.94 - 1.05 (m, 4H, 2 × CH_2) **^{13}C NMR ($CDCl_3$, 100 MHz)** δ 158.0 (BnO-C), 152.6 (BnO-C), 137.5 (C_q), 137.4 (C_q), 136.3 (C_q), 131.3 (ArC), 131.2 (ArC), 128.4 (ArC), 128.2 (ArC), 128.1 (ArC), 127.7 (ArC), 127.3 (ArC), 127.2 (ArC), 124.5 (C=C), 114.2 (ArC), 111.7 (ArC), 109.9 (ArC), 107.7 (C=C), 101.9 (ArC), 70.6 (CH_2), 69.6 (CH_2), 43.3 (CH_2), 29.5 (CH_2), 26.0 (CH_2), 8.9 (CH_3) **HRMS** (MALDI): Found 920.4589 (M), $C_{64}H_{60}N_2O_4$ requires 920.4553 **IR :** ν_{max} (KBr) cm^{-1}: 3032.9, 2925.3, 2858.4, 1612.1, 1505.2, 1478.9, 1453.9, 1379.2, 1283.0, 1173.8, 1022.5, 736.3 **MP :** 213-214 °C

8.4.34 1,8-bis(5-(Benzyloxy)-2-(4-(benzyloxy)phenyl)-3-methyl-1*H*-indol-1-yl)octane [266]

Column chromatography of [254] afforded a by-product as a white Solid (198 mg, 22%)

^{1}H NMR ($CDCl_3$, 400 MHz) δ 7.34 - 7.57 (m, 20H, Ar-H), 7.27 - 7.32 (m, 4H, Ar-H), 7.21 - 7.26 (m, 2H, Ar-H), 7.15 (s, 2H, Ar-H), 7.05 - 7.12 (m, 4H, Ar-H), 6.99 (m, 2H, Ar-H), 5.17 (s, 4H, 2 × CH_2), 5.11 (s, 4H, 2 × CH_2), 3.95 (t, *J* = 7.03 Hz, 4H, 2 × CH_2), 2.21 (s, 6H, 2 × CH_3), 1.43 - 1.65 (m, 4H, 2 × CH_2), 1.21 - 1.41 (m, 4H, 2 × CH_2), 0.81 - 0.96 (m, 4H, 2 × CH_2) **^{13}C NMR ($CDCl_3$, 100 MHz)** δ 158.0 (BnO-C), 152.6 (BnO-C), 137.5 (C_q), 137.4 (C_q), 136.3 (C_q), 131.3 (ArC), 128.2 (ArC), 128.1 (ArC), 127.7 (ArC), 127.3 (ArC), 127.2 (ArC), 127.1 (ArC), 124.6 (C=C), 114.2 (ArC), 111.6 (ArC), 109.8 (ArC), 107.6 (C=C), 101.9 (ArC), 70.6 (CH_2), 69.6 (CH_2), 43.4 (CH_2), 29.3 (CH_2), 28.4 (CH_2), 26.2 (CH_2), 8.9 (CH_3) **HRMS** (EI): Found 949.4931 $(M+H)^+$, $C_{66}H_{65}N_2O_4$ requires 949.4939 **IR :** ν_{max} (KBr) cm^{-1}: 3063.67, 3033.1, 2926.1, 2855.9, 1613.9, 1505.7, 1479.7, 1455.6, 1379.8, 1288.2, 1242.0, 1025.9, 735.5 **MP :** 136-139 °C

8.4.35 1,12-bis(5-(Benzyloxy)-2-(4-(benzyloxy)phenyl)-3-methyl-1*H*-indol-1-yl)dodectane [267]

Column chromatography of [255] afforded a by-product as a white Solid (280 mg, 30%)

^{1}H NMR ($CDCl_3$, 400 MHz) δ 7.48 - 7.57 (m, 7H, Ar-H), 7.23 - 7.47 (m, 19H, Ar-H), 7.15 (s, 2H, Ar-H), 7.08 - 7.13 (m, 4H, Ar-H), 6.95 - 7.02 (m, 2H, Ar-H), 5.18 (s, 4H, 2 × CH_2), 5.14 (s, 4H, 2 × CH_2), 3.98 (t, *J* = 7.28 Hz, 4H, 2 × CH_2), 2.22 (s, 6H, 2 × CH_3), 1.53 - 1.69 (m, 4H, 2 × CH_2), 1.07 - 1.20 (m, 16H, 8 × CH_2) **^{13}C NMR ($CDCl_3$, 100 MHz)** δ 158.0 (BnO-C), 152.6 (BnO-C), 137.6 (C_q), 137.4 (C_q), 136.4 (C_q), 131.3 (ArC), 128.3 (ArC), 128.2 (ArC), 128.1 (ArC), 127.7 (ArC), 127.3 (ArC), 127.2 (ArC), 127.1 (ArC), 124.6 (C=C), 114.2 (ArC), 111.6 (ArC), 109.9 (ArC), 107.6 (C=C), 101.9 (ArC), 70.6 (CH_2), 69.6 (CH_2), 43.5 (CH_2), 29.7 (CH_2), 29.1 (CH_2), 29.0 (CH_2), 28.7 (CH_2), 26.4 (CH_2), 8.9 (CH_3) **HRMS** (EI): Found 1005.5560 $(M+H)^+$, $C_{70}H_{73}N_2O_4$ requires 1005.5565 **IR :** ν_{max} (KBr) cm^{-1}: 3063.4, 3033.1, 2926.0, 2854, 1613.4, 1506.0, 1478.9, 1454.6, 1386.5, 1287.4, 1242.3, 1174.4, 1026.2, 734.9 **MP :** 132-135 °C

8.4.36 General method for the debenzylation of the di-indole conjugates

The appropriate di-indole [263]-[267] (200 mg) was dissolved in MeOH:EtOAc (1:4) (20 mL) and transferred to a 3-neck flask. To the flask was added a small spatula tipful of $Pd(OH)_2$ (~20 mg) and placed under a H_2 atmosphere. The reaction was monitored *via* TLC until the starting material had disappeared (10 – 60 min). The reaction mixture was filtered through celite and the solvent was evaporated under reduced pressure to obtain a brown oil. The material was purified *via* flash chromatography on silica gel to afford the product.

8.4.37 1,1'-(Butane-1,4-diyl)bis(2-(4-hydroxyphenyl)-3-methyl-1*H*-indol-5-ol) [268]

As per general method 8.4.36, the protected indole conjugate [263] (200 mg, 0.224 mmol) and a small spatula tipful of $Pd(OH)_2$ (20 mg) were reacted under a hydrogen atmosphere for 30 min. The material was purified *via* flash chromatography over silica gel (DCM:EtOAc, gradient 2:1 to 1:1) to afford the product as a yellow solid (79 mg, 67%)

^{1}H NMR (CD_3OD, 400 MHz) δ 6.86 - 6.96 (m, 6H, Ar-H), 6.78 - 6.85 (m, 6H, Ar-H), 6.66 (d, *J* = 8.53 Hz, 2H, Ar-H), 3.69 - 3.80 (m, 4H, 2 × CH_2), 2.06 (s, 6H, 2 × CH_3), 1.20 - 1.38 (m, 6H, 2 × CH_2, 2 × OH), 1.08 - 1.18 (m, 4H, 2 × CH_2), 0.91 (br s, 2H, 2 × OH) **^{13}C NMR (CD_3OD, 100 MHz)** δ 158.4 (C-OH), 151.3 (C-OH), 139.6 (C_q), 133.2 (C_q), 132.9 (ArC), 130.8 (C_q), 124.9 (C=C), 116.3 (ArC), 112.0 (ArC), 111.2 (ArC), 108.5 (C=C), 103.9 (ArC), 44.0 (CH_2), 28.0 (CH_2), 9.6 (CH_3) **HRMS** (EI): Found 533.2421 $(M+H)^+$, $C_{34}H_{35}N_2O_4$ requires 533.2435 **IR :** ν_{max} (KBr) cm^{-1}: 3428.5 (br), 2921.2, 2857.1, 1614.5, 1560.0, 1508.1, 1457.2, 1359.7, 1229.3, 1201.0, 1168.1, 836.9 **MP :** 128-129 °C

8.4.38 1,1'-(Pentane-1,5-diyl)bis(2-(4-hydroxyphenyl)-3-methyl-1*H*-indol-5-ol) [269]

As per general method 8.4.36, the protected indole conjugate [264] (200 mg, 0.220 mmol) and a small spatula tipful of $Pd(OH)_2$ (~20 mg) were reacted under a hydrogen atmosphere for 30 min. The material was purified *via* flash chromatography over silica gel (DCM:EtOAc, gradient 2:1 to 1:1) to afford the product as a yellow solid (63 mg, 53%)

^{1}H NMR (CD_3OD, 400 MHz) δ 7.03 (d, *J* = 9.03 Hz, 2H, Ar-H), 6.93 (s, 2H, Ar-H), 6.71 - 6.82 (m, 10H, Ar-H), 3.80 (t, *J* = 6.27 Hz, 4H, 2 × CH_2), 3.34 (br. s., 2H, 2 × OH), 2.06 (s, 6H, 2 × CH_3), 1.11 - 1.22 (m, 4H, 2 × CH_2), 0.34 - 0.45 (m, 2H, CH_2) **^{13}C NMR (CD_3OD, 100 MHz)** δ 158.2 (C-OH), 151.3 (C-OH), 139.9 (C_q), 133.0 (C_q), 132.9 (ArC), 130.8 (C_q), 125.1 (C=C), 116.3 (ArC), 111.9 (ArC), 111.4 (ArC), 108.1 (C=C), 104.0 (ArC), 44.1 (CH_2), 30.4 (CH_2), 23.7 (CH_2), 9.6 (CH_3) **HRMS** (EI): Found 547.2579 $(M+H)^+$, $C_{35}H_{35}N_2O_4$ requires 547.2591 **IR :** ν_{max} (KBr) cm^{-1}: 3429.9, 2928.1, 2859.9, 1614.9, 1508.3, 1461.8, 1353.3, 1231.0, 1168.9, 837.58 **MP :** 131-133 °C

8.4.39 1,1'-(Hexane-1,6-diyl)bis(2-(4-hydroxyphenyl)-3-methyl-1*H*-indol-5-ol) [270]

As per general method 8.4.36, the protected indole conjugate [265] (200 mg, 0.217 mmol) and a small spatula tipful of $Pd(OH)_2$ (20 mg) were reacted under a hydrogen atmosphere for 30 min. The material was purified *via* flash chromatography on silica gel (DCM:EtOAc, gradient 2:1 to 1:1) to afford the product as a yellow solid (90 mg, 74%)

^{1}H NMR ($CDCl_3$, 400 MHz) δ 7.00 - 7.14 (m, 6H, Ar-H), 6.81 - 6.95 (m, 6H, Ar-H), 6.72 (d, *J* = 8.53 Hz, 2H, Ar-H), 3.85 (t, *J* = 6.27 Hz, 4H, 2 × CH_2), 2.10 (s, 6H, 2 × CH_3), 1.24 - 1.40 (m, 6H, 2 × CH_2, 2 × OH), 0.71 - 0.84 (m, 4H, 2 × CH_2) **^{13}C NMR (CD_3OD, 100 MHz)** δ 158.5 (C-OH), 151.3 (C-OH), 139.7 (C_q), 133.0 (ArC), 130.8 (C_q), 125.1 (C=C), 116.4 (ArC), 112.0 (ArC), 111.2 (ArC), 108.2 (C=C), 103.9 (ArC), 44.4 (CH_2), 30.8 (CH_2), 27.2 (CH_2), 9.6 (CH_3) **HRMS** (EI): Found 561.2731 $(M+H)^+$, $C_{36}H_{37}N_2O_4$ requires 561.2748 **IR :** ν_{max} (KBr) cm^{-1}: 3425.1 (br.), 2925.8, 2850.2, 1614.5, 1508.15, 1460.8, 1354.9, 1231.62, 1168.7, 837.0 **MP :** 123-124 °C

8.4.40 1,1'-(Octane-1,8-diyl)bis(2-(4-hydroxyphenyl)-3-methyl-1*H*-indol-5-ol) [271]

As per general method 8.4.36, the protected indole conjugate [266] (200 mg, 0.210 mmol) and a small spatula tipful of $Pd(OH)_2$ (20 mg) were reacted under a hydrogen atmosphere for 30 min. The material was purified *via* flash chromatography over silica gel (DCM:EtOAc, gradient 2:1 to 1:1) to afford the product as a yellow solid (75 mg, 61%)

^{1}H NMR (CD_3OD, 400 MHz) δ 7.06 - 7.22 (m, 6H, Ar-H), 6.81 - 6.96 (m, 6H, Ar-H), 6.72 (d, *J* = 8.53 Hz, 2H, Ar-H), 3.86 - 4.00 (m, 4H, 2 × CH_2), 2.11 (s, 6H, 2 × CH_3), 1.07 - 1.52 (m, 12H, 4 × CH_2, OH), 0.79 - 1.00 (m, 4H, 2 × CH_2) **^{13}C NMR (CD_3OD, 100 MHz)** δ 158.5 (C-OH), 151.4 (C-OH), 139.7 (C_q), 133.0 (ArC), 130.9 (C_q), 125.1 (C=C), 116.4 (ArC), 112.0 (ArC), 111.2 (ArC), 108.2 (C=C), 103.9 (ArC), 44.6 (CH_2), 34.1 (CH_2), 29.8 (CH_2), 27.5 (CH_2), 9.7 (CH_3) **HRMS** (EI): Found 589.3090 $(M+H)^+$, $C_{38}H_{41}N_2O_4$ requires 589.3061 **IR :** ν_{max} (KBr) cm^{-1}: 3438.5 (br), 2922.7, 2854.3, 1638.4, 1614.5, 1508.2, 1456.9, 1384.1, 1239.9, 1168.9, 838.3 **MP :** 83-86 °C

8.4.41 1,1'-(Dodecane-1,12-diyl)bis(2-(4-hydroxyphenyl)-3-methyl-1*H*-indol-5-ol) [272]

As per general method 8.4.36, the protected indole conjugate [267] (200 mg, 0.199 mmol) and a small spatula tipful of $Pd(OH)_2$ (20 mg) were reacted under a hydrogen atmosphere for 30 min. The material was purified *via* flash chromatography on silica gel (DCM:EtOAc, gradient 2:1 to 1:1) to afford the product as a yellow solid (74 mg, 58%)

^{1}H NMR (CD_3OD, 400 MHz) δ 7.09 - 7.26 (m, 6H, Ar-H), 6.82 - 6.98 (m, 6H, Ar-H), 6.71 (d, *J* = 7.03 Hz, 2H, Ar-H), 3.92 - 4.06 (m, 4H, 2 × CH_2), 2.12 (s, 6H, 2 × CH_3), 1.42 - 1.60 (m, 4H, 2 × CH_2), 1.24 - 1.40 (m, 8H, 4 × CH_2), 0.99 - 1.16 (m, 8H, 4 × CH_2) (OH not observed) **^{13}C NMR (CD_3OD, 100 MHz)** δ 158.5 (C-OH), 151.4 (C-OH), 139.8 (C_q), 133.0 (ArC), 130.9 (C_q), 125.1 (C=C), 116.4 (ArC), 112.0 (ArC), 111.2 (ArC), 108.2 (C=C), 103.9 (ArC), 44.6 (CH_2), 30.9 (CH_2), 30.57 (CH_2), 30.56 (CH_2), 30.2 (CH_2), 27.7 (CH_2), 9.6 (CH_3) **HRMS** (EI): Found 645.3661 $(M+H)^+$, $C_{42}H_{49}N_2O_4$ requires 645.3687 **IR :** ν_{max} (KBr) cm^{-1}: 3401.6 (br), 2922.7, 2853.0, 1614.6, 1508.2, 1463.7, 1372.5, 1234.0, 1165.5, 834.6 **MP :** 139-140 °C

8.4.42 6-(Benzyloxy)-2-(4-(benzyloxy)phenyl)-3-(4-bromobutyl)-3-methyl-3*H*-indole [273]

Column chromatography of [251] afforded a by-product as a yellow solid (179 mg, 17%)

^{1}H NMR ($CDCl_3$, 400 MHz) δ 8.11 (d, *J* = 8.53 Hz, 2H, Ar-H), 7.61 (d, *J* = 8.03 Hz, 1H, Ar-H), 7.34 - 7.54 (m, 10H, Ar-H), 7.10 (d, *J* = 8.53 Hz, 2H, Ar-H), 6.98 - 7.04 (m, 1H, Ar-H), 6.95 (d, *J* = 2.01 Hz, 1H, Ar-H), 5.17 (s, 2H, CH_2), 5.15 (s, 2H, CH_2), 3.15 (t, *J* = 7.03 Hz, 2H, CH_2), 2.26 (dt, *J* = 4.52, 12.80 Hz, 1H, 0.5 × CH_2), 2.03 (dt, *J* = 4.02, 12.80 Hz, 1H, 0.5 × CH_2), 1.53 - 1.70 (m, 5H, CH_2, CH_3), 0.84 - 1.03 (m, 2H, CH_2) **^{13}C NMR ($CDCl_3$, 100 MHz)** δ 179.1 (C=N), 160.2 (C-OBn), 157.0 (C-OBn), 147.3 (C_q), 146.7 (C_q), 136.5 (C_q), 136.0 (C_q), 129.0, 128.2, 128.2, 127.8, 127.7, 127.6, 127.2, 127.1, 126.0 (C_q), 120.3, 114.5, 113.1, 108.2, 70.2 (CH_2), 69.6 (CH_2), 57.3 ($C(CH_3)$), 38.0 (CH_2), 32.4 (CH_2), 32.3 (CH_2), 24.6 (CH_3), 22.6 (CH_2) **HRMS** (EI): Found 554.1714 $(M+H)^+$, $C_{33}H_{35}BrNO_2$ requires 554.1689 **IR :** ν_{max} (KBr) cm^{-1}: 3064.6, 3032.6, 2930.3, 2858.6, 1604.3, 1505.8, 1454.1, 1379.8, 1247.9, 1174.0, 1023.7, 831.8 **MP :** 84-86 °C

8.4.43 6-(Benzyloxy)-2-(4-(benzyloxy)phenyl)-3-(5-bromopentyl)-3-methyl-3*H*-indole [274]

Column chromatography of [252] afforded a by-product as a yellow solid (97 mg, 9%)

^{1}H NMR ($CDCl_3$, 400 MHz) δ 8.12 (d, *J* = 8.53 Hz, 2H, Ar-H), 7.60 (d, *J* = 8.03 Hz, 1H, Ar-H), 7.35 - 7.54 (m, 10H, Ar-H), 7.10 (d, *J* = 8.53 Hz, 2H, Ar-H), 6.99 (d, *J* = 8.53 Hz, 1H, Ar-H), 6.94 (d, *J* = 2.01 Hz, 1H, Ar-H), 5.17 (s, 2H, CH_2), 5.14 (s, 2H, CH_2), 3.22 (t, *J* = 6.78 Hz, 2H, CH_2), 2.25 (dt, *J* = 3.51, 4.52 Hz, 1H, 0.5 × CH_2), 2.02 (dt, *J* = 4.02, 12.80 Hz, 1H, 0.5 × CH_2), 1.54 - 1.66 (m, 5H, CH_2, CH_3), 1.17 - 1.27 (m, 2H, CH_2), 0.76 - 0.95 (m, 2H, CH_2) **^{13}C NMR ($CDCl_3$, 100 MHz)** δ 179.3 (C=N), 160.2 (C-OBn), 157.0 (C-OBn), 146.8 (C_q), 136.5 (C_q), 136.0 (C_q), 129.1, 128.2, 128.2, 127.7, 127.6, 127.2, 127.1, 120.2, 114.5,

112.9, 108.2, 70.2 (CH_2), 69.7 (CH_2), 57.5 ($C(CH_3)$), 38.8 (CH_2), 33.3 (CH_2), 31.7 (CH_2), 27.7 (CH_2), 24.6 (CH_3), 22.9 (CH_2) **HRMS** (EI): Found 590.1688 $(M+H)^+$, $C_{34}H_{34}BrNNaO_2$ requires 590.1671 **IR :** ν_{max} (KBr) cm^{-1}: 3064.3, 3032.5, 2928.7, 2859.5, 1604.6, 1505.8, 1454.4, 1379.9, 1249.8, 1023.9, 836.8 **MP :** 81-84 °C

8.4.44 6-(Benzyloxy)-2-(4-(benzyloxy)phenyl)-3-(6-bromo-*n*-hexanoyl)-3-methyl-3*H*-indole [275]

Column chromatography of [253] afforded a by-product as a yellow solid (133 mg, 12%)

^{1}H NMR ($CDCl_3$, 400 MHz) δ 8.13 (d, *J* = 8.53 Hz, 2H, Ar-H), 7.61 (d, *J* = 8.53 Hz, 1H, Ar-H), 7.33 - 7.54 (m, 10H, Ar-H), 7.10 (d, *J* = 9.03 Hz, 2H, Ar-H), 7.00 (dd, *J* = 2.26, 8.28 Hz, 1H, Ar-H), 6.94 (d, *J* = 2.01 Hz, 1H, Ar-H), 5.17 (s, 2H, CH_2), 5.07 - 5.15 (m, 2H, CH_2), 3.28 (t, *J* = 6.78 Hz, 2H, CH_2), 2.20 (dt, *J* = 3.76, 12.92 Hz, 1H, 0.5 × CH_2), 2.01 (dt, *J* = 3.76, 12.92 Hz, 1H, 0.5 × CH_2), 1.54 - 1.70 (m, 5H, CH_2, CH_3), 1.03 - 1.23 (m, 4H, 2 × CH_2), 0.73 - 0.95 (m, 2H, CH_2) **^{13}C NMR ($CDCl_3$, 400 MHz)** δ 179.4 (C=N), 160.3 (C-OBn), 157.0 (C-OBn), 146.9 (C_q), 136.5 (C_q), 136.0 (C_q), 129.2, 128.2, 128.2, 127.7, 127.6, 127.2, 127.1, 120.1, 114.5, 112.9, 108.2, 70.2 (CH_2), 69.7 (CH_2), 57.5 ($C(CH_3)$), 38.8 (CH_2), 33.4 (CH_2), 32.0 (CH_2), 28.2 (CH_2), 27.1 (CH_2), 24.6 (CH_3), 23.4 (CH_2) **HRMS** (EI): Found 584.2000 $(M+H)^+$, $C_{35}H_{27}BrNO_2$ requires 582.2002 **IR :** ν_{max} (KBr) cm^{-1}: 3064.8, 3032.8, 2928.9, 2864.9, 1604.9, 1505.8, 1462.7, 1380.2, 1248.7, 1173.5, 1023.6, 836.7 **MP :** 79-82 °C

8.4.45 6-(Benzyloxy)-2-(4-(benzyloxy)phenyl)-3-(8-bromooctyl)-3-methyl-3*H*-indole [276]

Column chromatography of [254] afforded a by-product as a yellow solid (156 mg, 13%)

^{1}H NMR ($CDCl_3$, 400 MHz) δ 8.13 (d, *J* = 8.53 Hz, 2H, Ar-H), 7.61 (d, *J* = 8.03 Hz, 1H, Ar-H), 7.34 - 7.54 (m, 10H, Ar-H), 7.10 (d, *J* = 8.53 Hz, 2H, Ar-H), 6.99 (d, *J* = 8.03 Hz, 1H, Ar-H), 6.94 (s, 1H, Ar-H), 5.17 (s, 2H, CH_2), 5.13 (s, 2H, CH_2), 3.35 (t, *J* = 6.78 Hz, 2H, CH_2), 2.16 - 2.28 (m, 1H, 0.5 × CH_2), 1.95 - 2.05 (m, 1H, 0.5 × CH_2), 1.69 - 1.86 (m, 2H, CH_2), 1.56 (s, 3H, CH_3), 1.21 - 1.41 (m, 5H, 3 × CH_2), 1.03 - 1.16 (m, 6H, 3 × CH_2) **^{13}C NMR ($CDCl_3$, 100 MHz)** δ 179.5 (C=N), 159.6 (C-OBn), 155.4 (C-OBn), 147.6 (C_q), 136.4 (C_q), 136.0 (C_q), 129.3, 128.2, 128.2, 127.7, 127.6, 127.2, 127.1, 120.0, 114.5, 112.8, 108.3, 70.2 (CH_2), 69.7 (CH_2), 57.6 ($C(CH_3)$), 39.0 (CH_2), 33.6 (CH_2), 32.2 (CH_2), 29.0 (CH_2), 28.3 (CH_2), 28.0 (CH_2), 27.5 (CH_2), 24.7 (CH_3), 23.5 (CH_2) **HRMS** (EI): Found 610.2339 $(M+H)^+$, $C_{37}H_{41}BrNO_2$ requires 610.2315 **IR :** ν_{max} (KBr) cm^{-1}: 3064.7, 3032.9, 2928.2, 2855.8, 1604.1, 1505.8, 1454.3, 1379.6, 1241.9, 1174.4, 1023.6, 827.1 **MP :** 79-82 °C

8.4.46 6-(Benzyloxy)-2-(4-(benzyloxy)phenyl)-3-(12-bromododecyl)-3-methyl-3*H*-indole [277]

Column chromatography of [255] afforded a by-product as a yellow solid yellow solid (140 mg, 11%)

^{1}H NMR ($CDCl_3$, 400 MHz) δ 8.14 (d, *J* = 8.03 Hz, 2H, Ar-H), 7.62 (d, *J* = 7.53 Hz, 1H, Ar-H), 7.34 - 7.54 (m, 10H, Ar-H), 7.10 (d, *J* = 8.53 Hz, 2H, Ar-H), 6.99 (d, *J* = 8.53 Hz, 1H, Ar-H), 6.94 (s, 1H, Ar-H), 5.17 (s, 2H, CH_2), 5.13 (s, 2H, CH_2), 3.41 (t, *J* = 6.78 Hz, 2H, CH_2), 2.17 - 2.28 (m, 1H, 0.5 × CH_2), 1.96 - 2.07 (m, 1H, 0.5 × CH_2), 1.84 (quin, *J* = 14.30 Hz, 2H, CH_2), 1.56 (s, 3H, CH_3), 1.35 - 1.45 (m, 2H, CH_2), 1.00 - 1.34 (m, 14H, 7 × CH_2), 0.73 - 0.94 (m, 2H, CH_2) **^{13}C NMR ($CDCl_3$, 100 MHz)** δ 179.6 (C=N), 160.0 (C-OBn), 152.2 (C-OBn), 144.4 (C_q), 136.4 (C_q), 136.0 (C_q), 129.3, 128.2, 128.2, 127.7, 127.6, 127.2, 127.1, 126.8, 125.4, 120.0, 114.5, 112.8, 108.3, 70.2 (CH_2), 69.7 (CH_2), 57.6 ($C(CH_3)$), 39.1 (CH_2), 34.5 (CH_2), 33.7 (CH_2), 32.4 (CH_2), 29.2 (CH_2), 29.0 (CH_2), 28.9 (CH_2), 28.6 (CH_2), 28.3 (CH_2), 27.7 (CH_2), 24.7

(CH_2), 24.2 (CH_3), 23.7 (CH_2) **HRMS** (EI): Found 666.2943 $(M+H)^+$, $C_{41}H_{49}BrNO_2$ requires 666.2941 **IR :** ν_{max} (KBr) cm^{-1}: 3064.8, 3022.9, 2922.7, 2853.9, 1604.1, 1507.0, 1462.8, 1379.3, 1249.2, 1173.9, 1024.1, 836.8 **MP :** 85-88 °C

8.4.47 1-(benzyloxy)-4-(bromomethyl)benzene [279]

To a solution of benzylalcohol [302] (2.5 g, 11.67 mmol) in DCM (30 mL) was placed under a nitrogen atomosphere and was cooled to 0°C at which time PBr_3 (1.1 ml, 11.67 mmol) was added dropwise. The mixture was left to stir for 1 hour at RT after which $NaHCO_3$ was added dropwise. The resulting solution was washed with water (30 mL). The aqueous layer extracted with DCM (20 mL × 2). The organic layers were combined and washed with brine (50 mL) and dried over Na_2SO_4. The solvent was evaporated to yield an orange oil. The crude mixture was then purified using column chromatography over silica gel (DCM) to afford the product as an off-white solid (2.97 g, 92 %).

^{1}H-NMR 400MHz ($CDCl_3$): δ 7.41 - 7.50 (m, 4H, Ar-H), 7.32 - 7.40 (m, 3H, Ar-H), 6.98 (d, *J* = 8.53 Hz, 2H, Ar-H), 5.10 (s, 2H, CH_2), 4.54 (s, 2H, CH_2) **^{13}C-NMR 100MHz** ($CDCl_3$): δ 158.4, 136.2, 128.6, 114.7, 69.6 (CH_2), 34.2 (CH_2) **IR:** ν_{max} (KBr) cm^{-1}:3467.5, 1639.7, 1614.2, 1515.4, 1454.4, 1383.6, 1252.5, 1006.9, 737.4, 698.9 **HRMS** (EI): Found 197.0958 $(M-Br)^-$, $C_{14}H_{13}O^-$ requires 197.0972; **M.P.**: 83-85 °C

8.4.48 1-((2-Bromoethoxy)methyl)benzene [281]

To a suspension of NBS (0.68 g, 3.84 mmol) in dry DCM (7 ml) was added PPh_3 (1g, 3.83 mmol) in 5 ml DCM in the dark at -78 °C. The mixture was stirred until all the NBS was dissolved. A solution of 2-(benzyloxy)ethanol [306] (0.5 g, 0.46 mL, 3.28 mmol) in DCM (4 ml) was added dropwise. The cooling bath was removed and the reaction was stirred for 1 hour at RT until the solution turned orange. The reaction was quenched with the addition of methanol (4 ml) and toulene (5 ml). The mixture was then evaporated under reduced pressure till all the MeOH had been removed. The brown oil was dissolved in EtOAc (20 mL) and washed with water (20 mL × 2), brine (40 mL) and dried over Na_2SO_4. The solvent was evaporated *in vacuo* to afford a brown oil. Column chromatography over silica gel (DCM:*n*-Hexane, 1:4) eluted the product as a white solid. (620 mg, 88 %).

^{1}H-NMR 400MHz ($CDCl_3$): δ 6.51 – 6.83 (m, 5H, Ar-H), 5.11 (s, 2H, CH_2), 3.91 (t, *J* = 7.5 Hz, 2H, CH_2), 3.50 (t, *J* = 7.5 Hz, 2H, CH_2) **^{13}C-NMR 100MHz** ($CDCl_3$): δ 137.5 (C_q), 128.6 (ArC), 127.8 (ArC), 127.4 (ArC), 72.0 (CH_2), 69.2 (CH_2), 31.0 (CH_2) **IR:** ν_{max} (KBr) cm^{-1}: 3489.3, 3089.2, 2891.3, 1501.8, 14431, 1089.4, 693.4 **HRMS** (EI): Found 458.1747 $(M+Na)^+$, $C_{29}H_{25}NNaO_3$ requires 458.1732; **M.P.**: 100-101 °C

8.4.49 5-(Bromomethyl)-1,2,3-trimethoxybenzene [282]

To a solution of benzylalcohol [305] (2 g, 10 mmol) in DCM (30 mL) was placed under a nitrogen atomosphere and was cooled to 0°C at which time PBr_3 (1.045 mL, 11 mmol) was added dropwise. The mixture was left to stir for 1 hour at RT after which $NaHCO_3$ was added dropwise. The resulting solution was washed with water (30 mL). The aqueous layer extracted with DCM (20 mL × 2). The organic layers were combined and washed with brine (50 mL) and dried over Na_2SO_4. The solvent was evaporated to yield an orange oil. The crude mixture was then purified using column chromatography over silica gel (DCM:EtOAc, gradient 5:1 to 3:1) to afford the product as an off-white solid (2.37 g, 91 %).

^{1}H-NMR 400MHz ($CDCl_3$): δ 6.64 (s, 2H, Ar-H), 4.49 (s, 2H, CH_2), 3.89 (s, 6H, 2 × OCH_3), 3.87 (s, 3H, OCH_3) **^{13}C-NMR 100MHz** ($CDCl_3$): δ 152.8, 132.7, 105.6 (Ar-C), 60.4 (OCH_3), 55.7 (OCH_3), 33.9 (CH_2) **IR:**

ν_{max} (KBr) cm^{-1}: 2997.9, 2938.7, 2837.6, 1591.1, 1506.7, 1459.5, 1420.9, 13314.6, 1242.0, 1125.0, 1005.9, 833.0, 666.5 **HRMS** (EI): Found 261.0118 $(M+Na)^+$, $C_{10}H_{13}BrNaO_3$ requires 261.0121 **M.P.**: 71-73 °C

8.4.50 5-(Benzyloxy)-2-(4-(benzyloxy)phenyl)-1-butyl-3-methyl-1*H*-indole [284]

To a round bottomed flask was added NaH (0.19 g, 4.76 mmol) and THF (20 mL) at 0°C under a nitrogen atmosphere. To the flask was added indole [248] (0.5 g, 1.19 mmol) in THF (10 mL) and the mixture was allowed to stir for 10 minutes at 0°C. To the reaction mixture was then added 1-bromobutane [278] (0.179 g, 0.14 mL, 1.307 mmol) and left to stir for a further 30 minutes. The reaction was then refluxed for 2 hours. To the reaction mixture was added water dropwise till the fizzing ceased. The mixture was then evaporated under reduced pressure till all the THF had been removed. The brown oil was dissolved in EtOAc (20 mL) and washed with water (20 mL × 2), brine (40 mL) and dried over Na_2SO_4. The solvent was evaporated *in vacuo* to afford a brown resin. Column chromatography over silica gel (*n*-Hexane:DCM, gradient 4:1 to 2:1) to afford the product as a pink solid (284 g, 50 %).

^{1}H-NMR 400MHz ($CDCl_3$); δ 7.50 - 7.58 (m, 4H, Ar-H), 7.31 - 7.49 (m, 8H, Ar-H), 7.25 - 7.31 (m, 1H, Ar-H), 7.09 - 7.18 (m, 3H, Ar-H), 7.01 (d, *J* = 9.03 Hz, 1H, Ar-H), 5.19 (s, 2H, CH_2), 5.17 (s, 2H, CH_2), 4.01 (t, *J* = 7.28 Hz, 2H, CH_2), 2.23 (s, 3H, CH_3), 1.61 (quin, *J* = 7.40 Hz, 2H, CH_2), 1.18 (sxt, *J* = 7.33 Hz, 2H, CH_2), 0.81 (t, *J* = 7.28 Hz, 3H, CH_3) **^{13}C-NMR 100MHz** ($CDCl_3$): 158.0 (COBn), 152.6 (COBn), 137.6 (C_q), 137.4 (C_q), 136.4 (ArC), 131.3 (ArC), 131.3 (ArC), 128.3 (ArC), 128.2 (ArC), 128.1 (ArC), 127.7 (ArC), 127.3 (ArC), 127.2 (ArC), 124.6 (C=C), 114.2 (ArC), 111.6 (ArC), 109.9 (ArC), 107.6 (C=C), 101.9 (ArC), 70.6 (CH_2), 69.7 (CH_2), 43.3 (CH_2), 31.8 (CH_2), 19.6 (CH_2), 13.3 (CH_3), 8.9 (CH_3) **IR:** ν_{max} (KBr) cm^{-1}: 3418.7, 2956.3, 2933.3, 2871.5, 1609.5, 1480.3, 1461.3, 1379.6, 1204.9, 1017.5, 829.8, 698.6 **HRMS** (EI): Found 476.2585 $(M+H)^+$, $C_{33}H_{34}NO_2$ requires 475.2584 **M.P.**: 148 -150 °C

8.4.51 1-(4-(Benzyloxy)benzyl)-5-(benzyloxy)-2-(4-(benzyloxy)phenyl)-3-methyl-1*H*-indole [285]

To a round bottomed flask was added NaH (0.250 g, 6.2 mmol) dissolved in THF (20 mL) and was allowed to stir for 10 min at 0°C under a nitrogen atmosphere. To the reaction mixture was added indole [248] (1 g, 2.38 mmol) dissolved in THF (10 mL). The mixture was stirred at 0°C for 10 minutes after which benzylbromide compound [279] (0.989 g, 3.57 mmol) was added dropwise. The mixture was left to stir at 0°C for a further 30 minutes before being refluxed for 2 hours. The mixture was then evaporated under reduced pressure till all the THF had been removed. The brown oil was dissolved in EtOAc (20 mL) and washed with water (20 mL × 2), brine (40 mL) and dried over Na_2SO_4. The solvent was evaporated *in vacuo* to afford a brown resin. Column chromatography over silica gel (*n*-Hexane:DCM, gradient 4:1 to 2:1) to afford the product as a yellow solid (0.99 g, 68 %).

^{1}H-NMR 400MHz ($CDCl_3$): δ 7.31 - 7.57 (m, 12H, Ar-H), 7.22 - 7.31 (m, 3H, Ar-H), 7.20 (d, *J* = 2.01 Hz, 1H, Ar-H), 7.13 (d, *J* = 9.03 Hz, 2H, Ar-H), 7.01 - 7.09 (m, 2H, Ar-H), 6.83 - 7.01 (m, 6H, Ar-H), 5.09 - 5.21 (m, 6H, 3 × CH_2), 5.01 - 5.08 (m, 3H, 3 × CH_2), 2.30 (s, 3H, CH_3) **^{13}C-NMR 100MHz** ($CDCl_3$): δ 158.5 (COBn), 157.8 (COBn), 153.3 (COBn), 138.3, 137.8, 137.0, 136.8, 132.1, 131.7, 131.0, 130.4, 129.1, 128.6, 128.5, 128.5, 128.0, 127.9, 127.7, 127.6, 127.5, 127.5, 127.3, 124.6 (C=C), 115.1, 114.9, 114.7, 112.3, 110.8, 108.4 (C=C), 102.4, 71.0 (CH_2), 70.0 (CH_2), 47.1(CH_2), 9.5 (CH_3) **IR:** ν_{max} (KBr) cm^{-1}: 3062.9, 3032.7, 2916.4, 1610.4, 1509.0, 1454.7, 1240.5, 1174.6, 1024.9, 1024.9, 835.0, 736.7, 696.3 **HRMS** (EI): Found 458.1747 $(M+Na)^+$, $C_{29}H_{25}NNaO_3$ requires 458.1732 **M.P.**: 65-68°C

8.4.52 1-(4-Fluorobenzyl)-5-(benzyloxy)-2-(4-(benzyloxy)phenyl)-3-methyl-1*H*-indole [286]

To a round bottomed flask was added NaH (0.114 g, 4.76 mmol) suspended in THF (20 mL) and was allowed to stir for 10 min at 0°C under a nitrogen atmosphere. To the reaction mixture was added indole [248] (1 g, 2.38 mmol) dissolved in THF (10 mL). The mixture was stirred at 0°C for 10 minutes after which benzylbromide compound [280] (0.45 g, 0.29 mL, 2.38 mmol) was added dropwise. The mixture was left to stir at 0°C for a further 30 minutes before being refluxed for 2 hours. The mixture was then evaporated under reduced pressure till all the THF had been removed. The brown oil was dissolved in EtOAc (20 mL) and washed with water (20 mL × 2), brine (40 mL) and dried over Na_2SO_4. The solvent was evaporated *in vacuo* to afford a brown resin. Column chromatography over silica gel (*n*-Hexane:DCM, gradient 4:1 to 2:1) to afford the product as a yellow solid (0.72 g, 68 %).

^{1}H-NMR 400MHz ($CDCl_3$): δ 7.33 - 7.59 (m, 10H, Ar-H), 7.17 - 7.32 (m, 3H, Ar-H), 7.02 - 7.13 (m, 3H, Ar-H), 6.87 - 6.99 (m, 5H, Ar-H), 5.07 - 5.24 (m, 6H, 3 × CH_2), 2.29 (s, 3H, CH_3) **^{3}C-NMR 100MHz** ($CDCl_3$): δ 162.6 (C-F), 161.0 (COH), 158.6 (COH), 153.4, 138.2, 137.8, 136.8, 134.3, 132.0, 131.6, 129.2, 128.6, 128.5, 128.1, 127.7, 127.6, 127.6, 127.6, 127.5, 124.5 (C=C), 115.4, 115.3, 114.7, 112.4, 110.6, 108.7 (C=C), 102.5, 71.0 (CH_2), 70.0 (CH_2), 46.9 (CH_2), 9.5 (CH_3) **IR:** ν_{max} (KBr) cm^{-1}: 3380.3, 2923.7, 1613.4, 1505.9, 1462.3, 1220.2, 1171.9, 1016.0, 837.9, 735.0 **HRMS** (EI): Found 528.2329 $(M+H)^+$, $C_{36}H_{31}FNO_2$ requires 528.2333 **M.P.**: 60-62 °C

8.4.53 5-(Benzyloxy)-1-(2-(benzyloxy)ethyl)-2-(4-(benzyloxy)phenyl)-3-methyl-1*H*-indole [287]

To a round bottomed flask was added NaH (0.06 g, 2.4 mmol) suspended in THF (20 mL) and was the suspention was allowed to stir for 10 min at 0 °C under a nitrogen atmosphere. To the reaction mixture was added indole [248] (0.5 g, 1.2 mmol) dissolved in THF (10 mL). The mixture was stirred at 0°C for 10 minutes after which alkylbromide compound [281] (0.24 g, 1.2 mmol) was added dropwise. The mixture was left to stir at 0°C for a further 30 minutes before being refluxed for 2 hours. The mixture was then evaporated under reduced pressure till all the THF had been removed. The brown oil was dissolved in EtOAc (20 mL) and washed with water (20 mL × 2), brine (40 mL) and dried over Na_2SO_4. The solvent was evaporated *in vacuo* to afford a brown resin. Column chromatography over silica gel (DCM:EtOAc, gradient 4:1 to 2:1) eluted the product as a yellow solid (0.285 g, 43 %).

^{1}H-NMR 400MHz ($CDCl_3$): δ 7.24 - 7.57 (m, 10H, Ar-H), 7.13 - 7.19 (m, 4H, Ar-H), 7.07 (d, *J* = 8.53 Hz, 2H, Ar-H), 6.99 (dd, *J* = 2.26, 8.78 Hz, 1H, Ar-H), 6.51 - 6.80 (m, 5H, Ar-H), 5.17 (d, *J* = 12.05 Hz, 4H, 2 × CH_2), 4.76 (s, 2H, CH_2) 4.22 (t, *J* = 6.27 Hz, 2H, CH_2), 3.82 (t, *J* = 6.27 Hz, 2H, CH_2), 2.20 (s, 3H, CH_3) **^{13}C-NMR 100MHz** ($CDCl_3$): δ; 158.1 (COH), 152.7 (COH), 137.5, 137.4, 136.4, 131.5, 128.5, 128.2, 128.1, 127.9, 127.8, 127.7, 127.4, 127.3, 127.2, 127.1, 124.2 (C=C), 114.2, 111.7, 110.0, 108.1 (C=C), 102.0, 72.6 (CH_2), 70.6 (CH_2), 69.6 (CH_2), 68.3 (CH_2), 43.3 (CH_2), 8.9 (CH_3) **IR:** ν_{max} (KBr) cm^{-1}: 2935.8, 1614.5, 1594.6, 1508.3, 1450.4, 1331.6, 1236.2, 1125.0, 998.4, 839.9 **HRMS** (EI): Found 554.2683 $(M+H)^+$, $C_{38}H_{36}NO_3$ requires 554.2690; **M.P.**: 69-71 °C

8.4.54 1-(3,4,5-Trimethoxybenzyl)-5-(benzyloxy)-2-(4-(benzyloxy)phenyl)-3-methyl-1*H*-indole [288]

To a round bottom flask was added NaH (0.084 g, 3.6 mmol) suspended in THF (20 mL) and the mixture was allowed to stir for 10 min at 0 °C under a nitrogen atmosphere. To the reaction mixture

was added indole [248] (0.5 g, 1.2 mmol) dissolved in THF (10 mL). The mixture was stirred at 0 °C for 10 minutes after which 3,4,5-trimethoxybenzylbromide [282] (0.6 g, 2.38 mmol) was added dropwise. The mixture was left to stir at 0°C for a further 30 minutes before being refluxed for 2 hours. The mixture was then evaporated under reduced pressure till all the THF had been removed. The brown oil was dissolved in EtOAc (20 mL) and washed with water (20 mL × 2), brine (40 mL) and dried over Na_2SO_4. The solvent was evaporated *in vacuo* to afford a brown resin. Column chromatography over silica gel (DCM:EtOAc, gradient 5:1 to 3:1) eluted the product as a yellow solid (0.367 g, 51 %).

^{1}H-NMR 400MHz ($CDCl_3$): δ 7.33 - 7.57 (m, 10H, Ar-H), 7.27 - 7.32 (m, 2H, Ar-H), 7.15 - 7.20 (m, 2H, Ar-H), 7.07 (d, *J* = 8.53 Hz, 2H, Ar-H), 6.95 (dd, *J* = 2.51, 8.53 Hz, 1H, Ar-H), 6.21 (s, 2H, Ar-H), 5.17 (s, 2H, CH_2), 5.13 (s, 4H, 2 × CH_2), 3.82 (s, 3H, OCH_3), 3.70 (s, 6H, OCH_3), 2.29 (s, 3H, CH_3) **^{13}C-NMR 100MHz** ($CDCl_3$): δ 158.1 (COBn), 152.9 (COBn), 152.8 (COBn), 137.9 (C_q), 137.3 (C_q), 136.3 (C_q), 133.9 (C_q), 131.9 (C_q), 131.3 (C_q), 128.8 (C_q), 128.2 (C_q), 128.1 (ArC), 127.7 (ArC), 127.3 (ArC), 127.2 (ArC), 127.1 (ArC), 124.2 (C=C), 114.3 (ArC), 111.9 (ArC), 110.3 (ArC), 108.2 (C=C), 102.7 (ArC), 102.0 (ArC), 70.5 (CH_2), 69.6 (CH_2), 60.4 (OCH_3), 55.6 (OCH_3), 47.4 (CH_2), 9.1 (CH_3) **IR:** ν_{max} (KBr) cm^{-1}:3420.7, 2935.8, 1614.5, 1594.6, 1508.3, 1450.4, 1331.6, 1236.2, 1125.0, 998.4, 839.9 **HRMS** (EI): Found 622.2588 $(M+Na)^+$, $C_{25}H_{25}NNaO_5$ requires 622.2569; **M.P.**: 73-76 °C

8.4.55 1,4-Bis((5-(Benzyloxy)-2-(4-(benzyloxy)phenyl)-3-methyl-1*H*-indol-1-yl)methyl)benzene [289]

Indole [248] (1 g, 2.38 mmol) pre-dissolved in THF (10 mL) was added dropwise to a stirring mixture of NaH (10 eq., 571 mg, 23.8 mmol) in THF (10 mL) at 0 °C under N_2 atmosphere. The mixture was stirred for 10 min, at which point the α,α-dibromo-*p*-xylene [283] (0.5 eq., 310 mg, 1.19 mmol) was added and the mixture was stirred for 30 min at 0 °C. The reaction was refluxed for a further 30 min under N_2 atmosphere, the mixture was allowed to cool at which point water was added dropwise until the solution became clear. The solvent was evaporated under reduced pressure to obtain a brown oil. The resin was dissolved in DCM (50 mL) and the extract was washed with water (3 × 50 mL), brine (50 mL) and dried over Na_2SO_4. The solvent was evaporated under reduced pressure to obtain a brown oil. The material was purified *via* flash chromatography on silica gel (DCM:EtOAc, gradient 4:1 to 3:1) to afford the product as a yellow solid. (1.4 g, 63%)

^{1}H NMR ($CDCl_3$, 400 MHz) δ 8.01 - 8.16 (m, 4H, Ar-H), 7.30 - 7.52 (m, 22H, Ar-H), 7.02 - 7.13 (m, 4H, Ar-H), 6.85 - 6.94 (m, 2H, Ar-H), 6.74 - 6.84 (m, 2H, Ar-H), 5.99 - 6.10 (m, 4H, Ar-H), 5.15 (s, 4H, 2 × CH_2), 5.12 (s, 2H, CH_2), 5.09 (s, 2H, CH_2), 3.05 - 3.22 (m, 4H, 2 × CH_2), 1.61 (s, 6H, 2 × CH_3) **^{13}C NMR ($CDCl_3$, 100 MHz)** δ 160.1 (C-OBn), 151.8 (C-OBn), 145.8 (C_q), 136.5 (C_q), 136.0 (C_q), 133.3 (C_q), 129.4, 128.2, 128.1, 127.9, 127.7, 127.6, 127.2, 127.1, 127.1, 120.1, 114.4, 113.6, 108.9, 108.7, 70.0 (CH_2), 69.7 (CH_2), 23.9 (CH_3) **HRMS** (EI): Found 941.4326 $(M+H)^+$, $C_{66}H_{57}N_2O_4$ requires 941.4313 **IR :** ν_{max} (KBr) cm^{-1}: 3438.9 (br.), 3032.0, 2925.9, 2862.0, 1605.5, 1505.3, 1453.1, 1277.5, 1245.5, 1189.5, 1003.8, 839.9, 695.8 **MP :** 130-133 °C

8.4.56 1-Butyl-2-(4-hydroxyphenyl)-3-methyl-1*H*-indol-5-ol [292]

To a round bottomed flask was added indole compound [278] (200 mg, 0.476 mmol) and EtOAc (50 mL). To this was added a small spatula tipful of 10 % Pd/C (20 mg) and the mixture was placed under a hydrogen atmosphere for 1 week. The reaction mixture was then filtered through a bed of celite

and the solvent evaporated. Column chromatography over silica gel (DCM:EtOAc, gradient 4:1 to 2:1) to afford the product as a green solid (131 mg, 70 %).

^{1}H-NMR 400MHz ($CDCl_3$): δ ; 7.19 - 7.28 (m, 3H, Ar-H), 7.03 (s, 1H, Ar-H), 6.94 - 7.00 (m, 2H, Ar-H), 6.84 (d, *J* = 8.53 Hz, 1H, Ar-H), 5.76 (br. s., 1H, OH), 5.03 (br. s, 1H, OH), 3.98 (t, *J* = 7.28 Hz, 2H, CH_2), 2.18 (s, 3H, CH_3), 1.58 (quin, *J* = 7.28 Hz, 2H, CH_2), 1.16 (sxt, *J* = 7.50 Hz, 2H, CH_2), 0.80 (t, *J* = 7.50 Hz, 3H, CH_3) **^{13}C-NMR 100MHz** ($CDCl_3$): δ; 155.0 (ArC-OH), 148.5 (ArC-OH), 138.0 (C_q), 131.4 (ArC), 131.2 (C_q), 128.7 (C_q), 124.3 (C=C), 114.9 (ArC), 110.4 (ArC), 109.8 (ArC), 107.2 (C=C), 103.0 (ArC), 65.6 (CH_2), 43.2 (CH_2), 31.8 (CH_2), 19.6 (CH_2), 13.2 (CH_3), 8.9 (CH_3) **IR:** ν_{max} (KBr) cm^{-1}: 3337.8, 2958.7, 2930.3, 1614.7, 1508.3, 1464.2, 1361.8, 1207.2, 918.36, 830.24 **HRMS** (EI): Found 294.1494 (M-H), $C_{19}H_{20}NO_2$ requires 294.1500 **M.P.**: 71-74 °C

8.4.57 1-(4-Hydroxybenzyl)-2-(4-hydroxyphenyl)-3-methyl-1*H*-indol-5-ol [293]

To a round bottomed flask was added indole compound [285] (300 mg, 0.487 mmol) and EtOAc (50 mL). To this was added a small spatula tipful of $Pd(OH)_2/C$ (20 mg) and the mixture was placed under a hydrogen atmosphere for 1 h. The reaction mixture was then filtered through a bed of celite and the solvent evaporated. Column chromatography over silica gel (DCM:EtOAc, gradient 4:1 to 2:1) to afford the product as a green solid (137 mg, 82 %).

^{1}H-NMR 400MHz (DMSO-d_6): δ ; 9.65 (br. s., 1H, OH), 9.23 (br. s., 1H, OH), 8.67 (br. s., 1H, OH), 7.16 (d, *J* = 8.80 Hz, 2H, Ar-H), 7.07 (d, *J* = 8.80 Hz, 1H, Ar-H), 6.86 (d, *J* = 8.80 Hz, 2H, Ar-H), 6.80 (d, *J* = 2.20 Hz, 2H, Ar-H), 6.67 (d, *J* = 8.80 Hz, 2H, Ar-H), 6.53 - 6.60 (m, 2H, Ar-H), 5.06 (s, 2H, CH_2), 2.10 (s, 3H, CH_3) **^{13}C-NMR 100MHz** (DMSO-d_6): δ; 157.4 (COH), 156.5 (COH), 151.1 (COH), 138.3, 131.7, 131.0, 129.4, 129.2, 127.6, 122.5 (C=C), 115.6, 115.3, 111.5, 111.1, 106.6 (C=C), 102.8, 46.5 (CH_2), 9.7 (CH_3) **IR:** ν_{max} (KBr) cm^{-1}: 3336.87, 2976.2, 1613.9, 1513.3, 1466.7, 1353.2, 1207.1, 1171.7, 1099.4, 920.0, 839.1 **HRMS** (EI): Found 380.1064 $(M+Cl)^-$, $C_{22}H_{19}ClNO_3$ requires 380.1053 **M.P.**: 50-53 °C

8.4.58 1-(4-Fluorobenzyl)-2-(4-hydroxyphenyl)-3-methyl-1*H*-indol-5-ol [294]

To a round bottomed flask was added indole compound [286] (300 mg, 0.568 mmol) and EtOAc (50 mL). To this was added a small spatula tipful of $Pd(OH)_2/C$ (20 mg) and the mixture was placed under a hydrogen atmosphere for 1 h. The reaction mixture was then filtered through a bed of celite and the solvent evaporated. Column chromatography over silica gel (DCM:EtOAc, gradient 4:1 to 2:1) to afford the product as a green solid (154 mg, 78 %).

^{1}H-NMR 400MHz ($CDCl_3$): δ ; 7.18 (d, *J* = 8.03 Hz, 2H, Ar-H), 7.00 - 7.07 (m, 2H, Ar-H), 6.85 - 6.94 (m, 6H, Ar-H), 6.75 (d, *J* = 8.53 Hz, 1H, Ar-H), 5.15 (s, 2H, CH_2), 2.24 (s, 3H, CH_3) **^{13}C-NMR 100MHz** ($CDCl_3$): δ; 160.2 (OH), 155.0 (COH), 148.9, 138.1, 133.8, 131.6, 131.4, 129.1, 127.2, 127.1, 123.8 (C=C), 115.1, 114.9, 114.9, 110.9, 110.2, 107.9 (C=C), 103.1, 65.5, 46.5 (CH_2), 9.0 (CH_3) **IR:** ν_{max} (KBr) cm^{-1}: 3349.8, 2933.3, 1701.1, 1614.3, 1459.2, 1358.6, 1252.9, 912.0, 839.0 **HRMS** (EI): Found 346.1249 $(M-H)^-$, $C_{22}H_{17}FNO_2$ requires 346.1249 **M.P.**: 57-59 °C

8.4.59 1-(2-Hydroxyethyl)-2-(4-hydroxyphenyl)-3-methyl-1*H*-indol-5-ol [295]

To a round bottomed was added indole compound [281] (200 mg, 0.361 mmol) and EtOAc (50 mL). To this was added a small spatula tipful of $Pd(OH)_2/C$ (20 mg) and the mixture was placed under a hydrogen atmosphere for 1 h. The reaction mixture was then filtered through a bed of celite and the solvent evaporated. Column chromatography over silica gel (DCM:EtOAc, gradient 4:1 to 2:1) eluted the product as a green solid (72 mg, 71 %).

^{1}H-NMR 600MHz (DMSO-d_6): δ 9.61 (br. s, 2H, OH), 8.62 (br. s, 1H, OH), 7.20 (d, *J* = 8.07 Hz, 3H, Ar-H), 6.86 (d, *J* = 8.80 Hz, 2H, Ar-H), 6.73 - 6.77 (m, 1H, Ar-H), 6.59 - 6.63 (m, 1H, Ar-H), 4.72 (t, *J* = 5.14 Hz, 2H, CH_2), 3.93 (t, *J* = 6.60 Hz, 2H, CH_2), 2.01 (s, 3H, CH_3) **^{13}C-NMR 150MHz** (DMSO-d_6): δ 156.5 (COH), 153.1 (COH), 150.6 (COH), 145.0 (C_q), 137.6 (C_q), 132.1 (C_q), 131.6 (ArC), 128.3 (C=C), 121.9 (ArC), 114.4 (ArC), 110.8 (ArC), 105.6 (C=C), 102.5 (ArC), 101.6 (ArC), 59.7 (CH_2), 45.7 (CH_2), 9.47 (CH_3) **IR:** ν_{max} (KBr) cm^{-1}: 3271.7, 2920.3, 1614.7, 1468.8, 1367.5, 1260.8, 1233.0, 1167.6, 1021.4, 918.6, 834.8 **HRMS** (EI): Found 284.1288 $(M+H)^+$, $C_{17}H_{18}NO_3$ requires 284.1281 **M.P.**: 122-124 °C

8.4.60 1-(3,4,5-Trimethoxybenzyl)-2-(4-hydroxyphenyl)-3-methyl-1H-indol-5-ol [296]

To a round bottomed flask was added indole compound [288] (200 mg, 0.333 mmol) and EtOAc (50 mL). To this was added a small spatula tipful of $Pd(OH)_2/C$ (20 mg) and the mixture was placed under a hydrogen atmosphere for 1 h. The reaction mixture was then filtered through a bed of celite and the solvent evaporated. Column chromatography over silica gel (DCM:MeOH, gradient 50:1 to 40:1) eluted the product as a green solid (123 mg, 88 %).

^{1}H-NMR 600MHz (DMSO-d_6): δ 9.68 (br. s., 1H, OH), 8.69 (br. s., 1H, OH), 7.18 - 7.27 (m, 3H, Ar-H), 6.90 (d, *J* = 8.28 Hz, 2H, Ar-H), 6.81 (d, *J* = 2.26 Hz, 1H, Ar-H), 6.62 (dd, *J* = 2.07, 8.47 Hz, 1H, Ar-H), 6.19 (s, 2H, Ar-H), 5.11 (s, 2H, CH_2), 3.52 - 3.62 (m, 9H, OCH_3), 2.12 (s, 3H, CH_3) **^{13}C-NMR 150MHz** (DMSO- d_6): δ 157.2 (COH), 152.6 (COH), 150.8 (C_q), 138.0 (C_q), 136.2 (C_q), 134.2 (C_q), 131.5 (ArC), 130.9 (C_q), 129.2 (ArC), 122.2 (C=C), 115.4 (ArC), 111.3 (ArC), 110.8 (ArC), 106.7 (C=C), 103.8 (ArC), 102.5 (ArC), 59.8 (OCH_3), 55.6 (OCH_3), 46.6 (CH_2), 9.4 (CH_3) **IR:** ν_{max} (KBr) cm^{-1}: 3271.7, 2920.3, 1614.7, 1468.8, 1367.5, 1260.8, 1233.0, 1167.6, 1021.4, 918.6, 834.8 **HRMS** (EI): Found 442.1642 $(M+Na)^+$, $C_{25}H_{25}NNaO_5$ requires 442.1630; **M.P.**: 146-149 °C

8.4.61 1,1'-(1,4-Phenylenebis(methylene))bis(2-(4-hydroxyphenyl)-3-methyl-1*H*-indol-5-ol) [297]

The di-indole [289] (200 mg) was dissolved in MeOH:EtOAc (1:4) (20 mL) and transferred to a 3-neck flask. To the flask was added a small spatula tipful of $Pd(OH)_2$ (20 mg) and the mixture was placed under a H_2 atmosphere. The reaction was monitored *via* TLC until the starting material had disappeared (30 min). The reaction mixture was filtered through celite and the solvent was evaporated under reduced pressure to obtain a brown oil. The material was purified *via* flash chromatography on silica gel (DCM:EtOAc, gradient 2:1 to 1:1) to afford the product as a yellow solid. (87 mg, 71%)

^{1}H NMR (DMSO-d_6, 400 MHz) δ 9.99 (br. s, 2H, OH), 9.55 (br. s, 1H, OH), 9.39 (br. s, 1H, OH), 7.89 - 8.02 (m, 4H, Ar-H), 7.04 - 7.12 (m, 2H, Ar-H), 6.80 - 6.90 (m, 4H, Ar-H), 6.67 - 6.70 (m, 1H, Ar-H), 6.57 - 6.63 (m, 2H, Ar-H), 6.47 - 6.52 (m, 1H, Ar-H), 6.03 - 6.21 (m, 4H, Ar-H), 3.08 - 3.22 (m, 4H, 2 × CH_2), 1.46 (s, 6H, 2 × CH_3) **^{13}C NMR (DMSO-d_6, 151 MHz)** δ 159.2 (C-OH), 159.1 (C-OH), 155.2 (C-OH), 155.1 (C-OH), 146.7, 146.3, 146.0, 145.6, 134.4, 134.4, 129.7, 129.5, 128.0, 127.7, 124.6, 124.5, 119.8, 119.7, 115.4, 115.3, 114.1, 109.8, 109.4, 57.8, 57.6, 42.9 (CH_2), 42.8 (CH_2), 24.3 (CH_3), 23.8 (CH_3) **HRMS** (EI): Found 581.2431 $(M+H)^+$, $C_{38}H_{33}N_2O_4$ requires 581.2435 **IR :** ν_{max} (KBr) cm^{-1}: 3422.9 (br.), 3033.1, 2928.9, 2841.0, 1605.5, 150`8.3, 1453.1, 1277.5, 1245.5, 1189.5, 1003.8, 839.9, 695.8 **MP :** 111-113 °C

8.4.62 3-(4-(Benzyloxy)benzyl)-5-(benzyloxy)-2-(4-(benzyloxy)phenyl)-3-methyl-3*H*-indole [298]

Column chromatography of [285] afforded a byproduct [298] as a yellow solid (439 mg, 30 %)

^{1}H-NMR 400MHz ($CDCl_3$): δ 8.18 (d, *J* = 8.53 Hz, 2H, Ar-H), 7.26 - 7.57 (m, 16H, Ar-H), 7.14 (d, *J* = 9.03 Hz, 2H, Ar-H), 6.88 - 7.00 (m, 2H, Ar-H), 6.46 - 6.61 (m, 4H, Ar-H), 5.07 - 5.24 (m, 4H, 2 × CH_2), 4.91 (s, 2H, CH_2), 3.21 - 3.39 (m, 2H, CH_2), 1.72 (s, 3H, CH_3) **^{13}C-NMR 100MHz** ($CDCl_3$): δ 179.0 (C=N), 160.4 (COBn), 157.3 (COBn), 156.9 (COBn), 146.4, 137.0, 136.5, 130.3, 129.8, 128.6, 128.6, 128.4, 128.4, 128.1, 128.0, 127.8, 127.5, 127.5, 127.4, 120.7, 114.8, 114.0, 113.8, 109.4, 70.5 (CH_2), 70.1 (CH_2), 69.7 (CH_2), 43.9 (CH_2), 24.2 (CH_3) **IR:** ν_{max} (KBr) cm^{-1}: 3430.0, 3042.3, 2929.1, 2863.7, 1604.8, 1506.2, 1454.1, 1246.5, 1023.5, 835.9, 665.8 **HRMS** (EI): Found 458.1747 $(M+Na)^+$, $C_{29}H_{25}NNaO_3$ requires 458.1732 **M.P.**: 67-69 °C

8.4.63 3-(4-Fluorobenzyl)-5-(benzyloxy)-2-(4-(benzyloxy)phenyl)-3-methyl-3*H*-indole [299]

Column chromatography of [286] afforded a byproduct [299] as a yellow solid (288 mg, 23 %)

^{1}H-NMR 400MHz δ 8.15 (d, *J* = 8.80 Hz, 2H, Ar-H), 7.26 - 7.63 (m, 11H, Ar-H), 7.07 - 7.21 (m, 2H, Ar-H), 6.86 - 7.01 (m, 2H, Ar-H), 6.61 (t, *J* = 8.80 Hz, 2H, Ar-H), 6.47 (dd, *J* = 5.50, 8.44 Hz, 2H, Ar-H), 5.03 - 5.26 (m, 4H, 2 × CH_2), 3.39 (d, *J* = 13.94 Hz, 2H, 0.5 × CH_2), 3.27 (d, *J* = 13.94 Hz, 2H, 0.5 × CH_2), 1.56 - 1.78 (m, 3H, CH_3) **^{13}C-NMR 100MHz** ($CDCl_3$): δ; 178.6 (C=N), 160.7 (COH), 157.0 (COH), 146.1, 137.0, 136.5, 131.6, 130.6, 130.6, 129.7, 128.7, 128.6, 128.2, 128.0, 127.6, 127.5, 120.8, 114.9, 114.3, 114.2, 114.1, 109.3, 70.5 (CH_2), 70.1 (CH_2), 57.8 (C_q), 44.0 (CH_2), 24.3 (CH_3) **IR:** ν_{max} (KBr) cm^{-1}: 3064.9, 3034.1, 2928.6, 2868.1, 1603.9, 1508.4, 1454.3, 1454.3, 1250.8, 1221.3, 1171.1, 1017.4, 835.3, 738.1, 697.3 **HRMS** (EI): Found 528.2341$(M+H)^+$, $C_{36}H_{31}FNO_2$ requires 528.2333 **M.P.**: 80-82 °C

8.4.64 3-(3,4,5-Trimethoxybenzyl)-5-(benzyloxy)-2-(4-(benzyloxy)phenyl)-3-methyl-3*H*-indole [300]

Column chromatography (DCM:EtOAc, gradient 5:1 to 3:1) of [288] afforded a byproduct [300] as a yellow solid (122 mg, 17 %)

^{1}H-NMR 400MHz ($CDCl_3$): δ 8.13 (d, *J* = 8.53 Hz, 2H, Ar-H), 7.34 - 7.54 (m, 13H, Ar-H), 7.11 (d, *J* = 8.53 Hz, 2H, Ar-H), 7.04 (d, *J* = 2.01 Hz, 1H, Ar-H), 6.95 (dd, *J* = 2.26, 8.28 Hz, 1H, Ar-H), 5.70 (s, 2H, CH_2), 5.19 (s, 2H, CH_2), 5.13 (s, 2H, CH_2), 3.82 (s, 3H, OCH_3) 3.70 (s, 6H, 2 × OCH_3), 3.35 (m, 2H, CH_2), 1.76 (s, 3H, CH_3) **^{13}C-NMR 100MHz** ($CDCl_3$): δ 178.3 (C=N), 156.9 (COBn), 151.5 (COBn), 146.2 (C_q), 136.5 (C_q), 136.0 (C_q), 135.9 (C_q), 130.9 (C_q), 129.4 (ArC), 128.3 (ArC), 128.2 (ArC), 127.8 (ArC), 127.7 (ArC), 127.1 (ArC), 127.0 (ArC), 120.4 (ArC), 114.4 (ArC), 113.0 (ArC), 109.0 (ArC), 105.6 (ArC), 70.2 (CH_2), 69.6 (CH_2), 60.3 (OCH_3), 58.4 (C_q), 55.1 (OCH_3), 44.7 (CH_2), 24.0 (CH_3) **IR:** ν_{max} (KBr) cm^{-1}: 3032.2, 2935.5, 2835.6, 1591.7, 1507.6, 1463.9, 1245.2, 1125.0, 1012.6, 835.2, 736.2 **HRMS** (EI): Found 622.2537 $(M+Na)^+$, $C_{25}H_{25}NNaO_5$ requires 622.2569; **M.P.**: 84-86 °C

8.4.65 5-(Benzyloxy)-2-(4-(benzyloxy)phenyl)-1-(4-(bromomethyl)benzyl)-3-methyl-1*H*-indole [301]

Column chromatography of [289] afforded a byproduct [301] as a yellow solid (420 mg, 22%)

^{1}H NMR ($CDCl_3$, 400 MHz) δ 7.33 - 7.60 (m, 10H, Ar-H), 7.23 - 7.32 (m, 4H, Ar-H), 7.19 (s, 1H, Ar-H), 7.02 – 7.08 (m, 3H, Ar-H), 6.89 - 6.99 (m, 3H, Ar-H), 5.21 (s, 2H, CH_2), 5.17 (s, 2H, CH_2), 5.12 (s, 2H, CH_2), 4.47 (s, 2H, CH_2), 2.25 - 2.33 (m, 3H, CH_3) **^{13}C NMR ($CDCl_3$, 100 MHz)** δ 158.1 (C-OBn), 152.9 (C-OBn), 138.6 (C_q), 137.9 (C_q), 137.3 (C_q), 136.3 (C_q), 136.0 (C_q), 131.6, 131.2, 128.9, 128.7, 128.2, 128.1, 127.7, 127.3, 127.2, 127.1, 126.0, 124.0 (C=C), 114.3, 111.9, 110.3, 108.2 (C=C), 102.0, 70.5 (CH_2), 69.6 (CH_2), 46.9 (CH_2), 32.9 (CH_2), 9.1 (CH_3) **HRMS** (EI): Found 602.1680 $(M+H)^+$, $C_{37}H_{33}BrNO_2$

requires 602.1689 **IR :** ν_{max} (KBr) cm^{-1}: 3438.1 (br.), 3029.2, 2996.6, 2862.0, 2360.0, 2346.3, 1607.7, 1506.3, 1479.7, 1240.2, 1179.1, 1016.6, 1003.0, 698.1 **MP :** 87-88 °C

8.4.66 (4-(Benzyloxy)phenyl)methanol [303]

$NaBH_4$ (0.53 g, 14.13 mmol) was added to a solution of 4-benzyloxybenzaldehyde [302] (3 g, 14.13 mmol) in 50 ml methanol. After stirring for 1 hour, 1 M HCl was added dropwise to the reaction mixture till the $NaBH_4$ was neutralised. The reaction mixture was evaporated under reduced pressure to remove the MeOH and the resulting solution was redissolved in EtOAc (50 mL). The organic layer was washed with water (30 mL), brine (30 mL) and dried over Na_2SO_4. The solvent was evaporated to dryness to afford the product as a white solid with did not require further purfication. (2.86 g, 95 %).

^{1}H-NMR 400MHz ($CDCl_3$): δ 7.39 - 7.50 (m, 4H, Ar-H), 7.37 (d, *J* = 7.03 Hz, 1H, Ar-H), 7.32 (d, *J* = 8.03 Hz, 2H, Ar-H), 7.00 (d, *J* = 8.53 Hz, 2H, Ar-H), 5.10 (s, 2H, CH_2), 4.63 (s, 2H, CH_2), 1.80 (br. s., 1H, OH) **^{13}C-NMR 100MHz** ($CDCl_3$): δ 157.9 (COH), 136.5 (C_q), 132.9 (C_q), 128.3 (ArC), 128.2 (ArC), 127.6 (ArC), 127.0 (ArC), 114.5 (ArC), 69.6 (CH_2), 64.6 (CH_2) **IR:** ν_{max} (KBr) cm^{-1}: 3391.0, 2866.3, 1610.2, 1512.7, 1453.9, 1453.9, 1382.3, 1245.5, 999.1, 811.7, 739.2, 695.9 **HRMS** (EI): Found 237.0882 $(M+Na)^+$, $C_{14}H_{14}NaO_2$ requires 237.0891 **M.P.**: 84-85 °C

8.4.67 (3,4,5-Trimethoxyphenyl)methanol [305]

$NaBH_4$ (0.636 g, 16.83 mmol) was added to a solution of 3,4,5-trimethoxybenzaldehyde [304] (3 g, 15.3 mmol) in 50 ml methanol. After stirring for 1 hour, 1 M HCl was added dropwise to the reaction mixture till the $NaBH_4$ was neutralised. The reaction mixture was evaporated under reduced pressure to remove the MeOH and the resulting solution was redissolved in EtOAc (50 mL). The organic layer was washed with water (30 mL), brine (30 mL) and dried over Na_2SO_4. The solvent was evaporated to dryness to afford the product as a white solid with did not require further purfication. (2.87 g, 98 %).

^{1}H-NMR 400MHz ($CDCl_3$): δ 6.57 (s, 2H, Ar-H), 4.59 (s, 2H, CH_2), 3.73 - 3.92 (m, 9H, 3 × OCH_3), 2.47 (br. s, 1H, OH) **^{13}C-NMR 100MHz** ($CDCl_3$): δ 152.8, 136.5, 103.2 (Ar-C), 64.8 (OCH_3), 60.4 (OCH_3), 55.5 (CH_2) **IR:** ν_{max} (KBr) cm^{-1}: 3422.3, 2940.4, 2839.0, 1593.2, 1507.5, 1459.0, 1421.2, 1331.6, 1236.4, 1125.0, 1006.4, 828.6 **HRMS** (EI): Found 221.0781 $(M+Na)^+$, $C_{10}H_{14}NaO_4$ requires 221.0790; **M.P.**: 36-38 °C

8.5 Synthesis of the acrylic acid analogues

8.5.1 General procedure for reflux syntheses of Perkin products

A mixture of the necessary benzaldehyde (1eq.), the necessary phenylacetic acid (700 mg, 1eq.), acetic anhydride (2 mL) and triethylamine (1 mL) were heated to reflux of 3 h. After acidification with concentrated hydrochloric acid (5 mL), the resulting solid was filtered off and recrystallised to yield an appropriate acrylic yields

8.5.2 General procedure for microwave syntheses of Perkin products

A mixture of the necessary benzaldehyde (1 eq.), the necessary phenylacetic acid (700 mg, 1 eq.), acetic anhydride (2 mL) and triethylamine (1 mL) were reacted in the microwave reactor at a 120 °C and for 30 min. After acidification with concentrated hydrochloric acid (~ 5 mL), the resulting solid was filtered off and recrystallised to yield an appropriate acrylic yields.

8.5.3 (*E*)-3-(3-Hydroxy-4-methoxyphenyl)-2-(3,4,5-trimethoxyphenyl)acrylic acid [150][496]

Reflux

As per general method 8.5.1, 3-hydroxy-4-methoxybenzaldehyde [308] (470 mg, 3.09 mmol), 3,4,5-trimethoxyphenylacetic acid [307] (700 mg, 3.09 mmol) were reacted. Recrystallisation from methanol afforded the acrylic acid as fine yellow soild (578 mg, 51 %)

Microwave

As per general method 8.5.2, 3-hydroxy-4-methoxybenzaldehyde [308] (470 mg, 3.09 mmol), 3,4,5-trimethoxyphenylacetic acid [307] (700 mg, 3.09 mmol) were reacted. Recrystallisation from methanol afforded the acrylic acid as fine yellow solid (710 mg, 64 %)

^{1}H-NMR 400MHz (DMSO-d_6): δ 12.45(br s, 1H, COOH), 8.98(br s, 1H, OH), 7.57(s, 1H, C=CH), 6.81 (d, 1H, J= 8.5 Hz, Ar-H), 6.60 (d, 1H, J= 8.5 Hz, Ar-H), 6.53 (s, 1H, Ar-H), 6.44 (s, 2H, Ar-H), 3.73 (s, 3H, OCH_3), 3.71 (s, 3H, OCH_3), 3.69 (s, 6H, OCH_3) **^{13}C-NMR 100MHz** (DMSO-d_6): δ 55.45 (OCH_3), 55.91 (OCH_3), 60.12 (OCH_3), 106.65, 111.49, 117.19, 122.99, 127.02, 130.31, 132.18, 136.90, 139.13, 145.84, 148.89, 153.09, 168.61 (COOH) **IR:** ν_{max} (KBr) cm^{-1}: 3423.9(w), 2939.8, 1671.3, 1585.2, 1509.6, 1455.3, 1411.1, 1268.3, 1239.3, 1126.2 **HRMS (EI):** Found 383.1103 $(M+Na)^+$, $C_{19}H_{20}O_7Na$ requires 383.1107. **M.P.:** 237-239 °C

8.5.4 (*E*)-2-(3,4,5-trimethoxyphenyl)-3-(4-methoxyphenyl)acrylic acid [310][564]

Reflux

As per general method 8.5.1, anisaldehyde (700 mg, 5.1 mmol), 3,4,5-trimethoxyphenylacetic acid (1.153 mg, 5.1 mmol) were reacted. Recrystallisation from methanol afforded the acrylic acid as fine yellow solid (710 mg, 40 %)

Microwave

As per general method 8.5.2, anisaldehyde (374 mg, 0.36 ml, 3.09 mmol), 3,4,5-trimethoxyphenylacetic acid (700 mg, 3.09 mmol) were reacted. Recrystallisation from methanol afforded the acrylic acid as fine yellow solid (488 mg, 45 %)

^{1}H-NMR 400MHz (DMSO-d_6): δ 12.48 (br s, 1H, COOH), 7.68 (s, 1H, C=CH), 7.06 (d, 2H, J=9Hz, Ar-H), 6.82 (d, 2H, J=9Hz, Ar-H), 6.46 (s, 2H, Ar-H), 3.72 (s, 6H, OCH_3), 3.68 (s, 6H, OCH_3) **^{13}C-NMR 100MHz** (DMSO-d_6): δ 55.19 (OCH_3), 55.93 (OCH_3), 60.15 (OCH_3), 106.53, 113.88, 126.75, 130.52, 132.08, 132.27, 136.86, 138.72, 153.96, 160.01, 168.51 (COOH) **IR:** ν_{max} (KBr) cm^{-1}: 2994, 2942, 2630, 1664, 1604, 1582, 1508, 1464, 1414, 1253, 1242, 1180, 1127, 1029, 1008, 830 **HRMS** (EI): Found 345.1246 $(M+H)^+$, $C_{19}H_{21}O_6$ requires 344.1260. **M.P.**: 212 °C

8.5.5 (*E*)-3-(Benzo[d][1,3]dioxol-5-yl)-2-(4-methoxyphenyl)acrylic acid [311][550]

Reflux

As per general method 8.5.1, piperonal (700 mg, 4.7 mmol), 4-methoxyphenylacetic acid (781 mg, 4.7 mmol) were reacted. Recrystallisation from methanol afforded the acrylic acid as fine brown solid (542 mg, 39 %)

Microwave

As per general method 8.5.2, piperonal (463 mg, 3.09 mmol), 4-methoxyphenylacetic acid (513 mg, 3.09 mmol) were reacted. Recrystallisation from methanol afforded the acrylic acid as fine brown solid (440 mg, 47 %)

^{1}H-NMR 400MHz (DMSO-d_6): δ 12.49 (br s, 1H, COOH), 7.65 (s, 1H, C=CH), 7.08 (d, 2H, J=8.5Hz, Ar-H), 6.96 (d, 2H, J=8.5Hz, Ar-H), 6.82 (m, 2H, Ar-H), 6.39 (s, 1H, Ar-H), 5.97 (s, 2H, O-CH_2-O), 3.81 (s, 3H, OCH_3) **^{13}C-NMR 100MHz** (DMSO-d_6): δ 55.06 (OCH_3), 101.36 (O-CH_2-O), 108.28, 108.77, 114.07, 126.39, 128.42, 128.65, 130.68, 130.79, 138.59, 147.08, 148.98, 158.63, 168.73 (COOH) **IR:** ν_{max} (KBr) cm^{-1}: 3436.26, 3937.78, 1666.24, 1611.23, 1506.29, 1482.99, 1424.59, 1348.6, 1288.4, 1272.55, 1240.78, 1179.56, 1030.93, 921.74 **HRMS** (EI): Found 321.0742 $(M+Na)^+$, $C_{17}H_{14}O_5Na$ requires 321.0739. **M.P.**: 232-233 °C

8.5.6 (*E*)-3-(4-Methoxy-3-nitrophenyl)-2-(3,4,5-trimethoxyphenyl)acrylic acid [312][550]

Reflux

As per general method 8.5.1, 3-nitro-4-methoxybenzaldehyde (700 mg, 4mmol), 3,4,5-trimethoxyphenylacetic acid (900 mg, 4 mmol) were reacted. Recrystallisation from methanol afforded the acrylic acid as fine yellow solid (781 mg, 50 %)

Microwave

As per general method 8.5.2, 3-nitro-4-methoxybenzaldehyde (559 mg, 3.09 mmol), 3,4,5-trimethoxyphenylacetic acid (700 mg, 3.09 mmol) were reacted. Recrystallisation from methanol afforded the acrylic acid as fine yellow needles (790 mg, 65 %)

^{1}H-NMR 400MHz (DMSO-d_6): δ 12.767 (br s, 1H, COOH), 7.73 (s, 1H, C=CH), 7.56 (d, 1H, J=2Hz, Ar-H), 7.42 (dd, 1H, J=2Hz, Ar-H), 7.28 (d, 1H, J=9Hz, Ar-H), 6.49 (s, 2H, Ar-H), 3.90 (s, 3H, OCH_3), 3.71 (s, 9H, OCH_3) **^{13}C-NMR 100MHz** (DMSO-d_6): δ 56.04 (OCH_3), 56.86 (OCH_3), 60.15(OCH_3), 106.47, 114.26, 126.54, 127.80, 131.32, 133.39, 136.19, 136.37, 137.34, 138.74, 152.29, 153.42, 168.03 (COOH) **IR:** ν_{max} (KBr) cm^{-1}: 3435.90(w), 2941.68, 166.97, 1613.30, 1583.52, 1536.82, 1563.01, 1412.93, 1290.72, 1265.98, 1242.35, 1127.96, 1015.19, 997.24 **HRMS** (EI): Found 412.1010 $(M+Na)^+$, $C_{19}H_{19}NO_8Na$ requires 412.1008. **M.P.**: 220-222 °C

8.5.7 (*E*)-3-(3-Fluoro-4-methoxyphenyl)-2-(3,4,5-trimethoxyphenyl)acrylic acid [313][281]

Reflux

As per general method 8.5.1, 3-fluoro-4-methoxybenzaldehyde (700 mg, 4.5 mmol), 3,4,5-trimethoxyphenylacetic acid (900 mg, 4 mmol) were reacted. Recrystallisation from methanol afforded the acrylic acid as fine yellow solid (710 mg, 43 %)

Microwave

As per general method 8.5.2, 3-fluoro-4-methoxybenzaldehyde (476 mg, 3.09 mmol), 3,4,5-trimethoxyphenylacetic acid (700 mg, 3.09 mmol) were reacted. Recrystallisation from methanol afforded the acrylic acid as fine yellow solid (732 mg, 65 %)

^{1}H-NMR 400MHz (DMSO-d_6): δ 12.65 (br s, 1H, COOH), 7.67 (s, 1H, C=CH), 7.09 (t, 1H, J=9 Hz, Ar-H), 7.00 (d, 1H, J=7 Hz, Ar-H), 6.83 (dd, 1H, J=2 Hz, Ar-H), 6.47 (s, 2H, Ar-H), 3.81 (s, 3H, OCH_3), 3.72 (s, 9H, OCH_3) **^{13}C-NMR 100MHz** (DMSO-d_6): δ 56.46 (OCH_3), 60.65 (OCH_3), 65.40 (OCH_3), 106.92, 113.92,117.34, 117.54, 127.77, 128.28, 132.28, 132.44, 148.31, 153.75, 168.73 (COOH) **IR:** ν_{max} (KBr) cm^{-1}: 3448, 2998, 2942, 2626, 1667, 1616, 1516, 1506, 1414, 1278, 1257, 1129, 1024, 1003, 924, 818, 772. **HRMS** (EI): Found 363.1144 $(M+H)^+$, $C_{19}H_{20}O_6F$ requires 363.1166 **M.P.**: 203-205 °C

8.5.8 (*E*)-3-(3,4,5-Trimethoxyphenyl)-2-(3,5-dimethoxyphenyl)acrylic acid [314]

Reflux

As per general method 8.5.1, 3,4,5-trimethoxybenzaldehyde (700 mg, 3.57 mmol), 3,5-dimethoxyphenylacetic acid (700 mg, 3.57 mmol) were reacted. Recrystallisation from methanol afforded the acrylic acid as fine brown solid (340 mg, 25 %)

Microwave

As per general method 8.5.2, 3,4,5-trimethoxybenzaldehyde (606 mg, 3.09 mmol), 3,5-dimethoxyphenylacetic acid (606 mg, 3.09 mmol) were reacted. Recrystallisation from methanol afforded the acrylic acid as fine brown solid (411 mg, 35 %)

^{1}H-NMR 400MHz ($CDCl_3$): δ 7.83 (s, 1H, C=CH), 6.49 (d, 1H, 2.5Hz, Ar-H), 6.46-6.47 (m, 4H, Ar-H), 3.85 (s, 3H, OCH_3), 3.78 (s, 6H, OCH_3), 3.62 (s, 6H, OCH_3) **^{13}C-NMR 100MHz** ($CDCl_3$): δ 171.66 (COOH), 160.91, 152.20, 141.76, 139.00, 137.14, 129.80, 128.71, 107.93, 106.95, 99.94, 60.45 (OCH_3), 55.25(OCH_3), 55.01(OCH_3) **IR:** ν_{max} (KBr) cm^{-1}: 3439.53, 2938.98, 2633.47, 1683.93, 1590.82, 1502.72, 1419.53, 1251.12, 1157.00 **HRMS** (EI): Found 373.1329 $(M-H)^-$, $C_{20}H_{21}O_7$ requires 373.1366 **M.P.**: 234-236 °C

8.5.9 (*E*)-2,3-*bis*(3,4,5-Trimethoxyphenyl)acrylic acid [315]

Reflux

As per general method 8.5.1, 3,4,5-trimethoxybenzaldehyde (700 mg, 3.59 mmol), 3,4,5-trimethoxyphenylacetic acid (744 mg, 3.59 mmol) were reacted. Recrystallisation from methanol afforded the acrylic acid as fine yellow solid (484 mg, 33 %)

Microwave

As per general method 8.5.2, 3,4,5-trimethoxybenzaldehyde (606 mg, 3.09 mmol), 3,4,5-trimethoxyphenylacetic acid (700 mg, 3.09 mmol) were reacted. Recrystallisation from methanol afforded the acrylic acid as fine yellow solid (1.2 g, 96 %)

^{1}H-NMR 400MHz ($CDCl_3$): δ 7.85 (s, 1H, C=CH), 6.53 (s, 2H, Ar-H), 6.42 (s, 2H, Ar-H), 3.88 (s, 3H, OCH_3), 3.85 (s, 3H, OCH_3), 3.83 (s, 6H, 2 × OCH_3), 3.63 (s, 6H, 2 × OCH_3) **^{13}C-NMR 100MHz** (DMSO-d_6): δ 171.4 (COOH), 160.9, 153.1, 152.2, 141.7, 139.0, 137.1, 129.8, 128.7, 107.9, 106.9, 99.9, 60.5 (OCH_3), 60.4 (OCH_3), 55.2(O CH_3), 55.0 (OCH_3) **IR:** ν_{max} (KBr) cm^{-1}: 3440.90, 2938.31, 1668.56, 1580.98, 1505.11, 1413.46, 1272.44, 1240.40 **HRMS** (EI): Found 405.1452 $(M+H)^+$, $C_{21}H_{25}O_8$ requires 405.1471. **M.P.**: 169-172 °C

8.5.10 (*E*)-3-(3-Hydroxy-4-methoxyphenyl)-2-(3,5-dimethoxyphenyl)acrylic acid [316][508]

Reflux

As per general method 8.5.1, 3-hydroxy-4-methoxybenzaldehyde (548 mg, 3.6 mmol), 3,5-dimethoxyphenylacetic acid (710 mg, 3.6 mmol) were reacted. Recrystallisation from methanol afforded the acrylic acid as fine brown solid (90 mg, 7 %)

^{1}H-NMR 400MHz ($CDCl_3$): δ 7.82 (s, 1H, C=CH), 7.29 (s, 1H, Ar-H), 6.72 (s, 2H, Ar-H), 6.50 (s, 1H, Ar-H), 6.42 (s, 2H Ar-H), 5.48 (br s, 1H, OH), 3.89 (s, 3H, OCH_3), 3.79 (s, 6H, OCH_3) **^{13}C-NMR 100MHz** ($CDCl_3$): δ 55.38 (OCH_3), 55.88 (OCH_3), 100.44, 106.56, 107.24, 107.46, 100.18, 106.76, 124.46, 127.58, 129.31, 137.51, 142.15, 145.69, 147.94, 161.13, 172.47 (COOH) **IR:** ν_{max} (KBr) cm^{-1}: 3364.7, 2936.8, 2840.9, 2627.1, 1682.3, 1601.1, 1506.1, 1441.2, 1423.0, 1265.1, 1205.1, 1153.4, 1063.9, 1024.9, 800.7 **HRMS** (EI): Found 353.1001 $(M+Na)^+$, $C_{18}H_{18}O_6Na$ requires 353.1001. **M.P.**: 226-229 °C

8.5.11 (*E*)-3-(3,4-Dihydroxyphenyl)-2-(3,4,5-trimethoxyphenyl)acrylic acid [317][508]

Microwave

As per general method 8.5.2, 3,4-dihydroxybenzaldehyde (427 mg, 3.09 mmol), 3,4,5-trimethoxyphenylacetic acid (700 mg, 3.09 mmol) were reacted. Recrystallisation from methanol afforded the acrylic acid as fine yellow solid (390 mg, 36 %)

^{1}H-NMR 400MHz (DMSO-d_6): δ 12.44 (br s, 1H, COOH), 7.55 (s, 1H, C=CH), 6.61-6.48 (m, 3H, Ar-H), 6.43 (s, 2H, Ar-H), 3.69 (s, 9H, O CH_3) **^{13}C-NMR 100MHz** (DMSO-d_6): δ 168.71 (COOH), 153.04, 147.18, 144.79, 139.54, 136.83, 132.32, 129.24, 125.66, 123.45, 117.55, 115.22, 106.73, 60.12 (O CH_3), 55.91 (O CH_3) **IR:** ν_{max} (KBr) cm^{-1}: 3414.1, 2941.1, 1678.1, 1593.1, 1505.6, 1412.7, 1288.9, 1117.6, 986.4, 809.9 **HRMS** (EI): Found 369.0956 $(M+Na)^+$, $C_{18}H_{18}O_7Na$ requires 369.0950. **M.P.**: 189-193 °C

8.5.12 (*E*)-3-(3-Hydroxyphenyl)-2-(3,4,5-trimethoxyphenyl)acrylic acid [318]

Microwave

As per general method 8.5.2, 3-hydroxybenzaldehyde (377 mg, 3.09 mmol), 3,4,5-trimethoxyphenylacetic acid (700 mg, 3.09 mmol) were reacted. Recrystallisation from methanol afforded the acrylic acid as fine yellow soild (711 mg, 60 %)

^{1}H-NMR 400MHz (DMSO-d_6): δ 7.61 (s, 1H, C=CH), 7.05 (t, 1H, 8Hz, Ar-H), 6.67 (dd, 1H, 8Hz, 1Hz, Ar-H), 6.54-6.52 (m, 2H, Ar-H), 6.44 (s, 2H, Ar-H), 3.70 (s, 3H, O CH_3), 3.67 (s, 6H, O CH_3) **^{13}C-NMR 100MHz** (DMSO-d_6): δ 168.40 (COOH), 157.02, 152.93, 139.05, 136.96, 135.59, 132.96, 131.72, 129.19, 121.28, 116.85, 116.27, 106.74, 60.12 (O CH_3), 55.91 (O CH_3) **IR:** ν_{max} (KBr) cm^{-1}: 3362.7, 2941.0 2836.0, 2627.4, 1681.6, 1584.8, 1411.8, 1239.2, 1125.0, 997.3, 965.6, 688.2 **HRMS** (EI): Found 353.1003 $(M+Na)^+$, $C_{18}H_{18}O_6Na$ requires 353.1003. **M.P** 230-231 °C

8.5.13 (*E*)-2-(3,4,5-Trimethoxyphenyl)-3-(3,4-dimethoxyphenyl)acrylic acid [319]

Microwave

As per general method 8.5.2, 3,4-dimethoxybenzaldehyde (513 mg, 3.09 mmol), 3,4,5-trimethoxyphenylacetic acid (700 mg, 3.09 mmol) were reacted. Recrystallisation from methanol afforded the acrylic acid as fine yellow solid (532 mg, 45 %)

^{1}H-NMR 400MHz (DMSO-*d6*): δ 12.50 (br s, 1H, COOH), 7.67 (s, 1H, C=CH), 6.88 (s, 2H, Ar-H), 6.54 (s, 1H, Ar-H), 6.49 (s, 2H, Ar-H), 3.73 (s, 3H, O CH_3), 3.70 (s, 6H, O CH_3), 3.67 (s, 3H, O CH_3), 3.36 (s, 3H, O CH_3) **^{13}C-NMR 100MHz** (DMSO-d_6): δ 168.43 (COOH), 153.34, 149.81, 147.85, 139.08, 136.80, 132.52, 130.50, 126.79, 125.21, 112.25, 111.20, 106.64, 59.95 (O CH_3), 56.02 (O CH_3), 55.42 (O CH_3), 54.50 (O CH_3) **IR:** ν_{max} (KBr) cm^{-1}: 3003.3, 2941.7, 1664.2, 1583.9, 1413.1, 1266.2, 1241.7, 1126.8, 1023.8, 921.8, 816.8 **HRMS** (EI): Found 397.1269 $(M+Na)^+$, $C_{20}H_{22}O_7Na$ requires 397.1263. **M.P.**: 198-200 °C

8.5.14 (*E*)-3-(2,3,4-Trimethoxyphenyl)-2-(3,4,5-trimethoxyphenyl)acrylic acid [320]

Microwave

As per general method 8.5.2, 2,3,4-trimethoxybenzaldehyde (607 mg, 3.09 mmol), 3,4,5-trimethoxyphenylacetic acid (700 mg, 3.09 mmol) were reacted. Recrystallisation from methanol afforded the acrylic acid as fine yellow solid (374 mg, 30 %)

^{1}H-NMR 400MHz (DMSO-d_6): δ 7.91 (s, 1H, C=CH), 6.61 (d, 1H, 9Hz, Ar-H), 6.46 (m, 3H, Ar-H), 3.86 (s, 3H, O CH_3), 3.74 (s, 6H, OCH_3), 3.70 (s, 3H, O CH_3), 3.68 (s, 6H, OCH_3) **^{13}C-NMR 100MHz** (DMSO-d_6): δ 168.96 (COOH), 154.79, 153.48, 153.36, 141.88, 137.35, 133.34, 132.05, 124.97, 121.23, 108.20, 107.30, 61.95 (O CH_3), 60.88 (O CH_3), 60.58 (OCH_3), 56.40 (O CH_3), 56.31 (O CH_3) **IR:** ν_{max} (KBr) cm^{-1}: 3440.90, 2938.31, 1668.56, 1580.98, 1505.11, 1413.46, 1272.44, 1240.40 **HRMS** (EI): Found 427.1370 $(M+Na)^+$, $C_{21}H_{24}O_8Na$ requires 427.1369 **M.P.**: 222-225 °C

8.5.15 (*E*)-2-(3-Hydroxy-4-methoxyphenyl)-3-(3,4,5-trimethoxyphenyl)acrylic acid [321]

Microwave

As per general method 8.5.2, 3,4,5-trimethoxybenzaldehyde (323 mg, 1.64 mmol), 3-hydroxy-4-methoxyphenylacetic acid (300 mg, 1.64 mmol) were reacted. Recrystallisation from methanol afforded the acrylic acid as fine yellow solid (230 mg, 38 %)

^{1}H-NMR 400MHz ($CDCl_3$): δ 7.83 (s, 1H, C=CH), 6.93 (d, 1H, 8Hz, Ar-H), 6.89 (d, 1H, 2Hz, Ar-H), 6.79 (dd, 1H, 8Hz, 2Hz, Ar-H), 6.42 (s, 2H, Ar-H), 3.92 (s, 3H, O CH_3), 3.84 (s, 3H, O CH_3), 3.61 (s, 6H, O CH_3) **^{13}C-NMR 100MHz** ($CDCl_3$): δ 176.95 (COOH), 152.14 147.84, 145.95, 145.61, 141.66, 138.71, 136.91, 129.89, 129.14, 128.31, 121.14, 115.73, 110.63, 107.86, 60.44, 55.60, 55.20 **IR:** ν_{max} (KBr) cm^{-1}: 3401.6, 2939.0, 2838.2, 1683.2, 1580.5, 1508.6, 1419.7, 1334.5, 1270.1, 1126.7, 999.6 **HRMS** (EI): Found 383.1125 $(M+Na)^+$, $C_{19}H_{20}O_7Na$ requires 383.1107 **M.P.**: 237-239 °C

8.5.16 (*E*)-3-(4-Hydroxy-3,5-dimethoxyphenyl)-2-(3,4,5-trimethoxyphenyl)acrylic acid [322]

Microwave

As per general method 8.5.2, 3,5-dimethoxy-4-hydroxybenzaldehyde (350 mg, 1.91 mmol), 3,4,5-trimethoxyphenylacetic acid (433 mg, 1.91 mmol) were reacted. Recrystallisation from methanol afforded the acrylic acid as pale yellow solid (400 mg, 48 %)

^{1}H-NMR 400MHz ($CDCl_3$): δ 7.86 (s, 1H, C=CH), 6.52 (s, 2H, Ar-H), 6.44 (s, 2H, Ar-H), 3.86 (s, 3H, O CH_3), 3.83 (s, 6H, O CH_3), 3.59 (s, 6H, O CH_3) **^{13}C-NMR 100MHz** ($CDCl_3$): δ 171.94 (C=O CH_3), 168.05 (COOH), 153.40, 151.32, 141.59, 137.23, 131.51, 130.88, 130.35, 139.41, 107.34, 105.99, 60.34 (O CH_3), 55.77 (OCH_3), 55.37 (O CH_3), 19.97 (C=O CH_3) **IR:** ν_{max} (KBr) cm^{-1}: 3438.9, 2942.4, 1765.4,

1676.7, 1594.8, 1506.7, 1420.4, 1272.3, 1236.7, 1127.5, 999.8, 906.9 **HRMS** (EI): Found 455.1321 $(M+Na)^+$, $C_{22}H_{24}O_9Na$ requires 455.1318. **M.P.**: 212-214 °C

8.5.17 (E)-3-(3-Acetoxyphenyl)-2-(3,4,5-trimethoxyphenyl)acrylic acid [323]

Microwave

As per general method 8.5.2, vanillin (350 mg, 2.3 mmol), 3,4,5-trimethoxyphenylacetic acid (520 mg, 2.3 mmol) were reacted. Recrystallisation from methanol afforded the acrylic acid as fine yellow solid (515 mg, 56 %)

^{1}H-NMR 400MHz ($CDCl_3$): δ 7.88 (s, 1H, C=CH), 6.95 (d, 1H, 8Hz, Ar-H), 6.88 (dd, 1H, 18Hz, 2Hz, Ar-H), 6.65 (s, 2H, Ar-H), 6.50 (s, 2H, Ar-H), 3.88 (s, 3H, O CH_3), 3.81 (s, 6H, O CH_3), 2.30 (s, 3H, C=O CH_3) **^{13}C-NMR 100MHz** ($CDCl_3$): δ 171.72 (C=O CH_3), 153.36, 150.13, 141.07, 140.40, 137.21, 132.37, 130.80, 130.36, 124.46, 122.28, 113.19, 105.96, 60.38 (O CH_3), 55.72 (O CH_3), 54.88 (O CH_3), 20.18 (C=O CH_3) **IR:** ν_{max} (KBr) cm^{-1}: 3362.7, 2941.0 2836.0, 2627.4, 1681.6, 1584.8, 1411.8, 1239.2, 1125.0, 997.3, 965.6, 688.2 **HRMS** (EI): Found 395.1110 $(M+Na)^+$, $C_{20}H_{20}O_7Na$ requires 395.1107 **M.P.**: 176-180 °C

8.5.18 (E)-2-(3,4,5-Trimethoxyphenyl)-3-(naphthalen-5-yl)acrylic acid [324]

Microwave

As per general method 8.5.2, 1-napthaldehyde (483 mg, 0.420 mL, 3.09 mmol), 3,4,5-trimethoxyphenylacetic acid (700 mg, 2.3 mmol) were reacted. Recrystallisation from methanol afforded the acrylic acid as fine yellow solid (400 mg, 36 %)

^{1}H-NMR 400MHz ($CDCl_3$): δ 8.31 (s, 1H, C=CH), 8.04 (d, 1H, 8Hz, Ar-H), 7.94 (d, 1H, 8Hz, Ar-H), 7.84 (d, 1H, 8Hz, Ar-H), 7.57 (q(5), 2H, 8Hz, Ar-H), 7.32 (t, 1H, 8Hz, Ar-H), 7.11 (d, 1H, 8Hz, Ar-H), 6.36 (s, 2H, Ar-H), 3.59 (s, 3H, O CH_3), 3.45 (s, 6H, OCH_3) **^{13}C-NMR 100MHz** ($CDCl_3$): δ 168.10 (COOH), 152.22, 137.05, 136.75, 136.02, 132.88, 132.39, 131.08, 130.99, 128.47, 127.00, 126.71, 126.14, 125.19, 124.05, 107.44, 59.97 (O CH_3), 55.61 (O CH_3), 48.58 (OCH_3) **IR:** ν_{max} (KBr) cm^{-1}: 3435.50, 2937.78, 1664.26, 1581.88, 1504.78, 1454.14, 1411.09, 1287.35, 1239.16, 1127.39, 1005.19 **HRMS** (EI): Found 387.1216 $(M+Na)^+$, $C_{22}H_{20}O_5Na$ requires 387.1208. **M.P.**: 238-240 °C

8.5.19 (E)-2-(3,4,5-Trimethoxyphenyl)-3-(5-methylthiophen-2-yl)but-2-enoic acid [325]

Microwave

As per general method 8.5.2, 5-methyl-2-thiophenecarboxaldehyde (389 mg, 0.337 mL, 3.09 mmol), 3,4,5-trimethoxyphenylacetic acid (700 mg, 2.3 mmol) were reacted. Recrystallisation from methanol afforded the acrylic acid as a dark yellow solid (375 mg, 36 %)

^{1}H-NMR 400MHz (DMSO-d_6): δ 7.87 (s, 1H, C=CH), 7.24 (d, 1H, 3.6Hz, Thio-H), 6.74 (d, 1H, 3.6Hz, Thio-H), 6.47 (s, 2H, Ar-H), 3.72 (s, 9H, O CH_3), 2.31 (s, 3H, CH_3) **^{13}C-NMR 100MHz** (DMSO-d_6): δ 15.23 (CH_3), 55.93 (O CH_3), 60.20 (O CH_3), 106.94, 125.42, 128.27, 130.99, 133.25, 134.85, 136.05, 137.44, 153.36, 168.10 (C=O) **IR:** ν_{max} (KBr) cm^{-1}: 3426.13, 2998.75, 2537.61, 1662.03, 1581.35, 1412.40, 1283.72, 1128.23 **HRMS** (EI): Found 357.0763 $(M+Na)^+$, $C_{17}H_{18}O_5NaS$ requires 357.0773. **M.P.**: 212-217 °C

8.5.20 (E)-3-(Furan-3-yl)-2-(3,4,5-trimethoxyphenyl)acrylic acid [326]

Microwave

As per general method 8.5.2, 3-furaldehyde (296mg, 0.26ml, 3.09mmol), 3,4,5-trimethoxyphenylacetic acid (700mg, 2.3mmol) were reacted. Recrystallisation from methanol afforded the acrylic acid as a dark brown solid (460mg, 49%)

^{1}H-NMR 400MHz (DMSO-d_6): 7.90 (s, 1H, C=CH), 7.74 (s, 1H, C=CH), 7.29-7.25 (m , 1H, C=CH), 6.86 (m, 1H, C=CH), 6.38 (s, 2H, Ar-H), 3.92 (s, 3H, OCH_3), 3.81 (s, 6H, OCH_3) **^{13}C-NMR 100MHz** (DMSO-d_6): 168.3 (COOH), 153.0 ($COCH_3$), 143.7, 143.6, 139.0, 138.4, 138.0, 124.4, 108.2 (CCH_2), 105.1, 60.8 (OCH_3), 56.1 (OCH_3) **IR:** ν_{max} (KBr) cm^{-1}: 3447.5, 2938.9, 2627.6, 1674.9, 1582.2, 1504.8, 1909.5, 1504.8, 1909.5, 1236.5, 1127.5, 1007.9, 803.2 **HRMS** (EI): Found 327.0839 $(M+Na)^+$, $C_{16}H_{16}O_6Na$ requires 327.0845 **M.P.**: 188-191 °C

8.5.21 2-(3,5-Dimethoxyphenyl)acetic acid [328]

A concentrated solution of hydrochloric acid (50 mL) was added to the benzylic cyanide [334] (3.135 g, 17.6 mmol). After 2.5 h at reflux, water (50 mL) was added and the reaction mixture was allowed to cool to room temperature. The aqueous phase was extracted with dichloromethane (50 mL × 3), brine (50 mL), dried over sodium sulphate and evaporated to dryness *in vacuo* to yield product. The material was purified *via* flash chromatography on silica gel (*n*-Hexane:EtOAc, 1:1) to afford the product as a white solid. (2.14 g, 61 %)

^{1}H-NMR 400MHz ($CDCl_3$): 6.46 (s, 2H, Ar-H), 6.41 (s, 1H, Ar-H), 3.81 (s, 6H, O CH_3), 3.61 (s, 2H, CH_2) **^{13}C-NMR 100MHz** ($CDCl_3$): 177.68 (COOH), 160.89, 135.27, 107.48, 99.43, 55.35 (O CH_3), 41.30 (CH_2) **IR:** ν_{max} (KBr) cm^{-1}: 2910.72, 1702.38, 1606.56, 1207.33, 1150.42 **HRMS** (EI): Found 197.0711 $(M+H)^+$, $C_{10}H_{13}O_4$ requires 197.0736. **M.P.**: 101-103 °C

8.5.22 2-(3-Hydroxy-4-methoxyphenyl)acetic acid [329]

A concentrated solution of hydrochloric acid (100 mL) was added to the deprotected benzylic cyanide [339] (3 g, 18.38 mmol). After 2.5 h at reflux, water (50 mL) was added and the reaction mixture was allowed to cool to room temperature. The aqueous phase was extracted with dichloromethane (50 mL × 3), brine (50 mL), dried over sodium sulphate and evaporated to dryness *in vacuo* to yield product. The material was purified *via* flash chromatography on silica gel (*n*-Hexane:EtOAc, 1:1) to afford the product as a white solid. (700 mg, 21 %)

^{1}H-NMR 400MHz ($CDCl_3$): 6.86 (d, 1H, 8.5Hz, Ar-H), 6.78 (d, 1H, 2Hz, Ar-H), 6.73 (dd, 1H, 8.5Hz, 2Hz, Ar-H), 3.84 (s, 3H, O CH_3), 3.47 (s, 2H, CH_2) **^{13}C-NMR 100MHz** ($CDCl_3$): 174.90 (COOH), 147.10 (CO CH_3), 146.51 (COH), 127.82, 120.56, 116.36, 111.80, 55.46 (O CH_3), 40.34 (CH_2) **IR:** ν_{max} (KBr) cm^{-1}: 3393.6, 3029.6, 294.8, 1695.2, 1515.0, 1406.9, 1277.2, 1131.5, 1026.5, 776.0 **HRMS** (EI): Found 181.0567 $(M-H)^-$, $C_9H_9O_4$ requires 181.0579. **M.P.**: 130-131 °C

8.5.23 3-(Benzyloxy)-4-methoxybenzaldehyde [330]

To a solution of KOH (1.3 g, 20 mmol) in ethanol (12 mL) was added 3-hydroxy-4-methoxybenzaldehyde [335] (2 g, 10 mmol) and benzyl bromide (4.4 g, 10 mmol). The solution was heated under reflux for 6 h and then evaporated to dryness *in vacuo* to yield product. The material was purified *via* flash chromatography on silica gel (*n*-Hexane:EtOAc, 4:1) to afford the product as a cream solid. (1.3 g, 53 %)

^{1}H-NMR 400MHz ($CDCl_3$): 9.834 (s, 1H, CHO), 7.496-7.285 (m, 7H, Ar-H), 7.01 (d, 1H, J=8Hz, Ar-H), 5.20 (s, 2H, CH_2), 3.978 (s, 3H, OCH_3) **^{13}C-NMR 100MHz** ($CDCl_3$): 190.58 (CHO), 155.05, 148.70,

136.30, 129.98, 128.65, 128.15, 127.51, 126.95, 111.30, 110.78, 70.83 (CH_2), 56.21 (OCH_3) **IR:** ν_{max} (KBr) cm^{-1}: 2910.72, 1702.38, 1606.56, 1207.33, 1150.42 **HRMS** (EI): Found 265.0831 $(M+Na)^+$, $C_{15}H_{14}O_3Na$ requires 265.0841. **M.P.**: 61-64 °C

8.5.24 (3,5-Dimethoxyphenyl)methanol [332]

$LiAlH_4$ (2.33 g, 61.42 mmol) was added to a solution of 3,5-dimethoxybenzaldehyde [331] (5.6 g, 30.7 mmol) in 100 mL of THF. After stirring for 3 h, acetic acid was added (1 mL). To this $NaHCO_3$ (10 g) in 50 mL of water was added to neutralize the residual aqueous extract. The resulting mixture was filtered through celite. It was extractred with ethyl acetate (100 mL × 3), brine (100 mL), dried over sodium sulphate and evaporated to dryness *in vacuo* to yield product as a white solid. The material did not require further purification. (5.05 g, 98 %)

^{1}H-NMR 400MHz ($CDCl_3$):6.52 (s, 2H, Ar-H), 6.38 (s, 1H, Ar-H), 4.61 (s, 2H, CH_2), 3.79 (s, 6H, 2 × OCH_3) **^{13}C-NMR 100MHz** ($CDCl_3$): 160.46, 142.98, 104.08, 99.11, 64.76 (CH_2OH), 54.88 (O CH_3) **IR:** ν_{max} (KBr) cm^{-1}: 3343.1, 2933.4, 1678.0, 1598.1, 1504.3, 1456.1, 1383.3, 1005.6, 806.9, 697.1, 640.5 **HRMS** (EI): Found 169.0775 $(M+H)^+$, $C_9H_{13}O_3$ requires 169.0786. **M.P.**: 63-65 °C

8.5.25 1-(Bromomethyl)-3,5-dimethoxybenzene [333]

A solution of the benzylic alcohol [332] (1.8 g, 10.62mmol), in DCM (30 mL), was cooled to 0 °C at which time PBr_3 (1 M in DCM) (1 mL, 10.62 mmol) was added. After 1 h at room temperature saturated $NaHCO_3$ was added dropwise and the aqueous layer was extracted with dichloromethane (50 mL × 3). It was then extraxtred with ethyl acetate (50 mL × 3), brine (50 mL), dried over sodium sulphate and evaporated to dryness *in vacuo* to yield product as a white solid. The material did not require further purification. (1.97 g, 80 %)

^{1}H-NMR 400MHz ($CDCl_3$): 6.56 (d, 2H, *J*= 2 Hz, Ar-H), 6.41 (t, 1H, *J*= 2 Hz, Ar-H), 4.42 (s, 2H, CH_2), 3.82 (s, 6H, OCH_3) **^{13}C-NMR 100MHz** ($CDCl_3$): 33.2 (CH_2), 54.9 (O CH_3), 100.13, 106.49, 139.27, 160.44 **IR:** ν_{max} (KBr) cm^{-1}: 3003.4, 2969.9, 2936.5, 1609.4, 1517.8, 1162.3, 1006.8, 811.6, 696.4 **HRMS** (EI): Found 230.9942 $(M+H)^+$, $C_9H_{12}BrO_2$ requires 230.9942 **M.P.**: 67-70 °C

8.5.26 2-(3,5-Dimethoxyphenyl)acetonitrile [334]

To a solution of the benzylic bromide [333] (1.5 g, 6.49 mmol) in DMF (25 mL), was added sodium cyanide (0.33 g, 6.73 mmol). After 1h water was added and the aqueous layer. It was extracted with ethyl acetate (50 mL × 3), brine (50 mL), dried over sodium sulphate and evaporated to dryness in vacuo to yield product as a white solid. The material did not require further purification. (1.1 g, 74 %)

^{1}H-NMR 400MHz ($CDCl_3$): 6.48 (s, 2H, Ar-H), 6.42 (s, 1H, Ar-H), 3.81 (s, 6H, O CH_3), 3.70 (s, 2H, CH_2) **^{13}C-NMR 100MHz** ($CDCl_3$): 160.83, 131.50, 117.32 (CN), 105.56, 99.41, 54.98 (O CH_3), 54.94 (O CH_3), 23.30 CH_2) **IR:** ν_{max} (KBr) cm^{-1}: 2941.6, 2246.4, 1590.4, 1515.4, 1289.7, 1238.2, 1141.8, 1009.2 **HRMS** (EI): Found 178.0780 $(M+H)^+$, $C_{10}H_{12}NO_2$ requires 178.0790. **M.P.**: 74-78 °C

8.5.27 (3-(Benzyloxy)-4-methoxyphenyl)methanol [336]

$NaBH_4$ (0.5 g, 13.2 mmol) was added to a solution of 4-benzyloxy-3-methoxybenzaldehyde [330] (3 g, 12.3 mmol) in 50 mL of methanol. After stirring for 3 h, acetic acid was added (1 mL). To this $NaHCO_3$ (10 g) in 50 mL of water was added to neutralize the residual aqueous extract. It was extraxtred with ethyl acetate (50 mL × 3), brine (50 mL), dried over sodium sulphate and evaporated to dryness *in vacuo* to yield product as a white solid. The material did not require further purification. (2.86 g, 95 %)

^{1}H-NMR 400MHz ($CDCl_3$): 7.48-7.28 (m, 5H, Ar-H), 7.05-6.87 (m, 3H, Ar-H), 5.18 (s, 2H, CH_2), 4.59(s, 2H, CH_2), 3.90 (s, 3H, CH_3) **^{13}C-NMR 100MHz** ($CDCl_3$): 149.26, 148.29, 137.06, 135.35, 128.57, 127.88, 120.04, 113.11, 111.70, 70.95 (CH_2), 65.23 (CH_2OH), 56.11(O CH_3) **IR:** ν_{max} (KBr) cm^{-1}: 3204.17, 1591.6, 1425.3, 1240.7, 1157.8, 1008.6, 754.0 **HRMS** (EI): Found 267.1007 $(M+Na)^+$, $C_{15}H_{16}O_3Na$ requires 267.0997 **M.P.**: 65-66 °C

8.5.28 1-((5-(Bromomethyl)-2-methoxyphenoxy)methyl)benzene [337]

A solution of the benzylic alcohol [336] (4.692 g, 19.09 mmol), in dichloromethane (30 mL), was cooled to 0 °C at which time PBr_3 (1 M in DCM) (1.8 mL, 19.09 mmol) was added. After 1 h at room temperature saturated $NaHCO_3$ was added dropwise and the aqueous layer was extracted with dichloromethane (50 mL × 3). It was extraxtred with ethyl acetate (50mL × 3), brine (50 mL), dried over sodium sulphate and evaporated to dryness *in vacuo* to yield product as a white solid. The material did not require further purification. (5.46 g, 93 %)

^{1}H-NMR 400MHz ($CDCl_3$): 7.38-7.48 (m, 5H, Ar-H), 6.85-7.00 (m, 3H, Ar-H), 5.18 (s, 2H, CH_2), 4.48 (s, 2H, CH_2), 3.91 (s, 3H, O CH_3) **^{13}C-NMR 100MHz** ($CDCl_3$): 149.94, 148.25, 136.79, 130.15, 128.82, 128.60, 127.98, 127.44, 122.16, 114.78, 111.59, 77.06 (CH_2), 56.05 (O CH_3), 34.36 (CH_2Br) **IR:** ν_{max} (KBr) cm^{-1}: 3444.0, 3033.4, 3969,1609.4, 1517.8, 1162.3, 1006.8, 811.6, 696.4 **HRMS** (EI): Found 307.0255 $(M+H)^+$, $C_{15}H_{15}BrO_2$ requires 307.0255 **M.P.**: 77-78 °C

8.5.29 2-(3-(Benzyloxy)-4-methoxyphenyl)acetonitrile [338]

To a solution of the benzylic bromide [337] (5.46 g, 17.78 mmol) in DMF (40 mL), was added sodium cyanide (1.127 g, 23 mmol). After 1h water was added and the aqueous layer. It was extracted with ethyl acetate (50 mL × 3), brine (50 mL), dried over sodium sulphate and evaporated to dryness in vacuo to yield product white solid. The material did not require further purification. (3.95 g, 87 %)

^{1}H-NMR 400MHz (DMSO-d_6): 7.47 (d, 2H, J=7Hz, Ar-H), 7.41 (t, 2H, J=7Hz, Ar-H), 7.36 (d, 1H, 7Hz, Ar-H), 7.06 (s, 1H, Ar-H), 7.00 (m, 1H, Ar-H), 6.90 (m, 1H, Ar-H), 5.07 (s, 2H, CH_2), 3.92 (s, 2H, CH_2), 3.77 (s, 3H, O CH_3) **^{13}C-NMR 100MHz** (DMSO-d_6): 149.52, 148.53, 136.67, 128.65, 128.05, 127.40, 122.04, 120.80, 118.12, 113.70, 112.08, 71.13 (CH_2), 56.10 (O CH_3), 23.16 (CH_2NC) **IR:** ν_{max} (KBr) cm^{-1}: 2936.6, 2246.4, 1590.4, 1515.4, 1289.7, 1238.2, 1141.8, 1009.1, 794.7, 705.4 **HRMS** (EI): Found 276.1005 $(M+Na)^+$, $C_{16}H_{15}NO_2Na$ requires **M.P.**: 77-78 °C

8.5.30 2-(3-Hydroxy-4-methoxyphenyl)acetonitrile [339]

The benzylic cyanide [338] (3 g, 11.84 mmol) was dissolved in a 50/50 mixture of methanol and ethyl acetate (20 mL). To this solution Pd/C Black (80 mg) was added and placed in a hydrogen environment under 3 bar pressure for 24 h. The resulting mixture was filtered through celite. The solution was evaporated to dryness *in vacuo* to yield product. To this water (20 mL) was added. The aqueous phase was extracted with ethyl acetate (20 mL × 3), brine (50 mL), dried over sodium sulphate and evaporated to dryness *in vacuo* to yield product. The material was purified *via* flash chromatography on silica gel (*n*-Hexane:EtOAc, 1:1) to afford the product as a white solid. (1.5 g, 77 %)

^{1}H-NMR 400MHz ($CDCl_3$): 6.89 (s, 1H, Ar-H), 6.84 (s, 2H, Ar-H), 3.91(s, 3H, O CH_3), 3.67 (s, 2H, CH_2) **^{13}C-NMR 100MHz** ($CDCl_3$): 146.03 (C$\underline{O}$ CH_3), 145.60 (C$\underline{O}$H), 122.36, 119.11, 117.88 (CN), 113.91, 110.72, 55.60 (O CH_3), 22.44 (CH_2CN) **IR:** ν_{max} (KBr) cm^{-1}: 3416.3, 2936.5, 2249.9, 1717.8, 1592.8, 1515.1, 1263.6, 1140.1, 1023.5, 698.1 **HRMS** (MS Cl+): Found $C_9H_9NO_2$ $(M+H)^+$, 164.0619 requires 164.0633. **M.P.**: 106-107 °C

8.5.31 2-(3-(Benzyloxy)-4-methoxyphenyl)acetic acid [340]

Conc. hydrochloric acid (100 mL) was added to the benzylic cyanide [338] (3.2 g, 12.63 mmol). After 2.5 h at reflux, water (50 mL) was added and the reaction mixture was allowed to cool to room temperature. The aqueous phase was extracted with dichloromethane (50 mL × 3), brine (50 mL), dried over sodium sulphate and evaporated to dryness *in vacuo* to yield product. The material was purified *via* flash chromatography on silica gel (DCM:EtOAc, 1:1) to afford the product as a white solid. (700 mg, 20 %)

^{1}H-NMR 400MHz (DMSO-d_6): 7.28 (t, 3H, 8Hz, Ar-H), 7.20 (d, 1H, 7.5Hz, Ar-H), 7.11 (d, 2H, 7.5Hz, Ar-H), 6.85 (s, 1H, Ar-H), 6.66 (s, 1H, Ar-H), 3.98 (s, 2H, CH_2), 3.84 (s, 3H, CH_3), 3.52 (s, 2H, CH_2) **^{13}C-NMR 100MHz** (DMSO-d_6):176.73 (COOH), 145.43, 143.64, 139.85, 130.47, 128.69, 128.03, 125.68, 124.42, 116.48, 112.72, 55.46(O CH_3), 38.26, 27.34 **IR:** ν_{max} (KBr) cm^{-1}: 3400.9, 3020.3, 2544.3, 1696.3, 1519.5, 1291.3, 1098.3, 935.3, 876.4, 725.4 **HRMS** (EI): Found 271.1038 $(M-H)^-$, $C_{16}H_{15}O_4$ requires 271.1049 **M.P.**: 126-129 °C

8.5.32 (*E/Z*)-3-(3-Hydroxy-4-methoxyphenyl)acrylic acid [342][511]

A mixture of 3-hydroxy-4-methoxybenzaldehyde [335] (6234 mg, 4.1 mmol), malonic acid [341] (1.706 g, 16.4 mmol), piperidine (1.395 g, 1.62 mL, 16.4 mmol) and acetic acid (2.5 mL) was added to a 5 mL microwave tube. The tube was shaken well and irradiated under *via* the microwave 20 min (150 W, 130 °C). The cooled mixture was poured into ice-cold water (20 mL) and extracted with ethyl acetate (3 × 20 mL). The organic layer was washed with saturated sodium chloride and dried over sodium sulfate. The solvent was evaporated under reduced pressure to obtain a brown resin. The material was purified *via* flash chromatography on silica gel (*n*-Hexane:EtOAc, 2:1) to afford the product as a white solid. (white solid, 72%)

^{1}H-NMR 400MHz (DMSO-d_6):12.20 (br-s, 1H, COOH), 9.19 (br-s, 1H, OH), 7.47-7.43 (d, 1H, 16Hz, C=CH), 7.08 (s, 2H, Ar-H), 6.95-6.93 (d, 1H, 8Hz, Ar-H), 6.27-6.23 (d, 1H, 16Hz, C=CH), 3.80 (s, 3H, O CH_3) **^{13}C-NMR 100MHz** (DMSO-d_6): 167.79 (COOH), 149.83, 146.64, 144.21, 127.04, 121.00, 116.20, 114.06, 111.92, 55.59 (O CH_3) **IR:** ν_{max} (KBr) cm^{-1}: 3394.86, 2940.68, 1703.60, 1519.51, 1445.77, 1276.98 **HRMS** (EI): Found 193.0561 $(M-H)^-$, $C_{10}H_9O_4$ requires 193.0571. **M.P.**:233-234 °C

8.5.33 3-(3-Hydroxy-4-methoxyphenyl)propanoic acid [343][510]

Compound [343] (200 mg) was dissolved in EtOAc (20 mL) to this was added 10% Pd/C. The mixture was allowed to stir for 1 h under a hydrogen atmosphere and monitored by TLC until all the starting material had reacted. The reaction mixture was filtered through celite. The solvent was evaporated under reduced pressure to obtain the product as a white solid which did not require further purification (162 mg, 80%)

^{1}H-NMR 400MHz (DMSO-d_6): 12.08 (br-s, 1H, COOH), 8.82 (br-s, 1H, OH), 6.79 (d, 1H, 8Hz, Ar-H), 6.63 (s, 1H, Ar-H), 6.58 (d, 1H, 9Hz, Ar-H), 3.72 (s, 3H, O CH_3), 2.67 (t, 2H, 7.5Hz, CH_2), 2.44 (t, 2H, 7.5Hz, CH_2) **^{13}C-NMR 100MHz** (DMSO-d_6): 173.86 (COOH), 146.26, 145.91, 133.45, 118.59, 118.59, 115.61, 112.23, 55.64 (O CH_3), 35.54 (CH_2), 29.72 (CH_2) **IR:** ν_{max} (KBr) cm^{-1}: 3350 (OH), 1700 (COOH) **HRMS** (EI): Found 195.0726 $(M-H)^-$, $C_{10}H_{11}O_4$ requires 196.0736 **M.P.**: 146-150 °C

8.5.34 (*E/Z*)-3-(3,4,5-Trimethoxyphenyl)acrylic acid [344][511]

A mixture of 3,4,5-trimethoxybenzaldehyde [335a] (804 mg ,4.1 mmol), malonic acid [341] (1.706 g, 16.4 mmol), piperidine (1.395 g, 1.62 mL, 16.4 mmol) and acetic acid (2.5 mL) was added to a 5 mL microwave tube. The tube was shaken well and irradiated under *via* the microwave 8 min (150 W,

130 °C). The cooled mixture was poured into ice-cold water (20 mL) and extracted with ethyl acetate (3 × 20 mL). The organic layer was washed with saturated sodium chloride and dried over sodium sulfate. The solvent was evaporated under reduced pressure to obtain a brown resin. The material was purified *via* flash chromatography on silica gel (*n*-Hexane:EtOAc, 2:1) to afford the product as a white solid (956 mg, 84%)

^{1}H-NMR 400MHz ($CDCl_3$): δ 7.74-7.70 (d, 1H, *J*= 5.5Hz, C=CH), 6.80 (s, 2H, Ar-H), 6.39-6.35 (d, 1H, 5.5Hz, C=CH), 3.92 (s, 9H, OCH_3) **^{13}C-NMR 100MHz** ($CDCl_3$): δ 171.90 (COOH), 153.00, 146.65, 129.02, 115.97, 105.03, 60.55 (OCH_3), 55.71(OCH_3) **IR:** ν_{max} (KBr) cm^{-1}: 2945.74, 1719.94, 1687.73, 1629.03, 1584.20, 1416.49, 1285.90, 1123.54, 998.07 **HRMS** (EI): Found 261.0752 $(M+Na)^+$, $C_{12}H_{14}O_5Na$ requires 261.0739 **M.P.**: 126-127 °C

8.5.35 3-(3,4,5-Trimethoxyphenyl)propanoic acid [345][510]

Compound [344] (200 mg) was dissolved in EtOAc (20 mL) to this was added 10% Pd/C was added. The mixture was allowed to stir for 1 h under a hydrogen atmosphere and monitored by TLC until all the starting material had reacted. The reaction mixture was filtered through celite. The solvent was evaporated under reduced pressure to obtain the product as a white solid which did not require further purification (142 mg, 65%)

^{1}H-NMR 400MHz ($CDCl_3$): 6.68 (s, 2H, Ar-H), 3.78 (s, 6H, OCH_3), 3.65 (s, 3H, OCH_3), 2.69 (t, 2H, J=7.5Hz, CH_2), 2.47 (t, 2H, J=7.5Hz, CH_2) **^{13}C-NMR 100MHz** ($CDCl_3$): 171.36 (COOH), 145.62, 132.85, 118.39, 118.78, 115.61, 111.23, 56.88(OCH_3), 55.64 (OCH_3), 34.74 (CH_2), 28.22 (CH_2) **IR:** ν_{max} (KBr) cm^{-1}:2921.03, 2854.23, 1698.42, 1584.11, 1526.41, 1473.69, 1430.85, 1253.94, 1135.37 **HRMS** (EI): Found 263.0752 $(M+Na)^+$, $C_{12}H_{16}O_5Na$ requires 263.0739 **M.P.**: 103-104 °C

8.5.36 (*E*)-3-(3-Methoxy-4-hydroxyphenyl)-2-(3,4,5-trimethoxyphenyl)acrylic acid [346]

Microwave

As per general method 8.5.2, 4-hydroxy-3-methoxybenzaldehyde (470 mg, 3.09 mmol), 3,4,5-trimethoxyphenylacetic acid (700 mg, 3.09 mmol) were reacted. Recrystallisation from methanol afforded the acrylic acid as fine yellow needles (923 mg, 83%)

^{1}H-NMR (DMSO-d_6, 400MHz): 12.45(br s, 1H, COOH), 8.98(br s, 1H, OH), 7.57(s, 1H, C=CH), 6.81 (d, *J*= 7 Hz, 1H, Ar-H), 6.60 (d, *J*= 7 Hz, 1H, Ar-H), 6.53 (s, 1H, Ar-H), 6.44 (s, 2H, Ar-H), 3.73 (s, 3H, OCH_3), 3.71 (s, 3H, OCH_3), 3.69 (s, 6H, OCH_3) **^{13}C-NMR (DMSO-d_6, 100MHz):** 168.61 (COOH), 153.09, 148.89, 145.84, 139.13, 136.90, 132.18, 130.31, 127.02, 122.99, 117.19, 111.49, 106.65, 60.12 (OCH_3), 55.91 (OCH_3), 55.45 (OCH_3) **IR:** ν_{max} (KBr) cm^{-1}: 3423.9 (br), 2939.8, 1671.3, 1585.2, 1509.6, 1455.3, 1411.1, 1268.3, 1239.3, 1126.2 **HRMS (EI):** Found 383.1103 $(M+Na)^+$, $C_{19}H_{20}O_7Na$ requires 383.1107. **M.P.:** 237-239ºC

8.5.37 (*E*)-3-(4-Methoxyphenyl)-1-piperazin-1-yl-2-(3,4,5-trimethoxyphenyl)propenone [347]

A sample of the acrylic acid [310] (1 eq. 505 mg, 1.38 mmol) and HOBt (1 eq., 188 mg, 1.38 mmol) was dissolved in dry DCM (10 mL) under an inert atmosphere followed by the addition of DCC (1 eq., 288 mg, 1.38 mmol) and DMF (1 mL), the mixture was allowed stir for 30 min. To the reaction flask was added piperazine (5 eq., 601 mg, 6.8 mmol) in dry DCM (10 mL) and was left stirring over night under an inert atmosphere. The reaction mixture was then filtered to remove the urea by-product. The organic layer was then washed with 2 M HCl (3 × 20 mL). The aqueous layer was then basified 2 M NaOH and extracted with DCM. The organic layer was then washed with water (20 mL), brine (20 mL), dried over Na_2SO_4 and evaporated to dryness in vacuum to yield product. The material was purified *via* flash chromatography on silica gel (DCM:EtOAc, 2:1) to afford the product a white solid. (210 mg, 37%)

^{1}H-NMR (DMSO-d_6, 100MHz): 7.11 (d, *J*= 8.5 Hz, 2H, Ar-H), 6.75 (d, *J*= 8.5 Hz, 2H, Ar-H), 6.65 (s, 1H, C=CH), 6.54 (s, 2H, Ar-H), 3.87 (s, 3H, OCH_3), 3.78 (s, 3H, OCH_3), 3.72 (s, 6H, Ar-H), 3.72 (br s, 4H, $N(CH_2)_2$), 2.90 (br s, 4H, $N(CH_2)_2$) **^{13}C-NMR (DMSO-d_6, 100MHz):** 170.00 (C=O), 158.97 ($COCH_3$), 153.02 ($COCH_3$), 137.41 (C=CH), 134.06, 130.50, 130.36, 129.91, 126.92 (C=CH), 113.13, 105.38, 60.53 (OCH_3), 55.70 (OCH_3), 54.80 (OCH_3), ($N(CH_2)_2$ peaks not visable) **IR:** ν_{max} (KBr) cm^{-1}: 2939.4, 2837.2, 2740.0, 2468.5, 2052.1, 2158.0, 1611.1, 1503.7, 1460.1, 1380.1, 1177.6, 1032.3, 1006.7, 1073.5, 940.5, 701.5, 667.4 **HRMS** (EI):. Found 413.2092 $(M+H)^+$, $C_{23}H_{29}N_2O_5$ requires 413.2076 **M.P.**: 77-79 °C

8.5.38 (*E*)-3-(3-Fluoro-4-methoxyphenyl)-1-piperazin-1-yl-2-(3,4,5-trimethoxyphenyl)propenone [348]

A sample of the acrylic acid [313] (1 eq., 500 mg, 1.38 mmol) and HOBt (1 eq., 186 mg, 1.38 mmol) was dissolved up in dry DCM (10 mL) under an inert atmosphere followed by the addition of DCC (1 eq., 289 mg, 1.38 mmol) and DMF (1 mL), the mixture was allowed stir for 30 min. To the reaction flask was added piperazine (5 eq., 601 mg, 6.8 mmol) in dry DCM (10 mL) and was left stirring over night under an inert atmosphere. The reaction mixture was then filtered to remove the urea by-product. The reaction mixture was then filtered to remove the urea by-product. The organic layer was then washed with 2 M HCl (3 × 20 mL). The aqueous layer was then basified 2 M NaOH and extracted with DCM. The organic layer was then washed with water (20 mL), brine (20 mL), dried over Na_2SO_4 and evaporated to dryness in vacuum to yield product. The material was purified *via* flash chromatography on silica gel to afford the product as a white solid. (190 mg, 32%)

^{1}H-NMR (DMSO-d_6, 400MHz): 6.92 (s, 1H, Ar-H), 6.91 (s, 1H, Ar-H), 6.80 (t, *J*= 6.5 Hz, 1H, Ar-H), 6.58 (s, 1H, C=CH), 6.53 (s, 2H, Ar-H), 3.87 (s, 6H, OCH_3), 3.73 (s, 6H, OCH_3), 3.71 (br s, 4H, $N(CH_2)_2$), 2.89 (br s, 4H, $N(CH_2)_2$) **^{13}C-NMR (DMSO-d_6, 100MHz):** 169.56 (C=O), 153.12 ($COCH_3$), 152.48 ($COCH_3$), 150.03, 147.08, 137.74 (C=CH), 135.48, 129.77, 128.65, 127.24 (C=CH), 125.61, 125.58, 116.39, 116.20, 112.25, 105.34, 60.57 (OCH_3), 55.77 (OCH_3), 55.69 (OCH_3), ($N(CH_2)_2$ signals not visable) **IR:** ν_{max} (KBr) cm^{-1}: 3058.8, 2836.8, 2934.9, 1598.5, 1580.4, 1439.7, 1412.7, 1276.1, 1236.8, 1126.7, 1006.4, 1150.7, 902.4, 931.9, 972.8 **HRMS** (EI): Found 431.1995 $(M+H)^+$, $C_{23}H_{28}FN_2O_5$ requires 431.1982 **M.P.**: 79-80 °C

8.5.39 (*E*)-3-(3-Hydroxy-4-methoxyphenyl)-1-piperazin-1-yl-2-(3,4,5-trimethoxyphenyl)propenone [349]

A sample of the acrylic acid [150] (1 eq., 505 mg, 1.38 mmol) and HOBt (1 eq., 188 mg, 1.38 mmol) was dissolved dry DCM (10 mL) under an inert atmosphere followed by the addition of DCC (1 eq., 288 mg, 1.38 mmol) and DMF (1 mL), the mixture was allowed stir for 30 min. To the reaction flask was added piperazine (5 eq., 601mg, 6.8 mmol) in dry DCM (10 mL) and was left stirring overnight under an inert atmosphere. The reaction mixture was then filtered to remove the urea by-product. The organic layer was then washed with 2 M HCl (3 × 20 mL). The aqueous layer was then basified 2 M NaOH and extracted with DCM. The organic layer was then washed with water (20 mL), brine (20 mL), dried over Na_2SO_4 and evaporated to dryness in vacuum to yield product. The material was purified *via* flash chromatography on silica gel to afford the product as a cream solid. (98 mg, 16 %)

^{1}H-NMR (DMSO-d_6, 400MHz): 6.76 (s, 1H, Ar-H), 6.68 (s, 2H, Ar-H), 6.57 (s, 1H, C=CH), 6.55 (s, 2H, Ar-H), 3.86 (s, 3H, OCH_3), 3.85 (s, 3H, OCH_3), 3.72 (s, 6H, OCH_3), 3.70 (br s, 4H, $N(CH_2)_2$), 2.88 (br s, 4H, $N(CH_2)_2$) **^{13}C-NMR (DMSO-d_6, 100MHz):** 169.98 (C=O), 152.95 ($COCH_3$), 146.30 ($COCH_3$), 144.82 ($COCH_3$), 137.46 (C=CH), 134.31, 130.20, 129.87, 127.68 (C=CH), 121.56, 115.07, 115.07, 109.84, 105.45, 60.52 (OCH_3), 55.73 (OCH_3), 55.41 (OCH_3), ($N(CH_2)_2$ peaks not visable) **IR:** ν_{max} (KBr) cm^{-1}: 3000.03, 2935.70, 2838.75, 1635.80, 1579.36, 1605.99, 1380.11, 1321.78, 1284.20, 1177.41,

1284.29, 1151.39, 1031.62, 998,06, 905.61, 809.88, 830.18. **HRMS** (EI):. Found 429.2041 $(M+H)^+$, $C_{23}H_{29}N_2O_6$ requires 429.2026 **M.P.**: 83 °C

8.5.40 (*E*)-3-(4-Hydroxy-3-methoxyphenyl)-1-piperazin-1-yl-2-(3,4,5-trimethoxyphenyl)propenone [350]

A sample of the acrylic acid [346] (1 eq., 200 mg, 0.555 mmol) and HOBt (1 eq., 75 mg, 0.555 mmol) was dissolved in dry DCM (10 mL) under an inert atmosphere followed by the addition of DCC (1 eq., 114 mg, 0.555 mmol) and DMF (1 mL), the mixture was allowed stir for 30 min. To the reaction flask was added piperazine (5 eq., 236 mg, 2.77 mmol) in dry DCM (10 mL) and was left stirring overnight under an inert atmosphere. The reaction mixture was then filtered to remove the urea by-product. The organic layer was then washed with 2M HCl (3 × 20 mL). The organic layer was then washed with water (20 mL), brine (20 mL), dried over Na_2SO_4 and evaporated to dryness in vacuo to yield product. The material was purified *via* flash chromatography on silica gel to afford the product as a cream solid. (10 mg, 4 %)

^{1}H-NMR (DMSO-d_6, 400MHz): 6.76 (s, 1H, Ar-H), 6.68 (s, 2H, Ar-H), 6.57 (s, 1H, C=CH), 6.55 (s, 2H, Ar-H), 3.86 (s, 3H, OCH_3), 3.85 (s, 3H, OCH_3), 3.72 (s, 6H, OCH_3), 3.70 (br s, 4H, $N(CH_2)_2$), 2.88 (br s, 4H, $N(CH_2)_2$) **^{13}C-NMR (DMSO-d_6, 100MHz):** 169.98 (C=O), 152.95 ($COCH_3$), 146.30 ($COCH_3$), 144.82 ($COCH_3$), 137.46 (C=CH), 134.31, 130.20, 129.87, 127.68 (C=CH), 121.56, 115.07, 115.07, 109.84, 105.45, 60.52 (OCH_3), 55.73 (OCH_3), 55.41 (OCH_3), ($N(CH_2)_2$ peaks not visable) **IR:** ν_{max} (KBr) cm^{-1}: 3058.82, 2836.80, 2934.99, 1597.33, 1344.33, 1134.22, 1273.2, 1054.2, 1032.22, 1021.1, 1003.23, 932.22, 847.33, 944.33, 803.44, 812.33, 735.33, 8534.323, 653.29, 683.33. **HRMS** (EI): Found 429.2041 $(M+H)^+$, $C_{23}H_{29}N_2O_6$ requires 429.2026 **M.P.**: 82-83°C

8.5.41 (*E*)-3-(4-Methoxyphenyl)-1-[4-((E)-3-phenylallyl)-piperazin-1-yl]-2-(3,4,5-trimethoxyphenyl)propenone [351]

A sample of the acrylic acid [310] (1 eq., 500 mg, 1.38 mmol) and HOBt (1 eq., 186 mg, 1.38 mmol) was dissolved in dry DCM (10 mL) under an inert atmosphere followed by the addition of DCC (1 eq., 280 mg, 1.38 mmol) and DMF (1 mL) and was allowed stirr for 30 min. To the reaction flask was added *trans*-1-cinnamylpiperazine (5 eq., 1.38 g, 6.8 mmol) in dry DCM (10 mL) and was left stirring over night under an inert atmosphere. The reaction mixture was then filtered to remove the urea by-product. The organic layer was then washed with 2M HCl (3 × 20 mL). The organic layer was then washed with water (20 mL), brine (20 mL), dried over Na_2SO_4 and evaporated to dryness in vacuo to yield product. The material was purified *via* flash chromatography on silica gel to afford the product as a brown resin. (119 mg, 16 %)

^{1}H-NMR (DMSO-d_6, 400MHz): 7.33 (m, 2H, Ar-H), 7.31 (t, 2H, Ar-H), 7.27 (m, 1H, Ar-H), 7.13 (d, *J*= 8.5 Hz, 2H, Ar-H), 6.75 (d, *J*= 6.5 Hz, 2H, Ar-H), 6.52 (s, 1H, C=CH), 6.56 (s, 2H, Ar-H) 6.54 (d, *J*= 6.5 Hz, 1H, C=CH), 6.24 (m, 1H, C=CH), 3.88 (s, 3H, OCH_3), 3.79 (s, 3H, OCH_3), 3.71 (s, 6H, OCH_3), 3.79-3.61 (m, 4H, $N(CH_2)_2$), 3.17 (d, 2H, CH_2), 2.53-2.37 (m, 4H, $N(CH_2)_2$) **^{13}C-NMR (DMSO-d_6, 100MHz):** 169.89 (C=O), 158.91 ($COCH_3$), 152.96 ($COCH_3$), 137.34 (C=CH), 134.30 (C=CH), 130.49, 129.80, 128.20 (C=CH), 127.56, 127.04, 126.02, 113.11, 105.40, 60.53 (OCH_3), 60.24 (CH_2), 55.68 (OCH_3), 54.80 (OCH_3), 53.31 ($N(CH_2)_2$), 52.22 ($N(CH_2)_2$) **IR:** ν_{max} (KBr) cm^{-1}: 2934.33, 2744.4, 2211.45, 1568.64, 1464.33, 1644.24, 1159.16, 1063.43, 1032.11, 955.39, 944.32, 932.33, 902.23, 863.77, 841.33, 832.22, 799.73. **HRMS** (EI): Found 529.2684 $(M+H)^+$, $C_{32}H_{37}N_2O_5$ requires 529.2702

8.5.42 (*E*)-3-(3-Fluoro-4-methoxyphenyl)-1-[4-((E)-3-phenylallyl)-piperazin-1-yl]-2-(3,4,5-trimethoxyphenyl)propenone [352]

A sample of the acrylic acid [313] (1 eq., 500 mg, 1.38 mmol) and HOBt (1 eq., 186 mg, 1.38 mmol) was dissolved in dry DCM (10 mL) under an inert atmosphere followed by the addition of DCC (1 eq., 280 mg, 1.38 mmol) and DMF (1 mL), the mixture was allowed stirr for 30 min. To the reaction flask was added *trans*-1-Cinnamylpiperazine (5 eq., 1.38 g, 6.8 mmol) in dry DCM (10 mL) and was left stirring over night under an inert atmosphere. The reaction mixture was then filtered to remove the urea by-product. The organic layer was then washed with 2M HCl (3 × 20 mL). The organic layer was then washed with water (20 mL), brine (20 mL), dried over Na_2SO_4 and evaporated to dryness in vacuum to yield product. The material was purified *via* flash chromatography on silica gel to afford the product as a brown solid. (142mg, 19%)

^{1}H-NMR (DMSO-d_6, 400MHz): 7.37 (m, 2H, Ar-H), 7.32 (t, 2H, Ar-H), 7.26 (m, 1H, Ar-H), 6.93 (d, *J*= 7 Hz, 1H, Ar-H), 6.90 (s, 1H, Ar-H), 6.80 (s, 1H, Ar-H), 6.58 (s, 1H, C=CH), 6.54 (s, 2H, Ar-H), 6.55-6.52 (m, 1H, C=CH), 6.62-6.22 (m, 1H, C=CH), 3.88 (s, 3H, OCH_3), 3.86 (s, 3H, OCH_3), 3.72 (s, 6H, OCH_3), 3.81-3.60 (m, 4H, $N(CH_2)_2$), 3.20 (d, *J*= 5 Hz, 2H, CH_2), 2.56-2.38 (m, 4H, $N(CH_2)_2$) **^{13}C-NMR (DMSO-d_6, 100MHz):** 169.44 (C=O), 153.03 ($COCH_3$), 152.48 (CF), 146.96 ($COCH_3$), 146.84 ($COCH_3$), 137.62 (C=CH), 135.98 (C=CH), 135389, 129.98 (C=CH), 128.31, 128.17, 127.69, 127.37, 125.91, 125.52, 116.41, 116.21, 112.23, 105.38, 60.56 (OCH_3), 60.34 (CH_2), 55.72 (OCH3), 53.31 ($N(CH_2)_2$), 52.42 ($N(CH_2)_2$) **IR:** ν_{max} (KBr) cm^{-1}: 3094.44, 2847.33, 1934.4, 1544.24, 1532.33, 1477.29, 1302.3, 1127.22, 1102.2, 1163.33, 1183.33, 944.33, 945.3, 857.33, 756.33, 621.34 **HRMS** (EI):. Found 546.2544 $(M+H)^+$, $C_{32}H_{35}FN_2O_5$ requires 546.2530 **M.P.**: 126-129°C

8.5.43 (*E*)-3-(4-Methoxyphenyl)-1-(4-phenylpiperazin-1-yl)-2-(3,4,5-trimethoxyphenyl)propenone [353]

A sample of the acrylic acid [310] (1 eq., 500 mg, 1.38 mmol) and HOBt (1 eq., 186 mg, 1.38 mmol) was dissolved in dry DCM (10 mL) under an inert atmosphere followed by the addition of DCC (1 eq., 280 mg, 1.38 mmol) and DMF (1 mL), the mixture was allowed stirr for 30 min. To the reaction flask was added 1-phenylpiperazine (5 eq., 1.119 g, 1.054 mL, 6.8 mmol) in dry DCM (10 mL) and was left stirring over night under an inert atmosphere. The reaction mixture was then filtered to remove the urea by-product. The organic layer was then washed with 2M HCl (3 × 20 mL). The organic layer was then washed with water (20 mL), brine (20 mL), dried over Na_2SO_4 and evaporated to dryness in vacuo to yield product. The material was purified *via* flash chromatography on silica gel to afford the product as a brown solid. (203 mg, 29 %)

^{1}H-NMR (DMSO-d_6, 400MHz): 7.34 (s, 2H, Ar-H), 7.22 (s, 2H, Ar-H), 7.04 (s, 2H, Ar-H), 6.93 (s, 2H, Ar-H), 6.83 (s, 1H, Ar-H), 6.63 (s, 1H, C=CH), 6.50 (s, 2H, Ar-H), 3.90 (s, 6H, OCH_3), 3.87-3.82 (br s, 4H, $N(CH_2)_2$), 3.75 (s, 6H, OCH_3), 3.25-3.12 (m, 4H, $N(CH_2)_2$) **^{13}C-NMR (DMSO-d_6, 100MHz):** 169.56 (C=O), 153.18 ($COCH_3$), 137.80 (C=CH), 129.81, 129.22, 127.51, 125.65 (C=CH), 116.43, 116.23, 112.26, 105.39, 60.60 ($COCH_3$), 55.81 ($COCH_3$) 33.45 ($N(CH_2)_2$), 25.13 ($N(CH_2)_2$) **IR:** ν_{max} (KBr) cm^{-1}: 299.22, 2833.23,2432.33, 1704.33,1873.99, 1789.33, 1647.64, 1528.33, 1384.33, 1267.21, 1301.55, 1145.54, 1038.44, 1022.52, 984.66, 604.33 **HRMS** (EI):. Found 511.2204 $(M+Na)^+$, $C_{29}H_{32}N_2NaO_5$ requires 511.2209 **M.P.**: 126-129 °C

8.5.44 (*E*)-3-(3-Fluoro-4-methoxyphenyl)-1-(4-phenylpiperazin-1-yl)-2-(3,4,5-trimethoxyphenyl)propenone [354]

A sample of the acrylic acid [313] (1 eq., 500 mg, 1.38 mmol) and HOBt (1 eq., 186 mg, 1.38 mmol) was dissolved in dry DCM (10 mL) under an inert atmosphere followed by the addition of DCC (1 eq.,

285 mg, 1.38 mmol) and DMF (1 mL), the mixture was allowed stirr for 30min. To the reaction flask was added 1-phenylpiperazine (5 eq., 1.119 g, 1.057 mL, 6.9mmol) in dry DCM (10 mL) and was left stirring over night under an inert atmosphere. The reaction mixture was then filtered to remove the urea by-product. The organic layer was then washed with 2 M HCl (3 × 20 mL). The organic layer was then washed with water (20 mL), brine (20 mL), dried over Na_2SO_4 and evaporated to dryness in vacuo to yield product. The material was purified *via* flash chromatography on silica gel to afford the product as a brown resin. (227 mg, 31 %)

^{1}H-NMR (DMSO-d_6, 400MHz): 7.35 (s, 2H, Ar-H), 7.07 (s, 2H, Ar-H), 6.93 (s, 3H, Ar-H), 6.83 (s, 1H, Ar-H), 6.65 (s, 1H, C=CH), 6.52 (s, 2H, Ar-H), 3.89 (s, 6H, OCH_3), 3.89-3.80 (m, 4H, $N(CH_2)_2$), 3.75 (s, 6H, OCH_3), 3.24-3.11 (m, 4H, $N(CH_2)_2$) **^{13}C-NMR (DMSO-d_6, 100MHz):** 169.56 (C=O), 153.18 ($COCH_3$), 137.80 (C=CH), 129.81, 129.22, 127.51, 125.65 (C=CH), 116.43, 116.23, 112.26, 105.39, 60.60 ($COCH_3$), 55.81 ($COCH_3$) 33.45 ($N(CH_2)_2$), 25.13 ($N(CH_2)_2$) **IR:** ν_{max} (KBr) cm^{-1}: 2994.33,2746.44, 2245.3, 1633.34,1535.33,1366.32, 1098.34,1970.49, 1095.4, 948.43, 985.23, 901.3, 833.3, 823.3, 743.4, 618.43, 532.88 **HRMS** (EI):. Found 529.2109 $(M+Na)^+$, $C_{29}H_{31}FN_2NaO_5$ requires 529.2115 **M.P.**: 112-115 °C

8.5.45 (*E*)-3-(4-Hydroxy-3-methoxyphenyl)-1-(4-phenylpiperazin-1-yl)-2-(3,4,5-trimethoxyphenyl)propenone [355]

A sample of the acrylic acid [150] (1 eq., 500 mg, 1.38 mmol) and HOBt (1 eq., 186 mg, 1.38 mmol) was dissolved in dry DCM (10 mL) under an inert atmosphere followed by the addition of DCC (1 eq., 280 mg, 1.38 mmol) and DMF (1 mL), the mixture was allowed stirr for 30 min. To the reaction flask was added piperazine (5 eq., 1.38 g, 6.8 mmol) in dry DCM (10 mL) and was left stirring over night under an inert atmosphere. The reaction mixture was then filtered to remove the urea by-product. The organic layer was then washed with 2M HCl (3 × 20 mL). The aqueous layer was then basified 2 M NaOH and extracted with DCM. The organic layer was then washed with water (20 mL, brine (20 mL), dried over Na_2SO_4 and evaporated to dryness in vacuo to yield product. The material was purified *via* flash chromatography on silica gel to afford the product as a brown solid. (199 mg, 28%)
^{1}H-NMR (DMSO-d_6, 400MHz): 7.30 (s, 2H, Ar-H), 6.96 (s, 3H, Ar-H), 6.82 (s, 1H, Ar-H), 6.70 (s, 2H, Ar-H), 6.64 (s, 1H, C=CH), 6.60 (s, 2H, Ar-H), 3.88 (s, 6H, OCH_3), 3.88-3.73 (m, 4H, $N(CH_2)_2$), 3.73 (s, 6H, OCH_3), 3.20-3.07 (m, 4H, $N(CH_2)_2$) **^{13}C-NMR (DMSO-d_6, 100MHz):** 169.95 (C=O), 152.95 ($COCH_3$), 146.09 ($COCH_3$), 144.73 ($COCH_3$), 137.51 (C=CH), 134.68, 130.31, 129.84, 127.89 (C=CH), 121.58, 116.59, 115.03, 109.76, 105.55, 60.54 (OCH_3), 55.74 (OCH_3), 55.45 (OCH_3) ($N(CH_2)_2$ peaks not visable) **IR:** ν_{max} (KBr) cm^{-1}: 2994.33, 2884.3, 2779,33, 2742.33, 1684.33,1543.34. 1428.22, 1326.22, 1125.29, 1293.33, 1009,23, 982.22, 830.32, 839.32, 734.23, 645.44, 573.33 **HRMS** (EI):. Found 527.2141 $(M+Na)^+$, $C_{29}H_{32}N_2NaO_6$ requires 527.2158 **M.P.**: 121-125 °C

8.5.46 (*E*)-3-(4-Hydroxy-3-methoxyphenyl)-1-(4-phenylpiperazin-1-yl)-2-(3,4,5-trimethoxyphenyl)propenone [356]

A sample of the acrylic acid [346] (1 eq., 500 mg, 1.38 mmol) and HOBt (1 eq., 186 mg, 1.38 mmol) was dissolved in dry DCM (10 mL) under an inert atmosphere followed by the addition of DCC (1 eq., 280 mg, 1.38 mmol) and DMF (1 mL), the mixture was allowed stirr for 30min. To the reaction flask was added 1-phenylpiperazine (5 eq., 1.119 g, 1.054 mL, 6.8 mmol) in dry DCM (10 mL) and was left stirring overnight under an inert atmosphere. The reaction mixture was then filtered to remove the urea by-product. The organic layer was then washed with 2 M HCl (3 × 20 mL). The organic layer was then washed with water (20 mL), brine (20 mL), dried over Na_2SO_4 and evaporated to dryness in

vacuum to yield product. The material was purified *via* flash chromatography on silica gel to afford the product as a brown solid. (229 mg, 31 %)

^{1}H-NMR (DMSO-d_6, 400MHz): 7.29 (s, 2H, Ar-H), 7.07 (s, 1H, Ar-H), 6.91 (s, 3H, Ar-H), 6.74 (s, 2H, Ar-H), 6.65 (s, 1H, C=CH), 6.51 (s, 2H, Ar-H), 3.90 (s, 12H, OCH_3), 3.89-3.80 (m, 4H, $N(CH_2)_2$), 3.24-3.11 (m, 4H, $N(CH_2)_2$) **^{13}C-NMR (DMSO-d_6, 100MHz):** 168.71 (C=O), 153.02 ($COCH_3$), 146.19 ($COCH_3$), 145.69 ($COCH_3$), 137.86 (C=CH), 133.35, 128.90, 127.36, 127.19, 123.33 (C=CH), 123.33, 105.54, 102.54, 60.51 (OCH_3), 55.78 (OCH_3), 55.49 (OCH_3), 40.59 ($N(CH_2)_2$), 33.47 ($N(CH_2)_2$) **IR:** ν_{max} (KBr) cm^{-1}: 3003.33, 2740.44,2345.33, 2232.23,2045.32, 1747.33, 1522.33, 1642.33, 1587.32, 1548.2, 1427.3, 1254.33,1234.22,1087.39,839.33, 756.45, 665.4 **HRMS** (EI):. Found 527.2161 $(M+Na)^+$, $C_{29}H_{32}N_2NaO_6$ requires 527.2158 **M.P.**: 79-98 °C

8.5.47 (*E*)-1-(4-Acetylpiperazin-1-yl)-3-(4-methoxyphenyl)-2-(3,4,5-trimethoxyphenyl)propenone [357]

A sample of the acrylic acid [310] (1 eq., 200 mg, 0.551 mmol) and HOBt (1 eq., 74 mg, 0.551 mmol) was dissolved in dry DCM (10 mL) under an inert atmosphere followed by the addition of DCC (1 eq., 113.6 mg, 0.551 mmol) and DMF (1 mL) and was allowed stirr for 30min. To the reaction flask was added 1-acetyl-piperazin (5 eq., 353.7 mg, 2.76 mmol) in dry DCM (10 mL) and was left stirring over night under an inert atmosphere. The reaction mixture was then filtered to remove the urea by-product. The organic layer was then washed with 2 M HCl (3 × 20 mL). The organic layer was then washed with water (20 mL), brine (20 mL), dried over Na_2SO_4 and evaporated to dryness in vacuo to yield product. The material was purified *via* flash chromatography on silica gel to afford the product as a brown resin. (30 mg, 12 %)

^{1}H-NMR (DMSO-d_6, 100MHz): 7.10 (s, 1H, Ar-H), 7.08 (s, 1H, Ar-H), 6.73 (s, 1H, Ar-H), 6.65 (s, 1H, C=CH), 6.52 (s, 2H, Ar-H), 3.84 (s, 3H, OCH_3), 3.75 (s, 3H, OCH_3), 3.69 (s, 6H, 2 × OCH_3), 3.57 (br s, 8H, $(N(CH_2)_2)$, 2.08 (s, 3H, $NCOCH_3$) **^{13}C-NMR (DMSO-d_6, 100MHz):** 170.17 (C=O), 168.72 (C=O), 159.00 ($COCH_3$), 153.02 ($COCH_3$), 137.41 (C=CH), 134.06, 130.49, 130.34, 130.14, 126.81 (C=CH), 113.12, 105.35, 60.52 (OCH_3), 55.68 (OCH_3), 54.77 (OCH_3), 45.56 ($N(CH_2)_2$), 40.84 ($N(CH_2)_2$), 20.89 ($C=OCH_3$) **IR:** ν_{max} (KBr) cm^{-1}: 3088.33,2764.33,2543.1,1543.22,9873.34, 974,33,789.55,876.75, 769.86 **HRMS** (EI):. Found 477.2005 $(M+Na)^+$, $C_{25}H_{30}N_2NaO_6$ requires 477.2002.

8.5.48 (*E*)-1-(4-Acetylpiperazin-1-yl)-3-(3-fluoro-4-methoxyphenyl)-2-(3,4,5-trimethoxyphenyl)propenone [358]

A sample of the acrylic acid [313] (1 eq., 200 mg, 0.52 mmol) and HOBt (1 eq., 74.5 mg, 0.52 mmol) was dissolved in dry DCM (10 mL) under an inert atmosphere followed by the addition of DCC (1 eq., 113.8 mg, 0.52 mmol) and DMF (1 mL) and was allowed stirr for 30min. To the reaction flask was added 1-acetyl-piperazin (5 eq., 353.7 mg, 2.76 mmol) in dry DCM (10 mL) and was left stirring over night under an inert atmosphere. The reaction mixture was then filtered to remove the urea by-product. The organic layer was then washed with 2M HCl (3 × 20 mL). The organic layer was then washed with water (20 mL), brine (20 mL), dried over Na_2SO_4 and evaporated to dryness in vacuum to yield product. The material was purified *via* flash chromatography on silica gel to afford the product as a white solid. (59mg, 23%)

^{1}H-NMR (DMSO-d_6, 400MHz) 6.93 (s, 1H, Ar-H), 6.90 (s, 1H, Ar-H), 6.81 (m, 1H, Ar-H), 6.62 (s, 1H, C=CH), 6.54 (s, 2H, Ar-H), 3.88 (s, 3H, OCH_3), 3.87 (s, 3H, OCH_3), 3.71 (s, 6H, 2 × OCH_3), 3.61-3.48 (m, 8H, $N(CH_2)_2$), 2.11 (s, 3H, $C=OCH_3$) **^{13}C-NMR (DMSO-d_6, 100MHz):** 169.78 (C=O), 168.76 (C=O), 153.17 ($COCH_3$), 147.03 ($COCH_3$), 137.78 (C=CH), 135.51, 129.75, 127.45, 127.38, 125.61 (C=CH), 116.42, 116.22, 112.25, 105.33, 60.59 (OCH_3), 55.78 (OCH_3), 55.69 (OCH_3), 20.90 ($C=OCH_3$), $(N(CH_2)_2$ not

visable) **IR:** ν_{max} (KBr) cm^{-1}: 2843.33,3452.44, 2456.33, 2334.33, 1987.45, 1894.44,1745.44, 1876.4, 1745.09,1454.2,1004.44, 957.88, 876.33, 764.33, 734.33, 908.44, 648.43 **HRMS** (EI):. Found 495.1910 $(M+Na)^+$, $C_{25}H_{29}N_2FNaO_6$ requires 495.1907 **M.P.**: 121-125°C

8.5.49 (*E*)-1-(4-Acetylpiperazin-1-yl)-3-(3-hydroxy-4-methoxyphenyl)-2-(3,4,5-trimethoxyphenyl)propenone [359]

A sample of the acrylic acid [150] (200 mg, 0.555 mmol, 1 eq.) and HOBt (79.5 mg, 0.555 mmol, 1 eq.) was dissolved up in dry DCM (10 mL) under an inert atmosphere followed by the addition of DCC (114 mg, 0.555 mmol, 1 eq.) and 1 mL DMF and was allowed stir for 30 min. To the reaction flask was added 1-acetyl-piperazin (355 mg, 2.77 mmol, 5 eq.) in 10 mL dry DCM and was left stirring over night under an inert atmosphere. The reaction mixture was then filtered to remove the urea by-product. The organic layer was then washed with 2M HCl (3 x 20mL). The organic layer was then washed with water (20 mL), brine (20 mL), dried over Na_2SO_4 and evaporated to dryness in vacuo to yield product. The material was purified *via* flash chromatography on silica gel (DCM:EtOAc, 2:1) to afford the product as a white solid. (41 mg, 15 %)

^{1}H-NMR (DMSO-d_6, 400MHz) 6.75 (s, 1H, Ar-H), 6.63 (s, 2H, Ar-H), 6.56 (s, 1H, C=CH), 6.51 (s, 2H, Ar-H), 3.80 (s, 3H, OCH_3), 3.79 (s, 3H, OCH_3), 3.66 (s, 6H, OCH_3), 3.52-3.42 (m, 8H, $N(CH_2)_2$), 2.04 (s, 3H, $COCH_3$) **^{13}C-NMR (DMSO-d_6, 100MHz):** 170.22 (C=O), 168.87 (C=O), 152.98 ($COCH_3$), 146.56 ($COCH_3$), 144.98 ($COCH_3$), 137.41 (C=CH), 134.12, 130.19, 130.12, 127.43, 121.46, 115.20, 109.95, 105.39, 60.44 (OCH_3), 55.35 (OCH_3), 53.34 (OCH_3), 45.51 ($N(CH_2)_2$), 40.78 ($N(CH_2)_2$), 20.79 ($C=OCH_3$) **IR:** ν_{max} (KBr) cm^{-1}: 3243.22,2645.44,2345.32, 2534.77, 1534.33,1534.991635.54, 1436.32,1325.44, 1298.33, 1154.44, 1098.33, 987.44, 983.33, 876.47, 854.98, **HRMS** (EI):. Found 493.1933 $(M+Na)^+$, $C_{25}H_{30}N_2NaO_7$ requires 493.1951 **M.P.**: 124-126 °C

8.5.50 (*E*)-1-(4-Acetylpiperazin-1-yl)-3-(4-hydroxy-3-methoxyphenyl)-2-(3,4,5-trimethoxyphenyl)propenone [360]

A sample of the acrylic acid [346] (200 mg, 0.555 mmol, 1 eq.) and HOBt (74.5 mg, 1.38 mmol, 1 eq.) where dissolved up in dry DCM (10 mL) under an inert atmosphere followed by the addition of DCC (113.8 mg, 0.555 mmol, 1 eq.) and 1 mL DMF and was allowed stir for 30min. To the reaction flask was added 1-acetyl-piperazin (355 mg, 2.77 mmol, 5 eq.) in 10 mL dry DCM and was left stirring over night under an inert atmosphere. The reaction mixture was then filtered to remove the urea by-product. The organic layer was then washed with 2 M HCl (3 x 20 mL). The organic layer was then washed with water (20 mL), brine (20 mL), dried over Na_2SO_4 and evaporated to dryness in vacuo to yield product. The material was purified *via* flash chromatography on silica gel (DCM:EtOAc, 2:1) to afford the product as a cream solid. (30 mg, 11 %)

^{1}H-NMR (DMSO-d_6, 400MHz) 6.98 (s, 1H, Ar-H), 6.89 (s, 2H, Ar-H), 6.69 (s, 1H, C=CH), 6.57 (s, 2H, Ar-H), 3.89 (s, 3H, OCH_3), 3.87 (s, 3H, OCH_3), 3.86 (s, 6H, OCH_3), 3.73-3.62 (m, 4H, $(N(CH_2)_2$), 3.35-3.39 (m, 4H, $N(CH_2)_2$), 2.09 (s, 3H, $C=OCH_3$) **^{13}C-NMR (DMSO-d_6, 100MHz):** 168.89 (C=O), 168.66 (C=O), 153.09 ($COCH_3$), 146.25 ($COCH_3$), 145.77 ($COCH_3$), 137.97 (C=CH), 132.04, 130.55 (C=CH), 127.42, 123.38, 114.34, 113.81, 111.069, 105.46, 102.57, 60.50 (OCH_3), 55.79 (OCH_3), 55.77 (OCH_3), 45.61 ($N(CH_2)_2$), 40.76 ($N(CH_2)_2$), 20.78 ($C=OCH_3$) **IR:** ν_{max} (KBr) cm^{-1}: 2564.33, 1534.33,1423.66, 1264.33, 1266.31, 1143.22, 11432.2, 1152.11,1086.22, 992.22, 876.33, 765.33, 762.2, 659.6 **HRMS** (EI):. Found 493.1951 $(M+Na)^+$, $C_{25}H_{30}N_2NaO_7$ requires 493.1951 **M.P.**: 215-220°C

8.5.51 (*E*)-Methyl-3-(3-hydroxy-4-methoxyphenyl)-2-(3,4,5-trimethoxyphenyl)acrylate [361]

To a microwave vial was added acrylic acid [150] (495 mg, 1.29 mmol), 4 mL $HCl_{(conc.)}$ and 3 mL methanol. The reaction mixture was allowed to react under microwave irradiation for 30 min at a temperature of 105 °C. The microwave cap was removed and allowed to stir till the precipitate formed. The mixture was then filtered and the precipitate was then dried. The precipitate was purified *via* flash chromatography on silica gel (DCM:EtOAc, 2:1). (220 mg, 42 %)

^{1}H-NMR (DMSO-d_6, 400MHz): 7.61 (s, 1H, C=CH), 6.82 (d, *J*= 6.8 Hz, 1H, Ar-H), 6.63 (d, 1H, Ar-H), 6.54 (s, 1H, Ar-H), 6.46 (s, 2H, Ar-H), 3.74 (s, 3H, OCH_3), 3.72 (s, 3H, OCH_3), 3.70 (s, 3H, $C{=}OOCH_3$), 3.69 (s, 6H, OCH_3) **^{13}C-NMR (DMSO-d_6, 100MHz)** 167.55 (C=O), 153.18 ($COCH_3$), 149.11 ($COCH_3$), 145.87 ($COCH_3$), 139.82, 137.05 (C=CH), 131.48, 129.21, 126.73 (C=CH), 123.23, 117.25, 111.49, 106.67, 60.13 (OCH_3), 55.94 (OCH_3), 55.46 ($C{=}OCH_3$) **IR:** ν_{max} (KBr) cm^{-1}: 3325.22, 3421.23, 2654.23, 2654.23, 2098.34, 1698.33, 1332.43, 1423.32, 1234.21, 1134.54, 998.32, 900.34, 876.32, 765.33, 704.32, 632.29, 672.32, 603.23 **HRMS** (EI):. Found 397.1258 $(M+Na)^+$, $C_{20}H_{22}O_7Na$ requires 397.1263 **M.P.**: 172-176 °C

8.5.52 (*E*)-Methyl-3-(4-methoxyphenyl)-2-(3,4,5-trimethoxyphenyl)acrylate [363]

To a microwave vial was added acrylic acid [310] (800 mg, 2.31 mmol), 4 mL $HCl_{(conc.)}$ and 3 mL methanol. The reaction was allowed to react under microwave irradiation for 30 min at a temperature of 105 °C. The microwave cap was removed and allowed to stir till the precipitate formed. The mixture was then filtered and the precipitate was then dried. The precipitate was purified *via* flash chromatography on silica gel to afford the product as a white solid. (437 mg, 49.5 %)

^{1}H-NMR (DMSO-d_6, 400MHz) 7.69 (s, 1H, C=CH), 7.06 (m, 2H, Ar-H), 6.82 (d, *J*= 7 Hz, 2H, Ar-H), 6.49 (s, 2H, Ar-H), 3.81 (s, 3H, OCH_3), 3.72 (s, 3H, $COOCH_3$), 3.71 (s, 9H, OCH_3) **^{13}C-NMR (DMSO-d_6, 100MHz):** 167.22 (C=O), 153.38 ($COCH_3$), 153.29 ($COOCH_3$), 153.29 ($COCH_3$), 151.88, 148.19, 148.08, 138.33, 137.22 (C=CH), 131.10, 128.06, 126.98 (C=CH), 126.92, 117.19, 117.00, 113.46, 106.49, 60.19 (OCH_3), 56.00 (OCH_3), 52.19 ($C{=}OCH_3$) **IR:** ν_{max} (KBr) cm^{-1}:2893.33, 2764.11,2543.99, 2098.67, 1765.33, 1543.65, 1324.33, 1245.99, 1267.99, 1132.76, 1164.76, 1009.33, 900.43, 944.34, 875.34, 887.43, 664.32 **HRMS** (EI):. Found 381.1321 $(M+Na)^+$, $C_{20}H_{22}O_6Na$ requires 381.1314 **M.P.**: 186-188 °C

8.5.53 (*E*)-Methyl-3-(4-fluoro-3-methoxyphenyl)-2-(3,4,5-trimethoxyphenyl)acrylate [364]

To a microwave vial was added acrylic acid [313] (800 mg, 2.1 mmol), 4 mL $HCl_{(conc.)}$ and 3 mL methanol. The reaction was allowed to react under microwave irradiation for 30 min at a temperature of 105 °C. The microwave cap was removed and allowed to stir till the precipitate formed. The mixture was then filtered and the precipitate was then dried. The precipitate was purified *via* flash chromatography on silica gel to afford the product as a white solid. (401 mg, 46 %)

^{1}H-NMR (DMSO-d_6, 400MHz): 7.69 (s, 1H, C=CH), 7.06 (m, 1H, Ar-H), 6.82 (d, *J*= 7.5 Hz, 1H, Ar-H), 6.49 (s, 2H, Ar-H), 3.81 (s, 3H, OCH_3), 3.72 (s, 3H, $COOCH_3$), 3.71 (s, 9H, OCH_3) **^{13}C-NMR (DMSO-d_6, 100MHz)** 167.22 (C=O), 153.38 ($COCH_3$), 153.29 ($COOCH_3$), 153.29 ($COCH_3$), 151.88, 148.19, 148.08, 138.33, 137.22 (C=CH), 131.10, 128.06, 126.98 (C=CH), 126.92, 117.19, 117.00, 113.46, 106.49, 60.19 (OCH_3), 56.00 (OCH_3), 52.19 ($COOCH_3$) **IR:** ν_{max} (KBr) cm^{-1}: 2453.88, 2412.56, 2431.23, 1665.99, 1543.76, 1324.3, 1134.98, 1187,1, 1098.34, 1087.33, 987.34, 977.34, 900.34, 765.33, 760.98, 653.34 **HRMS** (EI):. Found 399.1214 $(M+Na)^+$, $C_{20}H_{21}O_6FNa$ requires 399.1220 **M.P.**: 192-196 °C

8.5.54 (*E*)-Methyl-3-(4-hydroxy-3-methoxyphenyl)-2-(3,4,5-trimethoxyphenyl)acrylate [365]

To a microwave vial was added acrylic acid [346] (502 mg, 1.31 mmol), 4 mL $HCl_{(conc.)}$ and 3 mL methanol. The reaction was allowed to react under microwave irradiation for 30 min at a temperature of 105 °C. The microwave cap was removed and allowed to stirr till the precipitate formed. The mixture was then filtered and the precipitate was then dried. The precipitate was purified *via* flash chromatography on silica gel (*n*-hexane:EtOAc, 2:1) to afford the product as a cream solid. (188 mg, 36 %)

^{1}H-NMR (DMSO-d_6, 400MHz): 7.59 (s, 1H, C=CH), 7.04 (s, 1H, Ar-H), 6.82 (d, *J*= 7.5 Hz, 1H, Ar-H), 6.63 (d, 1H, Ar-H), 6.54 (s, 1H, Ar-H), 6.46 (s, 2H, Ar-H), 3.74 (s, 3H, OCH_3), 3.72 (s, 3H, OCH_3), 3.70 (s, 3H, $COOCH_3$), 3.67 (s, 6H, OCH_3) **^{13}C-NMR (DMSO-d_6, 100MHz):** 167.55 (C=O), 153.18 ($COCH_3$), 149.11 ($COCH_3$), 145.87 ($COCH_3$), 139.82, 137.05 (C=CH), 131.48, 129.21, 126.73 (C=CH), 123.23, 117.25, 111.49, 106.67, 60.13 (OCH_3), 55.94 (OCH_3), 55.46 ($COOCH_3$) **IR:** ν_{max} (KBr) cm^{-1}: 2897.33, 2431.32, 1765.32, 1534.3, 1765.23, 1654.23, 1342.25, 1435.26,12 43.87, 908.55, 978.55, 876.54, 769.8, 876.0, 764.7, 755.8 **HRMS** (EI): Found 397.1260 $(M+Na)^+$, $C_{20}H_{22}O_7Na$ requires 397.1263 **M.P.**: 170-174 °C

8.6 Synthesis of the anastrozole derivative

8.6.1 Methyl-3,5-dimethylbenzoate [369][531]

A mixture of [368] (10 g, 66.58 mmol) and conc. HCl (25 mL) was dissolved in MeOH (50 mL) and heated at reflux. The mixture was monitored via TLC; after 3 h the majority of starting material had reacted. The organic solvent was removed *in vacuo* and the aq. layer was neutralised with 8 M NaOH (aq.). To the aq. layer was added EtOAc (100 mL) and the organic layer was washed with 8 M NaOH (aq.) (2 × 100 mL), water (20 mL), brine (20 mL) and dried over Na_2SO_4. Solvent was removed *in vacuo* to afford a white solid. This did not require further purification (9.3 g, 85%). Some of the starting material was recovered *via* the baseification of the organic layer (1.47 g).

^{1}H NMR ($CDCl_3$, 400 MHz) δ 7.68 (s, 2H, Ar-H), 7.21 (s, 1H, Ar-H), 3.92 (s, 3H, OCH_3), 2.38 (s, 6H, 2 × CH_3) **^{13}C NMR ($CDCl_3$, 100 MHz)** δ 167.0 (C=O), 137.6, 134.1 (C_q), 129.5 (C_q), 126.8, 51.6 (OCH_3), 20.7 (CH_3) **HRMS (EI):** 165.0910 $(M+H)^+$, $C_{10}H_{13}O_2$ requires 165.0910 **IR :** ν_{max} (KBr) cm^{-1}: 3441.8 (br.), 2951.3, 1722.7, 1607.8, 1436.9, 1315.8, 1220.9, 1116.4, 1020.8, 876.2, 768.1 **MP:** 31-33 °C

8.6.2 Methyl-3-(bromomethyl)-5-methylbenzoate [370][531]

To a solution of ester [369] (5 g, 29.62 mmol) in CCl_4 (20 mL) was added NBS (5.25 g, 29.62 mmol) and benzoyl peroxide (66.6 mg, 0.274 mmol). The solution was refluxed until the orange colour disappeared; the mixture was allowed to cool and reduced *in vacuo* to a cloudy viscous oil. The oil was dissolved in DCM (50 mL) and was then washed with saturated Na_2SO_3 (aq) (50 mL), water (2 × 50 mL), and brine (50 mL). The solution was dried (Na_2SO_4), filtered and solvent removed *in vacuo* to leave clear residues. The material was purified *via* flash chromatography on silica gel to afford two products as a white cloudy solid. (Gradient: EtOAc/*n*-hexane 1:20 to 1:10) (3.9 g, 54%)

^{1}H NMR ($CDCl_3$, 400 MHz) δ 7.88 (s, 1H, Ar-H), 7.81 (s, 1H, Ar-H), 7.41 (s, 1H, Ar-H), 4.50 (s, 2H, CH_2Br), 3.93 (s, 3H, OCH_3), 2.41 (s, 3H, CH_3) **^{13}C NMR ($CDCl_3$, 100 MHz)** δ 166.2 (C=O), 138.5 (C_q), 137.6 (C_q), 133.8, 130.2 (C_q), 129.8, 126.8, 51.8 (OCH_3), 32.3 (CH_2), 20.7 (CH_3) **HRMS (EI):** 243.0005 $(M+H)^+$, $C_{10}H_{12}{}^{79}BrO_2$ requires 243.0015 **IR :** ν_{max} (KBr) cm^{-1}: 3435.7 (br.), 2951.4, 1721.6, 1607.7, 1436.2, 1317.2, 1223.3. 1113.9, 1019.0, 769.6 **MP:** 46-49 °C

8.6.3 Methyl-3,5-*bis*(bromomethyl)benzoate [371]

The material was purified of [370] *via* flash chromatography on silica gel afforded the byproduct as a white cloudy solid. (Gradient: EtOAc/*n*-hexane 1:20 to 1:10) (2.1 g, 22%)

^{1}H NMR ($CDCl_3$, 400 MHz) δ 8.02 (s, 2H, Ar-H), 7.64 (s, 1H, Ar-H), 4.53 (s, 4H, 2 × CH_2Br), 3.96 (s, 3H, OCH_3) **^{13}C NMR ($CDCl_3$, 100 MHz)** δ 165.5 (C=O), 138.5 (C_q), 133.4, 130.9 (C_q), 129.6, 52.0 (OCH_3), 31.4 (CH_2) **HRMS (EI):** 320.9112 $(M+H)^+$, $C_{10}H_{11}{}^{79}Br_2O_2$ requires 320.9120 **IR :** ν_{max} (KBr) cm^{-1}: 3433.9 (br.), 2950.2, 1727.5, 1603.3, 1435.7, 1320.8, 1230.7, 995.1, 698.3**MP:** 44-46 °C

8.6.4 Methyl-3-(cyanomethyl)-5-methylbenzoate [372][531]

With vigorous stirring a mixture of [370] (9.7 g, 39.9 mmol), NaCN (2.34 g, 47.88 mmol) with MeOH (30 mL) and distilled water (10 mL) was stirred at RT overnight. The organic fraction was separated and washed with water (2 × 50 mL) and brine (50 mL) then dried (Na_2SO_4) and the solvent removed *in vacuo* to leave a red/orange oil. The material was purified *via* flash chromatography on silica gel to afford an off white cloudy solid. (Gradient: EtOAc/*n*-hexane 1:20 to 1:10) (6.5 g, 86%)

^{1}H NMR ($CDCl_3$, 400 MHz) δ 7.83 (s, 1H, Ar-H), 7.80 (s, 1H, Ar-H), 7.37 (s, 1H, Ar-H), 3.93 (s, 3H, OCH_3), 3.78 (s, 2H, CH_2), 2.42 (s, 3H, CH_3) **^{13}C NMR ($CDCl_3$, 100 MHz)** δ 166.1 (C=O), 139.0 (C_q), 132.6, 130.5, 129.8 (C_q), 129.5, 125.8, 117.1 (CN), 51.8 (OCH_3), 22.9 (CH_2), 20.7 (CH_3) **HRMS (EI):** 212.0673 $(M+Na)^+$, $C_{11}H_{11}NNaO_2$ requires 212.0687 **IR :** ν_{max} (KBr) cm^{-1}: 3427.8 (br.), 2948.5, 2236.7 (CN), 1721.9, 1605.6, 1455.7, 1434.6, 1316.8, 1223.3, 1111.8, 766.9, 696.5, 574.9 **MP:** 55-57 °C

8.6.5 Methyl-3-(2-cyanopropan-2-yl)-5-methylbenzoate [373][531]

Under inert conditions, [372] (3.5 g, 18.5 mmol) was dissolved in dry DMF (10 mL) to give a yellow solution. With stirring this solution was cooled to 0 °C under inert conditions and NaH (10 % in mineral oil, 1.11 g, 46.25 mmol) was added gradually and the mixture was left to stir at 0 °C for 15 min. Iodomethane (5.8 mL, 40.7 mmol) was then added dropwise. The resulting suspension was left to stir at room temperature for 16 h. Propan-2-ol (2.5 mL) was carefully added to the reaction mixture followed by CH_2Cl_2 (25 mL). The mixture was then washed with water (2 × 25 mL), brine (25 mL) and dried over Na_2SO_4 and solvent removed *in vacuo* to leave a red/orange oil. The material was purified *via* flash chromatography on silica gel to afford a light yellow solid. (Gradient: EtOAc/*n*-hexane 1:25 to 1:10) (2.3 g, 54%)

^{1}H NMR ($CDCl_3$, 400 MHz) δ 7.91 (s, 1H, Ar-H), 7.83 (s, 1H, Ar-H), 7.54 (s, 1H, Ar-H), 3.94 (s, 3H, OCH_3), 2.45 (s, 3H, CH_3), 1.76 (s, 6H, 2 × CH_3)**^{13}C NMR ($CDCl_3$, 100 MHz)** δ 166.3 (C=O), 141.4 (C_q), 138.7 (C_q), 130.3 (C_q), 130.2, 129.2, 123.8 (CN), 122.6, 51.8 (OCH_3), 36.6 ($C(CH_3)2$), 28.6 (CH_3), 20.9 (CH_3) **HRMS (EI):** 240.0986 $(M+Na)^+$, $C_{13}H_{15}NNaO_2$ requires 240.1000 **IR :** ν_{max} (KBr) cm^{-1}: 3429.8 (br.), 2950.6, 2237.7, 1732.1, 1603.9, 1440.7, 1306.5, 1231.9, 1120.1, 771.7 **MP:** 52-54 °C

8.6.6 Methyl-3-(bromomethyl)-5-(2-cyanopropan-2-yl)benzoate [374][531]

To a solution of ester (5 g, 29.62 mmol) [373] in CCl_4 (20 mL) was added NBS (5.25 g, 29.62 mmol) and benzoyl peroxide (66.6 mg, 0.274 mmol). The solution was refluxed until the orange colour disappeared; the mixture was allowed to cool and reduced *in vacuo* to afford a cloudy viscous oil. The oil was dissolved in DCM (50 mL) and was then washed with saturated Na_2SO_3 (aq) (50 mL), water (2 × 50 mL), and brine (50 mL). The solution was dried (Na_2SO_4), filtered and solvent removed *in vacuo* to leave clear residues. The material was purified *via* flash chromatography on silica gel to afford a white cloudy solid. (Gradient: EtOAc/*n*-hexane 1:20 to 1:10) (3.9 g, 54%)

^{1}H NMR ($CDCl_3$, 400 MHz) δ 8.06 (s, 2H, Ar-H), 7.75 (s, 1H, Ar-H), 4.55 (s, 2H, CH_2), 3.97 (s, 3H, OCH_3), 1.79 (s, 6H, 2 × CH_3) **^{13}C NMR ($CDCl_3$, 100 MHz)** δ 165.5 (C=O), 142.2 (C_q), 138.7 (C_q), 131.1 (C_q),

129.9, 129.2, 125.6, 123.4 (CN), (OCH_3), 36.7 ($C(CH_3)_2$), 31.5 (CH_2), 28.6 (CH_3) **HRMS (EI):** 318.0094 $(M+Na)^+$, $C_{13}H_{14}{}^{79}BrNNaO_2$ requires 318.0100 **IR :** ν_{max} (KBr) cm^{-1}: 3433.5 (br.), 2986.8, 2232.2, 1719.8, 1600.5, 1428.8, 1309.5, 1237.3, 997.8, 767.8, 699.1 **MP:** 57-59 °C

8.6.7 Methyl-3-((1*H*-1,2,4-triazol-1-yl)methyl)-5-(2-cyanopropan-2-yl)benzoate [375][531]

A mixture of compound [374] (350 mg, 1.30 mmol), (123 mg, 1.77 mmol), K_2CO_3 (163 mg, 1.18 mmol), KI (15 mg, 90.4 µmol) and acetone (5 mL) were placed in a sealed microwave reaction vessel. The reaction mixture was heated using microwave energy (120 °C) for 1h. The reaction mixture was allowed to cool and was checked by TLC to confirm that the majority of starting material had reacted. The mixture was filtered and the solvent was removed *in vacuo*. The residues were taken up in EtOAc (5 mL) and washed with water (3 × 5 mL), brine (5 mL) and dried over Na_2SO_4 and solvent removed *in vacuo* to leave a dark brown residue. The material was purified *via* flash chromatography on silica gel to afford the product a yellow solid. (Gradient: MeOH/DCM 1:99 to 1:20) (330 mg, 89%)
^{1}H NMR ($CDCl_3$, 400 MHz) δ 8.22 (s, 1H, NCHN), 8.11 (s, 1H, NCHN), 8.03 (s, 1H, Ar-H), 7.90 (s, 1H, Ar-H), 7.66 (s, 1H, Ar-H), 5.45 (s, 2H, CH_2), 3.94 (s, 3H, OCH_3), 1.76 (s, 6H, 2 × CH_3) **^{13}C NMR ($CDCl_3$, 100 MHz)** δ 165.4 (C=O), 152.0 (NCHN), 142.9 (NCHN), 142.6 (C_q), 135.7 (C_q), 131.4 (C_q), 128.9, 128.0, 125.9, 123.3 (CN), 52.4 (CH_2), 52.1 (OCH_3), 36.7 ($C(CH_3)_2$), 28.6 (CH_3) **HRMS (EI):** 307.1156 $(M+Na)^+$, $C_{15}H_{16}N_4NaO_2$ requires 307.1171 **IR :** ν_{max} (KBr) cm^{-1}: 3414.9 (br.), 3120.9, 2980.3, 2243.3 (CN), 1719.8, 1602.4, 1507.1, 1462.9, 1435.7, 1306.1, 1235.6, 1140.8, 1015.4, 763.1, 679.6 **MP:** 78-80 °C

8.6.8 3-((1*H*-1,2,4-Triazol-1-yl)methyl)-5-(2-cyanopropan-2-yl)benzoic acid [376]

To a mixture of [375] (500 mg, 1.76 mmol) and 2 M NaOH (aq.) (10 mL) was dissolved in MeOH (10 mL) and was heated to reflux. The mixture was monitored *via* TLC, after 1h all traces of starting material had reacted. The organic solvent was removed *in vacuo.* The residue was re-dissolved in EtOAc (20 mL) and the organic layer was washed with 2 M HCl (aq.) (2 × 20 mL), water (20 mL) and brine (20 mL) and dried over Na_2SO_4. Solvent was removed *in vacuo* to afford a pale yellow solid. This product did not require further purification (0.470 g, 99%),
^{1}H NMR (DMSO-d_6, 400 MHz) δ 13.28 (br. s, 1H, COOH), 8.74 (s, 1H, NCHN), 8.04 (s, 1H, NCHN), 8.01 (s, 1H, Ar-H), 7.79 (s, 1H, Ar-H), 7.77 (s, 1H, Ar-H), 5.56 (s, 2H, CH_2), 1.71 (s, 6H, 2 × CH_3) **^{13}C NMR (DMSO-d_6, 100 MHz)** δ 166.6 (C=O), 152.0 (NCHN), 144.6 (NCHN), 142.5 (C_q), 137.8 (C_q), 131.8 (C_q), 129.3, 128.0, 125.4, 124.2 (C_q), 51.4 (CH_2), 36.7 ($C(CH_3)_2$), 28.2 (CH_3) **HRMS (EI):** 271.1196 $(M+H)^+$, $C_{14}H_{15}N_4O_2$ requires 271.1190 **IR :** ν_{max} (KBr) cm^{-1}: 3367.7, 2984.5, 2237.0, 1723.5, 1605.7, 1507.3, 1434.7, 1306.5, 1235.8, 1078.2, 747.6 **MP:** 89-91 °C

8.6.9 Methyl 3-((1*H*-imidazol-1-yl)methyl)-5-(2-cyanopropan-2-yl)benzoate [377]

A mixture of compound [374] (500 mg, 1.69 mmol), imidazole (138 mg, 2.03 mmol), K_2CO_3 (281 mg, 2.03 mmol), KI (20 mg, 120 µmol) and acetone (5 mL) were placed in a microwave reaction vessel and then sealed. The reaction mixture was heated using microwave energy (120 °C) for 1h. The reaction mixture was allowed to cool and checked by TLC to confirm that majority of starting material had reacted. The mixture was filtered and the solvent was removed *in vacuo*. The residues were taken up in EtOAc (5 mL) and washed with water (3 × 5 mL), brine (5 mL) and dried over Na_2SO_4 and solvent removed *in vacuo* to leave a dark brown residues. The material was purified *via* flash chromatography on silica gel to afford the product as a yellow solid. (Gradient: MeOH/DCM 1:99 to 1:20) (385 mg, 67%)

^{1}H NMR ($CDCl_3$, 400 MHz) δ 8.09 (s, 1H, CH), 7.80 (s, 1H, CH), 7.66 (s, 1H, Ar-H), 7.53 (s, 1H, CH), 7.16 (s, 1H, Ar-H), 6.96 (s, 1H, Ar-H), 5.23 (s, 2H, CH_2), 3.94 (s, 3H, OCH_3), 1.75 (s, 6H, 2 × CH_3) **^{13}C NMR ($CDCl_3$, 100 MHz)** δ 165.4 (C=O), 142.6 (C_q), 137.2 (NCHN), 131.4 (C_q), 129.7, 128.2, 127.4, 125.6, 123.3 (CN), 52.1 (OCH_3), 49.9 (CH_2), 36.7 ($C(CH_3)_2$), 28.5 (CH_3) **HRMS (EI):** 284.1398 $(M+H)^+$, $C_{16}H_{18}N_3O_2$ requires 284.1394 **IR :** ν_{max} (KBr) cm^{-1}: 3367.7 (br.), 2984.5, 2237.0, 1723.5, 1605.7, 1507.3, 1434.7, 1306.5, 1233.8, 1078.2, 747.6 **MP:** 77-79 °C

8.6.10 1-(Benzyloxy)-4-(bromomethyl)benzene [382]

Compound [389] (4 g, 18.6 mmol) was dissolved in dry DCM and was cooled to 0 °C under a N_2 atmosphere. To this was added PBr_3 (5.03 g, 2.15 mL, 18.6 mmol) and the reaction mixture was allowed to stir at 0 °C and the reaction was monitored *via* TLC. After 1h, all traces of starting material had reacted the reaction mixture was worked up with the addition of saturated $NaHCO_3$ (20 mL). The reaction mixture was extracted with the addition of saturated $NaHCO_3$ (20 mL), water (2 × 50 mL), brine (50 mL) and dried over Na_2SO_4. The solvent was evaporated under reduced pressure to afford the product as a brown solid. (5.05 g, 98%)

^{1}H NMR ($CDCl_3$, 400 MHz) δ 7.40 - 7.49 (m, 4H, Ar-H), 7.33 - 7.39 (m, 3H, Ar-H), 6.94 - 7.00 (m, 2H, Ar-H), 5.10 (s, 2H, CH_2), 4.53 (s, 2H, CH_2) **^{13}C NMR ($CDCl_3$, 100 MHz)** δ 158.4 (COBn), 136.2 (C_q), 130.0 (C_q), 129.8, 128.2, 127.6, 127.0, 114.7, 69.6 (CH_2), 33.5 (CH_2Br) **HRMS (EI):** 197.0970 $(M-Br)^-$, $C_{14}H_{13}O$ requires 197.0972 **IR :** ν_{max} (KBr) cm^{-1}: 3418.7 (br.), 1638.4, 1616.9, 1508.9, 1221.9, 607.4 **MP:** 89-91 °C

8.6.11 1-(4-(Benzyloxy)benzyl)-1*H*-1,2,4-triazole [383]

A mixture of [382] (1 g, 3.61 mmol), 1,2,4-triazole (1.5 eq., 0.374 g, 5.41 mmol), K_2CO_3 (1.5 eq., 0.747 g, 5.41 mmol) and KI (0.05 eq., 30 mg, 0.180 mmol) was dissolved in acetone and refluxed for 16 h, under a dry atmosphere. The mixture was allowed to cool and was filtered and the solvent was evaporated under reduced pressure to afford a pale oil. The oil was then dissolved in EtOAc (30 mL) and was washed with 1 M NaOH (30 mL), water (2 × 50 mL), brine (50 mL) and dried over Na_2SO_4. The solvent was evaporated under reduced pressure to afford a pale yellow resin. The material was purified *via* flash chromatography on silica gel (*n*-Hexane:EtOAc, gradient 5:1 to 1:1) to afford the product as a white solid. (431 mg, 45%)

^{1}H NMR ($CDCl_3$, 400 MHz) δ 8.05 (s, 1H, CH), 7.99 (s, 1H, CH), 7.32 - 7.47 (m, 5H, Ar-H), 7.22 - 7.28 (m, 2H, Ar-H), 6.97 - 7.03 (m, 2H, Ar-H), 5.29 (s, 2H, CH_2), 5.09 (s, 2H, CH_2) **^{13}C NMR ($CDCl_3$, 100 MHz)** δ 158.6 (C-OBn), 151.6 (NCHN), 142.4 (NCHN), 136.1 (C_q), 129.2, 128.2, 127.7, 127.0, 126.2, 114.9, 69.6 (CH_2), 52.8 (CH_2) **HRMS (EI):** 288.1122 $(M+Na)^+$, $C_{16}H_{15}N_3NaO$ requires 288.1113 **IR :** ν_{max} (KBr) cm^{-1}: 3551.4, 3472.9, 3413.8, 3101.7, 1638.6, 1615.7, 1513.4, 1241.9, 1141.8, 1016.3, 744.5, 683.7 **MP:** 104-107 °C

8.6.12 General method for the introduction of the 1,2,4-triazole ring

To a solution of the specific alcohol (1 eq.) in toluene (65 mL) was added 1,2,4-triazole (3 eq.) and p-TSA (200 mg) and the mixture was refluxed with a Dean-Stark trap. The source of heating was an open vessel microwave reactor (90-200 W). The mixture was refluxed for 4h and then was allowed to cool. The solvent was evaporated under reduced pressure to afford bright green oil. The oil was redissolved in EtOAc (30 mL) and washed with water (20 mL), brine (10 mL) and dried over Na_2SO_4. The solvent was evaporated under reduced pressure to afford the crude product. The crude product was purified *via* flash chromatography over silica gel to afford the desired product.

8.6.13 4-((4-(Benzyloxy)phenyl)(1*H*-1,2,4-triazol-1-yl)methyl)benzonitrile [384]

As per general method 8.6.12, [396] (1 eq., 3 g, 9.51 mmol), 1,2,4-triazole (3 eq., 1.69 g, 24.5 mmol) and *p*-TSA (300 mg) were reacted. The fixed microwave was set to 95 W for the duration of the reaction. The material was purified *via* flash chromatography on silica gel (DCM : EtOAC, gradient 25:1 to 10:1) to afford a pale yellow solid (2.33 g, 67%)

^{1}H NMR ($CDCl_3$, 400 MHz) δ 8.07 (s, 1H, CH), 7.99 (s, 1H, CH), 7.68 (d, *J* = 8.53 Hz, 2H, Ar-H), 7.33 - 7.48 (m, 5H, Ar-H), 7.19 (d, *J* = 8.53 Hz, 2H, Ar-H), 7.11 - 7.16 (m, 2H, Ar-H), 6.98 - 7.05 (m, 2H, Ar-H), 6.75 (s, 1H, CH), 5.10 (s, 2H, CH_2) **^{13}C NMR ($CDCl_3$, 100 MHz)** δ 159.0 (COBn), 152.2 (NCHN), 143.4 (NCHN), 135.9 (C_q), 132.2, 129.7, 128.3, 128.0, 127.8 (C_q), 127.0, 117.8 (C_q), 115.1, 111.9 (C_q), 69.7 (CH_2), 66.4 (CH) **HRMS (EI):** 365.1408 $(M-H)^-$, $C_{21}H_{17}N_4O$ requires 365.1408 **IR :** ν_{max} (KBr) cm^{-1}: 3443.3, 3118.4, 2920.5, 2227.9, 1608.4, 1561.4, 1511.5, 1418.9, 1394.6, 1217.4, 1169.2, 1154.5, 1039.1, 686.9, 569.2 **MP:** 79-81 °C

8.6.14 4-((4-(2-Bromoethoxy)phenyl)(1*H*-1,2,4-triazol-1-yl)methyl)benzonitrile [386]

As per general method 8.6.12, [401] (1 eq., 1 g, 3.01 mmol), 1,2,4-triazole (3 eq., 623 mg, 9.03 mmol) and *p*-TSA (150 mg) were reacted. The fixed microwave was set to 90 W for the duration of the reaction. The material was purified *via* flash chromatography on silica gel (DCM : EtOAC, gradient 10:1 to 5:1) to afford a yellow solid (588 mg, 51%)

^{1}H NMR ($CDCl_3$, 400 MHz) δ 8.06 (s, 1H, CH), 8.01 (s, 1H, CH), 7.68 (d, *J* = 8.53 Hz, 2H, Ar-H), 7.19 (d, *J* = 8.03 Hz, 2H, Ar-H), 7.15 (d, *J* = 8.53 Hz, 2H, Ar-H), 6.95 (d, *J* = 8.50 Hz, 2H, Ar-H), 6.76 (s, 1H, CH), 4.31 (t, *J* = 6.02 Hz, 2H, CH_2), 3.66 (t, *J* = 6.27 Hz, 2H, CH_2) **^{13}C NMR ($CDCl_3$, 100 MHz)** δ 158.3 ($COCH_2$), 152.1 (NCHN), 143.3 (NCHN), 132.2, 129.7, 128.6 (C_q), 127.8, 117.8 (C_q), 114.9, 111.9 (C_q), 67.5 (CH_2), 66.2 (CH), 28.4 (CH_2) **HRMS (EI):** 381.0346 $(M-H)^-$, $C_{18}H_{14}BrN_4O$ requires 381.0356 **IR :** ν_{max} (KBr) cm^{-1}: 3479.7, 2957.7, 2927.6, 2851.5, 2228.6, 1681.9, 1609.2, 1508.4, 1244.6, 1174.2, 1072.8, 1017.3, 832.2 **MP:** 133-135 °C

8.6.15 4-((4-(2-(Methylamino)ethoxy)phenyl)(1*H*-1,2,4-triazol-1-yl)methyl)benzonitrile [387]

Methylamine (2 M in THF) (~20 eq., 8 mL, 16.74 mmol) was added to the bromide compound [386] (320 mg, 0.837 mmol) in THF (8 mL) and sealed in a high pressure tube. The reaction mixture was heated to 60 °C while stirring for 48 h. The reaction mixture was allowed sufficient time to cool, allowing the internal pressure to decrease prior to opening the pressure tube. The solvent was evaporated under reduced pressure. The oil was dissolved in DCM (30 mL) and was washed with an pH 10 aq. Solution* (30 mL). The pH 10 aq. Solution* was extracted with DCM (2 × 30 mL). The organic layers were combined and washed with water (50 mL), brine (50 mL) and dried over Na_2SO_4. The solvent was evaporated under reduced pressure to obtain brown oil. The material was purified *via* flash chromatography on silica gel (DCM : MeOH, gradient 100:1 to 50:1) to afford brown resin (245 mg, 88%)

* pH 10 aq. Solution = 6 g of $NaHCO_3$ and 6 g of Na_2CO_3 per 100 mL of water

^{1}H NMR ($CDCl_3$, 400 MHz) δ 8.05 (s, 1H, CH), 7.96 (s, 1H, CH), 7.67 (d, *J* = 8.53 Hz, 2H, Ar-H), 7.17 (d, *J* = 8.53 Hz, 2H, Ar-H), 7.12 (d, *J* = 8.53 Hz, 2H, Ar-H), 6.95 (d, *J* = 9.03 Hz, 2H, Ar-H), 6.74 (s, 1H, CH), 4.11 (t, *J* = 5.02 Hz, 2H, CH_2), 2.98 - 3.05 (m, 2H, CH_2), 2.54 (s, 3H, NCH_3), 2.26 (br. s., 1H, NH) **^{13}C NMR ($CDCl_3$, 100 MHz)** δ 159.0 ($COCH_2$), 152.2 (NCHN), 143.4 (C_q), 143.1 (NCHN), 132.2, 129.6,

128.0, 127.8 (C_q), 117.8 (C_q), 114.7, 111.8 (C_q), 66.6 (CH_2), 66.3 (CH), 50.0 (CH_2), 35.7 (NCH_3) **HRMS (EI):** 334.1676 $(M+H)^+$, $C_{19}H_{20}N_5O$ requires 334.1662 **IR :** ν_{max} (KBr) cm^{-1}: 3455.2, 3122.4, 2230.0, 1610.6, 1508.4, 1274.9, 1248.6, 1139.0, 1011.4, 910.8, 732.4, 678.5

8.6.16 (4-(Benzyloxy)phenyl)methanol [389]

4-Benzyloxybenzaldehyde [388] (5 g, 23.55 mmol) was dissolved in MeOH (50 mL) and was cooled to 0 °C. To this was added $NaBH_4$ (0.89 g, 23.53 mmol) in small portions and the reaction mixture was left to stir at 0 °C. The reaction was monitored *via* TLC; after 15 min all starting material had reacted. To the flask was added 1 M HCl (5 mL) and the solvent was evaporated under reduced pressure to obtain a white semi-solid. The semi-solid was redissolved in EtOAc (100 mL) and was extracted with water (2 × 50 mL), brine (50 mL) and dried over Na_2SO_4. The solvent was evaporated under reduced pressure to afford the product as a white solid. (4.99 g, 99%)

^{1}H NMR ($CDCl_3$, 400 MHz) δ 7.26 - 7.51 (m, 7H, Ar-H), 6.97 - 7.04 (m, 2H, Ar-H), 5.11 (s, 2H, CH_2), 4.64 (s, 2H, CH_2) **^{13}C NMR ($CDCl_3$, 100 MHz)** δ 157.9 (COBn), 136.5 (C_q), 132.9 (C_q), 128.2, 128.2, 128.0, 127.6, 127.5, 127.0, 114.5, 114.2, 69.6 (CH_2), 64.6 (CH_2OH) **HRMS (EI):** 237.0895 $(M+Na)^+$, $C_{14}H_{14}NaO_2$ requires 237.0891 **IR :** ν_{max} (KBr) cm^{-1}: 3410.5 (br.), 2865.9, 1611.2, 1512.9, 1382.1, 1245.4, 1172.8, 1006.9, 810.3, 740.6, 695.7 **MP:** 90-93 °C

8.6.17 4-(4-Methoxybenzoyl)benzonitrile *via* the intermediate (4-methoxyphenyl) zinc(II) bromide [393]

To a 3 necked round bottomed flask containing dry ACN (20 mL), placed under a nitrogen atmosphere, was added $CoBr_2$ (330 mg, 1.5 mmol), $ZnBr_2$ (340 mg, 1.5 mmol), bromobenzene (0.16 mL, 1.5 mmol), Zn dust (3.25 g, 50 mmol) and TFA (50 µL). The mixture was stirred for 15 min and to this was added 4-bromoanisole [390] (2.8 g, 1.88 mL, 15 mmol) and the reaction mixture was stirred for a further 30 min at RT. On assumption of 50% formation of [391], the [391] was taken directly to the next reaction. To the 3 necked round bottomed flask was added $Ni(acac)_2$ (0.1g, 3.89 mmol) and 4-cyanobenzyl chloride [392] (0.5 g, 3.125 mmol) and the mixture was stirred for 30 min at RT. The mixture was then filtered *via* celite and the solvent was evaporated under reduced pressure to afford a yellow resin. The resin was then re-dissolved in EtOAc (20 mL) and extracted with water (30 mL). The aq. layer was extracted with EtOAc (2 × 20 mL), the organic layer were combined and washed with brine (40 mL) and dried over Na_2SO_4. The solvent was evaporated under reduced pressure to afford a yellow resin. The material was purified *via* flash chromatography over silica gel (*n*-hexane:EtOAc, gradient 5:1 to 1:1) to afford the product as a pale yellow solid. (445 mg, 25%)

^{1}H NMR ($CDCl_3$, 400 MHz) δ 7.78 - 7.87 (m, 6H, Ar-H), 7.00 (d, *J* = 8.53 Hz, 2H, Ar-H), 3.92 (s, 3H, OCH_3) **^{13}C NMR ($CDCl_3$, 100 MHz)** δ 193.3 (C=O), 163.4 (COMe), 141.6 (C_q), 132.2, 131.8, 131.7, 129.5, 128.5 (C_q), 117.7, 114.7 (C_q), 113.0, 55.2 (OCH_3) **HRMS (EI):** 238.0859 $(M+H)^+$, $C_{15}H_{12}NO_2$ requires 238.0863 **IR :** ν_{max} (KBr) cm^{-1}: 3422.3 (br.), 2233.2 (CN), 1653.1, 1617.0, 1285.2, 1170.4, 764.1 **MP:** 166-168 °C

8.6.18 4-(4-Hydroxybenzoyl)benzonitrile [394]

Method A.

Compound [393] (300 mg, 1.26 mmol) and pyridine hydrochloride (1.45 g, 12.6 mmol) was heated to 210 °C for 20 min. The mixture while still hot was poured in H_2O (35 mL) and filtered. The filtrate was washed with water (20 mL) followed by *n*-hexane (20 mL) and the solid was placed in a vacuum oven

overnight. The off white solid was purified *via* flash chromatography on silica gel (n-hexane:EtOAc, gradient 5:1 to 1:1) to afford a pale yellow solid. (149 mg, 53%)

Method B.

Protected letrozole analogue [384] (400 mg, 1.09 mmol) and a small spatula tipful of $Pd(OH)_2$ (20%, 20 mg) were reacted for 60 min under a hydrogen atmosphere. The material was purified *via* flash chromatography over silica gel (DCM : EtOAC, gradient 10:1 to 5:1) to afford the product as a brown solid (200 mg, 66%)

^{1}H NMR (DMSO-d_6, 400 MHz) δ 10.60 (br. s., 1H, OH), 8.01 (d, *J* = 8.03 Hz, 2H, Ar-H), 7.80 (d, *J* = 8.03 Hz, 2H, Ar-H), 7.67 (d, *J* = 8.53 Hz, 2H, Ar-H), 6.91 (d, *J* = 8.53 Hz, 2H, Ar-H) **^{13}C NMR (DMSO-d_6, 100 MHz)** δ 193.1 (C=O), 162.7 (COH), 142.2 (C_q), 132.8, 132.5, 129.5, 126.9 (C_q), 118.3 (C_q), 115.5, 113.8 (C_q) **HRMS (EI):** 222.0557 $(M-H)^-$, $C_{14}H_8NO_2$ requires 222.0561 **IR :** ν_{max} (KBr) cm^{-1}: 3409.4 (br.), 2333.4 (CN), 1641.9, 1607.0, 1284.2, 1169.6, 764.1 **MP:** 78-81 °C

8.6.19 4-(4-(Benzyloxy)benzoyl)benzonitrile [395]

To a solution of [394] (80 mg, 0.358 mmol) dissolved in ACN (5 mL) under a N_2 atmosphere was added K_2CO_3 (51 mg, 0.370 mmol) and stirred at RT. To the reaction mixture was added benzyl bromide (0.63 mg, 0.43 mL, 0.37 mmol) the mixture was allowed to react overnight. The reaction mixture was filtered and the solvent was evaporated under reduced pressure to afford a yellow resin. The resin was re-dissolved in DCM (10 mL) and extracted with the addition of saturated $NaHCO_3$ (10 mL), water (2 × 10 mL), brine (10 mL) and dried over Na_2SO_4. The solvent was evaporated under reduced pressure to afford the product as a pale yellow solid. (98 mg, 88%)

^{1}H NMR ($CDCl_3$, 400 MHz) δ 7.76 - 7.89 (m, 6H, Ar-H), 7.35 - 7.50 (m, 5H, Ar-H), 7.08 (d, *J* = 8.80 Hz, 2H, Ar-H), 5.18 (s, 2H, CH_2) **^{13}C NMR ($CDCl_3$, 100 MHz)** δ 193.3 (C=O), 162.6 (COBn), 141.6 (C_q), 135.5 (C_q), 132.2, 131.7, 129.5, 128.7, 128.3, 127.9, 127.1 (C_q), 117.7 (C_q), 114.7, 114.3, 69.8 (CH_2) **HRMS (EI):** 314.1159 $(M+H)^+$, $C_{21}H_{16}NO_2$ requires 314.1176 **IR :** ν_{max} (KBr) cm^{-1}: 2234.7 (CN), 1642.2, 1593.2, 1567.8, 1257.7, 1144.0, 1005.6, 992.4, 840.7, 703.8 **MP:** 142-145 °C

8.6.20 4-((4-(Benzyloxy)phenyl)(hydroxy)methyl)benzonitrile [396]

Route A

Compound [395] (80 mg, 0.255 mmol) was dissolved in MeOH (5 mL) and was cooled to 0 °C. To this solution was added $NaBH_4$ (11 mg, 0.3 mmol) in small portions and the solution was left stir at 0 °C. The reaction was monitored *via* TLC; after 15 min all starting material had reacted. To the flask was added 1 M HCl (0.5 mL) and the solvent was evaporated under reduced pressure to obtain a white semi-solid. The semi-solid was redissolved in EtOAc (10 mL) and was extracted with water (2 × 5 mL), brine (5 mL) and dried over Na_2SO_4. The solvent was evaporated under reduced pressure to afford a white solid. (76 mg, 95%)

Route B

As per general method, 8.6.21, 4-bromobenzonitrile [389] (1 eq., 1.31 g, 7.2 mmol), n-BuLi (3.328 mL, 2.5 M) and 4-benzyloxybenzaldehyde (1 eq., 1.52 g, 7.2 mmol) were reacted. The material was purified *via* flash chromatography on silica gel (*n*-hexane:EtOAc, gradient 5:1 to 1:1) over silica gel to afford the product as a yellow solid (1.99 g, 88%)

^{1}H NMR ($CDCl_3$, 400 MHz) δ 7.64 (d, *J* = 8.53 Hz, 2H, Ar-H), 7.52 (d, *J* = 8.03 Hz, 2H, Ar-H), 7.33 - 7.47 (m, 5H, Ar-H), 7.25 (d, *J* = 8.53 Hz, 2H, Ar-H), 6.97 (d, *J* = 9.03 Hz, 2H, Ar-H), 5.84 (br s, 1H), 5.07 (s, 2H, CH_2) **^{13}C NMR ($CDCl_3$, 100 MHz)** δ 158.3 (COBn), 148.6 (C_q), 136.2 (C_q), 134.9 (C_q), 131.8, 128.2, 127.7, 127.6, 127.0, 126.5, 118.5 (C_q), 114.7, 110.5 (C_q), 74.7 (CH), 69.6 (CH_2) **HRMS (EI):** 338.1143 $(M+Na)^+$, $C_{21}H_{17}NNaO_2$ requires 338.1157 **IR :** ν_{max} (KBr) cm^{-1}: 3469.1, 2234.9, 1605.2, 1506.7, 1230.7, 1007.1, 826.7 **MP:** 89-92 °C

8.6.21 General method for the synthesis of the di-aryl methanol pharmacophore

To a solution of the specific aryl-bromide [388], [398], [406]-[407] (1 eq.) in THF (28 mL) at -78 °C under a N_2 atmosphere was added n-BuLi dropwise and the mixture was allowed stir for 1h. After 1h to this mixture was added the specific benzaldehyde [397], [400], [403]-[405] (1 eq.) in THF (16 mL) and the solution was allowed stir for 1.5h at -78 °C. The mixture was allowed to warm to RT and stirred for 2h. The solvent was evaporated under reduced pressure to obtain a brown oil. The oil was redissolved in DCM (50 mL) and was extracted with water (50 mL). The aq. layer was extracted with DCM (2 × 50 mL) and the organic layers were combined and washed with brine (50 mL) and dried over Na_2SO_4. The solvent was evaporated under reduced pressure to afford a brown oil. The brown oil was purified *via* flash chromatography on silica gel to afford the desired product.

8.6.22 4-(2-Bromoethoxy)benzaldehyde [400]

To a solution of 4-hydroxbenzaldehyde [399] (5 g, 40 mmol) dissolved in DMF (100 mL) under a N_2 atmosphere was added K_2CO_3 (13.82 mg, 100 mmol) and stirred at RT. To the mixture was added 1,2-dibromoethane (37.8 g, 17.35 mL, 201 mmol) and was allowed react overnight. The reaction mixture was filtered and the mixture was dissolved in EtOAc (100 mL) and extracted with water (3 × 100 mL), brine (10 mL) and dried over Na_2SO_4. The solvent was evaporated under reduced pressure to afford the product as a white solid. (5.70 mg, 63%)

^{1}H NMR ($CDCl_3$, 400 MHz) δ 9.91 (s, 1H, CHO), 7.87 (d, *J* = 8.50 Hz, 2H, Ar-H), 7.04 (d, *J* = 8.53 Hz, 2H, Ar-H), 4.39 (t, *J* = 6.27 Hz, 2H, CH_2), 3.69 (t, *J* = 6.02 Hz, 2H, CH_2) **^{13}C NMR ($CDCl_3$, 100 MHz)** δ 190.3 (CHO), 162.6 ($COCH_2$), 131.6, 130.0 (C_q), 114.4, 67.5 (CH_2), 28.1 (CH_2) **HRMS (EI):** 228.9563 $(M+H)^+$, $C_9H_{10}BrO_2$ requires 228.9559 **IR :** ν_{max} (KBr) cm^{-1}: 1687.3, 1601.8, 1577.9, 1507.8, 1252.5, 1162.6, 1009.3, 831.3 **MP:** 57-60 °C

8.6.23 4-((4-(2-Bromoethoxy)phenyl)(hydroxy)methyl)benzonitrile [401]

As per general method 8.6.21, 4-bromobenzonitrile (1 eq., 1.31 g, 7.2 mmol), n-BuLi (3.328 mL, 2.5 M) and [400] (1 eq., 1.65 g, 7.2 mmol) were reacted. The material was purified *via* flash chromatography on silica gel (*n*-Hexane:EtOAc, gradient 5:1 to 1:1) to afford the product was a yellow solid (1.93 g, 81%)

^{1}H NMR ($CDCl_3$, 400 MHz) δ 7.63 (d, *J* = 8.53 Hz, 2H, Ar-H), 7.51 (d, *J* = 8.03 Hz, 2H, Ar-H), 7.26 (d, *J* = 8.53 Hz, 2H, Ar-H), 6.90 (d, *J* = 9.03 Hz, 2H, Ar-H), 5.84 (s, 1H, CH), 4.29 (t, *J* = 6.27 Hz, 2H, CH_2), 3.64 (t, *J* = 6.27 Hz, 2H, CH_2), 2.54 (br. s., 1H, OH) **^{13}C NMR ($CDCl_3$, 100 MHz)** δ 157.5 ($COCH_2$), 148.6 (C_q), 135.4 (C_q), 131.8, 127.7, 126.5, 118.4 (C_q), 114.6, 110.5 (C_q), 74.6 (CH), 67.4 (CH_2), 28.6 (CH_2) **HRMS (EI):** 330.0142 $(M-H)^-$, $C_{16}H_{13}BrNO_2$ requires 330.0135 **IR :** ν_{max} (KBr) cm^{-1}: 3434.7, 2917.0, 2228.4, 1609.7, 1510.1, 1243.0, 1174.2, 1016.9, 830.1, 665.9 **MP:** 111-112 °C

8.6.24 4-((4-(2-(1*H*-1,2,4-Triazol-1-yl)ethoxy)phenyl)(1*H*-1,2,4-triazol-1-yl)methyl)benzonitrile [402]

The material was purified *via* flash chromatography on silica gel (DCM : EtOAC, gradient 5:1 to 1:1) to afford a clear resin (223 mg, 22%)

^{1}H NMR ($CDCl_3$, 400 MHz) δ 8.23 (s, 1H, CH), 8.04 (s, 1H, CH), 7.97 (s, 1H, CH), 7.96 (s, 1H, CH), 7.66 (d, *J* = 8.53 Hz, 2H, Ar-H), 7.16 (d, *J* = 8.53 Hz, 2H, Ar-H), 7.11 (d, *J* = 8.53 Hz, 2H, Ar-H), 6.88 (d, *J* = 9.03 Hz, 2H, Ar-H), 6.73 (s, 1H, CH), 4.59 (t, *J* = 5.02 Hz, 2H, CH_2), 4.35 (t, *J* = 4.77 Hz, 2H, CH_2) **^{13}C NMR ($CDCl_3$, 100 MHz)** δ 158.0 ($COCH_2$), 152.2 (NCHN), 151.7 (NCHN), 143.2 (NCHN), 143.1 (NCHN), 132.2, 129.7, 128.9 (C_q), 127.8, 117.8 (C_q), 114.7, 111.9 (C_q), 66.1 (CH), 65.3 (CH_2), 48.7 (CH_2) **HRMS (EI):** 370.1415 $(M-H)^-$, $C_{20}H_{16}N_7O$ requires 370.1422 **IR :** ν_{max} (KBr) cm^{-1}: 3408.2, 3121.4, 2230.0, 1610.6, 1508.4, 1274.9, 1248.6, 1139.0, 1011.4, 910.8, 732.4, 678.5

8.6.25 4-(Hydroxy-(3,4,5-trimethoxyphenyl)methyl)benzonitrile [408]

As per general method 8.6.21, 4-bromobenzonitrile (1 eq., 1.31 g, 7.2 mmol), *n*-BuLi (3.328 mL, 2.5 M) and 3,4,5-trimethoxybenzaldehyde (1 eq., 1.41 g, 7.2 mmol) were reacted. The material was purified *via* flash chromatography on silica gel (*n*-hexane:EtOAc, gradient 5:1 to 1:1) to afford the product as a yellow solid (1.98 g, 92%)

^{1}H NMR ($CDCl_3$, 400 MHz) δ 7.63 (d, *J* = 8.53 Hz, 2H, Ar-H), 7.52 (d, *J* = 8.03 Hz, 2H, Ar-H), 6.54 (s, 2H, Ar-H), 5.78 (s, 1H, CH), 3.82 (s, 9H, OCH_3), 2.83 (br. s, 1H, OH) **^{13}C NMR ($CDCl_3$, 100 MHz)** δ 152.9 (C_q), 148.3 (C_q), 138.2 (C_q), 137.0 (C_q), 131.8, 126.5, 118.4 (C_q), 110.6 (C_q), 103.1, 75.1 (CH), 60.4 (OCH_3), 55.6 (OCH_3) **HRMS (EI):** 298.1089 $(M-H)^-$, $C_{17}H_{16}NO_4$ requires 298.1079 **IR :** ν_{max} (KBr) cm^{-1}: 3471.6, 2940.3, 2228.3, 1593.8, 1504.9, 1462.5, 1420.2, 1328.7, 1235.5, 1127.5, 1004.6, 732.8 **MP:** 119-123 °C

8.6.26 4-((3-(Benzyloxy)-4-methoxyphenyl)(hydroxy)methyl)benzonitrile [409]

As per general method 8.6.21, 4-bromobenzonitrile (1 eq., 1.31 g, 7.2 mmol), *n*-BuLi (3.328 mL, 2.5 M) and 3-benzyloxy-4-methoxybenzaldehyde (1 eq., 1.74 g, 7.2 mmol) were reacted. The material was purified *via* flash chromatography on silica gel (*n*-Hexane:EtOAc, gradient 5:1 to 1:1) to afford the product as a cream solid (2.01 g, 81%)

^{1}H NMR ($CDCl_3$, 400 MHz) δ 7.56 (d, *J* = 8.03 Hz, 2H, Ar-H), 7.30 - 7.41 (m, 7H, Ar-H), 6.84 - 6.90 (m, 2H, Ar-H), 6.80 (s, 1H, Ar-H), 5.72 (s, 1H, CH), 5.07 - 5.16 (m, 2H, CH_2), 3.88 (s, 3H, CH_3), 2.63 (br. s., 1H, OH) **^{13}C NMR ($CDCl_3$, 100 MHz)** δ 149.1 (COBn), 148.5 (C_q), 147.7 (C_q), 136.3 (C_q), 134.9 (C_q), 131.7, 128.1, 127.4, 126.8, 126.4, 119.3, 118.5 (C_q), 112.2, 111.1, 110.4 (C_q), 74.7 (CH), 70.4 (CH_2), 55.6 (OCH_3) **HRMS (EI):** 368.1266 $(M+Na)^+$, $C_{22}H_{19}NNaO_3$ requires 316.1263 **IR :** ν_{max} (KBr) cm^{-1}: 3514.7, 2227.7, 1607.9, 1511.1, 1253.1, 1223.1, 1137.5, 1017.9, 820.8, 754.8, 598.3 **MP:** 105-107 °C

8.6.27 4-((3-(Benzyloxy)-4-methoxyphenyl)(1*H*-1,2,4-triazol-1-yl)methyl)benzonitrile [409a]

As per general method 8.6.12, [409] (1 eq., 600 mg, 1.73 mmol), 1,2,4-triazole (3 eq., 360 mg, 5.21 mmol) and *p*-TSA (150 mg) were reacted. The fixed microwave was set to 120 W for the duration of the reaction. The material was purified *via* flash chromatography on silica gel (DCM : EtOAC, gradient 25:1 to 10:1) to afford a yellow solid (507 mg, 74%)

^{1}H NMR ($CDCl_3$, 400 MHz) δ 8.04 (s, 1H, CH), 7.88 (s, 1H, CH), 7.61 (d, *J* = 8.53 Hz, 2H, Ar-H), 7.30 - 7.37 (m, 5H, Ar-H), 7.06 (d, *J* = 8.03 Hz, 2H, Ar-H), 6.91 (d, *J* = 8.03 Hz, 1H, Ar-H), 6.76 (dd, *J* = 1.51, 8.03 Hz, 1H, Ar-H), 6.64 (d, *J* = 13.55 Hz, 2H, Ar-H), 5.10 (s, 2H, CH_2), 3.92 (s, 3H, OCH_3) **^{13}C NMR ($CDCl_3$, 100 MHz)** δ 151.9 (NCHN), 150.0 (C_q), 147.8 (C_q), 143.1 (NCHN), 135.9 (C_q), 132.1, 128.2, 127.7, 127.7, 127.6, 126.7, 121.5, 117.8 (C_q), 114.2, 111.8, 111.3 (C_q), 70.6 (CH_2), 66.5 (CH), 55.6 (OCH_3) **HRMS (EI):** 395.1516 $(M-H)^-$, $C_{24}H_{19}N_4O_2$ requires 395.1508 **IR :** ν_{max} (KBr) cm^{-1}: 3032.8, 2934.1, 2228.9, 1607.9, 1513.3, 1441.9, 1264.0, 1139.2, 1015.1, 738.6 **MP:** 91-93 °C

8.6.28 (3-(Benzyloxy)-4-methoxyphenyl)(3,4,5-trimethoxyphenyl)methanol [410]

As per general method 8.6.21, 5-bromo-1,2,3-trimethoxybenzene (1 eq., 1.78 g, 7.2 mmol), n-BuLi (3.328 mL, 2.5 M) and 3-benzyloxy-4-methoxybenzaldehyde (1 eq., 1.74 g, 7.2 mmol) were reacted. The material was purified *via* flash chromatography on silica gel (*n*-hexane:EtOAc, gradient 5:1 to 1:1) to afford the product as an orange oil (2.51 g, 85%)

^{1}H NMR ($CDCl_3$, 400 MHz) δ 7.38 - 7.43 (m, 2H, Ar-H), 7.35 ($t_{(app)}$, *J* = 7.28 Hz, 2H, Ar-H), 7.27 - 7.32 (m, 1H, Ar-H), 7.02 (s, 1H, Ar-H), 6.88 - 6.94 (m, 2H, Ar-H), 6.54 (s, 2H, Ar-H), 5.68 (s, 1H, CH), 5.14 (s, 2H, CH_2), 3.90 (s, 3H, OCH_3), 3.85 (s, 3H, OCH_3), 3.81 (s, 6H, OCH_3), 2.31 (br. s., 1H, OH) **^{13}C NMR ($CDCl_3$, 100 MHz)** δ 152.7 (COBn), 148.7 (C_q), 47.5 (C_q), 139.0 (C_q), 136.6 (C_q), 136.5 (C_q), 135.8 (C_q), 128.0, 127.4, 126.9, 119.1, 112.1, 111.0, 102.8, 75.4 (CH), 70.4 (CH_2), 60.4 (OCH_3), 55.6 (OCH_3) **HRMS (EI):** 433.1613 $(M+Na)^+$, $C_{24}H_{26}NaO_6$ requires 433.1627 **IR :** ν_{max} (KBr) cm^{-1}: 3499.5, 2937.8, 1591.5, 1505.1, 1455.5, 1418.7, 1330.1, 1260.7, 1232.3, 1128.6, 1024.2, 735.5, 699.5

8.6.29 1-((3-(Benzyloxy)-4-methoxyphenyl)(3,4,5-trimethoxyphenyl)methyl)-1*H*-1,2,4-triazole [410a]

As per general method 8.6.12, [410] (1 eq., 1 g, 2.43 mmol), 1,2,4-triazole (3 eq., 0.5 g, 7.3 mmol) and *p*-TSA (150 mg) were reacted. The fixed microwave was set to 150 W for the duration of the reaction. The material was purified *via* flash chromatography on silica gel (DCM : EtOAC, gradient 25:1 to 10:1) to afford a yellow solid (718 mg, 64%)

^{1}H NMR ($CDCl_3$, 400 MHz) δ 8.02 (s, 1H, CH), 7.83 (s, 1H, CH), 7.29 - 7.35 (m, 5H, Ar-H), 6.89 (d, *J* = 8.53 Hz, 1H, Ar-H), 6.69 - 6.74 (m, 1H, Ar-H), 6.66 (d, *J* = 2.01 Hz, 1H, Ar-H), 6.59 (s, 1H, CH), 6.23 (s, 2H, CH_2), 5.08 (s, 2H, CH_2), 3.91 (s, 3H, OCH_3), 3.86 (s, 3H, OCH_3), 3.72 (s, 6H, OCH_3) **^{13}C NMR ($CDCl_3$, 100 MHz)** δ 153.0 (COBn), 151.8 (NCHN), 149.5 (C_q), 147.6 (C_q), 143.0 (NCHN), 137.4 (C_q), 136.0 (C_q), 133.2 (C_q), 129.3 (C_q), 128.1, 127.6, 126.8, 120.9, 113.7, 111.2, 104.3, 77.0 (CH_2), 70.5 (CH), 67.0 (OCH_3), 60.4 (OCH_3), 55.6 (OCH_3), 55.5 (OCH_3) **HRMS (EI):** 484.1844 $(M+Na)^+$, $C_{26}H_{27}N_3NaO_5$ requires 484.1848 **IR :** ν_{max} (KBr) cm^{-1}: 3440.8, 2938.0, 1591.6, 1517.8, 1464.0, 1416.7, 1253.3, 1127.5, 1006.7, 698.0 **MP:** 98-100 °C

8.6.30 4-((1*H*-1,2,4-Triazol-1-yl)(3,4,5-trimethoxyphenyl)methyl)benzonitrile [411]

As per general method 8.6.12, [408] (1 eq., 800 mg, 2.28 mmol), 1,2,4-triazole (3 eq., 473 mg, 6.85 mmol) and p-TSA (200 mg) were reacted. The fixed microwave was set to 100 W for the duration of the reaction. The material was purified *via* flash chromatography on silica gel (DCM : EtOAC, gradient 25:1 to 10:1) to afford a yellow solid (503 mg, 63%)

^{1}H NMR ($CDCl_3$, 400 MHz) δ 8.11 (s, 1H, CH), 8.09 (s, 1H, CH), 7.70 (d, *J* = 7.53 Hz, 2H, Ar-H), 7.23 (d, *J* = 8.03 Hz, 2H, Ar-H), 6.73 (s, 1H, CH), 6.40 (s, 2H, Ar-H), 3.87 (s, 3H, OCH_3), 3.74 - 3.83 (m, 6H, OCH_3) **^{13}C NMR ($CDCl_3$, 100 MHz)** δ 153.4 (C_q), 152.0 (NCHN), 143.3 (NCHN), 142.8 (C_q), 138.2 (C_q), 132.2,

131.2 (C_q), 128.0, 117.7 (C_q), 112.1 (C_q), 105.2, 66.9 (CH), 60.5 (OCH_3), 55.8 (OCH_3) **HRMS (EI):** 349.1306 $(M-H)^-$, $C_{19}H_{17}N_4O_3$ requires 349.1301 **IR :** ν_{max} (KBr) cm^{-1}: 2940.5, 2229.4, 1592.9, 1505.5, 1462.7, 1434.5, 1334.1, 1240.7, 1125.0, 1008.9, 731.5, 678.2 **MP:** 144-146 °C

8.6.31 General method for the debenzylation of the letrozole analogues

The protected letrozole analogues was dissolved in EtOAc (20 mL) and transferred to a 3-necked flask. To the flask was added $Pd(OH)_2$ (20%) and the reaction mixture was placed under a H_2 atmosphere. The reaction was monitored *via* TLC until the starting material had disappeared (10 – 60 min). The reaction mixture was filtered through celite and the solvent was evaporated under reduced pressure to obtain brown oil. The material was purified *via* flash chromatography over silica gel to afford the product.

8.6.32 4-((3-Hydroxy-4-methoxyphenyl)(1*H*-1,2,4-triazol-1-yl)methyl)benzonitrile [412]

As per 8.6.31, Protected letrozole analogue [412a] (190 mg, 0.479 mmol) and a small spatula tipful of $Pd(OH)_2$ (20%, 20 mg) were reacted for 60 min under a hydrogen atmosphere. The material was purified *via* flash chromatography over silica gel (DCM : EtOAC, gradient 10:1 to 5:1) to afford the product as a white solid (120 mg, 82%)

^{1}H NMR ($CDCl_3$, 400 MHz) δ 8.07 (s, 1H, CH), 8.05 (s, 1H, CH), 7.68 (d, *J* = 8.53 Hz, 2H, Ar-H), 7.19 (d, *J* = 8.03 Hz, 2H, Ar-H), 6.88 (d, *J* = 8.03 Hz, 1H, Ar-H), 6.77 (s, 1H, CH), 6.66 - 6.74 (m, 2H, Ar-H), 3.93 (s, 3H, OCH_3) **^{13}C NMR ($CDCl_3$, 100 MHz)** δ 151.8 (NCHN), 146.9 (C_q), 145.9 (C_q), 143.2 (NCHN), 132.2, 128.6 (C_q), 127.8, 120.2, 117.8 (C_q), 114.5, 111.9 (C_q), 110.5, 66.5 (CH), 55.6 (OCH_3) **HRMS (EI):** 305.1039 $(M-H)^-$, $C_{17}H_{13}N_4O_2$ requires 305.1039 **IR :** ν_{max} (KBr) cm^{-1}: 3123.7, 2937.2, 2842.3, 2230.0, 1609.6, 1592.4, 1505.9, 1442.2, 1278.1, 1132.7, 1022.9, 790.5 **MP:** 168-170 °C

8.6.33 5-((1*H*-1,2,4-Triazol-1-yl)(3,4,5-trimethoxyphenyl)methyl)-2-methoxyphenol [413]

Protected letrozole analogue [413a] (200 mg, 4.33 mmol) and a small spatula tipful of $Pd(OH)_2$ (20%, 20 mg) were reacted for 60 min a hydrogen atmosphere. The material was purified *via* flash chromatography over silica gel (DCM : EtOAC, gradient 10:1 to 5:1) to afford the product as a white solid (122 mg, 76%)

^{1}H NMR ($CDCl_3$, 400 MHz) δ 8.04 (s, 1H, CH), 7.97 (s, 1H, CH), 6.86 (d, *J* = 8.53 Hz, 1H, Ar-H), 6.76 (d, *J* = 2.01 Hz, 1H, Ar-H), 6.67 (dd, *J* = 2.01, 8.03 Hz, 1H, Ar-H), 6.61 (s, 1H, CH), 6.33 (s, 2H, Ar-H), 3.90 (s, 3H, OCH_3), 3.85 (s, 3H, OCH_3), 3.77 (s, 6H, OCH_3) **^{13}C NMR ($CDCl_3$, 100 MHz)** δ 153.1 (COH), 151.6 (NCHN), 146.5 (C_q), 145.6 (C_q), 143.0 (NCHN), 137.4 (C_q), 133.2 (C_q), 130.0 (C_q), 119.6, 114.2, 110.4, 104.5, 67.1 (CH), 60.4 (OCH_3), 55.7 (OCH_3), 55.5 (OCH_3) **HRMS (EI):** 394.1383 $(M+Na)^+$, $C_{19}H_{21}N_3NaO_2$ requires 394.1279 **IR :** ν_{max} (KBr) cm^{-1}: 3389.1, 2936.5, 1591.1, 1508.3, 1461.2, 1276.8, 1127.5, 1010.3 **MP:** 61-63 °C

8.7 Synthesis of endoxifen-acrylic acid conjugates

8.7.1 DCC coupling reagent

General method for the synthesis of endoxifen-acrylic acid conjugates (2 step syntheses)

A mixture of the required acrylic acid (1 eq., 0.154 mmol), DCC (1eq., 0.154 mmol, 32 mg), and HOBt (1eq., 0.154 mmol, 21 mg) was suspended in 3 mL of anhydrous DCM and stirred for 10 min under a nitrogen atmosphere. The silyl-protected endoxifen analogue (4-[(Z)-1-[4-(*tert*-Butyl-dimethyl-

silanyloxy)-phenyl]-2-[4-(2-methylamino-ethoxy)-phenyl]-but-1-enyl]-phenol) [197] (75 mg, 1 eq., 0.154 mmol) was dissolved in 3 mL of anhydrous DCM and slowly added to the mixture *via* syringe. Reaction was allowed stir for 24-48 h. Reaction was monitored *via* TLC. The reaction mixture was diluted to 15 mL with anhydrous DCM and filtered to remove DCU. The filtrate was evaporated to dryness under reduced pressure. Purification was not required at this step.

Silyl deprotection

The residue was dissolved in 3 mL THF and stirred under nitrogen environment. A solution of 0.1 M TBAF (2 eq.) was added to the mixture and allowed to stir for 24 h. The mixture was evaporated to dryness under reduced pressure. The residue was dissolved in DCM and was washed with 10 % HCl solution. The resulting organic phase was dried over sodium sulphate and evaporated to dryness under vacuum. The material was purified *via* flash chromatography on silica gel.

8.7.2 EDC coupling reagant

A mixture of the required acrylic acid (1.2 eq), EDC (1.4 eq.), and HOBt (1.4 eq.) was suspended in anhydrous dichloromethane (3 mL) and stirred for 10 min under a nitrogen atmosphere. The protected endoxifen (1 eq.) [197] was dissolved in anhydrous dichloromethane (3 mL) and slowly added to the mixture *via* syringe. Reaction was allowed stir for 16 h. Reaction was monitored *via* TLC. The reaction mixture was diluted to 15 mL with anhydrous dichloromethane. To this mixture, water (20 mL) was added. The aqueous phase was extracted with DCM (20 mL x3), brine (50ml), dried over Na_2SO_4 and evaporated to dryness in *vacuo* to yield the crude product. The material was purified *via* flash chromatography on silica gel. (DCM : EtOAc)

Silyl deprotection

The residue was dissolved in 3 mL THF and stirred under nitrogen environment. A solution of TBAF (1M in THF, 1 eq.) was added to the mixture and allowed to stir for 1 h. The mixture was evaporated to dryness under reduced pressure. The material was purified *via* flash chromatography over silica gel to afford the product. (DCM : EtOAc)

8.7.3 (*E/Z*)-3-(3-Hydroxy-4-methoxyphenyl)-N-(2-(4-((*Z*)-1-(4-hydroxyphenyl)-2-phenylbut-1-en-1-yl)phenoxy)ethyl)-N-methyl-2-(3,4,5-trimethoxyphenyl) acrylamide [414]

A) As per general method (8.7.1), the acrylic acid analogue [150] was reacted with endoxifen [197]. The crude mixture was then taken to the next step without further purification. The final product was purified *via* flash chromatography over silica gel (DCM:EtOAc, gradient 6:1 to 3:1) to afford the product as a brown resin (82 %)

B) As per general method (8.7.2), the acrylic acid [150] (1.2 eq., 177 mg, 0.492 mmol), EDC (1.4 eq., 110 mg, 0.572 mmol), and HOBt (1.4 eq., 77.6 mg, 0.572 mmol) was reacted with endoxifen [197] (1 eq., 200 mg, 0.41 mmol). The crude product was afforded as a brown resin. The material was purified *via* flash chromatography over silica gel (DCM:EtOAc, gradient 20:1 to 10:1) to afford the product as a white solid. (289 mg, 85%)*. The product was then deprotected. The protected compound (156 mg, 0.188 mmol) was dissolved in 3 mL THF and stirred under nitrogen environment. A solution of TBAF (1M in THF, 1 eq., 0.188 mL, 0.188 mmol) was added to the mixture and allowed to stir for 1 h. The mixture was evaporated to dryness under reduced pressure. The material was purified *via* flash chromatography over silica gel (DCM:EtOAc, gradient 6:1 to 3:1)to afford the product as a white solid. (130 mg, 97 %).

^{1}H-NMR 400MHz ($CDCl_3$): 6.40-7.20 (m, 38H, Ar-H), 3.34-4.33 (m, 32H, OCH_3, CH_2, NCH_2, OCH_2), 3.04-3.24 (m, 6H, NCH_3), 2.47-2.52 (m, 4H, CH_2), 0.90-0.96 (m, 6H,CH_3) **^{13}C-NMR 100MHz** ($CDCl_3$): 13.17, 13.20, 24.45, 25312, 28.62, 33.44, 48.72, 55.44, 55.57, 60.50, 65.71, 105.58, 105.58, 109.76, 112.65, 113.40, 113.93, 114.64, 115.01, 121.52, 125.46, 127.37, 127.39, 128.07, 129.25, 129.58, 130.17, 130.23, 131.55, 131.59, 135.20, 137.33, 140.12, 142.12, 144.68, 145.96, 145.98, 152.83, 153.72, 154.66, 156.62 **IR:** ν_{max} (KBr) cm^{-1}: 3379.5, 2933.2, 1735.1, 1606.3, 1581.7, 1505.9, 1238.9, 1124.6, 1026.5, 833.4 **HRMS** (EI): Found 738.3019 $(M+Na)^+$, $C_{44}H_{45}NO_8Na$ requires 738.3043. **MP:** 67-68 °C

* Found 852.3916 $(M+Na)^+$, $C_{50}H_{59}NO_8NaSi$ requires 852.3908

8.7.4 (*E/Z*)-3-(Benzo[d][1,3]dioxol-5-yl)-N-(2-(4-((*Z*)-1-(4-hydroxyphenyl)-2-phenylbut-1-en-1-yl)phenoxy)ethyl)-2-(4-methoxyphenyl)-N-methylacrylamide [415]

A) As per general method (8.7.1), the acrylic acid analogue [311] was reacted with endoxifen [197]. The crude mixture was then taken to the next step without further purification. The final product was purified *via* flash chromatography over silica gel (DCM:EtOAc, gradient 6:1 to 3:1) to afford the product as a brown resin (94%)

B) As per general method (8.7.2), the acrylic acid [311] (1.2 eq., 176 mg, 0.492 mmol), EDC (1.4 eq., 110 mg, 0.572 mmol), and HOBt (1.4 eq., 77.6 mg, 0.572 mmol) was reacted with endoxifen [197] (1 eq., 200 mg, 0.41 mmol). The crude product was afforded as a brown resin. The material was purified *via* flash chromatography over silica gel (DCM:EtOAc, gradient 20:1 to 10:1) to afford the product as a white solid. (261 mg, 83%)*. The product was then deprotected. The protected compound (142 mg, 0.185 mmol) was dissolved in 3 mL THF and stirred under nitrogen environment. A solution of TBAF (1M in THF, 1 eq., 0.185 mL, 0.185 mmol) was added to the mixture and allowed to stir for 1 h. The mixture was evaporated to dryness under reduced pressure. The material was purified *via* flash chromatography over silica gel (DCM:EtOAc, gradient 6:1 to 3:1) to afford the product as a white solid (109 mg, 91 %)

^{1}H NMR (400 MHz, $CDCl_3$) δ 6.99 - 7.24 (m, 17H, Ar-H, C=CH), 6.34 - 6.88 (m, 25H, Ar-H), 5.87 (s, 4H, CH_2), 4.00 - 4.26 (m, 4H, CH_2), 3.59 - 3.86 (m, 10H, OCH_3, CH_2), 2.96 - 3.13 (m, 6H, NCH_3), 2.38 - 2.54 (m, 4H, CH_2), 0.87 - 0.96 (m, 6H, CH_3) **^{13}C NMR (101 MHz, $CDCl_3$)** δ 172.8 (C=O), 160.7 ($COCH_3$), 159.3 ($COCH_3$), 158.3 (COH), 154.9 (C_q), 154.0 (C_q), 148.0, 147.3 (C_q), 147.3 (C_q), 147.2 (C_q), 147.1 (C_q), 142.6 (C_q), 140.9 (C_q), 137.8 (C_q), 135.7 (C_q), 135.4 (C_q), 131.98 (ArC), 131.96, 130.6 (ArC), 130.3 (ArC), 130.2 (ArC), 130.1 (ArC), 129.7 (ArC), 129.7 (ArC), 129.5 (ArC), 127.81 (ArC), 127.79 (ArC), 125.9 (ArC), 124.0 (ArC), 115.1 (ArC), 114.4 (ArC), 114.2 (ArC), 113.9 (ArC), 113.2 (ArC), 109.1 (ArC), 108.1 (ArC), 108.1 (ArC), 101.0 (ArC), 100.2 (OCH_2O), 65.9 (CH_2), 60.4 (CH_2), 55.2 (OCH_3), 47.6 (CH_2), 38.7 (NCH_3) 25.6 (CH_2), 13.6 (CH_3) **IR:** ν_{max} (KBr) cm^{-1}: 3239.3, 2929.9, 1735.6, 1605.7, 1508.4, 1244.2, 1036.7, 835.5 **HRMS** (EI): Found 676.2685 $(M+Na)^+$, $C_{42}H_{39}NO_6Na$ requires 676.2675. **MP:** 84-86 °C

* Found 790.3566 $(M+Na)^+$, $C_{48}H_{53}NO_6NaSi$ requires 790.3540

8.7.5 (*E/Z*)-N-(2-(4-((*E*)-1-(4-Hydroxyphenyl)-2-phenylbut-1-en-1-yl)phenoxy)ethyl)-3-(4-methoxy-3-nitrophenyl)-N-methyl-2-(3,4,5-trimethoxyphenyl)acrylamide [416]

A) As per general method (8.7.1), the acrylic acid analogue [312] was reacted with endoxifen [197]. The crude mixture was then taken to the next step without further purification. The final product was purified *via* flash chromatography over silica gel (DCM:EtOAc, gradient 6:1 to 3:1) to afford the product as a brown resin (54%)

B) As per general method (8.7.2), the acrylic acid [312] (1.2 eq., 191 mg, 0.492 mmol), EDC (1.4 eq., 110 mg, 0.572 mmol), and HOBt (1.4 eq., 77.6 mg, 0.572 mmol) was reacted with endoxifen [197] (1 eq., 200 mg, 0.41 mmol). The crude product was afforded as a brown resin. The material was purified *via* flash chromatography over silica gel (DCM:EtOAc, gradient 20:1 to 10:1) to afford the product as a white solid. (309 mg, 88 %)*. The product was then deprotected. The protected compound (182 mg, 0.212 mmol) was dissolved in 3 mL THF and stirred under nitrogen environment. A solution of TBAF (1M in THF, 1 eq., 0.212 mL, 0.212 mmol) was added to the mixture and allowed to stir for 1 h. The mixture was evaporated to dryness under reduced pressure. The material was purified *via* flash chromatography over silica gel (DCM:EtOAc, gradient 6:1 to 3:1) to afford the product as a white solid. (146 mg, 93 %).

^{1}H NMR (400 MHz, $CDCl_3$) δ 7.58 - 7.73 (m, 2H, Ar-H), 6.99 - 7.17 (m, 12H, Ar-H, C=CH), 6.09 - 6.88 (m, 24H, Ar-H), 4.01 - 4.28 (m, 4H, CH_2), 3.53 - 3.93 (m, 28H, CH_2, OCH_3), 2.99 - 3.20 (m, 6H, NCH_3), 2.36 - 2.50 (m, 4H, CH_2), 0.84 - 0.96 (m, 6H, CH_3) **^{13}C-NMR 100MHz** ($CDCl_3$): δ 172.8 (C=O), 172.7 (C=O), 157.2, 156.3, 155.9, 155.1, 154.1, 153.2, 142.7, 142.6, 141.2, 141.1, 140.9, 137.8, 137.7, 137.1, 136.7, 136.3, 135.7, 135.3, 132.1, 132.0, 130.8, 130.7, 129.7, 127.8, 125.9, 115.1, 114.4, 113.9, 113.1, 113.1, 105.3, 105.3, 66.7, 66.4, 65.1, 64.8, 60.9, 60.5, 56.1, 49.2, 48.3, 48.2, 37.7, 37.6, 35.7, 35.7, 35.2, 35.1, 34.2, 34.1, 32.1, 32.0, 31.6, 31.6, 29.1, 29.0 (CH_2), 13.7 (CH_3) **IR:** ν_{max} (KBr) cm^{-1}: 3240.6, 2933.8, 1733.9, 1606.5, 1505.9, 1238.4, 1126.7, 834.2 **HRMS** (EI): Found 743.2974 $(M-H)^-$, $C_{44}H_{43}N_2O_9$ requires 743.2974 **MP:** 77-78 °C

* Found 881.3841 $(M+Na)^+$, $C_{50}H_{58}N_2O_9NaSi$ requires 881.3809

8.7.6 (*E/Z*)-3-(3-Fluoro-4-methoxyphenyl)-N-(2-(4-((*Z*)-1-(4-hydroxyphenyl)-2-phenylbut-1-en-1-yl)phenoxy)ethyl)-N-methyl-2-(3,4,5-trimethoxyphenyl) acrylamide [417]

A) As per general method (8.7.1), the acrylic acid analogue [313] was reacted with endoxifen. The crude mixture was then taken to the next step without further purification. The final product was purified *via* flash chromatography over silica gel (DCM:EtOAc, gradient 6:1 to 3:1) to afford the product as a yellow resin (53%)

B) As per general method (8.7.2), the acrylic acid [313] (1.2 eq., 178 mg, 0.492 mmol), EDC (1.4 eq., 110 mg, 0.572 mmol), and HOBt (1.4 eq., 77.6 mg, 0.572 mmol) were reacted with endoxifen [197] (1 eq., 200 mg, 0.41 mmol). The crude product was afforded as a brown resin. The material was purified *via* flash chromatography over silica gel (DCM:EtOAc, gradient 20:1 to 10:1) to afford the product as a white solid. (262 mg, 77 %)*. The product was then deprotected. The protected compound (142 mg, 0.185 mmol) was dissolved in 3

mL THF and stirred under nitrogen environment. A solution of TBAF (1M in THF, 1 eq., 0.185 mL, 0.185 mmol) was added to the mixture and allowed to stir for 1 h. The mixture was evaporated to dryness under reduced pressure. The material was purified *via* flash chromatography over silica gel (DCM:EtOAc, gradient 6:1 to 3:1) to afford the product as a white solid. (119 mg, 90%).

^{1}H NMR (400 MHz, $CDCl_3$) δ 6.97 - 7.20 (m, 13H, Ar-H, C=CH), 6.03 - 6.94 (m, 25H, Ar-H), 4.00 - 4.27 (m, 4H, CH_2), 3.50 - 3.92 (m, 28H, CH_2, OCH_3), 2.97 - 3.22 (m, 6H, NCH_3), 2.37 - 2.52 (m, 4H, CH_2), 0.81 - 0.98 (m, 6H, CH_3) **^{13}C NMR (101 MHz, $CDCl_3$) δ** 171.7 (C=O), 155.0 (C_q), 154.1 (C_q), 153.5 (C_q), 152.9 (C_q), 150.5 (C_q), 147.44 (C_q), 147.41 (C_q), 147.3 (C_q), 147.2 (C_q), 142.6 (C_q), 142.5 (C_q), 141.0 (C_q), 137.7 (C_q), 136.6 (C_q), 135.6 (C_q), 135.3 (C_q), 132.0 (ArC), 132.0 (ArC), 130.7 (ArC), 130.6 (ArC), 129.7 (ArC), 129.6 (ArC), 128.2 (C_q), 127.8 (ArC), 127.8 (ArC), 125.9 (ArC), 116.8 (ArC), 116.8 (ArC), 116.7 (ArC), 115.0 (ArC), 114.3 (ArC), 113.9 (ArC), 113.1 (ArC), 112.7 (ArC), 105.9 (ArC), 66.1 (OCH_3), 60.9 (CH_2), 60.4 (OCH_3), 56.1 (CH_2), 56.0 (OCH_3), 50.8, 38.9 (NCH_3), 25.6 (CH_2), 13.60 (CH_3), 13.56 (CH_3) **IR:** ν_{max} (KBr) cm^{-1}: 3252.0, 2960.9, 2934.4, 1735.2, 1606.2, 1581.1, 1238.6, 1126.9, 1005.3, 834.7 **HRMS** (EI): Found 718.3170 $(M+H)^+$, $C_{44}H_{45}NO_7F$ requires 718.3142. **MP:** 77-78 °C

* Found 854.3890 $(M+Na)^+$, $C_{50}H_{58}FNO_7NaSi$ requires 854.3864

8.7.7 (*E/Z*)-N-(2-(4-((*Z*)-1-(4-Hydroxyphenyl)-2-phenylbut-1-en-1-yl)phenoxy)ethyl)-3-(4-methoxyphenyl)-N-methyl-2-(3,4,5-trimethoxyphenyl)acrylamide [418]

A) As per general method (8.7.1), the acrylic acid analogue [310] was reacted with endoxifen [197]. The crude mixture was then taken to the next step without further purification. The final product was purified *via* flash chromatography over silica gel (DCM:EtOAc, gradient 6:1 to 3:1) to afford the product as a brown resin (55%)

B) As per general method, the acrylic acid [310] (1.2 eq., 169 mg, 0.492 mmol), EDC (1.4 eq., 110 mg, 0.572 mmol) (8.7.2), and HOBt (1.4 eq., 77.6 mg, 0.572 mmol) was reacted with endoxifen [197] (1 eq., 200 mg, 0.41 mmol). The crude product was afforded as a brown resin. The material was purified *via* flash chromatography over silica gel (DCM:EtOAc, gradient 20:1 to 10:1) to afford the product as a white solid. (303 mg, 91 %). The product was then deprotected. The protected compound (185 mg, 0.235 mmol) was dissolved in 3 mL THF and stirred under nitrogen environment. A solution of TBAF (1M in THF, 1 eq., 0.235 mL, 0.235 mmol) was added to the mixture and allowed to stir for 1 h. The mixture was evaporated to dryness under reduced pressure. The material was purified *via* flash chromatography over silica gel (DCM:EtOAc, gradient 6:1 to 3:1) to afford the product as a white solid. (152 mg, 93 %).

^{1}H NMR (400 MHz, $CDCl_3$) δ 6.98 - 7.17 (m, 18H, Ar-H, C=CH), 6.21 - 6.87 (m, 22H, Ar-H), 4.02 - 4.26 (m, 4H, CH_2), 3.50 - 3.91 (m, 28H, CH_2, OCH_3), 3.00 - 3.22 (m, 6H, NCH_3), 2.39 - 2.49 (m, 4H, CH_2), 0.85 - 0.94 (m, 6H, CH_3) **^{13}C NMR (101 MHz, $CDCl_3$) δ** 173.4 (C=O), 159.3 (C-O-CH_2), 159.3 (C-OH), 155.1 (C_q), 154.1 (C_q), 153.3 (C_q), 142.6 (C_q), 142.5 (C_q), 141.0 (C_q), 140.9 (C_q), 137.7 (C_q), 135.6 (C_q), 135.2 (C_q), 132.0 (ArC), 131.9 (ArC), 130.9 (ArC), 130.9 (ArC), 130.7 (ArC), 130.6 (ArC), 130.1 (ArC), 129.7 (ArC), 129.6 (ArC), 127.8 (ArC), 127.8 (ArC), 127.6 (ArC), 125.9 (ArC), 115.0 (ArC), 114.3 (ArC), 113.9 (ArC), 113.6 (ArC), 113.5 (ArC), 113.1 (ArC), 106.0 (ArC), 60.9 (OCH_3), 60.4 (CH_2), 56.0 (OCH_3), 55.2 (OCH_3), 50.1 (CH_2), 39.1 (NCH_3), 28.9 (CH_2), 25.6 (CH_2), 13.61 (CH_3) **IR:** ν_{max} (KBr) cm^{-1}: 3426.3, 3250.8,

2933.8, 1736.3, 1605.7, 1508.5, 1240.2, 1127.3, 1030.7, 829.7 **HRMS** (EI): Found 722.3102 $(M+Na)^+$, $C_{44}H_{45}NO_7Na$ requires 722.3094. **MP:** 66-68 °C

* Found 851.4042 $(M+Na)^+$, $C_{50}H_{60}N_2O_7NaSi$ requires 851.4067

8.7.8 (*E/Z*)-2-(3,5-Dimethoxyphenyl)-N-(2-(4-((*Z*)-1-(4-hydroxyphenyl)-2-phenylbut-1-en-1-yl)phenoxy)ethyl)-N-methyl-3-(3,4,5-trimethoxyphenyl)acrylamide [419]

As per general method (8.7.1), the acrylic acid analogue [314] was reacted with endoxifen [197]. The crude mixture was then taken to the next step without further purification. The final product was purified *via* flash chromatography over silica gel (DCM:EtOAc, gradient 6:1 to 3:1) to afford the product as a brown resin (33%).

^{1}H-NMR 400MHz ($CDCl_3$): δ 7.17-6.37 (m, 38H, Ar-H, C=CH), 4.25-4.09 (m, 38H, OCH_3, NCH_2, OCH_2), 3.23-3.05 (m, 6H, NCH_3), 2.52-2.48 (m, 4H, CH_2), 0.94-0.91 (m, 6H, CH_3) **^{13}C-NMR 100MHz** ($CDCl_3$): δ 160.56 (C=O), 154.86, 153.90, 152.22, 152.20, 140.38, 137.34, 137.30, 131.56, 131.52, 130.20, 130.13, 129.97, 129.23, 127.38, 125.44, 114.67, 113.95, 113.47, 112.71, 106.28, 106.25, 100.06, 60.45 (OCH_3), 55.34 (OCH_3), 54.94 (OCH_3), 53.01, 48.70 (NCH_3), 33.41 (CH_2), 28.63 (CH_2), 28.54 (CH_2), 25.10 (CH_2), 24.45 (CH_2), 13.22 (CH_3), 13.17 (CH_3) **IR:** ν_{max} (KBr) cm^{-1}: 3167.5, 2935.3, 1737.4, 1581.6, 1505.6, 1233.1, 1125.0, 1003.7 834.9 **HRMS** (EI): Found 752.3223 $(M+Na)^+$, $C_{45}H_{47}NO_8Na$ requires 752.3199

8.7.9 (*E/Z*)-N-(2-(4-((*Z*)-1-(4-Hydroxyphenyl)-2-phenylbut-1-en-1-yl)phenoxy)ethyl)-N-methyl-2,3-bis(3,4,5-trimethoxyphenyl)acrylamide [420]

A) As per general method (8.7.1), the acrylic acid analogue [315] was reacted with endoxifen [197]. The crude mixture was then taken to the next step without further purification. The final product was purified *via* flash chromatography over silica gel (DCM:EtOAc, gradient 6:1 to 3:1) to afford the product as a brown resin (43%).

B) As per general method (8.7.2), the acrylic acid [197] (1.2 eq., 198 mg, 0.492 mmol)), EDC (1.4 eq., 110 mg, 0.572 mmol), and HOBt (1.4 eq., 77.6 mg, 0.572 mmol) was reacted with endoxifen [197] (1 eq., 200 mg, 0.41 mmol). The crude product was afforded as a brown resin. The material was purified *via* flash chromatography over silica gel (DCM:EtOAc, gradient 20:1 to 10:1) to afford the product as a white solid. (315 mg, 88%)*. The product was then deprotected. The protected compound (158 mg, 0.18 mmol) was dissolved in 3 mL THF and stirred under nitrogen environment. A solution of TBAF (1M in THF, 1 eq., 0.18 mL, 0.18 mmol) was added to the mixture and allowed to stir for 1 h. The mixture was evaporated to dryness under reduced pressure. The material was purified *via* flash chromatography over silica gel (DCM:EtOAc, gradient 6:1 to 3:1) to afford the product as a white solid. (128 mg, 94%).

^{1}H NMR (400 MHz, $CDCl_3$) δ 6.97 - 7.19 (m, 14H, Ar-H, C=CH), 6.30 - 6.89 (m, 24H, Ar-H), 4.02 - 4.27 (m, 4H, CH_2), 3.52 - 3.95 (m, 40H, OCH_3), 2.98 - 3.29 (m, 6H, NCH_3), 2.37 - 2.53 (m, 4H, CH_2), 0.83 - 0.96 (m, 6H, CH_3) **^{13}C NMR (101 MHz, $CDCl_3$)** δ 171.3 (C=O), 155.0 (C_q), 154.1 (C_q), 153.4 (C_q), 152.7 (C_q), 152.7 (C_q), 142.6 (C_q), 142.5 (C_q), 141.0 (C_q), 137.8 (C_q), 137.8 (C_q), 137.6 (C_q), 136.6 (C_q), 135.6 (C_q), 135.2 (C_q), 132.0 (ArC), 131.9 (ArC), 130.6 (ArC), 130.6 (ArC), 130.5 (ArC), 129.6 (ArC), 129.6 (ArC), 127.8 (ArC), 125.9 (ArC), 115.0 (ArC), 114.3 (ArC), 113.9 (ArC), 113.1 (ArC), 106.7 (ArC), 106.6 (ArC), 106.1 (ArC), 106.1 (ArC), 60.9 (CH_2), 60.82 (OCH_3), 60.81 (OCH_3), 60.4 (OCH_3), 56.1 (OCH_3), 55.8

(OCH_3), 53.4, 47.7, 39.0 (NCH_3) 29.1 (CH_2), 29.0 (CH_2), 13.6 (CH_3), 13.56 (CH_3) **IR:** ν_{max} (KBr) cm^{-1}: 3167.5, 2935.3, 1737.4, 1581.6, 1505.6, 1233.1, 1125.0, 1003.7 834.9 **HRMS** (EI): Found 782.3301 $(M+Na)^+$, $C_{46}H_{49}NO_9Na$ requires 782.3305. **MP:** 77-78 °C

* Found 898.4193 $(M+Na)^+$, $C_{52}H_{63}NO_9NaSi$ requires 896.4170

8.7.10 (*E/Z*)-2-(3,5-Dimethoxyphenyl)-3-(3-hydroxy-4-methoxyphenyl)-N-(2-(4-((*Z*)-1-(4-hydroxyphenyl)-2-phenylbut-1-en-1-yl)phenoxy)ethyl)-N-methylacrylamide [421]

As per general method (8.7.1), the acrylic acid analogue [316] was reacted with endoxifen [197]. The crude mixture was then taken to the next step without further purification. The final product was purified *via* flash chromatography over silica gel (DCM:EtOAc, gradient 6:1 to 3:1) to afford the product as a brown resin (54%).

^{1}H-NMR 400MHz ($CDCl_3$): δ 7.19-6.37 (m, 40H, Ar-H, C=CH), 4.24-3.60 (m, 26H, OCH_3, O-CH_2, N-CH_2), 3.18-3.04 (m, 6H, NCH_3), 2.53- 2.47 (m, 4H, CH_2), 0.95-0.91 (m, 6H, CH_3) **^{13}C-NMR 100MHz** ($CDCl_3$): δ 160.44 (C=O), 156.55, 154.65, 153.69, 146.00, 145.98, 144.60, 144.58, 142.17, 140.49, 140.38, 137.38, 135.30, 135.15, 131.56, 130.18, 129.25, 127.98, 127.38, 127.35, 125.44, 121.62, 115.01, 114.63, 113.90, 113.48, 112.74, 109.71, 106.29, 100.13, 55.40 (OCH_3), 54.89 (OCH_3), 53.00 (CH_2), 48.75(NCH_3), 33.41 (O-CH_2), 28.61 ($\underline{C}H_2$-CH_3), 28.55 ($\underline{C}H_2$-CH_3), 25.11 (CH_2), 24.45 (CH_2), 13.21 (CH_3), 13.18 (CH_3) **IR:** ν_{max} (KBr) cm^{-1}: 3379.5, 2933.2, 1735.1, 1606.3, 1581.7, 1505.9, 1238.9, 1124.6, 1026.5, 833.4 **HRMS** (EI): Found 708.2925 $(M+Na)^+$, $C_{43}H_{43}NO_7Na$ requires 708.2937.

8.7.11 (*E/Z*)-3-(3,4-dihydroxyphenyl)-N-(2-(4-((*Z*)-1-(4-hydroxyphenyl)-2-phenylbut-1-en-1-yl)phenoxy)ethyl)-N-methyl-2-(3,4,5-trimethoxyphenyl)acrylamide [422]

A) As per general method (8.7.1), the acrylic acid analogue [317] was reacted with endoxifen [197]. The crude mixture was then taken to the next step without further purification. The final product was purified *via* flash chromatography over silica gel (DCM:EtOAc, gradient 6:1 to 3:1) to afford the product as a brown resin (37%).

B) As per general method (8.7.2), the acrylic acid [317] (1.2 eq., 170 mg, 0.492 mmol), EDC (1.4 eq., 110 mg, 0.572 mmol), and HOBt (1.4 eq., 77.6 mg, 0.572 mmol) was reacted with endoxifen [197] (1 eq., 200 mg, 0.41 mmol). The crude product was afforded as a brown resin. The material was purified *via* flash chromatography over silica gel (DCM:EtOAc, gradient 20:1 to 10:1) to afford the product as a white solid. (237 mg, 71 %)*. The product was then deprotected. The protected compound (157 mg, 0.192 mmol) was dissolved in 3 mL THF and stirred under nitrogen environment. A solution of TBAF (1M in THF, 1 eq., 0.192 mL, 0.192 mmol) was added to the mixture and allowed to stir for 1 h. The mixture was evaporated to dryness under reduced pressure. The material was purified *via* flash chromatography over silica gel to afford the product as a white solid. (113 mg, 84 %).

^{1}H-NMR 400MHz ($CDCl_3$): δ 7.13-6.49 (m, 38H, Ar-H, C=CH), 4.22-3.52 (m, 26H, OCH_3, O-CH_2, N-CH_2), 3.04-2.94 (m, 6H, NCH_3), 2.47(m, 4H, CH_2), 1.32-1.28 (m, 6H, CH_3) **^{13}C-NMR 100MHz** ($CDCl_3$): δ 156.62, 154.66, 153.66, 152.88, 145.98, 145.96, 144.60, 142.12, 137.33, 135.20, 132.01, 131.54, 130.22, 130.10, 129.58, 129.25, 128.00, 127.32, 127.30, 125.46, 121.50, 115.10, 114.64, 114.05, 113.40, 112.65, 109.76, 105.58, 65.71, 55.57, 55.44, 48.72, 33.44, 28.62, 25.31, 24.54, 13.22, 13.17

IR: ν_{max} (KBr) cm^{-1}: 3250.6, 2930.1, 1735.4, 1605.6, 1605.1, 1244.1, 1037.1, 835.6 **HRMS** (EI): Found 724.2881 $(M+Na)^+$, $C_{43}H_{43}NO_8Na$ requires 724.2886. **MP:** 69-63 °C

* Found 838.3751$(M+Na)^+$, $C_{49}H_{57}NO_8NaSi$ requires 838.3742

8.7.12 (*E/Z*)-3-(3-Hydroxyphenyl)-N-(2-(4-((*Z*)-1-(4-hydroxyphenyl)-2-phenylbut-1-en-1-yl)phenoxy)ethyl)-N-methyl-2-(3,4,5-trimethoxyphenyl)acrylamide [423]

As per general method (8.7.1), the acrylic acid analogue [318] was reacted with endoxifen [197]. The crude mixture was then taken to the next step without further purification. The final product was purified *via* flash chromatography over silica gel (DCM:EtOAc, gradient 6:1 to 3:1) to afford the product as a brown resin (45%).

^{1}H-NMR 400MHz ($CDCl_3$): δ 7.15-6.38 (m, 40H, Ar-H, C=CH), 4.27-3.45 (m, 26H, OCH_3, N-CH_2, O-CH_2), 3.26-3.07 (m, 6H, NCH_3), 2.49-2.47 (m, 4H, CH_2), 0.94-0.91 (m, 6H, CH_3) **^{13}C-NMR 100MHz** ($CDCl_3$): δ 171.96, 171.90, 156.64, 155.82, 154.44, 153.53, 152.67, 142.16, 142.65, 140.66, 140.52, 137.24, 137.15, 136.42, 136.28, 135.92, 135.28, 134.91, 131.59, 131.55, 130.25, 130.18, 129.82, 129.50, 129.45, 129.23, 128.87, 127.40, 125.56, 120.82, 120.68, 115.64, 114.94, 114.62, 113.91, 113.40, 112.66, 105.56, 105.47, 105.49, 65.83, 66.46, 55.60, 55.41, 53.01, 47.46, 38.71, 38.63, 28.63, 28.55, 13.20, 13.17 **IR:** ν_{max} (KBr) cm^{-1}: 3250.6, 2930.1, 1735.4, 1605.6, 1605.1, 1244.1, 1037.1, 835.6 **HRMS** (EI): Found 708.2937 $(M+Na)^+$, $C_{43}H_{43}NO_7Na$ requires 708.2937

8.7.13 (*E/Z*)-3-(3,4-Dimethoxyphenyl)-N-(2-(4-((*Z*)-1-(4-hydroxyphenyl)-2-phenylbut-1-en-1-yl)phenoxy)ethyl)-N-methyl-2-(3,4,5-trimethoxyphenyl)acrylamide [424]

A) As per general method (8.7.1), the acrylic acid analogue [319] was reacted with endoxifen [197]. The crude mixture was then taken to the next step without further purification. The final product was purified *via* flash chromatography over silica gel (DCM:EtOAc, gradient 6:1 to 3:1) to afford the product as a brown resin (31%).

B) As per general method (8.7.2), the acrylic acid [319] (1.2 eq., 184 mg, 0.492 mmol)), EDC (1.4 eq., 110 mg, 0.572 mmol), and HOBt (1.4 eq., 77.6 mg, 0.572 mmol) was reacted with endoxifen [197] (1 eq., 200 mg, 0.41 mmol). The crude product was afforded as a brown resin. The material was purified *via* flash chromatography over silica gel (DCM:EtOAc, gradient 20:1 to 10:1) to afford the product as a white solid. (300 mg, 87 %). The product was then deprotected. The protected compound (176 mg, 0.21 mmol) was dissolved in 3 mL THF and stirred under nitrogen environment. A solution of TBAF (1M in THF, 1 eq., 0.21 mL, 0.21 mmol) was added to the mixture and allowed to stir for 1 h. The mixture was evaporated to dryness under reduced pressure. The material was purified *via* flash chromatography over silica gel (DCM:EtOAc, gradient 6:1 to 3:1) to afford the product as a white solid. (139 mg, 91 %).

^{1}H NMR (400 MHz, $CDCl_3$) δ 6.99 - 7.19 (m, 13H. Ar-H, C=CH), 6.29 - 6.87 (m, 25H, Ar-H), 5.89 (br. s., 1H, OH), 4.02 - 4.26 (m, 4H, CH_2), 3.51 - 3.87 (m, 34H, OCH_3, CH_2), 2.98 - 3.24 (m, 6H, NCH_3), 2.38 - 2.51 (m, 4H, CH_2), 0.85 - 0.95 (m, 6H, CH_3) **^{13}C NMR (101 MHz, $CDCl_3$)** δ 171.6 (C=O), 161.0 (C-OCH_2), 154.9 (C_q), 154.0 (C_q), 152.7 (C_q), 152.6 (C_q), 142.6 (C_q), 141.0 (C_q), 137.9 (C_q), 137.7 (C_q), 136.7 (C_q), 135.7 (C_q), 132.0 (ArC), 130.6 (ArC), 130.4 (C_q), 129.7 (ArC), 129.6 (ArC), 127.8 (ArC), 127.8 (ArC), 125.9 (ArC), 115.0 (ArC), 114.3 (ArC), 113.9 (ArC), 113.2 (ArC), 106.8 (ArC), 106.7 (ArC), 100.5 (ArC), 60.8 (CH_2), 60.4 (OCH_3), 55.8 (OCH_3), 55.4 (OCH_3), 38.9 (NCH_3), 25.6 (CH_2), 13.6 (CH_3), 13.6 (CH_3) **IR:**

ν_{max} (KBr) cm^{-1}: 3242.0, 2934.9, 2837.9, 2837.6, 1736.1, 1600.2, 1505.9, 1421.4, 1239.7, 1155.4 833.2 **HRMS** (EI): Found 752.3210 $(M+Na)^+$, $C_{45}H_{47}NO_8Na$ requires 752.3199 **MP:** 63-66 °C

* Found 866.4046 $(M+Na)^+$, $C_{51}H_{61}NO_8NaSi$ requires 866.4046

8.7.14 (*E/Z*)-N-(2-(4-((*Z*)-1-(4-Hydroxyphenyl)-2-phenylbut-1-en-1-yl)phenoxy)ethyl)-N-methyl-3-(2,3,4-trimethoxyphenyl)-2-(3,4,5-trimethoxyphenyl)acrylamide [425]

As per general method (8.7.1), the acrylic acid analogue [320] was reacted with endoxifen [197]. The crude mixture was then taken to the next step without further purification. The final product was purified *via* flash chromatography over silica gel (DCM:EtOAc, gradient 6:1 to 3:1) to afford the product as a brown resin (26%).

^{1}H-NMR 400MHz ($CDCl_3$): δ 7.16-6.43 (m, 36H, Ar-H, C=CH), 4.12-3.55 (m, 40H, OCH3, N-CH_2, O-CH_2), 3.12-3.10 (m, 6H, NCH_3), 2.50-2.47 (m, 4H, CH_2), 0.94-0.91 (t, 6H, J=7.5Hz CH_3) **^{13}C-NMR 100MHz** ($CDCl_3$): δ 170.7 (C=O), 155.0 (C_q), 154.2 (C_q), 153.4 (C_q), 152.7 (C_q), 152.7 (C_q), 142.6 (C_q), 142.5 (C_q), 141.0 (C_q), 137.8 (C_q), 137.8 (C_q), 137.6 (C_q), 136.6 (C_q), 135.6 (C_q), 135.2 (C_q), 132.0 (ArC), 131.9 (ArC), 130.6 (ArC), 130.6 (ArC), 130.5 (ArC), 129.6 (ArC), 129.6 (ArC), 127.8 (ArC), 125.9 (ArC), 115.0 (ArC), 114.3 (ArC), 113.9 (ArC), 113.1 (ArC), 106.7 (ArC), 106.6 (ArC), 106.1 (ArC), 106.1 (ArC), 60.9 (CH_2), 60.82 (OCH_3), 60.81 (OCH_3), 60.4 (OCH_3), 56.1 (OCH_3), 55.8 (OCH_3), 53.4, 47.7, 39.0 (NCH_3) 29.1 (CH_2), 29.0 (CH_2), 13.6 (CH_3), 13.56 (CH_3) **IR:** ν_{max} (KBr) cm^{-1}: 3167.5, 2935.3, 1737.4, 1581.6, 1505.6, 1233.1, 1125.0, 1003.7 834.9 **HRMS** (EI): Found 782.3310 $(M+Na)^+$, $C_{46}H_{49}NO_9Na$ requires 782.3305.

8.7.15 (*E/Z*)-2-(3-Hydroxy-4-methoxyphenyl)-N-(2-(4-((*Z*)-1-(4-hydroxyphenyl)-2-phenylbut-1-en-1-yl)phenoxy)ethyl)-N-methyl-3-(3,4,5-trimethoxyphenyl)acrylamide [426]

A) As per general method (8.7.1), the acrylic acid analogue [321] was reacted with endoxifen [197]. The crude mixture was then taken to the next step without further purification. The final product was purified *via* flash chromatography over silica gel (DCM:EtOAc, gradient 6:1 to 3:1) to afford the product as a brown resin (21%).

B) As per general method (8.7.2), the acrylic acid [321] (1.2 eq., 177 mg, 0.492 mmol)), EDC (1.4 eq., 110 mg, 0.572 mmol), and HOBt (1.4 eq., 77.6 mg, 0.572 mmol) was reacted with endoxifen [197] (1 eq., 200 mg, 0.41 mmol). The crude product was afforded as a brown resin. The material was purified *via* flash chromatography over silica gel (DCM:EtOAc, gradient 20:1 to 10:1) to afford the product as a white solid. (289 mg, 85%)*. The product was then deprotected. The protected compound (137 mg, 0.16 mmol) was dissolved in 3 mL THF and stirred under nitrogen environment. A solution of TBAF (1M in THF, 1 eq., 0.16 mL, 0.16 mmol) was added to the mixture and allowed to stir for 1 h. The mixture was evaporated to dryness under reduced pressure. The material was purified *via* flash chromatography over silica gel (DCM:EtOAc, gradient 6:1 to 3:1) to afford the product as a white solid. (103 mg, 90 %). (DCM : EtOAc)

^{1}H NMR (400 MHz, $CDCl_3$) δ 6.99 - 7.19 (m, 15H, Ar-H, C=CH), 5.85 - 6.88 (m, 23H, Ar-H), 4.05 - 4.29 (m, 4H, CH_2), 3.49 - 3.89 (m, 28H, OCH_3, CH_2), 2.91 - 3.25 (m, 6H, NCH_3), 2.39 - 2.50 (m, 4H, CH_2), 0.85 - 0.94 (m, 6H, CH_3) **^{13}C NMR (101 MHz, $CDCl_3$)** δ 171.2 (C=O), 168.7 (COH), 154.9 (C_q), 154.0 (C_q), 153.4 (C_q), 151.7 (C_q), 151.7 (C_q), 135.7 (C_q), 133.3 (ArC), 132.0 (ArC), 131.9 (ArC), 130.7 (ArC), 130.6 (ArC), 129.6 (ArC), 129.6 (ArC), 128.3 (ArC), 127.9 (ArC), 127.8 (ArC), 125.9 (ArC), 115.0 (ArC), 114.3

(ArC), 113.9 (ArC), 113.1 (ArC), 106.1 (ArC), 106.0 (ArC), 60.8 (OCH_3), 60.4 (CH_2), 56.3 (OCH_3), 56.2 (OCH_3), 56.1 (OCH_3), 55.9 (OCH_3), 29.04 (CH_2), 28.97 (CH_2), 13.6 (CH_3), 13.57 (CH_3) **IR:** ν_{max} (KBr) cm^{-1}: 3428.1, 2935.6, 2346.1, 1766.2, 1596.7, 1508.0, 1239.8, 1127.5, 835.0 **HRMS** (EI): Found 716.3226 $(M+H)^+$, $C_{44}H_{46}NO_8$ requires 716.3223 **MP:** 81-83 °C

* Found 852.3920 $(M+Na)^+$, $C_{50}H_{59}NO_8NaSi$ requires 852.3908

8.7.16 (*E/Z*)-3-(4-Hydroxy-3,5-dimethoxyphenyl)-N-(2-(4-((*Z*)-1-(4-hydroxyphenyl)-2-phenylbut-1-en-1-yl)phenoxy)ethyl)-N-methyl-2-(3,4,5-trimethoxyphenyl)acrylamide [427]

A) As per general method (8.7.1), the acrylic acid analogue [322] was reacted with endoxifen [197]. The crude mixture was then taken to the next step without further purification. The final product was purified *via* flash chromatography over silica gel (DCM:EtOAc, gradient 6:1 to 3:1) to afford the product as a brown resin (35 %).

B) As per general method (8.7.2), the acrylic acid [322] (1.2 eq., 194 mg, 0.492 mmol)), EDC (1.4 eq., 110 mg, 0.572 mmol), and HOBt (1.4 eq., 77.6 mg, 0.572 mmol) was reacted with endoxifen [197] (1 eq., 200 mg, 0.41 mmol). The crude product was afforded as a brown resin. The material was purified *via* flash chromatography over silica gel (DCM:EtOAc, gradient 20:1 to 10:1) to afford the product as a white solid. (315 mg, 76 %)*. The product was then deprotected. The protected compound (158 mg, 0.18 mmol) was dissolved in 3 mL THF and stirred under nitrogen environment. A solution of TBAF (1M in THF, 1 eq., 0.18 mL, 0.18 mmol) was added to the mixture and allowed to stir for 1 h. The mixture was evaporated to dryness under reduced pressure. The material was purified *via* flash chromatography over silica gel (DCM:EtOAc, gradient 6:1 to 3:1) to afford the product as a white solid. (128 mg, 94 %).

^{1}H NMR (400 MHz, $CDCl_3$) δ 6.97 - 7.19 (m, 14H, Ar-H, C=CH), 6.30 - 6.89 (m, 24H, Ar-H), 4.02 - 4.27 (m, 4H, CH_2), 3.52 - 3.95 (m, 34H, CH_2, OCH_3), 2.98 - 3.29 (m, 6H, NCH_3), 2.37 - 2.53 (m, 4H, CH_2), 0.83 - 0.96 (m, 6H, CH_3) **^{13}C NMR (101 MHz, $CDCl_3$)** δ 171.3 (C=O), 155.0 (C_q), 154.1 (C_q), 153.4 (C_q), 152.7 (C_q), 152.7 (C_q), 142.6 (C_q), 142.5 (C_q), 141.0 (C_q), 137.8 (C_q), 137.8 (C_q), 137.6 (C_q), 136.6 (C_q), 135.6 (C_q), 135.2 (C_q), 132.0 (ArC), 131.9 (ArC), 130.6 (ArC), 130.6 (ArC), 130.5 (ArC), 129.6 (ArC), 129.6 (ArC), 127.8 (ArC), 125.9 (ArC), 115.0 (ArC), 114.3 (ArC), 113.9 (ArC), 113.1 (ArC), 106.7 (ArC), 106.6 (ArC), 106.1 (ArC), 106.1 (ArC), 60.9 (CH_2), 60.82 (OCH_3), 60.81 (OCH_3), 60.4 (OCH_3), 56.1 (OCH_3), 55.8 (OCH_3), 53.4, 47.7, 39.0 (NCH_3) 29.1 (CH_2), 29.0 (CH_2), 13.6 (CH_3), 13.56 (CH_3) **IR:** ν_{max} (KBr) cm^{-1}: 3167.5, 2935.3, 1737.4, 1581.6, 1505.6, 1233.1, 1125.0, 1003.7 834.9 **HRMS** (EI): Found 768.3133 $(M+Na)^+$, $C_{45}H_{47}NO_9Na$ requires 768.3149. **MP:** 76-79 °C

* Found 882.4022 $(M+Na)^+$, $C_{51}H_{61}NO_9NaSi$ requires 882.4013

8.7.17 (*E/Z*)-N-(2-(4-((*E*)-1-(4-Hydroxyphenyl)-2-phenylbut-1-en-1-yl)phenoxy)ethyl)-N-methyl-3-(naphthalen-1-yl)-2-(3,4,5-trimethoxyphenyl)acrylamide [428]

A) As per general method (8.7.1), the acrylic acid analogue [324] was reacted with endoxifen [197]. The crude mixture was then taken to the next step with out further purification. The final product was purified *via* flash chromatography over silica gel (DCM:EtOAc, gradient 6:1 to 3:1) to afford the product as a brown resin (23%).

B) As per general method (8.7.2), the acrylic acid [324] (1.2 eq., 179 mg, 0.492 mmol)), EDC (1.4 eq., 110 mg, 0.572 mmol), and HOBt (1.4 eq., 77.6 mg, 0.572 mmol) were reacted with endoxifen [197] (1 eq., 200 mg, 0.41 mmol). The crude product was afforded as a brown resin. The material was purified *via* flash chromatography over silica gel (DCM:EtOAc, gradient 20:1 to 10:1) to afford the product as a white solid. (225 mg, 66 %). The product was then deprotected. The protected compound (109 mg, 0.131 mmol) was dissolved in 3 mL THF and stirred under nitrogen environment. A solution of TBAF (1M in THF, 1 eq., 0.131 mL, 0.131 mmol) was added to the mixture and allowed to stir for 1 h. The mixture was evaporated to dryness under reduced pressure. The material was purified *via* flash chromatography over silica gel (DCM:EtOAc, gradient 6:1 to 3:1) to afford the product as a white solid. (79 mg, 84%).

^{1}H-NMR 400MHz ($CDCl_3$): δ 6.05 - 8.12 (m, 45H, Ar-H, C=CH), 4.04 - 4.39 (m, 4H, CH_2), 3.86 - 4.03 (m, 4H, CH_2), 3.71 - 3.79 (m, 6H, OCH_3), 3.15 - 3.44 (m, 18H, OCH_3, NCH_3), 2.43 - 2.56 (m, 4H, CH_2), 0.83 - 1.02 (m, 6H, CH_3) **^{13}C-NMR 100MHz** ($CDCl_3$): δ 172.0 (C=O), 171.9 (C=O), 157.2 (COH), 156.3 (COH), 155.0 (COH), 154.1 (C_q), 153.0 (C_q), 152.9 (C_q), 152.9 (C_q), 142.7 (C_q), 142.6 (C_q), 141.1 (C_q), 141.0 (C_q), 139.7 (C_q), 137.7 (C_q), 136.4 (C_q), 135.7 (C_q), 133.5 (C_q), 133.3 (C_q), 132.1, 132.0, 131.7 (C_q), 130.7, 130.7, 129.8, 129.7, 128.6, 128.6, 128.3, 128.3, 128.0, 127.9, 127.9, 127.8, 127.2, 127.1, 127.1, 126.4, 126.1, 126.0, 125.6, 124.5, 115.1, 114.4, 113.9, 113.2, 106.0, 106.0, 105.8, 105.8, 66.4 (OCH_3), 66.2 (OCH_3), 65.0 (OCH_3), 60.8 (OCH_3), 60.5(CH_2), 55.9 (OCH_3), 55.8 (OCH_3), 55.6 (OCH_3), 50.1 (CH_2), 47.8 (CH_2), 47.7 (CH_2), 39.2 (NCH_3), 39.1 (NCH_3), 29.1 (CH_2), 29.0 (CH_2), 13.7 (CH_3), 13.6 (CH_3) **IR:** ν_{max} (KBr) cm^{-1}: 3251.3, 2932.6, 1736.1, 1605.6, 1505.7, 1239.8, 1126.9, 834.4 **HRMS** (EI): Found 742.3152 $(M+Na)^+$, $C_{47}H_{45}NNaO_6$ requires 742.3145 **MP:** 68-71 °C

* Found 856.4039 $(M+Na)^+$, $C_{53}H_{59}NO_6NaSi$ requires 856.4009

8.7.18 (*E/Z*)-N-(2-(4-((*E*)-1-(4-Hydroxyphenyl)-2-phenylbut-1-en-1-yl)phenoxy)ethyl)-N-methyl-3-(5-methylthiophen-2-yl)-2-(3,4,5-trimethoxyphenyl)acrylamide [429]

A) As per general method (8.7.1), the acrylic acid analogue [325] was reacted with endoxifen [197]. The crude mixture was then taken to the next step without further purification. The final product was purified *via* flash chromatography over silica gel (DCM:EtOAc, gradient 6:1 to 3:1) to afford the product as a brown resin (34%).

B) As per general method (8.7.2), the acrylic acid [325] (1.2 eq., 165 mg, 0.492 mmol)), EDC (1.4 eq., 110 mg, 0.572 mmol), and HOBt (1.4 eq., 77.6 mg, 0.572 mmol) was reacted with endoxifen [197] (1 eq., 200 mg, 0.41 mmol). The crude product was afforded as a brown resin. The material was purified *via* flash chromatography over silica gel (DCM:EtOAc, gradient 20:1 to 10:1) to afford the product as a white solid. (184 mg, 56 %). The product was then deprotected. The protected compound (101 mg, 0.126 mmol) was dissolved in 3 mL THF and stirred under nitrogen environment. A solution of TBAF (1M in THF, 1 eq., 0.126 mL, 0.126 mmol) was added to the mixture and allowed to stir for 1 h. The mixture was evaporated to dryness under reduced pressure. The material was purified *via* flash chromatography over silica gel (DCM:EtOAc, gradient 6:1 to 3:1) to afford the product as a white solid. (70 mg, 81%).

^{1}H-NMR 400MHz ($CDCl_3$): δ 5.82 - 7.24 (m, 34H, Ar-H, C=CH), 3.99 - 4.33 (m, 4H, CH_2), 3.72 - 3.96 (m, 22H, CH_2, OCH_3), 2.97 - 3.37 (m, 6H, NCH_3), 2.43 - 2.56 (m, 4H, CH_2), 2.37 (d, *J* = 3.26 Hz, 6H, CH_3), 0.94 (s, 6H, CH_3) **^{13}C-NMR 100MHz** ($CDCl_3$): δ 171.3 (C=O), 157.1 (COH), 156.3 (COH), 154.9, 154.0, 153.6, 153.6, 142.8, 142.7, 142.6, 142.5, 141.1, 141.0, 138.3, 138.2, 137.7, 136.9, 136.0, 135.8, 135.4, 132.3, 132.3, 132.0, 131.4, 131.4, 130.7, 129.7, 127.9, 125.9, 125.7, 125.6, 124.7, 124.7, 115.1, 114.4, 113.9, 113.2, 106.4, 106.3, 61.0 (OCH_3), 60.5 (CH_2), 56.3 (OCH_3), 56.2 (OCH_3), 38.7 (NCH_3) (CH_2), 29.1 (CH_2), 29.0 (CH_2), 15.5 (CH_3), 13.7 (CH_3), 13.6 (CH_3) **IR:** ν_{max} (KBr) cm^{-1}: 3255.2, 2961.7, 2932.4, 1735.6, 1605.5, 1580.2, 1505.9, 1238.4, 1120.2, 834.0 **HRMS** (EI): Found 712.2720 $(M+Na)^+$, $C_{42}H_{43}NNaO_6S$ requires 712.2709 **MP:** 83-84 °C

* Found 826.3604 $(M+Na)^+$, $C_{48}H_{57}NO_6NaSiS$ requires 826.3574

8.7.19 (*E/Z*)-3-(Furan-3-yl)-N-(2-(4-((*E*)-1-(4-hydroxyphenyl)-2-phenylbut-1-en-1-yl)phenoxy)ethyl)-N-methyl-2-(3,4,5-trimethoxyphenyl)acrylamide [430]

A) As per general method (8.7.1), the acrylic acid analogue [326] was reacted with endoxifen [197]. The crude mixture was then taken to the next step without further purification. The final product was purified *via* flash chromatography over silica gel (DCM:EtOAc, gradient 6:1 to 3:1) to afford the product as a brown resin (7 %).

B) As per general method (8.7.2), the acrylic acid [326] (1.2 eq., 149 mg, 0.492 mmol)), EDC (1.4 eq., 110 mg, 0.572 mmol), and HOBt (1.4 eq., 77.6 mg, 0.572 mmol) was reacted with endoxifen [197] (1 eq., 200 mg, 0.41 mmol). The crude product was afforded as a brown resin. The material was purified *via* flash chromatography over silica gel (DCM:EtOAc, gradient 20:1 to 10:1) to afford the product as a white solid. (89 mg, 32 %). The product was then deprotected. The protected compound (70 mg, 0.09 mmol) was dissolved in 3 mL THF and stirred under nitrogen environment. A solution of TBAF (1M in THF, 1 eq., 0.09 mL, 0.09 mmol) was added to the mixture and allowed to stir for 1 h. The mixture was evaporated to dryness under reduced pressure. The material was purified *via* flash chromatography over silica gel to afford the product as a white solid. (29 mg, 50 %).

^{1}H-NMR 400MHz ($CDCl_3$) δ 7.55 - 7.66 (m, 2H, Ar-H, CCH_2), 5.90 - 7.47 (m, 40H, Ar-H, C=CH, $C=C_2$), 4.00 - 4.32 (m, 4H, CH_2), 3.66 - 3.99 (m, 22H, OCH_3, CH_2), 3.02 - 3.30 (m, 6H, NCH_3), 2.43 - 2.56 (m, 4H, CH_2), 0.90 - 1.00 (m, 6H, CH_3) **^{13}C-NMR 100MHz** ($CDCl_3$): δ 171.7 (C=O), 154.8 (COH), 153.9 (COH), 153.4, 153.3, 143.6 ($C=CH_2$), 142.9 ($C=CH_2$), 142.9, 142.6, 142.5, 141.1, 137.9, 137.7, 135.8, 135.6, 135.5, 135.5, 132.0, 130.7, 130.7, 129.7, 127.9, 126.0, 121.3, 121.3, 115.1, 114.4, 113.9, 113.1, 110.0, 106.0, 105.9, 66.2 (OCH_3), 61.0 (OCH_3), 60.5 (CH_2), 56.1 (OCH_3), 39.1 (NCH_3), 29.1 (CH_2), 29.0 (CH_2), 13.7 (CH_3), 13.6 (CH_3) **IR:** ν_{max} (KBr) cm^{-1}: not enough compound **HRMS** (EI): Found 682.2791 $(M+Na)^+$, $C_{41}H_{41}NNaO_7$ requires 682.2781 **MP:** 81-84 °C

* Found 796.3656 $(M+Na)^+$, $C_{47}H_{55}NO_7NaSi$ requires 796.3645

8.8 Synthesis of endoxifen-cinnamic acid/-3-phenylpropanoic acid conjugates

General method for the synthesis of endoxifen-acrylic acid conjugates (2 step syntheses)

8.8.1 DCC coupling reagent

A mixture of the appropicate cinnamic acid/3-phenylpropanoic acid (1 eq., 0.154 mmol), DCC (1 eq., 0.154 mmol, 32 mg), and HOBt (1 eq., 0.154 mmol, 21 mg) were suspended in 3 mL of anhydrous dichloromethane and stirred for 10 min under a nitrogen atmosphere. The silyl-protected endoxifen analogue (4-[(E/Z)-1-[4-(*tert*-butyldimethylsilanyloxy)phenyl]-2-[4-(2-methylaminoethoxy)phenyl] but-1-enyl]phenol) [197] (75 mg, 1 eq., 0.154 mmol) was dissolved in 3 mL of anhydrous DCM and slowly added to the mixture *via* syringe. Reaction was allowed stir for 24-48 h. Reaction was monitored *via* TLC. The reaction mixture was diluted to 15 mL with anhydrous DCM and filtered to remove DCU. The filtrate was evaporated to dryness under reduced pressure. Purification was not done at this step.

Silyl deprotection

The above residue was dissolved in 3 mL THF and stirred under nitrogen environment. A solution of 0.1 M TBAF (2 eq.) was added to the mixture and allowed to stir for 24 h. The mixture was evaporated to dryness under reduced pressure. The residue was dissolved in DCM and was washed with 10 % HCl solution. The resulting organic phase was dried over sodium sulphate and evaporated to dryness under vacuum. The material was purified *via* flash chromatography on silica gel.

8.8.2 EDC coupling reagant

A mixture of the appropicate cinnamic acid/3-phenylpropanoic acid (1.2 eq), EDC (1.4 eq.), and HOBt (1.4 eq.) were suspended in anhydrous dichloromethane (3 mL) and stirred for 10 min under a nitrogen atmosphere. The protected endoxifen (1 eq.) [197] was dissolved in anhydrous dichloromethane (3 mL) and slowly added to the mixture *via* syringe. Reaction was allowed stir for 16 h. Reaction was monitored *via* TLC. The reaction mixture was diluted to 15 mL with anhydrous dichloromethane. To this mixture, water (20 mL) was added. The aqueous phase was extracted with DCM (20 mL x3), brine (50ml), dried over Na_2SO_4 and evaporated to dryness in *vacuo* to yield the crude product. The material was purified *via* flash chromatography on silica gel. (DCM : EtOAc)

Silyl deprotection

The above residue was dissolved in 3 mL THF and stirred under nitrogen environment. A solution of TBAF (1M in THF, 1 eq.) was added to the mixture and allowed to stir for 1 h. The mixture was evaporated to dryness under reduced pressure. The material was purified *via* flash chromatography over silica gel to afford the product.

8.8.3 (*E/Z*)-3-(3-Hydroxy-4-methoxyphenyl)-N-(2-(4-((*Z*)-1-(4-hydroxyphenyl)-2-phenylbut-1-en-1-yl)phenoxy)ethyl)-N-methylacrylamide [435]

A) As per general method (8.8.1), the cinnamic acid/3-phenylpropanoic acid analogue [342] was reacted with endoxifen [197]. The crude mixture was then taken to the next step with out further purification. The final product was purified *via* flash chromatography over silica gel (DCM:EtOAc, gradient 6:1 to 3:1) to afford the product as a brown resin (56 %)

B) As per general method (8.8.2), the cinnamic acid [342] (1.2 eq., 118 mg, 0.492 mmol), EDC (1.4 eq., 110 mg, 0.572 mmol), and HOBt (1.4 eq., 77.6 mg, 0.572 mmol) was reacted with endoxifen [197] (1 eq., 200 mg, 0.41 mmol). The crude product was afforded as a brown resin. The material was purified *via* flash chromatography over silica gel (DCM:EtOAc, gradient 10:1 to 10:1) to afford the product as a white solid. (236 mg, 87 %). The product was then deprotected. The protected compound (126 mg, 0.189 mmol) was dissolved in 3 mL THF and stirred under nitrogen environment. A solution of TBAF (1M in THF, 1 eq., 0.189

mL, 0.189 mmol) was added to the mixture and allowed to stir for 1 h. The mixture was evaporated to dryness under reduced pressure. The material was purified *via* flash chromatography over silica gel (DCM:EtOAc, gradient 6:1 to 3:1) to afford the product as a white solid. (94 mg, 94 %).

^{1}H NMR (400 MHz, $CDCl_3$) δ 7.51 - 7.65 (m, 2H, C=CH), 6.91 - 7.18 (m, 18H, Ar-H), 6.62 - 6.87 (m, 13H, Ar-H), 5.79 - 6.52 (m, 7H, Ar-H, C=CH), 3.94 - 4.21 (m, 4H, CH_2), 3.80 - 3.92 (m, 8H, OCH_3, 0.5 × CH_2), 3.75 (s, 2H, CH_2), 3.03 - 3.34 (m, 6H, NCH_3), 2.45 (m, 4H, CH_2), 0.90 (t, *J* = 7.04 Hz, 6H, CH_3) **^{13}C NMR (101 MHz, $CDCl_3$)** δ 171.3 (C=O), 167.2 (C-OH), 167.2 (C_q), 157.2 (C_q), 156.3 (C_q), 155.0 (C_q), 154.1 (C_q), 148.2 (C_q), 145.8 (C_q), 143.0 (C_q), 142.7 (C=CH), 142.6 (C=CH), 140.9 (C_q), 140.8 (C_q), 137.8 (C_q), 136.6 (C_q), 136.2 (C_q), 135.7 (C_q), 135.3 (C_q), 132.0 (ArC), 132.0 (ArC), 130.7 (ArC), 130.6 (ArC), 129.7 (ArC), 128.7 (ArC), 127.8 (ArC), 125.8 (ArC), 121.9 (C=CH), 121.6 (C=CH), 115.4 (ArC), 115.1 (ArC), 114.3 (ArC), 113.9 (ArC), 113.1 (ArC), 112.6 (ArC), 112.6 (ArC), 110.5 (ArC), 66.8 , 66.5, 60.4 (CH_2), 56.0 (OCH_3), 48.6, 37.7 (NCH_3), 35.1 (NCH_3), 29.01 (CH_2), 28.99 (CH_2), 13.6 (CH_3) **IR:** ν_{max} (KBr) cm^{-1}: 3385.2, 2930.3, 1733.5, 1643.5, 1584.1, 1504.9, 1265.0, 1238.0, 1025.7, 834.0 **HRMS** (EI): Found 572.2413 $(M+Na)^+$, $C_{35}H_{35}NO_5Na$ requires 572.2441 **MP:** 77-78 °C

* Found 686.3317 $(M+Na)^+$, $C_{46}H_{49}NO_5NaSi$ requires 686.3278

8.8.4 (*E/Z*)-3-(3-hydroxy-4-methoxyphenyl)-N-(2-(4-(1-(4-hydroxyphenyl)-2-phenylbut-1-en-1-yl)phenoxy)ethyl)-N-methylpropanamide [436]

A) As per general method (8.8.1), the cinnamic acid/3-phenylpropanoic acid analogue [343] was reacted with endoxifen [197]. The crude mixture was then taken to the next step with out further purification. The final product was purified *via* flash chromatography over silica gel (DCM:EtOAc, gradient 6:1 to 3:1) to afford the product as a brown resin (60%)

B) As per general method (8.8.2), the 3-phenylpropanoic acid [343] (1.2 eq., 96.5 mg, 0.492 mmol), EDC (1.4 eq., 110 mg, 0.572 mmol), and HOBt (1.4 eq., 77.6 mg, 0.572 mmol) was reacted with endoxifen [197] (1 eq., 200 mg, 0.41 mmol). The crude product was afforded as a brown resin. The material was purified *via* flash chromatography over silica gel (DCM:EtOAc, gradient 20:1 to 10:1) to afford the product as a white solid. (234 mg, 85 %). The product was then deprotected. The protected compound (144 mg, 0.219 mmol) was dissolved in 3 mL THF and stirred under nitrogen environment. A solution of TBAF (1M in THF, 1 eq., 0.219 mL, 0.219 mmol) was added to the mixture and allowed to stir for 1 h The mixture was evaporated to dryness under reduced pressure. The material was purified *via* flash chromatography over silica gel (DCM:EtOAc, gradient 6:1 to 3:1) to afford the product as a white solid. (108 mg, 90 %). (DCM : EtOAc)

^{1}H NMR (400 MHz, $CDCl_3$) δ 7.01 - 7.20 (m, 12H, Ar-H), 5.57 - 6.86 (m, 20H, Ar-H), 3.50 - 4.17 (m, 13H, OCH3, CH_2), 2.40 - 3.09 (m, 18H, NCH_3, CH_2), 0.75 - 0.98 (m, 6H, CH_3) **^{13}C NMR (101 MHz, CHLOROFORM-d)** δ 172.91 (C=O), 172.85 (C=O), 157.2 (C_q), 156.3 (C_q), 156.0 (C_q), 154.9 (C_q), 154.0 (C_q), 145.5 (C_q), 145.5 (C_q), 145.5 (C_q), 145.0 (C_q), 145.0 (C_q), 142.7 (C_q), 142.6 (C_q), 141.0 (C_q), 140.9 (C_q), 137.8 (C_q), 137.8 (C_q), 136.6 (C_q), 136.1 (C_q), 135.8 (C_q), 135.7 (C_q), 135.4 (C_q), 134.4 (C_q), 134.4 (C_q), 132.0 (ArC), 132.0 (ArC), 131.9 (ArC), 130.7 (ArC), 130.6 (ArC), 130.6 (ArC), 129.7 (ArC), 127.8 (ArC), 127.8 (ArC), 125.9 (ArC), 119.8 (ArC), 119.8 (ArC), 115.0 (ArC), 114.5 (ArC), 114.5 (ArC), 114.3 (ArC), 113.9 (ArC), 113.1 (ArC), 113.1 (ArC), 110.7 (ArC), 110.7 (ArC), 66.6 (CH_2), 66.3 (CH_2), 64.9

(CH_2), 60.4 (CH_2), 55.9 (OCH_3), 49.1 (CH_2), 48.2 (CH_2), 48.1 (CH_2), 37.6 (NCH_3), 37.5 (NCH_3), 35.6 (CH_2), 35.5 (CH_2), 35.1 (CH_2), 35.0 (CH_2), 34.2, 34.1, 31.0 (CH_2), 30.7 (CH_2), 30.6 (CH_2), 29.0 (CH_2), 28.98 (CH_2), 13.6 (CH_3), 13.6 (CH_3) **IR:** ν_{max} (KBr) cm^{-1}: 3441.1, 3232.4, 2931.4, 1733.5, 1607.4, 1508.4, 1272.0, 1239.5, 1029.1, 834.8 **HRMS** (EI): Found 574.2565 $(M+Na)^+$, $C_{35}H_{37}NO_5Na$ requires 574.2569 **MP:** 78-80 °C

* Found 688.3438 $(M+Na)^+$, $C_{41}H_{51}NO_5NaSi$ requires 688.3434

8.8.5 (*E/Z*)-N-(2-(4-((*Z*)-1-(4-Hydroxyphenyl)-2-phenylbut-1-en-1-yl)phenoxy)ethyl)-N-methyl-3-(3,4,5-trimethoxyphenyl)acrylamide [437]

A) As per general method (8.8.1), the cinnamic acid/3-phenylpropanoic acid analogue [344] was reacted with endoxifen [197]. The crude mixture was then taken to the next step without further purification. The final product was purified *via* flash chromatography over silica gel (DCM:EtOAc, gradient 6:1 to 3:1) to afford the product as a brown resin (36%)

B) As per general method (8.8.2), the cinnamic acid [344] (1.2 eq., 117 mg, 0.492 mmol), EDC (1.4 eq., 110 mg, 0.572 mmol), and HOBt (1.4 eq., 77.6 mg, 0.572 mmol) was reacted with endoxifen [197] (1 eq., 200 mg, 0.41 mmol). The crude product was afforded as a brown resin. The material was purified *via* flash chromatography over silica gel (DCM:EtOAc, gradient 20:1 to 10:1) to afford the product as a white solid. (258 mg, 89 %)*. The product was then deprotected. The protected compound (160 mg, 0.226 mmol) was dissolved in 3 mL THF and stirred under nitrogen environment. A solution of TBAF (1M in THF, 1 eq., 0.226 mL, 0.226 mmol) was added to the mixture and allowed to stir for 1 h. The mixture was evaporated to dryness under reduced pressure. The material was purified *via* flash chromatography over silica gel (DCM:EtOAc, gradient 6:1 to 3:1) to afford the product as a white solid. (127 mg, 95 %).

^{1}H NMR (400 MHz, $CDCl_3$) δ 7.53 - 7.65 (m, 2H, C=CH), 7.01 - 7.20 (m, 14H, Ar-H), 6.43 - 6.89 (m, 18H, Ar-H, C=CH), 3.96 - 4.25 (m, 4H, CH_2), 3.74 - 3.95 (m, 22H, OCH_3, CH_2), 3.04 - 3.39 (m, 6H, CH_3), 2.46 (q, *J* = 7.04 Hz, 4H, CH_2), 0.84 - 0.98 (m, 6H, CH_3) **^{13}C NMR (101 MHz, $CDCl_3$)** δ 169.6 (C=O), 153.4 (C_q), 153.3 (C_q), 132.0 (C=CH), 130.7 (ArC), 129.7 (ArC), 127.8 (ArC), 125.9 (ArC), 116.4 (C=CH), 115.0 (ArC), 114.3 (ArC), 113.9 (ArC), 113.1 (ArC), 105.4 (ArC), 105.1 (ArC), 60.9 (CH_2), 60.4 (OCH_3), 56.2 (OCH_3), 56.2 (OCH_3), 37.9 (NCH_3), 29.0 (CH_2), 13.6 (CH_3) **IR:** ν_{max} (KBr) cm^{-1}: 3236.4, 2934.8, 1735.4, 1647.2, 1583.3, 1506.3, 1240.5, 1089.3, 825.9 **HRMS** (EI): Found 616.2691 $(M+Na)^+$, $C_{37}H_{39}NO_6Na$ requires 616.2691 **MP:** 66-68 °C

* Found 730.3569 $(M+Na)^+$, $C_{43}H_{53}NO_6NaSi$ requires 730.3540

8.8.6 N-(2-(4-((*E/Z*)-1-(4-Hydroxyphenyl)-2-phenylbut-1-enyl)phenoxy)ethyl)-3-(3,4,5-trimethoxyphenyl)-N-methylpropanamide [438]

A) As per general method (8.8.1), the cinnamic acid/3-phenylpropanoic acid analogue [345] was reacted with endoxifen [197]. The crude mixture was then taken to the next step without further purification. The final product was purified *via* flash chromatography over silica gel (DCM:EtOAc, gradient 6:1 to 3:1) to afford the product as a brown resin (29%).

B) As per general method (8.8.2), the 3-phenylpropanoic acid [345] (1.2 eq., 118 mg, 0.492 mmol), EDC (1.4 eq., 110 mg, 0.572 mmol), and HOBt (1.4 eq., 77.6 mg, 0.572 mmol) was

reacted with endoxifen [197] (1 eq., 200 mg, 0.41 mmol). The crude product was afforded as a brown resin. The material was purified *via* flash chromatography over silica gel (DCM:EtOAc, gradient 20:1 to 10:1) to afford the product as a white solid. (264 mg, 92 %)*. The product was then deprotected. The protected compound (156 mg, 0.22 mmol) was dissolved in 3 mL THF and stirred under nitrogen environment. A solution of TBAF (1M in THF, 1 eq., 0.22 mL, 0.22 mmol) was added to the mixture and allowed to stir for 1 h. The mixture was evaporated to dryness under reduced pressure. The material was purified *via* flash chromatography over silica gel (DCM:EtOAc, gradient 6:1 to 3:1) to afford the product as a white solid. (121 mg, 93 %).

^{1}H-NMR 400MHz ($CDCl_3$): δ 7.18-6.40 (m, 30 H, Ar-H), 4.20-4.13 (m, 0.5*4H, CH_2-O-), 4.05-3.97 (m, 0.5*4H, CH_2-O-), 3.85-3.83 (m, 18H, OCH_3), 3.79-3.77 (m, 0.5*4H, CH_2-NCH_3), 3.70-3.66 (m, 0.5*4H, CH_2-NCH_3), 3.11 (s, 2/6*6H, NCH_3), 3.08 (s, 1/6*6H, NCH_3), 3.00 (s, 2/6*6H, NCH_3), 2.99 (s, 1/6*6H, NCH_3), 2.92 (m, 4H, Ar-CH_2), 2.80-2.58 (m, 4H, -O-CH_2), 2.52-2.48 (m, 4H, $\underline{CH_2}$-CH_3), 0.95 (t, 6H, 7.5Hz, CH_3) **^{13}C-NMR 100MHz** ($CDCl_3$): δ 170.27 (C=O), 156.75, 154.48, 152.11, 143.74, 142.31, 140.93, 137.36, 137.54, 136.15, 134.91, 133.88, 131.60, 131.40, 130.23, 130.19, 129.26, 127.38, 125.45, 119.39, 114.59, 144.10, 113.90, 113.42, 112.07, 110.25, 66.18 (CH_2-O), 65.88 (CH_2-O), 56.88(OCH_3), 55.64 (OCH_3), 55.50 (OCH_3), 53.01, 47.74 (CH_2), 37.24 (CH_3-N), 37.18 (CH_3-N), 35.17 (CH_2-O), 35.42 (CH_2-O), 33.86 (CH_3-N), 30.73 (CH_2-Ar), 30.52 (CH_2-Ar), 28.46 ($\underline{C}H_2$-CH_3), 13.60 (CH_3), 13.17 (CH_3) **IR:** ν_{max} (KBr) cm^{-1}: 3251.9, 2933.8, 1735.3, 1607.2, 1589.8, 1508.4, 1239.2, 1127.4, 833.7 **HRMS** (EI): Found 618.2691 $(M+Na)^+$, $C_{37}H_{41}NO_6Na$ requires 618.2691 **MP:** 73-75 °C

* Found 732.3723 $(M+Na)^+$, $C_{43}H_{55}NO_6NaSi$ requires 732.3696

8.9 Synthesis of Cyclofenil-acrylic acid conjugates

8.9.1 General method for the synthesis of protected Cyclofenil-acrylic acid conjugates

A mixture of the required acrylic acid [150] (1.2 eq), EDC (1.4 eq.), and HOBt (1.4 eq.) were suspended in anhydrous dichloromethane (3 mL) and stirred for 10 min under a nitrogen atmosphere. The appropriate cyclofenil derivative [216]-[220] (1 eq.) was dissolved in anhydrous dichloromethane (3 mL) and slowly added to the mixture *via* syringe. The reaction was allowed stir for 16 h. The reaction was monitored *via* TLC. The reaction mixture was diluted to 15 mL with anhydrous dichloromethane. To this water (20ml) was added. The aqueous phase was extracted with DCM (20ml x3), brine (50ml), dried over Na_2SO_4 and evaporated to dryness in *vacuo* to yield the crude product. The material was purified *via* flash chromatography on silica gel. (DCM : EtOAc)

8.9.2 (*E*)-N-(2-(4-((4-((*tert*-Butyldimethylsilyl)oxy)phenyl)(cyclopentylidene)methyl) phenoxy)ethyl)-3-(3-hydroxy-4-methoxyphenyl)-N-methyl-2-(3,4,5-trimethoxyphenyl) acrylamide [439]

As per general method (8.9.1), the acrylic acid [150] (1.2 eq., 196 mg, 0.54 mmol), EDC (1.4 eq., 120 mg, 0.63 mmol), and HOBt (1.4 eq., 85 mg, 0.63 mmol) were reacted with protected cyclofenil derivative [216] (1 eq., 200 mg, 0.45 mmol). The product was obtained as a brown resin. The material was purified *via* flash chromatography on silica gel (DCM:EtOAc, gradient 15:1 to 10:1) to afford the product as a yellow solid (284 mg, 81%)

^{1}H NMR ($CDCl_3$, 400 MHz) δ 6.97 - 7.16 (m, 4H, Ar-H, C=CH), 6.52 - 6.88 (m, 10H, Ar-H), 4.25 (m, 1H, 0.5 × OCH_2), 3.60 - 3.92 (m, 15H, 0.5 × OCH_2, NCH_2, 4 × OCH_3), 3.08 - 3.23 (m, 3H, NCH_3), 2.40 (s, 4H,

2 × CH_2), 1.69 (s, 4H, 2 × CH_2), 1.00 (s, 9H, 3 × CH_3), 0.22 (s, 6H, 2 × CH_3) **^{13}C NMR ($CDCl_3$, 100 MHz)** δ 169.0 (C=O), 153.2 (C-O-CH_2), 152.8 (C-O-Si), 145.8 (C_q), 144.6 (C_q), 141.8 (C_q), 129.9, 129.7, 118.9, 115.0, 113.2, 109.7, 105.5, 66.0 (CH_2), 60.5 (OCH_3), 55.4 (OCH_3), 38.6 (CH_2), 32.8 (CH_2), 26.5 (CH_2), 25.2 (CH_3), 17.7 ($\underline{C}(CH_3)_3$), -4.8 (CH_3) **HRMS (EI):** Found 780.3922 $(M+H)^+$, $C_{46}H_{58}NO_8Si$ requires 780.3926. **IR :** ν_{max} (KBr) cm^{-1}: 3350.9 (br.), 2954.2, 2936.7, 2859.3, 1603.9, 1581.5, 1505.9, 1463.8, 1242.5 (br.), 1127.1, 912.2 **MP:** 87-89 °C

8.9.3 (*E*)-N-(2-(4-((4-((*tert*-Butyldimethylsilyl)oxy)phenyl)(cyclon-hexaneylidene) methyl)phenoxy)ethyl)-3-(3-hydroxy-4-methoxyphenyl)-N-methyl-2-(3,4,5-trimethoxyphenyl)acrylamide [440]

As per general method (8.9.1), the acrylic acid [150] (1.2 eq., 189 mg, 0.526 mmol)), EDC (1.4 eq., 118 mg, 0.616 mmol), and HOBt (1.4 eq., 83 mg, 0.616 mmol) were reacted with protected cyclofenil derivative [217] (1 eq., 200 mg, 0.44 mmol). The product was obtained as a brown resin. The material was purified *via* flash chromatography on silica gel (DCM:EtOAc, gradient 15:1 to 10:1) to afford the product as a yellow solid (272 mg, 78%)

^{1}H NMR ($CDCl_3$, 400 MHz) δ 6.90 - 7.09 (m, 4H, Ar-H, C=CH), 6.52 - 6.85 (m, 10H, Ar-H), 4.17 - 4.29 (m, 1H, 0.5 × OCH_2), 3.57 - 3.91 (m, 15H, 0.5 × OCH_2, NCH_2, 4 × OCH_3), 3.07 - 3.26 (m, 3H, NCH_3), 2.18 - 2.30 (m, 4H, 2 × CH_2), 1.52 - 1.69 (m, 6H, 3 × CH_2), 1.00 (s, 9H, 3 × CH_3), 0.21 (s, 6H, 2 × CH_3) **^{13}C NMR ($CDCl_3$, 100 MHz)** δ 170.0 (C=O), 153.3 (C-O-CH_2), 152.8 (C-O-Si), 145.9 (C_q), 144.6 (C_q), 130.5, 130.3, 121.5, 118.8, 115.0, 113.1, 109.7, 105.5, 66.1 (CH_2), 60.5 (OCH_3), 55.4 (OCH_3), 32.0 (CH_2), 28.2 (CH_2), 26.4 (CH_2), 25.2 (CH_3), 17.7 ($\underline{C}(CH_3)_3$), -4.8 (CH_3) **HRMS (EI):** Found 794.4079 $(M+H)^+$, $C_{47}H_{60}NO_8Si$ requires 794.4083. **IR :** ν_{max} (KBr) cm^{-1}: 3350.9 (br.), 2930.1, 2855.3, 1604.3, 1581.7, 1505.9, 1463.7, 1240.6, 1127.3, 912.6 **MP:** 88-90 °C

8.9.4 (*E*)-N-(2-(4-((4-((*tert*-Butyldimethylsilyl)oxy)phenyl)(cycloheptylidene) methyl)phenoxy)ethyl)-3-(3-hydroxy-4-methoxyphenyl)-N-methyl-2-(3,4,5-trimethoxyphenyl)acrylamide [441]

As per general method (8.9.1), the acrylic acid [150] (1.2 eq., 185 mg, 0.516 mmol)), EDC (1.4 eq., 118 mg, 0.616 mmol), and HOBt (1.4 eq., 83 mg, 0.616 mmol) were reacted with protected cyclofenil derivative [218] (1 eq., 200 mg, 0.43 mmol). The product was obtained as a brown resin. The material was purified *via* flash chromatography on silica gel (DCM:EtOAc, gradient 15:1 to 10:1) to afford the product as a yellow solid (284 mg, 81%)

^{1}H NMR ($CDCl_3$, 400 MHz) δ 6.93 - 7.12 (m, 4H, Ar-H, C=CH), 6.50 - 6.86 (m, 10H, Ar-H), 5.64 (br. s., 1H, OH), 4.17 - 4.27 (m, 1H, 0.5 × OCH_2), 3.55 - 3.95 (m, 15H, 0.5 × OCH_2, NCH_2, 4 × OCH_3), 3.06 - 3.24 (m, 3H, NCH_3), 2.24 - 2.37 (m, 4H, 2 × CH_2), 1.49 - 1.64 (m, 8H, 4 × CH_2), 0.99 (s, 9H, 3 × CH_3), 0.20 (s, 6H, 2 × CH_3) **^{13}C NMR ($CDCl_3$, 100 MHz)** δ 172.1 (C=O), 156.6 (C-OH), 153.7 (C-OSi), 153.3 (C-OCH_2), 146.4 (C_q), 145.1 (C_q), 139.7 (C_q), 137.9 (C_q), 136.8 (C_q), 136.3 (C_q), 135.9 (C_q), 130.5, 130.3, 129.9, 128.6 (C_q), 122.0, 119.4, 115.5, 113.7, 110.2, 105.8, 66.5 (CH_2), 60.9 (OCH_3), 56.0 (OCH_3), 55.9 (OCH_3), 47.7 (CH_2), 39.0 (NCH_3), 33.5 (CH_2), 33.4 (CH_2), 29.4 (CH_2), 28.2 (CH_2), 28.1 (CH_2), 25.7 (CH_3), 18.2 ($\underline{C}(CH_3)_3$), -4.4 (CH_3) **HRMS (EI):** Found 830.4050 $(M+Na)^+$, $C_{48}H_{61}NNaO_8Si$ requires 830.4064. **IR :** ν_{max} (KBr) cm^{-1}: 3436.1 (br.), 2928.7, 2854.8, 1631.2, 1604.1, 1581.4, 1505.9, 1463.4, 1240.2, 1126.3, 839.5 **MP:** 84-86 °C

8.9.5 (*E*)-N-(2-(4-((4-((*tert*-Butyldimethylsilyl)oxy)phenyl)(cyclooctylidene) methyl)phenoxy)ethyl)-3-(3-hydroxy-4-methoxyphenyl)-N-methyl-2-(3,4,5-trimethoxyphenyl)acrylamide [442]

As per general method (8.9.1), the acrylic acid [150] (1.2 eq., 180 mg, 0.5 mmol)), EDC (1.4 eq., 118 mg, 0.616 mmol), and HOBt (1.4 eq., 83 mg, 0.616 mmol) were reacted with protected cyclofenil derivative [219] (1 eq., 200 mg, 0.416 mmol). The product was afforded as a brown resin. The material was purified *via* flash chromatography on silica gel (DCM:EtOAc, gradient 15:1 to 10:1) to afford the product as a yellow solid (243 mg, 71%)

^{1}H NMR ($CDCl_3$, 400 MHz) δ 6.95 - 7.15 (m, 4H, Ar-H, C=CH), 6.51 - 6.87 (m, 10H, Ar-H), 4.17 - 4.27 (m, 1H, 0.5 × OCH_2), 3.56 - 3.94 (m, 15H, 0.5 × OCH_2, NCH_2, 4 × OCH_3), 3.05 - 3.23 (m, 3H, NCH_3), 2.20 - 2.34 (m, 4H, 2 × CH_2), 1.62 - 1.73 (m, 2H, CH_2), 1.48 - 1.61 (m, 8H, 4 × CH_2), 0.99 (s, 9H, 3 × CH_3), 0.20 (s, 6H, 2 × CH_3) **^{13}C NMR ($CDCl_3$, 100 MHz)** δ 171.1 (C=O), 156.4 (C-OH), 153.1 (C-OSi), 152.8 (C-OCH_2), 145.9 (C_q), 144.7 (C_q), 139.5 (C_q), 136.6 (C_q), 135.7 (C_q), 135.4 (C_q), 129.7, 129.4, 128.1 (C_q), 121.5, 119.1, 115.0, 113.4, 109.7, 105.5, 66.1 (CH_2), 60.5 (OCH_3), 60.0 (OCH_3), 55.6 (OCH_3), 55.4 (OCH_3), 47.2 (CH_2), 38.6 (NCH_3), 32.1 (CH_2), 32.0 (CH_2), 26.1 (CH_2), 26.0 (CH_2), 25.9 (CH_2), 25.8 (CH_2), 25.2 (CH_3), 17.7 ($\underline{C}(CH_3)_3$), -4.9 (CH_3) **HRMS (EI):** Found 844.4200 $(M+Na)^+$, $C_{49}H_{63}NNaO_8Si$ requires 844.4221. **IR :** ν_{max} (KBr) cm^{-1}:3425.7 (br.), 2929.0, 2856.1, 1633.8, 1603.9, 1581.6, 1505.9, 1463.7, 1240.2, 1126.2, 838.3 **MP:** 89-91 °C

8.9.6 (*E*)-N-(2-(4-((4-((*tert*-butyldimethylsilyl)oxy)phenyl)(4-methylcyclon-hexaneylidene)methyl)phenoxy)ethyl)-3-(3-hydroxy-4-methoxyphenyl)-N-methyl-2-(3,4,5-trimethoxyphenyl)acrylamide [443]

As per general method, the acrylic acid [150] (1.2 eq., 189 mg, 0.526 mmol)), EDC (1.4 eq., 118 mg, 0.616 mmol), and HOBt (1.4 eq., 83 mg, 0.616 mmol) were reacted with protected cyclofenil derivative [220] (1 eq., 200 mg, 0.429 mmol). The product was afforded as a brown resin. The material was purified *via* flash chromatography on silica gel (DCM:EtOAc, gradient 15:1 to 10:1) to afford the product as a yellow solid (294 mg, 85%).

^{1}H NMR ($CDCl_3$, 400 MHz) δ 6.88 - 7.09 (m, 4H, Ar-H, C=CH), 6.53 - 6.86 (m, 10H, Ar-H), 5.50 - 5.89 (br. s., 1H, OH), 4.23 (m, 1H, 0.5 × OCH_2), 3.57 - 3.92 (m, 15H, 0.5 × OCH_2, NCH_2, 4 × OCH_3), 3.07 - 3.24 (m, 3H, NCH_3), 2.50 - 2.64 (m, 2H, CH_2), 1.87 - 2.00 (m, 2H, CH_2), 1.72-1.78 (m, 2H, CH_2), 1.05 - 1.14 (m, 2H, CH_2), 1.00 (s, 9H, 3 × CH_3), 0.91 - 0.97 (m, 3H, CH_3), 0.21 (s, 6H, 2 × CH_3) **^{13}C NMR ($CDCl_3$, 100 MHz)** δ 171.7 (C=O), 156.3 (C-OH), 153.3 (C-OSi), 152.8 (C-OCH_2), 145.9 (C_q), 144.7 (C_q), 137.5 (C_q), 135.9 (C_q), 135.4 (C_q), 133.1, 130.5, 130.3, 128.1 (C_q), 121.5, 118.8, 115.0, 113.1, 109.7, 105.5, 66.1 (CH_2), 60.5 (OCH_3), 60.0 (OCH_3), 55.6 (OCH_3), 55.4 (OCH_3), 47.2 (CH_2), 38.5 (NCH_3) 36.4 (CH_2), 32.3 (CH), 31.3 (CH_2), 25.2 (CH_3), 21.6 (CH_3), 17.7 ($\underline{C}(CH_3)_3$), -4.8 (CH_3) **HRMS (EI):** Found 808.4211 $(M+H)^+$, $C_{48}H_{62}NO_8Si$ requires 808.4239. **IR :** ν_{max} (KBr) cm^{-1}:3436.6 (br.), 2929.1, 2852.2, 1628.9, 1604.4, 1581.8, 1505.9, 1463.4, 1239.6, 1126.1, 839.5 **MP:** 89-93 °C

8.9.7 General method for deprotection of *tert*-butyldimethylsilyl (TBDMS) ether group

The appropriate silyl ether [439]-[443] was dissolved in a minimum amount of THF (~3 mL) while stirring under N_2. An equimolar quantity of TBAF (1 M in THF) was added and the mixture was allowed to stir for 30 min. The reaction was monitored *via* TLC. The solvent was evaporated to dryness. The residue was redissolved in DCM (20 mL) and washed with a 10% HCl solution (10 mL).

The organic phase was dried over Na_2SO_4 and evaporated to dryness in *vacuo*. The residue is purified *via* flash chromatography on silica gel to afford the products.

8.9.8 (*E*)-N-(2-(4-(Cyclopentylidene(4-hydroxyphenyl)methyl)phenoxy)ethyl)-3-(3-hydroxy-4-methoxyphenyl)-N-methyl-2-(3,4,5-trimethoxyphenyl)acrylamide [444]

As per general deprotection method (8.9.7), protected cyclofenil-acrylic acid derivative [439] (150 mg, 0.192 mmol) and TBAF (1 M in THF) (0.192 mmol, 0.192 mL) were reacted together in THF (3 mL). The residue is purified *via* flash chromatography on silica gel (DCM:EtOAc, gradient 5:1 to 2:1) to afford the product as a yellow solid (116 mg, 91%).

^{1}H NMR ($CDCl_3$, 400 MHz) δ 6.96 - 7.14 (m, 4H, Ar-H, C=CH), 6.47 - 6.91 (m, 10H, Ar-H), 4.19 - 4.28 (m, 1H, 0.5 × OCH_2), 3.56 - 3.95 (m, 15H, 0.5 × OCH_2, NCH_2, 4 × OCH_3), 3.10 - 3.26 (m, 3H, NCH_3), 2.31 - 2.45 (m, 4H, 2 × CH_2), 1.62 - 1.74 (m, 4H, 2 × CH_2) **^{13}C NMR ($CDCl_3$, 100 MHz)** δ 171.5 (C=O), 156.1 (C-OH), 153.7 (C-OCH_2), 152.9, 145.9, 144.6, 141.7, 136.3, 135.5, 135.2, 131.3, 129.9, 128.0, 121.6, 115.0, 114.4, 113.2, 109.7, 105.5, 66.0 (CH_2), 60.5 (OCH_3), 55.6 (OCH_3), 55.4 (OCH_3), 47.4 (CH_2), 32.8 (CH_3), 29.3 (CH_2), 26.5 (CH_2) **HRMS (EI):** Found 688.2868 $(M+Na)^+$, $C_{40}H_{43}NNaO_8$ requires 688.2886. **IR :** ν_{max} (KBr) cm^{-1}: 3433.5 (br.), 2933.4, 2862.0, 1603.9, 1508.1, 1408.8, 1238.4, 1125.3, 835.2 **MP:** 159-162 °C

8.9.9 (*E*)-N-(2-(4-(Cyclon-hexaneylidene(4-hydroxyphenyl)methyl)phenoxy)ethyl)-3-(3-hydroxy-4-methoxyphenyl)-N-methyl-2-(3,4,5-trimethoxyphenyl)acrylamide [445]

As per general deprotection method (8.9.7), protected cyclofenil-acrylic acid derivative [440] (150 mg, 0.189 mmol) and TBAF (1 M in THF) (0.189 mmol, 0.189 ml) were reacted together in THF (3 mL). The residue was purified *via* flash chromatography on silica gel (DCM:EtOAc, gradient 5:1 to 2:1) to afford the product as a yellow solid (119 mg, 93%).

^{1}H NMR ($CDCl_3$, 400 MHz) δ 6.87 - 7.07 (m, 4H, Ar-H), 6.50 - 6.84 (m, 10H, Ar-H), 4.17 - 4.31 (m, 1H, 0.5 × CH_2), 3.54 - 3.95 (m, 15H, 0.5 × CH_2, CH_2, 3 × OCH_3), 3.08 - 3.24 (m, 3H, NCH_3), 2.17 - 2.30 (m, 4H, 2 × CH_2), 1.50 - 1.67 (m, 6H, 3 × CH_2) **^{13}C NMR ($CDCl_3$, 100 MHz)** δ 172.1 (C=O), 154.0 (C-OH), 152.9 (C-OCH_2), 146.0 (C_q), 144.7 (C_q), 137.8 (C_q), 137.3 (C_q), 135.2 (C_q), 134.9 (C_q), 132.9 (C_q), 130.5, 130.5, 129.6, 128.0 (C_q), 121.6, 115.0, 114.3, 113.2, 109.7, 105.5, 66.0 (CH_2), 60.5 (OCH_3), 60.0 (OCH_3), 55.6 (OCH_3), 55.4 (OCH_3), 47.3 (CH_2), 38.7 (CH_3), 32.0 (CH_2), 28.2 (CH_2), 26.4 (CH_2) **HRMS (EI):** Found 702.3026 $(M+Na)^+$, $C_{41}H_{45}NNaO_8$ requires 702.3043. **IR :** ν_{max} (KBr) cm^{-1}: 3425.4 (br.), 2926.5, 2847.3, 1605.2, 1582.5, 1510.9, 1449.1, 1273.8, 1237.5, 1125.7, 1026.9, 835.4 **MP:** 166-170 °C

8.9.10 (*E*)-N-(2-(4-(Cycloheptylidene(4-hydroxyphenyl)methyl)phenoxy)ethyl)-3-(3-hydroxy-4-methoxyphenyl)-N-methyl-2-(3,4,5-trimethoxyphenyl)acrylamide [446]

As per general deprotection method (8.9.7), protected cyclofenil-acrylic acid derivative [441] (150 mg, 0.185 mmol) and TBAF (1 M in THF) (0.185 mmol, 0.185 ml) were reacted together in THF (3 mL). The residue is purified *via* flash chromatography on silica gel (DCM:EtOAc, gradient 5:1 to 2:1) to afford the product as a yellow solid (113 mg, 98%).

^{1}H NMR ($CDCl_3$, 400 MHz) δ 6.92 - 7.12 (m, 4H, Ar-H, C=CH), 6.49 - 6.84 (m, 10H, Ar-H), 4.16 - 4.26 (m, 1H, 0.5 × OCH_2), 3.53 - 3.93 (m, 15H, 0.5 × OCH_2, NCH_2, 4 × OCH_3), 3.07 - 3.23 (m, 3H, NCH_3), 2.24

- 2.38 (m, 4H, 2 × CH_2), 1.52 - 1.62 (m, 8H, 4 × CH_2) **^{13}C NMR ($CDCl_3$, 100 MHz)** δ 172.2 (C=O), 156.6 (C-OH), 154.3 (C-OCH_2), 153.3, 146.4 (C_q), 145.1 (C_q), 139.6 (C_q), 137.8 (C_q), 136.9 (C_q), 136.2 (C_q), 135.8 (C_q), 135.6 (C_q), 130.5, 130.4, 130.1, 128.5 (C_q), 122.0, 115.5, 114.9, 113.7, 110.2, 106.1, 66.4 (CH_2), 60.9 (OCH_3), 60.5 (CH_2), 56.0 (OCH_3), 55.9 (OCH_3), 53.5 (CH_2), 50.1 (CH_2), 47.8 (CH_2), 39.1 (NCH_3), 33.4 (CH_2), 29.4 (CH_2), 28.1 (CH_2) **HRMS (EI):** Found 716.3185 $(M+Na)^+$, $C_{42}H_{47}NNaO_8$ requires 716.3199. **IR :** ν_{max} (KBr) cm^{-1}: 3437.4 (br.), 2923.4, 2842.2, 160.3, 1582.3, 1506.0, 1410.0, 1273.7, 1238.2, 1125.3, 831.2 **MP:** 162-163 °C

8.9.11 (*E*)-N-(2-(4-(Cyclooctylidene(4-hydroxyphenyl)methyl)phenoxy)ethyl)-3-(3-hydroxy-4-methoxyphenyl)-N-methyl-2-(3,4,5-trimethoxyphenyl)acrylamide [447]

As per general deprotection method (8.9.7), protected cyclofenil-acrylic acid derivative [442] (150 mg, 0.182 mmol) and TBAF (1 M in THF) (0.182 mmol, 0.182 ml) were reacted together in THF (3 mL). The residue was purified *via* flash chromatography on silica gel (DCM:EtOAc, gradient 5:1 to 2:1) to afford the product as a yellow solid (102 mg, 79%).

^{1}H NMR ($CDCl_3$, 400 MHz) δ 6.92 - 7.13 (m, 4H, Ar-H, C=CH), 6.50 - 6.86 (m, 10H, Ar-H), 4.16 - 4.25 (m, 1H, 0.5 × OCH_2), 3.51 - 3.95 (m, 15H, 0.5 × OCH_2, NCH_2, 4 × OCH_3), 3.05 - 3.24 (m, 3H, NCH_3), 2.17 - 2.36 (m, 4H, 2 × CH_2), 1.62 - 1.74 (m, 2H, CH_2), 1.45 - 1.61 (m, 8H, 4 × CH_2) **^{13}C NMR ($CDCl_3$, 100 MHz)** δ 172.4 (C=O), 156.6, 153.8 (C-OH), 152.9 (C-OCH_2), 146.0, 144.7, 139.4, 139.4, 137.3, 135.6, 135.2, 133.9, 129.6, 129.6, 121.6, 115.0, 114.6, 113.4, 109.8, 105.5, 65.9 (CH_2), 60.5 (OCH_3), 60.1 (CH_2), 55.5 (OCH_3), 55.4 (OCH_3), 39.1 (NCH_3), 32.0 (CH_2), 26.1 (CH_2), 25.9 (CH_2), 25.8 (CH_2) **HRMS (EI):** Found 730.3336 $(M+Na)^+$, $C_{43}H_{49}NNaO_8$ requires 730.3356. **IR:** ν_{max} (KBr) cm^{-1}: 3437.6 (br.), 2927.9, 2847.3, 1604.1, 1582.3, 1505.9, 1274.6, 1238.3, 1125.6, 831.6 **MP:** 158-159 °C

8.9.12 (*E*)-3-(3-Hydroxy-4-methoxyphenyl)-N-(2-(4-((4-hydroxyphenyl)(4-methylcyclon-hexaneylidene)methyl)phenoxy)ethyl)-N-methyl-2-(3,4,5-trimethoxyphenyl)acrylamide [448]

As per general deprotection method (8.9.7), protected cyclofenil-acrylic acid derivative [443] (150 mg, 0.186 mmol) and TBAF (1 M in THF) (0.186 mmol, 0.186 ml) were reacted together in THF (3 mL). The residue was purified *via* flash chromatography on silica gel (DCM:EtOAc, gradient 5:1 to 2:1) to afford the product as a yellow solid (110 mg, 86%).

^{1}H NMR ($CDCl_3$, 400 MHz) δ 6.87 - 7.06 (m, 4H, Ar-H), 6.51 - 6.84 (m, 10H, Ar-H), 4.17 - 4.27 (m, 1H, 0.5 × CH_2), 3.54 - 3.94 (m, 15H, 0.5 × OCH_2, NCH_2, 4 × OCH_3), 3.08 - 3.25 (m, 3H, NCH_3), 2.49 - 2.64 (m, 2H, CH_2), 1.93 (t, J = 11.54 Hz, 2H, CH_2), 1.76 (d, J = 10.54 Hz, 2H, CH_2), 1.55 - 1.68 (m, 1H, CH), 1.01 - 1.15 (m, 2H, CH_2), 0.87 - 0.98 (m, 3H, CH_3) **^{13}C NMR ($CDCl_3$, 100 MHz)** δ 172.2 (C=O), 154.1 (C-OH), 152.8 (C-OCH_2), 146.0 (C-OH), 144.7 (C_q), 137.4 (C_q), 134.8 (C_q), 133.1 (C_q), 130.5, 130.5, 128.0 (C_q), 121.6, 115.0, 114.3, 113.2, 109.8, 105.5, 65.9 (CH_2), 60.5 (OCH_3), 60.1 (OCH_3), 55.5 (OCH_3), 55.4 (OCH_3), 47.4 (CH_3), 38.7 (NCH_3), 36.4 (CH_2), 32.3 (CH), 31.3 (CH_2), 21.6 (CH_3) **HRMS (EI):** Found 694.3359 $(M+H)^+$, $C_{42}H_{48}NO_8$ requires 694.3374. **IR :** ν_{max} (KBr) cm^{-1}: 3421.5 (br.), 2912.0, 2840.1, 1605.5, 1582.3, 1508.4, 1454.1, 1274.2, 1237.9, 1125.8, 830.8 **MP:** 158-161 °C

8.10 Synthesis of Indole-acrylic acid conjugates

8.10.1 General method for the synthesis of protected Indole-acrylic acid conjugates

A mixture of the required acrylic acid [150] (1.2 eq), EDC (1.4 eq.), and HOBt (1.4 eq.) were suspended in anhydrous dichloromethane (3 mL) and stirred for 10 min under a nitrogen atmosphere. The protected indole (1 eq.) [256]-[260] was dissolved in anhydrous dichloromethane (3 mL) and slowly added to the mixture *via* syringe. Reaction was allowed stir for 16 h. Reaction was monitored *via* TLC. The reaction mixture was diluted to 15 mL with anhydrous dichloromethane. To this mixture, water (20 mL) was added. The aqueous phase was extracted with DCM (20 mL x3), brine (50ml), dried over Na_2SO_4 and evaporated to dryness in *vacuo* to yield the crude product. The material was purified *via* flash chromatography on silica gel.

8.10.2 (2*E*)-N-[4-[5-(benzyloxy)-2-[4-(benzyloxy)phenyl]-3-methyl-1*H*-indol-1-yl]butyl]-3-(3-hydroxy-4-methoxyphenyl)-N-methyl-2-(3,4,5-trimethoxyphenyl)prop-2-enamide [449]

As per general method (8.10.1), the acrylic acid [150] (1.2 eq., 171 mg, 0.475 mmol)), EDC (1.4 eq., 106 mg, 0.554 mmol), and HOBt (1.4 eq., 75 mg, 0.554 mmol) were reacted with indole [256] (1 eq., 200 mg, 0.396 mmol). The crude product was afforded as a brown resin. The material was purified *via* flash chromatography on silica gel (DCM:EtOAc, gradient 10:1 to 5:1) to afford the product as a yellow solid (285 mg, 85%)

^{1}H NMR ($CDCl_3$, 400 MHz) δ 7.32 - 7.55 (m, 10H, Ar-H), 7.25 - 7.31 (m, 3H, Ar-H), 7.06 - 7.16 (m, 3H, Ar-H), 6.95 - 7.01 (m, 1H, Ar-H), 6.43 - 6.79 (m, 6H, Ar-H), 5.17 (s, 4H, CH_2), 5.14 (s, 2H, CH_2), 3.95 - 4.11 (m, 2H, CH_2), 3.85 (s, 6H, 2 × OCH_3), 3.66 (s, 6H, 2 × OCH_3), 3.13 - 3.38 (m, 2H, CH_2), 2.84 (s, 3H, NCH_3), 2.20 (s, 3H, CH_3), 1.33 - 1.68 (m, 4H, 2 × CH_2) **^{13}C NMR ($CDCl_3$, 100 MHz)** δ 171.5 (C=O), 158.5 (C-O-Bn), 153.2 (C-O-Bn), 153.0 (C_q), 146.3 (C_q), 145.1 (C_q), 137.8 (C_q), 137.7 (C_q), 136.7, (C_q) 136.0 (C_q), 131.6, 130.6, 129.4, 128.9, 128.6, 128.5, 128.1, 127.7, 127.6, 127.6, 124.8 (C_q), 121.9, 115.3, 114.7, 112.2, 110.2, 108.4 (C_q), 105.9, 102.5, 71.0 (CH_2), 70.0 (CH_2), 60.9 (OCH_3), 56.1 (OCH_3), 55.8 (OCH_3), 53.4 (CH_2), 43.4 (CH_2), 36.3 (NCH_3), 29.7 (CH_2), 27.2 (CH_2), 9.3 (CH_3) **HRMS** (EI): Found 847.3937 $(M+H)^+$, $C_{53}H_{55}N_2O_8$ requires 847.3953 **IR :** ν_{max} (KBr) cm^{-1}: 3237.0 (br.), 2932.o, 2863.0, 1614.3, 1579.9, 1506.5, 1454.0, 1276.5, 1238.9, 1125.0, 1025.2, 737.2 **MP :** 86-89 °C

8.10.3 (2*E*)-N-[5-[5-(Benzyloxy)-2-[4-(benzyloxy)phenyl]-3-methyl-1*H*-indol-1-yl]pentyl]-3-(3-hydroxy-4-methoxyphenyl)-N-methyl-2-(3,4,5-trimethoxyphenyl) prop-2-enamide [450]

As per general method (8.10.1), the acrylic acid [150] (1.2 eq., 167 mg, 0.450 mmol)), EDC (1.4 eq., 104 mg, 0.540 mmol), and HOBt (1.4 eq., 73 mg, 0.540 mmol) were reacted with indole [257] (1 eq., 200 mg, 0.386 mmol). The product was afforded as a brown resin. The material was purified *via* flash chromatography on silica gel (DCM:EtOAc, gradient 10:1 to 5:1) to afford the product as a yellow solid (293 mg, 91%)

^{1}H NMR ($CDCl_3$, 400 MHz) δ 7.05 - 7.66 (m, 16H, Ar-H), 6.99 (s, 1H, Ar-H), 6.80 (s, 1H, Ar-H), 6.45 - 6.73 (m, 5H, Ar-H), 5.17 (s, 2H, CH_2), 5.14 (s, 2H, CH_2), 3.59 - 4.11 (m, 14H, CH_2, 4 × OCH_3), 3.13 - 3.41 (m, 2H, CH_2), 2.90 (s, 3H, NCH_3), 2.21 (s, 3H, CH_3), 0.82 - 1.77 (m, 6H, 3 × CH_2) **^{13}C NMR ($CDCl_3$, 100 MHz)** δ 172.0 (C=O), 158.1 (C-O-Bn), 152.8 (C-O-Bn), 152.6 (C_q), 145.9 (C_q), 144.7 (C_q), 137.3 (C_q), 136.3 (C_q), 135.8 (C_q), 131.3, 131.2, 128.9, 128.4, 128.2, 128.1, 127.7, 127.3, 127.2, 127.2, 124.5 (C_q), 121.5, 115.0, 114.3, 111.7, 109.7, 107.8 (C_q), 105.6, 102.0, 70.6 (CH_2), 69.6 (CH_2), 60.5 (OCH_3), 55.7 (OCH_3), 55.4 (OCH_3), 36.3 (NCH_3), 29.4 (CH_2), 23.7 (CH_2), 8.9 (CH_3) **HRMS** (EI): Found 861.4122

$(M+H)^+$, $C_{54}H_{55}N_2O_8$ requires 861.4109 **IR :** ν_{max} (KBr) cm^{-1}: 3237.5 (br.), 3064.3, 3033.0, 2934.8, 2249.0, 1768.0, 1613.9, 1580.4, 1505.9, 1479.4, 1412.1, 1275.5, 1235.6, 1126.4, 1026.3, 910.2, 733.8 **MP :** 81-83 °C

8.10.4 (*E*)-N-(6-(5-(Benzyloxy)-2-(4-(benzyloxy)phenyl)-3-methyl-1*H*-indol-1-yl)hexyl)-3-(3-hydroxy-4-methoxyphenyl)-N-methyl-2-(3,4,5-trimethoxyphenyl)acrylamide [451]

As per general method (8.10.1), the acrylic acid [150] (1.2 eq., 162 mg, 0.450 mmol), EDC (1.4 eq., 101 mg, 0.525 mmol), and HOBt (1.4 eq., 71 mg, 0.525 mmol) were reacted with indole [258] (1 eq., 200 mg, 0.375 mmol). The product was afforded as a brown resin. The material was purified *via* flash chromatography on silica gel (DCM:EtOAc, gradient 10:1 to 5:1) to afford the product as a yellow solid (288 mg, 88%)

^{1}H NMR ($CDCl_3$, 400 MHz) δ 7.27 - 7.57 (m, 12H, Ar-H), 7.23 (d, *J* = 8.53 Hz, 1H, Ar-H), 7.07 - 7.16 (m, 3H, Ar-H), 6.98 (d, *J* = 8.53 Hz, 1H, Ar-H), 6.79 (s, 1H, Ar-H), 6.68 (s, 2H, Ar-H), 6.50 - 6.61 (m, 3H, Ar-H), 5.10 - 5.20 (m, 4H, 2 × CH_2), 3.63 - 4.05 (m, 14H, CH_2, 3 × OCH_3), 3.19 - 3.41 (m, 2H, CH_2), 2.89 - 2.99 (m, 3H, CH_3), 2.20 (s, 3H, CH_3), 0.96 - 1.65 (m, 8H, 4 × CH_2) **^{13}C NMR ($CDCl_3$, 100 MHz)** δ 170.5 (C=O), 158.0 (C-O-Bn), 152.8 (C-O-Bn), 152.6 (C_q), 145.8 (C_q), 144.6 (C_q), 137.5 (C_q), 137.4 (C_q), 136.3 (C_q), 135.6 (C_q), 131.3, 131.2, 129.0, 128.4, 128.2, 128.1, 128.1, 127.7, 127.3, 127.2, 124.5 (C_q), 121.5, 114.9, 114.2, 111.7, 109.8, 109.7, 107.7 (C_q), 105.6, 101.9, 76.9, 70.6 (CH_2), 69.6 (CH_2), 60.5 (OCH_3), 55.7 (OCH_3), 55.4 (OCH_3), 43.3 (CH_2), 29.5 (CH_2), 26.1 (CH_2), 26.0 (CH_2), 8.9 (CH_3) **HRMS** (EI): Found 875.4262 $(M+H)^+$, $C_{55}H_{58}N_2O_8$ requires 875.4262 **IR :** ν_{max} (KBr) cm^{-1}: 3437.8 (br.), 2931.6, 2858.6, 1614.1, 1580.2, 1506.7, 1454.1, 1276.1, 1239.1, 1129.9, 1025.5, 697.4 **MP :** 66-69 °C

8.10.5 (*E*)-N-(8-(5-(Benzyloxy)-2-(4-(benzyloxy)phenyl)-3-methyl-1*H*-indol-1-yl)octyl)-3-(3-hydroxy-4-methoxyphenyl)-N-methyl-2-(3,4,5-trimethoxyphenyl)acrylamide [452]

As per general method (8.10.1), the acrylic acid [150] (1.2 eq., 115 mg, 0.321 mmol), EDC (1.4 eq., 72 mg, 0.375 mmol), and HOBt (1.4 eq., 72 mg, 0.375 mmol) were reacted with indole [259] (1 eq., 150 mg, 0.267 mmol). The product was afforded as a brown resin. The material was purified *via* flash chromatography on silica gel (DCM:EtOAc, gradient 10:1 to 5:1) to afford the product as a yellow solid (204 mg, 85%)

^{1}H NMR ($CDCl_3$, 400 MHz) δ 7.21 - 7.57 (m, 14H, Ar-H), 7.08 - 7.17 (m, 3H, Ar-H), 6.99 (d, *J* = 9.03 Hz, 1H, Ar-H), 6.81 (s, 1H, Ar-H), 6.68 (s, 2H, Ar-H), 6.52 - 6.62 (m, 3H, Ar-H), 5.17 (s, 2H, CH_2), 5.15 (s, 2H, CH_2), 3.93 - 4.02 (m, 2H, CH_2), 3.87 (s, 6H, 2 × OCH_3), 3.71 (s, 6H, 2 × OCH_3), 3.25 - 3.47 (m, 2H, CH_2), 2.97 (s, 3H, CH_3), 2.21 (s, 3H, CH_3), 1.00 - 1.65 (m, 12H, 6 × CH_2) **^{13}C NMR ($CDCl_3$, 100 MHz)** δ 171.3 (C=O), 158.0 (C-O-Bn), 152.8 (C-O-Bn), 152.6 (C_q), 145.8 (C_q), 144.7 (C_q), 137.5 (C_q), 137.4 (C_q), 136.4 (C_q), 135.9 (C_q), 131.3, 131.2, 128.7, 128.3, 128.2, 128.1, 127.7, 127.3, 127.2, 124.6 (C_q), 121.4, 115.0, 114.2, 111.6, 109.9, 109.7, 107.6 (C_q), 105.6, 101.9, 70.6 (CH_2), 69.7 (CH_2), 60.5 (OCH_3), 55.7 (OCH_3), 55.4 (OCH_3), 43.4 (CH_2), 36.2 (NCH_3), 29.6 (CH_2), 28.8 (CH_2), 28.7 (CH_2), 26.3 (CH_2), 8.9 (CH_3) **HRMS** (EI): Found 903.4573 $(M+H)^+$, $C_{57}H_{63}N_2O_8$ requires 903.4579 **IR :** ν_{max} (KBr) cm^{-1}: 3439.2 (br.), 2929.7, 2852.2, 1614.5, 1580.5, 1580.5, 1507.0, 1454.1, 1240.9, 1125.8, 835.9 **MP :** 82-83 °C

8.10.6 (*E*)-N-(12-(5-(Benzyloxy)-2-(4-(benzyloxy)phenyl)-3-methyl-1*H*-indol-1-yl)dodecyl)-3-(3-hydroxy-4-methoxyphenyl)-N-methyl-2-(3,4,5-trimethoxyphenyl)acrylamide [453]

As per general method (8.10.1), the acrylic acid [150] (1.2 eq., 105 mg, 0.2918 mmol), EDC (1.4 eq., 65 mg, 0.340 mmol), and HOBt (1.4 eq., 46 mg, 0.340 mmol) were reacted with indole [260] (1 eq., 150 mg, 0.243 mmol). The product was afforded as a brown resin. The material was purified *via* flash chromatography over silica gel (DCM:EtOAc, gradient 10:1 to 5:1) to afford the product as a yellow solid (212 mg, 91%)

^{1}H NMR ($CDCl_3$, 400 MHz) δ 7.23 - 7.57 (m, 13H, Ar-H), 7.08 - 7.17 (m, 3H, Ar-H), 6.99 (d, *J* = 8.53 Hz, 1H, Ar-H), 6.81 (s, 1H, Ar-H), 6.69 (s, 2H, Ar-H), 6.54 - 6.62 (m, 3H, Ar-H), 5.17 (s, 2H, CH_2), 5.15 (s, 2H, CH_2), 3.98 (t, *J* = 6.78 Hz, 3H, CH_2), 3.83 - 3.91 (m, 6H, 2 × OCH_3), 3.72 (s, 6H, 2 × OCH_3), 3.27 - 3.49 (m, 2H, CH_2), 2.94 - 3.02 (m, 3H, NCH_3), 2.21 (s, 3H, CH_3), 1.08 - 1.65 (m, 20H, 10 × CH_2) **^{13}C NMR ($CDCl_3$, 100 MHz)** δ 170.5 (C=O), 158.0 (C-O-Bn), 152.8 (C-O-Bn), 152.6 (C_q), 145.8 (C_q), 144.6 (C_q), 137.6 (C_q), 137.4 (C_q), 136.4 (C_q), 131.3, 131.2, 128.7, 128.3, 128.2, 128.1, 127.7, 127.3, 127.1, 124.6 (C_q), 121.4, 115.0, 114.2, 111.6, 109.9, 109.7, 107.6 (C_q), 105.6, 101.9, 70.6 (CH_2), 69.6 (CH_2), 60.5 (OCH_3), 55.7 (OCH_3), 55.4 (OCH_3), 43.5 (CH_2), 36.5 (NCH_3), 29.7 (CH_2), 29.1 (CH_2), 29.1 (CH_2), 29.0 (CH_2), 28.7 (CH_2), 26.4 (CH_2), 8.9 (CH_3) **HRMS** (EI): Found 959.5191 $(M+H)^+$, $C_{61}H_{71}N_2O_8$ requires 959.5205 **IR :** ν_{max} (KBr) cm^{-1}: 3439.3 (br.), 2927.5, 2853.1, 1614.4, 1580.8, 1505.9, 1454.7, 1240.3, 1125.0, 1026.4, 737.4 **MP :** 60-62 °C

8.10.7 General method for debenzylation of the protected indole conjugates

The protected indole conjugate [449]-[453] was dissolved in MeOH:EtOAc (1:4) (20 mL) and transferred to a 3-neck flask. To the flask was added $Pd(OH)_2$ the mixture was placed under a H_2 atmosphere. The reaction was monitored *via* TLC until the starting material had disappeared (10 – 60 min). The reaction mixture was filtered through celite and the solvent was evaporated under reduced pressure to obtain brown oil. The material was purified *via* flash chromatography on silica gel. (DCM : EtOAc)

8.10.8 (*E*)-N-(4-(5-Hydroxy-2-(4-hydroxyphenyl)-3-methyl-1*H*-indol-1-yl)butyl)-3-(3-hydroxy-4-methoxyphenyl)-N-methyl-2-(3,4,5-trimethoxyphenyl)acrylamide [454]

As per general method (8.10.7), protected indole conjugate [449] (150 mg, 0.177 mmol) and a small spatula tipful of $Pd(OH)_2$ (20 mg) were reacted under a hydrogen atmosphere for 30 min. The material was purified *via* flash chromatography on silica gel (DCM:EtOAc, gradient 3:1 to 1:1) to afford the product as a yellow solid (105 mg, 89%)

^{1}H NMR (CD_3OD, 600 MHz) δ 7.00 – 7.24 (m, 3H, Ar-H), 6.76 - 6.94 (m, 4H, Ar-H), 6.35 - 6.74 (m, 6H, Ar-H), 3.87 - 4.05 (m, 2H, CH_2), 3.48 - 3.85 (m, 12H, 4 × OCH_3), 3.11 - 3.36 (m, 2H, CH_2), 2.68 - 2.85 (m, 3H, NCH_3), 2.10 (s, 3H, CH_3), 1.06 - 1.56 (m, 4H, CH_2) **^{13}C NMR (CD_3OD, 150 MHz)** δ 173.8 (C=O), 173.7 (C=O), 173.0 (C=O), 172.9 (C=O), 169.5, 157.5, 157.4, 153.8, 153.7, 153.6, 153.5, 150.4, 148.2, 146.5, 146.2, 138.5, 138.4, 138.3, 138.1, 137.2, 137.0, 136.1, 135.9, 135.7, 135.6, 133.0, 132.9, 131.9, 131.8, 131.1, 131.0, 130.2, 130.0, 129.8, 129.7, 128.5, 128.4, 127.9, 127.6, 123.9, 123.8, 121.9, 120.4, 120.3, 116.4, 116.3, 116.0, 115.8, 115.3, 111.7, 111.6, 111.4, 111.1, 111.0, 110.1, 110.0, 107.5, 107.4, 107.2, 107.0, 106.4, 106.1, 105.3, 102.9, 102.8, 60.3 (OCH_3), 60.2 (OCH_3), 60.1 (OCH_3), 55.7 (OCH_3), 55.6 (OCH_3), 55.5 (OCH_3), 55.3 (CH_2), 53.8 (CH_2), 51.3 (CH_2), 51.1 (CH_2), 50.6

(CH_2), 49.3 (CH_2), 46.3 (CH_2), 43.3 (CH_2), 40.9 (CH_2), 40.6 (CH_2), 35.7 (NCH_3), 34.4 (NCH_3), 32.9 (NCH_3), 31.8 (NCH_3), 27.2 (CH_2), 27.1 (CH_2), 27.0 (CH_2), 26.9 (CH_2), 25.5 (CH_2), 25.3 (CH_2), 24.2 (CH_2), 24.0 (CH_2), 8.5 (CH_3) **HRMS** (EI): Found 667.3016 $(M+H)^+$, $C_{39}H_{43}N_2O_8$ requires 667.3014 **IR :** ν_{max} (KBr) cm^{-1}: 3423.2 (br.), 2935.7, 1614.1, 1584.1, 1508.6, 1461.3, 1273.5, 1237.6, 1122.6 **MP :** 109-111 °C

8.10.9 (*E*)-N-(5-(5-Hydroxy-2-(4-hydroxyphenyl)-3-methyl-1*H*-indol-1-yl)pentyl)-3-(3-hydroxy-4-methoxyphenyl)-N-methyl-2-(3,4,5-trimethoxyphenyl)acrylamide [455]

As per general method (8.10.7), protected indole conjugate [450] (150 mg, 0.174 mmol) and a small spatula tipful of $Pd(OH)_2$ (20 mg) were reacted under a hydrogen atmosphere for 30 min. The material was purified *via* flash chromatography on silica gel (DCM:EtOAc, gradient 3:1 to 1:1) to afford the product as a yellow solid (93 mg, 79%)

^{1}H NMR ($CDCl_3$, 600 MHz) δ 7.14 (s, 3H, Ar-H), 6.91 - 7.03 (m, 3H, Ar-H), 6.72 - 6.88 (m, 3H, Ar-H), 6.43 - 6.71 (m, 6H, Ar-H), 3.82 - 3.97 (m, 8H, CH_2, 2 × OCH_3), 3.59 - 3.71 (m, 6H, 2 × OCH_3), 3.13 - 3.41 (m, 2H, CH_2), 2.91 (s, 3H, CH_3), 2.11 (s, 3H, CH_3), 1.36 - 1.66 (m, 4H, 2 × CH_2), 1.06 - 1.20 (m, 2H, CH_2) **^{13}C NMR ($CDCl_3$, 150 MHz)** δ 171.9 (C=O), 156.3 (C-OH), 153.4 (C-OH), 153.3 (C_q), 153.2 (C_q), 149.4 (C_q), 146.5 (C_q), 145.1 (C_q), 138.4 (C_q), 137.8 (C_q), 135.7 (C_q), 131.7, 131.4 (C_q), 130.6, 129.8, 129.6, 129.2, 128.4, 128.4, 127.6, 123.9 (C_q), 121.9, 115.5, 111.0, 110.3, 110.0, 109.9, 107.4 (C_q), 106.1, 103.5, 60.9 (OCH_3), 56.1 (OCH_3), 55.9 (OCH_3), 50.8 (CH_2), 43.3 (CH_2), 36.8 (NCH_3), 29.6 (CH_2), 27.5 (CH_2), 23.9 (CH_2), 9.2 (CH_3) **HRMS** (EI): Found 681.3163 $(M+H)^+$, $C_{40}H_{45}N_2O_8$ requires 681.3170 **IR :** ν_{max} (KBr) cm^{-1}: 3423.4 (br.), 2934.4, 1732.6, 1611.6, 1583.6, 1508.6, 1461.5, 1272.9, 1238.6, 1122.6, 1026.1 **MP :** 87-89 °C

8.10.10 (*E*)-N-(6-(5-Hydroxy-2-(4-hydroxyphenyl)-3-methyl-1*H*-indol-1-yl)hexyl)-3-(3-hydroxy-4-methoxyphenyl)-N-methyl-2-(3,4,5-trimethoxyphenyl)acrylamide [456]

As per general method (8.10.7), protected indole conjugate [451] (150 mg, 0.171 mmol) and a small spatula tipful of $Pd(OH)_2$ were reacted under a hydrogen atmosphere for 30 min. The material was purified *via* flash chromatography on silica gel (DCM:EtOAc, gradient 3:1 to 1:1) to afford the product as a yellow solid (98 mg, 83%)

^{1}H NMR (CD_3OD, 600 MHz) δ 6.49 - 7.34 (m, 13H, Ar-H), 3.89 - 4.03 (m, 2H, CH_2), 3.55 - 3.87 (m, 12H, OCH_3), 3.18 - 3.37 (m, 2H, CH_2), 2.72 - 2.98 (m, 3H, NCH_3), 2.07 - 2.24 (m, 3H, CH_3), 1.35 - 1.56 (m, 3H, 1.5 × CH_2), 0.80 - 1.16 (m, 5H, 2.5 × CH_2) **^{13}C NMR (CD_3OD, 150 MHz)** δ 174.1 (C=O), 158.6, 154.9, 151.5, 149.4, 147.4, 139.8, 139.5, 137.1, 137.0, 133.0, 132.5, 131.2, 130.9, 129.7, 129.6, 129.1, 128.8, 125.1, 123.0, 117.1, 116.4, 116.1, 112.5, 112.3, 112.1, 111.2, 108.3, 107.7, 107.4, 106.6, 104.0, 61.4 (OCH_3), 56.8 (OCH_3), 56.8 (OCH_3), 56.6 (OCH_3), 56.5 (OCH_3), 54.9 (CH_2), 52.2 (CH_2), 44.5 (CH_2), 37.4 (NCH_3), 33.2 (NCH_3), 30.8 (CH_2), 28.7 (CH_2), 27.8 (CH_2), 27.4 (CH_2), 27.3 (CH_2), 27.1 (CH_2), 9.6 (CH_3) **HRMS** (EI): Found 695.3331 $(M+H)^+$, $C_{41}H_{47}N_2O_8$ requires 695.3327 **IR :** ν_{max} (KBr) cm^{-1}: 4413.4 (br.), 2932.3, 1611.6, 1582.7, 1508.1, 1461.6, 1272.4,1237.3, 1125.0, 1025.3, 839.8 **MP :** 104-106 °C

8.10.11 (*E*)-N-(8-(5-Hydroxy-2-(4-hydroxyphenyl)-3-methyl-1*H*-indol-1-yl)octyl)-3-(3-hydroxy-4-methoxyphenyl)-N-methyl-2-(3,4,5-trimethoxyphenyl)acrylamide [457]

As per general method (8.10.7), protected indole conjugate [457] (150 mg, 0.166 mmol) and a small spatula tipful of $Pd(OH)_2$ (20 mg) were reacted under a hydrogen atmosphere for 30 min. The

material was purified *via* flash chromatography on silica gel (DCM:EtOAc, gradient 3:1 to 1:1) to afford the product as a yellow solid (112 mg, 94%)

^{1}H NMR (CD_3OD, 600 MHz) δ 6.56 - 7.28 (m, 13H, Ar-H), 3.96 - 4.09 (m, 2H, CH_2), 3.64 - 3.91 (m, 12H, OCH_3), 3.31 - 3.51 (m, 2H, CH_2), 2.89 - 3.07 (m, 3H, NCH_3), 2.13 - 2.26 (m, 3H, CH_3), 1.47 - 1.62 (m, 3H, 1.5 × CH_2), 0.96 - 1.41 (m, 9H, 4.5 × CH_2) **^{13}C NMR (CD_3OD, 150 MHz)** δ 174.9 (C=O), 174.2 (C=O), 174.0 (C=O), 173.8 (C=O), 170.6, 160.1, 158.6, 155.0, 154.9, 154.7, 152.7, 151.5, 149.4, 147.7, 147.6, 147.4, 141.0, 139.8, 139.5, 139.4, 138.8, 138.3, 137.5, 137.1, 137.0, 134.2, 134.1, 133.0, 132.4, 132.3, 131.2, 130.9, 130.0, 129.7, 129.6, 129.1, 128.8, 126.7, 125.1, 124.6, 123.0, 121.5, 117.4, 117.1, 116.4, 116.1, 113.4, 112.7, 112.5, 112.2, 112.0, 111.3, 111.2, 108.5, 108.2, 108.1, 107.7, 107.4, 106.6, 106.5, 104.5, 104.0, 61.4 (OCH_3), 61.3 (OCH_3), 61.3 (OCH_3), 57.6 (OCH_3), 56.8 (OCH_3), 56.7 (OCH_3), 56.6 (OCH_3), 56.5 (OCH_3), 52.5 (CH_2), 52.3 (CH_2), 51.1 (CH_2), 44.5 (CH_2), 44.5 (CH_2), 42.1 (CH_2), 41.6 (CH_2), 37.4 (NCH_3), 36.2 (NCH_3), 34.5 (NCH_3), 33.2 (CH_2), 31.0 (CH_2), 30.8 (CH_2), 30.7 (CH_2), 30.2 (CH_2), 30.1 (CH_2), 30.0 (CH_2), 29.4 (CH_2), 28.8 (CH_2), 28.1 (CH_2), 27.9 (CH_2), 27.8 (CH_2), 27.6 (CH_2), 27.5 (CH_2), 9.6 (CH_3) **HRMS** (EI): Found 723.3639 $(M+H)^+$, $C_{43}H_{51}N_2O_8$ requires 723.3640 **IR :** ν_{max} (KBr) cm^{-1}: 3405.4 (br.), 2930.2, 2855.1, 1611.7, 1583.1, 1508.3, 1462.2, 1272.8, 1237.7, 1125.6, 1025.3 **MP :** 103-107 °C

8.10.12 (*E*)-N-(12-(5-Hydroxy-2-(4-hydroxyphenyl)-3-methyl-1*H*-indol-1-yl)dodecyl)-3-(3-hydroxy-4-methoxyphenyl)-N-methyl-2-(3,4,5-trimethoxyphenyl)acrylamide [458]

As per general method (8.10.7), protected indole conjugate [453] (150 mg, 0.156 mmol) and a small spatula tipful of $Pd(OH)_2$ (20 mg) were reacted under a hydrogen atmosphere for 30 min. The material was purified *via* flash chromatography over silica gel (DCM:EtOAc, gradient 3:1 to 1:1) to afford the product as a yellow solid (109 mg, 90%)

^{1}H NMR (CD_3OD, 600 MHz) δ 6.56 - 7.24 (m, 13H, Ar-H), 3.96 - 4.03 (m, 2H, CH_2), 3.65 - 3.86 (m, 12H, 4 × OCH_3), 3.38 - 3.53 (m, 2H, CH_2), 2.86 - 3.06 (m, 3H, NCH_3), 2.09 - 2.23 (m, 4H, 2 × CH_2), 0.81 - 1.70 (m, 20H, 10 × CH_2) **^{13}C NMR (CD_3OD, 150 MHz)** δ 174.9 (C=O), 174.2 (C=O), 158.6, 154.9, 154.7, 154.7, 151.4, 149.4, 147.6, 147.4, 139.8, 139.5, 138.3, 137.5, 137.0, 134.2, 133.0, 132.5, 131.3, 130.9, 129.7, 128.8, 125.1, 123.0, 121.5, 119.2, 117.4, 117.2, 116.4, 113.4, 112.8, 112.5, 112.0, 111.2, 108.2, 107.7, 107.4, 106.6, 106.5, 104.9, 104.4, 104.0, 97.7, 89.7, 61.4 (OCH_3), 61.3 (OCH_3), 61.3 (OCH_3), 56.8 (OCH_3), 56.8 (OCH_3), 56.6 (OCH_3), 56.5 (OCH_3), 52.5 (CH_2), 52.3 (CH_2), 51.1 (CH_2), 44.6 (CH_2), 42.1 (CH_2), 41.6 (CH_2), 37.4 (NCH_3), 36.1 (NCH_3), 34.5 (NCH_3), 33.2 (CH_2), 30.9 (CH_2), 30.9 (CH_2), 30.7 (CH_2), 30.7 (CH_2), 30.6 (CH_2), 30.6 (CH_2), 30.5 (CH_2), 30.1 (CH_2), 29.5 (CH_2), 29.0 (CH_2), 28.2 (CH_2), 27.9 (CH_2), 27.8 (CH_2), 27.7 (CH_2), 9.6 (CH_3) **HRMS** (EI): Found 779.4277 $(M+H)^+$, $C_{47}H_{59}N_2O_8$ requires 779.4266 **IR :** ν_{max} (KBr) cm^{-1}: 3422.7 (br.), 2926.8, 2852.7, 1614.8, 1586.6, 1508.9, 1462.2, 1272.3, 1237.1, 1122.6, 1026.5 **MP :** 89-92 °C

8.10.13 General method for synthesis of methoxy-indole-acrylic acid conjugates

A mixture of the required acrylic acid (1 eq.), DCC (1 eq.) and HOBt (1 eq.) was suspended in anhydrous DCM (3 mL) and stirred for 10 min under N_2 atmosphere. The phenylindole [459]-[461] was dissolved in anhydrous DCM (3 mL) and slowly added *via* syringe. The reaction mixture was allowed stirring for 16 h and was monitored using TLC. The reaction mixture was then diluted with DCM (15 mL) and filtered to remove the urea by-product. The filtrate was evaporated to dryness in

vacuo to afford the crude oil product which was then purified *via* flash chromatography over silicia gel to afford product. (DCM : EtOAc)

8.10.14 (*E*)-3-(3-Hydroxy-4-methoxyphenyl)-*N*-(4-(5-methoxy-2-(4-methoxyphenyl)-3-methyl-1*H*-indol-1-yl)butyl)-2-(3,4,5-trimethoxyphenyl)-N-methylacrylamide [459]

As per general method (8.10.13), the acrylic acid [150] (1 eq., 293 mg, 0.813 mmol), DCC (1 eq., 167 mg, 0.813 mmol), and HOBt (1 eq., 108 mg, 0.813 mmol) and [238] (286 mg, 0.813 mmol) were reacted together. The crude material was purified using flash chromotragphy over silica gel (DCM:EtOAC, gradient 6:1 to 3:1) to afford the product as a green foam (230 mg, 41%).

^{1}H NMR ($CDCl_3$, 400 MHz) δ 7.28 (d, *J*= 6.5 Hz, 3H, Ar-H), 7.28 (d, *J*= 6.5 Hz, 3H, Ar-H), 7.03(t, *J*= 5.5 Hz, 3H, Ar-H), 6.89(d, *J*= 8.5 Hz, 1H, Ar-H), 6.75 (s, 1H, Ar-H), 6.53 (s, 2H,Ar-H), 6.45 (s, 1H, Ar-H), 4.02 (t, *J*= 7 Hz, 2H, CH_2-N), 3.74-3.95 (m, 12H, 4OCH_3), 3.66 (s, 6H, OCH_3), 3.20-3.28 (m, 2H, CH_2-N), 2.85 (s, 3H, NCH_3), 2.21 (s, 3H, CH_3), 1.29-1.43 (m, 4H, 2 × CH_2) **^{13}C NMR ($CDCl_3$, 400 MHz)** δ 171.18 (C=O), 158.78 (C-OCH_3), 153.38 (C-OCH_3), 152.82 (C-OCH_3), 145.92 (C-OCH_3), 144.67 (C-OCH_3), 137.41, 135.44, 131.19 (Ar-C), 131.02, 130.20, 129.03 (Ar-C), 128.46, 128.01, 124.12, 121.43 (Ar-C), 114.99 (Ar-C), 113.48 (Ar-C), 111.11 (Ar-C), 109.76 (Ar-C), 105.52 (Ar-C), 100.38 (Ar-C), 60.51 (NCH_3), 55.65 (OCH_3), 55.58 (OCH_3), 55.44 (OCH_3), 54.87 (OCH_3), 46.00 (CH_2), 42.99 (NCH_3), 26.74 (CH_2), 25.00 (CH_2), 8.89 (CH_3) **HRMS (EI)**: Found 693.3266 $(M-H)^+$, $C_{41}H_{45}N_2O_8$ requires 693. 3245. **IR:** ν_{max} (KBr) cm^{-1}: 3052.61, 2936.76, 2836.69, 1614.72, 1581.16, 1506.22, 1483.33, 1462.86, 1412.25, 1276.13, 1245.74, 1174.66, 1126.42, 1033.08, 1006.11, 972.86, 905.21, 838.15, 800.22, 762.58, 735.09, 702.49

8.10.15 (*E*)-3-(3-hydroxy-4-methoxyphenyl)-*N*-(8-(5-methoxy-2-(4-methoxyphenyl)-3-methyl-1*H*-indol-1-yl) octyl)-2-(3,4,5-trimethoxyphenyl)-*N*-methylacrylamide [460]

As per general method (8.10.13), the acrylic acid [150] (1 eq., 176 mg, 0.49 mmol), DCC (1 eq., 101mg, 0.49 mmol), and HOBt (1 eq., 66 mg, 0.49 mmol) and [460] (200 mg, 0.49 mmol) were reacted together. The crude material was purified using flash chromotragphy over silica gel (DCM:EtOAC, gradient 6:1 to 3:1) to afford the product as a white foam (250 mg, 68%).

^{1}H NMR ($CDCl_3$, 400 MHz) δ 7.31 (d, *J*= 6.5 Hz, 2H, Ar-H), 7.29 (s, 1H, Ar-H), 7.05 (s, 2H, Ar-H), 7.02 (s, 1H, Ar-H), 6.84 (d, *J*= 8.5 Hz, 2H, Ar-H), 6.68 (s, 1H, Ar-H), 6.56 (s, 2H, Ar-H), 3.95 (t, *J*= 7 Hz, 2H, NCH_2), 3.80-3.93 (m, 12H, 4OCH_3), 3.71 (s, 6H, OCH_3), 3.12-3.33 (m, 2H, CH_2-N), 2.91 (s, 3H, NCH_3), 2.21 (s, 3H, CH_3), 1.21-1.39 (m, 14H, 7CH_2),**^{13}C NMR ($CDCl_3$, 400 MHz)** δ 171.16 (C=O), 158.71 ($COCH_3$), 153.32 ($COCH_3$), 152.79 ($COCH_3$), 145.81 ($COCH_3$), 144.67 ($COCH_3$), 137.54, 131.26 (Ar-C), 131.01, 128.64, 128.31, 124.34, 121.41 (Ar-C), 114.95 (Ar-C), 113.33 (Ar-C), 110.92 (Ar-C), 109.89 (Ar-C), 109.72 (Ar-C), 107.53, 105.97 (Ar-C), 100.19 (Ar-C), 60.52 (OCH_3), 55.66 (OCH_3), 55.58 (OCH_3), 55.44 (OCH_3), 54.87 (NCH_2), 43.39 (CH_2), 33.27 (NCH_3), 29.60 (CH_2), 28.76 (CH_2), 28.64 (CH_2), 26.28 (CH_2), 25.07 (CH_2), 24.41 (CH_2), 8.91 (CH_3) **HRMS (EI):** Found751.3876 $(M+H)^+$, $C_{45}H_{55}N_2O_8$ requires 751.3880 **IR:** ν_{max} (KBr) cm^{-1}**:** 2931.26, 2855.09, 1614.65, 1580.59, 1507.79, 1483.12, 1461.42, 1412.41, 1275.81, 1246.57, 1174.14, 1126.93, 1033.52, 904.89, 836.51, 797.35, 734.39.

8.10.16 (*E*)-3-(3-hydroxy-4-methoxy-2-(4-methoxyphenyl)-3-methyl-1*H*-indol-1-yl)dodecyl)-2-(3,4,5- trimethoxyphenyl)-*N*-methylacrylamide [461]

As per general method (8.10.13), the acrylic acid [150] (1 eq., 155 mg, 0.43 mmol), DCC (1 eq., 88mg, 0.43 mmol), and HOBt (1 eq., 58 mg, 0.43 mmol) and [240] (200 mg, 0.43 mmol) were reacted

together. The crude material was purified using flash chromotragphy over silica gel (DCM:EtOAC, gradient 6:1 to 3:1) to afford the product as a white foam (180 mg, 52%).

^{1}H NMR ($CDCl_3$, 400 MHz) δ 7.31 (d, *J*= 6.5 Hz, 2H, Ar-H), 7.25 (t, *J*= 7 Hz, 4H, Ar-H), 7.05 (s, 2H, Ar-H), 7.02 (s, 1H, Ar-H), 6.90 (d, *J*= 8.5 Hz, 1H, Ar-H), 6.81 (s, 1H, Ar-H), 6.68 (s, 1H, Ar-H), 6.59 (s, 1H, Ar-H), 6.56 (s, 1H, Ar-H), 3.97 (t, *J*= 7 Hz, 2H, NCH_2), 3.92 (s, 6H, OCH_3), 3.90 (s, 3H, OCH_3), 3.88 (s, 3H, OCH_3), 3.80-3.86 (m, 6H, OCH_3), 3.32-3.38 (m, 2H, NCH_2), 2.99 (s, 3H, CH_3), 2.22 (s, 3H, CH_3), 1.11-1.35 (m, 20H, 10 × CH_2) **^{13}C NMR ($CDCl_3$, 400 MHz)** δ 171.23 (C=O), 158.70 (C-OCH_3), 153.30 (C-OCH_3), 152.79 (C-OCH_3), 145.84 (C-OCH_3), 144.69 (C-OCH_3), 137.57, 131.27 (Ar-C), 131.01, 128.30, 124.36, 121.40 (Ar-C), 115.00 (Ar-C), 113.31 (Ar-C), 110.89 (Ar-C), 109.90 (Ar-C), 109.73 (Ar-C), 107.49, 105.57 (Ar-C), 100.18 (Ar-C), 60.52 (OCH_3), 55.66 (OCH_3), 55.58 (OCH_3), 55.43 (OCH_3), 54.85 (CH_2), 43.47 (CH_2), 33.31 (NCH_3), 29.65 (CH_2), 29.08 (CH_2), 28.99 (CH_2), 28.69 (CH_2), 26.36 (CH_2), 25.10 (CH_2), 24.44 (CH_2), 8.91 (CH_3) **HRMS (EI):** Found 807.4532 $(M+H)^+$, $C_{49}H_{63}N_2O_8$ requires 807.4506. **IR:** ν_{max} (KBr) cm^{-1}: 2928.30, 2853.89, 1770.35, 1614.93, 1580.69, 1508.08, 1483.23, 1460.27, 1412.54, 1275.62, 1246.76, 1174.19, 1127.44, 1034.48, 904.81, 835.58, 796.82, 762.66, 735.48, 704.53

8.11 Synthesis of Endoxifen-anastrozole conjugate

8.11.1 (*Z*)-3-((1*H*-Imidazol-1-yl)methyl)-N-(2-(4-(1-(4-((*tert*-butyldimethylsilyl)oxy) phenyl)-2-phenylbut-1-en-1-yl)phenoxy)ethyl)-5-(2-cyanopropan-2-yl)-N-methylbenzamide [462]

A mixture of the required acid [150] (1 eq., 40 mg, 0.148 mmol), DCC (1 eq., 30.53 mg, 0.148 mmol) and HOBt (1 eq., 20 mg, 0.148 mmol) was suspended in anhydrous DCM (3 mL) and stirred for ten minutes under N_2. The endoxifen analogue [197] (1 eq., 72 mg, 0.148 mmol) was dissolved in anhydrous DCM (3 mL) and slowly added *via* syringe. The reaction mixture was allowed to stirr for 16 hours. The reaction was monitored using TLC. The reaction mixture was then diluted with DCM (15 mL) and filtered to remove the urea by-product. The filtrate was evaporated to dryness in *vacuo* to afford the crude oil product which used directly in the next reaction.

HRMS (EI): 762.3811 $(M+Na)^+$, $C_{45}H_{53}N_5NaO_3Si$ requires 762.3815

8.11.2 (*E*)-3-((1*H*-1,2,4-Triazol-1-yl)methyl)-5-(2-cyanopropan-2-yl)-N-(2-(4-(1-(4-hydroxyphenyl)-2-phenylbut-1-en-1-yl)phenoxy)ethyl)-N-methylbenzamide [463]

The silyl ether [462] (80 mg, 0.108 mmol) was dissolved in a minimum amount of THF (3 mL) while stirred under N_2. An equimolar quantity of TBAF (0.108 mL, 0.108 mmol) was added and the mixture was allowed stir for 16 h. The reaction was monitored *via* TLC. The solvent was evaporated to dryness. The residue was redissolved in DCM (20 mL) and washed with a 10% HCl solution (10 mL). The organic phase was dried over Na_2SO_4 and evaporated to dryness in *vacuo*. The residual material was purified *via* flash chromatography on silica gel (DCM:EtOAc, gradient 25:1 to 10:1) to afford the product as a yellow solid. (33 mg, 49%)

^{1}H NMR ($CDCl_3$, 400 MHz) δ 7.85 - 8.38 (m, 2H, 2 × NCHN), 7.34 - 7.62 (m, 2H, Ar-H), 7.03 - 7.28 (m, 8H, Ar-H, C=CH), 6.67 - 6.94 (m, 4H, Ar-H), 6.43 - 6.61 (m, 2H, Ar-H), 5.28 - 5.44 (m, 2H, CH_2), 3.60 - 4.37 (m, 4H, 2 × CH_2), 3.00 - 3.23 (m, 3H, NCH_3), 2.42 - 2.56 (m, 2H, CH_2), 1.64 - 1.77 (m, 12H, CH_3), 0.89 - 0.98 (m, 3H, CH_3) **^{13}C NMR ($CDCl_3$, 100 MHz)** δ 169.9 (C=O), 154.7 (C_q), 153.9 (NCHN), 142.5 (NCHN), 142.2 (C_q), 137.2 (C_q), 135.6 (C_q), 131.6, 131.5, 130.2, 130.2, 129.3, 129.2, 127.4, 125.6, 125.5, 125.3, 123.7, 123.7, 123.3 (CN), 114.6, 113.9, 113.5, 112.7, 65.9 (CH_2), 65.4, 52.5 (CH_2), 47.4

(CH_2), 39.3 (NCH_3), 36.7 ($C(CH_3)_2$), 32.9, 28.6 (CH_2), 28.5 (CH_3), 13.2 (CH_3) **HRMS (EI):** 648.2921 $(M+Na)^+$, $C_{39}H_{39}N_5NaO_3$ requires 648.2951 **IR :** ν_{max} (KBr) cm^{-1}: 3436.9 (br.), 3236.4, 2965.5, 2930.1, 2231.5 (CN), 1628.9, 1602.6, 1505.9, 1441.3, 1234.6, 1234.6, 1168.7, 1135.2, 835.8, 730.5 **MP:** 92-94 °C

8.12 Synthesis of letrozole-cytotoxic agent conjugate

8.12.1 (*E*)-N-(2-(4-((4-Cyanophenyl)(1*H*-1,2,4-triazol-1-yl)methyl)phenoxy)ethyl)-3-(3-hydroxy-4-methoxyphenyl)-N-methyl-2-(3,4,5-trimethoxyphenyl)acrylamide [464]

A mixture of the required acyrilic acid [150] (1.2 eq., 165 mg, 0.448 mmol), EDC (1.4 eq., 85.5 mg, 0.598 mmol), and HOBt (1.4 eq., 60 mg, 0.598 mmol) were suspended in 3 mL of anhydrous dichloromethane and stirred for 10 min under a nitrogen atmosphere. The letrozole derivative [387] (1 eq., 124 mg, 0.373 mmol) was dissolved in 3ml of anhydrous dichloromethane and slowly added to the mixture *via* a syringe. The reaction was allowed stir for 16 h and was monitored *via* TLC. The reaction mixture was diluted to 15 ml with anhydrous dichloromethane. To this mixture, water (20 mL) was added. The aqueous phase was extracted with DCM (20 mL x 3), brine (50 mL), dried over Na_2SO_4 and evaporated to dryness in *vacuo* to yield the crude product. The crude product was afforded as a brown resin. The material was purified *via* flash chromatography over silica gel (DCM : EtOAc, gradient 40:1 to 20:1) to afford the product as a yellow resin (196 mg, 78%)

^{1}H NMR ($CDCl_3$, 600 MHz) δ 8.08 (s, 1H, NCHN), 8.01 (s, 1H, NCHN), 7.69 (d, *J* = 8.28 Hz, 2H, Ar-H), 7.07 - 7.24 (m, 4H, Ar-H), 6.94 (s, 2H, Ar-H), 6.49 - 6.81 (m, 7H, Ar-H, CH, C=CH), 4.28 (s, 2H, CH_2), 3.80 - 3.94 (m, 8H, OCH_3, CH_2), 3.67 (s, 6H, OCH_3), 3.09 - 3.20 (m, 3H, NCH_3) **^{13}C NMR ($CDCl_3$, 150 MHz)** δ 164.0 (C=O), 153.4 (C_q), 152.1 (NCHN), 146.5 (C_q), 145.2 (C_q), 143.6 (NCHN), 135.8 (C_q), 132.7, 130.2, 128.4 (C_q), 128.3, 121.9, 118.2 (C_q), 115.5, 115.2, 112.5 (C_q), 110.3 (C_q), 106.1, 77.2 (CH), 66.9 (OCH_3), 65.9 (CH_2), 61.0 (OCH_3), 56.1 (OCH_3), 55.9 (OCH_3), 53.4 (CH_2), 38.9 (NCH_3) **HRMS (EI):** 698.2592 $(M+Na)^+$, $C_{38}H_{37}N_5NaO_7$ requires 698.2591 **IR :** ν_{max} (KBr) cm^{-1}: 3434.8, 3300.5, 2938.2, 2230.4 (CN), 1610.5, 1581.5, 1508.4, 1412.8, 1275.4, 1240.5, 1125.9, 1008.2, 911.8, 731.2

Bibliography

1. National Cancer Ireland Registry. *Cancer in Ireland 2011*; National Ireland Registry of Ireland: 2011.
2. Pöhls, U. G.; Fasching, P. A.; Beck, H.; Kaufmann, M.; Kiechle, M.; von Minckwitz, G.; Paepke, S.; Schultz-Zehden, B.; Schwarz-Boeger, U.; Beckmann, M. W. *Oncol Rep.* **2005,** 14, 1605-13.
3. Nogrady, T.; Weaver, D. F. *Medicinal Chemistry: A Molecular and Biochemical Approach*. 3rd ed.; Oxford University Press: 2005.
4. Gelehrter, T. D. Patients and Populations: Medical Genetics. **2012**.
5. Agostinis, P.; Berg, K.; Cengel, K. A.; Foster, T. H.; Girotti, A. W.; Gollnick, S. O.; Hahn, S. M.; Hamblin, M. R.; Juzeniene, A.; Kessel, D.; Korbelik, M.; Moan, J.; Mroz, P.; Nowis, D.; Piette, J.; Wilson, B. C.; Golab, J. *CA Cancer J Clin.* **2011,** 61.
6. Cancer.org. Monoclonal antibodies. http://www.cancer.org/treatment/treatmentsandsideeffects/treatmenttypes/immunotherapy/immunotherapy-monoclonal-antibodies (08/07/2012).
7. Ophardt, C. E. Anti-Cancer Drugs I. In Elmhurst College: 2003; Vol. CHM 110 - Env. Issues, CHM 103 - Org&Bio.
8. Brown, J. M.; Wilson, W. R. *Nature Reviews Cancer* **2004,** 4, 437-47.
9. Gottesman, M. M. *Annu. Rev. Med.* **2012,** 53, 615–27.
10. Barinaga, M. *Science* **1997.,** 278, 1036–39.
11. Nabholtz, J. M.; Slamon, D. *Semin. Oncol.* **2001.,** 28 (Suppl 3), 1-12.
12. Pastan, I.; Kreitman, R. J. *Adv. Drug. Deliv. Rev.* **1998,** 31, 53–88.
13. Druker, B. J.; Sawyers, C. L.; Kantarjian, H.; et al. *N. Engl. J. Med.* **2001,** 344, 1038–42.
14. American Cancer Society. Chemotherapy Principles: An Indepth Discussion of the Techniques and Its Role in Cancer Treatment. In 2011 (http://www.cancer.org/acs/groups/cid/documents/webcontent/002995-pdf.pdf).
15. Smith, H. J. *Smith and Williams Introduction to the Principles of Drug Design and Action*. 4th ed.; CRC Talyor & francis: London, 2006.
16. Kingston, D. G. I. *Anticancer Agents from Natural Products*. CRC Lewis Publishers: Boca Raton, Florida, 2005.
17. Cyclacel Pharmaceuticals, I. Cell Cycle. In graph_cell_cycle, Ed. 2012.
18. Woolley, D. W. *A Study of antimetabolites*. John Wiley & Sons, Inc.: New York, 1952.
19. Dijkmans, B. A.; Jansen, G. *Nucleosides Nucleotides Nucleic Acids* **2004,** 8, 1083-88.
20. Peters, G. J.; van der Wilt, C. L.; van Moorsel, C. J. A.; Kroep, J. R.; Bergman, A. M.; Ackland, S. P. *Pharmacology & Therapeutics* **2000,** 87, 227–253.
21. Palchaudhuri, R.; Hergenrother, P. J. *Current Opinion in Biotechnology* **2007,** 18, 497-503.
22. Lerman, L. S. *J Mol Biol* **1961,** 3, 18-30.
23. Jonathan, B. C. *Biopolymers* **1997,** 44, 201-15.
24. van Maanen, M. J.; Smeets, C. J. M.; Beijnen, J. H. *Cancer Treatment Review* **2000,** 26, 257-68.
25. Wei, L. L.; Mangel, W. F.; Katzenellenbogen, B. S. *Journal of Steriod Biochemistry* **1985,** 23, 875-81.
26. Inlow, R. O.; Joesten, M. D. *Journal of inorganic and Nuclear Chemistry* **1975,** 37, 2353-57.
27. Shealy, Y. F.; Krauth, C. A.; Laster, W. R. J. *J. Med. Chem.* **1984,** 27, 664-70.
28. Lam, H. P.; Begleiter, A.; Goldenberg, G. J.; Wong, C.-M. *J. Med. Chem.* **1979,** 22, 200-02.
29. Soloway, A. H.; Brumbaugh, R. J.; Witial, D. T. *Journal of Theoretical Biology* **1983,** 102, 361-73.
30. Crooke, S. T.; Brader, W. T. *Cancer Treatment Review* **1976,** 3, 121-39.
31. Hartley, J. A. *Expert Opin. Investig. Drugs* **2011,** 20, 733-44.
32. Farmer, J. D.; Gustafson, G. R.; Conti, A. *Nucleic Acids Res.* **1991,** 19, 899-905.
33. Bose, D. S.; Thompson, A. S.; Ching, J.; et al. *J Am Chem Soc* **1992,** 114, 4939-41.
34. Smellie, M.; Kelland, L. R.; Thurston, D. E.; et al. *Br. J. Cancer* **1994,** 70, 48-53.

35. McHugh, M. M.; Kuo, S. R.; Walsh-O'Beirne, M. H.; Liu, J. S.; Melendy, T.; Beerman, T. A. *Biochemistry* **1999,** 38, 11508-15.
36. Parker, C.; Waters, R.; Leighton, C.; Hancock, J.; Sutton, R.; Moorman, A. V.; Ancliff, P.; Morgan, M.; Masurekar, A.; Goulden, N.; Green, N.; Révész, T.; Darbyshire, P.; Love, S.; Saha, V. *Lancet* **2010,** 376, 2009-17.
37. Hande, K. R. *European Journal of Cancer* **1998,** 34, 1514-21.
38. Robinson, H. M.; Bratlie-Thoresen, S.; Brown, R.; Gillespie, D. A. *Cell Cycle* **2007,** 6, 1265-7.
39. Brown, T. Nucleic Acids Book. In Ltd, A., Ed. University of Southampton: http://www.atdbio.com/nucleic-acids-book, 2012.
40. Chen, J.; Stubble, J. *J. Nature Reviews Cancer* **2005,** 5, 102-12.
41. Rowinsky, E. K.; Donehower, R. C. *Pharmacol. Ther.* **1991,** 52, 35-84.
42. Poruchynsky, M. S.; Wang, E. E.; Rudin, C. M.; Blagosklonny, M. V.; Fojo, T. *Cancer Res.* **1998,** 58, 3331-38.
43. Liu, X. M.; Wang, L. G.; Kreis, W.; Budman, D. R.; Adams, L. M. *Br. J. Cancer* **2001,** 85, 1403-11.
44. Dustin, P. *Sci. Am.* **1980,** 243, 66-7.
45. Krasenti, E.; Vernos, I. *Science* **2001,** 294, 543-47.
46. Hait, W. N.; Rubin, E.; Goodin, S. *Chemother. Biol. Response Modif. Cancer* **2001,** 19, 59-83.
47. Pellegrini, F.; Budman, D. R. *Cancer Investigation* **2005,** 23, 264-73.
48. Heath, V. L.; Bicknell, R. *Nat Rev Clin Oncol* **2009,** 6, 395-404.
49. Denga, Z. T.; Fenga, T.; Wanga, P.; Qia, X.; Chena, X. H.; Lia, Y. X.; Songa, C. L.; Gengb, M. Y.; Lia, J. *Biochemical Pharmacology* **2011,** 82, 1832-42.
50. Zwick, E.; Bange, J.; Ullrich, A. *Endocr. Relat. Cancer,* **2001,** 8.
51. Mayo Clinic. http://www.mayoclinic.com/health/monoclonal-antibody/CA00082 (12/18/12).
52. Menard, S.; Pupa, S. M.; Campiglio, M.; Tagliabue, E. *Oncogene* **2003,** 22, 6570-78.
53. Hudis, C. A. *N Engl J Med.* **2007,** 357, 39-51.
54. Albanell, J.; Codony, J.; Rovira, A.; Mellado, B.; Gascon, P. *Advances in Experimental Medicine and Biology* **2003,** 542, 253-68.
55. Jemal, A.; Siegel, R.; Xu, J.; Ward, E. *CA Cancer J. Clin.* **2010,** 60, 277-300.
56. Pasqualini, J. R.; Chetrite, G. S. *Journal of Steroid Biochemistry & molecular Biology* **2005,** 93, 221-36.
57. Higgins, M. J.; Baselga, J. *The Journal of Clinical Investigation* **2011,** 121, 3797-3803.
58. Palchaudhuri, J. R.; Chetrite, G. S.; Blacker, C.; Feinstein, M. C.; Delalonde, L.; Talbi, M.; Maloche, C. *J. Clin, Endocrinol. Metab.* **1996,** 81, 1460-64.
59. Chetrite, G. S.; Cortes-Prieto, J.; Philippe, J. C.; Wright, F.; Pasqualini, J. R. *J. Steroid Biochem. Molec. Biol.* **2000,** 72, 23-27.
60. McGuire, W. L.; Chamness, G. C.; Fuqua, S. A. W. *J. Steroid Biochem. Molec. Biol.* **1992,** 43, 243-47.
61. Fuqua, S. A. W.; Greene, G. L.; McGuire, W. L. *Cancer Res.* **1992,** 52, 483-86.
62. Castles, C. G.; Fuqua, S. A. W.; Klotz, D. M.; Hill, S. M. *Cancer Res.* **1993,** 53, 5934-39.
63. Edwards, D. P.; Chamness, G. C.; McGuire, W. L. *Biochim. Biophys. Acta.* **1979,** 560, 457-86.
64. Litherland, S.; Jackson, I. M. *Cancer Treat. Rev.* **1988,** 15, 183-94.
65. Gruber, C. J.; Tschugguel, W.; Schneeberger, C.; Huber, J. C. *N. Engl. J. Med.* **2002,** 346, 340-52.
66. Scallen, T. J.; Noland, B. J.; Gavey, K. L.; Bassn, N. M.; Ocknern, R. K.; Chanderbhan, R.; Vahouny, G. V. *J. Biol. Chem.* **1985,** 260, 4733-39.
67. Kallen, C. B.; Billheimer, J. T.; Summers, S. A.; Stayrook, S. E.; Lewis, M.; Strauss, J. F. *J. Biol. Chem.* **1998,** 273, 26285-88.
68. Simpson, E. R.; Zhao, Y.; Agarwal, V. R.; Michael, M. D.; Bulun, S. E.; Hinshelwood, M. M.; Gramah-Lorence, S.; Sun, S.; Fisher, T.; Mendelson, C. R. *Recent Progress in Hormone Research* **1997,** 52, 185-213.

69. Bruch, H. R.; Wolf, L.; Budde, R.; Romalo, G.; Schweikert, H. U. *Journal of Clinical Endocrinology and Metabolism* **1992,** 75, 101-05.
70. Bayard, F.; Clamens, S.; Delsol, G.; Blaes, N.; Maret, A.; Ciba, F. *Foundation Symposium* **1995,** 191, 122-32.
71. Sasano, H.; Uzuki, M.; Sawai, T.; Nagura, H.; Matsunaga, G.; Kashimoto, O.; Harada, N. *Journal of Bone and Mineral Research* **1997,** 12, 1416-23.
72. Naftolin, F.; Ryan, K. J.; Davies, I. J.; Reddy, V. V.; Flores, F.; Petro, Z.; Kuhn, M.; White, R. J.; Takaoka, Y.; Wolin, L. *Recent Progress in Hormone Research* **1975,** 31, 295-319.
73. Labrie, F.; Belanger, A.; Cusan, L.; Candas, B. *Journal of Clinical Endocrinology and Metabolism* **1997,** 82, 2403-09.
74. Siiteri, P. K.; MacDonald, P. C. *Handbook of Physiology*. Eds RO Greep & EB Astwood. Washington: American Physiology Society.: 1973; Vol. 2.
75. Riggins, R. B.; Bouton, A. H.; Liu, M. C.; Clarke, R. *Vitam. Horm.* **2005,** 71, 201-37.
76. Jordan, V. C. *Steroids* **2007,** 72, 829-42.
77. Jordan, V. C. *J. Med. Chem.* **2003,** 7, 1081-1111.
78. Karamouzis, M. V.; Konstantinopoulos, P. A.; Badra, F. A.; Papavassiliou, A. G. *Breast Cancer Research and Treatment* **2008,** 107, 195-210.
79. Swedenborg, E.; Power, K. A.; Cai, W.; Pongratz, I.; Ruegg, J. *Cellular and Molecular Life Sciences,* **2009,** 66, 3873-94.
80. Welboren, W. J.; Sweep, F. C.; Span, P. N.; Stunnenberg, H. G. *Endocrine-Related Cancer Investigation* **2009,** 16, 1073-89.
81. Ascenzi, P.; Bocedi, A.; Marino, M. *Molecular Aspects of Medicine* **2006,** 27, 299-402.
82. Green, S.; Walter, P.; Kumar, V.; Krust, A.; J-M., B.; Argos, P.; Chambon, P. *Nature* **1986,** 320, 134-39.
83. Kuiper, G. G.; Enmark, E.; Pelto-Huikko, M.; Nilsson, S.; Gustafsson, J. A. *Proc. Natl. Acad. Sci. USA* **1996,** 93, 5925-30.
84. Witkowska, H. E.; Carlquist, M.; Engström, O. *Steroids* **1997,** 62, 621-31.
85. Enmark, E.; Pelto-Huikko, M.; Grandien, K. *J. Clin. Endocrinol Metab.* **1997,** 82, 4258-65.
86. Beato, M. *Cell* **1989,** 56, 335-44.
87. Berry, M.; Metzger, D.; Chambon, P. *The EMBO Journal* **1990,** 9, 2811-18.
88. Tora, L.; White, J.; Brou, C. *Cell* **1989,** 59, 477-87.
89. Tsai, M. J.; O'Malley, B. W. *Annual Review of Biochemistry* **1994,** 63, 451-86.
90. Schwabe, J. W.; Chapman, L.; Finch, J. T.; Rhodes, D.; Neuhaus, D. *Structure* **1993,** 1, 187-204.
91. Glass, C. K.; Rosenfeld, M. G. *Genes and Development* **2000,** 14, 121-41.
92. Johnston, S. R.; Lu, B.; Scott, G. K.; et al. *Clinical Cancer Research* **1999,** 5, 251-56.
93. Webb, P.; Nguyen, P.; Valentine, C.; et al. *Molecular Endocrinology* **1999,** 13, 1672-85.
94. Paech, K.; Webb, P.; Kuiper, G. G.; et al. *Science* **1997,** 277, 1508-1.
95. Kumar, R.; Zakharov, M. N.; Khan, S. H.; Miki, R.; Jang, H.; Toraldo, G.; Singh, R.; Bhasin, S.; Jasuja, R. *Journal of Amino Acids* **2011,** 2011, 1-7.
96. Greschik, H.; Wurtz, J.-M.; S., S.; Bourguet, W.; van Dorsselaer, A.; Moras, D. *Molecular Cell* **2002,** 9, 303-13.
97. Pike, A. C. W. *Best Practice & Clinical Endocrinology & Metabolism* **2006,** 20, 1-14.
98. Ascenzi, P.; Bocedi, A.; Marino, M. *J. Molecular Aspects of Medicine* **2006,** 27, 299-402.
99. McDonnell, D. P. *Clin Cancer Res* **2005,** 11, 871-77.
100. Brzozowski, A. M.; Pike, A. C. W.; Dauter, Z.; et al. *Nature* **1997,** 389, 753-758.
101. Warnmark, A.; Treuter, E.; Gustafsson, J.-A.; et al. *The Journal of Biological Chemistry* **2003,** 277, 21862-68.
102. Shiau, A. K.; Barstad, D.; Loria, P. M.; Cheng, L.; Kushner, P. J.; Agard, D. A.; Greene, G. L. *Cell* **1998,** 85, 927-37.
103. Shiau, A. K.; Barstad, D.; Radek, J. T.; et al. *Nature Structural Biology* **2002,** 9, 359-64.

104. Pike, A. C. W.; Brzozowski, A. M.; Walton, J.; Hubbard, R. E.; Thorsell, A. G.; Li, Y. L.; Gustafsson, J. A.; Carlquist, M. *Structure* **2001,** 9, 145-53.
105. Anstead, G. M.; Carlson, K. E.; Katzenellenbogen, J. A. *Steroids* **1997,** 62, 268-303.
106. Meyers, R. A. *Cancer : from mechanisms to therapeutic approaches*. Wiley-VCH: Weinheim, 2007.
107. Bohl, M. *Z Natutforsch* **1987,** 42c, 221-24.
108. VC., J. *Nat Rev Cancer.* **2007,** 7, 46-53.
109. Morrow, M.; Jordan, V. C. *J Surg Oncol.* **2007,** 95, 4-5.
110. Cummings, S. R.; Eckert, S.; Krueger, K. A.; et al. *JAMA* **1999,** 281, 2189-97.
111. Komm, B. S.; Kharode, Y. P.; Bodine, P. V. *Endocrinology.* **2005,** 146, 3999-4008.
112. Stump, A. L.; Kelley, K. W.; Wensel, T. M. *Ann Pharmacother.* **2007,** 41, 833-39.
113. Hall, J. M.; McDonnell, D. P. *Menopausal Medicine* **2008,** 15, 1-6.
114. Meegan, M. J.; Lloyd, D. G. *Curr Med Chem* **2003,** 10.
115. Bryant, H. *Endocr Metab Dis* **2002,** 3.
116. Marttunen, M. B.; Hietanen, P.; Titinen, A.; Roth, H.-J.; Viinikka, L.; Ylikorkala, O. *Calcif Tissue Int* **1999,** 65, 365-68.
117. O'Regan, R. M.; Cisneros, G. M.; England, G. M.; MacGregor, J. L.; Muenzner, H. D.; Assikis, V. J. *J Natl Cancer Inst* **1998,** 90, 1552-55.
118. Shapiro, C. L.; Recht, A. *N Engl J Med* **2001,** 344, 1997-2008.
119. Diez-Perez, A. *Arq Bras Endocrinol Metab* **2006,** 50, 720-34.
120. Katzenellenbogen, J. A.; Carlson, K. E.; Katzenellenbogen, B. S. *J. Steroid Biochem. Molec. Biol.* **1985,** 22, 589.
121. Einer, J. *N. Acta Pharmacol. Toxicol.* **1965,** 23, 365.
122. Willson, T. M.; Henke, B. R.; Momtahen, T. M.; Charifson, P. S.; Batchelor, K. W.; Lubahn, D. B.; Moore, L. B.; Oliver, B. B.; Sauls, H. R.; Triantafillou, J. A.; Wolfe, S. G.; Baer, P. G. *J. Med. Chem.* **1994,** 37, 1550-52.
123. Black, L. J.; Sato, M.; Rowley, E. R.; Magee, D. E.; Bekele, A.; Williams, D. C.; et al. *J Clin Invest* **1994,** 93, 63-39.
124. Frolik, C. A.; Bryant, H. U.; Black, E. C.; Magee, D. E.; Chandrasekhar, S. *Bone* **1996,** 18, 621-27.
125. Anzano, M. A.; Peer, C. W.; Smith, J. M.; Mullen, L. T.; Shrader, M. W.; Logsdon, D. L. *J Natl Cancer Inst* **1996,** 88, 123-25.
126. Eli Lilly and Company. *Lilly Reports on Outcome of Phase III Study of Arzoxifene". Press Release.*; 2009-08-18.
127. Ke, H. Z.; Paralkar, V. M.; Grasser, W. A.; Crawford, D. T.; Qi, H.; Simmons, H. A.; et al. *Endocrinology* **1998,** 139, 2068-76.
128. Witte, R. S.; Pruitt, B.; Tormey, D. C.; Moss, S.; Rose, D. P.; Falkson, G.; et al. *Cancer* **1986,** 57.
129. Ji, Q.; Wang, J.; Yang, C.; Hui, X.; Yan, X.; Wu, X.; Xie, Y.; Wang, M. W. *Bioorganic & Medicinal Chemistry Letters* **2005,** 15, 2891-2893.
130. McDevitt, R. E.; Malamas, M. S.; Manas, E. S.; Unwalla, R. J.; Xu, Z. B.; Miller, C. P.; Harris, H. A. *Bioorganic & Medicinal Chemistry Letters* **2005,** 15, 3137-3142.
131. Ullrich, J. W.; Unwalla, R. J.; Singhaus, R. R. J.; Harris, H. A.; Mewshaw, R. E. *Bioorganic & Medicinal Chemistry Letters* **2007,** 17, 118-22.
132. Dykstra, K. D. *Bioorganic & Medicinal Chemistry Letters* **2007,** 17, 2322-28.
133. Goldstein, S. R.; Nanavati, N. *Am J Obstet Gynecol* **2002,** 187, 521-27.
134. Sutherland, M. K.; Brady, H.; Gayo-Fung, L. M.; Leisten, J.; Lipps, S. G.; McKie, J. A. *Calcif Tissue Int* **2003,** 72, 710-16.
135. Labrie, F.; Labrie, C.; Belanger, A.; Simard, J.; Giguere, V.; Tremblay, A.; et al. *J Steroid Biochem Mol Biol* **2001,** 79, 213-25.
136. Gutman, M.; Couillard, S.; Roy, J.; Labrie, F.; Candas, B.; Labrie, C. *Int J Cancer* **2002,** 99, 273-78.

137. Richardson, T. I.; Dodge, J. A.; Wang, Y.; Durbin, J. D.; Krishnan, V.; Norman, B. H. *Bioorg. Med. Chem.* **2007,** 17, 5563-66.
138. Richardson, T. I.; Norman, B. H.; Lugar, C. W.; Jones, S. A.; Wang, Y.; Durbin, J. D.; Krishnan, V.; Dodge, J. A. *Bioorganic & Medicinal Chemistry Letters* **2007,** 17, 3570-3574.
139. Richardson, T. I.; Dodge, J. A.; Wang, Y.; Durbin, J. D.; Krishnan, V.; Norman, B. H. *Bioorganic & Medicinal Chemistry Letters* **2007,** 17, 5563-5566.
140. Simons, R.; Gruppen, H.; Bovee, T. F. H.; Verbruggen, M. A.; Vincken, J.-P. *Food Funct* **2012,** 3, 810-27.
141. Yazaki, K.; K., S.; Tsurumaru, Y. *Phytochemistry* **2009,** 70, 1739-45.
142. Jiang, Q.; Payton-Stewart, F.; Elliott, S.; Driver, J.; Rhodes, L. V.; Zhang, Q.; Zheng, S.; Bhatnagar, D.; Boue, S. M.; CollinsBurow, B. M.; Sridhar, J.; Stevens, C.; McLachlan, J. A.; Wiese, T. E.; Burow, M. E.; Wang, G. *J. Med. Chem.* **2010,** 53, 6153-63.
143. Halabalaki, M.; Alexi, X.; Aligiannis, N.; Lambrinidis, G.; Pratsinis, H.; Florentin, I.; Mitakou, S.; Mikros, E.; Skaltsounis, A. L.; Alexis, M. N. *Planta Med* **2006,** 72, 488-93.
144. Djiogue, S.; Halabalaki, M.; Alexi, X.; Njamen, D.; Fomum, Z. T.; Alexis, M. N.; Skaltsounis, A. L. *J. Nat. Prod.* **2009,** 72, 1603-07.
145. Kretzschmar, G.; Zierau, O.; Wober, J.; Tischer, S.; Metz, P.; Vollmer, G. *J. Steroid Biochem. Mol. Biol.* **2010,** 118, 1-6.
146. Djiogue, S.; Njamen, D.; Halabalaki, M.; Kretzschmar, G.; Beyer, A.; Mbanya, J. C.; Skaltsounis, A. L.; Vollmer, G. *J. Steroid Biochem. Mol. Biol.* **2010,** 120, 184-91.
147. Tan, Q. *Bioorganic & Medicinal Chemistry Letters* **2005,** 15, 1675-1681.
148. Liu, J.; Birzin, E. T.; Chan, W.; et al. *Bioorganic & Medicinal Chemistry Letters* **2005,** 15, 715-18.
149. Vu, A. T.; Cohna, S. T.; Manasa, E. S.; Harrisb, H. A.; Mewshawa, R. E. *Bioorganic & Medicinal Chemistry Letters* **2005,** 15, 4520-25.
150. Vu, A. T.; Campbell, A. N.; Harris, H. A.; Unwalla, R. J.; Manas, E. S.; Mewshaw, R. E.; Adams, L. M. *Bioorganic & Medicinal Chemistry Letters* **2007,** 17, 4053-56.
151. Blizzard, T. A.; DiNinno, F.; Morgan, J. D.; Chen, H. Y.; et. al. *Bioorganic & Medicinal Chemistry Letters* **2005,** 15, 107-.
152. Tan, Q.; Birzin, E. T.; Chan, W.; al, E. *Bioorganic & Medicinal Chemistry Letters* **2004,** 14, 3753-55.
153. Zhuang, S.; Zhang, J.; Zhang, F.; Zhang, Z.; Wen, Y.; Liu, W. *Bioorganic & Medicinal Chemistry Letters* **2011,** 21, 7298-305.
154. Wilkening, R. R.; Ratcliffe, R. W.; Fried, A. K.; Meng, D.; Sun, W.; Colwell, L.; Lambert, S.; Greenlee, M.; Nilsson, S.; Thorsell, A.; Mojena, M.; Tudela, C.; Frisch, K.; Chan, W.; Birzin, E. T.; Rohrer, S. P.; Hammond, M. L. *Bioorganic & Medicinal Chemistry Letters* **2006,** 16, 3489–94.
155. Wildonger, K. J. *Bioorganic & Medicinal Chemistry Letters* **2006,** 16, 4462-66.
156. Wilkening, R. R.; Ratcliffe, R. W.; Fried, A. K.; Meng, D.; Sun, W.; Colwell, L.; Lambert, S.; Greenlee, M.; Nilsson, S.; Thorsell, A.; Mojena, M.; Tudela, C.; Frisch, K.; Chan, W.; Birzin, E. T.; Rohrer, S. P.; Hammond, M. L. *Bioorganic & Medicinal Chemistry Letters* **2006,** 16, 3896-901.
157. Parker, D. L.; Meng, D.; Ratcliffe, R. W.; Wilkening, R. R.; Sperbeck, D. M.; Greenlee, M. L.; Colwell, L. F.; Lambert, S.; Birzin, E. T.; Frisch, K.; Rohrer, S. P.; Nilsson, S.; Thorsell, A. G.; Hammond, M. L. *Bioorganic & Medicinal Chemistry Letters* **2006,** 16, 4652-56.
158. Hwang, K. J.; O'Neil, J. P.; Katzenellenbogen, J. A. *J. Org. Chem.* **1992,** 57, 1262.
159. Meyers, M. J.; Sun, J.; Carlson, K. E.; Katzenellenbogen, B. S.; Katzenellenbogen, J. A. *J. Med. Chem.* **1999,** 42, 2456.
160. Tedesco, R.; Youngman, M. K.; Wilson, S. R.; Katzenellenbogen, J. A. *Bioorganic & Medicinal Chemistry Letters* **2001,** 11, 1281-84.

161. Stauffer, S. R.; Coletta, C. J.; Tedesco, R.; Nishiguchi, G.; Carlson, K.; Sun, J.; Katzenellenbogen, B. S.; Katzenellenbogen, J. A. *j Med. Chem.* **2000,** 43, 4934-47.
162. Harrington, W. R.; Sheng, S.; Barnett, D. H.; Petz, L. N.; Katzenellenbogen, J. A.; Katzenellenbogen, B. S. *Mol. Cell Endocrinol.* **2003,** 206, 13-22.
163. Alexi, X. *Journal of Steroid Biochemistry & Molecular Biology* **2009,** 117, 159-67.
164. De Angelis, M.; Stossi, F.; Carlson, K. A.; Katzenellenbogen, B. S.; Katzenellenbogen, J. A. *J Med Chem.* **2005,** 48, 1132-44.
165. Malamas, M. S.; Manas, E. S.; McDevitt, R. E.; Gunawan, I.; Xu, Z. B.; Collini, M. D.; Miller, C. P.; Dinh, T.; Henderson, R. A.; Keith, J. C. J.; Harris, H. A. *jinbJournal of Medicinal Chemistry* **2004,** 47, 5021-40.
166. Compton, D. R.; Sheng, S.; Carlson, K. E.; Rebacz, N. A.; Lee, I. Y.; Katzenellenbogen, B. S.; Katzenellenbogen, J. A. *J. Med. Chem.* **2004,** 47, 5872-93.
167. Bradbury, S. P.; Mekenyan, O. G.; Ankley, G. T. *Environ. Toxicol. Chem.* **1998,** 17, 15-25.
168. Lloyd, D. G.; Smith, H. M.; O'Sullivan, T.; Knox, A. S.; Zisterer, D. M.; Meegan, M. J. *Medicinal Chemistry* **2006,** 2, 147-68.
169. Meegan, M. J.; Hughes, R. B.; Lloyd, D. G.; Williams, D. C.; Zisterer, D. M. *J. Med. Chem.* **2001,** 44, 1072-84.
170. Bowler, J.; Lilley, T. J.; Pittam, J. D.; Wakeling, A. E. *Steroids* **1989,** 54, 71-99.
171. Johnston, S. J.; Cheung, K. L. *Curr Med Chem* **2010,** 17, 902-14.
172. Wakeling, A. E.; Bowler, J. *Journal of Endocrinology* **1987,** 112, R7-R10.
173. Wakeling, A. E.; Dukes, M.; Bowler, J. A. *Cancer Res.* **1991,** 51, 3867-73.
174. Dodwell, D.; Wardley, A.; Johnston, S. *Breast.* **2006,** 15.
175. Dowsett, M. *Clin Cancer Res.* **2003,** 9, 502s-10s.
176. Robertson, J. F.; Nicholson, R. I.; Bundred, N. J.; et al. *Cancer Res.* **2001,** 61, 6739-46.
177. Gjerde, J.; Kisanga, E. R.; Hauglid, M.; Holm, P. I.; Mellgrn, G.; Lien, E. A. *J. Chromatography A* **2005,** 1082, 6-14.
178. Stearns, V.; Johnson, M. D.; Rae, J. M.; et al. *J Natl Cancer Inst.* **2003,** 95, 1758-64.
179. Borges, S.; Desta, Z.; Li, L.; al., e. *Clin Pharmacol Ther.* **2006,** 80, 61-74.
180. Briest, S.; Stearns, V. *Clinical Advances in Hematology & Oncology* **2009,** 7, 185-92.
181. Jordan, V. C. *Nature reviews cancer* **2007,** 7, 46-53.
182. Labrie, F.; Belanger, A.; Luu-The, V.; Labrie, C.; Simond, J.; Cusan, L.; Gomez, J. L.; Candas, B. *Steroids* **1998,** 63, 322-28.
183. Labrie, F.; Belanger, A.; Cusan, L.; Gomez, J. L.; Candas, B. *Journal of Clinical Endocrinology and Metabolism* **1997,** 82, 2396-2402.
184. Sasano, H.; Frost, A. R.; Saitoh, R.; Harada, N.; Poutanen, M.; Vihko, R.; Bulun, S. E.; Silverberg, S. G.; Nagura, H. *Journal of Clinical Endocrinology and Metabolism* **1996,** 81, 4042-46.
185. Geisler, J.; Berntsen, H.; Lonning, P. *J Steroid Biochem Mol Biol* **2000,** 72, 259-64.
186. Chetrite, G.; Cortes-Prieto, J.; Philippe, J.; Wright, F.; Pasqualini, J. *J Steroid Biochem Mol Biol* **2000,** 72, 23-27.
187. Van Landeghem, A. A. J.; Poortman, J.; Nabuurs, M.; Thijssen, J. H. H. *Cancer Res* **1985,** 45, 2907-12.
188. Yue, W.; Zhou, D.; Chen, S.; Brodie, A. *Cancer Res* **1994,** 54, 5092-95.
189. Dowsett, M. *Endocrine-Related Cancer* **1999,** 6, 181-85.
190. Johnson, S. R. D., Dowsett, M. *Nat Rev Cancer.* **2003,** 3, 821-31.
191. Di Salle, E.; Ornati, G.; Giudici, D.; al., e. *J Steroid Biochem Mol Biol* **1992,** 43, 137-43.
192. Rockville, M. D. *NDA 20753 (Exemestane) Medical Review.*; U.S. Food and Drug Administration: 1999.
193. Njar, V. C.; Brodie, A. M. *Drugs* **1999,** 58, 233-55.
194. Miller, W. R. *Cancer Treat Rev* **1989,** 16, 83-93.

195. Gale, K. E.; Andersen, J. W.; Tormey, D. C.; Mansour, E. G.; Davis, T. E.; Horton, J.; Wolter, J. M.; Smith, T. J.; Cummings, F. J. *Cancer* **1994,** 73, 354-61.
196. Smith, I. E.; Harris, A. L.; Morgan, M.; Gazet, J. C.; McKinna, J. A. *Cancer Res* **1982,** 42, 3430S–33S.
197. Stein, R. C.; Dowsett, M.; Headley, A. *Cancer Chemother Pharmacol* **1990,** 26, 75-78.
198. Steele, R. E.; Mellor, L. B.; Sawyer, W. K.; Wasvary, J. M.; Browne, L. J. *Steroids* **1987,** 50, 147-61.
199. Ankley, G. T.; Kahl, M. D.; Jensen, K. M.; Hornung, M. W.; Korte, J. J.; Makynen, E. A.; Leino, R. L. *Toxicol. Sci.* **2002,** 67, 121-30.
200. Lonning, P. E.; Jacobs, S.; Jones, A.; Haynes, B.; Powles, T.; Dowsett, M. *Br J Cancer* **1991,** 63, 789-93.
201. Cepa, M. M. D. S.; Tavares da Silva, E. J.; Correia-da-Silva, G.; Roleira, F. M. F.; Teixeira, N. A. A. *J. Med. Chem.* **2005,** 48, 6379-85.
202. Goss, P. E. *Breast Cancer Research and Treatment* **1998,** 49, S59-S65.
203. Kellokempu-Lehitinen, P.; Huovinen, R.; Johansson, R. *Cancer* **1987,** 60, 2367.
204. Falkson, C. I.; Falkson, H. I. *Ann. Oncol.* **1996,** 7, 465.
205. Babu, B. R.; Vaz, A. D. *Biochemistry* **1997,** 36, 7209.
206. Recanatini, M.; Bisi, A.; Cavalli, A.; Belluti, F.; Gobbi, S.; Rampa, A.; Valenti, P.; Palzer, M.; Palusczak, A.; Hartmann, R. W. *J. Med. Chem.* **2001,** 44, 672.
207. Cavalli, A.; Recanatini, M. *J. Med. Chem.* **2002,** 45, 251.
208. Plourde, P. V.; Dyroff, M.; Dowsett, M.; Demers, L.; Yates, R.; Webster, A. *J Steroid Biochem Mol Biol* **1995,** 153, 175-79.
209. Geisler, J.; King, N.; Dowsett, M.; Ottestad, L.; Lundgren, S.; Walton, P.; Kormeset, P. O.; Lonning, P. E. *Br J Cancer* **1996,** 74, 1286-91.
210. Bonneterre, J.; Thurlimann, B.; Robertson, J. F.; Krzakowski, M.; Mauriac, L.; Koralewski, P.; Vergote, I.; Webster, A.; Steinberg, M.; Euler, v. *J. Clin Oncol* **2000,** 18.
211. Buzdar, A.; Nabholtz, J. M.; Robertson, J., F.; Thurlimann, B.; Bonneterre, J.; von Euler, M.; Steinberg, M.; Webster, A. *Proc ASCO* **2000,** 19, 154a.
212. Dixon, J. M.; Renshaw, L.; Bellamy, C.; Stuart, M.; Hoctin-Boes, G.; Miller, W. R. *Clin Cancer Res* **2000,** 6, 2229-35.
213. Jakesz, R.; Jonat, W.; Gnant, M.; Mittlboeck, M.; Greil, R.; Tausch, C.; Hilfrich, J.; Kwasny, W.; Menzel, C.; Samonigg, H.; Seifert, M.; Gademann, G.; Kaufmann, M.; Wolfgang, J. *Lancet* **2005,** 366, 455-62.
214. Bhatnagar, A. S. *Breast Cancer Res Treat* **2007,** 105, 7-17.
215. Haynes, B. P.; Dowsett, M.; Miller, W. R.; Dixon, J. M.; Bhatnagar, A. S. *J Steroid Biochem Mol Biol* **2003,** 87, 35-45.
216. Bhatnagar, A. S.; Batzl, C.; Hausler, A.; Schieweck, K.; Lang, M.; Trunet, P. F. *Pharmacology of non-steroidal aromatase inhibitors.* . Pasqualini, J.R., Katzenellenbogen, B.S.: Marcel Dekker, New York, 1996.
217. Bhatnagar, A. S.; Hausler, A.; Schieweck, K.; Lang, M.; Bowman, R. *J Steroid Biochem Mol Biol* **1990,** 37, 1021-27.
218. Mouridsen, H.; Gershanovich, M.; Sun, Y.; Pe´rez-Carrio´n, R.; Boni, C.; Monnier, A.; Apffelstaedt, J.; Smith, R.; Sleeboom, H. P.; Jaenicke, F.; Pluzanska, A.; Dank, M.; Becquart, D.; Bapsy, P. P.; Salminen, E.; Snyder, R.; Chaudri-Ross, H.; Lang, R.; Wyld, P.; Bhatnagar, A. *J Clin Oncol* **2003,** 21, 2101-09.
219. Thurlimann, B.; Keshaviah, A.; Coates, A. S.; Mouridsen, H.; Mauriac, L.; Forbes, J. F.; Paridaens, R.; Castiglione-Gertsch, M.; Gelber, R. D.; Rabaglio, M.; Smith, I.; Wardly, A.; Price, K. N.; Goldhirsch, A. *N Engl J Med* **2005,** 353, 2747-57.
220. Bubert, C.; Woo, L. W.; Sutcliffe, O. B.; Mahon, M. F.; Chander, S. K.; Purohit, A.; Reed, M. J.; Potter, B. V. *ChemMedChem* **2008,** 3, 1708-30.

221. Woo, L. W.; Jackson, T.; Putey, A.; Cozier, G.; Leonard, P.; Acharya, K. R.; Chander, S. K.; Purohit, A.; Reed, M. J.; Potter, B. V. *J. Med. Chem.* **2010,** 53, 2155-70.
222. Gobbi, S.; Cavalli, A.; Bisi, A.; Recanatini, M. *Curr. Top. Med. Chem.* **2008,** 8, 869-87.
223. Recanatini, M.; Bisi, A.; Cavalli, A.; Belluti, F.; Gobbi, S.; Rampa, A.; Valenti, P.; Palzer, M.; Palusczak, A.; Hartmann, R. W. *J. Med. Chem.* **2001,** 44, 672-80.
224. Leonetti, F.; Favia, A.; Rao, A.; Aliano, R.; Paluszcak, A.; Hartmann, R. W.; Carotti, A. *J. Med. Chem.* **2004,** 47, 6792-803.
225. Harris, R. E.; Chlebowski, R. T.; Jackson, R. D.; Frid, D. J.; Ascenseo, J. L.; Anderson, G.; Loar, A.; Rodabough, R. J.; White, E.; McTiernan, A. *Cancer Res.* **2003,** 63, 6096.
226. Nakatsugi, S.; Ohta, T.; Kawamori, T.; Mutoh, M.; Tanigawa, T.; Watanabe, K.; Sugie, S.; Sugimura, T.; Wakabayashi, K. *Jpn. J. Cancer Res* **2000,** 91.
227. Diaz-Cruz, E. S.; Shapiro, C. L.; Brueggemeier, R. W. *J. Clin. Endocrinol. Metab.* **2005,** 90, 2563.
228. Chen, B.; Su, B.; Chen, S. *Biochem. Pharmacol.* **2009,** 77, 1787.
229. Su, B.; Darby, M. V.; Brueggemeier, R. W. *J. Comb. Chem.* **2008,** 10, 475.
230. Su, B.; Diaz-Cruz, E. S.; Landini, S.; Brueggemeier, R. W. *J. Med. Chem.* **2006,** 49, 1413.
231. Su, B.; Chen, S. *Bioorganic & Medicinal Chemistry Letters* **2009,** 19.
232. Chen, B.; Su, B.; S., C. *Biochemical Pharmacology* **2009,** 77, 1787-94.
233. Lu, W. J.; Xu, C.; Pei, Z.; Mayhoub, A. S.; Cushman, M.; Flockhart, D. A. *Breast Cancer Res Treat* **2012,** 133, 99-109.
234. Jin, Y.; Desta, Z.; Stearns, V.; Ward, B.; Ho, H.; Lee, K. H.; Skaar, T.; Storniolo, A. M.; Li, L.; Araba, A.; Blanchard, R.; Nguyen, A.; Ullmer, L.; Hayden, J.; Lemler, S.; Weinshilboum, R. M.; Rae, J. M.; Hayes, D. F.; Flockhart, D. A. *J Natl Cancer Inst* **2005,** 97, 30-39.
235. Lien, E. A.; Wester, K.; Lonning, P. E.; Solheim, E.; Ueland, P. M. *Br J Cancer* **1991,** 63, 641-45.
236. Lu, W. J.; Desta, Z.; Flockhart, D. A. *Breast Cancer Res Treat.* **2012,** 131, 473-81.
237. Santen, R. J.; Leszczynski, D.; Tilson-Mallet, N.; Feil, P. D.; Wright, C.; Manni, A.; Santner, S. J. *Ann NY Acad Sci* **1986,** 464, 126-37.
238. Li, P. K.; Pillai, R.; Dibbelt, L. *Steroids* **1995,** 60, 301-06.
239. Reed, M. J.; Purohit, A. *Endocr Relat Cancer* **1993,** 45, 51-62.
240. Reed, M. J.; Purohit, A. *Sanders, M. Smith, J. Design of enzyme inhibitors as drugs*. Oxford: Oxford University Press: 1994; Vol. 2, p 481-94.
241. Reed, M. J.; Purohit, A.; Howarth, N. M.; Potter, B. V. L. *Drugs Future* **1994,** 19, 673-80.
242. Howarth, N. M.; Purohit, A.; Reed, M. J. *J Med Chem.* **1994,** 37, 219-21.
243. Maltais, R.; Poirier, D. *Steroids* **2011,** 76, 929-48.
244. Ishida, H.; Nakata, T.; Suzuki, M.; Shiotsu, Y.; Tanaka, H.; Sato, N. *Breast Cancer Res Treat* **2007,** 106, 215-17.
245. Ishida, H.; Nakata, T.; Sato, N.; Li, P. K.; Kuwabara, T.; Akinaga, S. *Breast Cancer Res Treat* **2007,** 104, 211-19.
246. Schwarz, S.; Kosemund, D.; Müller, G.; Richter, M.; Peters, O.; Droescher, P.; al., e. Ent-steroids as selectively effective estrogens. 2000.
247. Schwarz, S.; Mueller, G.; Kosemund, D.; Richter, M.; Peters, O.; Scherlitz-Hofmann, I.; et al. C13-substituted estra-1,3,5,(10)-trien-3-yl sulfamates, methods of preparing same, and pharmaceutical compositions containing these compounds. 2003.
248. Jinbo, Y.; Inoue, Y. Novel estradiol derivatives. . 2000.
249. Leese, M. P.; Leblond, B.; Newman, S. P.; Purohit, A.; Reed, M. J.; Potter, B. V. L. *J Steroid Biochem Mol Biol* **2005,** 94.
250. Potter, B. V. L.; Reed, M. J. Thioether-sulfamate steroids as steroid sulfatase inhibitors and anti-cancer compounds. 2002.
251. Reed, J. E.; Woo, L. W. L.; Robinson, J. J.; Leblond, B.; Leese, M. P.; Purohit, A.; Reed, M. J. *Biochem Biophys Res Commun* **2004,** 317, 169-75.
252. Ciobanu, L. C.; Luu-The, V.; Martel, C.; Labrie, F.; Poirier, D. *Cancer Res* **2003,** 63.

253. Fischer, D. S.; Woo, L. W. L.; Mahon, M. F.; Purohit, A.; Reed, M. J.; Potter, B. V. L. *Bioorganic & Medicinal Chemistry Letters* **2003,** 11, 1685-700.
254. Foster, P. A.; Newman, S. P.; Chander, S. K.; Stengel, C.; Jhalli, R.; Woo, L. W. L.; et al. *Clin Cancer Res* **2006,** 12, 5543-49.
255. Woo, L. W. L.; Fischer, D. S.; Sharland, C. M.; Trusselle, M.; Foster, P. A.; Chander, S. K.; et al. *Mol Cancer Ther* **2008,** 7, 2435-44.
256. Ahmed, S.; James, K.; Owen, C. P.; Patel, C. K.; Patel, M. *Bioorganic & Medicinal Chemistry Letters* **2001,** 11, 841-44.
257. Anderson, C. J.; Lucas, L. J. H.; Widlanski, T. S. *J Am Chem Soc* **1995,** 117.
258. Billich, A.; Schreiner, E. P.; Wolff-Winiski, B. Benzoxa- and benzthiazoles. 2001.
259. Koizumi, N.; Okada, M.; Iwashita, S.; Takegawa, S.; Nakagawa, T.; Takahashi, H. Phenyl sulfamate derivatives. 2001.
260. Okada, M.; Nakagawa, T.; Iwashita, S.; Takegawa, S.; Fujii, T.; Koizumi, N.; al., e. *J Steroid Biochem Mol Biol* **2004,** 87, 141-48.
261. Reed, M. J.; Potter, B. V. L. Compound. 2005.
262. Saito, T.; Kinoshita, S.; Fujii, T.; Bandoh, K.; Fuse, S.; Y., Y.; al., e. *J Steroid Biochem Mol Biol* **2004,** 88, 167-73.
263. Schreiner, E. P.; Wolff, B.; Winiski, A. P.; Billich, A. *Bioorganic & Medicinal Chemistry Letters* **2003,** 13, 4313-16.
264. Stanway, S. J.; Delavault, P.; Purohit, A.; Woo, L. W. L.; Thurieau, C.; Potter, B. V. L.; et al. *The Oncologist* **2007,** 12, 370-74.
265. Stanway, S. J.; Purohit, A.; Woo, L. W. L.; Sufi, S.; Vigushin, D.; Ward, R.; et al. *Clin Cancer Res* **2006,** 12, 1585-92.
266. Boivin, R. P.; Luu-The, V.; Lachance, R.; Labrie, F.; Poirier, D. *J Med Chem* **2000,** 43, 4465-78.
267. Ciobanu, L. C.; Boivin, R. P.; Luu-The, V.; Poirier, D. *Eur J Med Chem* **2001,** 36, 659-71.
268. Fournier, D.; Poirier, D. *Bioorganic & Medicinal Chemistry Letters* **2009,** 19, 693-96.
269. Jutten, P.; Schumann, W.; Hartl, A.; Heinisch, L.; Grafe, U.; Werner, W. *Bioorganic & Medicinal Chemistry Letters* **2002,** 12, 1339-42.
270. Jutten, P.; Schumann, W.; Hartl, A.; Dahse, H. M.; Grafe, U. *J Med Chem Biol* **2007,** 50, 3661-66.
271. Okada, M.; Nakagawa, T.; Iwashita, S.; Takegawa, S.; Fujii, T.; Koizumi, N. *J. Steroid Biochem. Mol. Biol.* **2003,** 87, 141-48.
272. Jackson, T.; Woo, L. W. L.; Trusselle, M. N.; Purohit, A.; Reed, M. J.; Potter, B. V. L. *Chem. Med. Chem.* **2008,** 3, 603-18.
273. Woo, L. W. L.; Jackson, T.; Putey, A.; Cozier, A.; Philip Leonard, P.; Acharya, R. K.; Chander, S. K.; Purohit, A.; Reed, M. J.; Potter, B. V. *J. Med. Chem.* **2010,** 53, 2155-70.
274. Hammond, J.; Cai, D.; Verhey, K. J. *Curr Opin Cell Biol.* **2008,** 20, 71-76.
275. Jordan, M. A.; Wilson, W. *Nat Rev Cancer.* **2004,** 4, 253-65.
276. Cragg, G. M.; Kingston, D. G. I.; Newman, J. N. *Anticancer agents from natural products*. Taylor & Francis group, NY: 2005.
277. Pettit, G. R.; Singh, S. B.; Niven, M. L.; Hamel, E.; Schmidt, J. M. *J. Nat. Prod.* **1987,** 50, 119-131.
278. Pettit, G. R.; Singh, S. B.; Cragg, G. M. *J. Org. Chem.* **1985,** 50, 3404-3406.
279. Pettit, G. R.; Singh, S. B. *Can J Chem* **1987,** 65, 2390-98.
280. Pettit, G. R.; Singh, S. B.; Hamel, E.; Lin, C. M.; Alberts, D. S.; Garcia-Kendall, D. *Experientia* **1989,** 45, 209-11.
281. Gaukroger, K.; Hadfield, J. A.; Hepworth, L. A.; Lawrence, N. J.; McGrown, A. T. *J. Org. Chem.* **2001,** 66, 8135.
282. Nan, N.-H. *Curr Med Chem* **2003,** 10, 1697-722.
283. Tron, G. C.; Pirali, T.; Sorba, G.; Pagliai, F.; Busacca, S.; Genazzani, A. A. *J. Med. Chem.* **2006,** 29, 2579-88.

284. Iyer, S.; Chaplin, D. J.; Rosenthal, D. S.; Boulares, A. H.; Li, L. Y.; Smulson, M. E. *Cancer Res.* **1998,** 58, 4510.
285. Dark, G. G.; Hill, S. A.; Prise, V. E.; Tozer, G. M.; Pettit, G. R.; Chaplin, D. J. *Cancer Res.* **1997,** 57, 1829.
286. Zhao, S.; Moore, J. V.; Waller, M. L.; McGown, A. T.; Hadfield, J. A.; Pettit, G. R.; Hastings, D. L. *Eur. J. Nucl. Med.* **1999,** 26, 231.
287. Cirla, A.; Mann, J. *Nat. Prod. Rep.* **2003,** 20, 558-64.
288. Pinney, K. G.; et al. *Bioorg. Med. Chem.* **2000,** 8, 2417-25.
289. Ohsumi, K. *J. Med. Chem.* **1998,** 41, 3022.
290. Ohsumi, K. *Anti-Cancer Drug Design* **1999,** 14, 539.
291. Siles, R.; Hadimani, M.; Pinney, K. G. Cancer chemotherapy; prodrug strategies for enhanced bioavailability and selectivity of vasclur targeting agents. In *58th Southwest Regional Meeting of The American Chemical Society*, Austin, TX, 2002; p abstract 236.
292. Pettit, G. R.; et al. *J. Med. Chem.* **2003,** 46, 525.
293. Lawrence, N. J.; et al. *J. Fluorine Chem.* **2003,** 123, 101.
294. Davis, P. D. Compositions with vascular damaging activity. 2002.
295. Gaukroger, K. *Bioorg. Med. Chem.* **2003,** 1, 3003.
296. Pettit, G. R.; et al. *J. Med. Chem.* **1998,** 41, 1688.
297. Pettit, G. R.; et al. *J. Med. Chem.* **2000,** 43, 2731.
298. Medarde, M.; et al. *Eur J Med Chem* **1998,** 33, 71.
299. Andres, C. J.; et al. *Bioorg. Med. Chem.* **1993,** 3, 565.
300. Shirai, R. *Bioorg. Med. Chem.* **1994,** 4, 699.
301. Pettit, G. R.; et al. *J. Nat. Prod.* **2000,** 63, 696.
302. Pettit, G. R.; et al. *Anti-Cancer Drug Design* **2000,** 15, 361.
303. Ducki, S.; et al. *Bioorg. Med. Chem.* **1998,** 8, 1051.
304. Wang, L.; et al. *J. Med. Chem.* **2002,** 45, 1697.
305. Hatanaka, T.; et at. *Bioorg. Med. Chem.* **1998,** 8, 3371.
306. Zou, Y.; Xiao, C.-F.; Zhong, R.-Q.; Wei, W.; Huang, W.-M.; He, S.-J. *Journal of Chemical Research,* **2008,** 2008, 354-56.
307. Medina, J. C.; et al. Pentafluorobenzenesulfonamides and analogs. 1999.
308. Flynn, B. L.; Hamel, E.; Jung, M. K. *J. Med. Chem.* **2002,** 45, 2670.
309. Gastpar, R.; et. al. *J. Med. Chem.* **1998,** 41, 4965.
310. Chen, Z.; et al. *J. Org. Chem.* **2000,** 65.
311. Ghatak, A.; et al. *Tetrahedron Lett.* **2003,** 44, 4145.
312. Goldbrunner, M.; et al. *J. Med. Chem.* **1997,** 40, 3524.
313. Li, Q.; et al. *Bioorg. Med. Chem.* **2002,** 12, 465.
314. Greene, L. M.; Nathwani, S. M.; Bright, S. A.; Fayne, D.; Croke, A.; Gagliardi, M.; McElligott, A. M.; O'Connor, L.; Carr, M.; Keely, N. O.; O'Boyle, N. M.; Carroll, P.; Sarkadi, B.; Conneally, E.; Lloyd, D. G.; Lawler, M.; Meegan, M. J.; Zisterer, D. M. *J Pharmacol Exp Ther.* **2010,** 335, 302-13.
315. Bedford, S. B.; Quarterman, C. P.; Rathbone, D. L.; Slack, J. A.; Griffin, R. J.; Stevens, M. F. G. *6* **1996,** 2.
316. Pettit, G. R.; et al. *Anti-Cancer Drug Design* **1995,** 10, 299-309.
317. Brown, R. T.; Fox, B. W.; Hadfield, J. A.; et al. *J. Chem. Soc. Perkin Trans.* **1995,** 1, 577.
318. Ohsumi, K.; Nakagawa, R.; Fukuda, Y.; Hatanaka, T.; Morinaga, Y.; Nihei, Y.; Ohishi, K.; Suga, Y.; Akiyama, Y.; Tsuji, T. *J. Med. Chem.* **1998,** 41, 3022-30.
319. Chaplin, D. J.; Pettit, G. R.; Hill, S. A. *Anticancer Res.* **1999,** 19, 189-95.
320. Hatanaka, T.; Fujita, K.; Ohsumi, K.; Nakagawa, R.; Fukuda, Y.; Nihei, Y.; Suga, Y.; Akiyama, Y.; Tsuji, T. *Bioorg Med Chem Lett.* **1998,** 8, 3371-74.
321. Ohsumi, K.; Nakagawa, R.; Fukuda, Y.; Hatanaka, T.; Morinaga, Y.; Nihei, Y.; Ohishi, K.; Suga, Y.; Akiyama, Y.; Tsuji, T. *J Med Chem.* **1998,** 41, 3022-32.

322. Lippert, J. W. I. *Bioorg. Med. Chem.* **2007,** 15, 605-15.
323. Sinhababu, A. K.; Thakker, D. R. *Adv. Drug. Deliv. Rev.* **1996,** 19, 241-73.
324. Garnett, M. C. *Adv. Drug. Deliv. Rev.* **2001,** 53, 171-216.
325. Denny, W. A. *Eur J Med Chem* **2001,** 36, 577-95.
326. El Alaoui, A.; Saha, N.; Schmidt, F.; Monneret, C.; Florent, J.-C. *Bioorg. Med. Chem.* **2006,** 14, 5012-17.
327. Jaracz, S.; Chen, J.; Kuznetsova, L. V.; OJima, I. *Bioorg. Med. Chem.* **2005,** 13, 5043-54.
328. Maeda, H.; Fang, J.; Inutsuka, T.; Kitamoto, Y. *Int. Immunopharmacol* **2003,** 3, 319.
329. Maeda, H.; Matsumura, Y.; Oda, T.; Sasamoto, K. *Protein Tailoring for Food and Medical Uses*. Marcel Dekker: New York: 1986.
330. Emerich, D. F.; Thanos, C. G. *Journal of Drug Targeting* **2007,** 15, 163-83.
331. Lee, J. H.; Nan, A. Combination Drug Delivery Approaches in Metastatic Breast Cancer. *Journal of Drug Delivery* **2012,** 2012, 1-17.
332. Panchal, R. G. *Biochem. Pharmacol.* **1998,** 55, 247-52.
333. Zangemeister-Wittke, U. *Pathobiology* **2005,** 72, 279-86.
334. Wu, A. M.; Senter, P. D. *Nat. Biotechnol.* **2005,** 23, 1137-46.
335. Ricart, A. D.; Tolcher, A. W. *Nat. Clin. Pract. Oncol.* **2007,** 4, 245-55.
336. Carter, P. J.; Senter, P. D. *Cancer J.* **2008,** 14, 154-69.
337. Rohrer, T. *Chem. Rundschau* **2008,** 9, 26-28.
338. Ducry, L.; Stump, B. *Bioconjugate Chem.* **2010,** 21, 5-13.
339. Trail, P. A.; Willner, D.; Lasch, S. J.; Henderson, A. J.; Hofstead, S.; Casazza, A. M.; Firestone, R. A.; Hellstrom, I.; Hellstrom, K. E. *Science* **1993,** 261, 212-15.
340. Dubowchik, G. M.; Firestone, R. A.; Padilla, L.; Willner, D.; Hofstead, S. J.; Mosure, K.; Knipe, J. O.; Lasch, S. J.; Trail, P. A. *Bioconjugate Chem.* **2002,** 13, 885-69.
341. Hamann, P. R.; Hinman, L. M.; Beyer, C. F.; Lindh, D.; Upeslacis, J.; Flowers, D. A.; Bernstein, I. *Bioconjugate Chem.* **2002,** 13, 40-46.
342. Hamann, P. R.; Hinman, L. M.; Hollander, I.; Beyer, C. F.; Lindh, D.; Holcomb, R.; Hallett, W.; Tsou, H.-R.; Upeslacis, J.; Shochat, D.; Mountain, A.; Flowers, D. A.; Bernstein, I. *Bioconjugate Chem.* **2002,** 13, 47-58.
343. Hollander, I.; Kunz, A.; Hamann, P. R. *Bioconjugate Chem.* **2008,** 19, 358-61.
344. Higashide, E.; Asai, M.; Ootsu, K.; et al. *Nature* **1977,** 270, 721-22.
345. Cassady, J. M.; Chan, K. K.; Floss, H. G.; et al. *Chem Pharm Bull (Tokyo)* **2004,** 52, 1-26.
346. Yu, T. W.; Bai, L.; Clade, D.; et al. *Proc Natl Acad Sci U S A* **2002,** 99, 7968-73.
347. Tassone, P.; Goldmacher, V. S.; Neri, P.; et al. *Blood* 104, 3688-96.
348. Wang, L.; Amphlett, G.; Blattler, W. A.; et al. *Protein Sci* **2005,** 14, 2436-46.
349. Barginear, M. F.; Budman, D. R. *The Open Breast Cancer Journal* **2009,** 1, 25-30.
350. Blättler, W. A.; Chari, R. V. J.; Vite, G. D.; Altmann, K. H. *Anticancer Agents – Frontiers in Cancer Chemotherapy,*. American Chemical Society, Washington: 2001.
351. Moser, U. *J. Appl. Cosmet.* **2002,** 20, 137.
352. Heird, W. C.; Lapillonne, A. *Annu. Rev. Nutr.* **2005,** 25, 549.
353. Bradley, M. O.; Webb, N. L.; Anthony, F. H.; Devanesan, P.; Witman, P. A.; Hemamalini, S.; Chander, M. C.; Baker, S. D.; He, L.; Horwitz, S. B.; Swindell, C. S. *Clin. Cancer Res.* **2001,** 7, 3229-38.
354. Sun, L. Design, Synthesis, Biological Evaluation and Molecular Modeling of Novel Taxane-based Anticancer Agents and Paclitaxel Mimics. Stony Brook University, ProQuest, 2008.
355. Bai, L.; Zhu, R.; Chen, Z.; Gao, L. *J of Biochem.Pharm.* **2006,** 71, 1265-71.
356. Elnakat, H.; Ratnam, M. *Adv. Drug Delivery Rev.* **2004,** 56.
357. Sudimack, J.; Lee, R. J. *Adv. Drug Delivery Rev.* **2000,** 41, 147-62.
358. Weitman, S. D.; Lark, R. H.; Coney, L. R.; Fort, D. W.; Frasca, V.; Zurawski, V. R.; Kamen, B. A. *Cancer Res.* **1992,** 52, 3396-401.

359. Pasut, G.; Canal, F.; Dalla Via, L.; Arpicco, S.; Veronese, F. M.; Schiavon, O. *J. Controlled Release* **2008,** 127, 239-48.
360. Prabaharan, M.; Grailer, J. J.; Pilla, S.; Steeber, D. A.; Gong, S. Q. *Biomaterials* **2009,** 30, 5757-66.
361. Lee, R. J.; Low, P. S. *Biochim. Biophys. Acta.* **1995,** 1233, 134-44.
362. Wang, S.; Lee, R. J.; Cauchon, G.; Gorenstein, D. G.; Low, P. S. *Proc. Natl. Acad. Sci. U.S.A.* **1995,** 92, 3318-22.
363. Leamon, C. P.; Low, P. S. *J. Drug Targeting* **1994,** 2, 101-12.
364. Rund, L. A.; Cho, B. K.; Manning, T. C.; Holler, P. D.; Roy, E. J.; Kranz, D. M. *Int. J. Cancer* **1999,** 83, 141-49.
365. Hong, S.; Leroueil, P. R.; Majoros, I. J.; Orr, B. G.; Baker, J. R.; Holl, M. M. B. *Chem. Biol.* **2007,** 14, 107-15.
366. Jaracz, S.; et al. ***Bioorg. Med. Chem.*** **2005,** 13, 5043-54.
367. Herrlich, P.; Sleeman, J.; Wainwright, D.; Konig, H.; Sherman, L.; Ponta, H. *Cell Adhes. Commun.* **1998,** 6.
368. Lee, H.; Lee, K.; Park, T. G. *Bioconjugate Chem.* **2008,** 19, 1219-25.
369. Curran, S.; Murray, G. I. *Eur. J. Cancer* **2000,** 36, 1621-30.
370. Egeblad, M.; Werb, Z. *Nat. Rev. Cancer* **2002,** 2, 161-74.
371. Stearns, M. E.; Wang, M. *Cancer Res* **1993,** 53, 878-83.
372. Giambernardi, T. A.; Grant, G. M.; Taylor, G. P.; Hay, R. J.; Maher, V. M.; McCormick, J. J.; Klebe, R. J. *Matrix Biol.* **1999,** 16, 483-96.
373. Bremer, C.; Tung, C. H.; Weissleder, R. *Nat. Med.* **2001,** `7, 743-48.
374. Kratz, F.; Drevs, J.; Bing, G.; Stockmar, C.; Scheuermann, K.; Lazar, P.; Unger, C. *Bioorg. Med. Chem.* **2001,** 11, 2001-16.
375. Holle, L.; Song, W.; Holle, E.; Wei, Y.; Wagner, T.; Yu, X. *Int. J. Oncol.* **2003,** 2, 93-98.
376. Yokoyama, M.; Okano, T.; Sakurai, Y.; Fukushima, S.; Okamoto, K.; Kataoka, K. *J. Drug Target.* **1999,** 7, 171-86.
377. Burkhart, D. J.; Kalet, B. T.; Coleman, M. P.; Post, G. C.; Koch, T. H. *Molecular Cancer Therapeutics* **2004,** 3, 1593.
378. Maeda, H.; Wu, J.; Sawa, T.; Matsumura, Y.; Hori, K. *J. Contr. Release* **2000,** 65, 271-84.
379. Jabr-Milane, L. S.; van Vlerken, L. E.; Yadav, S.; Amiji, M. M. *Cancer Treat. Rev.* **2008,** 34, 592-602.
380. Cao, N.; Feng, S. S. *Biomaterials* **2008,** 29, 3856-65.
381. Zhang, Y.; Zhuo, R. X. *Biomaterials* **2005,** 26, 6736-42.
382. Gong, C.; We, X.; Wang, X.; Wang, Y.; Guo, G.; Mao, Y.; Luo, F.; Qian, Z. *Nanotechnology* **2010,** 21, 215103.
383. Xu, B.; Yuan, J.; Ding, T.; Gao, Q. *Polym. Bull.* **2010,** 64, 537-51.
384. Ge, H.; Hu, Y.; Jiang, X.; Cheng, D.; Yuan, Y.; Bi, H.; Yang, C. *J. Pharm. Sci.* **2002,** 91, 1463-73.
385. Gou, M.; Zheng, X.; Men, K.; Zhang, J.; Zheng, L.; Wang, X.; Luo, F.; Zhao, Y.; Zhao, X.; Wei, Y.; Qian, Z. *J. Phys. Chem. B* 113, 12928-33.
386. Cuong, N. V.; Hsieh, M. F.; Chen, Y. T.; Liau, I. *J. Biomater. Sci. Polym. Ed.* **2010**.
387. Park, J. W.; al., e. *Clin. Cancer Res.* **2002,** 8, 1172-81.
388. Katzenellenbogen, J. A.; Katzenellenbogen, B. S. *Breast Cancer Res Treat* **1982,** 2, 347-53.
389. Biersack, B.; Schobert, R. *Curr. Med. Chem.* **2009,** 16, 2314-37.
390. Meunier, B. *Acc. Chem. Res.* **2008,** 41, 69-77.
391. Katzenellenbogen, J. A.; Zablocki, J. A. Oestrogen and Antiestrogens: Concepts, Progress, and Evaluation. In Pharmacology and Clinical Uses of Inhibitors of Hormone Secretion and Action. In Wakeling, Ed. Bailliere Tindall, London.: 1987; pp 41-5.
392. Delbarre, A.; Oberlin, R.; Roques, B. P.; Borgna, J. L.; Rochefort, H.; Le, P. J. B.; Jacquemin-Sablon, A. *J Med Chem* **1985,** 18, 752-61.

393. Devraj, R.; Barrett, J. F.; Fernandez, J. A.; Katzenellenbogen, J. A.; Cushman, M. *J. Med. Chem.* **1996,** 39, 3367-74.
394. Dao, K.-L.; Hanson, R. N. *Bioconjugate Chem.* **2012,** 23, 2139-58.
395. Tsubura, A.; Lai, Y.-C.; Miki, H.; Sasaki, T.; Uehara, N.; Yuri, T.; Yoshizawa, K. *In Vivo* **2011,** 25, 11-22.
396. Eisenbrand, G.; Berger, M. R.; Fischer, J.; Schneider, M. R.; Tang, W.; Zeller, W. J. *Anti-Can. Drug Dev.* **1998,** 2, 351-59.
397. Prodromou, C.; Roe, S. M.; Piper, P. W.; Pearl, L. H. *Nat. Struct. Biol.* **1997,** 4, 477-82.
398. Annamalai, B.; Liu, X.; Gopal, U.; Isaacs, J. S. *Mol. Cancer. Res.* **2009,** 7, 1021-32.
399. Kuduk, S. D.; Zheng, F. F.; Sepp-Lorenzino, L.; Rosen, N.; Danishefsky, S. J. *Bioorganic & Medicinal Chemistry Letters* **1999,** 9, 1233-38.
400. Drablos, F.; Feyzi, E.; Aas, P. A.; Vaagbo, C. B.; Kavli, B.; Bratlie, M. S.; Pena-Diaz, J.; Otterlei, M.; Slupphaug, G.; Krokan, H. E. *DNA Repair* **2004,** 3.
401. Sharma, U.; Marquis, J.; Nicole Dinaut, A.; Hillier, S. M.; Fedeles, B.; Rye, P. T.; Essigmann, J. M.; Croy, R. G. *Bioorg. Med. Chem. Lett.* **2004,** 14, 3829-33.
402. Mitra, K.; Marquis, J. C.; Hillier, S. M.; Rye, P. T.; Zayas, B.; Lee, A. S.; Essigmann, J. M.; Croy, R. G. *J. Am. Chem. Soc.* **2002,** 124, 1862-63.
403. Al-Omar, A.; Abdou, S.; De, R. L.; Marsura, A.; Finance, C. *Bioorg. Med. Chem. Lett.* **1999,** 9, 1115-20.
404. Gianni, L.; Corden, B. J.; Myers, C. E. *Biochem. Toxicol.* **1983,** 5, 1-82.
405. Hartman, N. G.; Patterson, L. H.; Workman, P.; Suarato, A.; Angelucci, F. *Biochem Pharmacol.* **1990,** 40, 1164-67.
406. Kasiotis, K. M.; Magiatis, P.; Pratsinis, H.; Skaltsounis, A.-L.; Abadji, V.; Charalambous, A.; Moutsatsou, P.; Haroutounian, S. A. *Steroids* **2001,** 66, 785-91.
407. Levin, M. *Drug Today* **2001,** 37, 57-65.
408. Liu, C.; Strobl, J. S.; Bane, S.; Schilling, J. K.; McCracken, M.; Chatterjee, S. K.; Rahim-Bata, R.; Kingston, D. G. I. *J. Nat. Prod.* **2004,** 67, 152-59.
409. Barnes, K. R.; Kutikov, A.; Lippard, S. J. *Chem. Biol.* **2004,** 11, 557-64.
410. Kim, E.; Croy, R. G.; Essigmann, J. M. *J. Biol. Inorg. Chem.* **2007,** 12, S36.
411. Wolkenberg, S. E.; Boger, D. L. *Chem Rev* **2002,** 102, 2477-95.
412. Tomasz, M.; Das, A.; Tang, K. S.; Ford, M. G. J.; Minnock, A.; Musser, S. M.; Waring, M. J. *J. Am. Chem. Soc.* **1998,** 120, 11581-93.
413. Sami, S. M.; Iyengar, B. S.; Tarnow, S. E.; Remers, W. A.; Bradner, W. T.; Schurig, J. E. *J. Med. Chem.* **1984,** 27, 701-08.
414. Krohn, K.; Kulikowski, K.; Leclercq, G. *Journal of Medicinal Chemistry* **1989,** 32.
415. Kohle, H.; Krohn, K.; Leclercq, G. *J. Med. Chem.* **1989,** 32, 1538-47.
416. Fenick, D. J.; Taatjes, D. J.; Koch, T. H. *J. Med. Chem.* **1997,** 40, 2452-61.
417. Burke, P. J.; Koch, T. H. *J. Med. Chem.* **2004,** 47, 1193-1206.
418. Faye, J.-C.; Jozan, S.; Redeuilht, G.; Baulient, E.-E.; Bayard, F. *Proc. Natl. Acad. Sci. U.S.A.* **1983,** 80, 3158-62.
419. Burke, P. J.; Kalet, B. T.; Koch, T. H. *J. Med. Chem.* **2004,** 47, 6509-18.
420. Keely, N. O.; Zisterer, D. M.; Meegan, M. J. *Letters in Drug Design & Discovery* **2012,** 9, 295-304.
421. Keely, N. O. Design, synthesis and biochemical evalution of dual-acting, estrogen receptor conjugates. Trinity College Dublin, Ph.D. Thesis, 2008.
422. Top, S.; El Hafa, H.; Vessieres, A.; Quivy, J.; Vaissermann, J.; Hughes, D. W.; McGlinchey, M. J.; Thoreau, E.; Jaouen, G. *J. Am. Chem. Soc.* **1995,** 117, 8372-80.
423. Banerjee, S.; Das, T.; Chakraborty, S.; Samuel, G.; Korde, A.; Meera Venkatesh, H.; Pillai, M. R. A. *Bioorg. Med. Chem.* **2005,** 13, 4315-22.
424. Hunter, D. H.; Luyt, L. G. *Bioconjugate Chem.* **2000,** 11, 175-81.

425. Thompson, M. J.; Hutchinson, E. J.; Stratford, T. H.; Bowler, W. B.; Blackburn, G. M. *Tetrahedron Lett.* **2004,** 45, 1207-10.
426. Zovko, M.; Zorc, B.; Novak, P.; Tepes, P.; Centia-Cizmek, B.; Horvat, M. *International Journal of Pharmaceutics* **2004,** 285, 35-41.
427. Rickert, E. L.; Trebley, J. P.; Peterson, A. C.; Morrell, M. M.; Weatherman, R. V. *Biomacromolecules* **2007,** 8, 3608-12.
428. Reddel, R. R.; Sutherland, R. L. *Cancer Res.* **1983,** 43, 4613-24.
429. Burke PJ, K. T. Design, Synthesis, and Biological Evaluation of Doxorubicin-Formaldehyde Conjugates targeted to Breast Cancer Cells. *J. Med. Chem.* **2004,** 47, 1193-1206.
430. Ahmed N, D. C., Rousseau J, Benard F, van Lier JE, . *bioorg. Med. Chem. lett* **2007,** 17, 3212-3216.
431. Robertson, D. W.; Katzenellenbogen, J. A.; Long, D. J.; Rorke, E. A.; Katzenellenbogen, B. S. *Journal of Steriod Biochemistry* **1982,** 16, 1-13.
432. McKinley, N. F.; O'Shea, D. F. *J. Org. Chem.* **2006,** 71, 9552-55.
433. Potter, G. A.; McCague, R. J. *J. Org. Chem.* **1990,** 55, 6184-87.
434. McCague, R. J. *Chem. Research (S)* **1986**, 58-59.
435. Miller, R. B.; Al-Hassan, M. I. *J. Org. Chem.* **1985,** 50, 2121.
436. Minato, A.; Suzuki, K.; Tamao, K. *J. Am. Chem. Soc.* **1987,** 109, 1257-58.
437. Liron, F.; Gervais, M.; Peyrat, J.; Alami, M.; Brion, J. *Tetrahedron Lett.* **2003,** 44, 2789-94.
438. Shimizu, M.; Nakamaki, C.; Shimono, K.; Schelper, M.; Kurahashi, T.; Hiyama, T. *J. Am. Chem. Soc.* **2005,** 127, 12506.
439. Studemann, T.; Knochel, P. *Angew. Chem., Int. Ed. Engl.* **1997,** 36, 93.
440. Zhou, C.; Emrich, D. E.; Larock, R. C. *Org. Lett.* **2003,** 5, 1579.
441. Zhou, C.; Larock, R. C. *J. Org. Chem.* **2005,** 70, 3765.
442. Itami, K.; Kamei, T.; Toshida, J. *J. Am. Chem. Soc.* **2003,** 125, 14670.
443. Shiina, I.; Suzuki, M.; Yokoyama, K. *Tetrahedron Lett.* **2004,** 45, 965-67.
444. Coe, P. L.; Scriven, C. E. *J. Chem. Soc. Perkin Trans.* **1986,** I, 475-477.
445. Gauthier, S.; Mailhot, J.; Labrie, F. *J. Org. Chem.* **1996,** 61, 3890-93.
446. Detsi, A.; Koufaki, M.; Calogeropoulou, T. *J. Org. Chem.* **2002,** 67, 4608-11.
447. Hughes, R. B. PhD Thesis. Trinity College Dublin, 2000.
448. Lauhoff, S. M. PhD Thesis. Trinity College Dublin, 2002.
449. Smith, H. M. PhD Thesis. Trinity College Dublin, 2004.
450. Takeda, T. *Modern Carbonyl Olefination: Methods and Applications*. John Wiley & Sons: 2006.
451. Tyrlik, I.; Wolochowicz, I. *Bull. Soc. Chim. Fr.* **1973**, 2147-48.
452. Mukaiyama, T.; Sato, T.; Hanna, J. *Chem. Lett* **1973**, 1041-44.
453. McMurry, J. E.; Fleming, M. P. *J. Am. Chem. Soc.* **1974,** 96, 4708-09.
454. McMurry, J. E. *Chem. Rev.* **1989,** 89, 1513-24.
455. Lenoir, D. *Synthesis* **1989**, 883-897.
456. Laue, T. *Named Organic Reactions.* London, 2005; Vol. 2nd.
457. Dams, R.; Malinowski, M.; Greise, H. J. *J. Org. Chem.* **1982,** 47, 248-59.
458. Lauhoff SM. Trinity College Dublin, 2002.
459. Herriott AW, P. D. Phase transfer catalysis. Evaluation of catalysis. *J. Am. Chem. Soc.* **1975,** 97, 2345-2349.
460. Bedford, G. R.; Richardsonm D.N. *Nature* **1966,** 212, 733-34.
461. Atkins PW. *Elements of Physical Chemistry*. 3rd ed.; Oxford University Press: 1993.
462. Manns, J. E.; Brown, J. C. *Journal of Pharmaceutical and Biomedical Analysis* **1997,** 16, 847-52.
463. Murphy, C. S.; McCague, R.; Jordan, V. C. *Mol Pharmacol* **1991,** 39, 421-28.
464. Katzenellenbogen, B. S.; Eckert, R. L.; Peltz, S. W.; Mangel, W. F. *Cancer Res* **1984,** 44, 112-119.

465. Murphy, C. S.; McCague, R.; Jordan, V. C. *Mol Pharmacol.* **1990,** 38, 737-43.
466. Lim, Y. C.; Flockhart, D. A.; Skaar, T. C. *Cancer Chemother Pharmacol* **2005,** 55, 471-78.
467. Silfen, S. L.; Ciaccia, A. V.; Bryant, H. U. *Climacteric* **1999,** 2, 268-83.
468. McDonnell, D. P.; Connor, C. E.; Wijayaratne, A.; Chang, C. Y.; Norris, J. D. *Recent Prog Horm Res* **2002,** 27, 295–316.
469. Seo, J. W.; Comminos, J. S.; Chi, D. Y.; Kim, D. W.; Carlson, K. E.; Katzenellenbogen, J. A. *J. Med. Chem.* **2006**, 2496–2511.
470. Mason, R. M.; Lineham, J. D.; Phillipson, M. A.; Black, C. M. *Biochem. J.* **1984,** 223, 401-12.
471. Lancaster, C. A.; Fryer, P. R.; Griffiths, S.; Mason, R. M. *J. Cell Sci.* **1989,** 92, 271-80.
472. Gennari, L.; Merlotti, D.; De Paola, V.; Martini, G.; Nuti, R. *Therapeutics and Clinical Risk Management* **2008,** 4, 1229-42.
473. Komm, B. S.; Lyttle, C. R. *Ann NY Acad Sci* **2001,** 949, 317-26.
474. Miller, C. P.; Collini, M. D.; Tran, B. D. *J. Med. Chem.* **2001,** 44, 1654-7.
475. Gruber, C.; Gruber, D. *Curr Opin Investig Drugs* **2004,** 5, 1086-93.
476. Von Angerer, E.; Prekajac, J.; Strohmeier, J. *J. Med. Chem.* **1984,** 27, 1439-47.
477. Von Angerer, E.; Knebel, N.; Kager, M.; Ganss, B. *J. Med. Chem.* **1990,** 33, 2635-40.
478. Von Angerer, E.; Knebel, N. *J. Med. Chem.* **1988,** 31, 1675-79.
479. Lemke, T. *D, W. Foye's Principles of Medicinal Chemistry*. 6th ed ed.; Lippincott, Williams and Wilkins: 2006.
480. Clayden, J.; Greeves, N.; Warren, W. *Organic Chemistry*. Oxford University Press: Oxford, 2001; Vol. 1st.
481. Dewick, P. M. *Essentials of Organic Chemistry*. Wiley: New Yory, 2006; Vol. 1st.
482. Miller, C. P.; Harris, H. A.; Komm, B. S. *Drugs of the Future* **2002,** 27, 117.
483. Green. *Protective Groups in Organic Synthesis*. Wiley: 1981.
484. Wang, Z. Pearlman's Catalyst. In *Comprehensive Organic Name Reactions and Reagents*, John Wiley & Sons, I., Ed. John Wiley & Sons, Inc.: 2010; pp 2143–2146.
485. Jonville, M.-C.; Dive, G.; Angenot, L.; Bero, J.; Tits, M.; Ollivier, E.; Frédérich, M. Dimeric bisindole alkaloids from the stem bark of Strychnos nux-vomica L. *Phytochemistry* **2012,** In Print.
486. Chacon-Garcıa, L.; Martınez, R. *European Journal of Medicinal Chemistry* **2002,** 37, 261-266.
487. Ke-Jia, W.; Li-Xin, D.; Shu-Li, Y. *Org. Lett.* **2012,** 14, 3772-3775.
488. Chadwick, C. C.; Chippari, S.; Matelan, E.; Borges-Marcucci, L.; Eckert, A. M.; Keith, J. C.; Albert, L. M.; Leathurby, Y.; Harris, H. A.; Bhat, R. A. *Proc Natl Acad Sci U S A* **2005,** 102, 2543-2548.
489. Biswas, D. K.; Shi, Q.; Baily, S.; Strickland, I.; Ghosh, S.; Pardee, A. B.; Iglehart, J. D. *Proc Natl Acad Sci U S A* **2004,** 101, 10137-10142.
490. Biswas, D. K.; Iglehart, J. D. *J Cell Physiol* **2006,** 209, 645-652.
491. Tyree, C. M.; Zou, A.; Allegretto, E. A. *Steroid Biochem. Mol. Biol.* **2002,** 80, 291-97.
492. Valentine, J. E.; Kalkhoven, E.; White, R.; Hoare, S.; Parker, M. G. *J. Biol. Chem.* **2000,** 275, 25322-29.
493. Amos, L. A.; Klug, A. *J. Cell Science* **1974,** 14, 523-30.
494. Jordan, A.; Hadfield, J. A.; Lawrence, N. J.; McGown, A. T. *Medicinal Research Reviews* **1998,** 18, 259-96.
495. Sackett, D. L. *Pharmacol. Ther.* **1993,** 59, 163.
496. Cushman, M.; Nagarathnam, D.; Gopal, D.; He, H.; Lin, C. M.; Hamel, E. *J. Med. Chem.* **1992,** 35, 2293-96.
497. Pettit, G. R. *J. Natl. Prod.* **1996,** 59, 812-16.
498. Pettit, G. R.; Singh, S. B.; Boyd, M. R.; Hamel, E.; Pettit, R. K.; Schmidt, J. M.; Horgan, F. *J. Med. Chem.* **1995,** 38, 1666-72.
499. Robinson, J. E.; Taylor, R. J. K. *Chem. Commun.* **2007,** 32, 1617-19.

500. Gaukroger, K.; Hepworth, L. A.; Lawrence, N. J.; McGowen, A. T. *J. Org. Chem.* **2001,** 66, 8135-38.
501. Furstner, A. *Liebigs Ann. Chem.* **1996**, 2107-13.
502. Lawrence, N. J.; Hepworth, L. A.; Hadfield, J. A.; McGown, A. T.; Pritchard, R. G. *Synthesis* **1999**, 1656-60.
503. Furniss, B. S.; Hannaford, A. J.; Smith, P. W. G.; Tatchell, A. R. *Vogel's textbook of practical organic chemistry.* . Longman Scientific & Technical: 1989; Vol. 5.
504. Cushman, M. N., D.; Gopal, D.; He, H.; Lin, C. M.; Hamel, E. . *J. Med. Chem.* **1992,** 35, 2293.
505. Prakash S, K. M., Khan Z, Zaman A,. *Phytochemistry* **1985,** 24, 622-662.
506. Borrela C, T. S., Cacheta X, Guénardb D, Tillequina F, Kocha M, Michela S,. New antitubulin derivatives in the combretastatin A4 series: synthesis and biological evaluation. *Bioorganic & Medicinal Chemistry* 13, 3853-3864.
507. Gaukroger, K. H., J. A.; Hepworth, L. A.; Lawrence, N. J.; McGown, A. T. . *J. Org. Chem.* **2001,** 66, 8135.
508. Letcher, R. M. *J. Chem. Soc. Perkin Trans. 1* **1972**, 1941-46.
509. Chen, Y.; Zou, Y.; Sun, H.-Y.; Liu, X.-K.; Xiao, C.-F.; Sun, J.; He, S.-J.; Li, J. *Synthesis* **2011,** 2, 217-22.
510. McCorkindale, N. J.; Magrill, D. S.; Caddy, B.; Martin-Smith, M.; Smith, S. J.; Stenlake, J. B. *Tetrahedron Lett.* **1968,** 25, 5475-83.
511. Sinha, A. K.; Joshi, B. P. *Tetrahedron Lett.* **2007,** 63, 960-65.
512. Sinha AK, S. A., Joshi BP. *Tetrahedron* **2007,** 63, 960-965.
513. Vanjari, H.; Pande, R. *Journal of Pharmaceutical and Biomedical Analysis* **2003,** 33, 783-88.
514. Neilands, J. B. *Science* **1967,** 156, 1443-47.
515. Raetz, C. R. *J. Biol. Chem.* **2000,** 275, 11002-09.
516. Holland, K. P.; Elford, H. L.; Bracchi, V.; Annis, C. G.; Schuster, S. M.; Chakrabarti, D. *Antimicrob. Agents Chemother.* **1998,** 42, 2456-58.
517. Tabuchi, K.; Okubo, H.; Fujihira, K.; Tsuji, S.; Hara, A.; Kusakari, J. *Neurosci. Lett.* **2001,** 307, 29-32.
518. Leoni, F.; Zaliani, A.; Bertolini, G.; Porro, G.; Pagani, P.; Pozzi, P.; Dona, G.; Fossati, G.; Sozzani, S.; Azam, T.; Bufler, R.; Fantuzzi, G.; Goncharav, I.; Kim, S. H.; Pomerantz, B. J.; Reznikov, L. L.; Siegmund, B.; Dinarello, C. A.; Mascagni, P. *Proc. Natl. Acad. Sci. U.S.A.* **2002,** 99, 2995-3000.
519. Kikuchi, T.; Itoh, F.; Toyota, M.; Suzuki, H.; Yamamoto, H.; Fujita, M.; Hosokawa, M.; Imai, K. *Int. J. Cancer* **2002,** 97, 272-77.
520. Clements, J. M.; Beckett, R. P.; Brown, A.; Catlin, G.; Labell, M.; Palan, S.; Thomas, W.; Whittaker, M.; Wood, S.; Salama, S.; Baker, P. J.; Rodgers, H. F.; Barynin, V.; Rice, D. W.; Hunter, M. G. *Antimicrob. Agents Chemother.* **2001,** 45, 563-70.
521. Komatsu, Y.; Tomizaki, K. Y.; Tsukamoto, M.; Kato, T.; Nishino, N.; Sato, S.; Yamori, T.; Tsuruo, T.; Furumai, R.; Yoshida, M.; Horinouchi, S.; Hayashi, H. *Cancer Res.* **2001,** 61, 4459-66.
522. Riva, E.; Gagliardi, S.; Mazzoni, C.; Passarella, D.; Rencurosi, A.; Vigo, D.; Martinelli, M. *J. Org. Chem.* **2009,** 74, 3540-43.
523. Gissot, A.; Volonterio, A.; Zanda, M. *J. Org. Chem.* **2005,** 70, 6925-28.
524. Reddy, A. S.; Kumar, M. S.; Reddy, G. R. *Tetrahedron Letters* **2000,** 41, 6285-88.
525. Kumar, A.; Prasad, B.; Vinaya, K.; Chandrappa, S.; Thimmegowda, N. R.; Kumar, S.; Swarup, S.; Rangappa, K. S. *Eur J Med Chem* **2009,** 44, 1223-29.
526. Qun Li, H. L. S. *Expert Opinion in Pharmacotherapy* **2002,** 12, 1663-702.
527. O'Brien, J. Private communiation. In Kelly, P. M., Ed. 2010.
528. Winer, E. P.; Hudis, C.; Burstein, H. J.; et al. *J Clin Oncol* **2005,** 23, 619-29.
529. Edwards, P. N.; Large, M. S. (Substituted aralkyl) heterocyclic compounds. 1990.
530. Edwards, P. N.; Large, M. S. (Substituted aralkyl) heterocyclic compounds 2000.

531. Jackson, T.; Lawrence Woo, L. W.; Trusselle, M., N.; Chander, S. K.; Purohit, A.; Reed, M. J.; Potter, B. V. L. *Org. Biomol. Chem.* **2007,** 5, 2940-52.
532. Kikuchi, D.; Sakaguchi, S.; Ishii, Y. *J. Org. Chem.* **1998,** 63, 6023.
533. Doiron, J.; Soultan, A. H.; Richard, R.; Touré, M. M.; Picot, N.; Richard, R.; Cuperlovic-Culf, M.; Robichaud, G. A.; Touaibia, M. *European Journal of Medicinal Chemistry* **2011,** 46, 4010-24.
534. Johnson, D. S.; Li, J. J. *The Art of Drug Synthesis*. John Wiley & Sons: Hoboken, NJ., 2007.
535. Lang, M.; Batzl, C.; Furet, P.; Bowman, R.; Hausler, A.; Bhatnagar, A. *The Journal of Steroid Biochemistry and Molecular Biology* **1993,** 44, 421-28.
536. MacDonald, P. L.; Bigatti, E.; Rossetto, P.; Harel, Z. Process for the preparation of letrozole. 2006.
537. Kil, K. E.; Biegon, A.; Ding, Y. S.; Fischer, A.; Ferrieri, R. A.; Kim, S. W.; Pareto, D.; Schueller, M. J.; Fowler, J. S. *Nucl Med Biol* **2009,** 36, 215-23.
538. Kim, S.-H.; Rieke, R. D. *Tetrahedron Lett.* **2011,** 52, 1523-26.
539. Fillion, H.; Gosmini, C.; Perichon, J. *J. Am. Chem. Soc.* **2003,** 125, 3867-70.
540. Seka, S.; Buriez, O.; Nedelec, J. Y.; Perichon, J. *Chem. Eur. J.* **2534,** 8, 2534.
541. Murthi, K. K.; Dubay, M.; McClure, C.; Brizuela, L.; Boisclair, M. D.; Worland, P. J.; M.M., M.; Pal, K. *Bioorganic & Medicinal Chemistry Letters* **2000,** 10, 1037-41.
542. Misawa, T.; Aoyama, H.; Furuyama, T.; Dodo, K.; Sagawa, M.; Miyachi, H.; Kizaki, M.; Hashimoto, Y. *Chem. Pharm. Bull.* **2008,** 56, 1490-95.
543. Veillet, S.; Tomao, V.; Visinoni, F.; Chemat, F. *Analytica Chimica Acta* **2009,** 632, 203-07.
544. Pratt, R. F.; McLeish, M. J. *Biochemistry* **2010,** 49, 9688-97.
545. Rawlings, N. D.; Salvesen, G. *Handbook of Proteolytic Enzymes*. Elsevier Science, San Diego: 2012.
546. Richard, S. A.; Hollerton, J. C. Essential practical NMR for organic chemistry. In Wiley InterScience Chichester, West Sussex, U.K.: 2011.
547. Lloyd, D. G.; Smith, H. M.; O'Sullivan, T.; Zisterer, D. M.; Meegan, M. J. *Medicinal Chemistry* **2005,** 1, 335-53.
548. Lloyd, D. G.; Smith, H. M.; O'Sullivan, T.; Knox, A. S.; Zisterer, D. M.; Meegan, M. J. *Medicinal Chemistry* **2006,** 2, 147-68.
549. Cushman, M.; Nagarathnam, D.; Gopal, D.; Chakraborti, A. K.; Lin, C. M.; Hamel, E. *Medicinal Chemistry* **1991,** 34, 2579-88.
550. Borrel, C.; Thoret, S.; Cachet, X.; Guenard, D.; Tillequin, F.; Koch, M.; Michel, S. *Bioorg. Med. Chem.* **2005,** 13, 3853-64.
551. Pettit, G. R.; Singh, S. B.; Boyd, M. R.; Hamel, E.; Pettit, R. K.; Schmidt, J. M.; Hogan, F. *Medicinal Chemistry* **1995,** 38, 1666-72.
552. Mürdter1, T. E.; Kerb, R.; Turpeinen, M.; Schroth, W.; Ganchev, B.; Böhmer, G. M.; Igel, S.; Schaeffeler, E.; Zanger, U.; Brauch, H.; Schwab, M. *Hum. Mol. Genet.* **2012,** 21.
553. Cytoskeleton, Tubulin Polymerization Assay Kit *Cat. # BK006P* 2011, pp 1-18.
554. Michael L. Shelanski; Felicia Gaskin; Charles R. Cantor. Microtubule Assembly in the Absence of Added Nucleotides. *Proceedings of the National Academy of Sciences* **1973,** 70, 765-768.
555. James C. Lee; Serge N. Timasheff. *In vitro* reconstitution of calf brain microtubules: effects of solution variables. *Biochemistry* **1977,** 16, 1754-1764.
556. Chemical Computing Group Inc. MOE (The Molecular Operating Environment) Version 2012.10. *Available from: http://www.chemcomp.com [2012 Jul 15]* **2012**.
557. Wurtz, J.-M.; Bourguet, W.; Renaud, J.-P.; Vivat, V.; Chambon, P.; Moras, D.; Gronemeyer, H. *Nature Structural Biology* **1996,** 3, 87-94.
558. Pike, A. C. W.; Brzozowski, A. M.; Hubbard, R. E.; Bonn, T.; Thorsell, A.-G.; Engström, O.; Ljunggren, J.; Gustafsson, J.-A.; Carlquist, M. *EMBO Journal* **1999,** 18, 4608-18.
559. Ravelli, R. B.; Gigant, B.; Curmi, P. A.; Jourdain, I.; Lachkar, S.; Sobel, A.; Knossow, M. *Nature* **2004,** 428.
560. Ghosh, D.; Griswold, J.; Erman, M.; Pangborn, W. *Nature* **2009,** 457, 219-23.

561. Accelry's. DS Visualizer 3.1. **2012**.
562. Wilson, M. A.; Miller, D. W.; Ahmad, R.; McLendon, C.; Bandyopadhyay, S.; Baptista, M. J.; Ringe, D.; Petsko, G. A.; Cookson, M. R. *Proc.Natl.Acad.Sci.USA* **2004,** 101, 9103-08.
563. Limited, D. s. L. Method for the preparation of 5-benzyloxy-2-(4-benzyloxphenyl)-3-methyl-1h-indole. 1999.
564. Prakash, S. K. M.; Khan, Z.; Zaman, A. *Phytochemistry* **1985,** 24, 622-62.